South Australia South Australia South Australia South Australia

Open File Envelope

NUMBER 8785

ABSORBENT CLAY PROJECT

PROGRESS REPORTS

Submitted by

CSIRO. Division of Soils
1996

© 18/4/95

MINES AND ENERGY
SOUTH AUSTRALIA

This report was supplied as part of the requirement to hold a mineral or petroleum exploration tenement in the State of South Australia. MESA accepts no responsibility for statements made, or conclusions drawn, in the report or for the quality of text or drawings. All rights reserved under the copyright. No part of this publication may be reproduced, stored in a retrieval system or transmitted in any form or by any means (electronic, mechanical, photocopying, recording or otherwise) without the written permission of Mines and Energy South Australia, PO Box 151, Eastwood, SA 5063

Enquiries: Records Management
Mines and Energy South Australia
191 Greenhill Road, Parkside 5063
Telephone: (08) 274 7687
Facsimile: (08) 272 7597

ENVELOPE 8785

CONTENTS

		MESA NO.
REPORT:	**Churchman, G.J., Ferris, G.M., Keeling, J.L., McClure, S.G., Raven, M.D., Self, P.G. and Slade, P.G., 1994.** Absorbent clay project. Progress report no. 1. Characterisation of the selected clays.	**8785 R 1** Pgs 3-115
APPENDIX 1:	**Raven, M.D., Keeling, J.L., Self, P.G. and Slade, P.G., 1992.** Mineralogical analysis of composite samples from the Arumpo Bentonite Deposit.	Pgs 116-137
REPORT:	**Slade, P.G. and Kimber, R.W.L., 1994.** Absorbent clay project. Progress report no. 2. Results of the uptake of Ni, Cd, Cr, Pb and Benzene by selected clays.	**8785 R 2** Pgs 138-150
APPENDIX 1:	**Fazey, P.G., 1994.** X-ray fluorescence analyses of heavy metal cations.	Pgs 151-163
APPENDIX 2:	**Fiebiger, W. and Schellhorn, M., 1994.** Industrial minerals in soil sealants and waste dump linings.	Pgs 164-169
REPORTS:	**Slade, P.G., Taylor, R.M., Raven, M.D., Churchman, G.J., Fletcher, S., Urban, A.J., Kimber, R.W., Keeling, J.L., McClure, S.G. and Self, P.G., 1995.** Absorbent clay project. Progress report no. 3. Clays for the uptake of pollutants: modification, properties and assessment techniques.	**8785 R 3** Pgs 170-246
	Raven, M.D., Abolins, N., Keeling, J.L. and Self, P.G., 1995. Absorbent clay project. Mineralogical characterisation of Garford palaeochannel clays.	**8785 R 4** Pgs 247-364
	Self, P.G., Keeling, J.L. and Raven, M.D., 1996. Absorbent clay project. Additional report. Mineralogy and physical properties of samples containing palygorskite collected during the MESA 1995 drilling programme in the Garford palaeochannel, South Australia.	**8785 R 5** Pgs 365-529
APPENDIX 1:	Quantification of mineral content by x-ray diffraction.	Pgs 530-547
APPENDIX 2:	Mineralogy of all samples from the Garford palaeochannel.	Pgs 548-562
APPENDIX 3:	Laboratory method for separation of quartz and dolomite from Garford palaeochannel clay samples.	Pg. 563
APPENDIX 4:	Analyses of reference samples.	Pgs 564-574
APPENDIX 5:	Water sorption by Westinghouse method.	Pgs 575-576

END OF CONTENTS

DME 392/93
Env. 8785

000003

ABSORBENT CLAY PROJECT

PROGRESS REPORT No.1 TO MINES AND ENERGY, SOUTH AUSTRALIA

CHARACTERISATION OF THE SELECTED CLAYS

G.J. Churchman, G.M. Ferris, J.L. Keeling, S.G. McClure,

M.D. Raven, P.G. Self and P.G. Slade

CSIRO

Division of Soils

Commonwealth of Australia

June, 1994

SUMMARY

In January 1994, an agreement was made between Mines and Energy, South Australia and CSIRO Division of Soils to investigate the potential for local clays to effectively adsorb harmful or toxic substances.

Clays selected for study represented those readily available in South Australia. They included samples containing significant amounts of either smectite, kaolin, illite or palygorskite.

No commercial smectite deposits are known in South Australia and samples from the recently discovered Arumpo Deposit in New South Wales were included for testing. Pleistocene plastic clays of the Adelaide Plains have a significant smectite component, and representatives from Pooraka Formation, Keswick Clay and Hindmarsh Clay were collected for comparison. Keswick and Hindmarsh Clays were shown to have a relatively high content of clay-sized particles, around 50%, mostly as interstratified kaolinite/smectite with illite/mica and kaolinite. Arumpo is a relatively pure Na/Mg montmorillonite with minor interstratified illite.

A wide range of kaolin clays are available in South Australia. Those included in this investigation were poorly-crystalline, sedimentary kaolinite from Golden Grove and McLaren Vale, well-crystalline kaolinite from Birdwood, and mixed kaolinite/halloysite from Cromer and Woodside. The presence of tubular halloysite increases the surface area of kaolin and the range of pore sizes. Therefore, these clays are expected to perform better as sorbents than those with dominantly kaolinite. A relatively pure halloysite product from New Zealand China Clays Ltd was included for comparison.

Fine-grained, chemically precipitated illite clays appear to be relatively widespread as lacustrine deposits in Tertiary palaeodrainage channels in South Australia. The clays are characterised by relatively high iron contents and uniform, very fine-grained particles. These clays have not been used commercially, but have a relatively high surface area and may have potential as an absorbent. The sample selected for further investigation was from Muloorina near Lake Eyre South.

Palygorskite clays are also associated with palaeodrainage channels in South Australia. Pure palygorskite reported previously from Garford Palaeochannel was shown by this investigation to be a mixed illite/palygorskite clay. Mixed dolomite/palygorskite clay overlies the illite/palygorskite clay at Garford and examples of both types of clay will be included in sorption tests. Similar clays were investigated from the Maralinga site. These are under consideration for use in sealing shallow pits to be excavated for burial of soils contaminated by low levels of radioactive materials.

Data contained in this report will be the basis for selection of clays for comparative sorption studies in the next stage of the Absorbent Clay Project.

TABLE OF CONTENTS

GENERAL INTRODUCTION	1
THE SMECTITES	3
Introduction	3
Materials	5
Experimental	5
Results	6
FIGS. 2 TO 19	10
THE KAOLINS	29
Introduction	29
Materials	30
Experimental	31
Results	32
FIGS. 20 TO 30	36
ILLITE	61
Introduction	61
Material	61
Experimental	61
Results	61
FIGS. 31 AND 32	64
THE PALYGORSKITES	67
Introduction	67
Materials	68
Garford palygorskite	68
Maralinga palygorskite	74
Reference materials	74

Experimental 74
Mineralogy (XRD) 74
Chemistry 74
Differential thermal analysis (DTA) and thermogravimetric analysis (TGA) 75
Scanning electron microscopy 75
Results 75
Garford palygorskite 75
Maralinga palygorskite 77
Illite content and grain size of Garford clays 81
Results 81
FIGS. 33 TO 38 85

ACKNOWLEDGMENTS 106

REFERENCES 107

APPENDIX 1: Mineralogical analyses of composite samples from the Arumpo Bentonite Deposit. 110

GENERAL INTRODUCTION

In the past few years there has been an increasing interest in using both natural and modified clays for efficiently removing pollutants from water. Clays are potentially or actually being used in water purification, the containment of organic and inorganic pollutants around waste deposits and to form sealing layers around underground storage reservoirs.

Australia has large and diverse clay resources (Table 1, Fig. 1) but, owing to small local markets, high transportation costs, limited knowledge of properties, processing methods and markets, these are largely under utilised. As a result, we continue to import significant amounts of specialised clays and clay products as well as other absorbing agents such as diatomaceous earths and zeolites for domestic markets. To develop these resources to their full potential, both existing and innovative end uses need to be assessed, developed and marketed for individual deposits.

Ultimately this project aims to identify potential uses for a defined group of Australian clays including kaolinites, smectites, illites and palygorskites and products formed from them by different treatments. However, at present, insufficient basic data on the properties of Australian clays limits their potential for use. The present report characterises key properties of a group of predominantly South Australian clays selected for study by Mr J.L. Keeling, Senior Geologist, Mines and Energy, South Australia.

Table 1. Industrial clay and natural zeolite production in Australia 91/92 (tonnes)

	Qld	NSW	Vic	Tas	SA	WA	Total
Kaolin	120,000	80,000	65,000	20,000	10,000	7,000	302,000
Vermiculite							nil
Bentonite	50,000	15,000					65,000
Palygorskite						40,000	40,000
Zeolite		1,200					1,200
Total	170,000	96,200	65,000	20,000	10,000	47,000	408,200

Kaolin

1. Welpa Qld
2. Pittong/Lal Lal Vic
3. Gulgong NSW
4. Tonganah Tas
5. Williamstown SA
6. Greenbushes WA
7. Wingen NSW
8. Birdwood SA
9. Lal Lal Dyke Vic
10. Cromer SA
11. Poochera SA
12. Skardon River Qld
13. Gabbin WA
14. Lake Moore WA
15. Mount Hope SA

Vermiculite

16. Munglinup WA
17. Hillview NSW
18. Coonana WA

Bentonite

19. Gurulmundi Qld
20. Cressfield NSW
21. Yarraman Qld
22. Oakleigh Qld
23. Arumpo NSW

Palygorskite

24. Lake Narramyne WA
25. Peak Crossing Qld
26. Garford SA
27. Glendambo SA

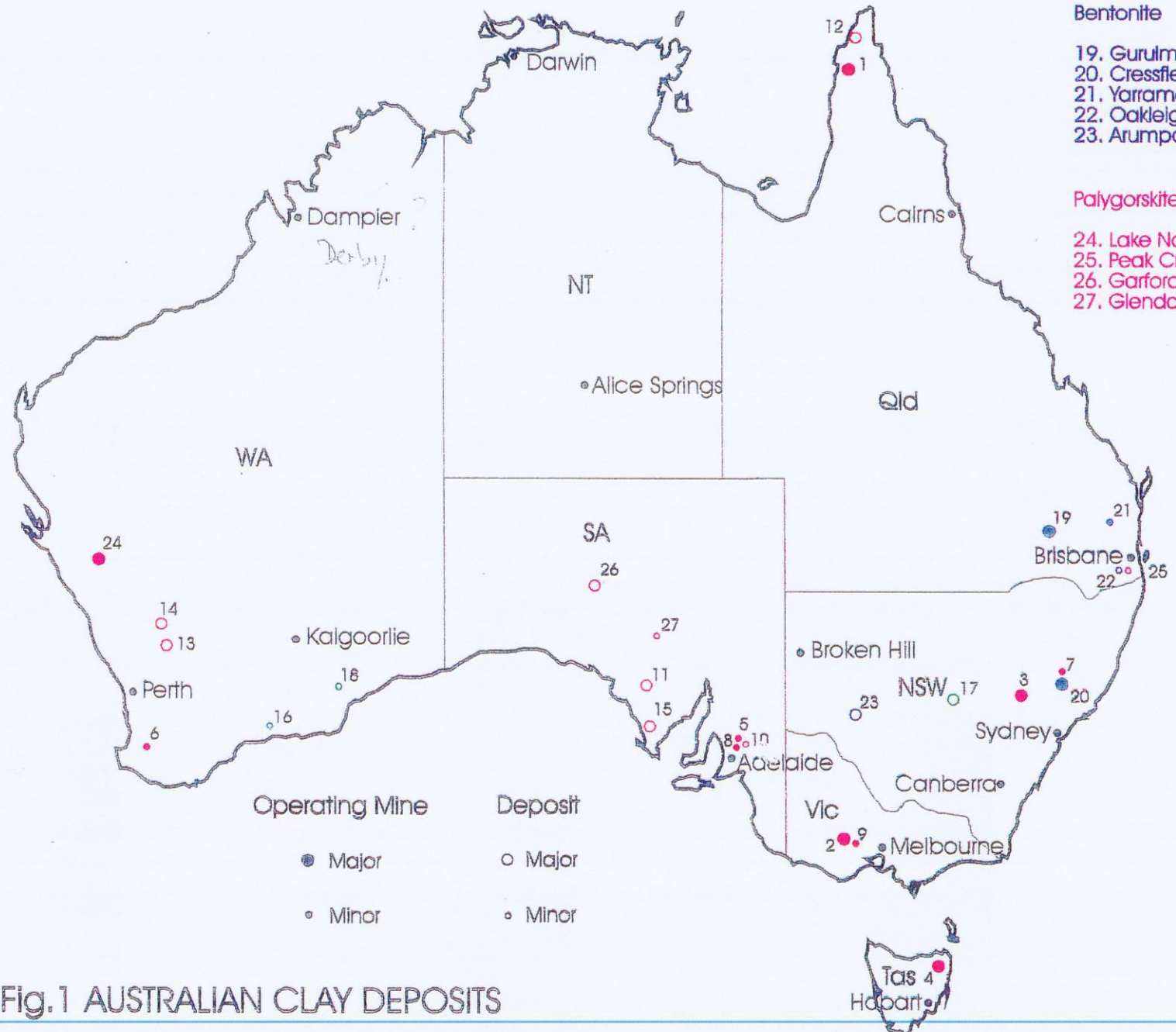


Fig.1 AUSTRALIAN CLAY DEPOSITS

000008

THE SMECTITES

Introduction

The smectites consist of sheets of aluminium atoms with oxygen atoms and hydroxyl groups and sheets of silicon atoms with oxygen atoms. The former comprise octahedrons, the corners of which are formed by the oxygen atoms and hydroxyl groups (in the ratio 2:1) and the centres by the aluminium atoms. The silica sheets are composed of tetrahedrons having oxygen atoms at the corners; the centres are occupied by the silicon atoms. The silica-tetrahedrons share corners with each other; terminal oxygens (at the edges and lines of fracture) being present as hydroxyl groups. The alumina-octahedrons also share corners. In the smectites the silica and alumina sheets are arranged in the order "silica-alumina-silica" and hence these clay minerals are referred to as 2:1 type phyllosilicates. On account of isomorphous substitutions (e.g. Si replaced by Al or Al replaced by Mg) the smectites are negatively charged. These negative charges are balanced by positively-charged interlayer cations which are hydrated to a variable degree. The following formula can be used to represent the end-member composition for the common smectite, montmorillonite:

$$(M^{+}_{y}\, nH_2O)(Al_{2-y})Mg_y)(Si_4)O_{10}(OH)_2$$

where M^{+} represents the positively-charged interlayer cation. Interlayer cations are exchangeable and the interlayer space is expandable so that it is capable of accommodating a wide range of inorganic and organic species. This property makes smectites attractive for absorption of toxic species.

Smectites occur as platy particles which are typically 10 Å thick and vary between 100 to 1000 Å across. In theory, the area of the planar surfaces is about 800 m^2/g which is indeed close to experimentally determined values.

Industrial applications of smectites are diverse and examples of these applications are given in Table 2.

Table 2. Industrial applications of smectite group minerals.

Rheological	drilling mud paint (to prevent settling, thixotropic paints) printing ink, thickening agent
Sorptive	pet litter, deodorising of poultry waste bleaching agent for mineral and vegetable oils spill absorbent (oil, grease, water, chemicals) beer and wine clarification pharmaceuticals (toxin absorption)
Catalytic	detergents desulphurisation of naphthalene ingrain agent for carbonless copy paper ozone decomposition
Binding	pelletising agent for iron ores and other metallic ores foundry bond clay pelletising animal feeds
Engineering	slurry trench excavation farm dam and irrigation channel sealant containment of toxic liquids
Other	cosmetics, crayons, general filler, polishing and cleaning agents

In order to compare the adsorption/absorption of a range of toxic organic compounds and inorganic cations by a group of clay minerals these had firstly to be characterised. However, also to be bourne in mind during this stage of the work was that the High Pressure Liquid Chromatographic method to be used subsequently to measure the uptake of the imbibed species requires the clays to be sized so that their particles were between 1-2 μm, or possibly down to 0.5 μm.

The clay sized fractions (< 2 μm) of the natural materials whose adsorption/absorption was to be tested were therefore subdivided into 1-2, 1-0.2 and < 0.2 μm fractions. In all cases, only small amounts of material occurred in the 1-2 μm range and hence the characterisations reported below focussed upon the 1-0.2 μm of the smectite containing materials.

Materials

1). Samples supplied by Mines and Energy, South Australia (MESA) (Fig. 2), consisted of the following:-

1. Material (Hindmarsh Clay) from Adelaide Subway Drill Hole CH8 (6-9.6m).
2. Material (Keswick and Hindmarsh Clay equivalents) from Commonwealth Law Courts Drill Hole CH1 (5.5-9.1 m and 11.9-16.0 m).
3. Material from Department of Agriculture Drill Hole CH1 (1.95 - 5.4m); referred to subsequently as Keswick Clay.
4. Pooraka Clay from type section - cliff section under Bridgeway Hotel, Pooraka.

2). Samples supplied by Brown Creek Gold NL from the Arumpo Bentonite Deposit in the Wentworth Shire Council area, NSW consisted of:

1. Material from Test Pit 1, upper seam, crushed and screened to -2 mm + 1 mm, (M010893).
2. ditto but disc pulverised, screened and sized to 100% <63μm, (M020593).
3. Material from bulk sample pit, upper seam, wet, sticky, plastic bentonite below north face of mill (BS-1).

3). For comparison, Wyoming Bentonite from the mineral collection of the Mineralogy Section of the CSIRO Division of Soils, Adelaide. Ref. cat. no. C2 S1 T8-9.

Experimental

After being lightly crushed in a large cast iron mortar, the materials from MESA were oven dried at 60°C. They were then homogenised by repeatedly being passed through a stainless steel sample splitter. All other materials were processed as received. 10 g portions of each material were dispersed in distilled water by shaking in a SPEX mill for 10 mins. The slurries were then poured into 400 ml beakers and ~150 mls of 1M NaCl added to each. They were left to stand for 2 hours and then, with the aid of centrifugation, repeatedly washed with deionised water until a stable (non-flocculating) suspension was obtained. The suspensions were transferred to measuring cylinders and allowed to stand in a constant temperature room for 15 hours when the < 2 μm particles were drawn off from the top 20 cm of the cylinders. By using centrifugation, this "clay sized" material was

further split into 1-2 μm, 1-0.2 μm and <0.2 μm fractions. The materials in each size range were then calcium saturated, carefully washed, dried at 105°C and weighed.

X-ray diffraction (XRD) analysis of the 1-0.2 μm fraction was carried out with a Philips PW1800 microprocessor-controlled diffractometer with CoKα radiation; variable divergence slits and a graphite monochromator.

Patterns were recorded in steps of 0.5°2θ with a 1 second counting time/step. Data were stored on computer discs for analysis by an IBM-compatible PC using the program XPLOT (Raven 1990).

X-ray fluorescence (XRF) analyses were carried out with a Philips PW1400 spectrometer. Cation exchange capacities were determined by saturating with Ba.

Results

Tables 3 and 4 show the weight percentages of particles in given size ranges for the Adelaide clays and the Arumpo bentonites respectively. Of note (Table 3), are the high percentages (40-90) of non clay sized materials in the Adelaide samples and also that the clay fractions of the samples contain substantial amounts of very fine particles. This last mentioned property of the Adelaide clays may enhance their adsorption of non-polar organic molecules.

Table 3. Summary of particle size distribution for Adelaide Clays

Size (μm)	Keswick	Pooraka	Com. Law Court 5.5-9.1 m	Com. Law Court 11.9-16.0 m	Adelaide Subway
> 2	50.8%	89.7%	42.9%	46.4%	48.5%
1-2	2.8	2.3	2.9	8.2	3.9
0.2-1	14.0	5.7	15.8	23.3	24.4
< 0.2	32.4	2.3	38.4	22.1	23.3

Table 4. Summary of particle size distributions for Arumpo Bentonites

	TP1(MO10893)	TP1(MO20593)	BS-1
> 2 μm	28.2%	27.9%	47.3%
1-2	5.1%	12.5%	1.0%
0.2-1	28.8%	44.0%	8.1%
< 0.2	38.0%	15.6%	43.6%

The XRD patterns of the non-oriented Adelaide clays (Figs. 3-7) broadly show these materials to consist of mixtures of quartz, kaolinite, muscovite and feldspar. The presence of smectite is not obvious. The non-oriented Arumpo clays (Figs. 8-10) are shown to be dominantly smectite with some quartz (especially in BS-1). Fig. 11 shows the diffraction pattern of the non-oriented Wyoming bentonite.

As is well known, the diffracted peak intensities of clay minerals may be very low unless they are oriented. Hence, for the present materials, oriented samples were produced by sucking down suspensions onto Millipore filters. Figs. 12-19 give the diffraction patterns of the oriented clay samples after they had been Mg-saturated and treated with glycerol in order to move the smectite lines away from those of chlorite or vermiculite.

The diffraction patterns of the oriented Adelaide clays are broadly similar but revealed, besides kaolinite, quartz and muscovite/illite, the presence of interstratified kaolinite/smectite (see the broad peaks at low angles).

No attempt was made to establish the exact nature of the interstratified system but from previous experience (Churchman *et al.*, 1994a) it would seem that the kaolinite/smectite ratio could be ~30:70.

The XRD pattern of the oriented Pooraka clay (Fig. 13) contains a sharp line corresponding to a basal spacing of 14.230 Å. None of the other Adelaide clays show a comparable spacing. When a second oriented specimen of the Pooraka clay was saturated with Ba, the line at 14.230 Å disappeared and a line corresponding to a spacing of 12.3 Å appeared. The presence of vermiculite rather than chlorite was therefore established.

For the oriented Arumpo bentonites (Mg-saturated and treated with glycerol) TP1 (M010893) and TP1 (MO20593), the XRD patterns are essentially the same; as might be expected because these samples differ only in the extent to which they were milled. The patterns show the presence of interstratified illite/smectite with minor kaolinite. For Arumpo bentonite (BS-1), besides the interstratified illite/smectite, there is rather more kaolinite and quartz present than in M010893 and M020593.

A Division of Soils Technical Report 83/1992 entitled "Mineralogical Analysis of Composite Samples from the Arumpo Bentonite Deposit" (see **Appendix 1**) discusses an analysis of the illite/smectite interstratification and shows that ~20% illite is interstratified with the smectite.

Table 5 shows the XRF analyses made upon the 1-0.2 μm fractions of the Adelaide and the Arumpo clays in order to obtain their cation exchange capacities (CECs). The CEC of a < 1 μm fraction of Wyoming bentonite was also determined and is shown in Table 5. By assuming that the CEC values of the smectites in the Adelaide and the Arumpo Clays are close to 100 meq/100g, often accepted as being reasonable for pure smectite, the measured CECs equate to the upper limits for the smectite concentrations in the 1-0.2 μm fractions. Illite and kaolinite also present, especially in the Adelaide clays, account for part of the exchange capacities and hence the CEC values will exceed the smectite concentrations.

Table 5. XRF Analyses and CEC Results (using Ba) for the 1 - 0.2 μm fractions of the clays listed

SAMPLE	Fe_2O_3 %	MnO %	TiO_2 %	CaO %	K_2O %	P_2O_5 %	SiO_2 %	Al_2O_3 %	MgO %	BaO %	SUM %	CEC-Ba meq/100g
Keswick Clay	7	0.02	1.24	0.04	2.3	< 0.1	39	18	2.0	3.5	74	45
Pooraka Clay	9	0.03	1.23	0.04	2.2	0.1	36	20	2.0	3.2	75	42
Com. Law Court (Upper)	8	0.02	1.60	0.03	2.4	0.1	39	20	1.5	3.0	76	39
Com. Law Court (Lower)	8	0.01	0.96	0.06	2.3	< 0.1	38	19	1.7	3.5	74	45
Subway Clay	9	0.02	0.97	0.04	2.0	0.1	39	21	1.5	2.6	76	33
Arumpo TP1 (M010893)	3	0.01	0.74	0.04	0.8	< 0.1	40	15	3.2	4.7	67	62
Arumpo TP1 (M020593)	3	0.01	0.58	0.03	0.6	< 0.1	39	15	2.9	5.2	66	68
Arumpo BS-1	4	0.01	1.55	0.04	1.3	< 0.1	42	18	2.6	4.9	75	64
Wyoming bentonite	4	0.02	0.15	0.08	< 0.1	< 0.1	46	18	2.7	7.0	77	92

FIGS. 2 TO 19

Fig. 2. Location of kaolin and smectite samples.

Fig. 3. XRD of Keswick clay - Dept. of Agriculture CH-1 1.95-5.4 m.

Fig. 4. XRD of Pooraka clay - Bridgeway Hotel.

Fig. 5. XRD of Commonwealth Law Court clay - 5.5-9.1 m.

Fig. 6. XRD of Commonwealth Law Court clay - 11.9-16.0 m.

Fig. 7. XRD of Adelaide Subway clay - CH8 6-9.6 m.

Fig. 8. XRD of Arumpo bentonite - TP-1 (MO 10893) +1mm-2mm.

Fig. 9. XRD of Arumpo bentonite - TP-1 (MO 20593) < 63 μm.

Fig. 10. XRD of Arumpo bentonite - BS-1.

Fig. 11. XRD of Wyoming montmorillonite - 1-2 μm fraction Ca-saturated.

Fig. 12. XRD of Keswick clay - 0.2-1 μm Mg-saturated and glycerolated.

Fig. 13. XRD of Pooraka clay - 0.2-1 μm Mg-saturated and glycerolated.

Fig. 14. XRD of Commonwealth Law Courts clay - 5.5-9.1 m - 0.2-1 μm Mg-saturated and glycerolated.

Fig. 15. XRD of Commonwealth Law Court clay - 11.9-16.0 m - 0.2-1 μm Mg-saturated and glycerolated.

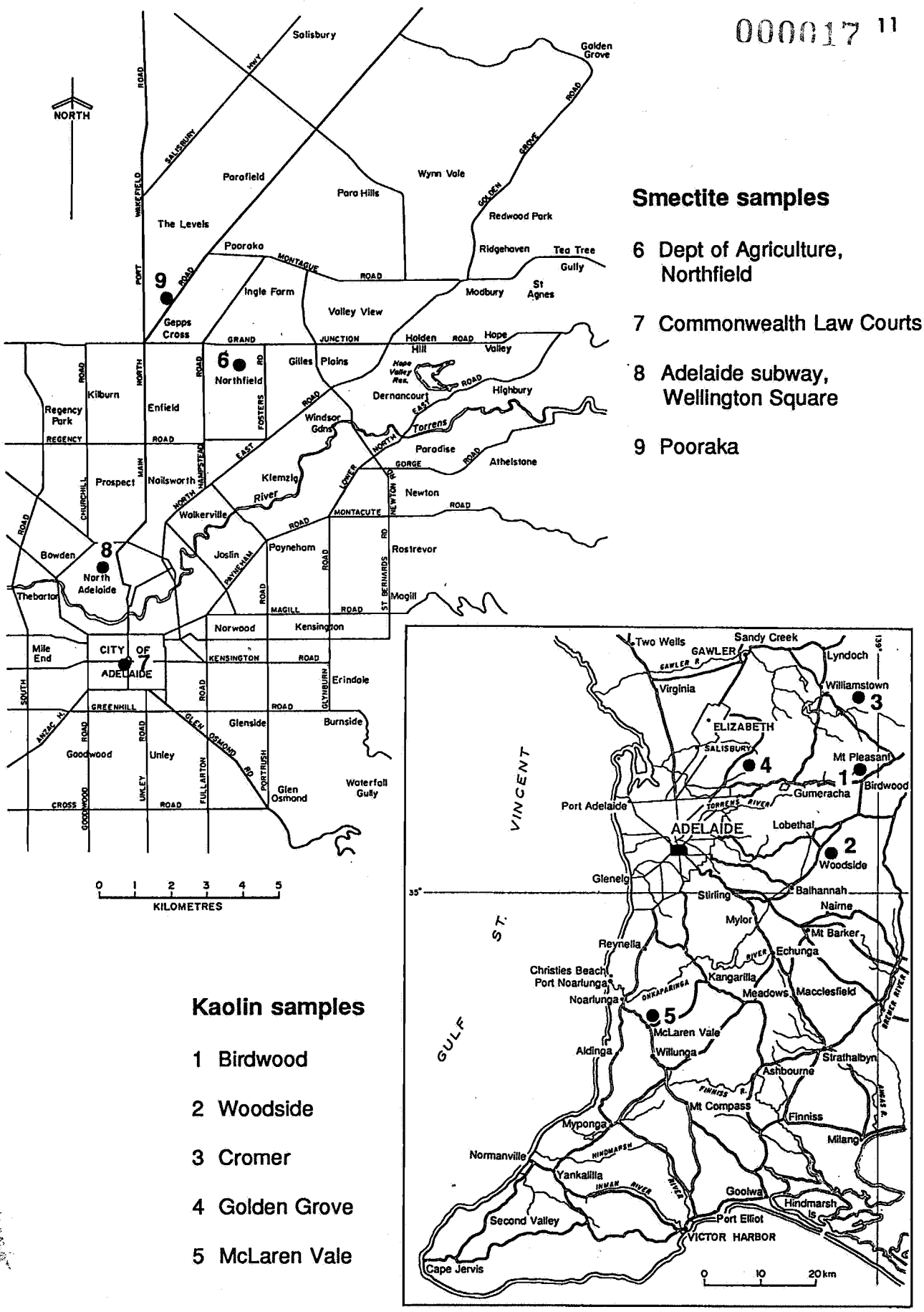
Fig. 16. XRD of Adelaide Subway clay - 0.2-1 μm Mg-saturated and glycerolated.

Fig. 17. XRD of Arumpo bentonite - TP-1 (MO 10893) - 0.2-1 μm Mg-saturated and glycerolated.

Fig. 18. XRD of Arumpo bentonite - TP-1 (MO 20593) - 0.2-1 μm Mg-saturated and glycerolated.

Fig. 19. XRD of Arumpo bentonite - BS-1 - 0.2-1 μm Mg-saturated and glycerolated.

000017 11



Smectite samples

6 Dept of Agriculture, Northfield

7 Commonwealth Law Courts

8 Adelaide subway, Wellington Square

9 Pooraka

Kaolin samples

1 Birdwood

2 Woodside

3 Cromer

4 Golden Grove

5 McLaren Vale

Figure 2

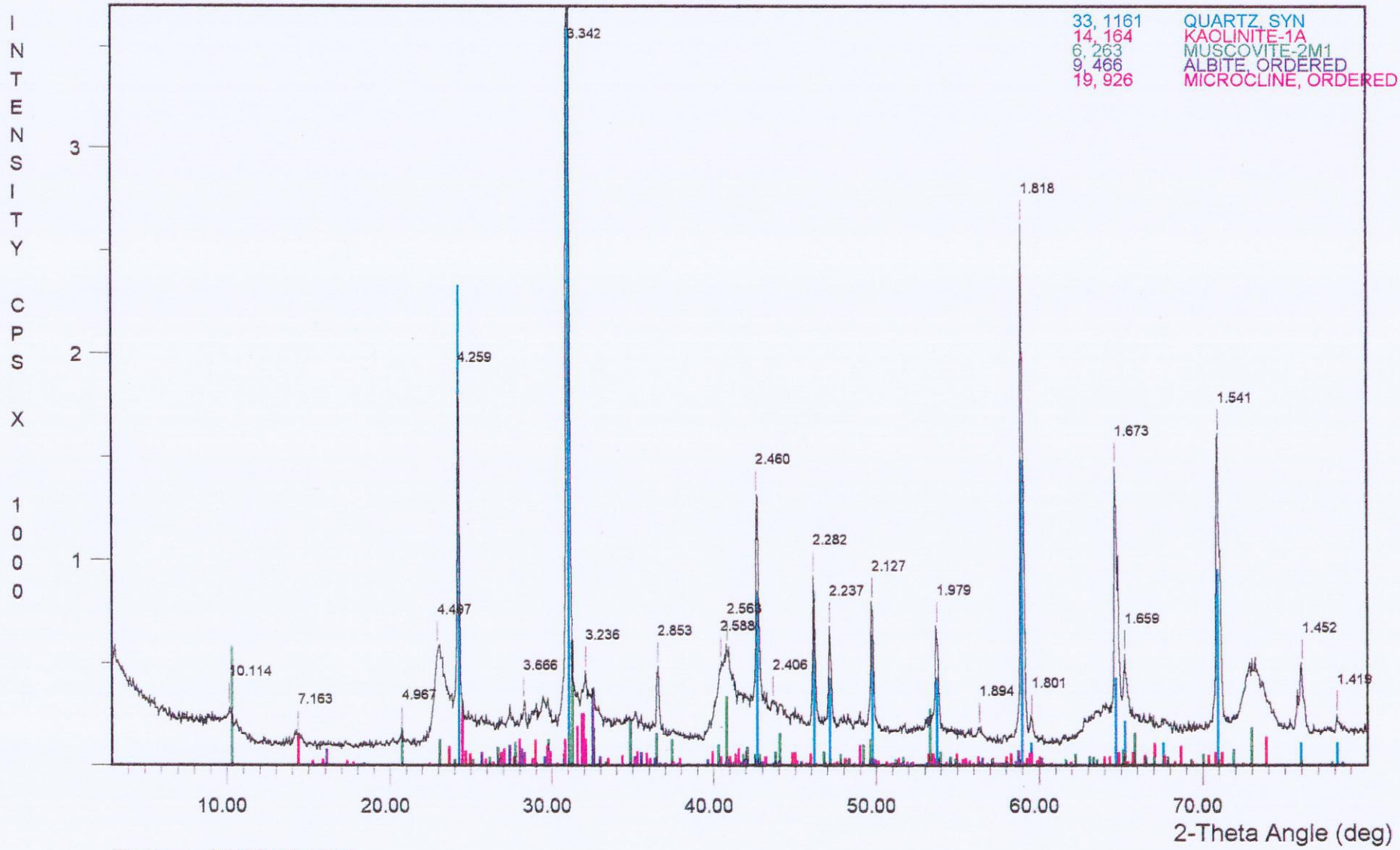
LOCATION OF KAOLIN AND SMECTITE SAMPLES ADELAIDE AREA

MINES AND ENERGY SOUTH AUSTRALIA

94-732

6805

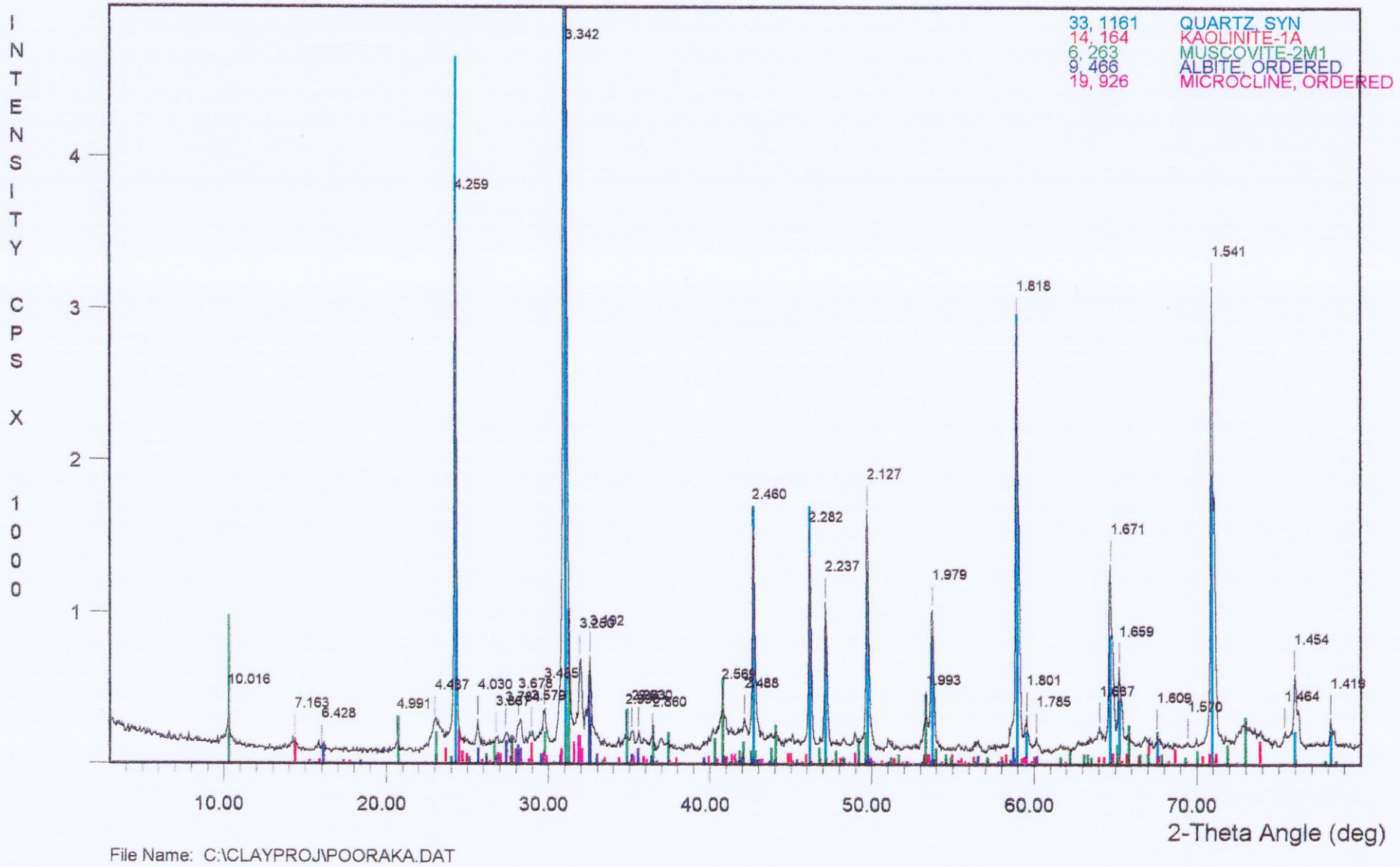
Fig. 3. Keswick clay - Dept. of Agriculture CH-1 1.95-5.4 m.



File Name: A:\KESWICK.DAT

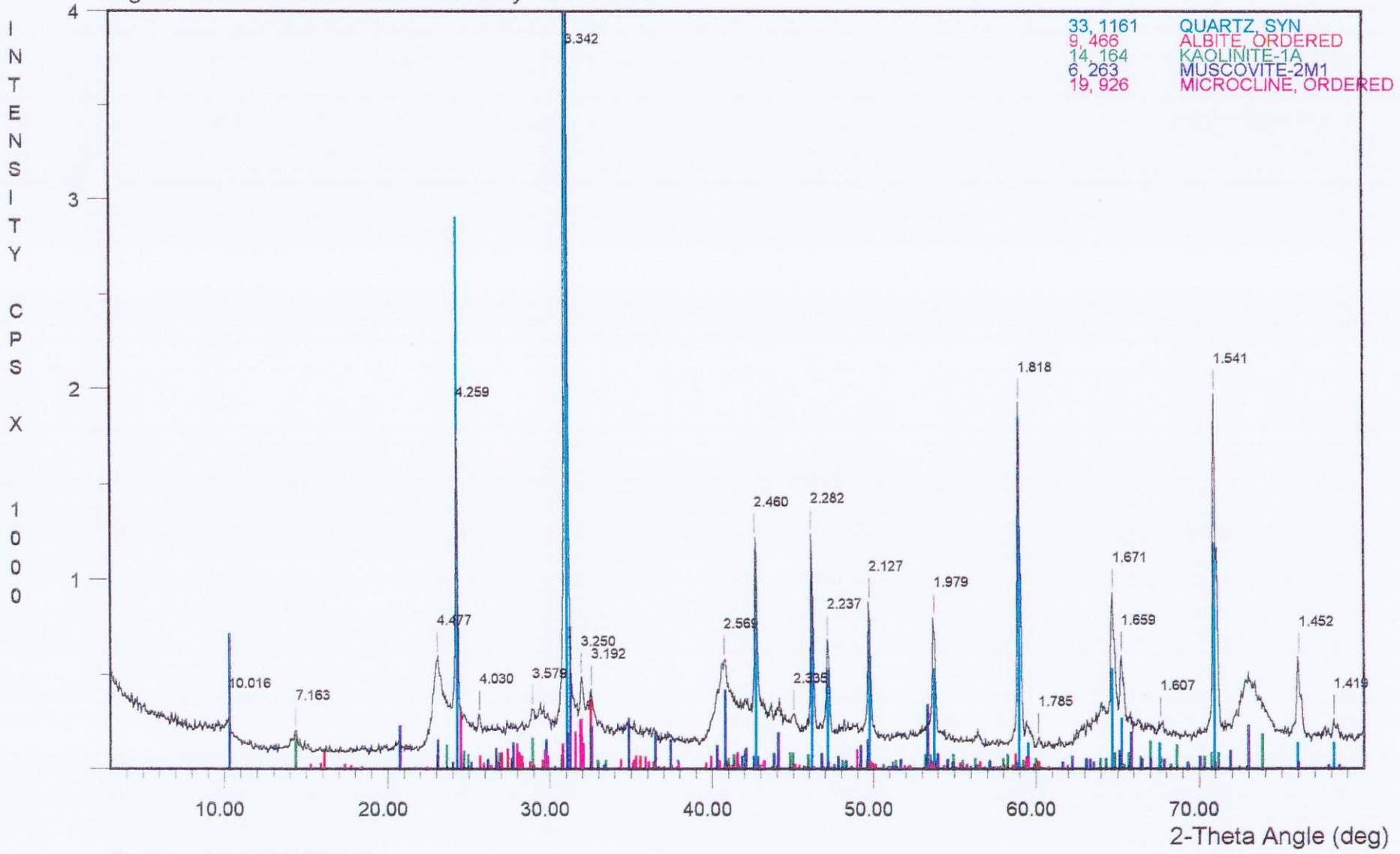
000018

Fig. 4. Pooraka clay - Bridgeway Hotel.



File Name: C:\CLAYPROJ\POORAKA.DAT

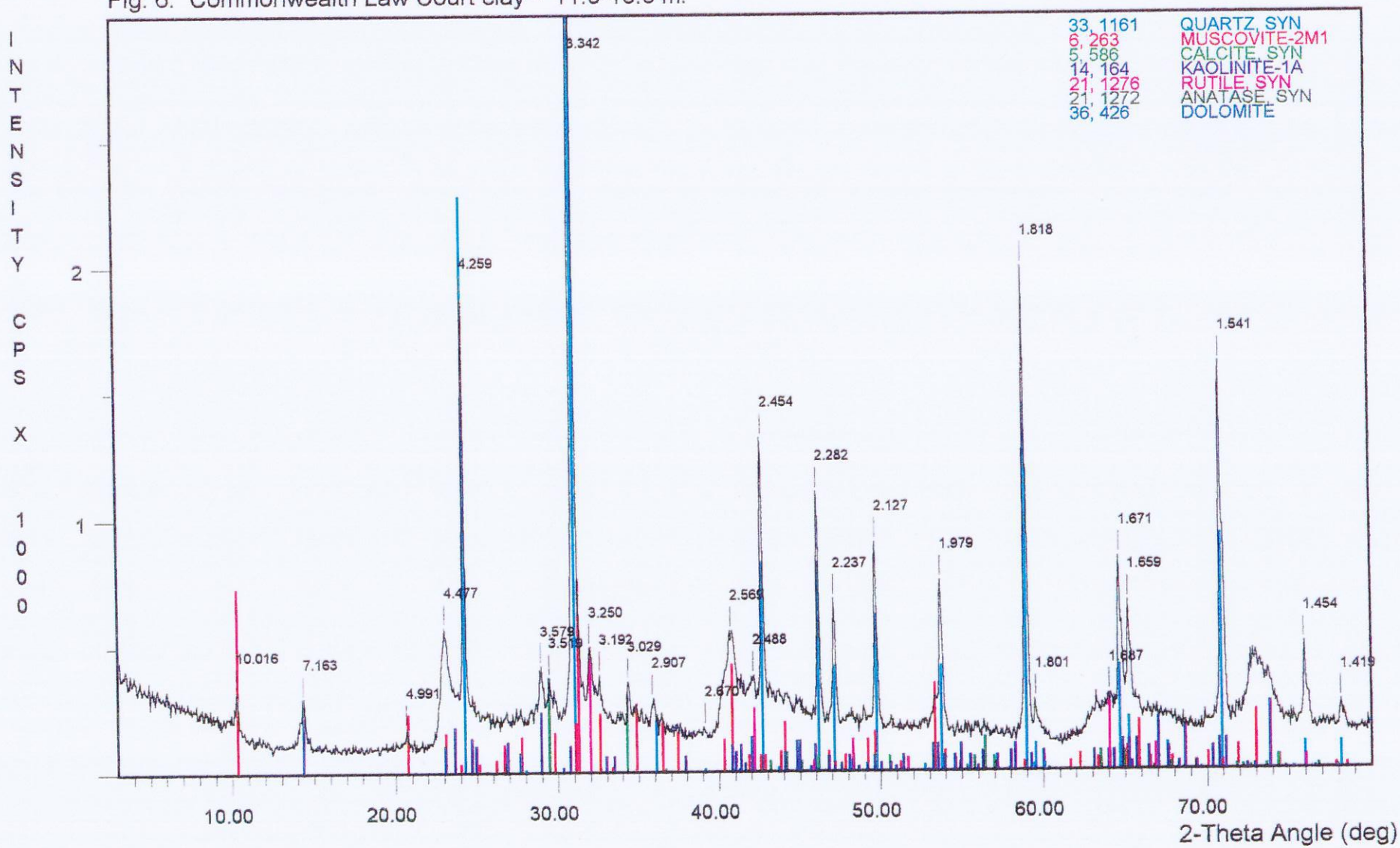
Fig. 5. Commonwealth Law Court clay - 5.5-9.1 m.



File Name: A:\LAWCOURT.DAT

000020

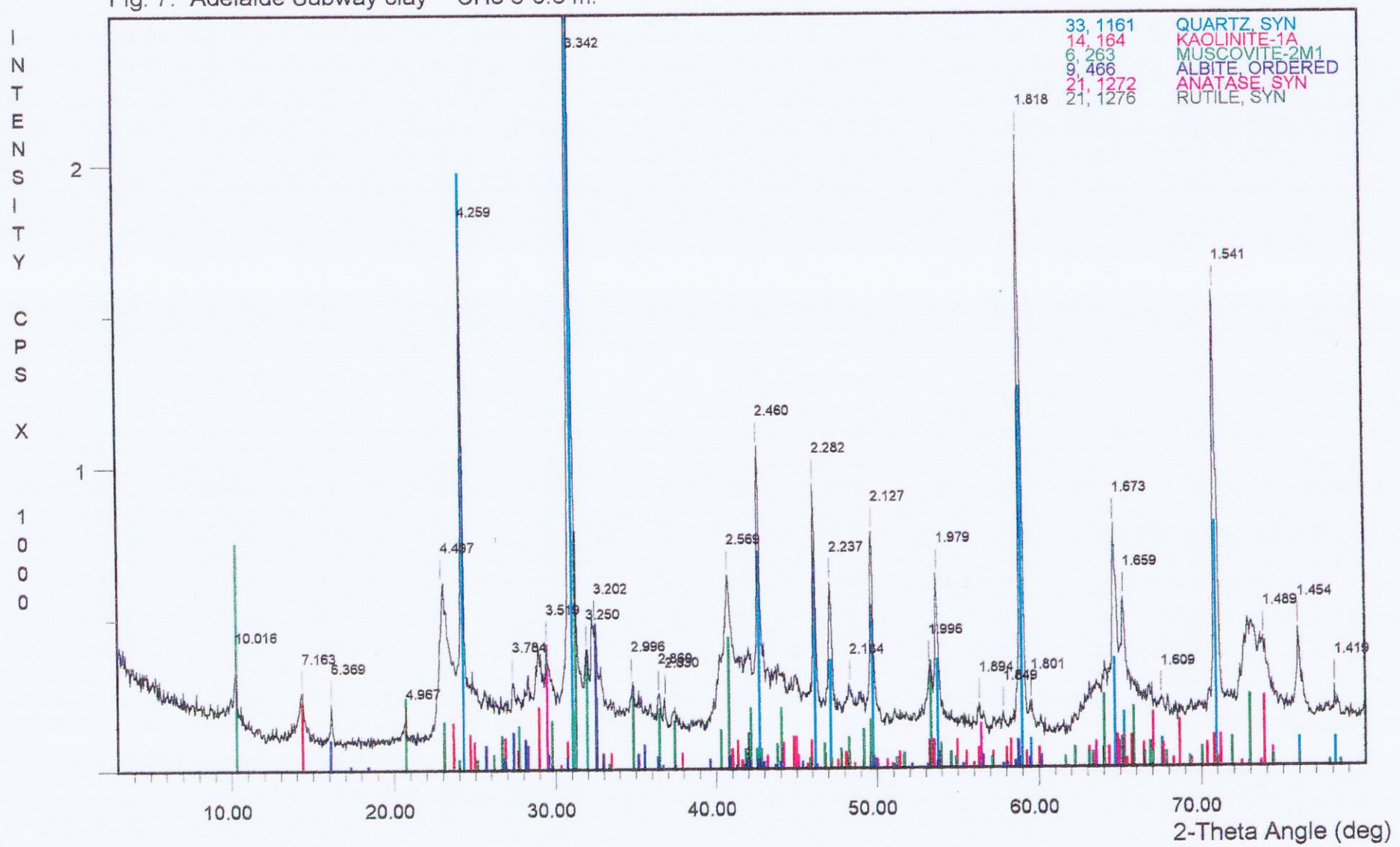
Fig. 6. Commonwealth Law Court clay - 11.9-16.0 m.



File Name: A:\LAWCOUR2.DAT

0000021

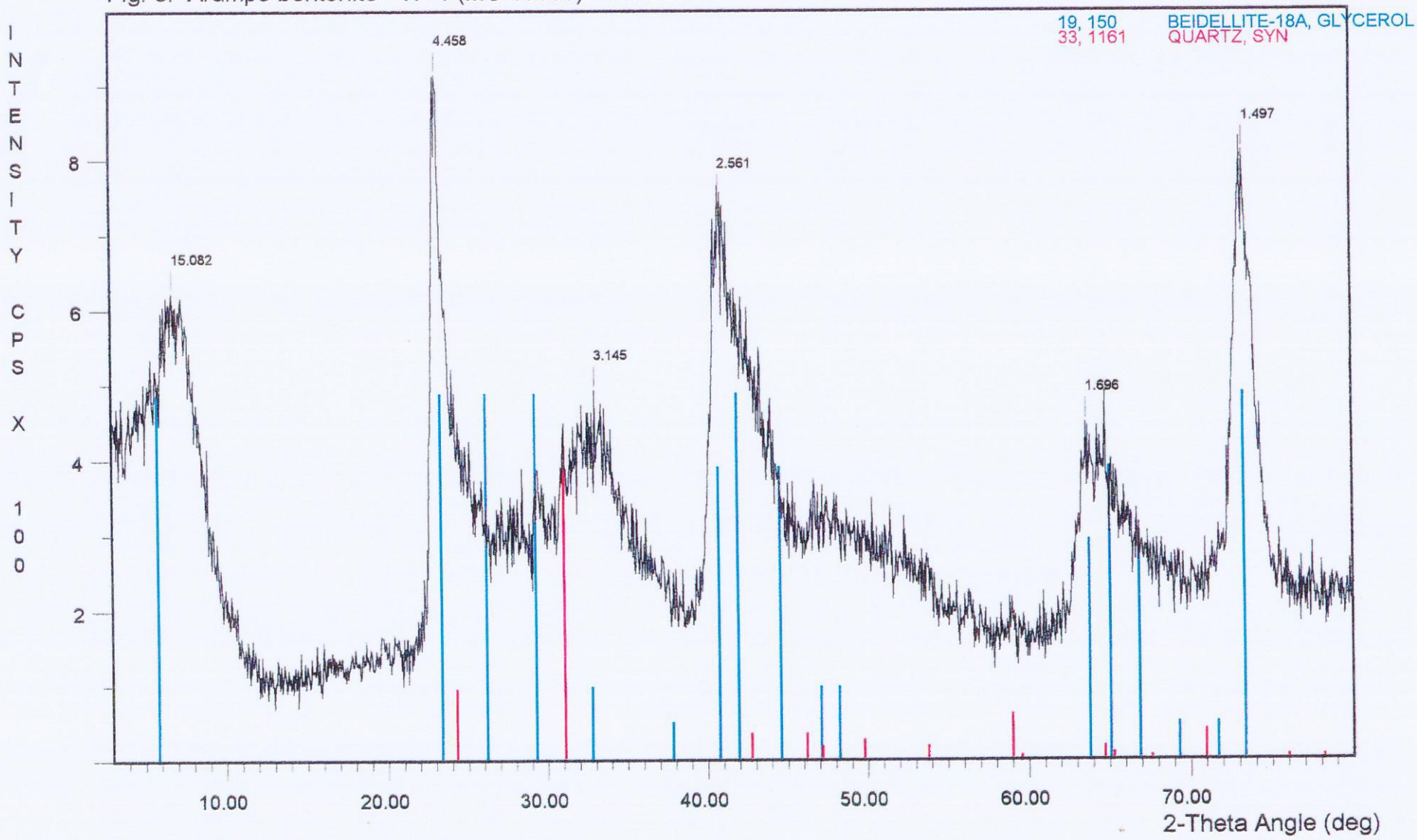
Fig. 7. Adelaide Subway clay - CH8 6-9.6 m.



File Name: A:\SUBWAY.DAT

16 2220000

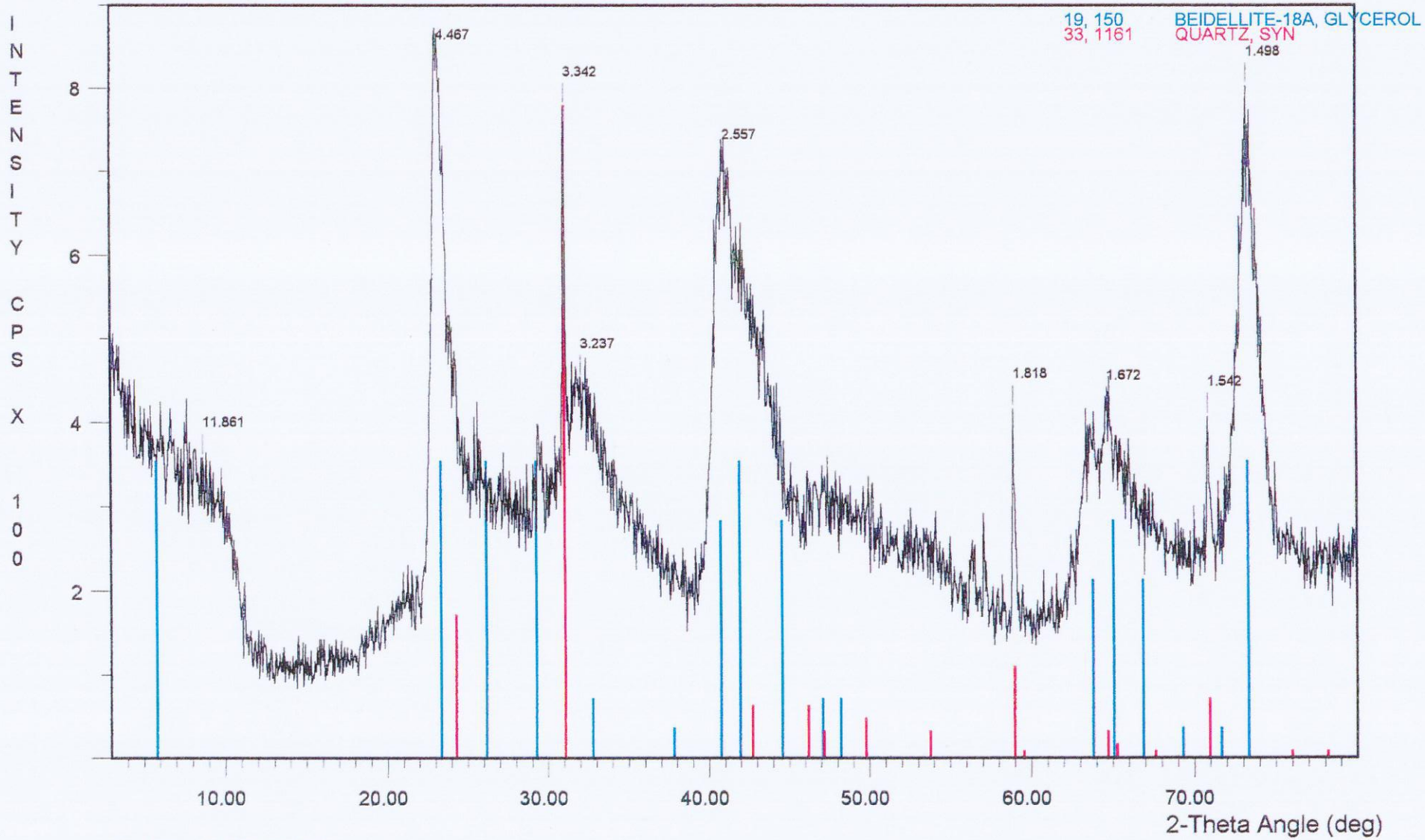
Fig. 8. Arumpo bentonite - TP-1 (MO 10893) +1mm-2mm.



File Name: A:\TP1-1-2.DAT

0000023 17

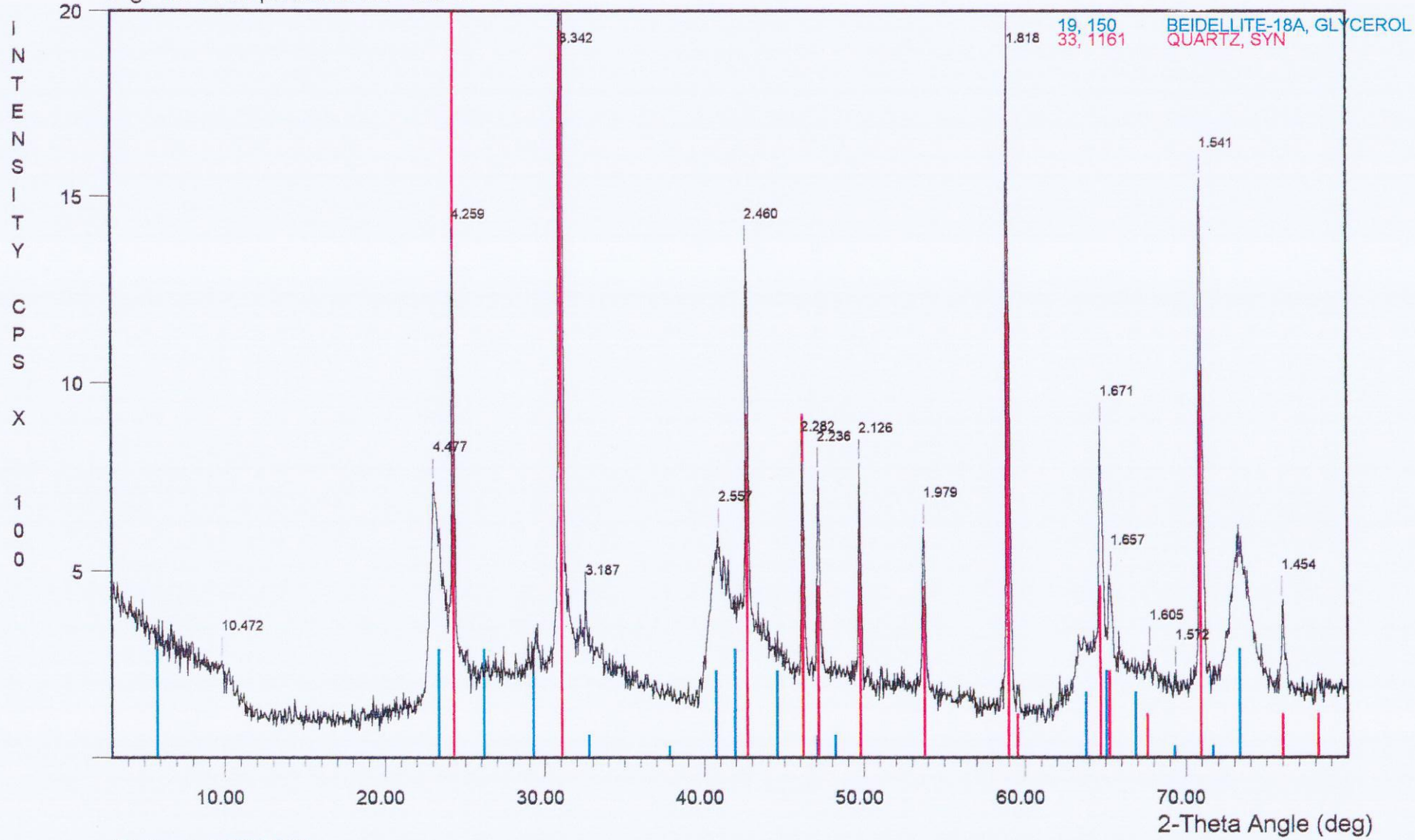
Fig. 9. Arumpo bentonite - TP-1 (MO 20593) <63 µm.



File Name: A:\TP1-63.DAT

0000024

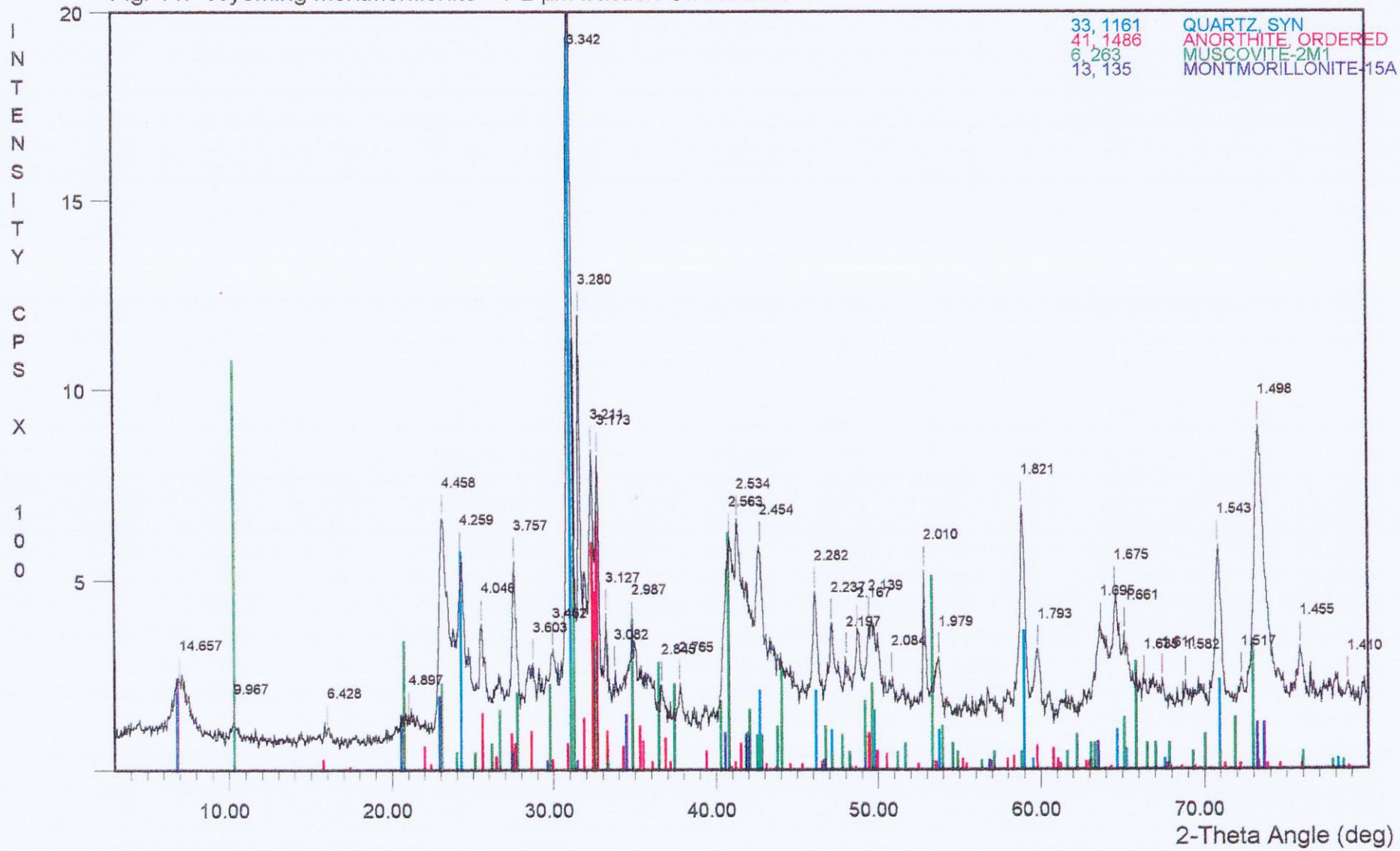
Fig. 10. Arumpo bentonite - BS-1.



File Name: A:\PS-1.DAT

0000025 19

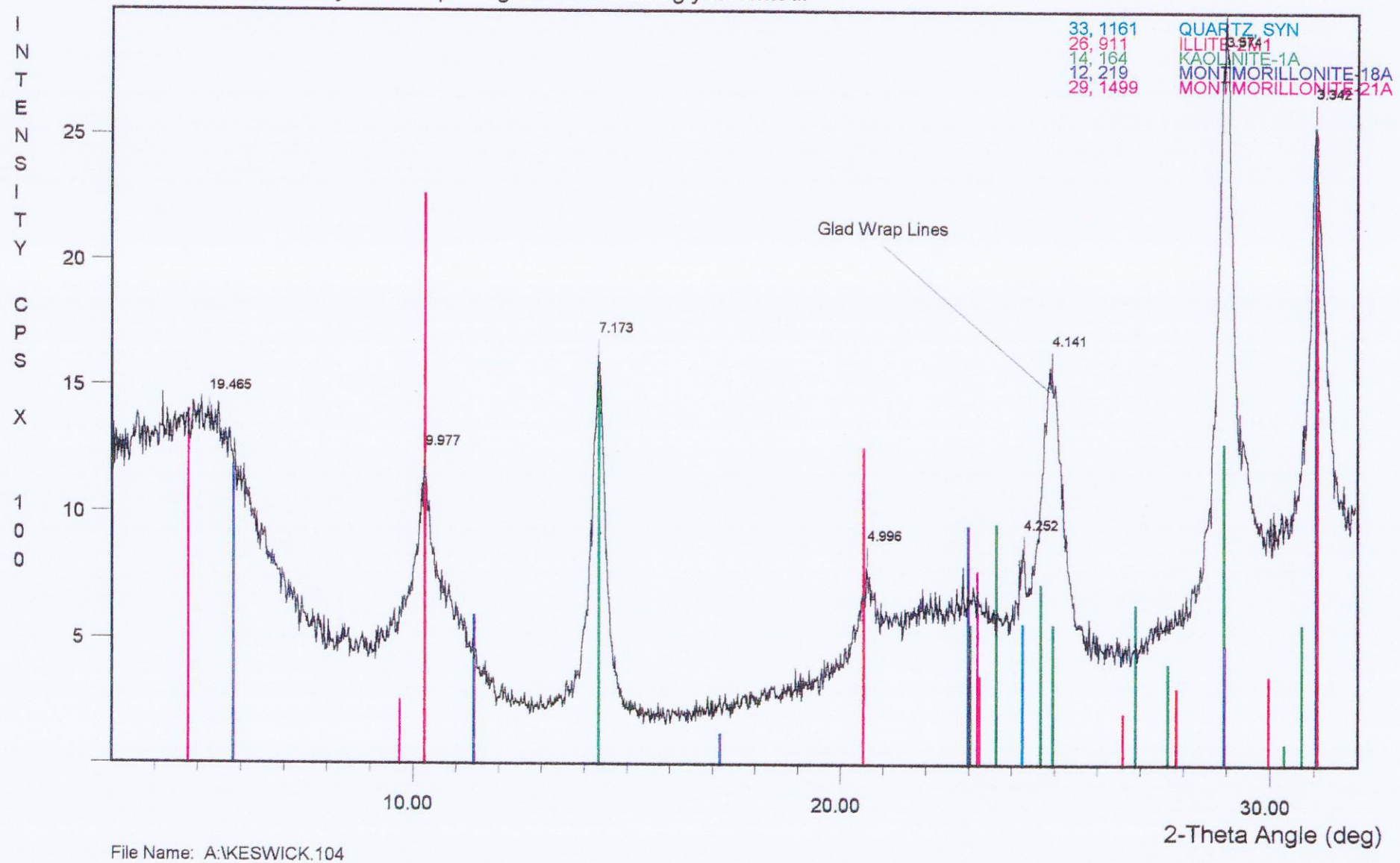
Fig. 11. Wyoming montmorillonite - 1-2 µm fraction Ca-saturated.



File Name: A:\WYOM-CA.DAT

000026

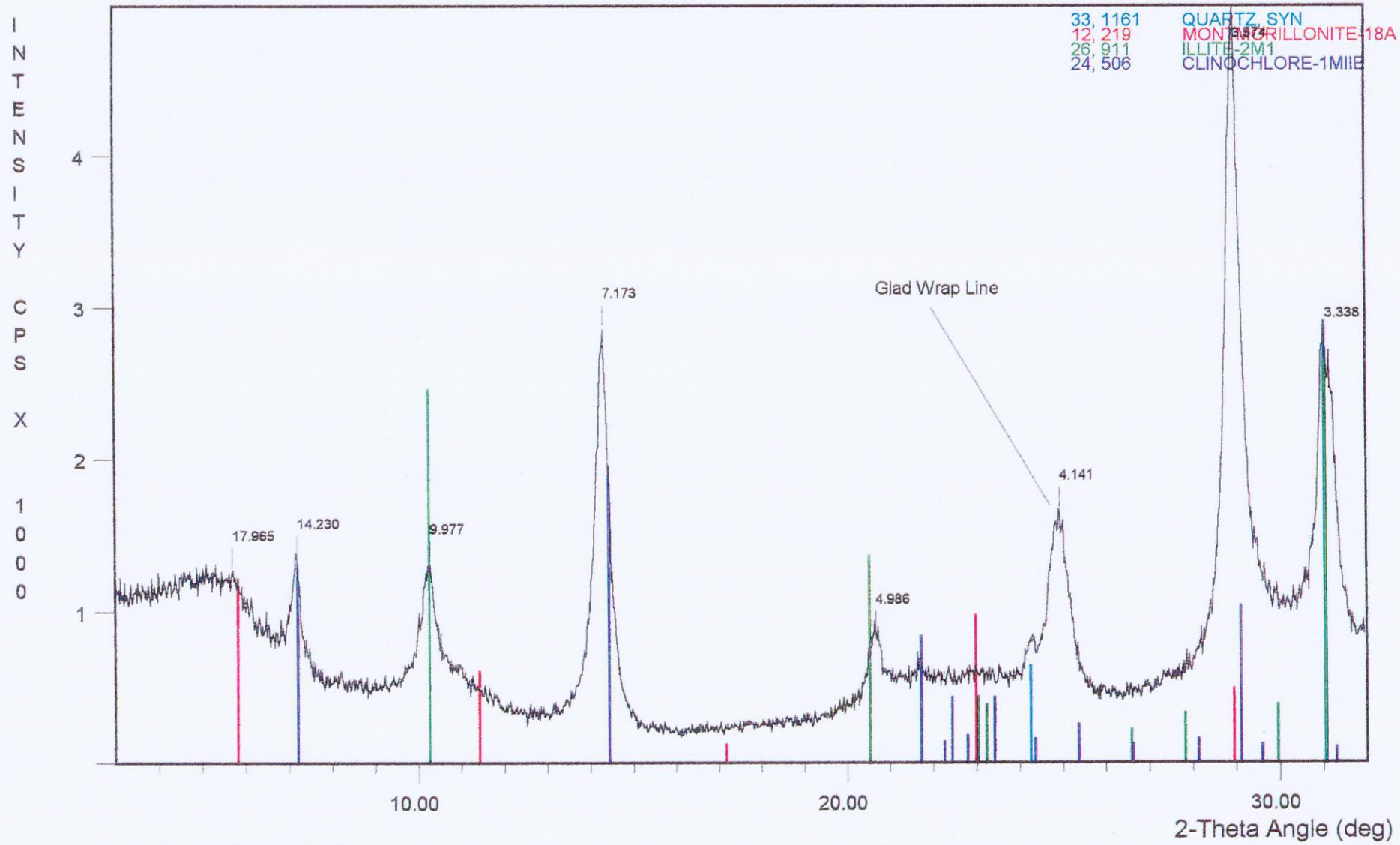
Fig. 12. Keswick clay - 0.2-1 µm Mg-saturated and glycerolated.



File Name: A:\KESWICK.104

000027

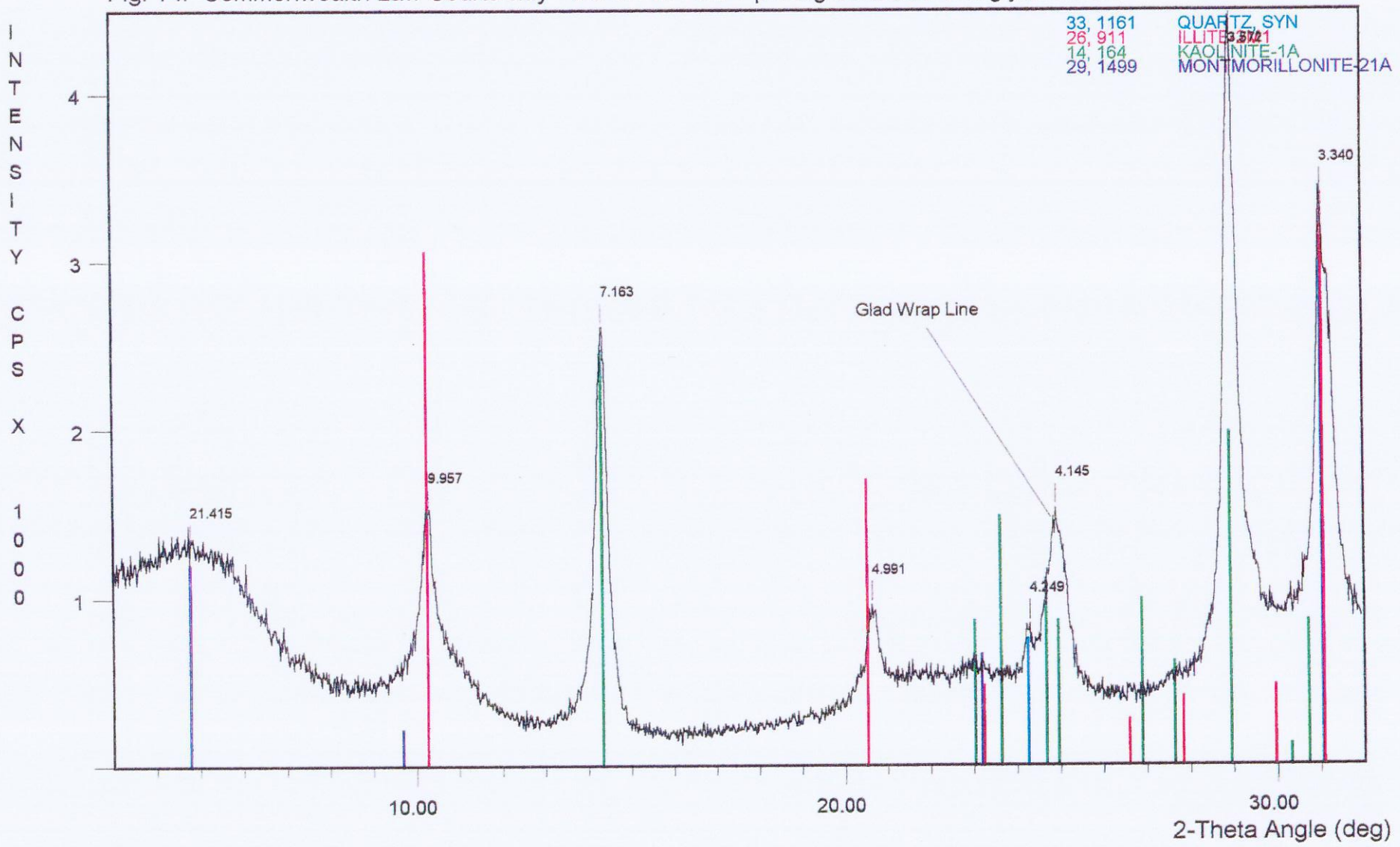
Fig. 13. Pooraka clay - 0.2-1 µm Mg-saturated and glycerolated.



File Name: A:\POORAKA.102

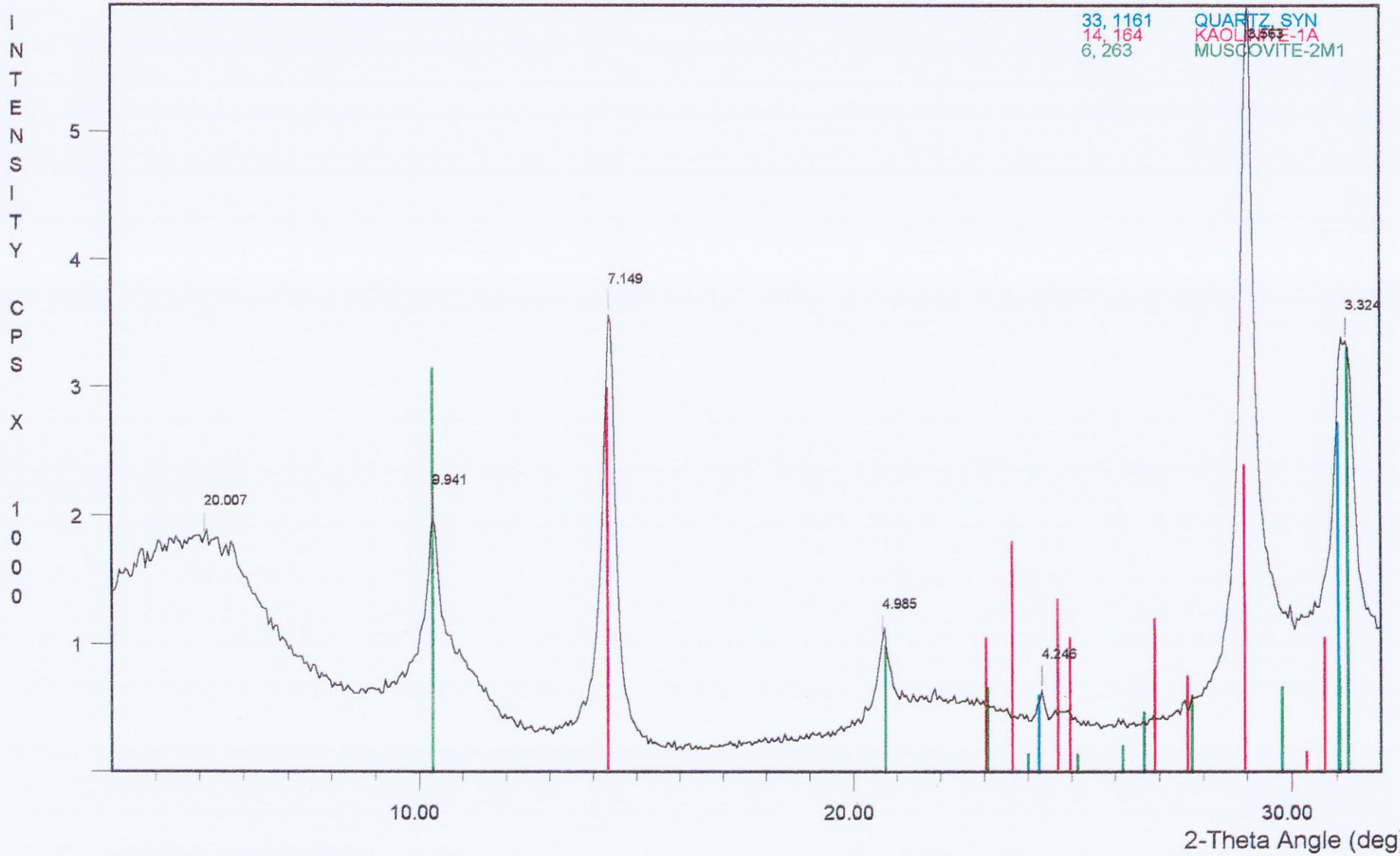
0000028
22

Fig. 14. Commonwealth Law Courts clay - 5.5-9.1 m - 0.2-1 µm Mg-saturated and glycerolated.



File Name: A:\LAW-OR.DAT

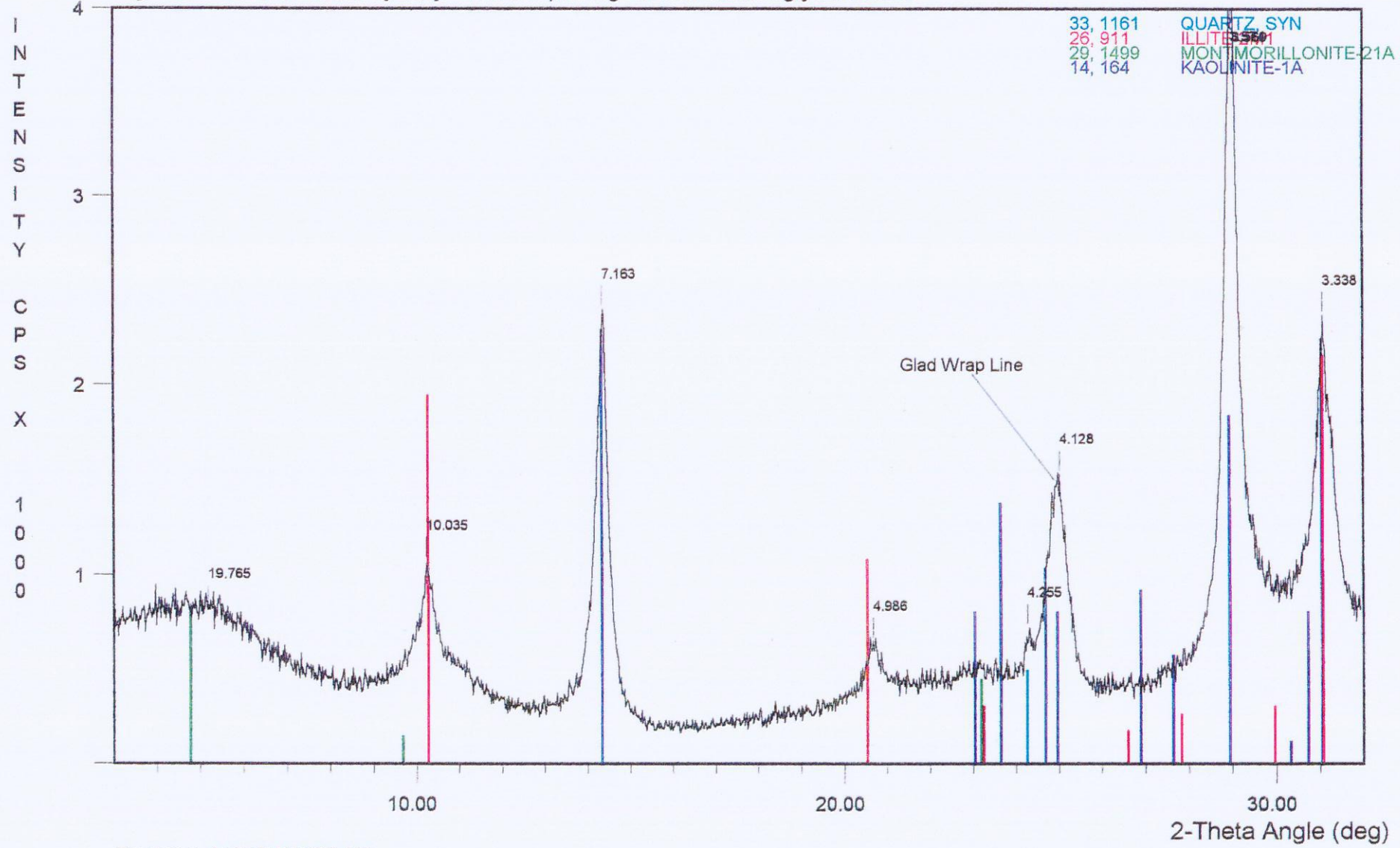
Fig. 15. Commonwealth Law Courts clay - 11.9-16.0 m - 0.2-1 µm Mg-saturated and glycerolated.



File Name: A:\COMLAW39.526

000030

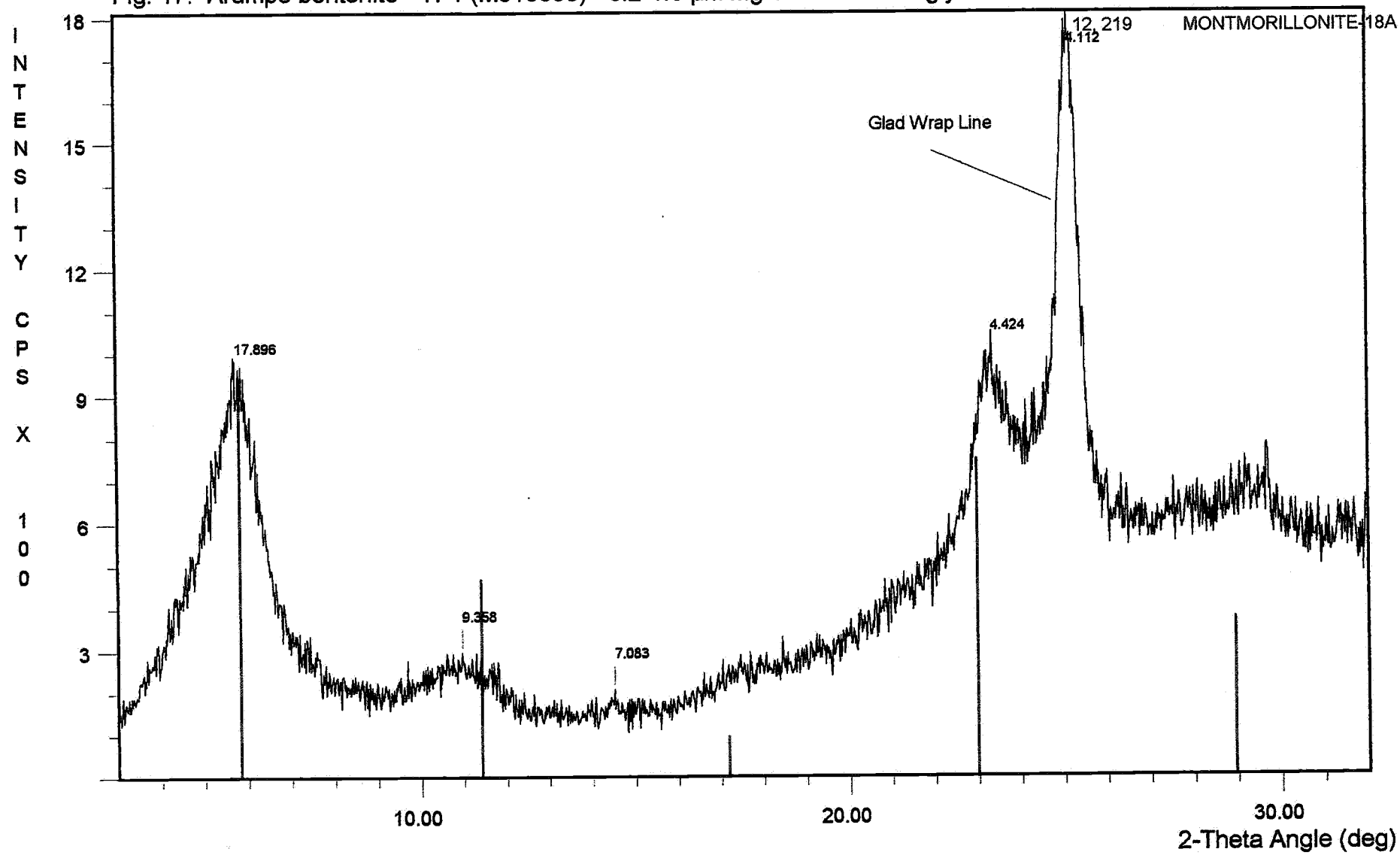
Fig. 16. Adelaide Subway clay - 0.2-1.0 µm Mg-saturated and glycerolated.



File Name: A:\SUBWAYOR.102

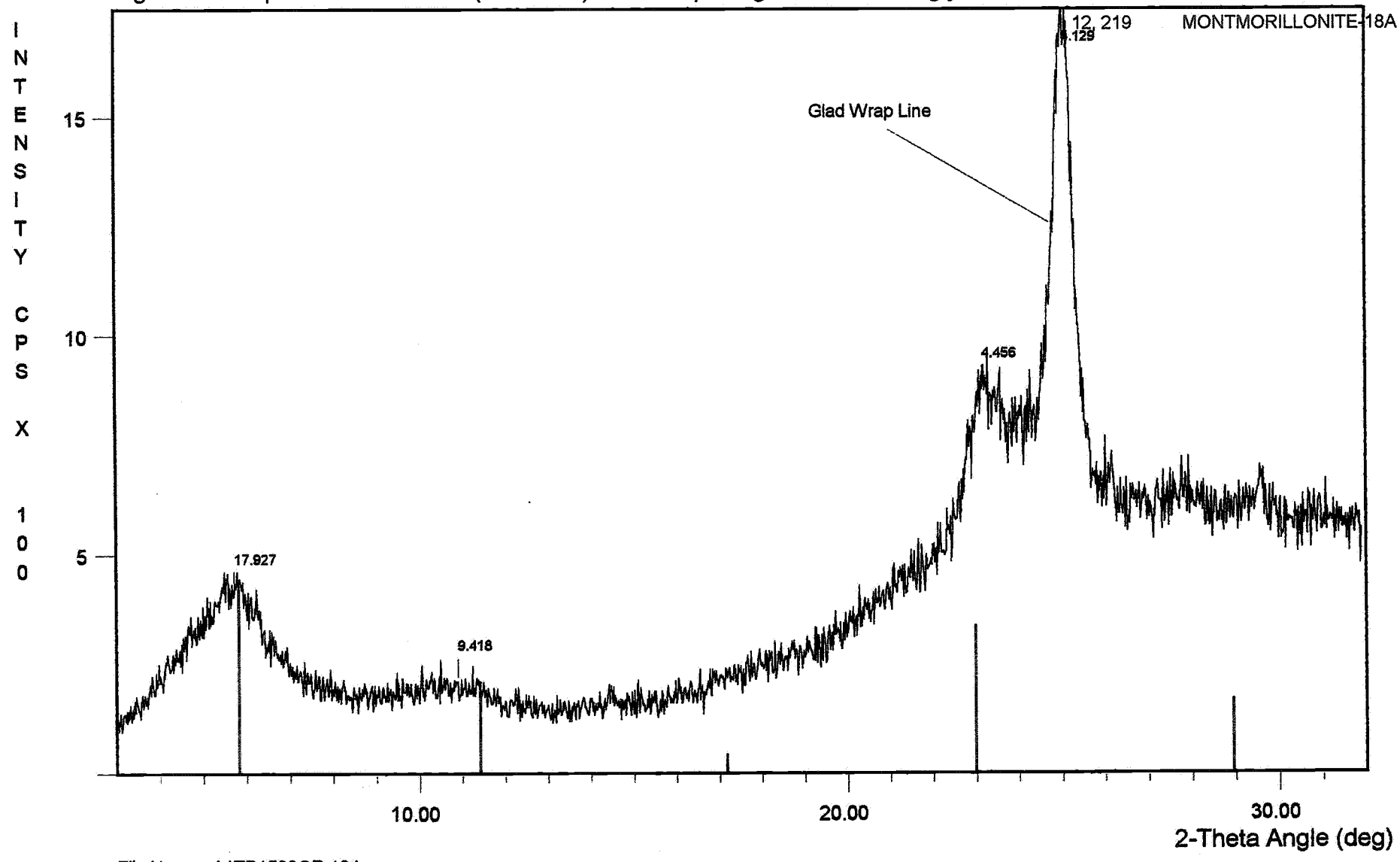
000031

Fig. 17. Arumpo bentonite - TP1 (M010893) - 0.2-1.0 µm Mg-saturated and glycerolated.



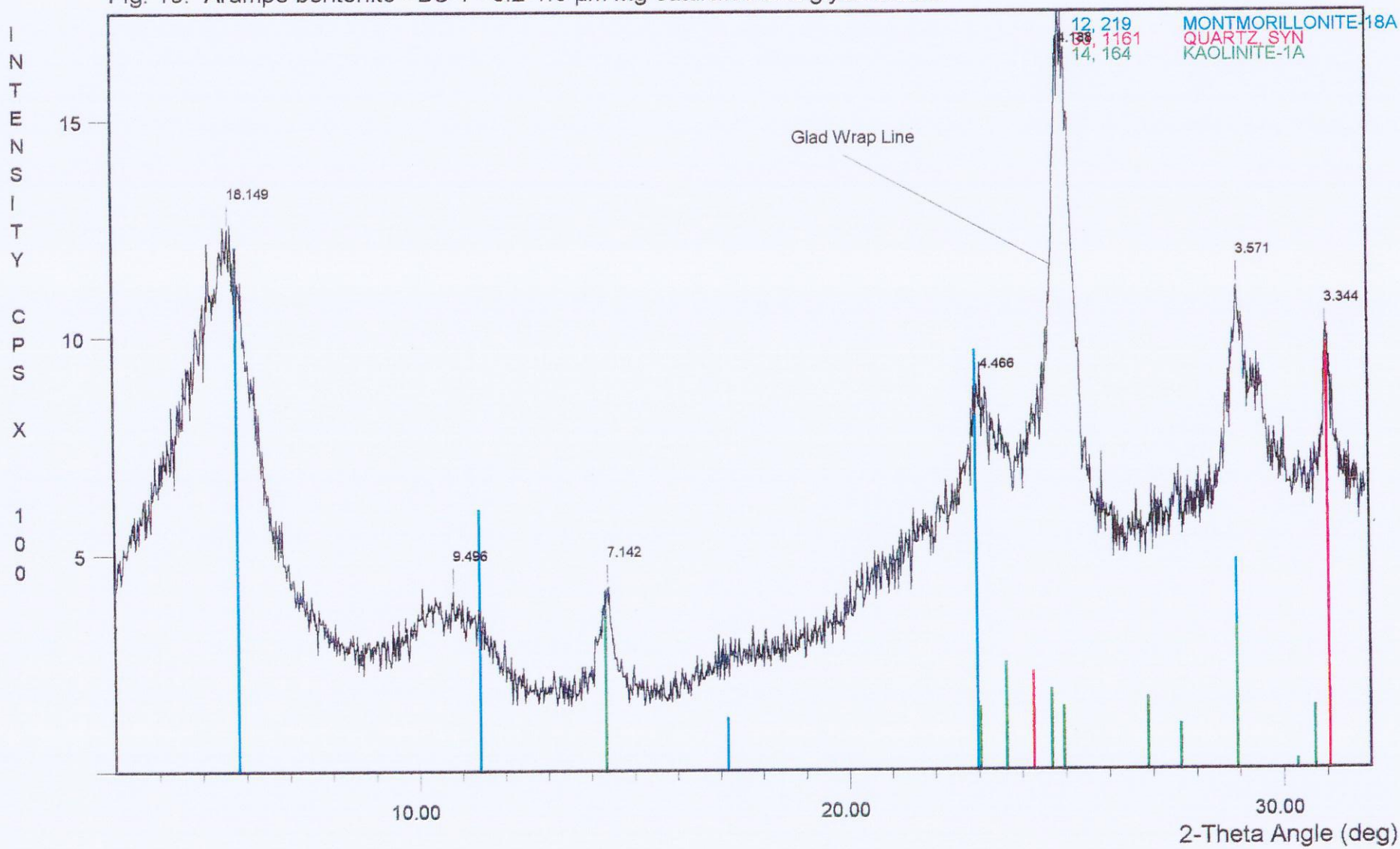
File Name: C:\CLAYPROJ\TP1893OR.103

Fig. 18. Arumpo Bentonite - TP1 (M020593) - 0.2-1.0 µm Mg-saturated and glycerolated.



File Name: A:\TP1593OR.104

Fig. 19. Arumpo bentonite - BS-1 - 0.2-1.0 µm Mg-saturated and glycerolated.



File Name: A:\BS-1OR.105

THE KAOLINS

Introduction

In the kaolin minerals, layers are comprised of sheets of silica tetrahedra linked to sheets of aluminium oxide/hydroxide octahedra in 1:1 coordination. The most widespread member of the kaolin group, kaolinite, has an ideal formula of $Si_2Al_2O_5(OH)_4$. Halloysite, which may contain water in its structure, to give an ideal formula of $Si_2Al_2O_5(OH)_5.2H_2O$, also occurs widely, but the other members of the group, dickite and nacrite, which both have the same ideal formula as kaolinite, are very rare.

Kaolin minerals show little substitution of their essential cations. As a result, they have only a low permanent negative charge (usually < 10 meq/100g). They can exhibit a pH-dependent component of charge which is comparable to their permanent charge and which can strongly affect their colloidal behaviour, so that, for instance, kaolin minerals do not disperse in acid solutions.

Kaolinites usually occur in platy, hexagonal-shaped particles which are large compared with those of most smectites. They are usually > 0.3 μm in length or width and > 0.05 μm thick. As a result, their specific surface area tends to be relatively low (between *c.* 6 and 40 m^2g^{-1}). They do not contain any fine pores.

Halloysites occur in particles with a variety of shapes. Tubular and spheroidal shapes are the most common. These particles may be smaller than those of kaolinites (*c.* 0.1 μm in length or width) but of similar thickness. Specific surface areas may be larger (*c.* 20-60 m^2g^{-1}) and they may contain fine pores (Churchman *et al.*, 1994b). Compared with kaolinites, halloysites offer more prospects for sorption, particularly of gases (see below).

Common industrial applications of kaolin group minerals are summarised in Table 6.

Table 6. Industrial applications of kaolin group minerals

Filler and pigment	paper filling paper coating (to improve surface characteristics, brightness and gloss) plastic (to improve surface finish and resistance to chemical attack) paint (as an extender of titanium dioxide) rubber (to improve strength, abrasion resistance and rigidity)
Ceramics	whiteware ceramics, porcelain enamels, insulators sanitaryware, wall and floor tiles fibreglass refractories white cement
Sorptive	adsorbent of oil and water medicines (toxin adsorption) carrier for fertilisers and insecticides
Catalytic	carrier of zeolite used in petroleum cracking precursor for zeolite manufacture
Other	cosmetics, pharmaceuticals

Materials

Samples supplied by MESA (Fig. 2) were as follows:-

1. Cromer - channel sample from the bottom of the pit face.
2. Woodside - from the western face of the northern pit.
3. Golden Grove - from lower face of Nubrik pit, Hancock Road.
4. McLaren Vale - face sample from east of pit access ramp.
5. Birdwood - from core of the anticline, Adelaide Brighton Cement Ltd. South Pit.

The location and geology of these deposits are as follows:

• Cromer - a bulk sample was collected from the western face of the open cut at the Cromer 'C' kaolin deposit located approximately 4km southeast of Mount Crawford. Here kaolin has been formed by deep weathering of fine grained schist of Cambrian age. Mineral leases over the deposit are held by Adelaide Brighton Cement Ltd, but there has been no production recorded in recent years.

• Woodside - a bulk sample of sandy clay was collected from the western face of the northern open cut. The kaolin formed from weathering quartz-biotite schist.
• Golden Grove - approximately 5 kg of kaolin was collected from a zone of pale yellow to pale grey plastic clay in Nubrik's Hancock Road clay pit, Golden Grove. Golden Grove is located approximately 25 km northeast of Adelaide City Centre and is the major supplier of construction sand and brick shale for the northern metropolitan area (McCallum and Keeling, 1993). The kaolin is sedimentary in origin, deposited as a lacustrine facies of fluviatile sediments of Middle Eocene age (McCallum, 1988, 1990; McCallum and Keeling, 1993)
• McLaren Vale - white plastic clay suitable for cream brick manufacture was discovered 3.5 km north of McLaren Vale township in 1974. The deposit is the only source of white plastic clay south of Adelaide and is a sedimentary deposit forming lenses to 10 m thickness in sand and silt of Eocene age (Keeling, 1984). A bulk sample was collected from the north eastern pit face.
• Birdwood - a bulk sample was collected from Adelaide Brighton Cement Ltd, South Pit, located approximately 3 km north of Birdwood township. The sample was taken from a high-grade zone within the core of a north plunging anticline (Keeling, 1993). Kaolin was derived from deep weathering of a pyritic, quartz-biotite schist within the Adelaidean Saddleworth Formation (Keeling, 1986, 1993).

For comparison, a sample of commercial halloysite clay product from Matauri Bay, Northland, New Zealand from New Zealand China Clays Ltd. was supplied by Commercial Minerals Ltd. Technical information for this product is given in Fig. 20.

Experimental

For the reasons given above with respect to the smectite-containing clays, the natural materials whose adsorption/absorption was to be tested were separated, initially into clay size (< 2 μm) fractions and subsequently into 1-2, 0.5-1 and < 0.5 μm sub-fractions. In one case, the clay fraction was separated into 1-2, 0.2-1 and < 0.2 μm sub-fractions.

10 g portions of each material were dispersed by shaking in a SPEX mill for 10 min. in a 50 ml of a solution that comprised 0.5% sodium hexametaphosphate (or "Calgon") and 1% sodium carbonate. Dispersion was often incomplete when NaCl was used as for the smectites. The slurry was transferred to a measuring cylinder and water added to enable separation of > 2 μm particles by sedimentation overnight. Suspended material was collected as the < 2 μm fraction. The sedimented material was resuspended and sedimentation continued until the resulting suspension was virtually clear. Using

centrifugation, the combined sample of all of the suspended material was then separated into 1-2, 0.5-1 and < 0.5 μm sub-fractions. In the case of the Woodside sample, 0.2-1 and < 0.2 μm sub-fractions were also obtained following dispersion with 1M NaCl.

XRD analyses of the < 2 and 1-2 μm fractions were carried out with a Philips 1800 microprocessor-controlled diffractometer with CoKα radiation, variable divergence slits and a graphite monochromator. Patterns were recorded in steps of 0.02°2θ with a 1 second counting time/step. Data were stored on computer discs for analysis by an IBM-compatible PC using the program XPLOT (Raven 1990).

XRF analyses were carried out with a Philips PW1400 spectrometer. CECs were determined by analysis for Ba after the samples had been saturated with this element.

Results

Table 7 shows the weight percentages of particles in given size ranges following dispersion of the different South Australian kaolin samples with "Calgon". The contents of coarse (> 2 μm) particles differ. 2 samples (Woodside and Cromer) have high (> 50%), 2 (Birdwood and the N.Z. halloysite) have low (< 20%), while the other 2 samples (Golden Grove and McLaren Vale) have intermediate values. The Birdwood sample has a higher content of fine (< 0.5 μm) particles than the other South Australian samples, but it has a lower proportion of these particles than the N.Z. halloysite (Fig. 20).

Table 7. Summary of particle size distributions for South Australian kaolin samples

Size Range (μm)	Proportion (wt %)				
	Cromer	Woodside	Golden Grove	McLaren Vale	Birdwood
>53	20.9	25.0	1.4	8.5	0.7
40-53	0.5	1.7	2.0	0.6	<0.5
20-40	1.0	8.1	7.7	3.9	1.6
15-20	0.7	3.0	2.3	1.9	<0.5
10-15	2.5	5.9	4.0	1.9	2.6
5-10	5.2	8.3	11.5	5.6	3.4
2-5	23.6	7.6	16.8	8.0	9.5
1-2	13.4	3.2	13.2	8.5	14.7
0.5-1	8.0	2.8	22.0	36.5	26.8
< 0.5	24.1	33.1	20.0	21.5	40.5

The XRD patterns of the non-oriented bulk samples of the South Australian kaolins (Fig. 21a-e) show that these include a very pure kaolinite (Birdwood), a largely kaolinitic sample which contains a trace of quartz (Cromer) and 3 samples in which, while kaolin minerals are dominant, mica is present and there is substantial quartz (Woodside, Golden Grove and McLaren Vale). The Golden Grove sample also contains a minor amount of a smectitic phase and, along with the McLaren Vale sample, a trace of rutile. The Woodside sample contains some feldspar and also some halite.

The XRD patterns of the oriented whole clay (< 2 μm) fractions (Figs. 22a-e) indicate that this fraction of 3 samples (Birdwood, Cromer and Woodside) comprises virtually pure kaolin. The clay fractions of the Golden Grove and McLaren Vale samples also comprise mica and rutile in minor proportions, while the clay fraction of the Golden Grove sample has some smectite and that of the McLaren Vale sample contains a trace of quartz.

The XRD patterns of the 1-2 μm fractions (Figs. 23a-e) largely reflect those of the corresponding whole clay fractions, except (1) there are relatively higher proportions of mica in the Golden Grove (Fig. 23c) and McLaren Vale (Fig. 23d) samples in this narrower size fraction, (2) there is a lower proportion of smectite in the narrower size fraction of the Golden Grove sample (cf. Figs. 23c and 22c), and (3) there are marked differences in line profiles between the 1-2 and < 2 μm fractions of the Cromer sample (cf. Figs. 23a and 22a) and also some differences between the line profiles of the corresponding fractions of the Woodside sample (cf. Figs. 23b and 22b). For the Cromer and Woodside samples, XRD patterns for the 1-2 μm fractions show peaks for (hkl) reflections that are generally sharper and stronger than in patterns for the < 2 μm fractions.

In order to help explain the differences in line profiles between the whole clay and 1-2 μm fractions for two of the samples, XRD patterns for the finest fractions were also obtained in these cases. The pattern for the < 0.2 μm fraction of the Woodside sample is shown in Fig. 24 and that for the < 0.5μm of the Cromer sample in Fig. 25. Compared with the pattern for the 1-2 μm fraction of the Woodside sample (Fig. 23b), that for the < 0.2 μm fraction of this sample (Fig. 24) shows broader and fewer peaks. It is typical for a halloysite while that for the coarser fraction is typical for a well-crystallised kaolinite. Similarly, for the Cromer sample, the pattern for the < 0.5μm fraction (Fig. 25) shows virtually none of the (hkl) peaks for well-crystallised kaolinite that are prominent in the pattern for the 1-2 μm.

Electron micrographs (Figs. 26-30) show that the Woodside and Cromer samples contain particles with tubular shapes typical of halloysites as well as particles with platy hexagonal shapes typical of kaolinites while the other South Australian samples contain only platy particles. Our earlier work on halloysites from Western Australia and New Zealand has shown that these contain a high proportion of fine pores (< *c.* 15 nm in diameter) (Churchman *et al.*, 1991; 1994b). These pores offer prospects for entraining large organic molecules. They could act in a similar way to zeolitic molecular sieves, except that the pores in zeolites are limited to very small sizes (< *c.* 1 nm) so that they can only be used to sorb or entrap small molecules of either cations or simple gases.

Table 8 gives the analyses of the various samples and also their whole clay (< 2μm) fractions by XRF. Their CECs are also given. An analysis of the New Zealand halloysite sample, as supplied, is also given for comparison. This material has been described by a German author in the scientific literature as "the whitest clay in the world" (Ney, 1983). The Cromer and Birdwood samples are particularly free of impurities, with

the Cromer sample, in particular, showing even lower proportions of Fe and Ti than the New Zealand halloysite.

Compared with smectites, the kaolin minerals have low CECs. The values for their clay fractions range from 4 or 5 meq/100g for the Birdwood, Cromer and Woodside samples to 9 or 11 meq/100g for the McLaren Vale and Golden Grove samples. The two higher values reflect the presence of accessory minerals besides kaolins in these particular samples.

Table 8. XRF analyses of bulk and clay fractions of kaolins

	SiO_2 %	TiO_2 %	Al_2O_3 %	Fe_2O_3 %	MgO %	CaO %	Na_2O %	K_2O %	CEC meq
Cromer Bulk	49.3	0.02	36.8	0.20	0.086	0.025	0.13	0.03	
Cromer <2μm	47.2	0.01	37.2	0.17	0.046	0.240	0.03	0.01	5
Woodside Bulk	52.0	1.91	26.6	0.66	0.200	0.067	0.50	0.60	
Woodside <2μm	45.4	0.21	38.1	0.63	0.060	0.300	0.02	0.02	5
Golden Grove Bulk	57.5	2.68	25.2	1.42	0.700	0.080	0.23	2.45	
Golden Grove <2μm	46.1	1.12	35.4	1.71	0.600	0.450	0.19	2.32	11
McLaren Vale Bulk	55.7	2.12	27.9	1.30	0.400	0.120	0.31	1.58	
McLaren Vale <2μm	45.3	1.19	36.2	1.42	0.300	0.270	0.25	1.42	9
Birdwood Bulk	63.5	1.26	24.1	0.54	0.058	0.017	0.17	0.09	
McLaren Vale <2μm	45.3	1.57	37.6	0.46	0.065	0.170	0.01	0.02	4
NZ halloysite Bulk	0.1	0.08	35.5	0.28	0.06	0.07	0.06	0.05	-

Compared with the smectites and also with Muloorina illite (see below), kaolinites tend to occur in larger particles and therefore have a lower specific surface available for sorption. Halloysites, however, may occur in smaller particles and have higher specific surface areas than kaolinites. Nevertheless, considerable research has demonstrated that kaolin minerals can be delaminated as a result of their intercalation by various reagents (e.g. Churchman and Carr, 1973; Lahav, 1990), enabling an increase in the extent of their surfaces available for sorption.

FIGS. 20 TO 30

Fig. 20. Technical information for Matauri Bay halloysite.

Fig. 21. XRD of non-oriented bulk kaolin samples:
a) Cromer 'C' kaolin deposit - Site 1.
b) Woodside kaolin deposit - Sample WOD1.
c) Golden Grove kaolin deposit - Site 2.
d) McLaren Vale kaolin deposit - Site 2.
e) Birdwood kaolin deposit - Site 1.

Fig. 22. XRD of Kaolin samples - < 2 μm, oriented, Mg-saturated, glycerolated:
a) Cromer 'C' - Site 1.
b) Woodside - Sample WOD1.
c) Golden Grove - Site 2.
d) McLaren Vale - Site 2.
e) Birdwood - Site 1.

Fig. 23. XRD of kaolin samples - 1-2 μm, oriented, Mg-saturated, glycerolated:
a) Cromer 'C' - Site 1.
b) Woodside - Sample WOD1.
c) Golden Grove - Site 2.
d) McLaren Vale - Site 2.
e) Birdwood - Site 1.

Fig. 24. XRD of Woodside sample WOD1 - < 0.2 μm, oriented, Mg-saturated, glycerolated.

Fig. 25. XRD of Cromer 'C' site 1 sample - < 0.5 μm, oriented, Mg-saturated, glycerolated.

Fig. 26. Scanning electron micrograph (SEM) (above) and transmission electron micrograph (TEM) (below) of samples from the Cromer "C" kaolin deposit. (Micrographs 164 and 16108).

Fig. 27. SEMs of Woodside sample WOD1. (Micrographs 646 and 647).

Fig. 28. SEM (above) and TEM (below) of samples from site 2 at the Golden Grove kaolin deposit. (Micrographs 356 and 15976).

Fig. 29. SEM (above) and TEM (below) of samples from site 2 at the McLaren Vale kaolin deposit. (Micrographs 336 and 16118).

Fig. 30. SEM (above) and TEM (below) of samples from site 1 at the Birdwood kaolin deposit. (Micrographs 127 and 16003).

Technical Information

PREMIUM and **FILTERCAKE** are hydrated aluminium silicates which have been specially prepared by a unique process to accentuate such features as high brightness and fine particle size.

A typical chemical analysis is:

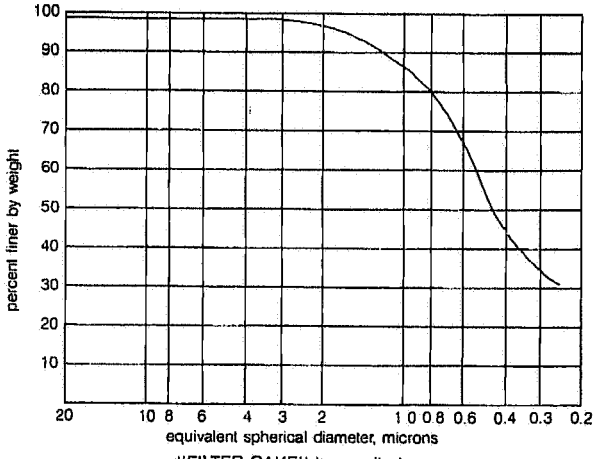
Loss on Ignition	SiO_2	Al_2O_3	Fe_2O_3	TiO_2	CaO	MgO	K_2O	Na_2O
13.8	50.1	35.5	0.28	0.08	0.07	0.06	0.05	0.06

GRIT	Less than 0.10 per cent on a 240 mesh BSS Screen for dispersed solution.
COLOUR	Brightness of 88.5 measured on an Elrepho photo-electric reflection photometer at 457 nanometers using Barium Sulfate as a standard.

WHITENESS INDEX	10 or less.
pH OF AQUEOUS SLURRY AT 20 PER CENT SOLIDS	4.8 — 5.0
SPECIFIC GRAVITY	2.55
REFRACTIVE INDEX	1.56
FLUORIDE ION	Less than 0.01% as F^- (B.C.R.A.)
CATION EXCHANGE CAPACITY	Approximately 10 milli equivalents/100gms of Clay
SURFACE AREA	Approximately 20m²/gm.
DISPERSABILITY	DISPERSABILITY — For ceramic applications the clay needs to be either ball milled or blunged under high shear.
	Casting Concentration = 55% wt % solids
	Wt % P84 grade Sodium Silicate to obtain 5 poise = 1.
	Casting Rate mm²/minute = 0.9

Typical Particle Size Distribution

New Zealand Halloysite

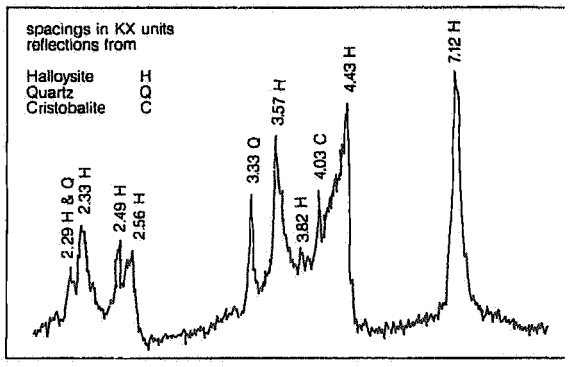


"FILTER CAKE" is supplied as extruded 25kg slabs, wrapped in polythene film

MOISTURE CONTENT	36 per cent (approximate)
MODULUS OF RUPTURE (dried at 110°C)	3.39MN/m² (B.C.R.A.) or 33.26kg/cm²
LINEAR SHRINKAGE:	
dried at 110°C	4.2%
fired at 1300°C	10.8%
REFRACTORINESS (P.C.E.)	Orton Cone 33-34 (1743-1763°C)

X-Ray Diffraction

New Zealand Halloysite
Randomly oriented sample

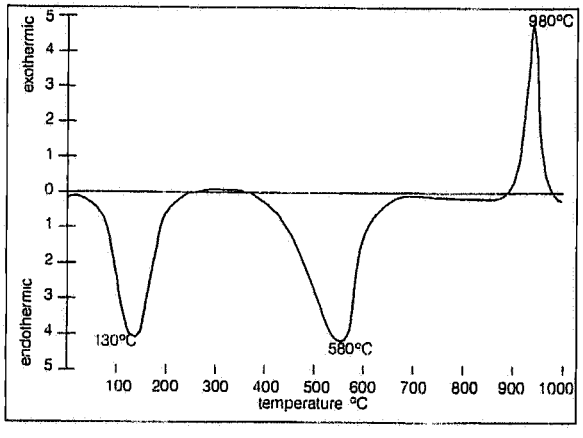


"PREMIUM" is supplied as a hammer milled powder in 30.0kg multiwall paper bags.

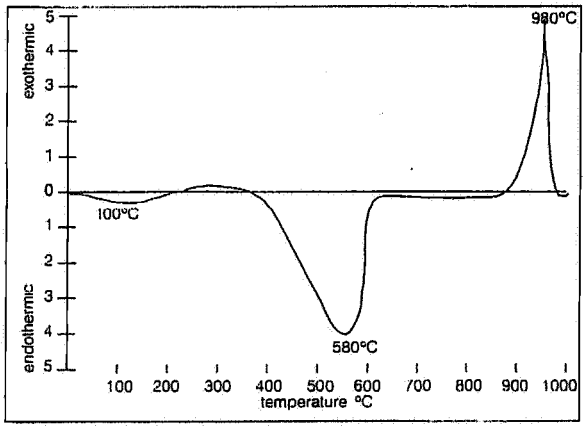
MOISTURE CONTENT	3 per cent (nominal)
MODULUS OF RUPTURE (dried at 110°C)	2.91 MN/m² B.C.R.A.) or 28.55kg/cm²
LINEAR SHRINKAGE:	
dried at 110°C	3.8%
fired at 1300°C	10.9%
REFRACTORINESS (P.C.E.)	Orton Cone 33-34 (1743-1763°C)

Differential Thermal Analysis

New Zealand Halloysite
Filter Cake



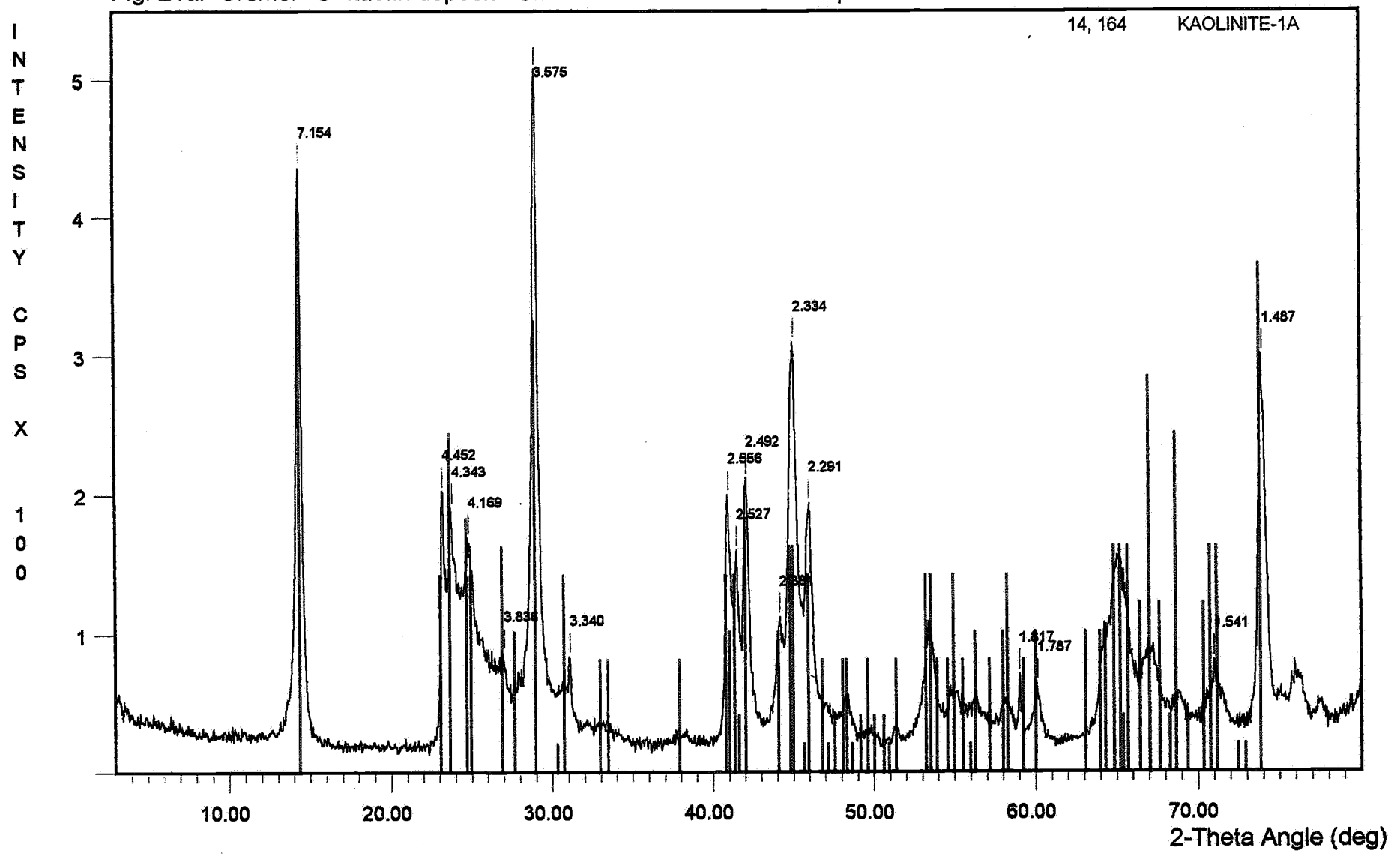
New Zealand Halloysite
Premium



"Every precaution is taken in production to ensure the clays conform to the above data but as the products are based on naturally occurring raw materials, minor variations may occur."

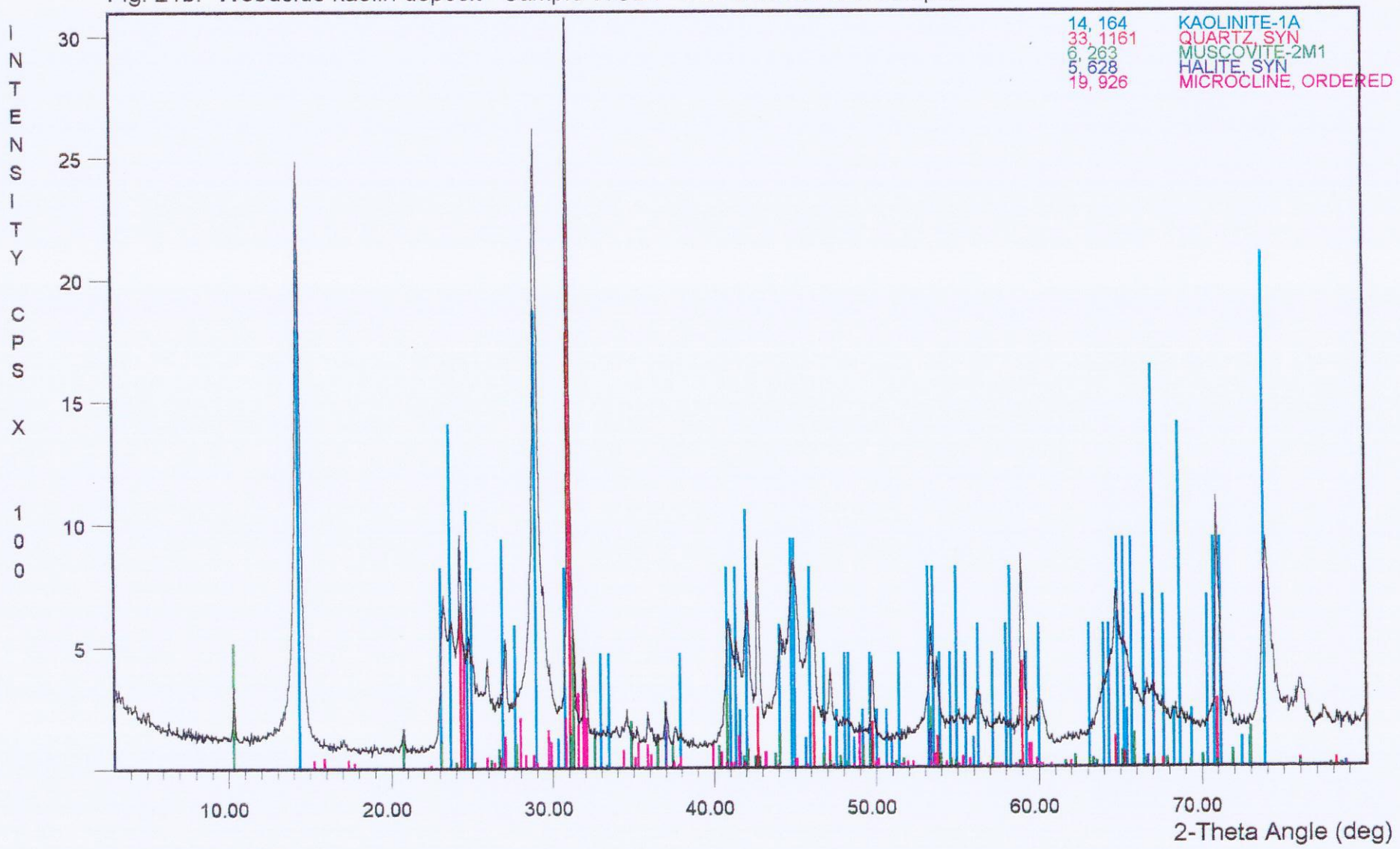
Fig. 20. Technical information for Matauri Bay halloysite.

Fig. 21a. Cromer "C" kaolin deposit - Site 1 - non-oriented bulk sample.



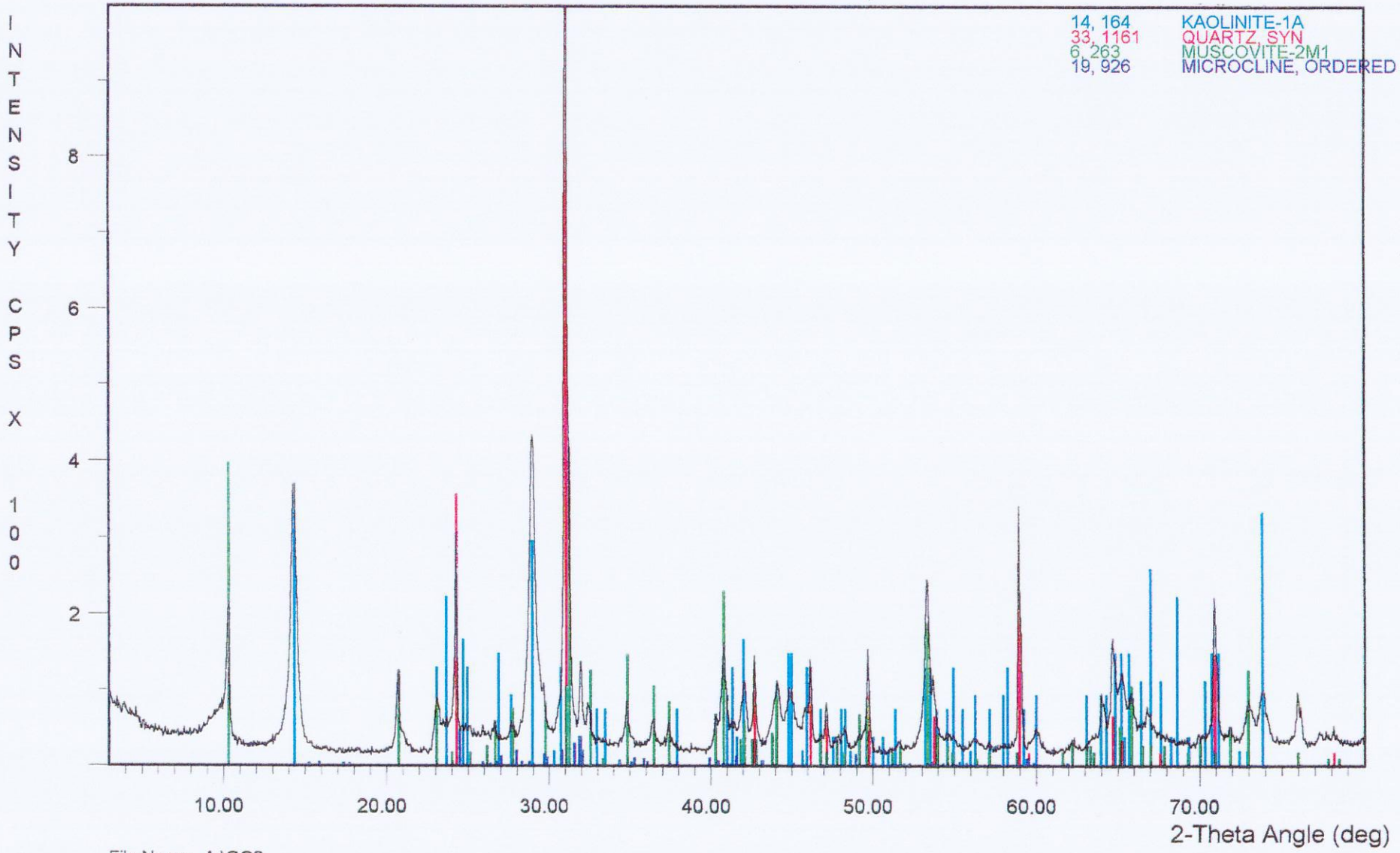
File Name: A:\CR1

Fig. 21b. Woodside kaolin deposit - Sample WOD1 - non-oriented bulk sample.



File Name: A:\WOD1

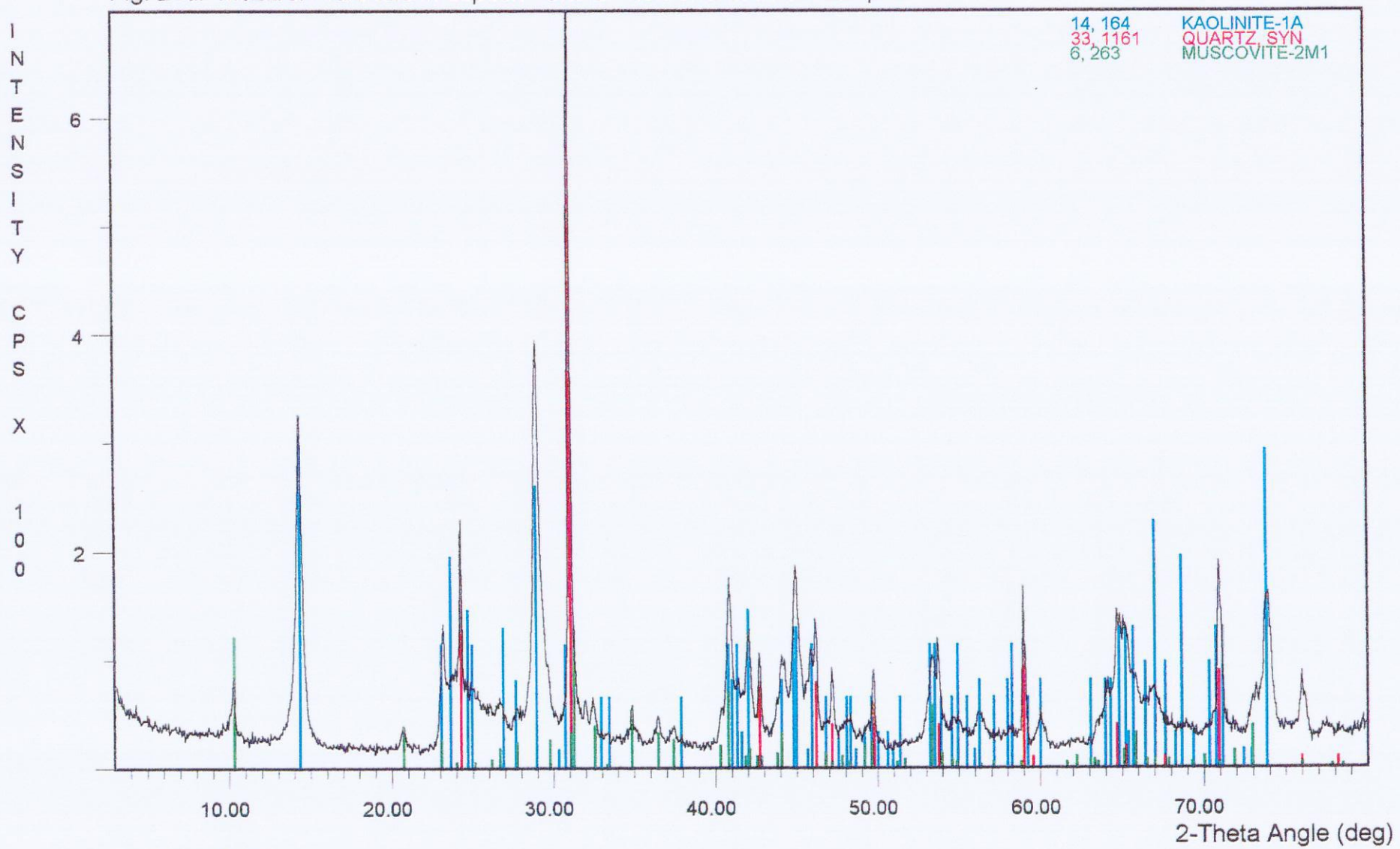
Fig. 21c. Golden Grove kaolin deposit - Site 2 - non-oriented bulk sample.



File Name: A:\GG2

0000047

Fig. 21d. McLaren Vale kaolin deposit - Site 2 - non-oriented bulk sample.



File Name: A:\MV2

Fig. 21e. Birdwood kaolin deposit - Site 1 - non-oriented bulk sample.

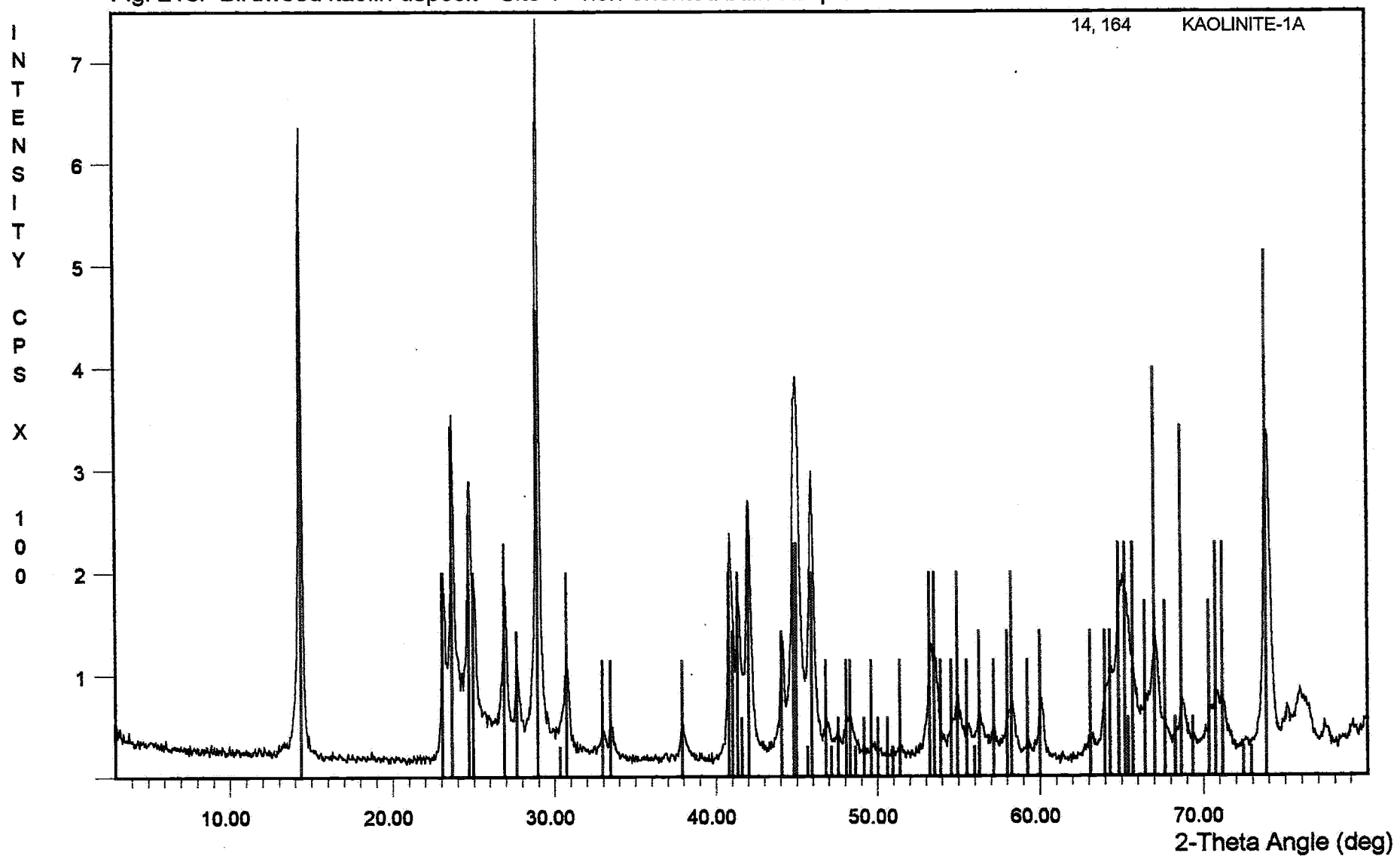
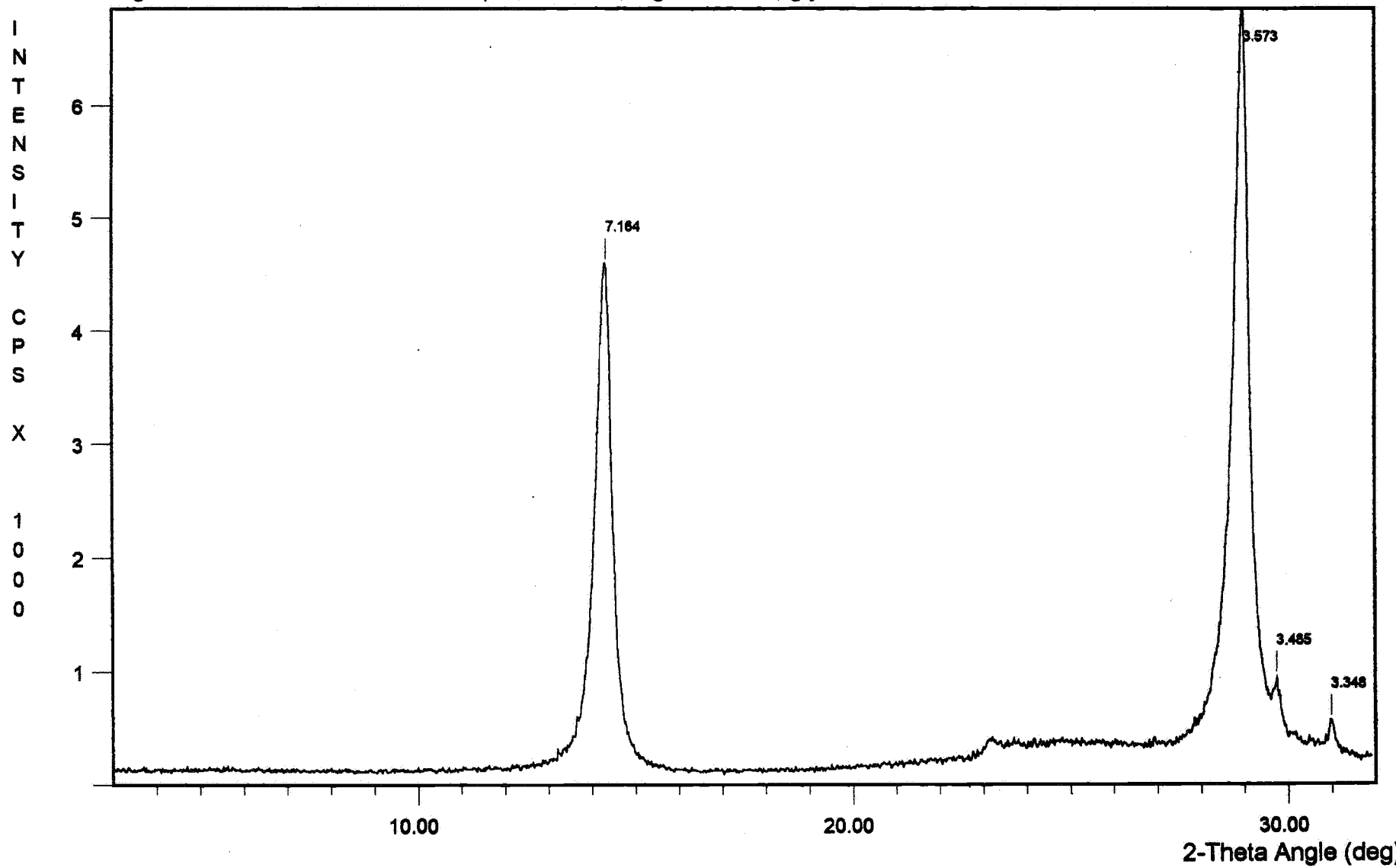
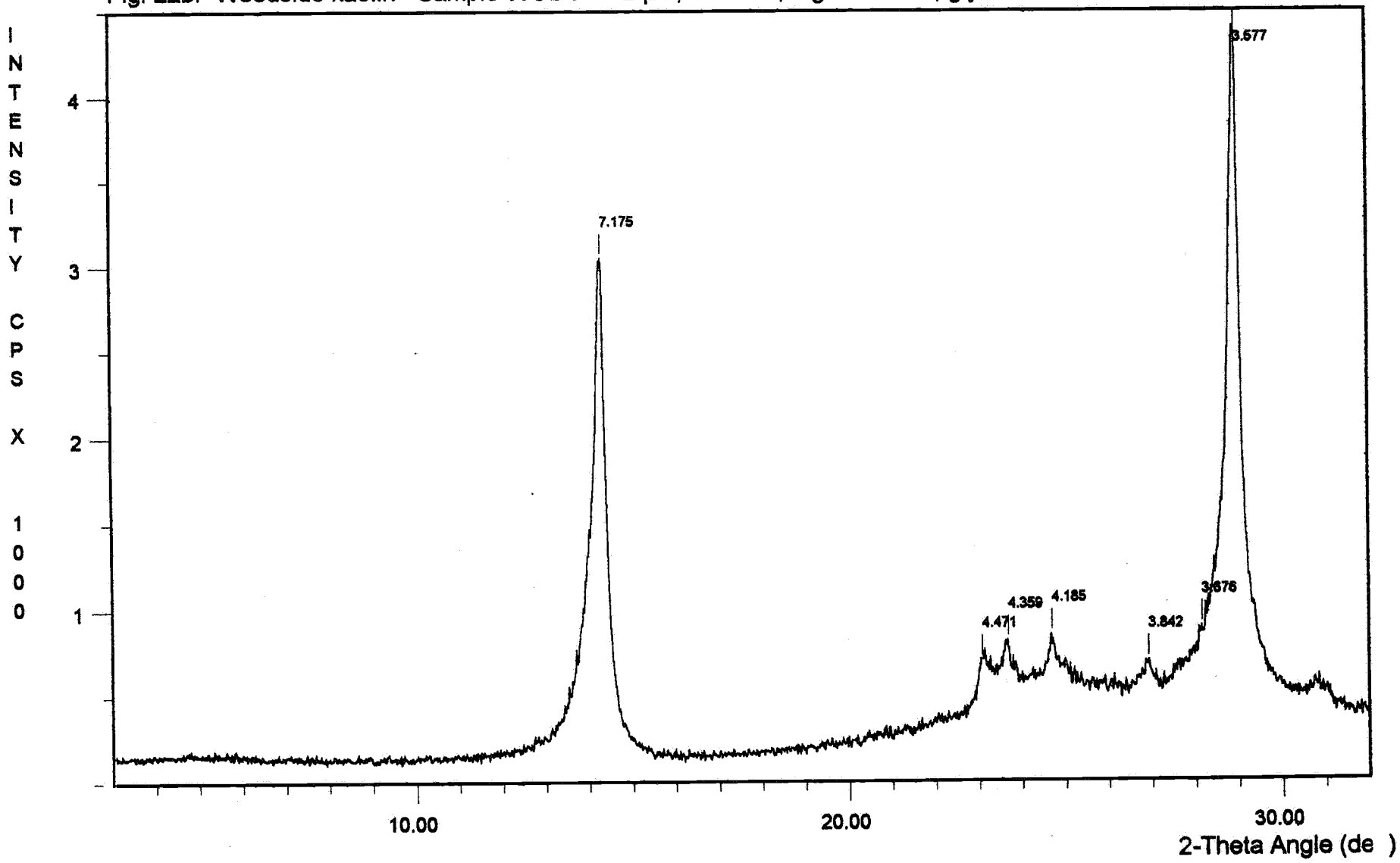


Fig. 22a. Cromer 'C' - Site 1 - < 2 µm, oriented, Mg-saturated, glycerolated.



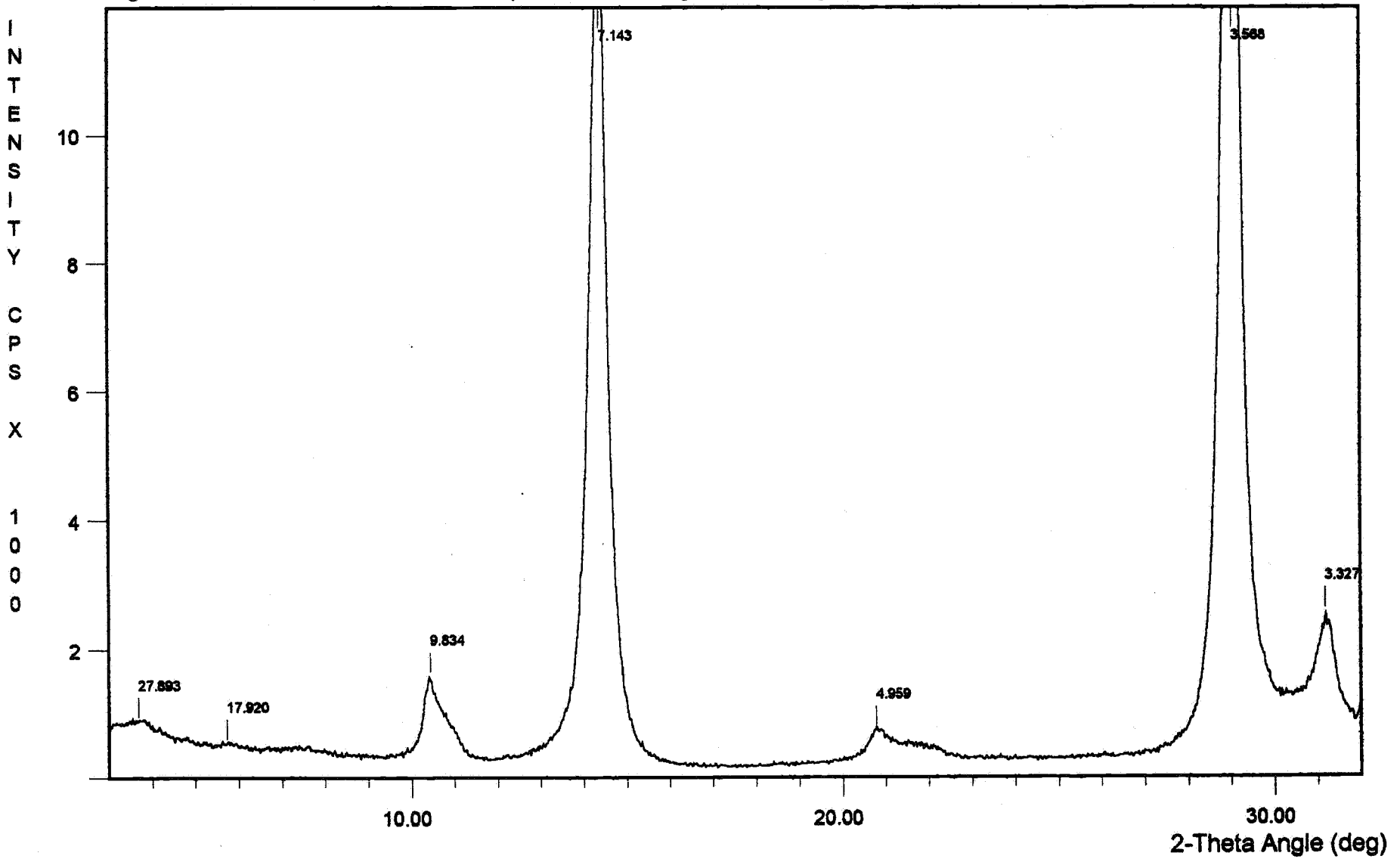
File Name: C:\CLAYPROJ\CR1.OCF

Fig. 22b. Woodside kaolin - Sample WOD1 - < 2 µm, oriented, Mg-saturated, glycerolated.



File Name: C:\CLAYPROJ\WODMGGL

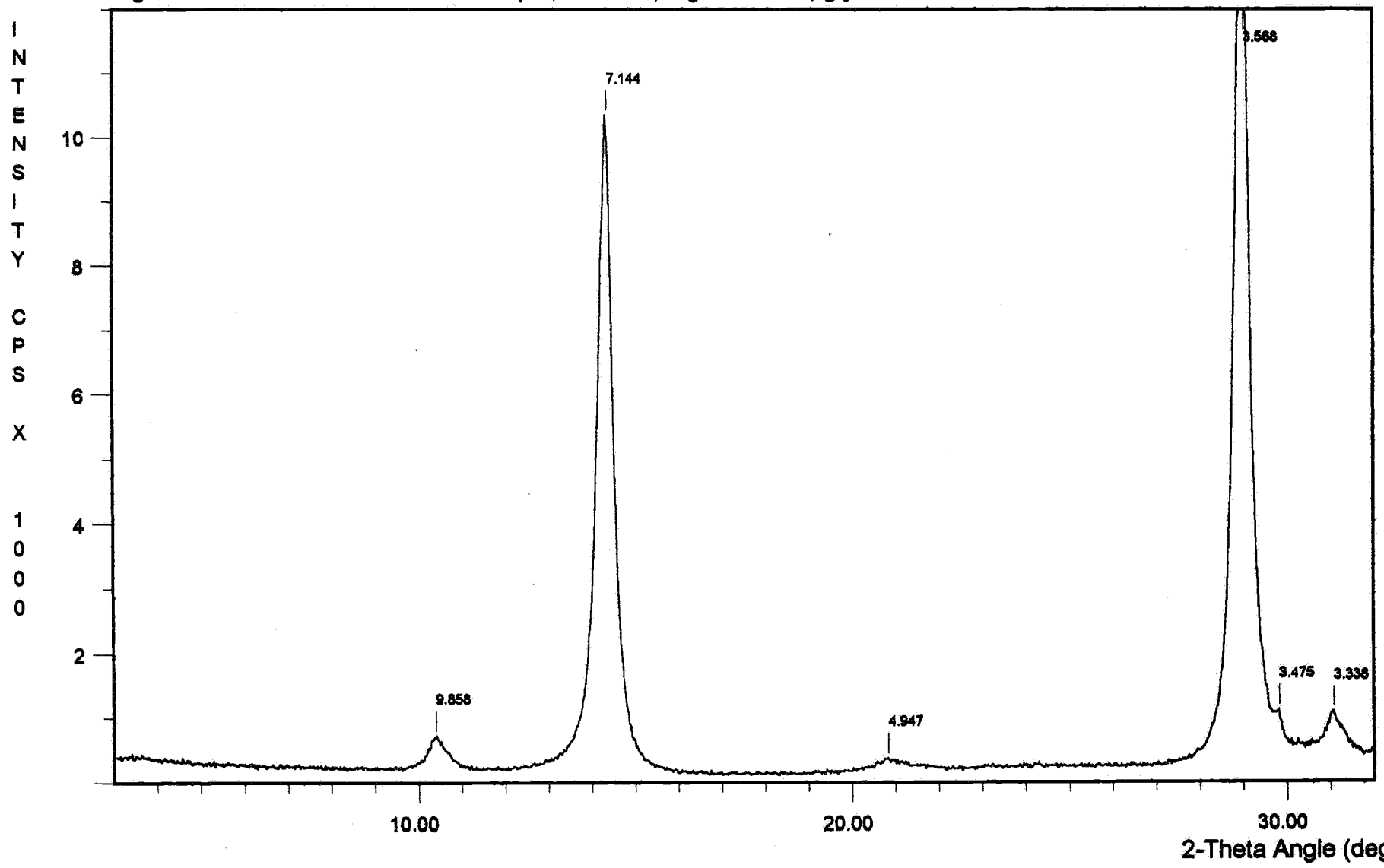
Fig. 22c. Golden Grove - Site 2 - < 2 µm, oriented, Mg-saturated, glycerolated.



File Name: A:\OCF\GG2.OCF

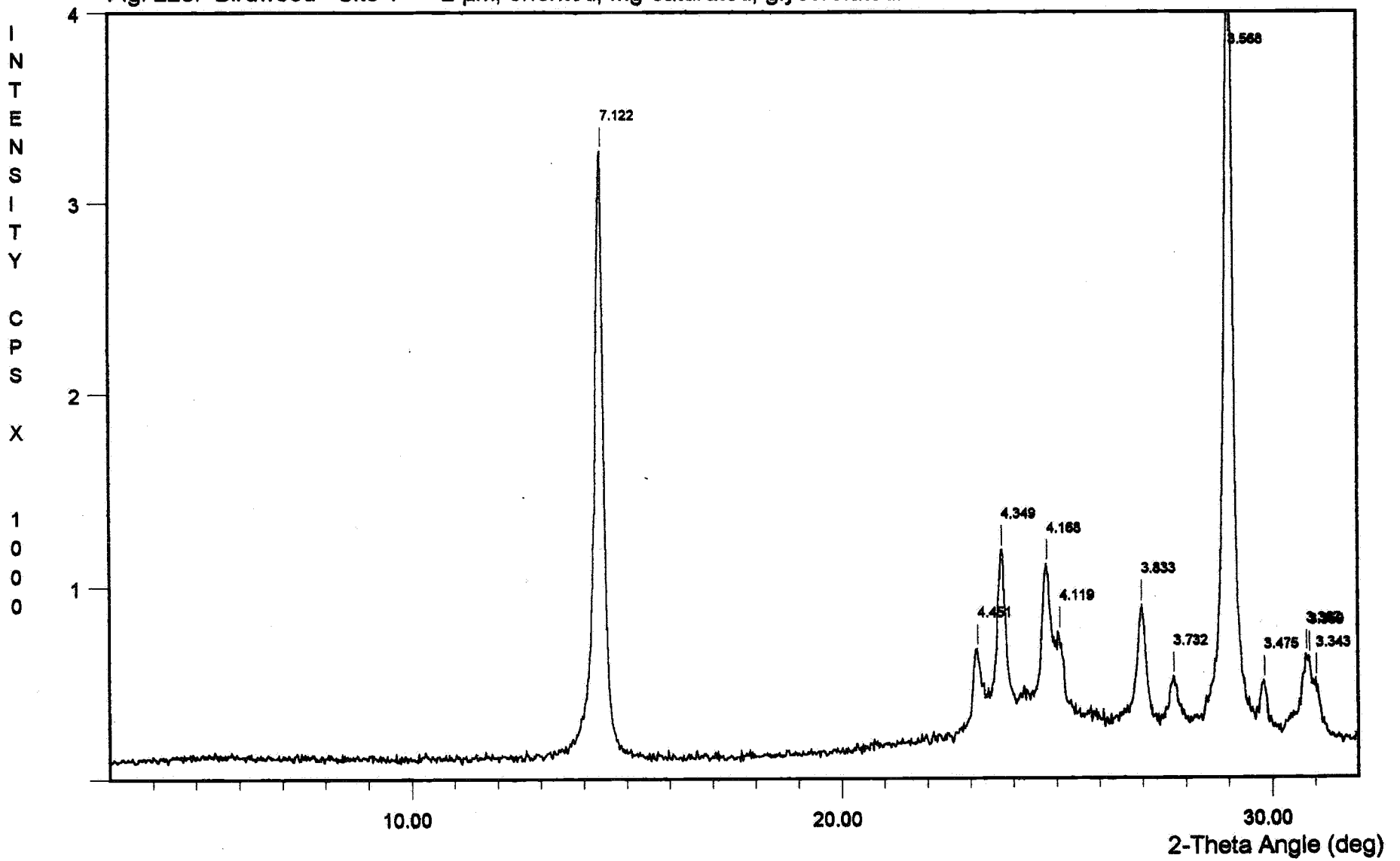
0000052

Fig. 22d. McLaren Vale - Site 2 - < 2 µm, oriented, Mg-saturated, glycerolated.



File Name: A:\OCF\MV2.OCF

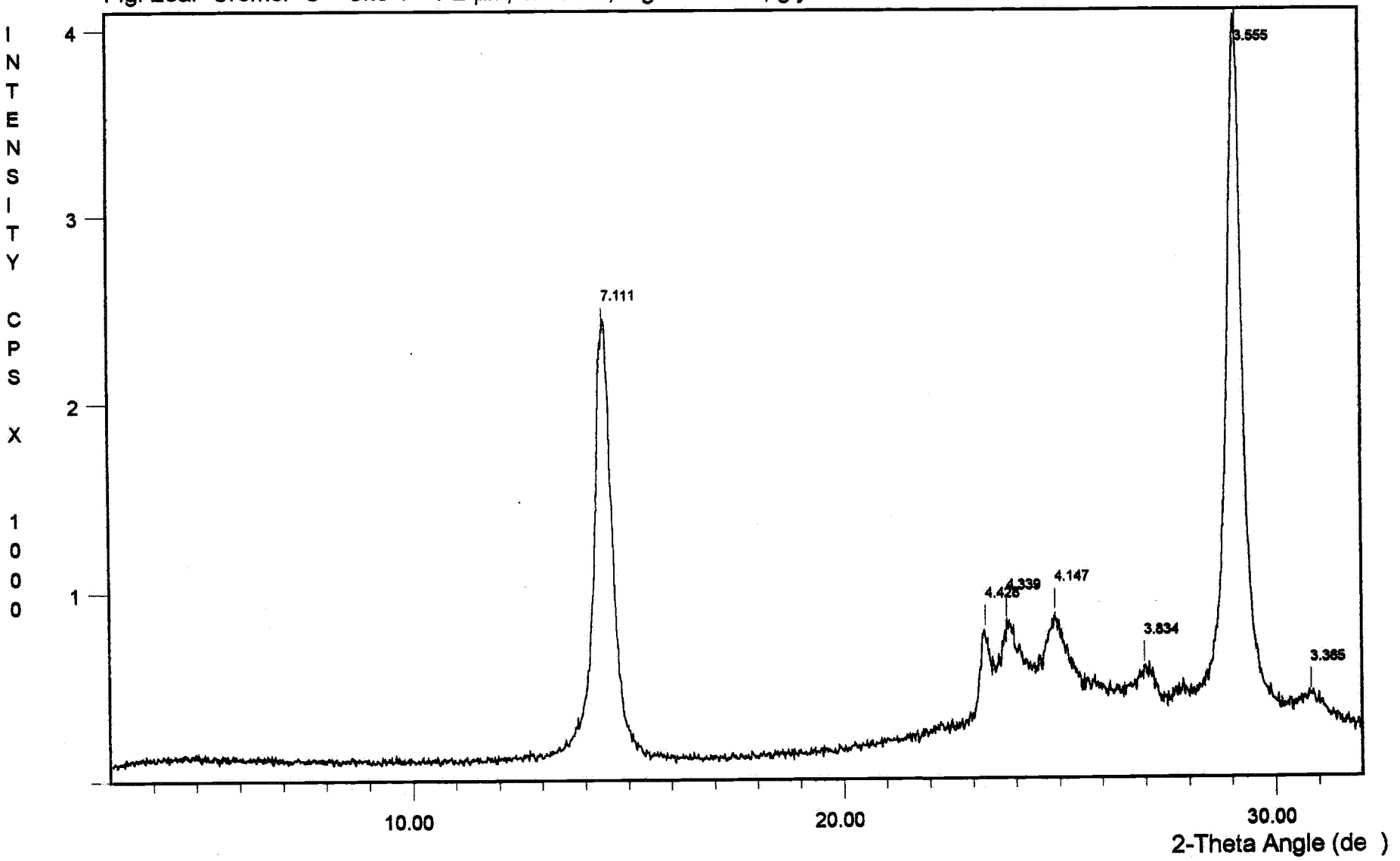
Fig. 22e. Birdwood - Site 1 - < 2 µm, oriented, Mg-saturated, glycerolated.



File Name: A:\OCF\BW1.OCF

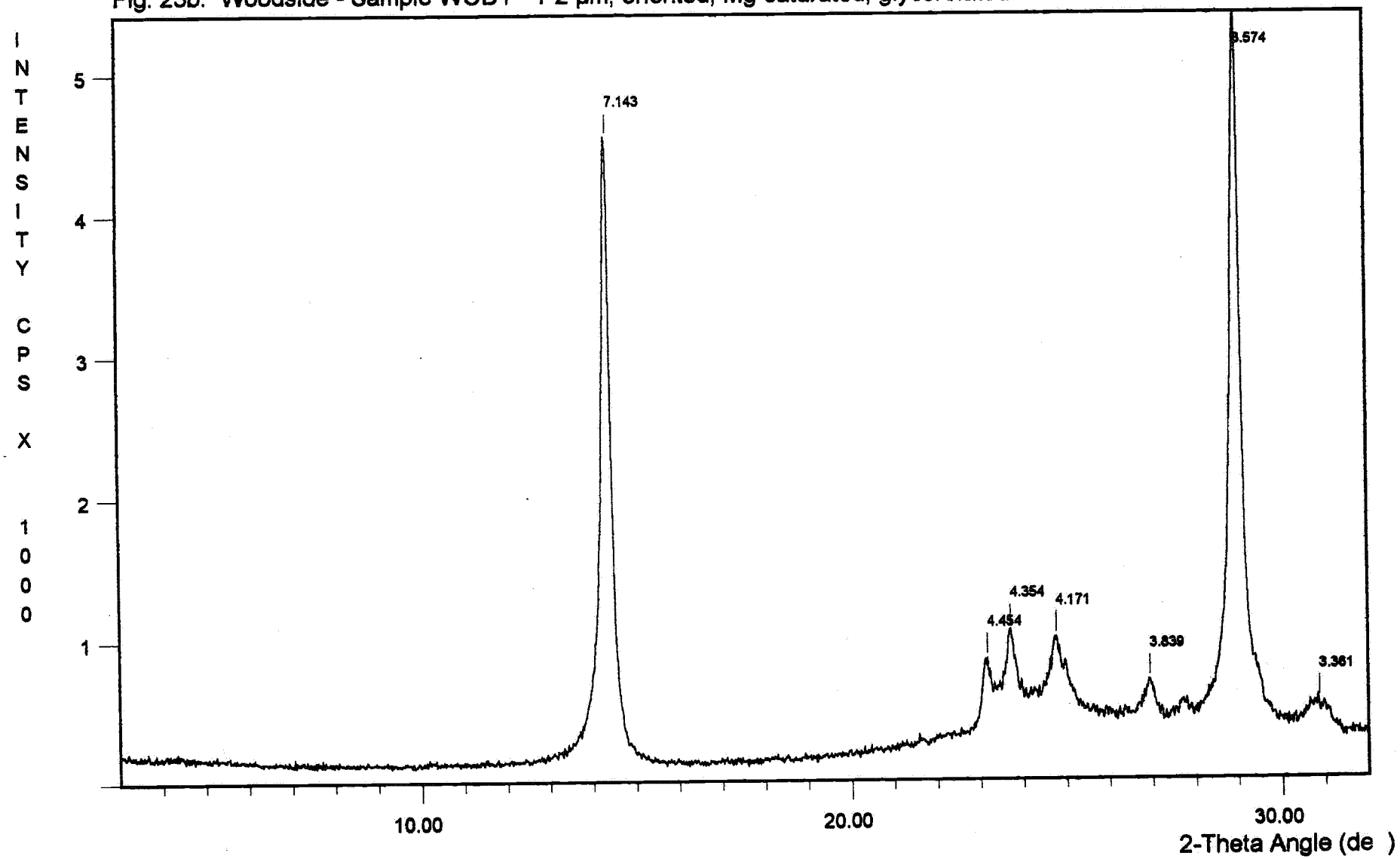
000054

Fig. 23a. Cromer 'C' - Site 1 - 1-2 µm, oriented, Mg-saturated, glycerolated.



000055

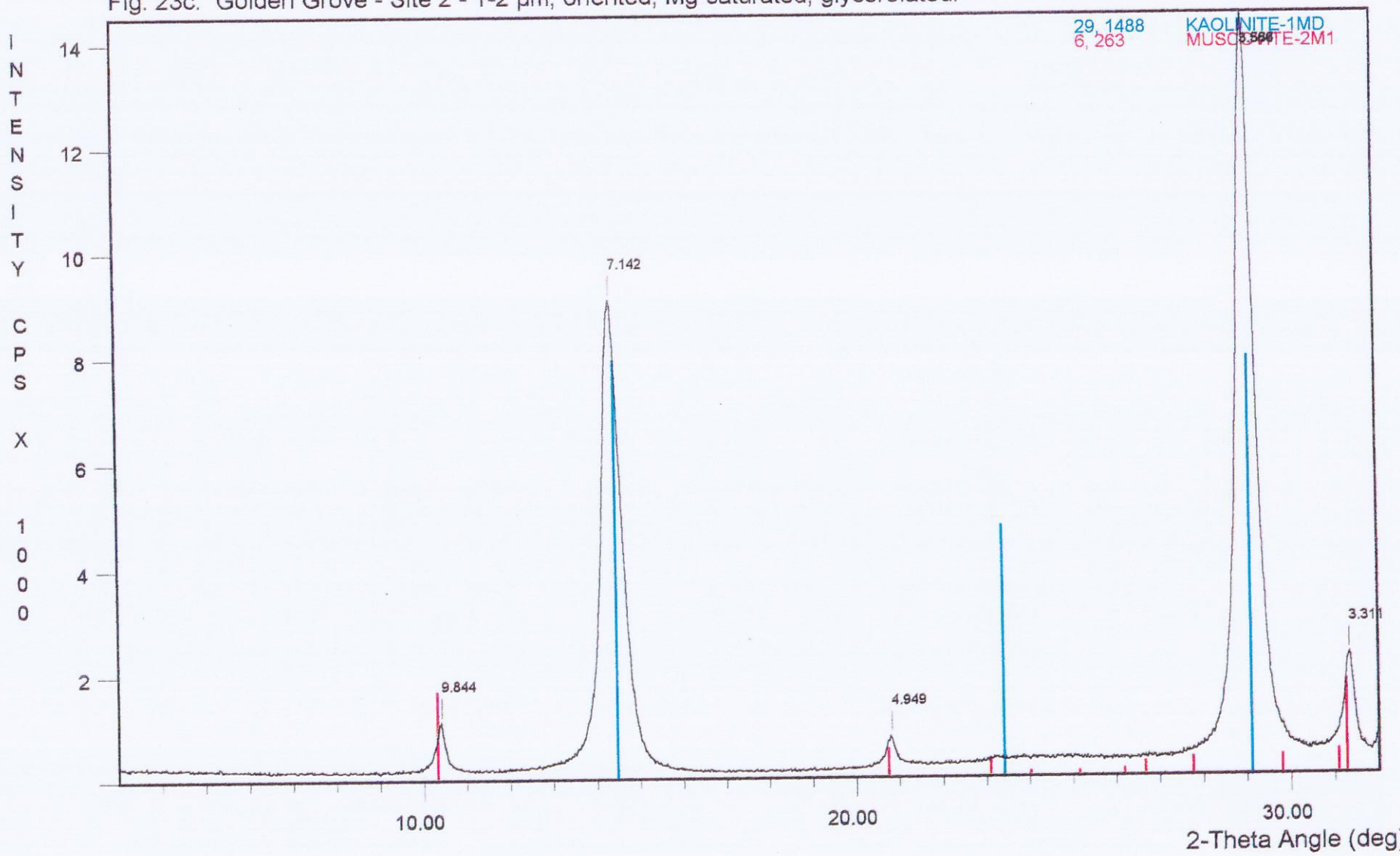
Fig. 23b. Woodside - Sample WOD1 - 1-2 µm, oriented, Mg-saturated, glycerolated.



File Name: C:\CLAYPROJ\KAOL1TO2.104

0000056
50

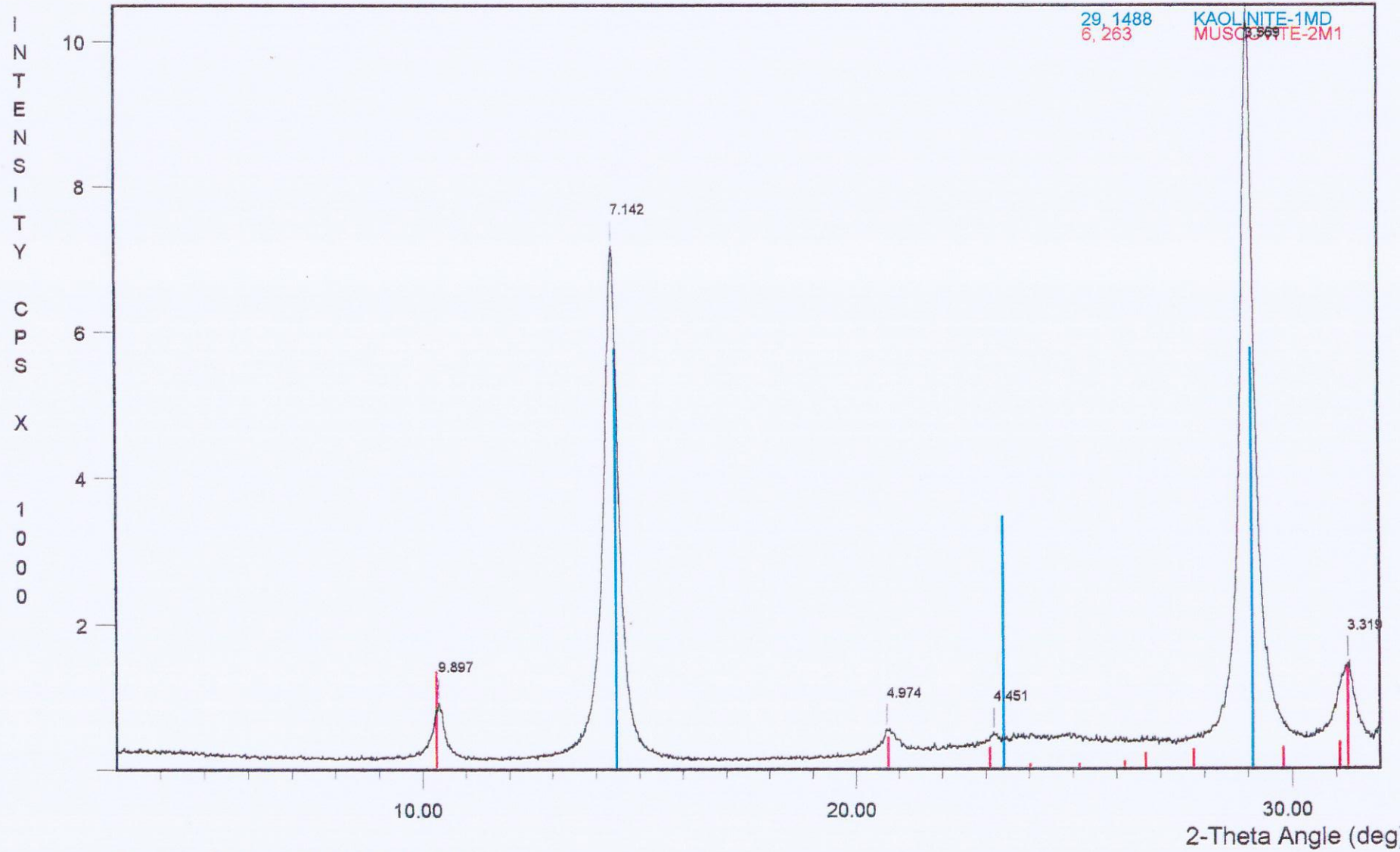
Fig. 23c. Golden Grove - Site 2 - 1-2 µm, oriented, Mg-saturated, glycerolated.



File Name: C:\CLAYPROJ\KAOL1TO2.102

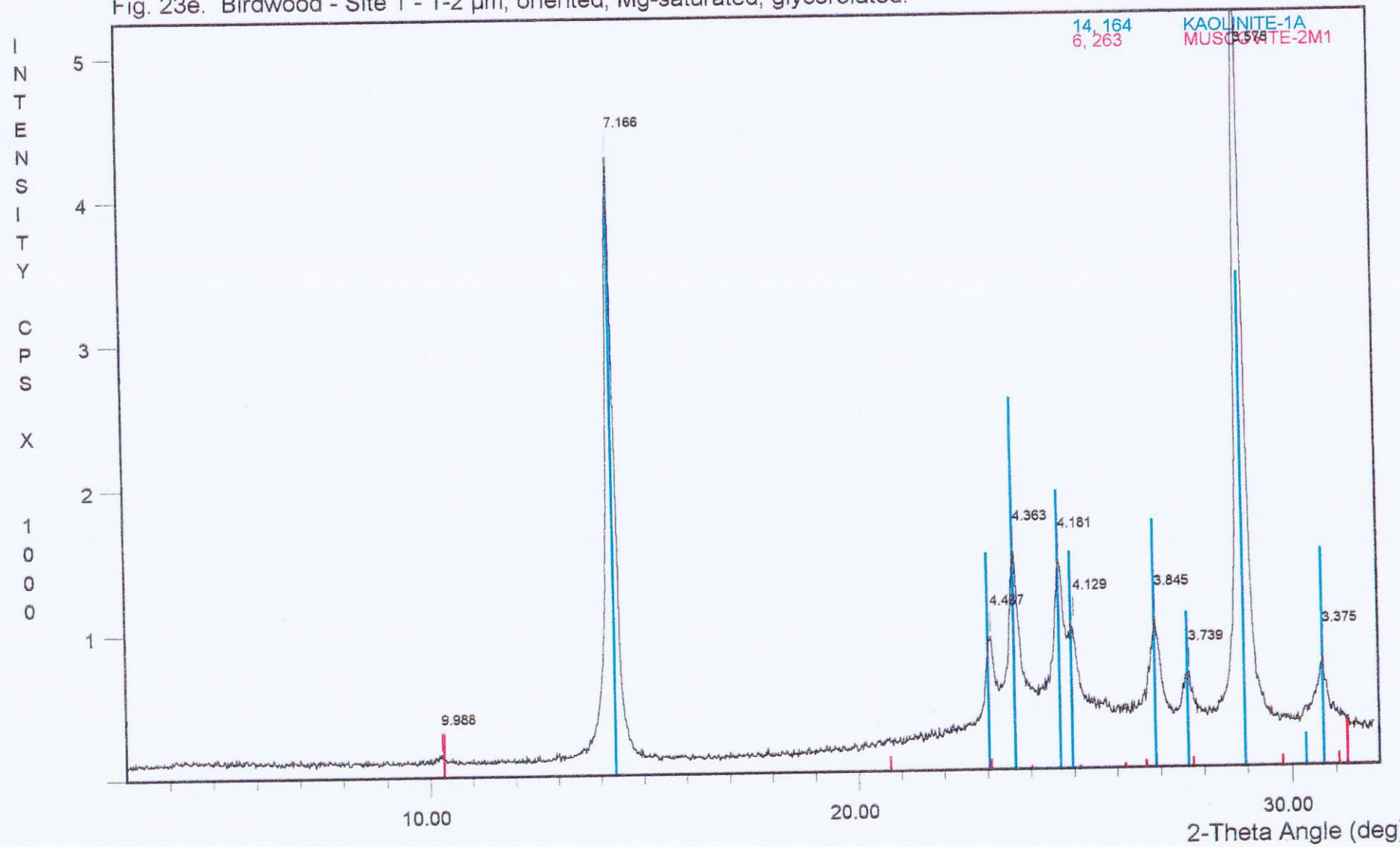
000057

Fig. 23d. McLaren Vale - Site 2 - 1-2 µm, oriented, Mg-saturated, glycerolated.



File Name: C:\CLAYPROJ\KAOL1TO2.106

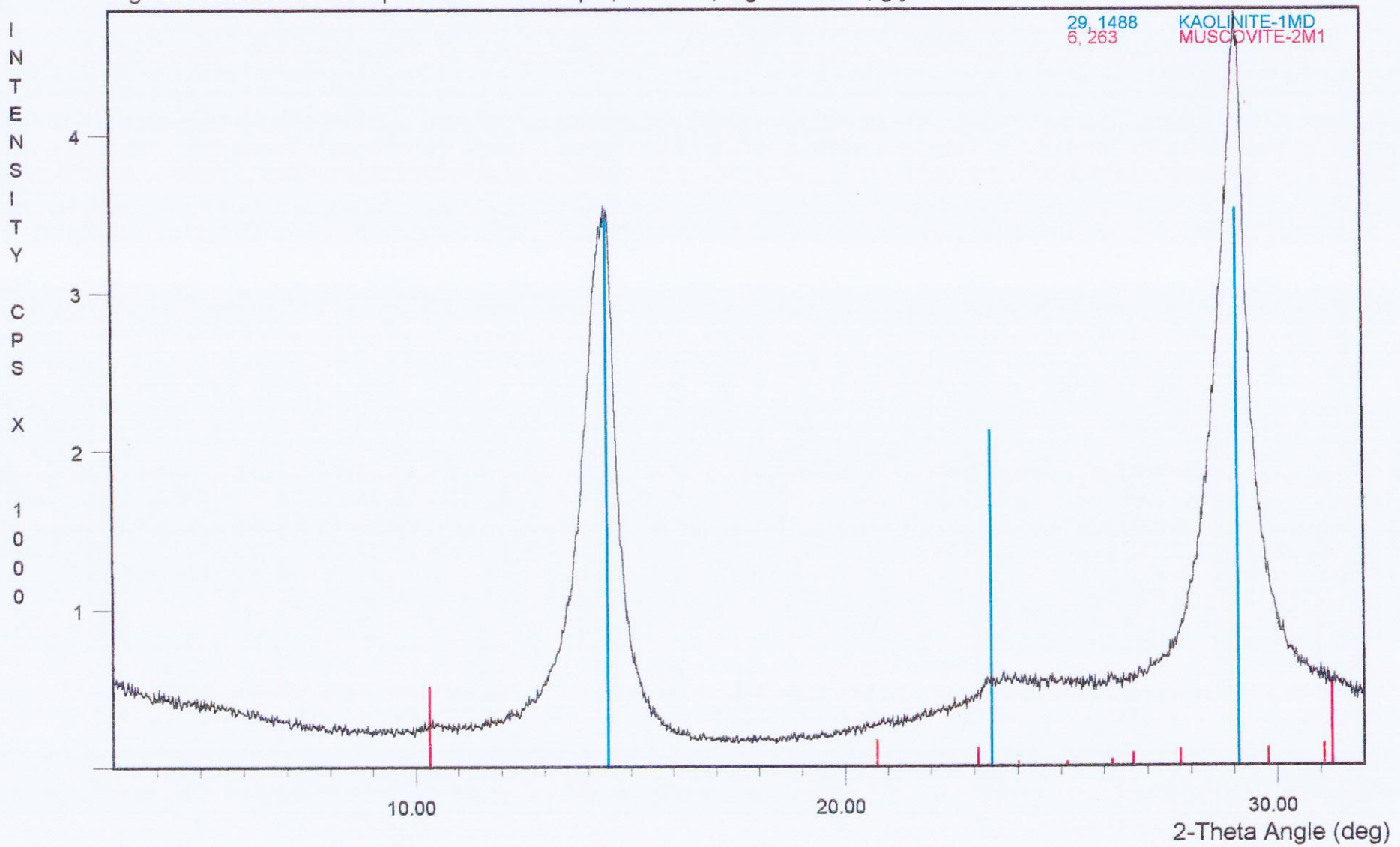
Fig. 23e. Birdwood - Site 1 - 1-2 µm, oriented, Mg-saturated, glycerolated.



File Name: C:\CLAYPROJ\KAOL1TO2.103

0000059

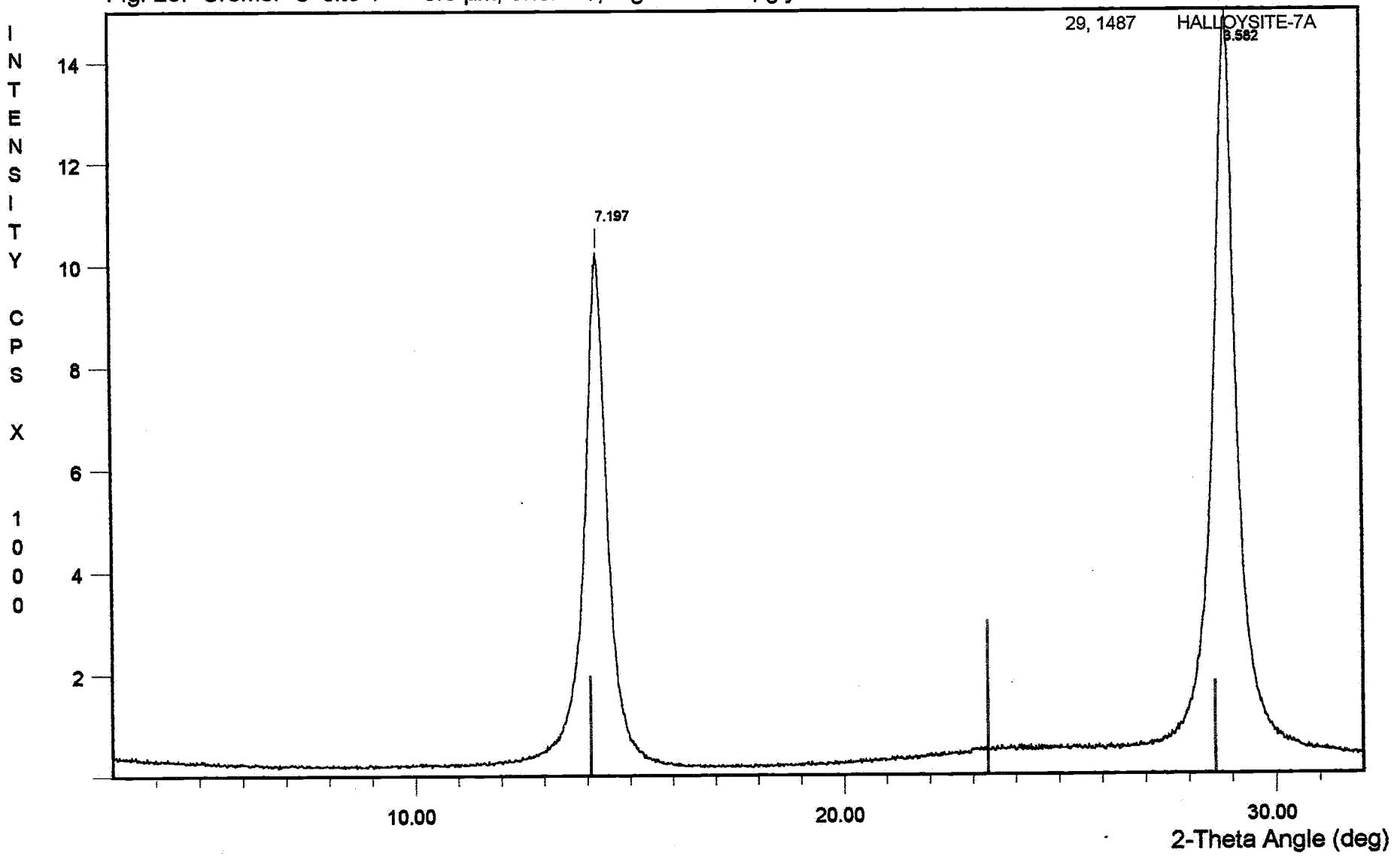
Fig. 24. Woodside - Sample WOD1 - < 0.2 µm, oriented, Mg-saturated, glycerolated.



File Name: C:\CLAYPROJ\WOODFINE

000060

Fig. 25. Cromer 'C' site 1 - < 0.5 µm, oriented, Mg-saturated, glycerolated.



File Name: C:\CLAYPROJ\CROFINE



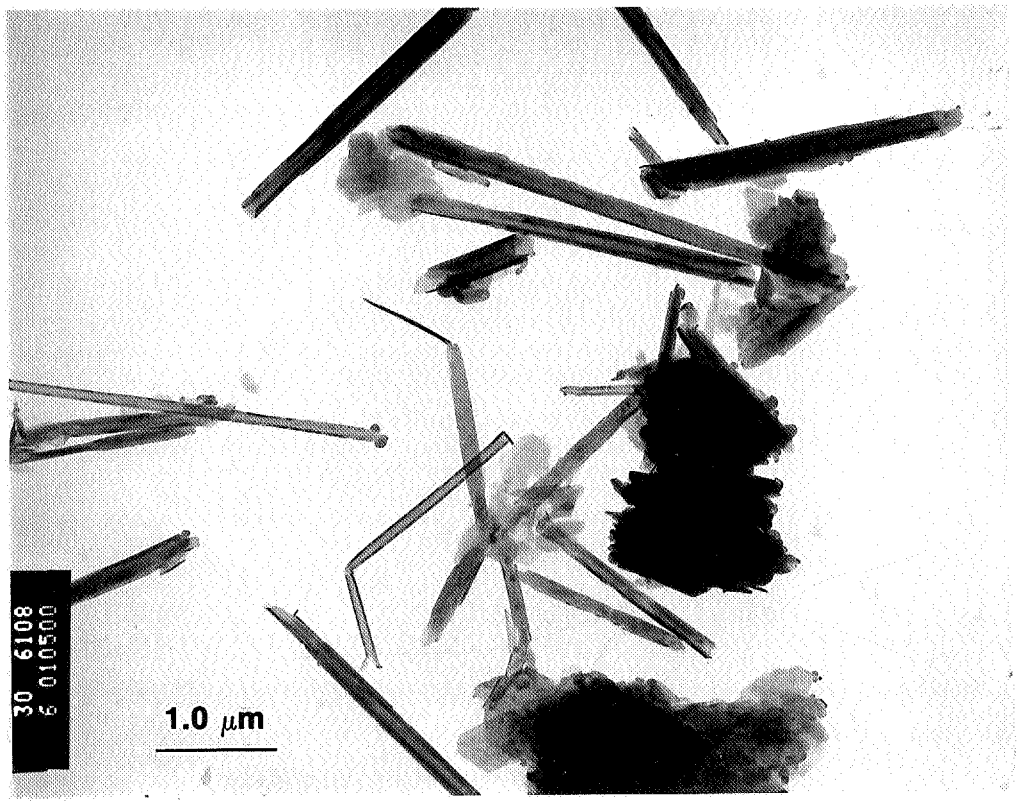


Fig. 26. Scanning electron micrograph (SEM) (above) and transmission electron micrograph (TEM) (below) of samples from the Cromer "C" kaolin deposit. (Micrographs 164 and 16108).

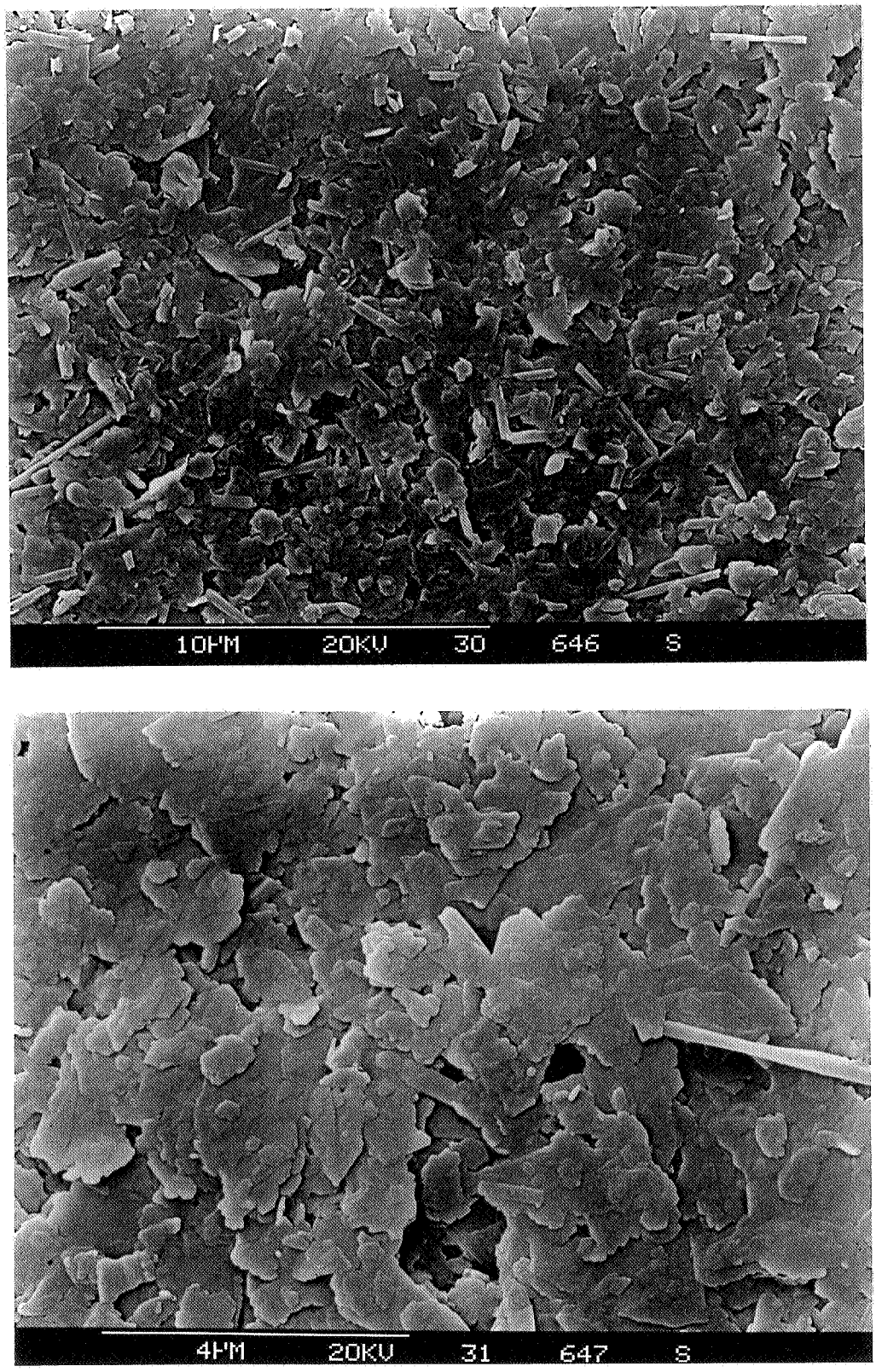
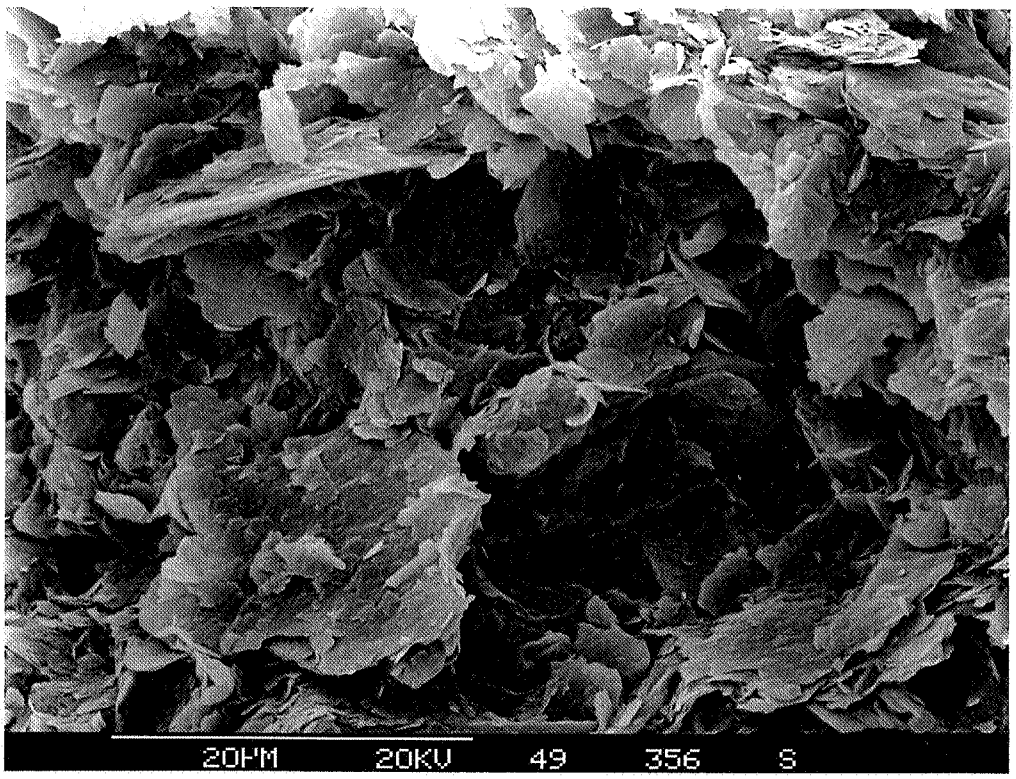


Fig. 27. SEMs of Woodside sample WOD1. (Micrographs 646 and 647).



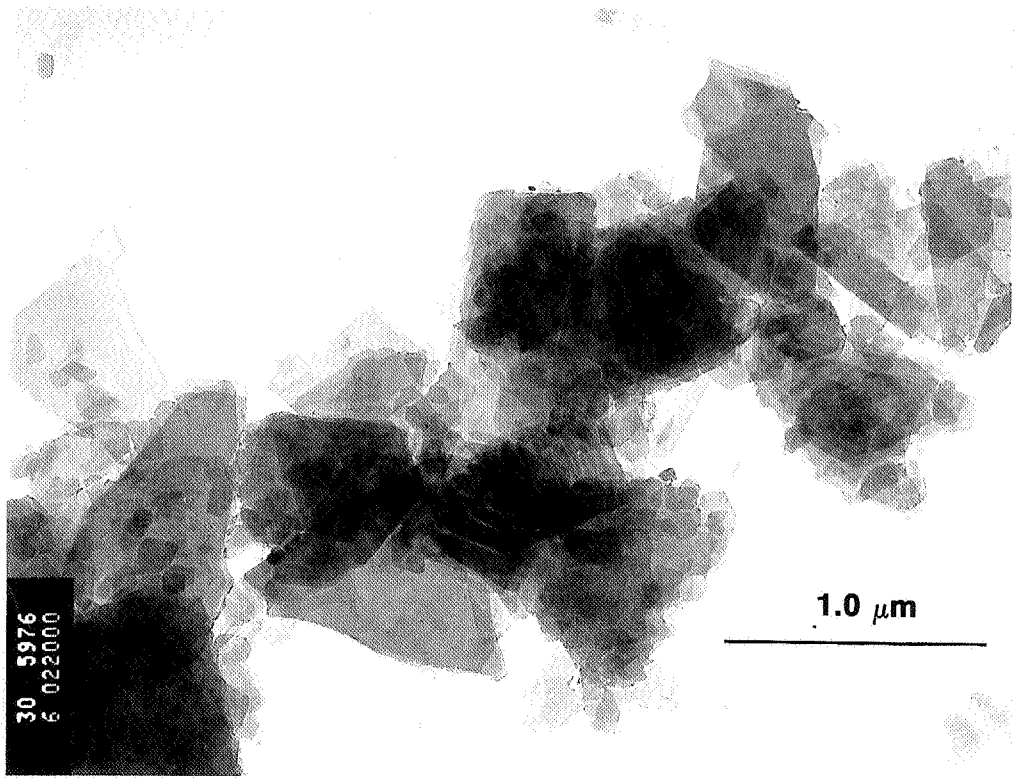


Fig. 28. SEM (above) and TEM (below) of samples from site 2 at the Golden Grove kaolin deposit. (Micrographs 356 and 15976).

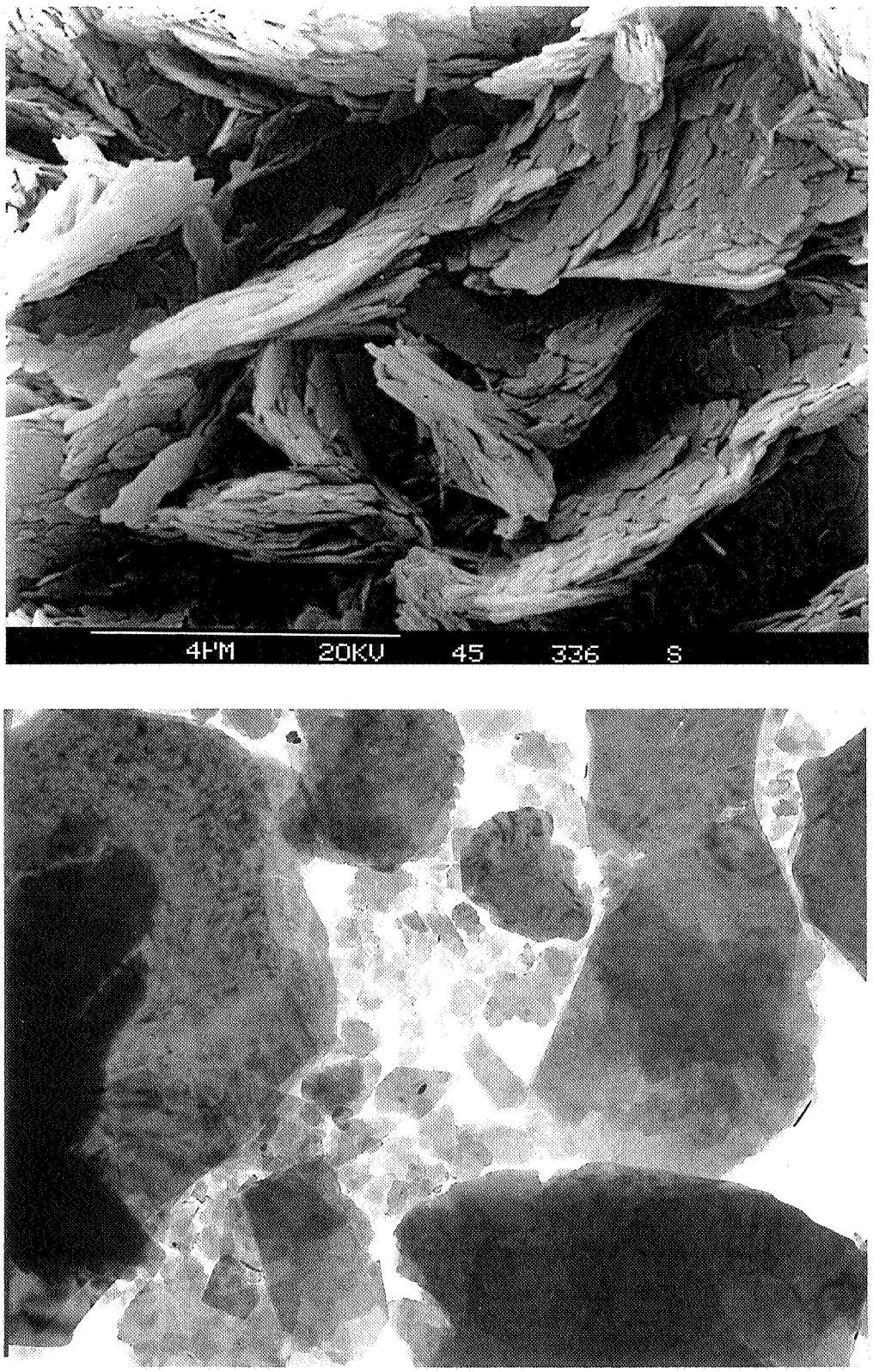
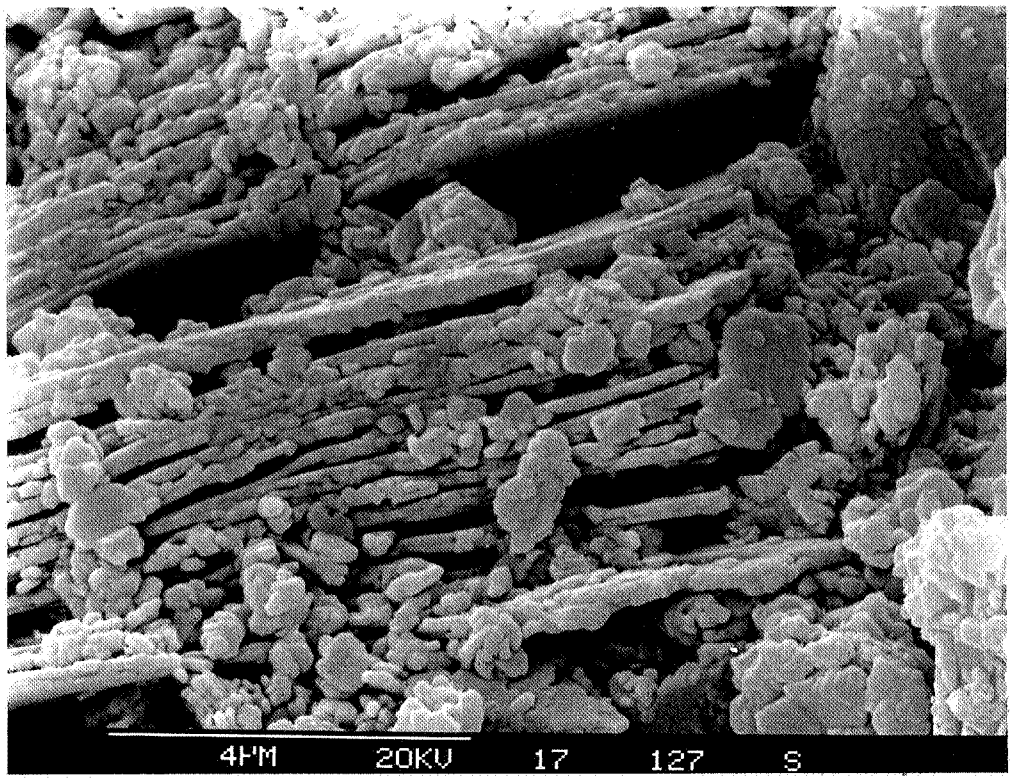


Fig. 29. SEM (above) and TEM (below) of samples from site 2 at the McLaren Vale kaolin deposit. (Micrographs 336 and 16118).



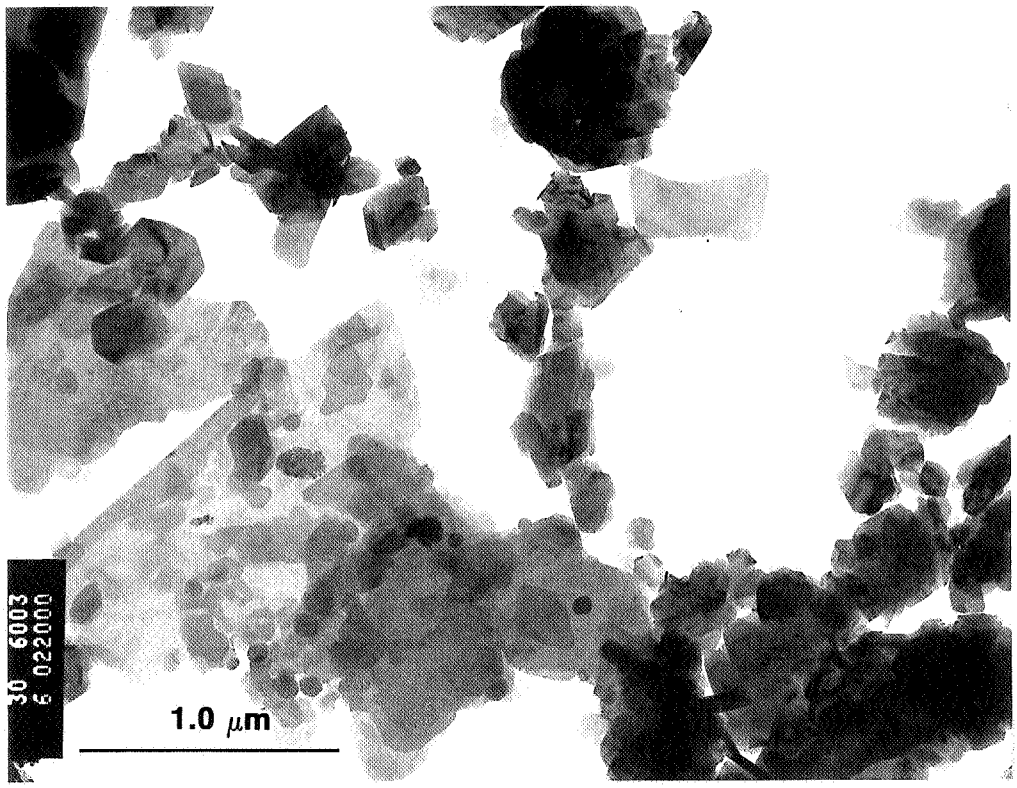


Fig. 30. SEM (above) and TEM (below) of samples from site 1 at the Birdwood kaolin deposit. (Micrographs 127 and 16003).

ILLITE

Introduction

Illites are clay-size micas. As for the micas generally, illite layers are comprised of sheets of octahedrally coordinated cations sandwiched between sheets of silica tetrahedra, giving 2:1 structures. In a typical illite, approximately 15% of Si in the tetrahedral sheets is substituted by Al and a similar proportion of Al in the octahedral sheet is substituted by Mg. As a result, illites have a high layer charge. Nevertheless, a large part of the layer charge is satisfied by potassium ions, which are strongly held in the interlayer region. There may be other elements present (e.g. Fe^{3+}) in the octahedral sheet and Ca and Na, as cations, in the interlayers. The net cation exchange capacity of illites usually does not exceed 40 meq/100g.

Illites occur in platy particles encompassing a wide range of sizes. Muloorina illite is of particular interest owing to its occurrence as very small particles, < 0.1 μm in length or width and only *c.* 0.006 μm thick. As a result, the sample has a high surface area, which is conducive to adsorption (see below).

Material

A green clayey illitic material from Muloorina Station, on the edge of Lake Eyre, South Australia, known as Muloorina illite, was studied. It is a lacustrine deposit of Oligocene age. The fractions and sub-fractions studied were taken from a "pit sample" from 76-91 cm.

Experimental

10g of the sample was dispersed in a slurry with 1M NaCl and separated into the clay-size (< 2 μm) fraction and also into 1-2, 0.2-1 and < 0.2 μm fractions. XRD and XRF determinations were carried out as for the kaolin samples.

Results

Table 9 shows the weight percentages of particles in given size ranges for the Muloorina illite. The sample comprises mainly extremely fine particles, with *c.* 90% of particles in the whole sample and *c.* 98% of those in the < 2 μm fraction being < 0.2 μm. The proportion of 1-2 μm fraction in the whole sample is almost negligible.

Table 9. Particle size distribution for Muloorina illite.

Size range (μm)	Fraction (wt%)
>2	8.6
1-2	0.2
0.2-1	1.5
<0.2	89.9

The XRD pattern of the whole clay (< 2 μm) fraction (Fig. 31) shows that illite is the dominant constituent, with minor quartz and kaolinite also present. The XRD pattern of a < 2 μm sample of another sample of Muloorina illite (Fig. 38c) was essentially similar except that there were no peaks for kaolinite in that case. Variation in the composition of Muloorina illite has been noted previously (Norrish and Pickering, 1983). In particular, palygorskite may occur along with illite. A peak for palygorskite at 10.4 Å may contribute to the low angle asymmetry of the 10 Å peak in Fig. 31. Interstratification with an expanded 2:1 aluminosilicate phase could also contribute to this peak and also to the high background at very low angles.

An XRD pattern was obtained of the 1-2 μm fraction sedimented on to a silicon wafer and treated with ethylene glycol and is shown in Fig. 32. Kaolinite is the dominant mineral in this fraction, which forms a minuscule part of the Muloorina sample.

An XRF analysis of a < 2 μm fraction of another sample of Muloorina illite is given in Table 17. The analysis is very similar to that for the < 0.05 μm fraction of a sample of Muloorina illite given by Norrish and Pickering (1983), except that the latter has a higher proportion of SiO_2, probably reflecting the higher proportion of illite compared with kaolinite in fine fractions.

Muloorina illite has only a moderate-low CEC (18 meq/100g - Table 17). However, illites have a high layer charge compared even with smectites.

Some recent work (Paulus *et al.*, 1992) has shown that synthetic micas can show highly selective extraction of radioactive elements like strontium and caesium from nuclear wastes. We have shown that the particular synthetic micas studied by Paulus *et al.* (1992) can been produced in our laboratory. However, this synthetic mica has a very different structure from a natural material like Muloorina illite. Nevertheless, Muloorina illite offers particularly attractive prospects because it consists of very small particles which

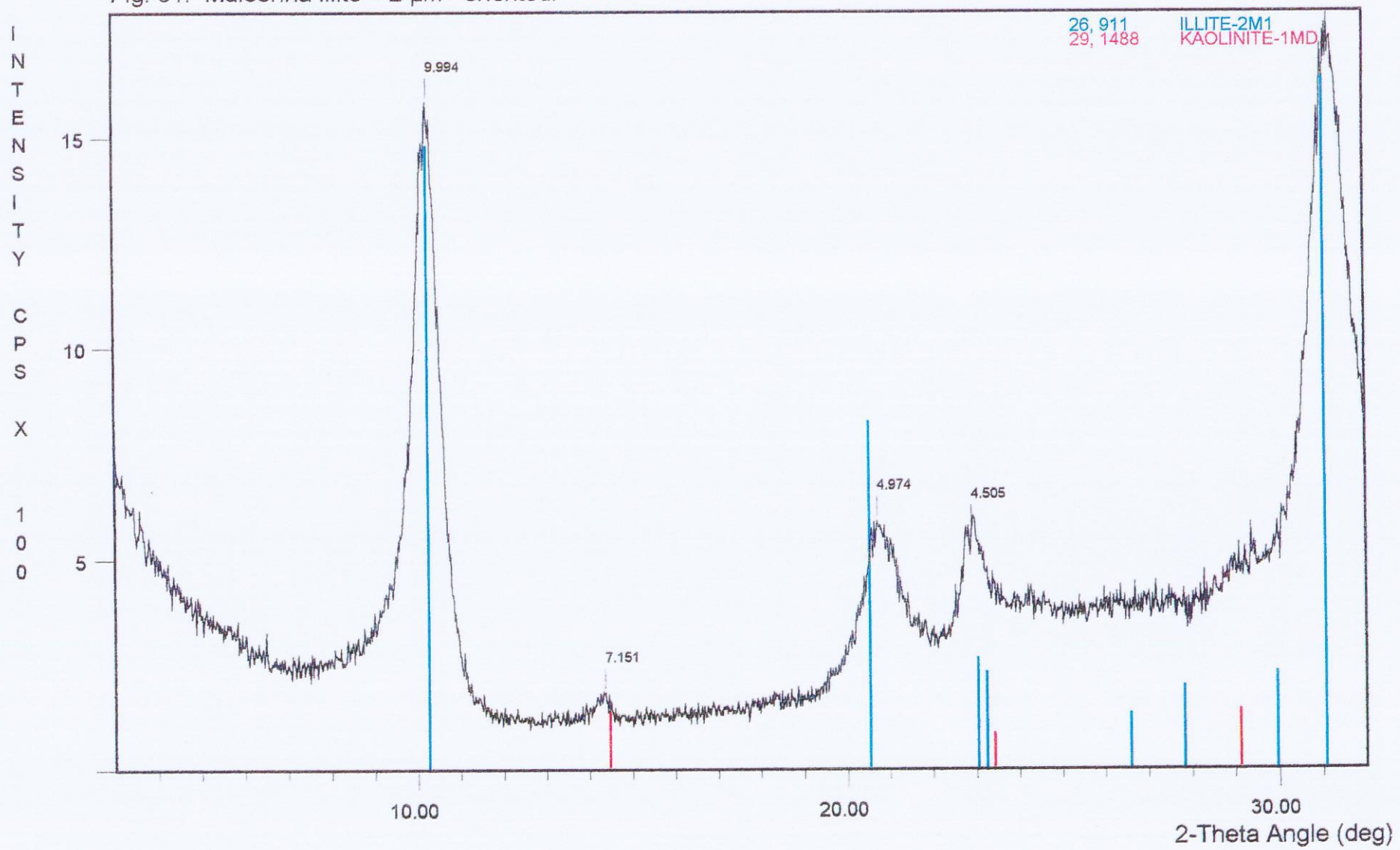
therefore present a very high specific surface area for sorption. Tiller and Smith (1990) measured the specific surface area of a bulk sample of Muloorina illite as 103 m^2g^{-1}.

FIGS. 31 TO 32

Fig. 31. XRD of Muloorina illite < 2μm - oriented.

Fig. 32. XRD of Muloorina illite 1-2 μm - sedimented on silicon wafer.

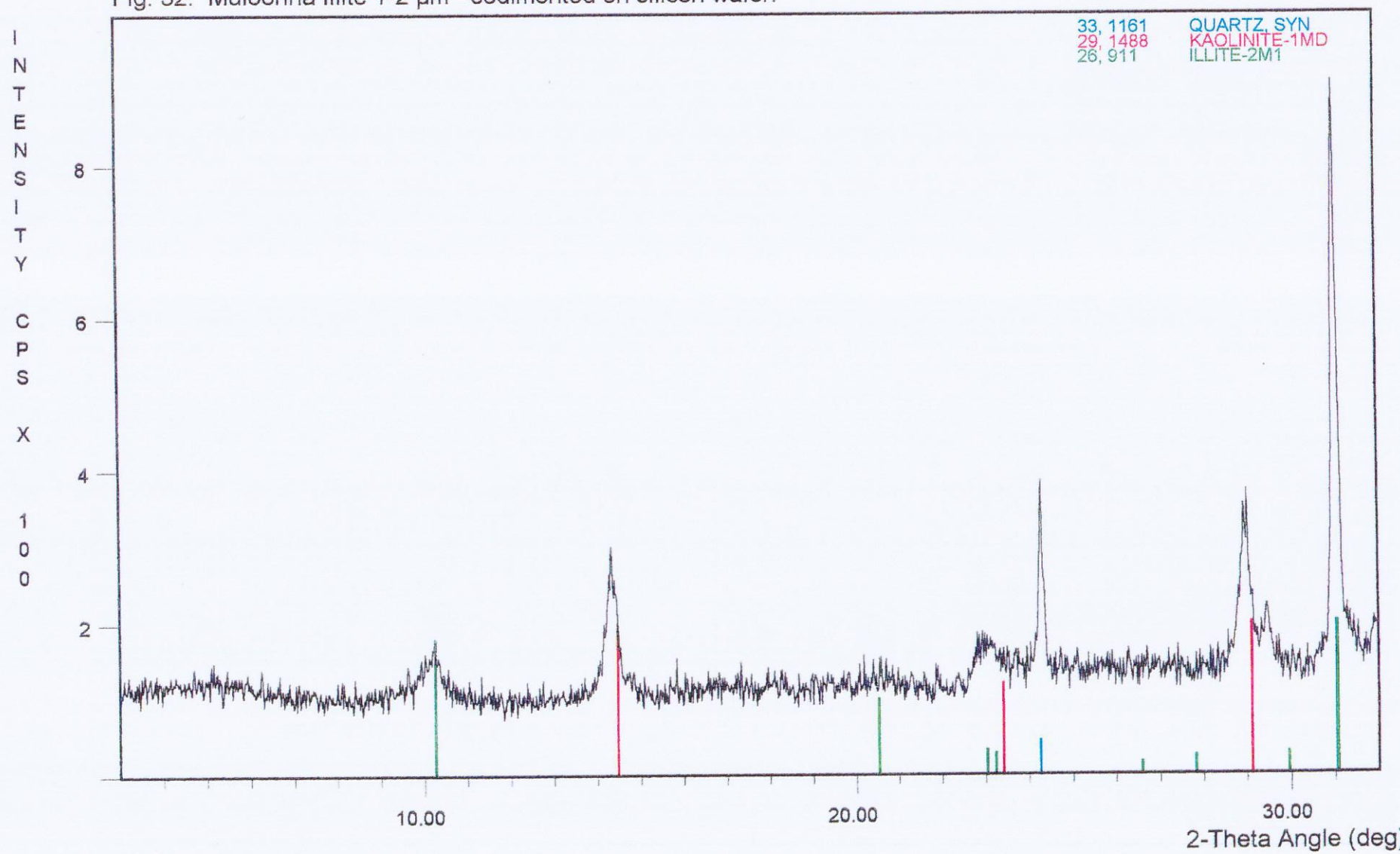
Fig. 31. Muloorina illite < 2 µm - oriented.



File Name: A:\MULCL

000071
65

Fig. 32. Muloorina Illite 1-2 µm - sedimented on silicon wafer.



File Name: A:\MUL1T02

99 270000

THE PALYGORSKITES

Introduction

Palygorskite, sometimes called attapulgite, is a fibrous Mg silicate with the ideal formula $Mg_5Si_8O_{20}(OH)_2(OH_2)_4 \cdot 4H_2O$. The palygorskite structure is made up of ribbons of the 2:1 phyllosilicate structure with one ribbon joined to another ribbon via an inversion of SiO_4 tetrahedra along a line of Si-O-Si bonds (Jones and Galan, 1984). The tetrahedral layer is continuous while the octahedral sheet is discontinuous along the y-axis producing channels (3.7Å by 6.4Å) between the layers that extend parallel to the fibre axis. The structure of palygorskite is closely related to that of sepiolite with the latter having wider channels (3.7Å by 10.6Å). The chemical composition of palygorskite can vary with Al^{3+} replacing Mg^{2+} in the octahedral layer or Si^{4+} in the tetrahedral layer. The charge imbalance caused by this substitution is countered by the presence of exchangeable Ca^{2+} or Mg^{2+} ions in the channels.

Palygorskite contains water in 4 forms (Bellat and Simonot-Grange, 1989):

1. water adsorbed on external surfaces,
2. zeolitic water in the centre of the channels,
3. structural water bound to Mg at the edges of the channels and
4. hydroxyl water in the octahedral ribbons.

On heating this water is lost from the structure at temperatures of ~105°C, 150 to 290°C, 450 to 500°C and above 800°C respectively.

Because of the fibrous nature of palygorskite, it has a high surface area and high porosity. These properties make it suitable for a variety of industrial applications. Table 10 outlines various industrial applications of palygorskite that utilise its sorptive, catalytic and rheological properties.

Table 10. Industrial applications of palygorskite grouped according to its physio-chemical properties

Sorptive	pet litter pesticide and herbicide carriers bleaching agents for mineral and vegetable oils filter aids (particularly in sugar refining) water treatment pharmaceutical (toxin absorption) animal-feed binders spill absorbents (oil, grease, water)
Catalytic	carbonless copying paper. catalyst carrier
Rheological	drilling mud thickeners for aqueous or organic liquids oil-bound foundry sands
Filling	reinforcing filler in rubber and foam

Materials

Garford palygorskite

A major deposit of palygorskite exists in the Garford Palaeochannel that is situated some 100 km southwest of Coober Pedy, South Australia. Previous x-ray diffraction (XRD) of bulk samples obtained from holes drilled in the palaeochannel showed a sequence of chemically precipitated dolomite and dolomitic clays overlying dominantly palygorskite clay (Benbow and Pitt, 1978; Robertson, 1984). Clay ranging in thickness from 5 to 10m is widespread in a series of dry playa lakes that, potentially, contain very large geological resources of palygorskite clay. In order to extend the results of previous work, samples were taken from auger holes drilled in March 1991. Logs of holes that intersected significant amounts of palygorskite are recorded in Table 11.

Table 11. Garford Palaeochannel, auger hole logs and mineralogy of bulk samples

Hole No	Sample interval (m)	Description	Mineralogy
P25	0.0 - 1.0	**CLAY**, white to pale yellow, minor yellow brown staining. Hard at surface but soft and slightly moist below 0.2m. Greyish patches at 1.0m.	Dol 75%, Paly 23%
	1.0 - 2.0	**CLAY**, white to pale yellow to pale orange, salty, rare quartz grains, minor yellow brown Fe oxides.	Dol 74%, Paly 18%
	2.0 - 3.0	**CLAY**, greenish grey and yellow, some darker grey patches, moist, moderately plastic, salty.	Dol 11%, Paly/Illite 83%
	3.0 - 4.0	**CLAY**, dark greenish grey, moderately - very plastic, trace of quartz sand (M). Colour less patchy than above.	Dol 12%, Paly/Illite 77%
	4.0 - 5.0	**CLAY**, dark greenish grey with rare black patches ~ 2mm across, shiny and magnetic. Very rare quartz grains (M-C).	Dol 2%, Paly/Illite 92%
	5.0 - 6.0	**CLAY**, dark greenish grey smooth, wet, very stiff. WATER CUT at ~5.8m. Even colour and texture, minor quartz grains. Pliable and waxy, soapy feel when wet, dark greyish green to grey. Pulled rods and cleaned off.	Dol 0%, Paly/Illite 94%
	6.0 - 7.0	**CLAY**, dark grey to greenish grey with yellow brown and red brown Fe oxide staining, wet.	Dol <1%, Paly/Illite 93%
	7.0 - 9.0	**CLAY**, dark olive green to grey, very plastic, cracks on drying.	Dol <1%, Paly/Illite 90%
		EOH 9.0m. Logged JLK 20 March 1991.	
P26	0.0 - 1.0	**CLAY**, white to pale yellow, dry easily crumbled.	Dol 75%, Paly 20%, Qtz 3%, Halite 1%, Celest <1%
	1.0 - 2.0	**CLAY**, white to pale yellow brown, dry becoming moist below 1.5m.	Dol 79%, Paly 19%, Tr Qtz, Halite, Celes, Kaolin
	2.0 - 3.0	**CLAY**, white to very pale yellow brown, some orange bands or patches, moist plastic.	Dol 67%, Paly 30%, Tr Qtz, Halite, Kaolin
	3.0 - 4.0	**CLAY**, white to pale yellow with minor orange specking.	Dol 37%, Celes 37%, Paly 25%, Tr Qtz, Halite
	4.0 - 5.0	**CLAY**, white to very pale yellow with minor orange Fe oxide patches, moist, plastic.	Dol 76%, Paly 21%, Tr Qtz, Halite, Celes, Kaolin
	5.0 - 6.0	**CLAY**, white to pale grey with rare grey quartz (C-VC) moist, plastic.	Dol 74%, Paly 24%, Tr Qtz, Halite, Celes, Kaolin
	6.0 - 6.5	**CLAY**, greyish green to yellowish green, even grained, smooth, plastic.	Illite/Paly 89%, Qtz 8%, Tr Dol, Halite, Anatase, Kaolin
		EOH 6.5m. Logged JLK 20 March 1991.	

Hole No	Sample interval (m)	Description	Mineralogy
P30	0.0 - 1.0	**CLAY**, white to pale grey with minor orange brown to yellow Fe staining, dry.	Dol 70%, Paly 16%
	1.0 - 2.0	**CLAY**, white to pale grey, moist. Rare scattered quartz grains (C), black patches (organic or Mn) and minor Fe patches that appear to infill root holes or burrows.	Dol 60%, Paly 32%
	2.0 - 3.0	**CLAY**, white to very pale grey, even colour, moist.	Dol 60%, Paly 38%
	3.0 - 4.0	**CLAY**, very pale grey, moist, plastic, smooth. WATER CUT.	Dol 40%, Paly 55%
	4.0 - 6.0	**CLAY**, dark greenish grey with minor yellow brown Fe patches, smooth stiff, good sample return.	Dol 30%, Illite/Paly 64%
		EOH 6.0m. Logged JLK 21 March 1991	
P31	0.0 - 1.3	**GYPSUM** sand (F-M), yellow brown to red brown with minor quartz sand (C). Colour greenish yellow to yellow brown below 0.7m.	
	1.3 - 2.0	**CLAY**, white to very pale grey, crumbly with low moisture, minor yellow brown staining.	
	2.0 - 3.5	**CLAY**, calcareous, white to very pale grey, moist.	Dol 90%, Paly 8%
	3.5 - 5.0	**CLAY**, very pale yellowish grey, moist plastic smooth with some small yellowish patches.	Dol 86%, Paly 10% Dol 80%, Paly 14%
	5.0 - 6.0	**CLAY,** very pale grey, smooth, plastic. WATER CUT. Flights pulled and cleaned.	Dol 74%, Paly 24%
	6.0 - 7.0	**CLAY**, grey green to grey with minor yellow orange patches, smooth, plastic.	Illite/Paly >95%.
	7.0 - 7.5	**CLAY**, dark grey green, smooth plastic with yellow orange to orange Fe oxide patches.	
		EOH 7.5m. Logged JLK 21 March 1991.	
P34	0.0 - 0.4	**GYPSUM** sand (F-M), mod CLAYEY, pale orange brown.	
	0.4 - 1.0	**CLAY,** white, dry, with minor yellow brown Fe oxide staining.	
	1.0 - 2.0	**CLAY**, white to very pale grey, to very pale yellow, dry, becoming slightly moist at 2.0m.	Dol 64%, Paly 28%
	2.0 - 3.0	**CLAY**, white to very pale grey, moist.	Dol 67%, Paly 27%
	3.0 - 4.0	**CLAY**, very pale greenish yellow, moist, slightly plastic. WATER CUT at ~3.8m.	Dol 54%, Paly 43%
	4.0 - 5.0	**CLAY**, white to very pale yellow, becoming pale greenish grey below 4.5m, mod. plastic.	Dol 70%, Paly/Illite 19%
	5.0 - 6.0	**CLAY**, very pale greenish yellow to very pale yellow, moist, plastic.	Dol 67%, Paly 29%
	6.0 - 6.5	**CLAY**, dark greenish grey with some orange brown patches, moist.	Dol 75%, Paly/Illite 21%
	6.5 - 7.5	**CLAY**, very pale yellow grey to pale pink, mod. plastic.	
		EOH 7.5m. Logged JLK 24 March 1991.	

Hole No	Sample interval (m)	Description	Mineralogy
P35	0.0 - 1.5	**SILT**, mod. SANDY (VF-M), gypsum orange brown.	
	1.5 - 2.0	**CLAY**, very pale orange brown, with minor quartz grains (M) and some coarse clear gypsum crystals.	
	2.0 - 3.0	**CLAY**, white to very pale grey, dry and hard with some quartz grains (M-VC).	Dol 67%, Paly 31%
	3.0 - 4.0	**CLAY**, white to very pale yellow, dry, clean.	Dol 70%, Paly 26%
	4.0 - 5.0	**CLAY**, pale grey green, dry to moist with pale yellow clay interbeds.	Dol 72%, Paly 26%
	5.0 - 6.0	**CLAY**, white to pale brown with thin dark grey green bands, moist.	Dol 58%, Paly 37%
	6.0 - 7.0	**CLAY**, white to pale yellowish grey with minor thin greyish bands, very moist, plastic. WATER CUT at ~6.0m.	Dol 45%, Paly 52%
	7.0 - 8.0	**CLAY**, white to pale greyish yellow with bands of dark greenish grey clay, moist, plastic.	Dol 31%, Paly/Illite 66%
	8.0 - 9.0	CLAY, white with pale yellow to orange brown patches of Fe oxides, plastic , stiff.	Dol 50%, Paly 48%
		EOH 9.0m. Logged JLK 24 March 1991.	
P36	0.0 - 1.0	**SILT**, gypsum, very pale orange brown with 10-20% quartz GRAVEL (F) and SAND (VC).	
	1.0 - 2.0	**SILT**, mod. SANDY (VF-F) pale orange brown gypsum.	
	2.0 - 3.0	**SILT**, mod. CLAYEY with sand sized gypsum crystals.	
	3.0 - 4.0	**CLAY**, pale grey to orange brown, minor quartz grains.	Dol 76%, Paly 21%
	4.0 - 5.0	**CLAY**, white to very pale grey, smooth with minor quartz sand (M-C), difficult sample return, water added.	Dol 72%, Paly 25%
	5.0 - 6.0	**CLAY**, white to very pale grey, slightly SANDY (F-C), mod. plastic.	Dol 82%, Paly 7%, Qtz 8%
	6.0 - 8.0	**CLAY**, white to very pale grey, slightly SANDY (F-C), mod. plastic, some grey-green bands.	Dol 66%, Paly 23%, Qtz 9%.
	8.0 - 9.0	**CLAY**, white to very pale yellow, mod. plastic with minor sandy interbeds.	Dol 71%, Paly 21%, Qtz 7%.
		EOH 9.0m. Logged JLK 24 March 1991.	

Hole No	Sample interval (m)	Description	Mineralogy
P37	0.0 - 1.0	**CLAY**, white to very pale greyish yellow, dry.	
	1.0 - 2.0	**CLAY**, very pale yellow, dry and powdery.	Dol 79%, Paly 13%
	2.0 - 3.0	**CLAY**, very pale yellow, grey and white, dry to slightly moist.	Dol 76%, Paly 10%, Qtz 10%
	3.0 - 4.0	**CLAY**, white, plastic, stiff, minor quartz sand (M-C). WATER CUT at ~3.0m.	Dol 52%, Paly 44%
	4.0 - 5.0	**CLAY**, greenish grey, plastic smooth.	Dol 48%, Paly 47%
	5.0 - 6.0	**CLAY**, white to very pale grey with greenish grey bands.	Dol 65%, Paly 30%
	6.0 - 7.5	**CLAY**, greenish grey becoming red brown with depth, smooth, plastic, no grit.	Dol 63%, Paly 33%, Dol 13%, Illite/Paly 82%
		EOH 7.5m. Logged JLK 24 March 1991.	
P38	0.0 - 1.0	**CLAY**, white to pale greenish grey, dry and powdery.	
	1.0 - 2.0	**CLAY**, white to very pale yellow with gypsum crystals, dry.	Dol 72%, Paly 26%
	2.0 - 3.0	**CLAY**, white to very pale greenish grey, moist smooth and mod. plastic. Very minor yellow brown patches.	
	3.0 - 4.0	**CLAY**, white to very pale yellowish grey, mod. plastic.	Dol 51%, Paly 40%
	4.0 - 5.0	**CLAY**, white to very pale greenish yellow with minor yellow brown patches.	Dol 66%, Paly 30%
	5.0 - 5.5	**CLAY**, pale greenish grey.	Dol 66%, Paly/Illite 30%
	5.5 - 6.3	**CLAY**, pale yellow grey to dark greenish grey.	
		EOH 6.3m. Logged JLK 24 March 1991.	

Hole No	Sample interval (m)	Description	Mineralogy
P42	0.0 - 0.3	**SAND** (F-M), gypsum, orange brown to red brown.	
	0.3 - 1.0	**CLAY**, white to very pale yellowish grey, dry.	Dol 40%, Paly 40%, Qtz 10%, Tr Halite
	1.0 - 2.0	**CLAY**, white to very pale grey, dry and crumbly or slightly moist. Fe oxides as yellow orange stringers.	Dol 75%, Paly 10%, Tr Qtz, Halite
	2.0 - 3.0	**CLAY**, very pale grey, slightly moist, crumbly.	Dol 50%, Paly/Illite 30%, Qtz 10%, Tr Halite, Celes
	3.0 - 5.0	**CLAY**, pale yellowish grey, moist, mod. plastic with rare quartz grains (C).	Dol 40%, Paly/Illite 40%, Tr Qtz, Halite, Celes
	5.0 - 6.0	**CLAY**, very pale yellowish grey to very pale greenish grey, soft, smooth and plastic but very sticky. WATER CUT.	Dol 50%, Illite/Paly 40%, Tr Halite, Qtz, Kaolin, Celes
	6.0 - 7.0	**CLAY**, dark greenish grey with some orange brown patches, plastic.	Paly/Illite 40%, Dol 40%, Qtz 10%, Tr Halite, Celes
	7.0 - 8.0	**CLAY**, greenish grey, becoming dark grey with depth, stiff, plastic.	Paly/Illite 40%, Kaolin 40%, Dol 10%, Qtz, Tr Halite, Anatase
	8.0 - 9.0	**CLAY**, dark grey, smooth and plastic, very stiff.	Qtz 30%, Kaolin 30%, Paly 20%, Dol 10%, Tr Halite, Anatase
		EOH 9.0m. Logged JLK 25 March 1991.	

Dol = dolomite; Kaolin = kaolinite; Paly = palygorskite; Qtz = quartz; Tr = trace; EOH = end of hole; JLK = John L. Keeling.

Maralinga palygorskite

In the Maralinga area, clays of equivalent age to the Garford Formation are a potential source of sealing material for pits proposed for burial of radioactively-contaminated soils. Green and grey clays were intersected during drilling in the Taranaki Site (Morris and Walker, 1993). As part of the engineering investigations, chemical analyses (but not the mineralogy) of the clays were determined by AMDEL. Samples from 5 holes (T3R, T4R, T5R, T9R and T13R) and pit sample TN2 were selected for mineralogical investigation as part of this project.

Reference materials

Several "reference materials" were selected so that the properties of Garford and Maralinga palygorskite could be compared with the properties of well characterised palygorskites and an illite. These reference materials included palygorskite from Lake Nerramyne, Western Australia (Rakich, 1990); O'Laddie, South Australia (see Oodlawirra Palygorskite Deposit, Olliver and Carr, 1977); Attapulgus, Georgia, USA (Bradley, 1940); Torrejon, Caceres, Spain (Galan *et al.*, 1975) and illite from Muloorina, South Australia (as described elsewhere in this report).

Experimental

Mineralogy (XRD)

A small portion of each sample, dried at 105°C, was crushed in an agate mortar and pestle with the resulting fine powders pressed into aluminium sample holders for XRD analysis. XRD patterns were recorded with a Philips PW1800 microprocessor-controlled diffractometer using CoKα radiation, variable divergence slit and a graphite monochromator. Diffraction patterns were recorded in steps of 0.05°2θ with a 1 second counting time per step. The data were logged to permanent files on an IBM PC for analysis (Raven, 1990). Estimates of abundance of non-clay minerals were determined by comparing peak intensities of samples with known concentrations with peak intensities of the unknown samples. Clay mineral contents were determined by difference.

Chemistry

The chemistry of selected samples was determined by XRF. Preparation of samples involved the 'grab' weight method, which comprised accurately weighing 0.28 g of finely ground powders into glass vials with 1.5 g of Norrish/Hutton lithium tetraborate and lanthanum oxide flux. The mixture was then fused into a Pt-Au crucible over an oxy-propane flame at approximately 1050°C and the molten material quench-pressed into a glass disk between a graphite mould and an aluminium plunger. The resulting glass disks were

analysed on a Philips PW1480 XRF system using a control program developed by Philips and algorithms developed by K. Norrish and P. Fazey (CSIRO, Division of Soils - personal communication).

Differential thermal analysis (DTA) and thermogravimetric analysis (TGA)

Two Garford clay samples (P25, 4-5m and P42, 1-2m) were analysed by DTA and TGA. Approximately 10 mg of sample were heated in Pt crucibles at 10°C/min under both static air and flowing nitrogen atmosphere from ambient to 1000°C using a Rigaku TG-DTA infrared heating apparatus (Thermoflex 8100 series).

Scanning electron microscopy

Small fragments of bulk samples were mounted on aluminium stubs using 'Araldite' and coated with a 30-60 nm film of gold. Specimens were examined using a Cambridge Stereoscan S250 SEM fitted with an energy dispersive x-ray (EDX) analyser. Three Garford Formation clay samples from drill holes P25, P34 and P42 were examined together with samples of "untreated" ore from Lake Nerramyne.

Results

Garford palygorskite

The mineralogy of the bulk samples from the Garford Palaeochannel (Table 11) showed mixtures of palygorskite with dolomite or illite. Palygorskite content ranged from minor to co-dominant. Minor to trace levels of quartz, halite, kaolin, anatase and celestine were also present. Selected diffraction patterns are shown in Fig. 33. A key feature of the mineralogy is the presence of illite in association with palygorskite (e.g. samples P25 and P42). Samples containing illite usually have a greenish colour. Illite has not been reported in previous studies presumably because XRD reflections from the basal planes of illite are overlapped by palygorskite reflections (Fig. 34). The content of illite in Garford palygorskite is discussed in more detail in a later section of this report.

Results of XRF major element analyses is presented in Table 12 together with chemical analyses of palygorskite from the Attapulgus Deposit, Georgia; the Torrejon Deposit, Caceres, Spain and Lake Nerramyne, Western Australia.

Table 12. Whole sample major element XRF analysis results (wt%) for selected Garford and reference palygorskites (Garford samples dried at 105°C)

	P25 4-5m	P34 3-4m	P42 1-2m	Lake Nerramyne	Georgia*	Spain**
SiO_2	52.5	59.8	65.6	61.0	55.03	51.50
TiO_2	0.55	0.58	0.65	0.80		
Al_2O_3	13.99	11.27	11.01	14.79	10.24	10.03
Fe_2O_3	5.89	4.98	3.05	4.94	3.53	2.36
MnO	0.017	0.030	0.004	0.014		
MgO	5.45	7.4	7.5	4.39	10.49	12.28
CaO	0.64	0.093	0.087	0.137		1.81
Na_2O	4.7	0.23	0.20	1.1		0.12
K_2O	3.76	1.89	1.01	2.05	0.47	0.13
P_2O_5	0.035	0.009	0.006	0.005		
SO_3	1.04	0.087	0.044	0.166		
ZrO_2	0.014	0.023	0.027	0.025		
Sr	0.120	0.002	0.002	0.005		
LOI	11.3	13.6	10.8	10.5	10.13	14.43

* - Attapulgus, Georgia, USA (Bradley, 1940)
** - Torrejon, Caceres, Spain (Galan *et al.*, 1975)

The DTA curve for P25(4-5m) shows a significant endothermic peak at 80-90°C together with a significant weight loss (Fig. 35a), due to the loss of adsorbed water. A second endothermic peak was recorded between 200-280°C, due to the loss of zeolitic water. A significant endothermic peak was recorded between 320-580°C which is the result of loss of structurally bound water, that causes the structure to fold (Serna *et al.*, 1975). A exothermic peak was recorded at 870°C, which is possibly due to the formation of clinoenstatite (Jones and Galan, 1989).

The DTA curve for P42 (1-2m) shows 2 endothermic peaks at 80°C and 120°C, and an endothermic peak at 220°C. These peaks resulted from the loss of adsorbed and zeolitic water in the palygorskite and decomposition of carbonate ions associated with magnesium in dolomite. There was only minor weight loss (Fig. 35b). A significant endothermic peak was recorded at approximately 600°C, which was possibly due to the decomposition of ions associated with calcium in dolomite. This was accompanied by a significant weight loss between 380-700°C (Fig. 35).

SEM examination of Garford samples showed the following morphological features:

- P25(4-5m) comprised oriented, compact mats composed of illite platelets 0.2 to 0.4 μm in diameter (Fig. 36a). Palygorskite fibres up to 1 μm in length appeared to be randomly interspersed amongst the illite platelets.
- P34(3-4m) (Fig. 36b) contained subrounded dolomite grains, 2 to 8 μm in diameter, coated by tightly-packed palygorskite fibres of average length 1 μm and diameter 0.1 μm. Palygorskite fibres also infill between dolomite grains.
- P42(1-2m) (Fig. 36c) comprised a high proportion of dolomite as subrounded grains, 2 - 5 μm in diameter, variably coated by palygorskite fibres. Palygorskite varied from short stumpy fibres < 0.2 μm in length to fibres of 1 μm length.
- The Lake Nerramyne sample (Fig. 36d) comprised interwoven mats of palygorskite fibres averaging 1.5 μm in length and between 0.08 to 0.14 μm in diameter. Individual fibres were up to 4 μm in length. By comparison, palygorskite from Lake Nerramyne showed a higher aspect ratio and overall greater fibre length and were more interwoven than palygorskite from Garford Palaeochannel.

Maralinga

Drillhole logs and chemical analyses reported in Morris and Walker (1993) are summarised in Tables 13 and 14 respectively. Mineralogical results are summarised in Table 15 and were estimated from XRD traces given in Figs. 37(a-f).

All holes examined penetrated profiles with high carbonate content with variable amounts of calcite and dolomite. Clay intersected at 3.6 - 5.0 m in T4R was a mixed illite/ palygorskite with illite dominant. An indurated clay in T5R at 2.8 - 3.4 m had a higher palygorskite to illite content but was siliceous. Clay recorded in T9R was mixed palygorskite/ illite but calcite and silica contents were high. In hole T13R, the clayey interval 2.4 - 4.6 m was high in dolomite together with illite/palygorskite. Samples were not available for the interval 4.6 - 5.0 m but chemical analyses indicate that clay content increases significantly below 4.6 m. Clay from pit sample TN2 (sample reference M316), had a high clay content that was again a mixed palygorskite/illite.

Mixed palygorskite/illite clays may form a suitable sealing material if compacted at the correct moisture content. The clays do not show high shrinkage and swelling associated with smectite group clays. Samples from the Taranaki site were very variable in silica and carbonate contents and there may be difficulty in recovering substantial quantities of clay with consistent properties.

Table 13. Logs of reverse circulation drillholes (Morris and Walker, 1993)

Hole	Depth (m)	Description
T3R	0.0-0.4	ROAD FILL, gravelly sand, brown.
	0.4-1.2	CALCRETE, lt brown, MS-S.
	1.2-1.6	LIMESTONE, grey to brown, strong.
	1.6-1.8	LIMESTONE, grey to brown, strong, qtz as f-m sand, rounded.
	1.8-2.0	LIMESTONE, grey to brown, strong, sand matrix to calc. clasts..
	2.0-3.6	LIMESTONE, grey to brown, strong.
	3.6-3.8	LIMESTONE, lt grey.
	3.8-5.0	LIMESTONE, grey to brown, strong.
T4R	0.0-0.4	ROAD FILL, calcrete gravel and fine to med. sand.
	0.4-1.2	CALCRETE, light brown.
	1.2-1.4	CARBONATES, predominantly calcite.
	1.4-3.6	CARBONATES predominantly dolomite as large light grey clasts in sandy matrix, quartz, fine - med. grained, subrounded.
	3.6-5.0	CLAY, dark greenish grey, moderately plastic.
T5R	0.0-0.4	ROAD FILL
	0.4-0.8	CALCRETE, lt. brown, MW-MS, plus qtz sand, med. grn., rounded.
	0.8-1.0	CALCRETE as above with clay, greenish brown, indurated.
	1.0-1.2	CALCRETE as above but qtz sand is fine, rounded.
	1.2-1.6	CALCRETE, lt. brown, MW-MS, plus qtz sand, med. grn., rounded.
	1.6-1.8	CALCRETE as above, calcrete lt grey to lt brown.
	1.8-2.6	CALCRETE, lt. brown, MW-MS, plus qtz sand, med. grn., rounded.
	2.6-2.8	CALCRETE as above with clay.
	2.8-3.4	CLAY, dark grey, indurated.
	3.4-5.0	DOLOMITE, lt. yellow, mauve, VS plus CLAY as above.
T9R	0.0-0.4	ROAD FILL, calcrete, lt. brown and sand, qtz, f-m.
	0.4-0.8	CALCRETE and sand.
	0.8-1.0	SAND, qtz, medium to fine grn., rounded.
	1.0-1.6	CALCRETE, lt. brown, nodular, MS-S.
	1.6-1.8	CALCRETE as above, with clay as black clasts to 3 mm.
	1.8-3.0	CALCRETE, lt. brown, nodular, MS-S.
	3.0-4.4	CALCRETE, brown to lt. green, S, with clay as green specks and clasts.
	4.4-4.6	CLAY, green, silty, dolomitic.
	4.6-4.8	CLAY, green, silty, dolomitic, with limestone, grey (60%).
	4.8-4.9	LIMESTONE and clay, as above.
T13R	0.0-0.4	ROAD FILL.
	0.4-2.2	CALCRETE, lt. brown, W-MS.
	2.2-3.0	CLAY, lt. grey, mod. plastic, plus calcrete.
	3.0-4.8	CLAY as above, mod. to high plasticity.
	4.8- 5.0	CLAY, dark green, very high plasticity.

Table 14. XRF of Maralinga samples (from Morris and Walker, 1993)

Hole	Depth	Sample no	SiO_2	Al_2O_3	MgO	CaO	LOI	CO_2	$MgCO_3$	$CaCO_3$	Total Carb-onates
T3R	2.8-3.6	M237	28.0	4.65	7.2	26.8	29.6	27.2	11	49	60
	3.6-4.2	M238	30.5	5.41	7.97	24	28	25.2	12	43	55
	4.2-5.0	M239	32.5	5.04	13.4	20.8	32.5	27.2	20	38	58
T4R	3.6-4.2	M246	40.0	11.3	4.67	15.4	29.9	14.4	6	25	32
	4.2-4.6	M247	39.1	11.3	4.48	14.5	17.3	12.8	6	22	28
	4.6-5.0	M248	50.4	13.4	5.16	3.39	16.7	3.5	4	3	7
T5R	2.2-2.6	M255	29.5	5.62	6.14	25.7	26.3	22.6	8	41	50
	2.6-2.8	M256	42	9.08	5.78	13.8	17.6	13.4	8	21	29
	2.8-3.0	M257	54.3	11.6	5.82	0.87	8.63	1.55	3	0	3
	3.0-3.4	M258	53.2	11.5	4.93	0.418	7.38	0.7	1	0	1
T9R	3.0-3.6	M130	24.4	3.49	1.2	36.2	31.4	28	2	62	63
	3.6-4.4	M131	27.5	4.5	1.95	29.9	29.7	22.8	3	49	51
	4.4-5.0	M132	35.5	5.66	2.3	22.3	26.4	18.4	3	38	41
T13R	2.2-3.4	M189	20	3.89	14.4	24.4	34.1	31.4	22	45	67
	3.4-4.6	M190	22.5	7.04	14.7	19.1	31.1	28.6	24	37	61
	4.6-4.8	M191	52.1	17.5	6.11	1.22	8.52	1.95	3	1	4
	4.8-5.0	M192	51.9	18.1	5.3	0.577	8.42	0.35	1	0	1

Table 15. Mineralogy of five drill holes at Maralinga

Hole	Depth	Sample no	Mineralogy
T3R	2.8-3.6	M237	Calcite (CD), dolomite (CD), quartz (M), illite (Tr), palygorskite (Tr)
	3.6-4.2	M238	Calcite (CD), dolomite (CD), quartz (M), illite (Tr), palygorskite (Tr)
	4.2-5.0	M239	Dolomite (D), quartz (M), calcite (Tr), illite (Tr), palygorskite (Tr)
T4R	3.6-4.2	M246	Calcite (D), quartz (SD), illite (SD), palygorskite (M), dolomite (M)
	4.2-4.6	M247	Calcite (D), illite (SD), quartz (M), palygorskite (M), dolomite (M)
	4.6-5.0	M248	Illite (D), palygorskite (SD), quartz (M), calcite (M), dolomite (Tr)
T5R	2.2-2.6	M255	Calcite (D), quartz (M), dolomite (M), illite (M), palygorskite (M)
	2.6-2.8	M256	Quartz (SD), calcite (SD), palygorskite (M), illite (M), dolomite (M)
	2.8-3.0	M257	Palygorskite (SD), illite (SD), quartz (SD), calcite (Tr), dolomite (Tr)
	3.0-3.4	M258	Palygorskite (CD), illite (CD), quartz (M), calcite (Tr), dolomite (Tr)
T9R	3.0-3.6	M130	Calcite (D), quartz (M), illite (Tr), palygorskite (Tr)
	3.6-4.4	M131	Calcite (D), quartz (SD), palygorskite (M), illite (Tr)
	4.4-5.0	M132	Calcite (D), quartz (SD), palygorskite (M), illite (M)
T13R	2.2-2.4	M177	Calcite (CD), dolomite (CD), quartz (M), palygorskite (Tr), illite (Tr),
	3.0-3.2	M181	Dolomite (D), palygorskite (Tr), illite (Tr), quartz (Tr), calcite (Tr)
	3.4-4.6	M190	Dolomite (D), illite (M), palygorskite (M), quartz (Tr)
Pit TN2		M316	Palygorskite (CD), illite (CD), calcite (M), quartz (M), dolomite (Tr)

D = dominant, CD = co-dominant, SD = sub-dominant, M = minor, Tr = trace.

Illite content and grain size of Garford clays

In order to determine the nature of illite in the Garford samples a high illite/palygorskite sample, P25(4-5m), was chosen for further study. A subsample of bulk cuttings from auger drillhole P25(4-5m) was lightly crushed in a large cast iron mortar, oven dried at 60°C, and then homogenised by repeatedly being passed through a stainless steel sample splitter. A 10 gm portion was dispersed in distilled water by shaking in a SPEX mill for 10 mins. The slurry was poured into a 400 ml beaker and ~150 mls of 1M NaCl added. This was left to stand for 2 hours and then, with the aid of centrifugation, repeatedly washed with deionised water to give a stable (non-flocculating) suspension. The suspension was transferred to a measuring cylinder and allowed to stand in a constant temperature room for 15 hours when the < 2 μm particles was drawn off from the top 20 cms of the cylinders. The < 2 μm fraction, obtained by gravity separation over 15 hours, was further divided using centrifugation into 2-0.5 μm, 0.5-0.2 μm, < 0.2 μm and < 0.02 μm fractions. The materials in each size range were then calcium saturated, carefully washed, dried at 105°C and weighed.

XRD and XRF analyses of each sample fraction were made using the same methods as described for the whole samples. Cation exchange capacities were determined by saturating with Ba.

Results

Table 16 gives the percentage weight fractions of particles in the various size ranges. XRD patterns from oriented specimens are shown in Fig. 38a. From the carefully prepared samples, X-ray reflections from 001 atomic planes of palygorskite (10.4 Å) and illite (10.0 Å) were readily resolved. The mineralogical compositions of the separate size fractions differed very little, although minor amounts of kaolinite and anatase were present in the > 2 μm and the 2-0.5 μm fractions. More importantly, each fraction was shown to comprise a mixture of palygorskite and illite, in an essentially fixed ratio.

Table 16. Summary of particle size distribution for Garford Palygorskite sample P25(4-5m)

Particle size range (μm)	Proportion (wt %)
> 2	27.1
2 - 0.5	14.7
0.5-0.2	25.0
< 0.2	33.2
< 0.02	nm

nm = not measurable

For reference purposes, the diffraction patterns of oriented samples of purified > 2 μm O'Laddie Palygorskite and Muloorina Illite were obtained; these patterns are given in Figs. 38b and 38c respectively.

In order to obtain an estimate of the amount of illite in the mixture, a reasonable assumption was made that the Garford illite was chemically similar to Muloorina illite. Both illite samples formed as chemical precipitates in palaeodrainage channels of Miocene age. By ratioing the K_2O contents of the sample from hole P25 and that of relatively pure Muloorina illite, an estimate of the composition of the mixture was made.

Table 17 shows the XRF analyses of the Garford clay (<0.2 μm fraction) and the Muloorina illite (< 2 μm fraction). The proportion of illite in the <0.2 μm fraction of Garford sample P25 4-5m is therefore = $\frac{5.1}{7.3}$ x 100 i.e. ~70%.

Table 17. XRF analyses of Garford clay P25(4-5m) (<0.2 μm fraction) and Muloorina Illite (< 2 μm fraction)

Sample	Fe_2O_3	MnO	TiO_2	CaO	K_2O	P_2O_5	SiO_2	Al_2O_3	MgO	BaO	Sum	CEC
Garford Clay	8	0.03	0.21	0.04	5.1	0.0	55	17	5.4	2.8	94	37
Muloorina Illite	13	0.04	0.54	0.06	7.3	0.1	52	17	4.1	1.3	95	18

Assuming that the chemical composition of Muloorina Illite approximates that of illite in the Garford Palaeochannel, then K_2O content could be used to estimate the proportion of illite present in other Garford samples. Alternatively, the results from Garford clay P25(4-5m) can be used as a calibration for the determination of illite content from the relative peak areas of XRD peaks from illite and palygorskite. The illite to palygorskite weight ratios for some Garford clays determined by comparing XRD peak areas standardised on sample P25(4-5m) are given in Table 18.

Table 18. Illite to palygorskite weight ratio in selected clays from the Garford Palaeochannel

Hole no	Sample interval (m)	Illite/paly
P25	0-1	0
	1-2	0.3
	2-3	1.3
	3-4	1.0
	4-5	2.3
	5-6	4.5
	6-7	1.9
	7-9	nr
P34		
	1-2	0.1
	2-3	0
	3-4	0.1
	4-5	0.5
	5-6	nr
	6-7	0.3

Hole no	Sample interval (m)	Illite/paly
P30	0-1	0
	1-2	0
	2-3	0.2
	3-4	1.2
	4-6	11.6
P42	0-1	0
	1-2	0
	2-3	0.1
	3-4	0.2
	4-5	0.2
	5-6	2.7
	6-7	1.8
	7-8	0.7
	8-9	nr

nr = not resolved.

FIGS. 33 TO 38

Fig. 33. Selected x-ray diffraction patterns of Garford Palaeochannel clays. a) Sample P25(4-5m) predominantly palygorskite and illite. b) Sample P42(3-4m) co-dominant dolomite and palygorskite-illite. c) Sample P26(2-3m) predominantly dolomite. For display purposes, muscovite 2M1 is used to approximate the x-ray pattern for illite.

Fig. 34. XRD pattern of Garford clay P25(4-5m) showing the overlap in palygorskite and illite reflections.

Fig. 35. DTA/TGA traces of two Garford clays: a) P25(4-5m) and b) P42(1-2m).

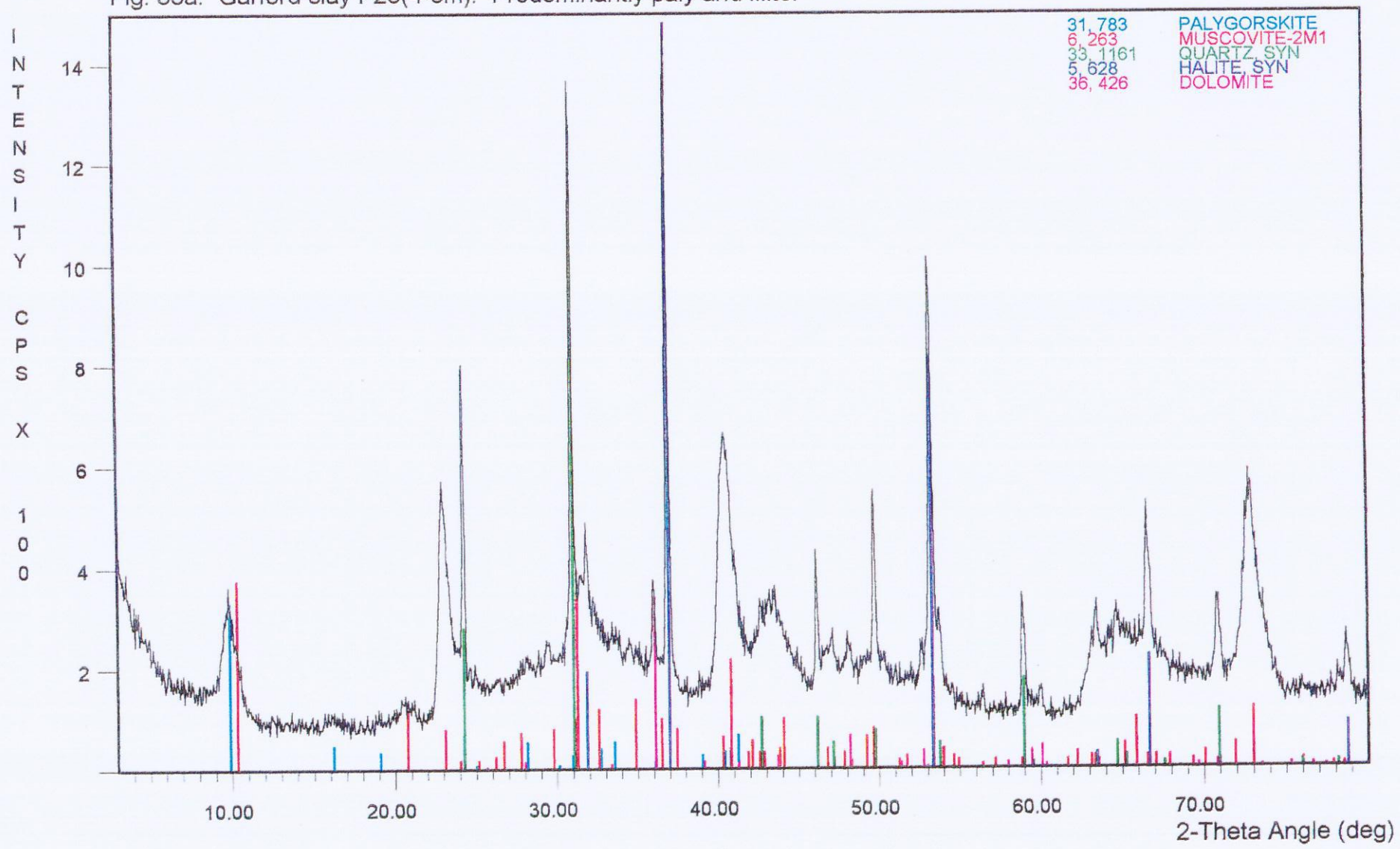
Fig. 36. SEM micrographs of Garford and Lake Nerramyne clays. a) P25(4-5m) (micrograph 1932), b) P34(3-4m) (micrograph 1935), c) P42(1-2m) (micrograph 1911) and d) Lake Nerramyne (micrograph 1918).

Fig. 37. XRD patterns of Maralinga clays. For display purposes, muscovite 2M1 is used to approximate the x-ray pattern for illite.

Fig. 38. XRD patterns of palygorskites and illites. a) Patterns from oriented samples from a range of size fractions separated from Garford clay P24(4-5m). b) O'Laddie palygorskite. c) Ba saturated Muloorina illite.

Fig. 33. Selected x-ray diffraction patterns of Garford Palaeochannel clays. a) Sample P25(4-5m) predominantly palygorskite and illite. b) Sample P42(3-4m) co-dominant dolomite and palygorskite-illite. c) Sample P26(2-3m) predominantly dolomite. For display purposes, muscovite 2M1 is used to approximate the x-ray pattern for illite.

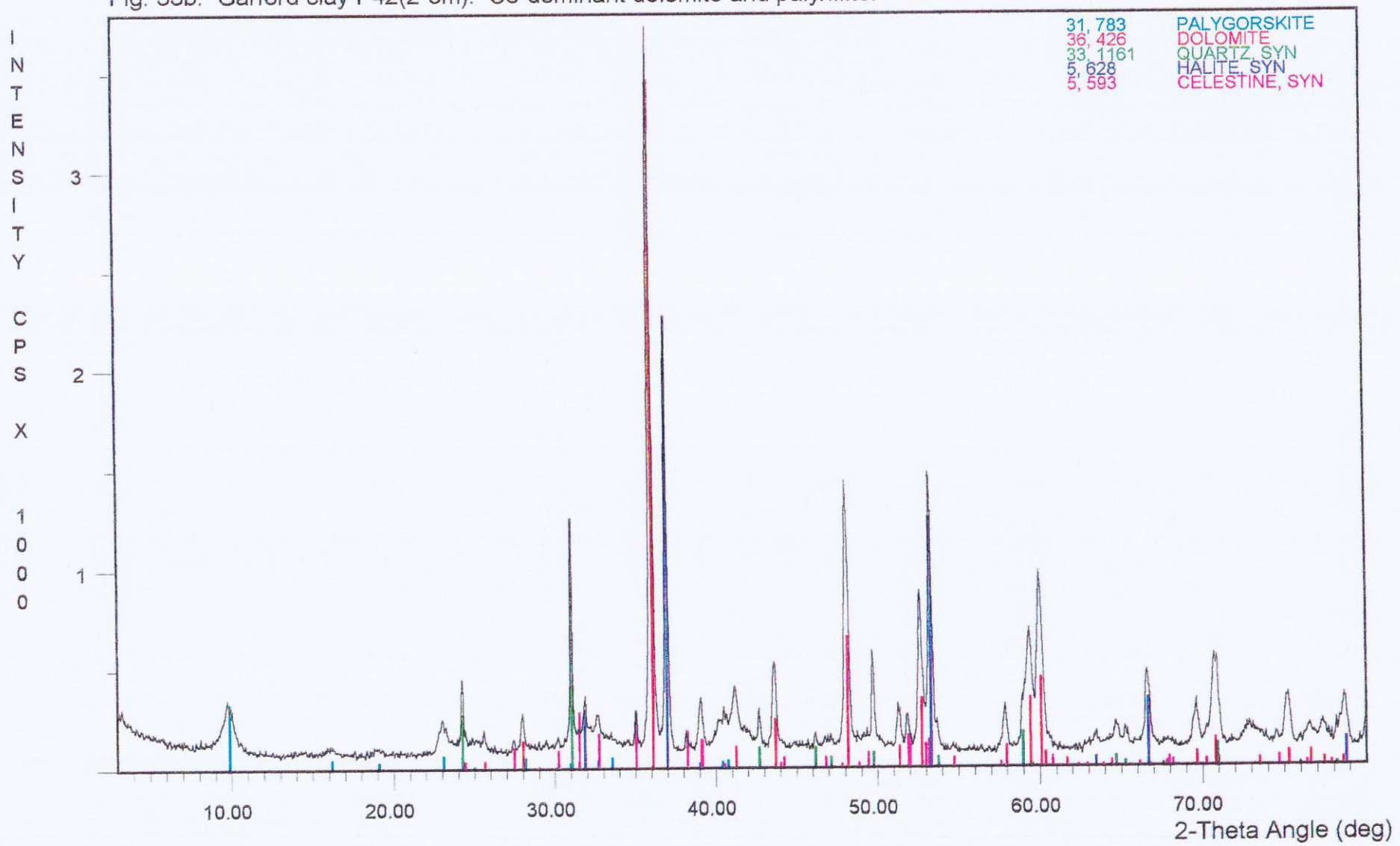
Fig. 33a. Garford clay P25(4-5m). Predominantly paly and illite.



File Name: A:\P254-5

0000093
87

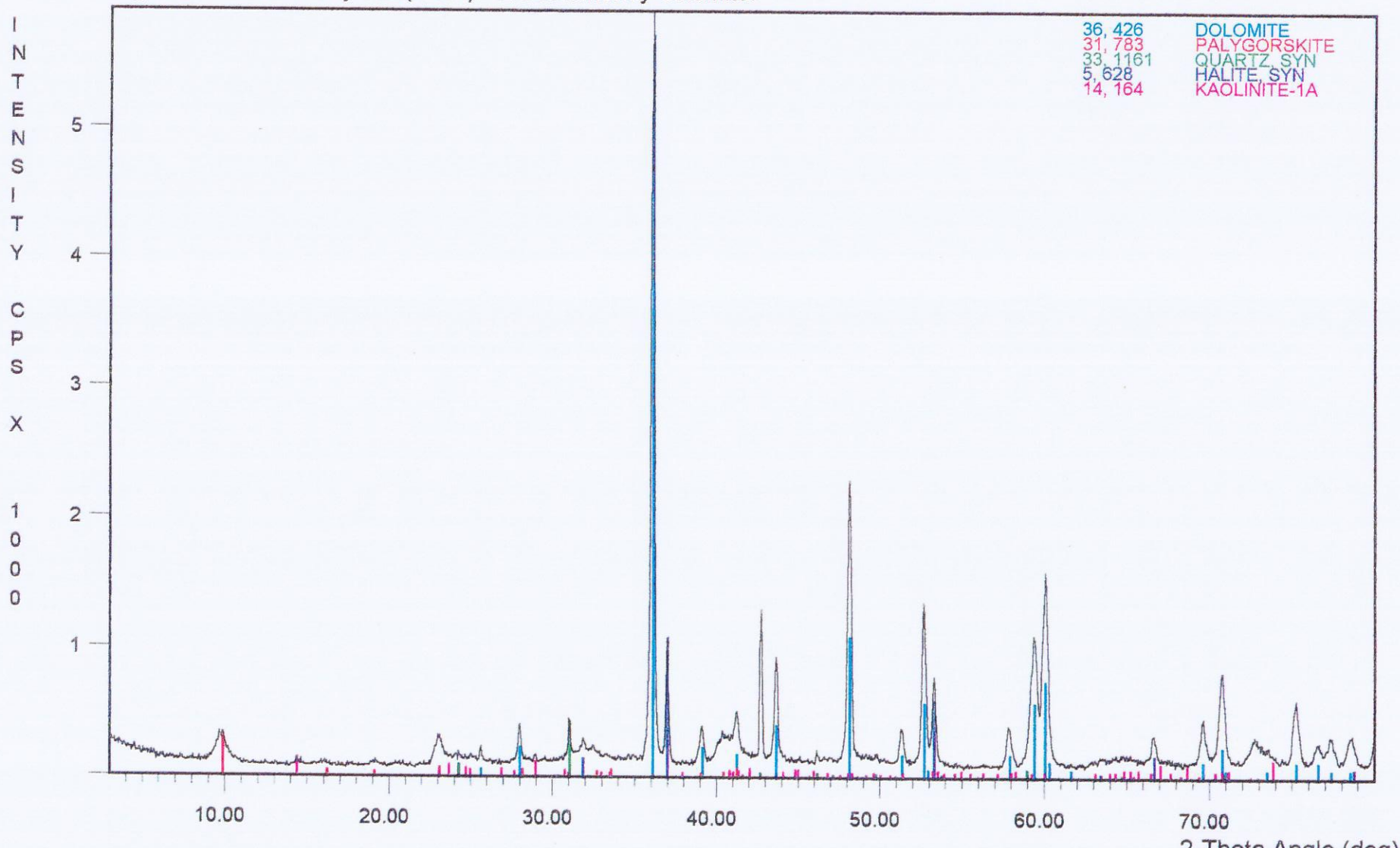
Fig. 33b. Garford clay P42(2-3m). Co-dominant dolomite and paly/illite.



File Name: A:\P423-4

0000094

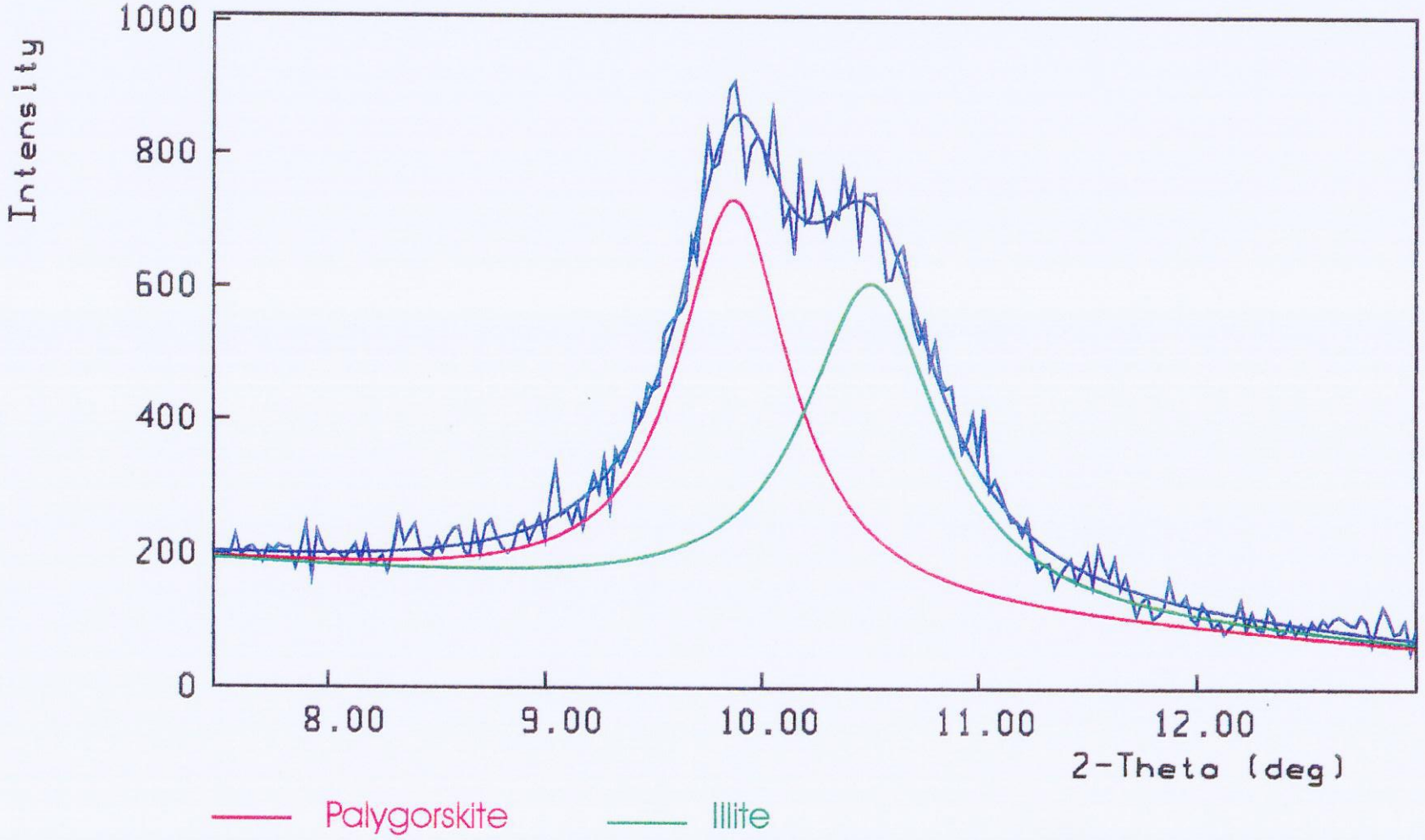
Fig. 33c. Garford clay P26(2-3m). Predominantly dolomite.



File Name: A:\P262-3.103

0000095

Fig. 34. XRD pattern of Garford clay P25(4-5m) showing the overlap in palygorskite and illite reflections.



0000096 90

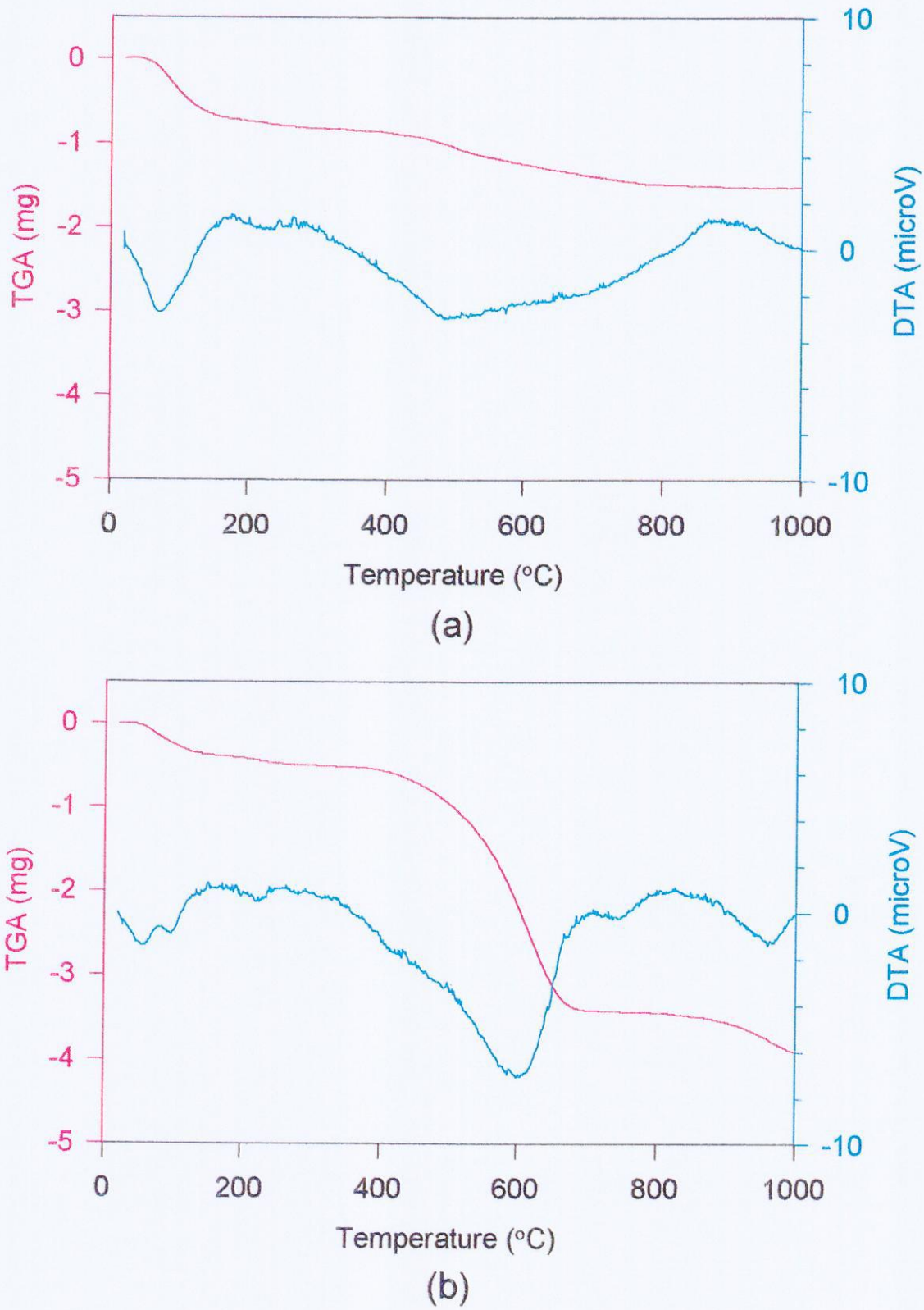
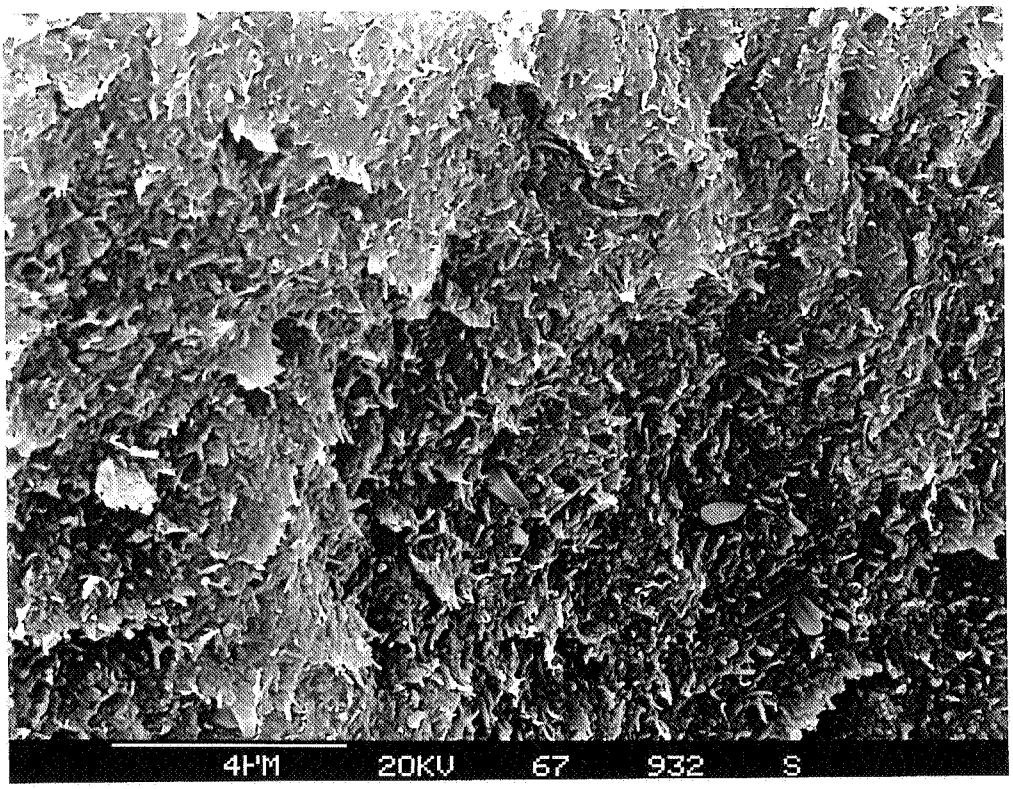
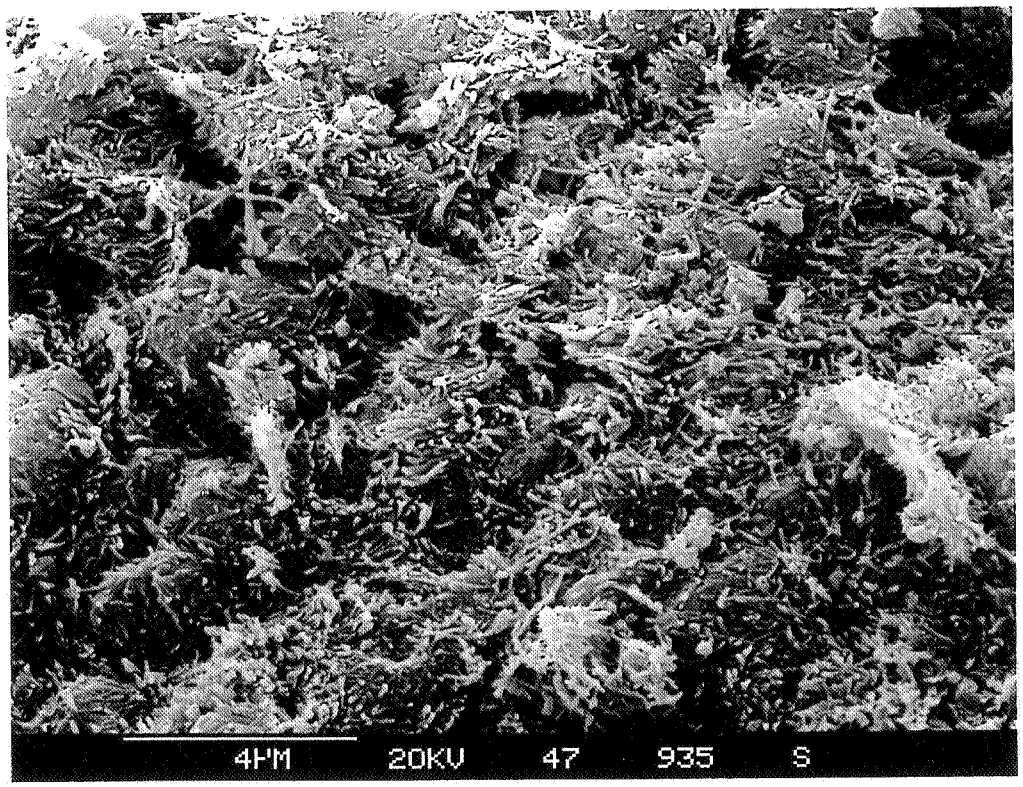


Fig. 35. DTA/TGA traces of two Garford clays: a) P25(4-5m) and b) P42(1-2m).

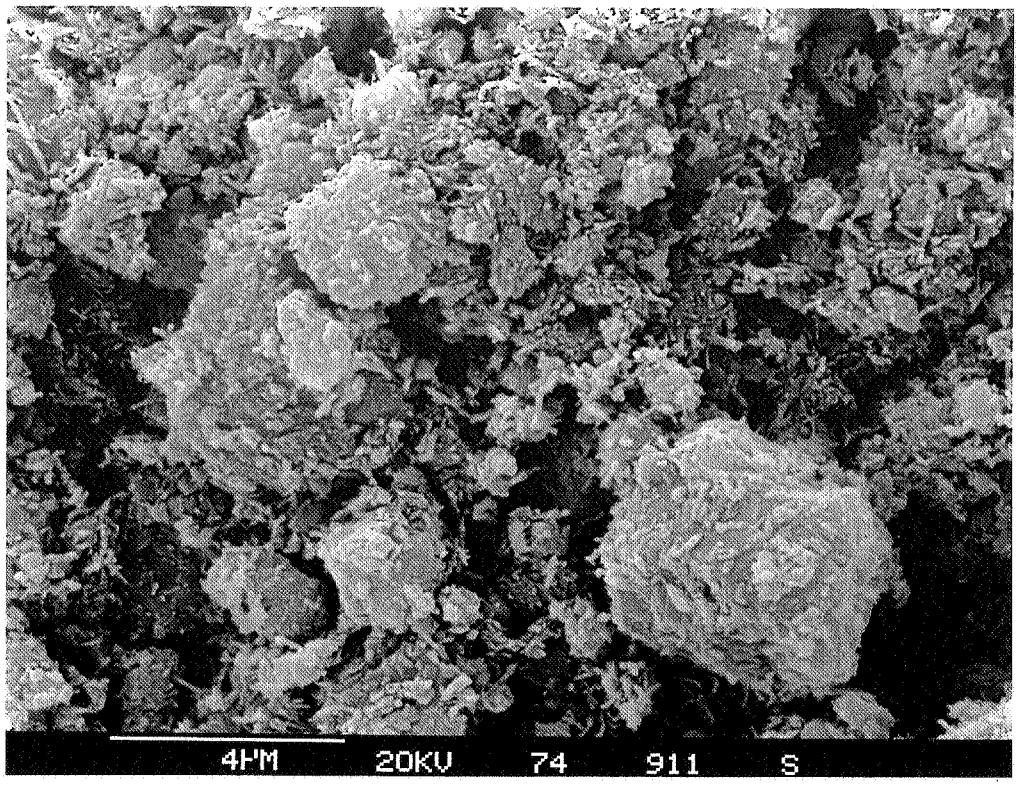
Fig. 36. SEM micrographs of Garford and Lake Nerramyne clays. a) P25(4-5m) (micrograph 1932), b) P34(3-4m) (micrograph 1935), c) P42(1-2m) (micrograph 1911) and d) Lake Nerramyne (micrograph 1918).



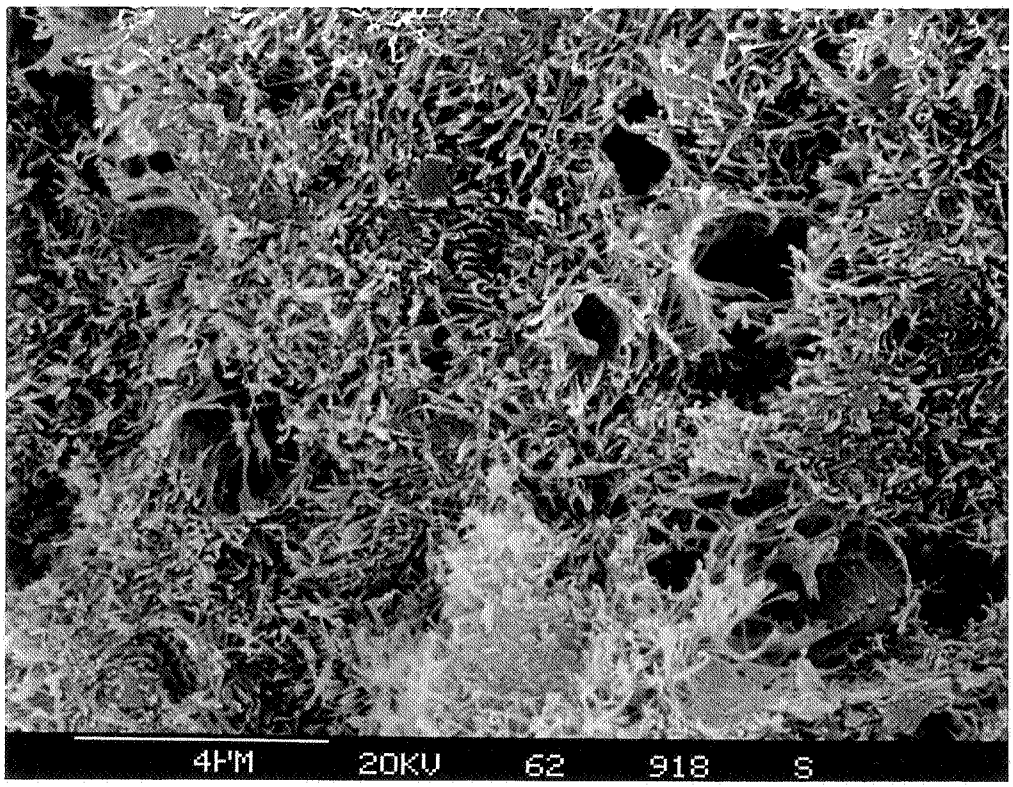
(a)



(b)



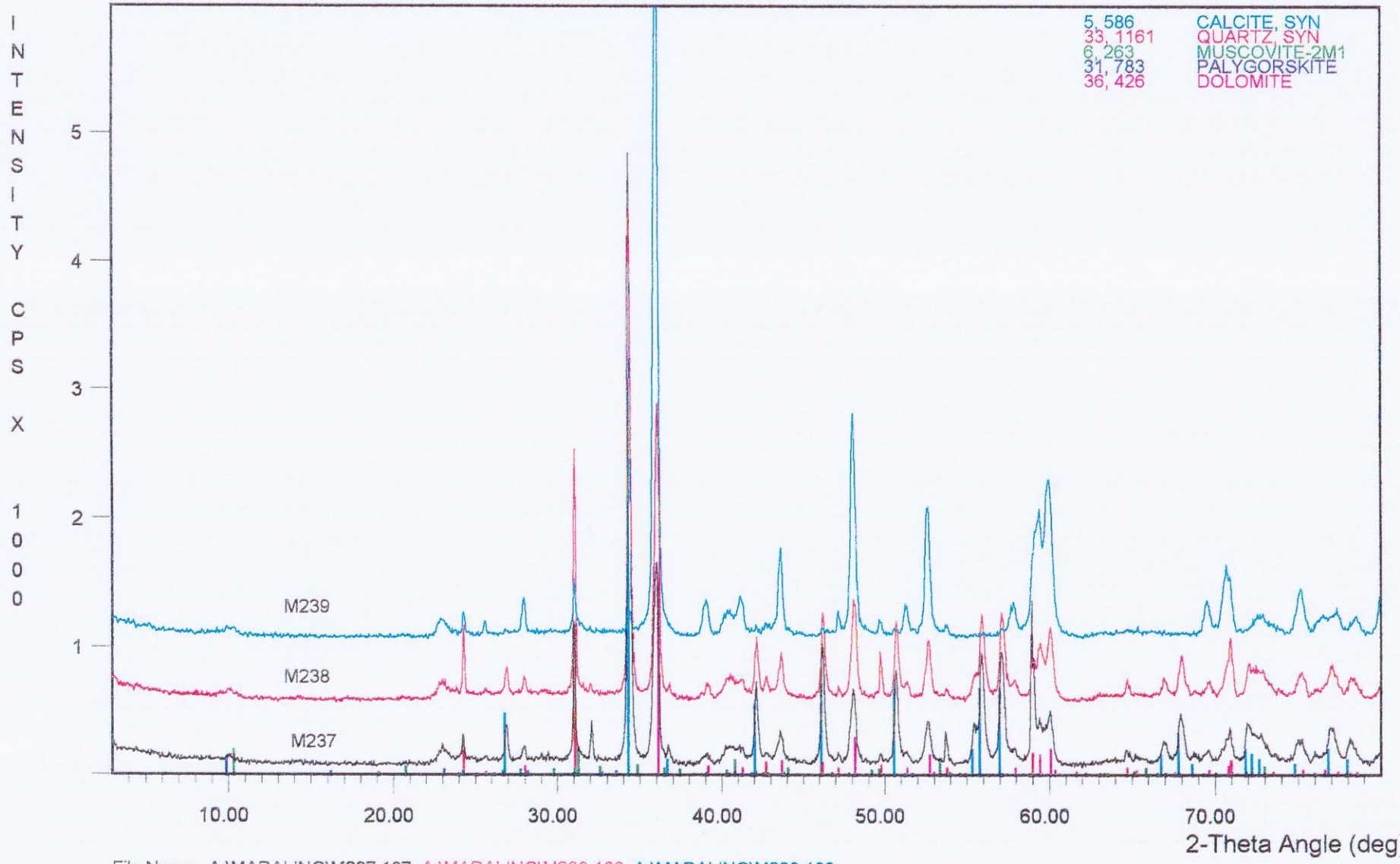
(c)



(d)

Fig. 37. XRD patterns of Maralinga clays. For display purposes, muscovite 2M1 is used to approximate the x-ray pattern for illite.

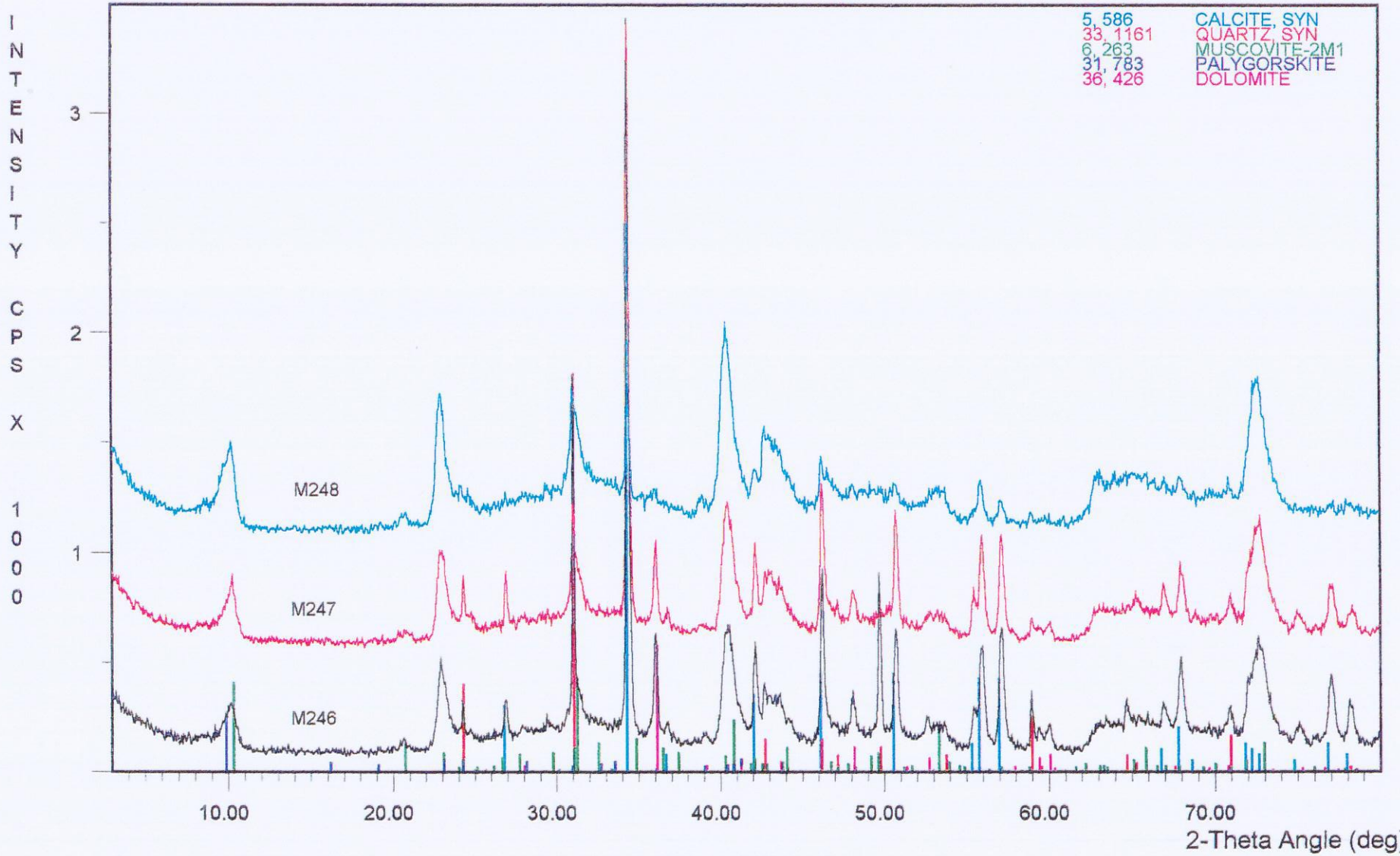
Fig. 37a. Maralinga clay samples M237, M238 and M239 from hole T3R.



File Name: A:\MARALING\M237.107 A:\MARALING\M238.108 A:\MARALING\M239.109

000102

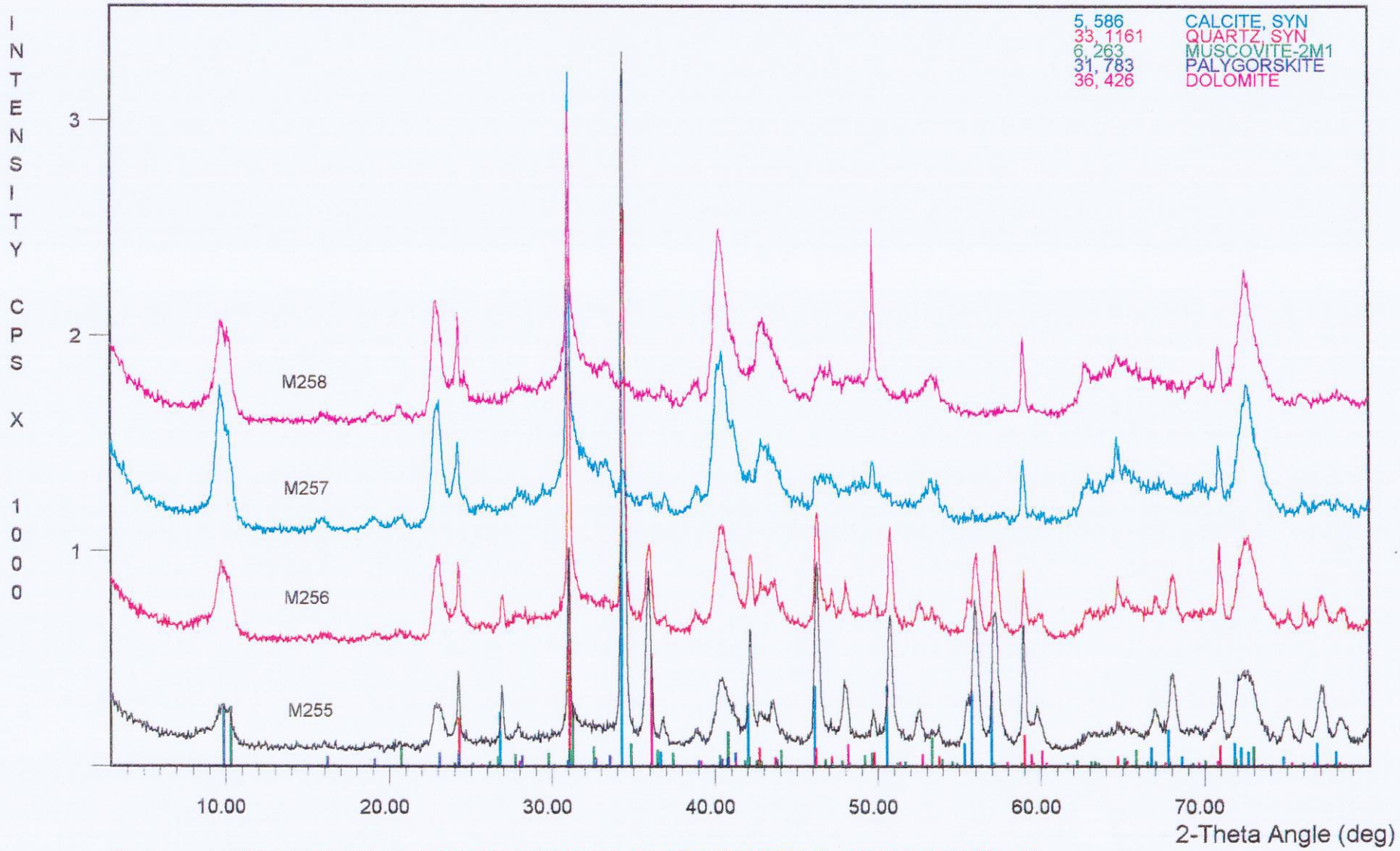
Fig. 37b. Maralinga clay samples M246, M247 and M248 from hole T4R.



File Name: A:\MARALING\M246.110 A:\MARALING\M247.111 A:\MARALING\M248.112

000103 97

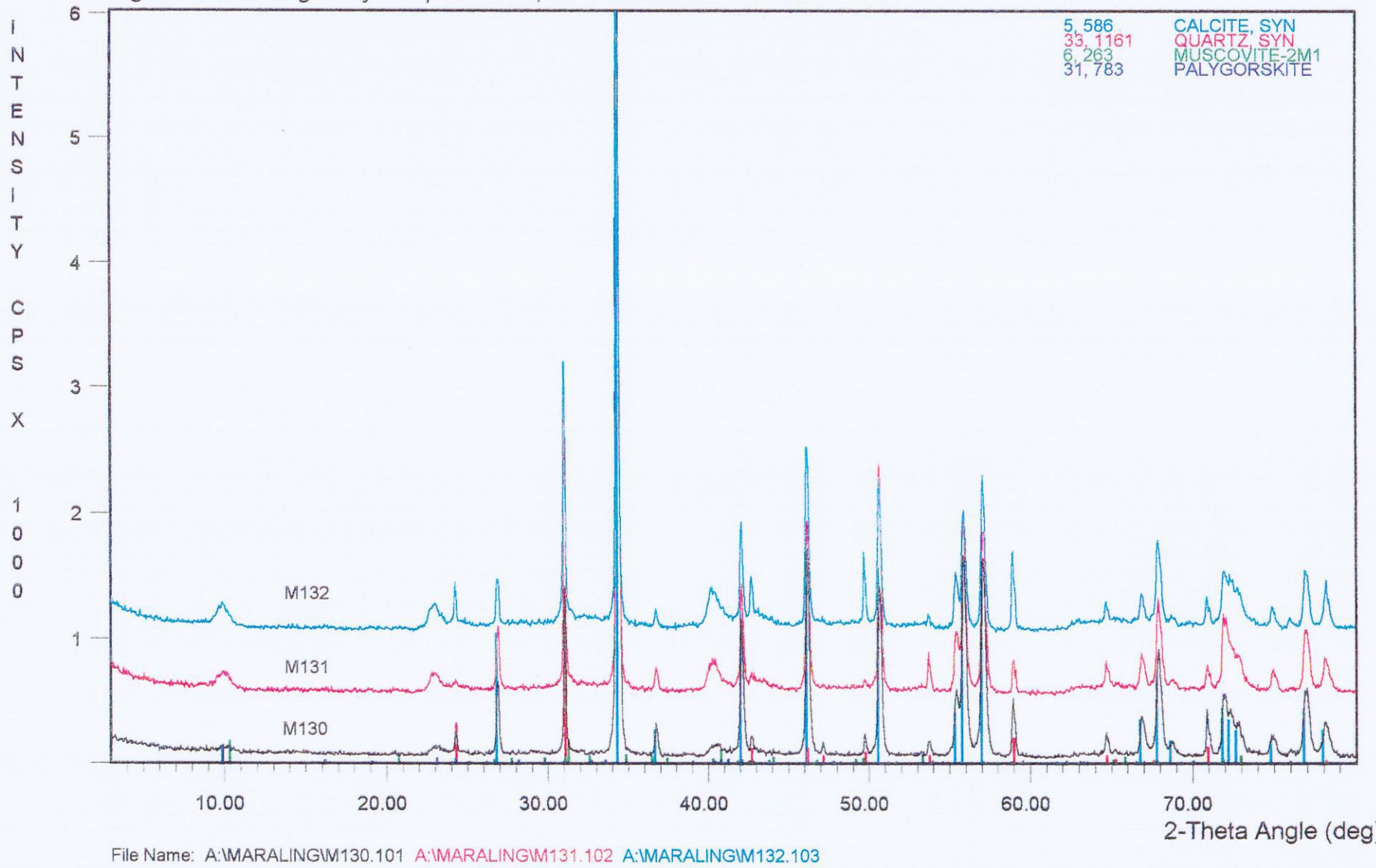
Fig. 37c. Maralinga clay samples M255, M256, M257 and M258 from hole T5R.



File Name: A:\MARALING\M255.113 A:\MARALING\M256.114 A:\MARALING\M257.115 A:\MARALING\M258.116

0001104
98

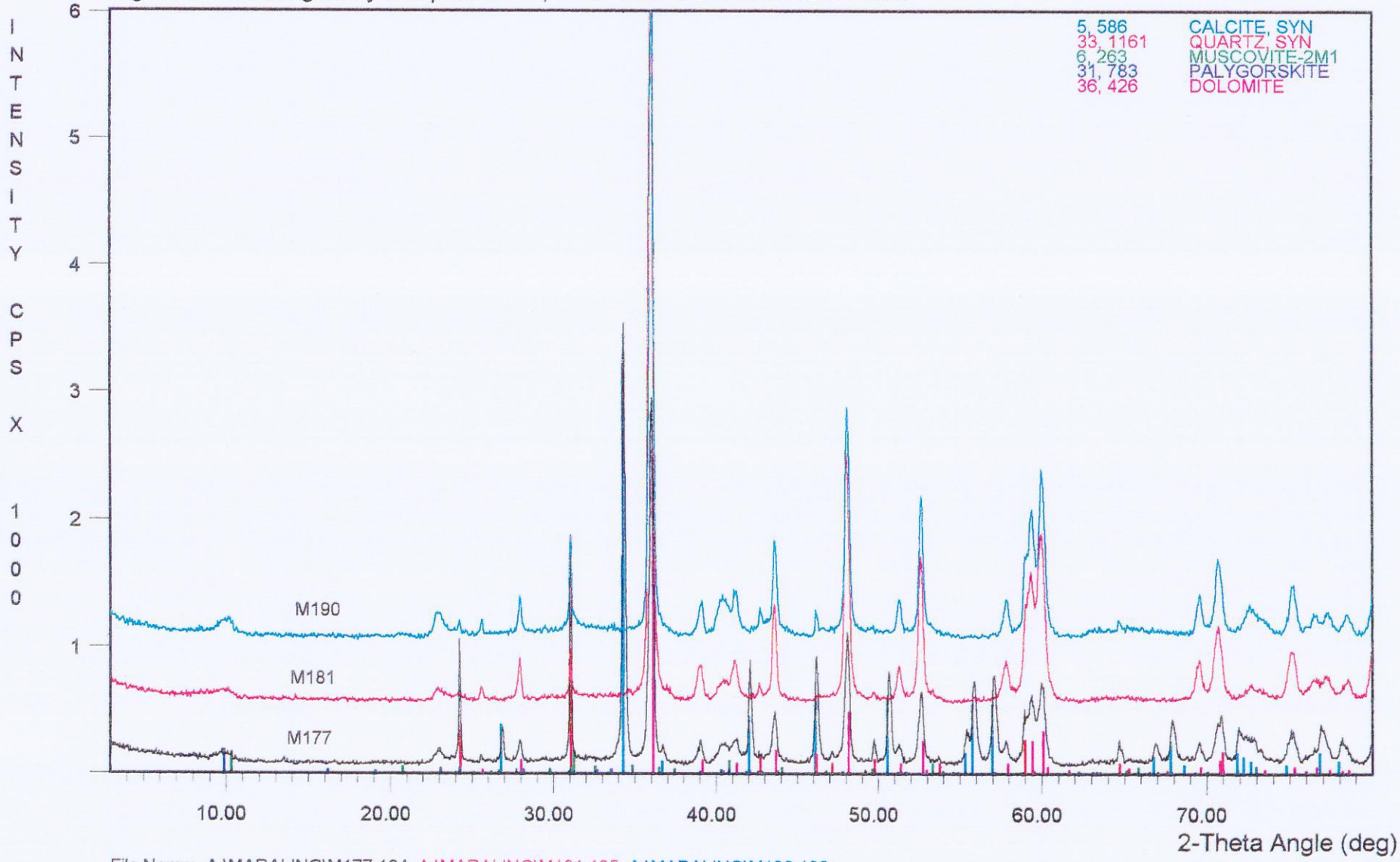
Fig. 37d. Maralinga clay samples M130, M131 and M132 from hole T9R.



File Name: A:\MARALING\M130.101 A:\MARALING\M131.102 A:\MARALING\M132.103

000105
99

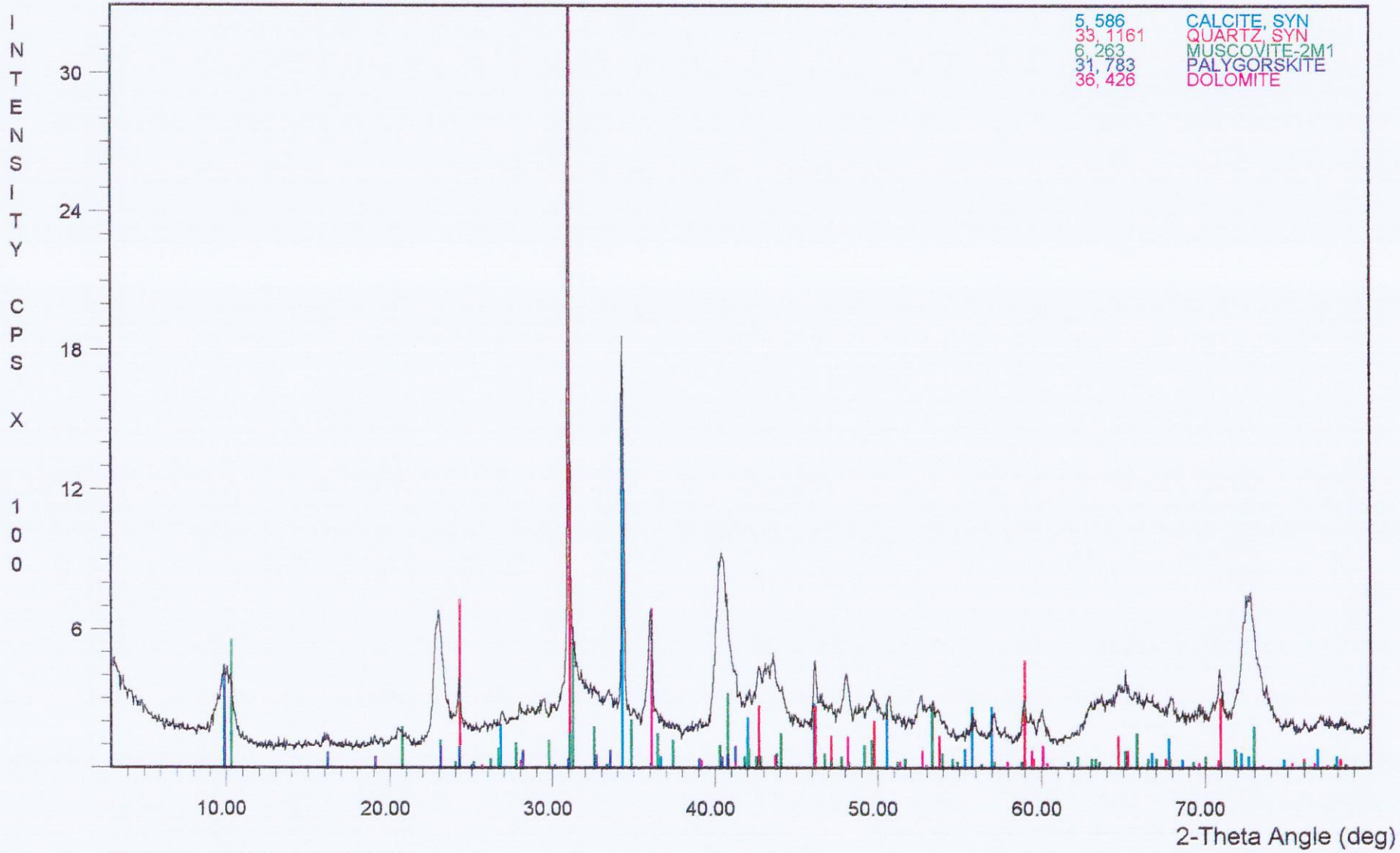
Fig. 37e. Maralinga clay samples M177, M181 and M190 from hole T13R.



File Name: A:\MARALING\M177.104 A:\MARALING\M181.105 A:\MARALING\M190.106

000106
100

Fig. 37f. Maralinga clay sample M316 from Pit TN2.

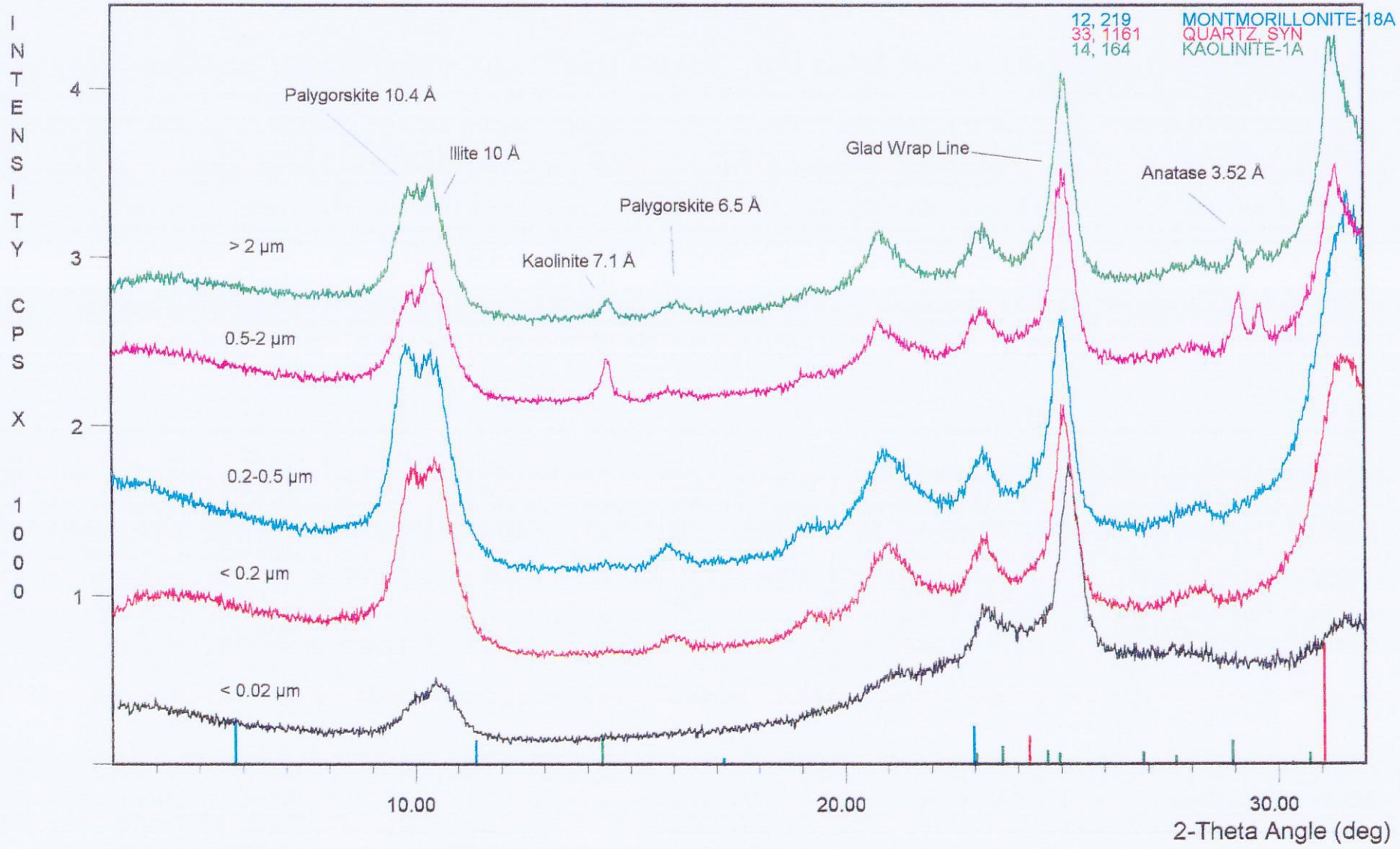


File Name: A:\MARALING\M316.117

000107

Fig. 38. XRD patterns of palygorskites and illites. a) Patterns from oriented samples from a range of size fractions separated from Garford clay P24(4-5m). b) O'Laddie palygorskite. c) Ba saturated Muloorina illite.

Fig. 38a. Garford clay P25(4-5m) < 0.02 to > 2 µm Ca-saturated.



File Name: A:\P25LP02 A:\P254-5L.2 A:\P254-5-5 A:\P254-5-2.NO2 A:\P254-5G2

0001109
103

Fig. 38b. O'Laddie palygorskite NaCl 0.05N HCl 5µm Ca-Sat.

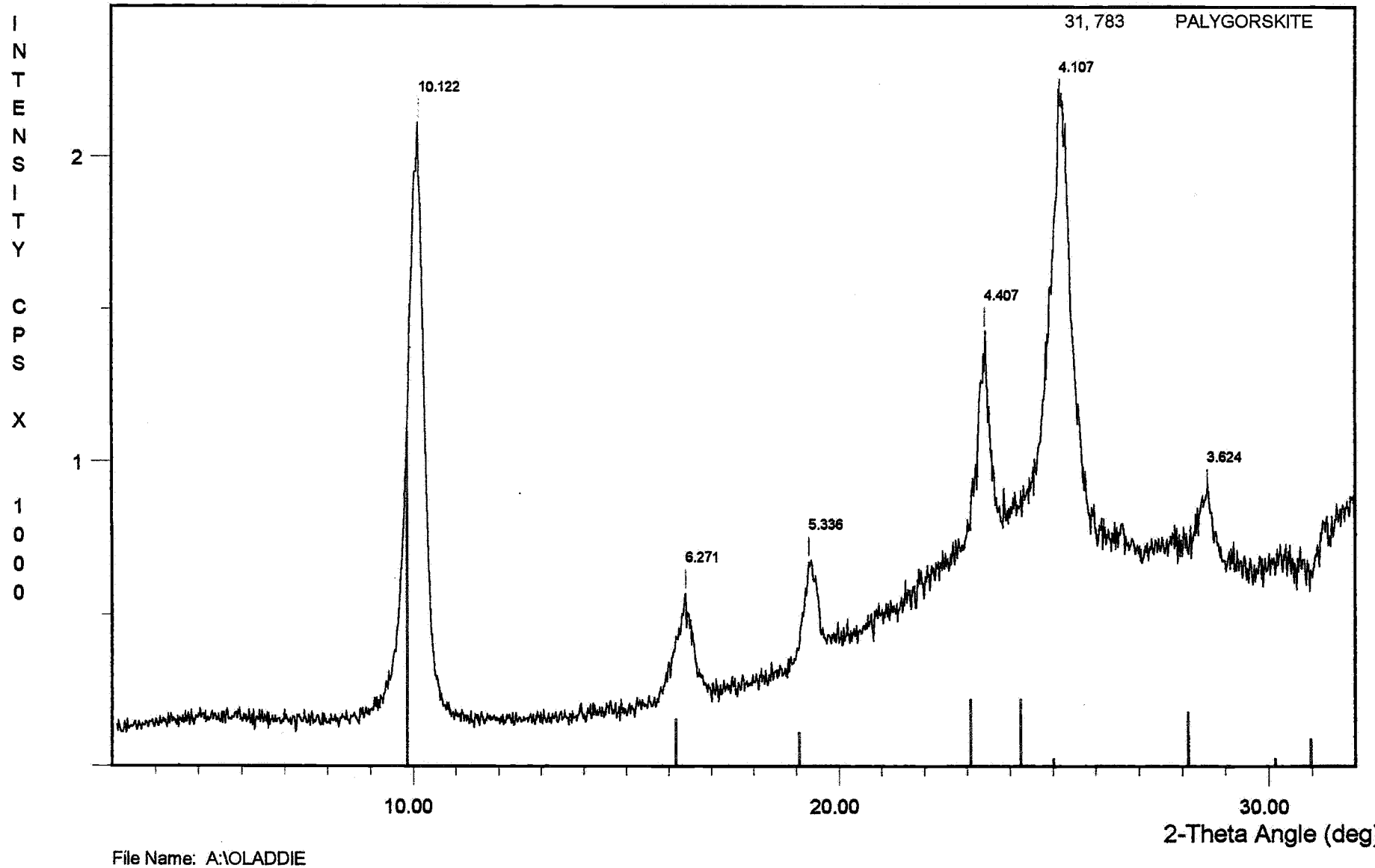
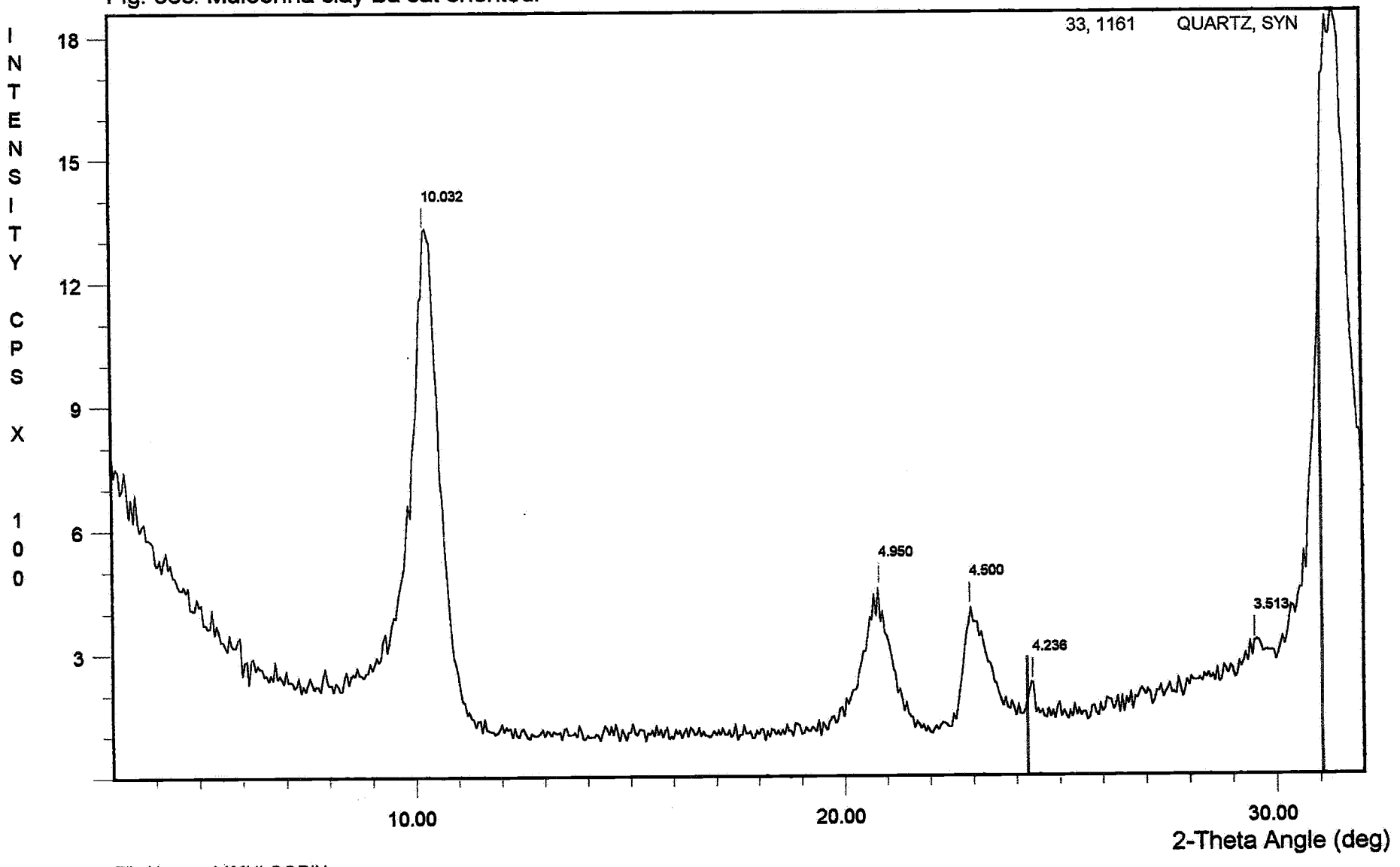


Fig. 38c. Muloorina clay Ba sat oriented.



File Name: A:\MULOORIN

ACKNOWLEDGMENTS

We acknowledge Mr P. Fazey for XRF analyses and Mr G. Riley for help in separating samples and XRD analyses. We also acknowledge Mrs B. Barovs for typing and Mr J. Coppi for photographic work.

REFERENCES

Bellat, J-P. and Simonot-Grange, M-H. (1989). Adsorption-desorption of water by sepiolite: characterization of zeolitic water. *In* Farmer, V.C. and Tardy, Y (eds.) *Proceedings of the 9th International Clay Conference, Strasbourg 1989.* Sci. Géol., Mém., **87**: 15-23.

Benbow, M.C. and Pitt, G.M. (1978). The Garford Formation. *South Australian Quarterly Geological Notes*, **59**: 7-10.

Bradley, W.F. (1940). The structural scheme of attapulgite. *American Mineralogist*, **44**: 495-500.

Churchman, G.J. and Carr, R.M. (1973). Dehydration of the washed potassium acetate complex of halloysite. *Clays and Clay Minerals*, **21**: 241-246.

Churchman, G.J., Davy, T.J., Aylmore, L.A.G. and Gilkes, R.J. (1991). Micropores in halloysites. *12th Biennial Conference of the Australian Clay Minerals Society, 1991. Program and Abstracts* p.5.

Churchman, G.J., Slade, P.G., Self, P.G. and Janik, L.J. (1994a). Nature of interstratified kaolin-smectite in some Australian soils. *Australian Journal of Soil Research*, **32**: 805-822.

Churchman, G.J., Davy, T.J., Aylmore, L.A.G., Gilkes, R.J. and Self, P.G. (1994b). Characteristics of fine pores in some halloysites. *Clay Minerals* (in review).

Galan, E., Brell, J.M., La Iglesia, A. and Roberston, R.H.S. (1975). The Caceres palygorskite deposit, Spain. *In*, Bailey, S.W. (ed.), *1975 International Clay Conference, Mexico, 1975.* Applied Publishing, Wilmette, Illinios: 91-94.

Jones, B.F. and Galan, E. (1988). Sepiolite and palygorskite. *In* Ribbe, P.H. (ed.), *Hydrous phyllosilicates (exclusive of micas). Reviews in Mineralogy*, **19**: 631-674.

Keeling, J.L. (1984). McLaren Vale white clay deposit. *Mineral Resources Review, South Australia*, **153**: 30-39.

Keeling, J.L. (1986). *Economic geology and mineralogy of Birdwood Kaolin, South Australia.* MSc Thesis, University of Hull (UK).

Keeling, J.L. (1993). Birdwood Kaolin Deposits p. 6-14 *In* (J.L. Keeling, ed.) *Deep Kaolinization in Amphibolite-Grade metamorphics, Adelaide Hills, Sedimentary kaolin at Golden Grove.* Field Guide for Pre- and post-conference 1 day tours F.3a and F.3b 18 and 24 July 1993. 10th International Clay Conference. Adelaide, Australia 18-23 July, 1993.

Lahav, N. (1990). Preparation of stable suspensions of delaminated kaolinite by combined dimethylsulfoxide-ammonium fluoride treatment. *Clays and Clay Minerals*, **38**: 219-222.

McCallum, W.S. (1988). Geology of the Golden Grove Extractive Industry area. *South Australia Department of Mines and Energy. Report Book* 88/46.

McCallum, W.S. (1990). Construction material resources - Golden Grove area. *South Australia. Mines and Energy Review* **157**: 90-91

McCallum, W.S. and Keeling, J.L. (1993). Golden Grove Sand and Clay Deposits p. 27-32 *In* (J.L. Keeling, ed.) *Deep Kaolinization in Amphibolite-Grade metamorphics, Adelaide Hills, Sedimentary kaolin at Golden Grove.* Field Guide for Pre- and post-conference 1 day tours F.3a and F.3b 18 and 24 July 1993. 10th International Clay Conference. Adelaide, Australia 18-23 July, 1993.

Morris, L.J. and Walker, S. (1993). Maralinga *in situ* vitrification investigation. *South Australia. Department of Mines and Energy Report* 93/49.

Ney, P. (1983). "The whitest clay in the world' - halloysite clay from Matauri Bay, New Zealand. *Berichte, Deutsche Keramische Gesellschaft*, **60**: 409-415.

Norrish, K. and Pickering, J.G. (1983). Clay minerals. *Soils: An Australian Viewpoint.* CSIRO Australia: Melbourne/Academic Press: London., 281-308.

Olliver, J.G. and Carr, S.G. (1977). Oodlawirra Palygorskite Deposit. *South Australia. Department of Mines and Energy Report* 77/15.

Paulus, W.J., Komarneni, S. and Roy, R. (1992). Bulk synthesis and selective exchange of strontium ions in $Na_4Mg_6Al_4Si_4O_{20}F_4$ mica. *Nature* **357**: 571-573.

Raven, M.D. (1990). XPLOT Version 3.2 - User Manual. Manipulation of X-ray Powder Diffraction data. *CSIRO Division of Soils Technical Memorandum No.* 24/1990. 26pp.

Rakich, P.B. (1990). Development of the attapulgite industry in Australia. *Proceedings of the 9th Industrial Minerals International Congress, Sydney, 1990.* Metal Bulletin PLC, London: 165-169.

Robertson, R.S. (1984). Reconnaissance sampling of palygorskite clay - Garford Palaeochannel - Coober Pedy. *South Australia. Department of Mines and Energy Report* 84/52.

Serna, C., Ahlrichs, J.L. and Serratosa, J.M. (1975). Folding in sepiolite crystals. *Clays and Clay Minerals*, **23**: 452-457.

Tiller, K.G. and Smith L.H. (1990). Limitations of EGME retention to estimate the surface area of soils. *Australian Journal of Soil Research* **28:** 1-26.

APPENDIX 1

CSIRO DIVISION OF SOILS

TECHNICAL REPORT NO. 83/1992

NOT FOR PUBLICATION
The material contained herein has not been refereed. It may be quoted as a personal communication following the written consent of the author.

CSIRO
AUSTRALIA

MINERALOGICAL ANALYSIS OF COMPOSITE SAMPLES FROM THE ARUMPO BENTONITE DEPOSIT

M D Raven, J L Keeling, P G Self and P G Slade

SUMMARY

The mineralogy of 7 composite samples from the Arumpo Bentonite Deposit were determined by XRD as dominantly smectite clay with minor quartz and anatase. Two samples also contained dolomite, one of which had accessory analcime. Further examination of sample Composite #1 showed the presence of 10% illite clay randomly interstratified in a smectite classified as a ***Wyoming-type*** montmorillonite.

Difficulties with dispersion of some clay lumps is due to physical properties of the clay rather than the presence of a cement. The presence of very fine grained particles resulting in extremely small micropores would be expected to give rise to higher bond strength between clay microaggregates. The presence of interstratified illite suggests that associated areas of smectite may have a higher tetrahedral lattice charge with stronger bonding of microaggregrates.

Dispersion of clay lumps was achieved by fine grinding and sodium saturation followed by washing and vigorous shaking.

INTRODUCTION

Seven composite bentonite samples from the Arumpo deposit, New South Wales were submitted by L C Barnes, Chief Geologist and Manager Technical Services, Commercial Minerals Ltd, on 3 September 1992 for semi-quantitative mineralogical analysis. Preliminary results were advised on 16 September 1992. A verbal request was received subsequently to assess the presence of interstratified illite and to examine clay lumps which could not be dispersed readily. Sample "Composite #1" was selected for further testing.

Mineralogy was determined by X-ray diffraction (XRD) aided by chemical analyses supplied by Commercial Minerals. Clay lumps from Composite #1 and sample #135033 were investigated using a variety of techniques including XRD, Scanning Electron Microscopy (SEM) and Transmission Electron Microscopy (TEM). Wyoming bentonite was used as a comparison for XRD and TEM investigations.

MINERALOGY OF COMPOSITE SAMPLES

The composite samples were prepared by grinding oven dried (105°C) sub-samples in an agate mortar and pestle and lightly pressing the powders into aluminium holders for XRD analysis.

XRD patterns were recorded with a Philips PW1800 microprocessor-controlled diffractometer (Self, 1989) using cobalt Kα radiation, variable divergence slit and a graphite monochromator. The diffraction patterns of the powdered materials were recorded in steps of 0.05° 2θ with a 1 second counting time per step. The patterns were logged to permanent data files on an IBM PC/XT computer for analysis (Raven 1990).

Quantitative analysis was made by comparing peak intensity data (XRD) with standard materials, and by rational analysis using chemical data. The smectite component was determined by difference.

Table 1 summarises the mineralogy determined from XRD traces. Very high smectite (montmorillonite) contents were determined for all samples, except Composite #4. Quartz levels were slightly higher compared with previously analysed samples (Raven *et al.*, 1992). Anatase was detected in all XRD patterns, and based on chemical data (Table 2), averaged 0.6%. Dolomite was found in samples Composite #4 and #5. Trace analcime ($Na[Si_2Al]O_6.H_2O$) was also present in Composite #4.

Table 1. Mineralogical Composition of Composite Arumpo Bentonites†

Comp #	*Smectite**	*Quartz*	*Anatase*	*Dolomite*	*Analcime*
1	95	4	<1	-	-
2	92	7	<1	-	-
3	92	7	<1	-	-
4	76	6	<1	16	<1
5	96	2	<1	<1	-
6	97	2	<1	-	-
7	93	6	<1	-	-

*smectite component contains 10-20% randomly interstratified illite layers.

†The term "bentonite" is used here as a commercial rock term and describes a clay consisting essentially of minerals of the smectite clay mineral group, and in which the dominant clay mineral is montmorillonite.

Table 2. Chemical Data of Composite Arumpo Bentonites (Supplied by Commercial Minerals)

Comp #	*SiO_2*	*TiO_2*	*Al_2O_3*	*Fe_2O_3*	*MgO*	*CaO*	*Na_2O*	*K_2O*	*LOI*	*Total*
1	61.4	0.6	19.1	4.3	4.5	0.05	1.3	1.1	7.9	100.2
2	63.3	0.5	16.7	4.7	4.7	0.03	1.3	1.1	7.0	99.3
3	63.3	0.6	17.2	4.1	4.3	0.07	1.4	1.3	6.8	99.1
4	53.5	0.7	13.1	3.0	8.2	4.9	1.7	1.2	13.9	100.2
5	62.0	0.6	19.1	3.9	5.3	0.3	1.6	1.3	7.7	101.8
6	61.1	0.6	19.3	4.3	4.6	0.06	1.4	1.3	7.5	100.2
7	62.8	0.6	19.2	5.0	3.8	0.05	1.1	1.1	7.1	100.8

MINERALOGY OF HARD LUMPS IN ARUMPO BENTONITE

Composite samples of Arumpo bentonite submitted for quantitative mineralogical analysis on 6 August, 1992 contained lumps of clay in the >75µm fraction which resisted slaking in water. The mineralogy of the coarse fraction was determined by XRD as smectite with around 4% quartz, essentially the same mineralogy as the finer grained fraction (Raven *et al.*, 1992). Additional samples recieved on 3 September, 1992 also contained similar clay lumps. These were accompanied by chemical analysis of the bulk material determined previously by Commercial Minerals, Technical Services Division (Table 2). This showed that in addition to Na^+, the clay also contained cations K^+ and Mg^{2+}. Disintegration and dispersion of the clay lumps might therefore be readily achieved by saturation of the exchange sites of the bentonite with Na^+ ions followed by repeated washing with distilled water. This procedure was tried without success and a more detailed analysis of the lumps was carried out to better characterise the smectite.

Diffraction analysis showed the lumps to be composed of smectite, quartz and anatase. No clear evidence for the presence of free illite (or mica) was found although the analytical chemical data, from Commercial Minerals Ltd, showed all samples to contain over 1% K_2O. By taking this analytical data and re-calculating it after 1) subtracting SiO_2 figures corresponding to the quartz percentages estimated by XRD and 2) anatase, as per the chemical analyses, a set of structural formulae for the composite samples were obtained. These all showed improbably low interlayer charges.

Sample Composite #1 was selected for a more thorough mineralogical analysis. Lumps totalling ~5g were selected and freed of adhering fine particles by washing with a stream of distilled water. The lumps were then broken up with a mortar and pestle, followed by vigorous shaking with water in a SPEX mill (for 10 minutes). The slurry was then treated with 1M NaCl and finally washed with the aid of repeated centrifugation until much of the

clay remained dispersed. The dispersed material was separated into two fractions, >2μm and <2μm. These were both calcium saturated and after being washed, until free of excess Cl^- ions, oven dried at 105°C. X-ray diffraction patterns of the separated fractions clearly showed the <2μm fraction (Fig. 1) was now free of quartz but still contained anatase. The coarse fraction was, correspondingly, quartz rich.

X-ray fluorescence analysis of the calcium saturated <2μm fraction (Table 3) showed that appreciable K_2O was still present, even though the procedure attempted to convert the clay to a homoionic (Ca) form. The question then arose as to how this K_2O was bound in the clay. The XRD pattern (Fig. 1) did not indicate the likely presence of any free illite (or mica). To investigate the source of the K_2O an oriented sample of the clay was Mg^{2+} saturated and then saturated with ethylene glycol. The XRD pattern of the treated clay (Fig. 2) showed a set of relatively broad peaks at positions which, on comparison with published data, (Brindley & Brown, 1984) corresponded to a randomly interstratified smectite-illite with approximately 10-20% illite layers. The XRD pattern of a similarly prepared sample of Wyoming bentonite (Fig. 3) also showed relatively broad peaks, but at positions consistent with pure smectite. Table 4 shows the shift in positions of the 2nd and 3rd order peaks for various proportions of random and regular interstratified smectite-illites.

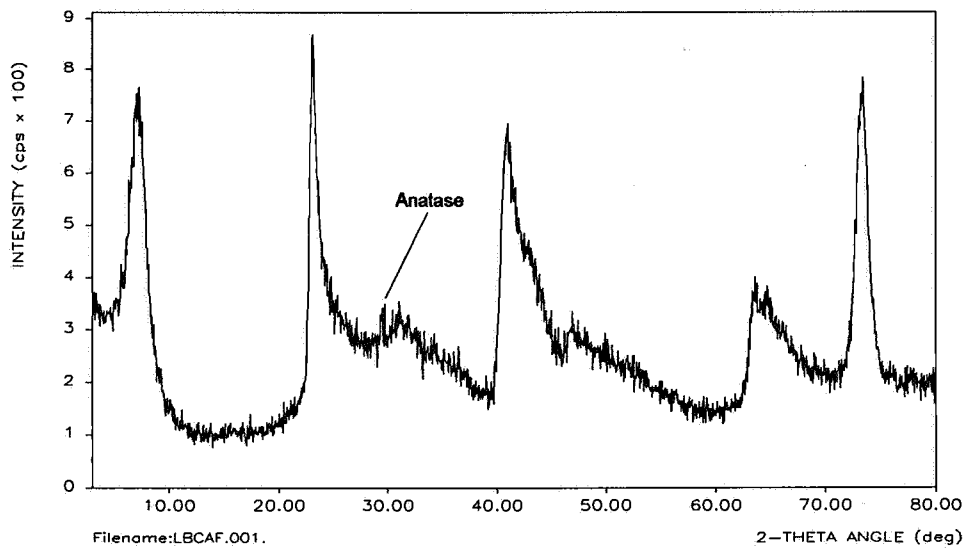


Figure 1. XRD Pattern (Non-Oriented) of <2μm Fraction of Composite #1 (Co Radiation)

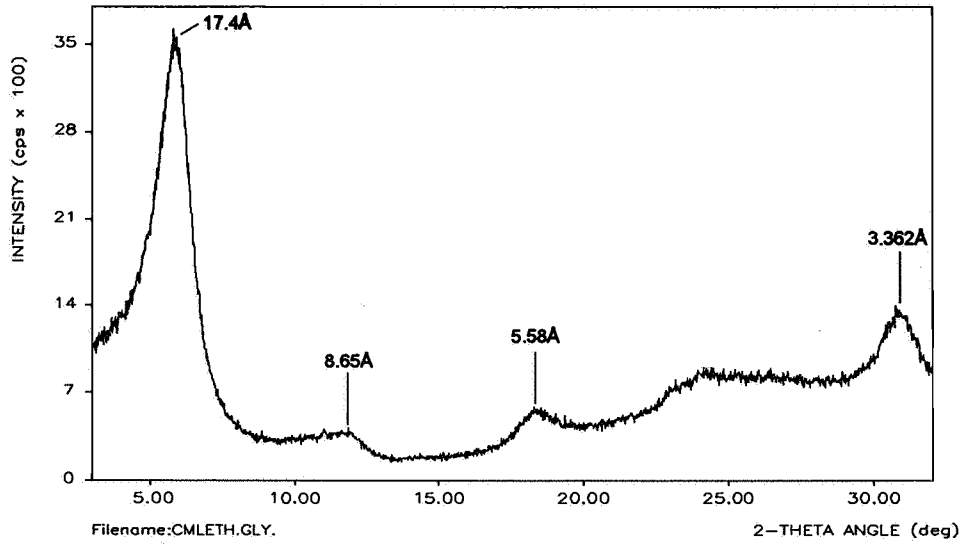


Figure 2. XRD Pattern (Oriented Mg saturated and Ethylene Glycol) of <2μm Fraction of Composite #1 (Co Radiation)

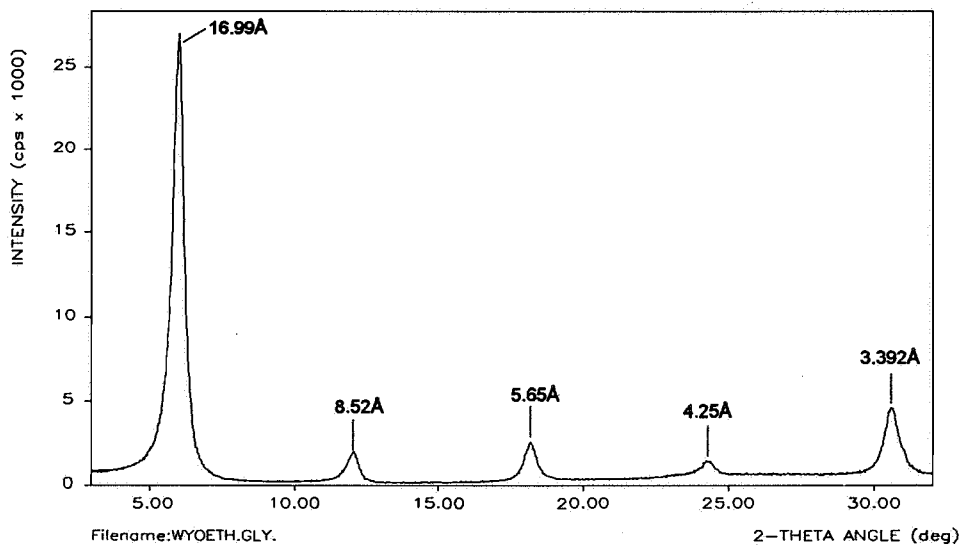


Figure 3. XRD Pattern (Oriented Mg saturated and Ethylene Glycol) of <2μm Fraction of Wyoming Bentonite (Co Radiation)

With this information, it was possible to calculate a structural formula for the smectite component. This necessitated a subtraction of the oxide components associated with the mica (illite) from the full analysis. The results (Table 3) show that the smectitic component of the interstratified system has a low tetrahedral charge (-0.02), is dioctahedral and carries a low overall surface charge (-0.77). This is similar to Wyoming montmorillonite which has corresponding values of -0.07 and -0.73 respectively.

Table 3. Structure Information for Arumpo Bentonite (<2μm Ca Saturated)

CHEMICAL ANALYSIS			*CLAY-MINERAL STRUCTURAL FORMULA* *2:1 layer clay (mica type)* *Oxygen equivalents per formula unit = 22*			
	weight %	*mole %*				
			Tetrahedral	Si	7.97825	
SiO_2	67.3400	74.0512		Al	0.02175	
Al_2O_3	19.9200	12.9085		Total		8.00000
Fe_2O_3	5.2300	2.1639				
MnO	0.0180	0.0168	*Octahedral*	Al	2.75976	
MgO	4.4300	7.2623		Fe^{3+}	0.46628	
CaO	2.9900	3.5228		Mn	0.00181	
Na_2O	0.0700	0.0746		Mg	0.78243	
				Total		4.01027
Total	99.9980	100.0000				
			Interlayer	Ca	0.37955	
				Na	0.01608	
				Total		0.39562
			Tetrahedral layer charge = -0.02175			
			Octahedral layer charge = -0.75342			
			Interlayer cation charge = 0.77517			

Table 4. Relationship Between Composition and Peak Position for Calculated Smectite(Glycol)-Illite Interstratifications (Spacings in Å)

	Random		*Ordered*	
% Illite	*d(002)*	*d(003)*	*d(002)*	*d(003)*
0	8.52	5.62	8.52	5.62
10	8.60	5.59	8.60	5.59
20	8.67	5.57	8.71	5.55
30	8.76	5.54	8.82	5.50
40	8.90	5.50	8.93	5.44
50	9.06	5.44	9.03	5.39
60	9.26	5.37	9.21	5.34
70	9.52	5.28	9.40	5.28
80	9.83	5.16	9.66	5.22
90	10.00	5.07	9.99	5.09
100	10.16	5.01	10.16	5.01

SCANNING ELECTRON MICROSCOPY

Method

Two samples were examined:

.Composite #1 - several hard waxy lumps were selected which would not disperse in water.

.Sample #135033 - particles from the +75µm fraction.

These were mounted onto aluminium stubs using "Araldite", dried at 105°C, then coated with 30nm of gold. The samples were examined using a Cambridge Instruments Steroscan S250 Scanning Electron Microscope to determine the nature and morphology of the particles and of any cementing agent.

Results

Composite #1. The sample consisted of very fine-grained clay particles giving a tight compact appearance with some clay ridges on the surface of grains (Fig. 4). Fissure type macropores up to 30µm length by 5µm width were occassionally developed along with micropores 2 to 5µm diameter which appeared to be aligned parallel to the orientation of fissure openings (Fig. 4).

In detail, the clay comprised sub-micron, thin, curved, sheet-like microaggregates (Figs 5 & 6). Contacts between microaggregates were indistinct and of the "coagulation type" (Grabowska-Olszewska *et al.*, 1984). Orientation of clay microaggregates was face-to-face and face-to-edge. Clay lining the macropores was present usually as larger aggregates, to 1µm across, and showed face-to-edge contact which resulted in a structure with a high proportion of micropores (Fig. 6). The bulk of the clay was finer grained comprising microaggregates of montmorillonite <0.1 to 1µm across which encompassed very fine-grained micropores (Fig. 7). No non-clay mineral cements were observed.

Sample #135033. The >75µm fraction contained predominantly rounded to angular grains of clay to 400µm across (Fig. 8). Individual grains comprised very fine-grained clay mineral as curved, sheet-like microaggregates ranging in size from <0.1 to 2µm (Figs 9-11) which were similar to sample "Composite #1". Coarse micropores were present as rounded or irregular voids occassionally larger than 5µm across (Fig. 9), but usually of the order of 1 to 2µm across (Fig. 10). Finer, sub-micron porosity predominated and formed as a result of face-to-edge microaggregate contact (Figs 10 & 11). No evidence as found for a non-clay mineral cement which might inhibit dispersion of the clay.

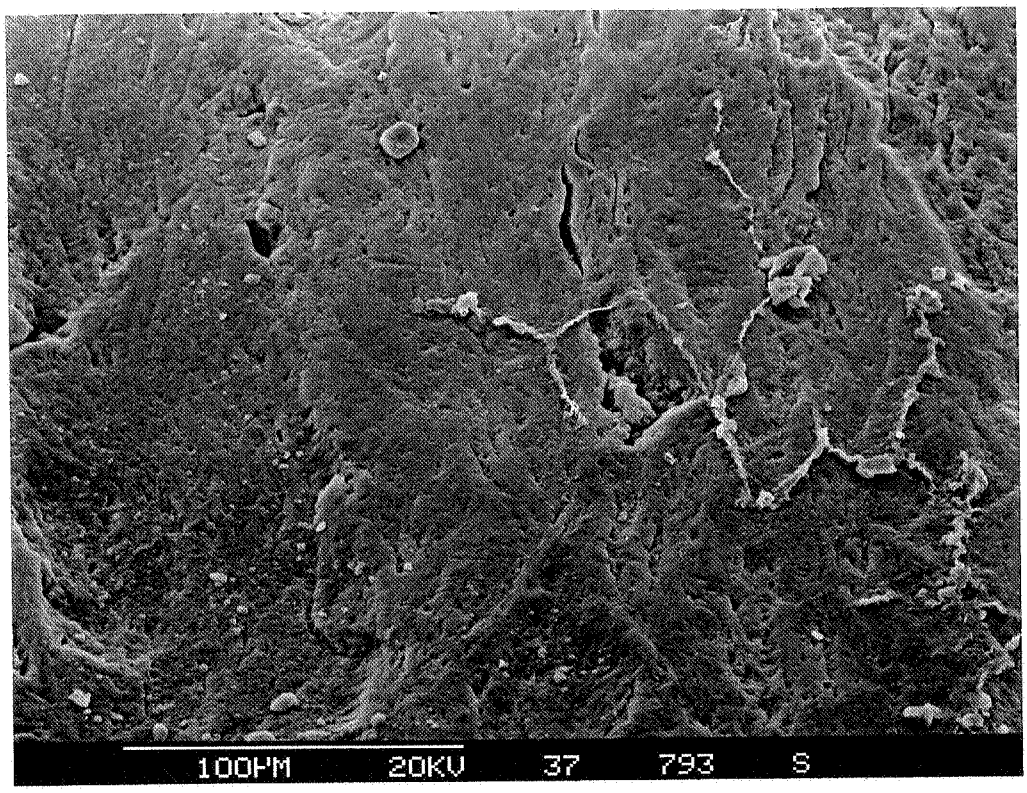


Fig. 4. ***Composite #1.*** **Scanning electron micrograph of the surface of a hard clay fragment composed of very fine-grained clay microaggregates and showing minor development of clay ridges and fissure-like porosity. Micropores, 2-5µm across can be seen which appear to be aligned roughly parallel to the fissures. Scale bar 100µm, photo. no. 37/793.**

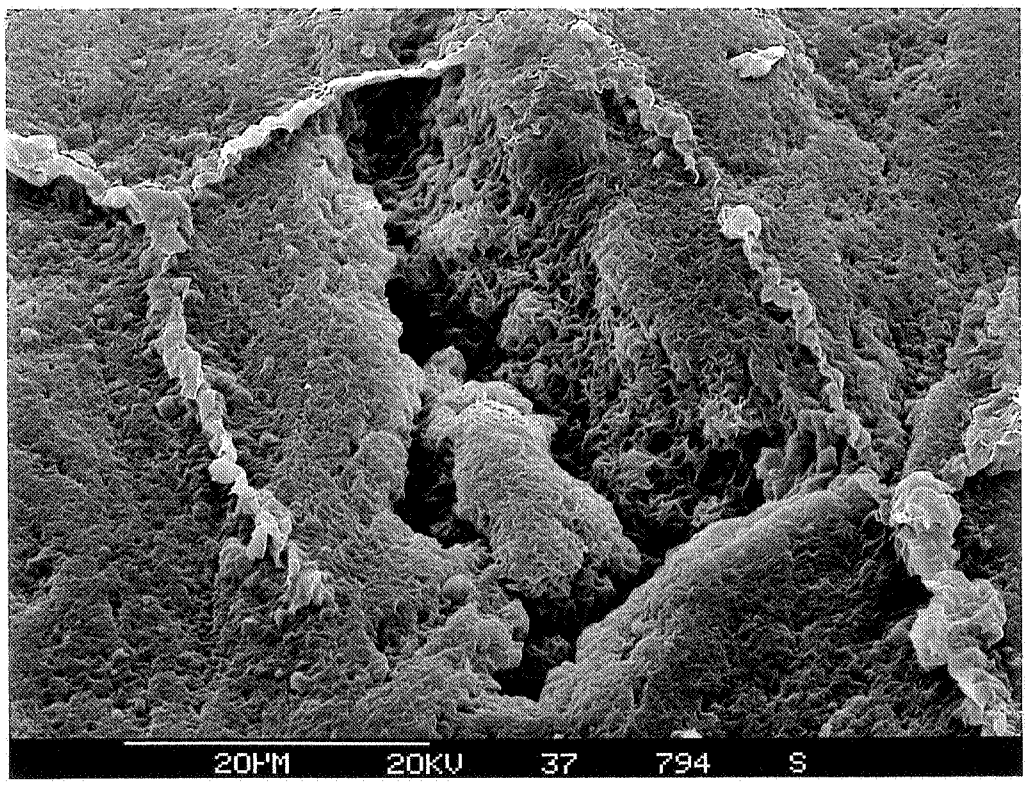


Fig. 5. Composite #1. Detail of Fig.4, showing fine grained montmorillonite with a fissure-like macropore (centre) partly surrounded by a thin clay ridge. Scale bar 20µm, photo. no. 37/794.

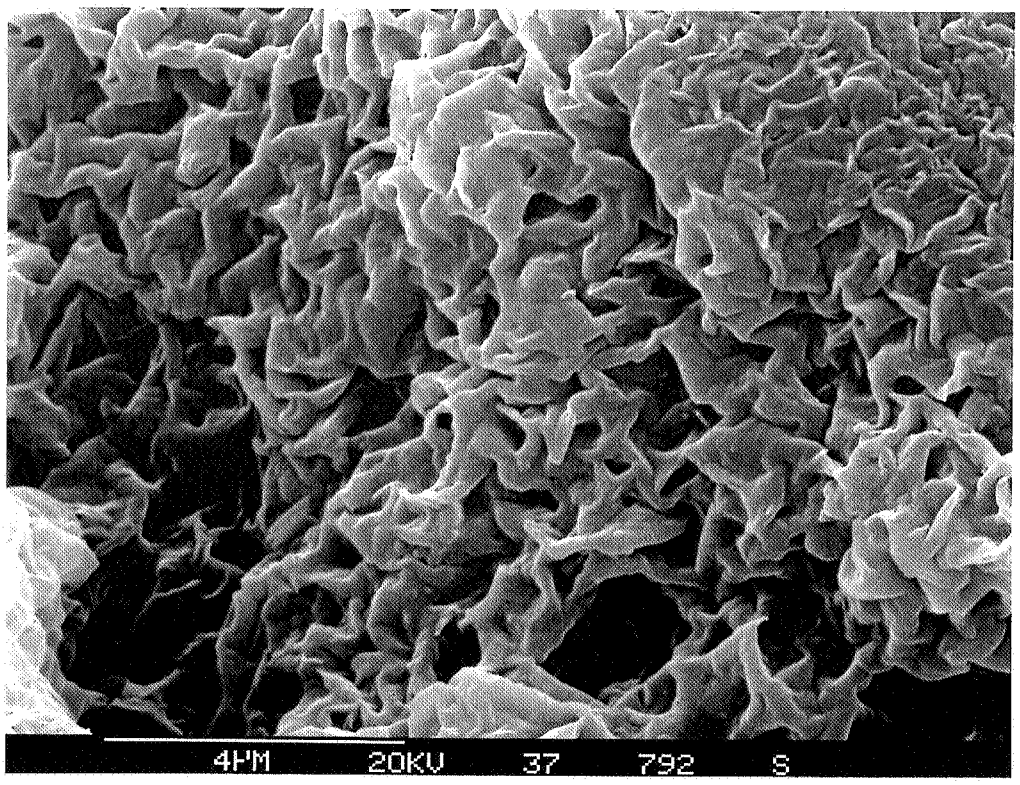


Fig. 6. ***Composite #1.*** **Detail of Fig. 5, showing clay microaggregates on the macropore surface. Microaggregates are thin, curved and sheet-like with face-to-edge arrangement and "coagulation-type" contacts. Bar scale 4μm, photo. no. 37/792.**

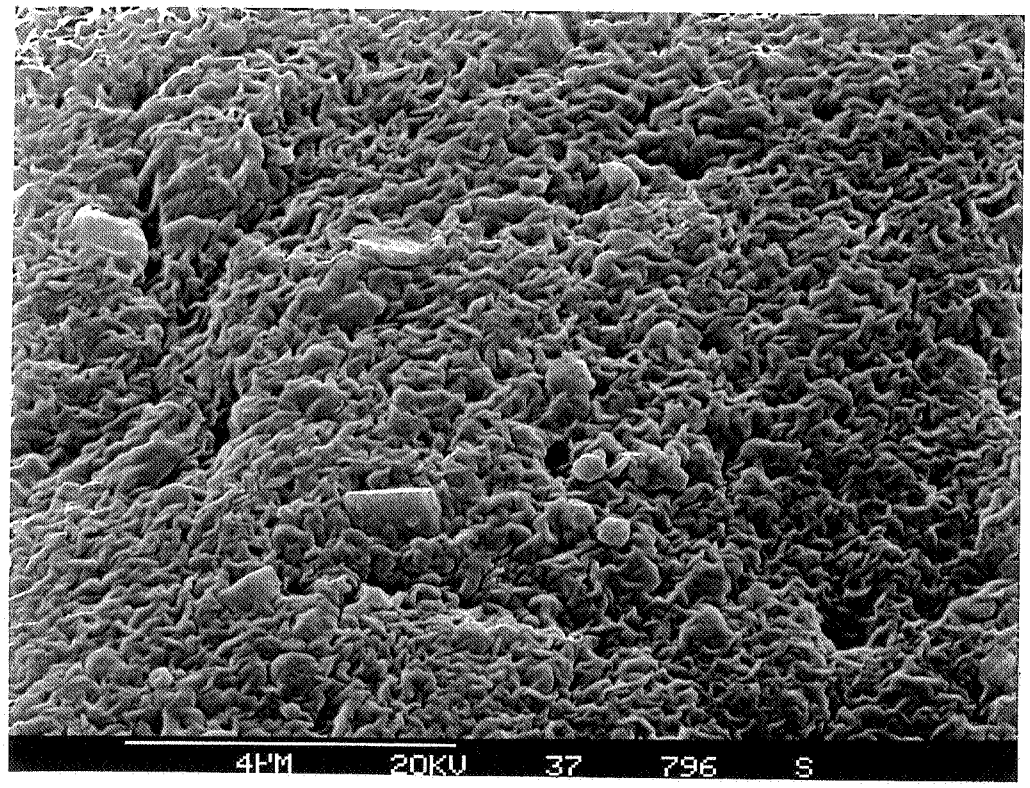


Fig. 7. ***Composite #1.*** **Typical surface of clay lump, showing clay microaggregates <0.1 to 1μm across with fine-grained micropores. Scale bar 4μm, photo. no. 37/796.**

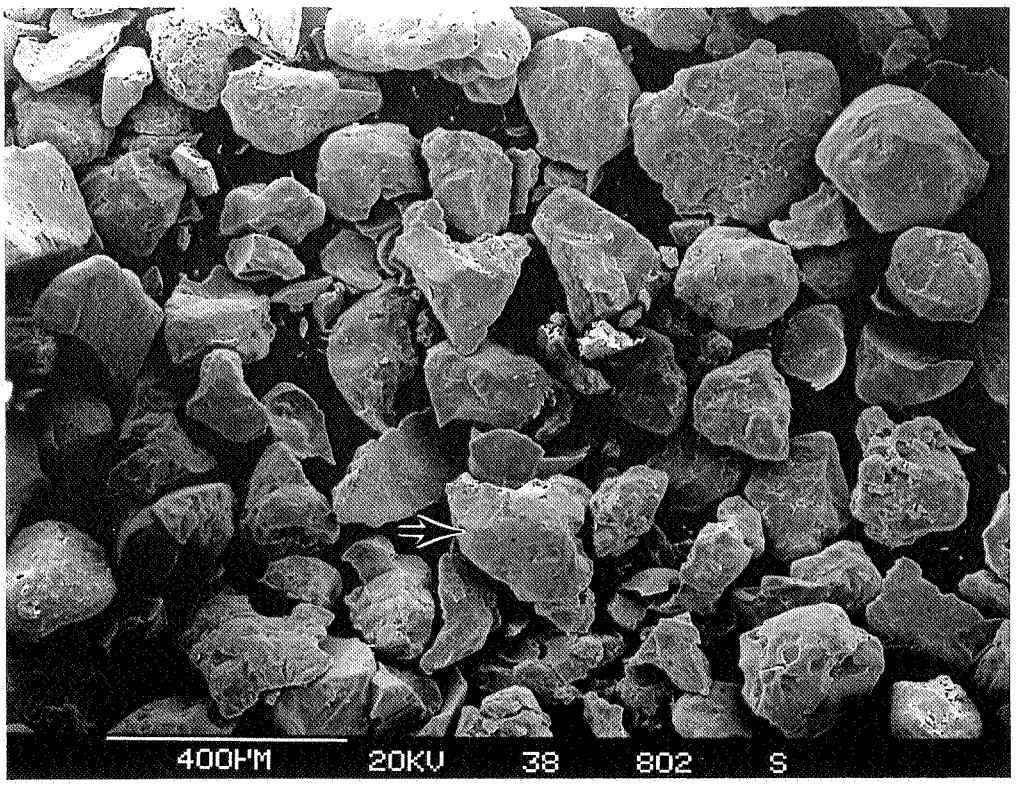


Fig. 8. ***Sample #135033.*** **>75µm size fraction: predominantly rounded to sub-angular clay particles to 400µm across. For detail of arrowed grain, see Fig. 9. Scale bar 400µm, photo. no. 38/802.**

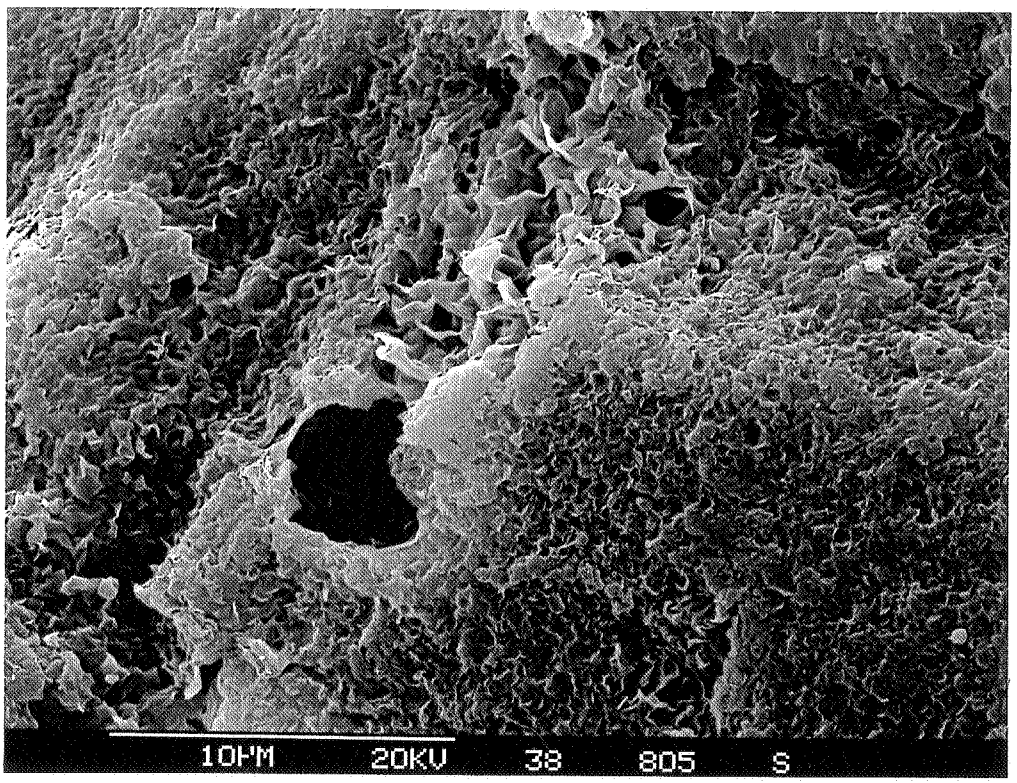


Fig. 9. ***Sample #135033.*** **Detail of the grain arrowed in Fig. 8, showing a 4µm wide micropore (centre left) with large, 1-2µm, curved clay flakes above the void showing face-to-edge arrangement and well developed microporosity, and fine-grained, sub-micron clay microaggregrates to the right. Scale bar 10µm, photo. no. 38/805.**

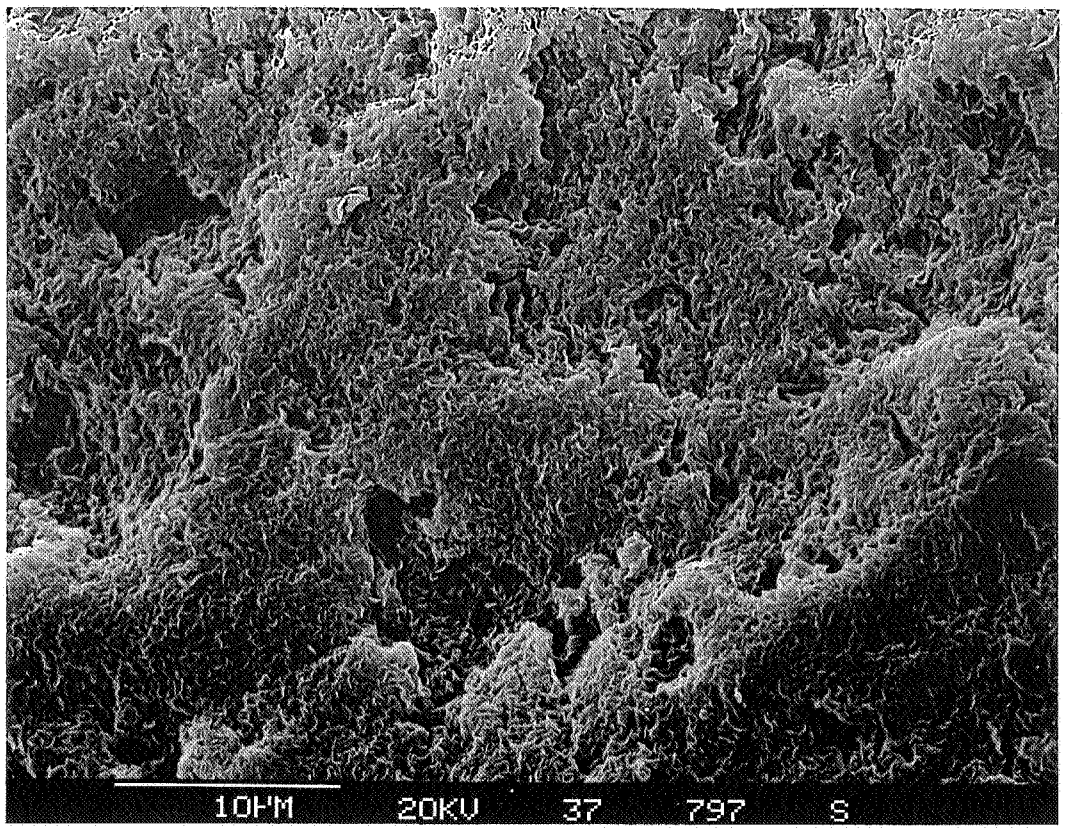


Fig. 10. ***Sample #135033.*** **Surface of a clay particle showing typical arrangement of fine-grained curved clay flakes showing irregular micropores in the size range 1-5µm. Scale bar 10µm, photo. no. 37/797.**

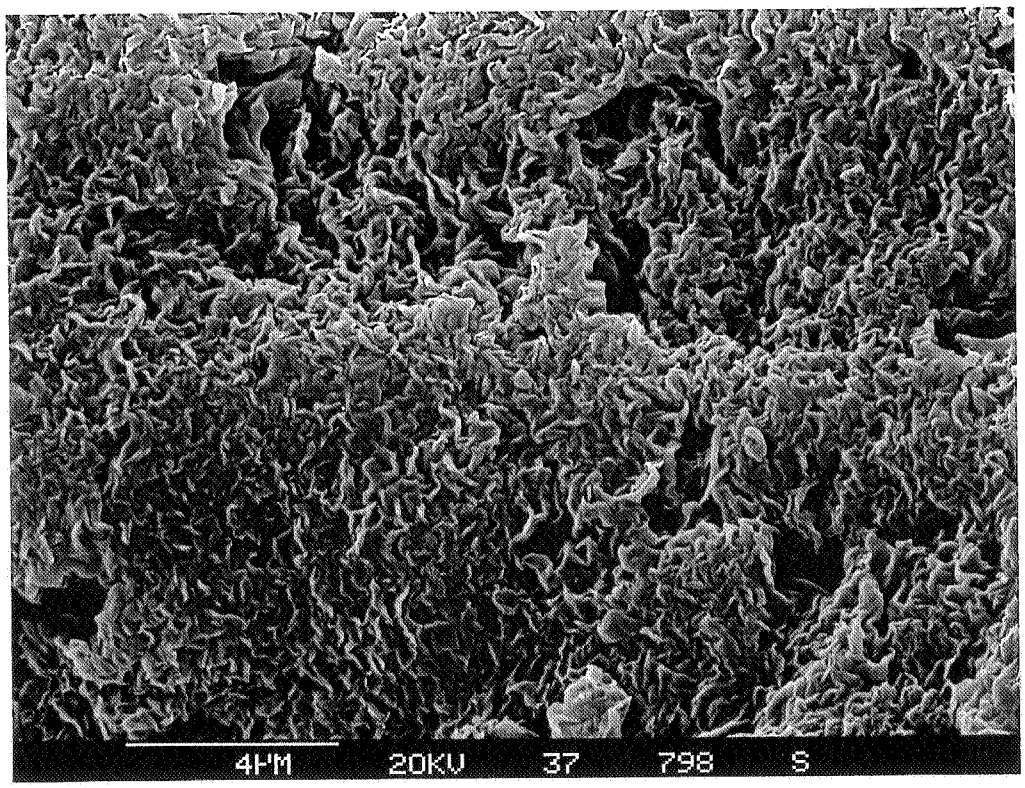


Fig. 11. ***Sample #135033.*** **Detail of the central portion of Fig. 10, showing fine-grained curved clay microaggregates and the very fine microporosity formed by face-to-edge and face-to-face arrangement of clay particles. Scale bar 4µm, photo.no. 37/798.**

TRANSMISSION ELECTRON MICROSCOPY (TEM)

Method

The sample examined by TEM was "Composite #1" which had been dispersed previously using NaCl and then Ca saturated. The sample was prepared by allowing a drop of the suspension, used to prepare an oriented XRD sample, to dry on a carbon support film mounted on a Cu grid. This was examined using a Philips 400 TEM fitted with a Link Systems energy dispersive X-ray analyser (EDX).

Results

The most immediately obvious feature of the sample when observed in the transmission electron microscope was the presence of sub-spherical particles (Fig. 12). These ranged in size from 0.2μm to 1μm and had an internal structure of balled up layers, not dissimilar to that of an onion. The sub-spherical particles were clay aggregates which had not been effectively dispersed, although some at least showed evidence of disaggregation and partial dispersion (Fig. 13).

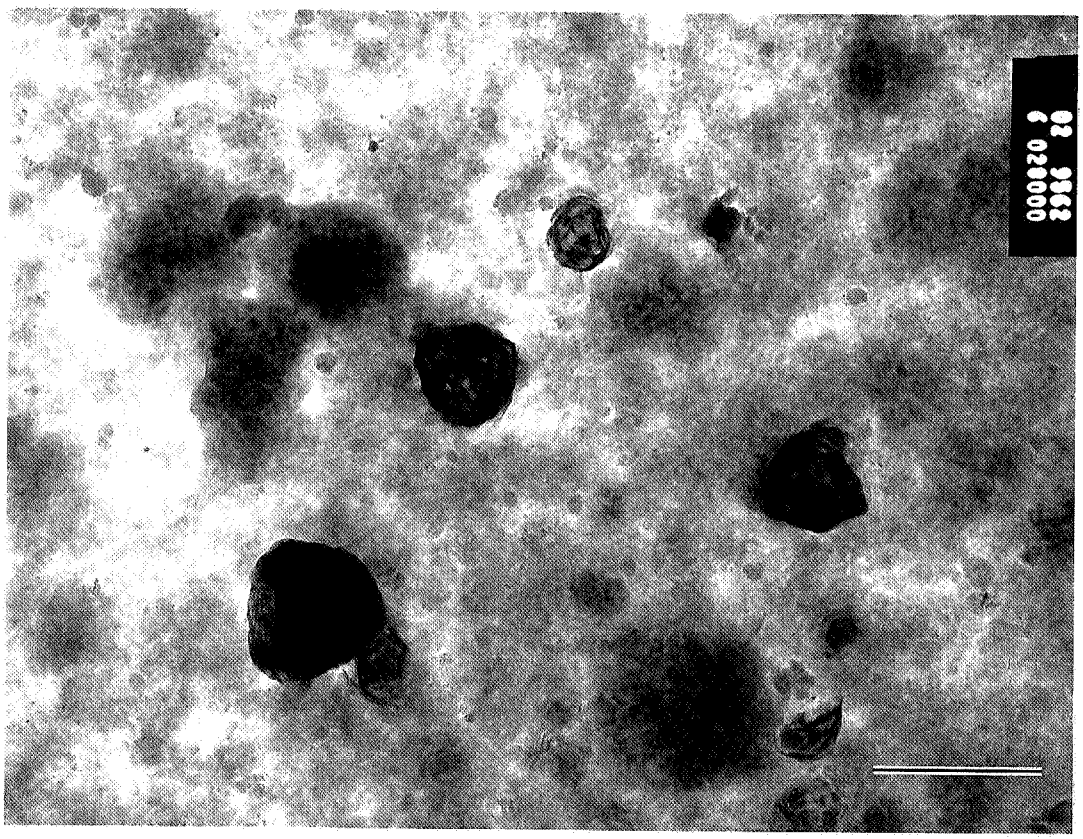


Fig. 12. ***Composite #1.*** **Transmission electron micrograph showing sub-spherical particles in a background of fine-grained clay platlets. Scale bar 0.5μm, photo. no. 9562.**

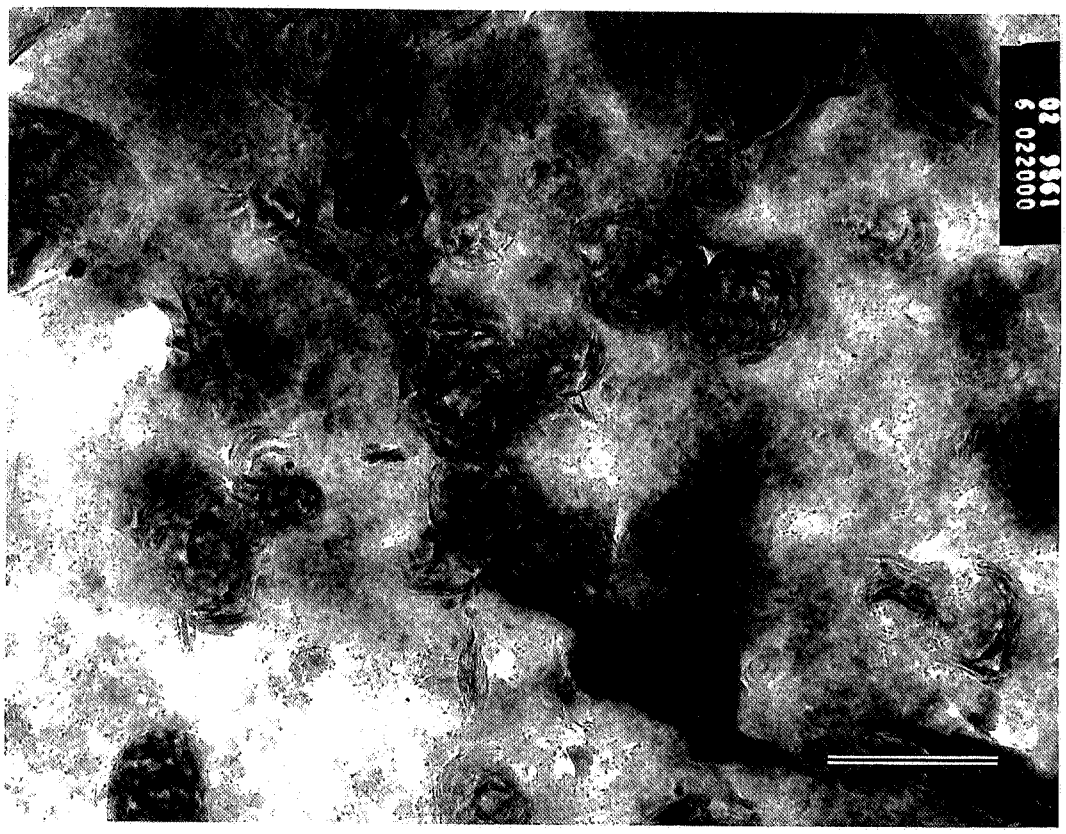


Fig. 13.: ***Composite #1.*** **Partially-dispersed, sub-spherical clay aggregates. Scale bar 0.5µm, photo. no. 9561.**

Although the sub-spherical particles were prominent, the majority of the sample comprised very fine-grained, thin platlets, 0.02µm to 0.3µm diameter (Fig. 14). Thickness of the particles ranged from 0.01µm to 0.1µm. Although the platlets were small, they were comparatively well formed and commonly showed straight edges that met at an angle of 120°.

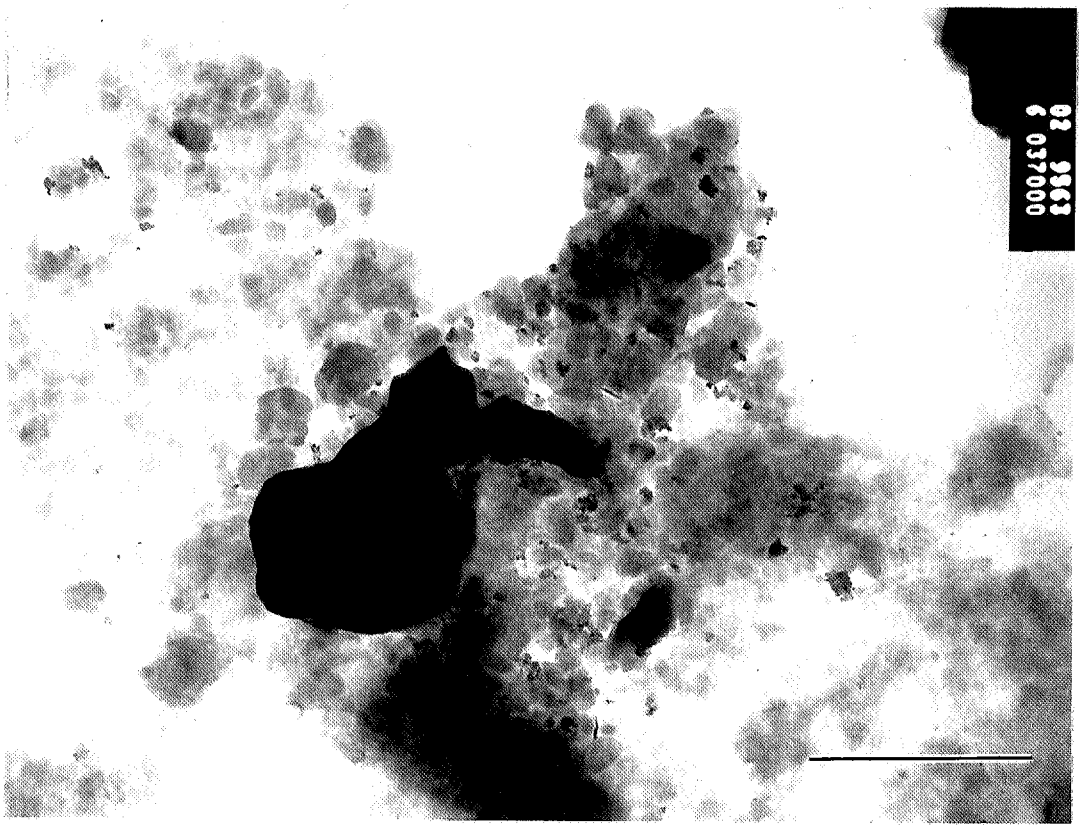


Fig. 14. ***Composite #1.*** **Large, sub-spherical clay aggregate and fine-grained clay particles. Scale bar 0.5µm, photo. no. 9563.**

EDX analysis of the sub-spherical particles and the platelets is shown in Fig. 15. The presence of K in both types of particles confirms a significant illitic component. Comparison of Fig. 15a with Fig. 15b indicates that the sub-spherical particles have a higher percentage of illite than the platelets. However, the number of particles examined by EDX is insufficient to make any definite conclusions about the concentration of K in the sub-spherical particles with respect to the concentration in the platelets.

EDX also showed that both types of particle contained Mg and probably some Fe. The proportion of iron present in the sample is uncertain due to iron contributed from electron and X-ray scattering from both the microscope pole pieces and specimen holder. Similarly, the Cr and Cu signals were generated from the specimen holder and are not attributable to the specimen. EDX analysis also showed the presence of fine particles of anatase and goethite, although in very minor amounts.

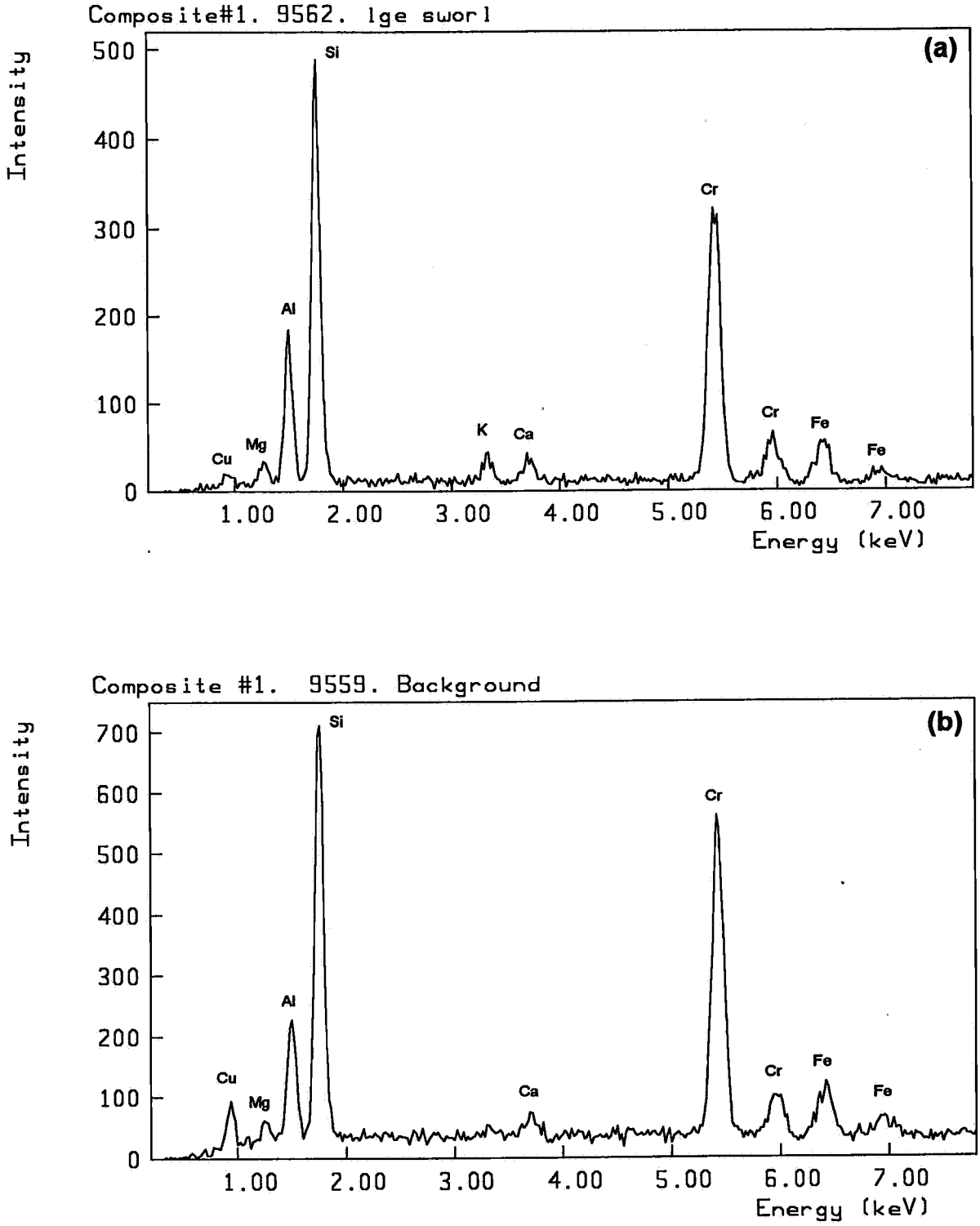


Fig. 15. EDX spectra from sample "Composite #1". (a) Spectrum from subspherical particle. (b) Spectrum from fine-grained platelet.

A third type of particle was also observed in "Composite #1". These were extremely fine-grained (<0.01μm to 0.04μm) and less electron transparent than other fine-grained platelets in the sample. Examples are shown in Fig. 16 and can also be seen on close inspection of Fig. 14. The loss of electron transparency may be due either to :- a relative increase in thickness, higher than average Fe content, or different mineralogy. EDX analyses of such fine-grained particles were difficult to obtain. For the group of particles marked A in Fig. 16, an attempted analysis is shown in Fig. 17a. This shows an increase in the ratio of Al to Si in the "dark" particles relative to the other fine-grained particles (compare Fig. 17a with Fig. 15b).

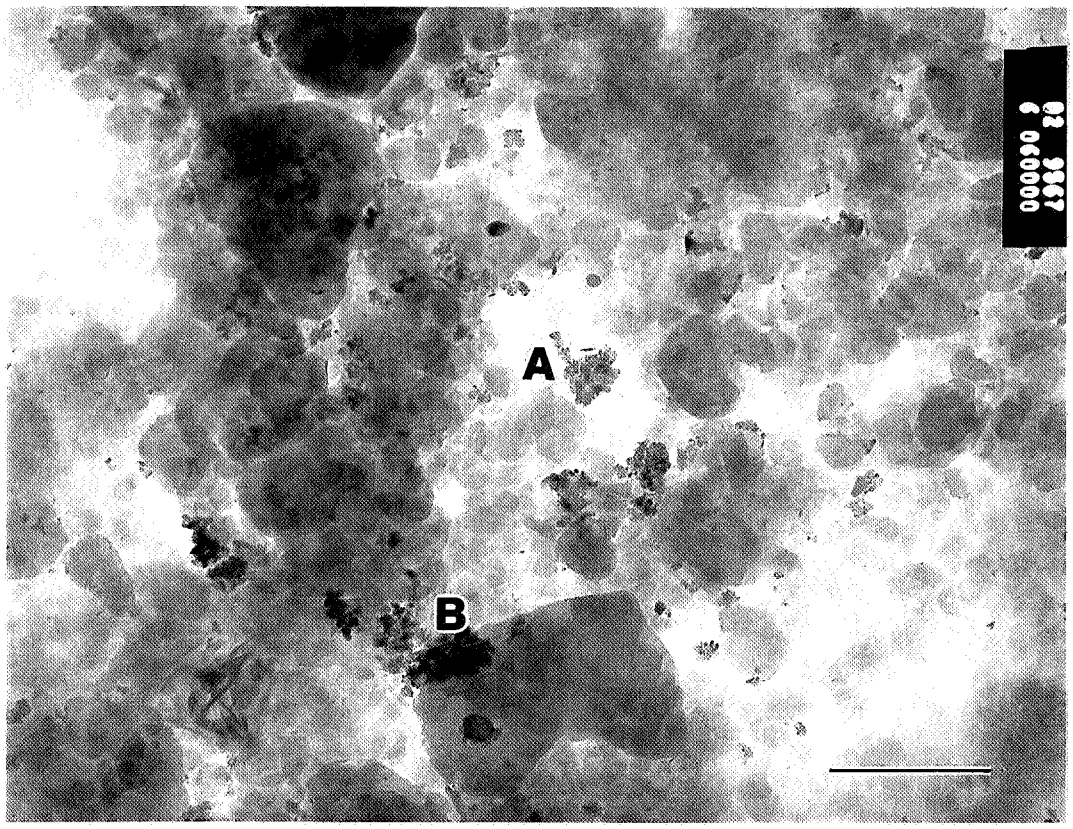


Fig. 16. ***Composite #1.*** **Transmission electron micrograph showing fine-grained particles with relatively low electron transparency (e.g. group of particles marked A). EDX spectra in Fig. 17 where obtained from regions marked A and B. Scale bar 0.2μm, photo. no. 9567.**

An increased Al:Si ratio in the dark particles is confirmed by EDX analysis (Fig. 17b) of a relatively large dark particle labelled B in Fig. 16. EDX results indicate that the particle is relatively high in Al and low in Mg (compare Fig. 17b with Fig. 15). The ratio of Al:Si in particle "B" is approximately 0.75 suggesting it has a beidellitic or kaolinitic component.

There was no evidence found during the TEM investigation for the presence of any silica cement.

000133

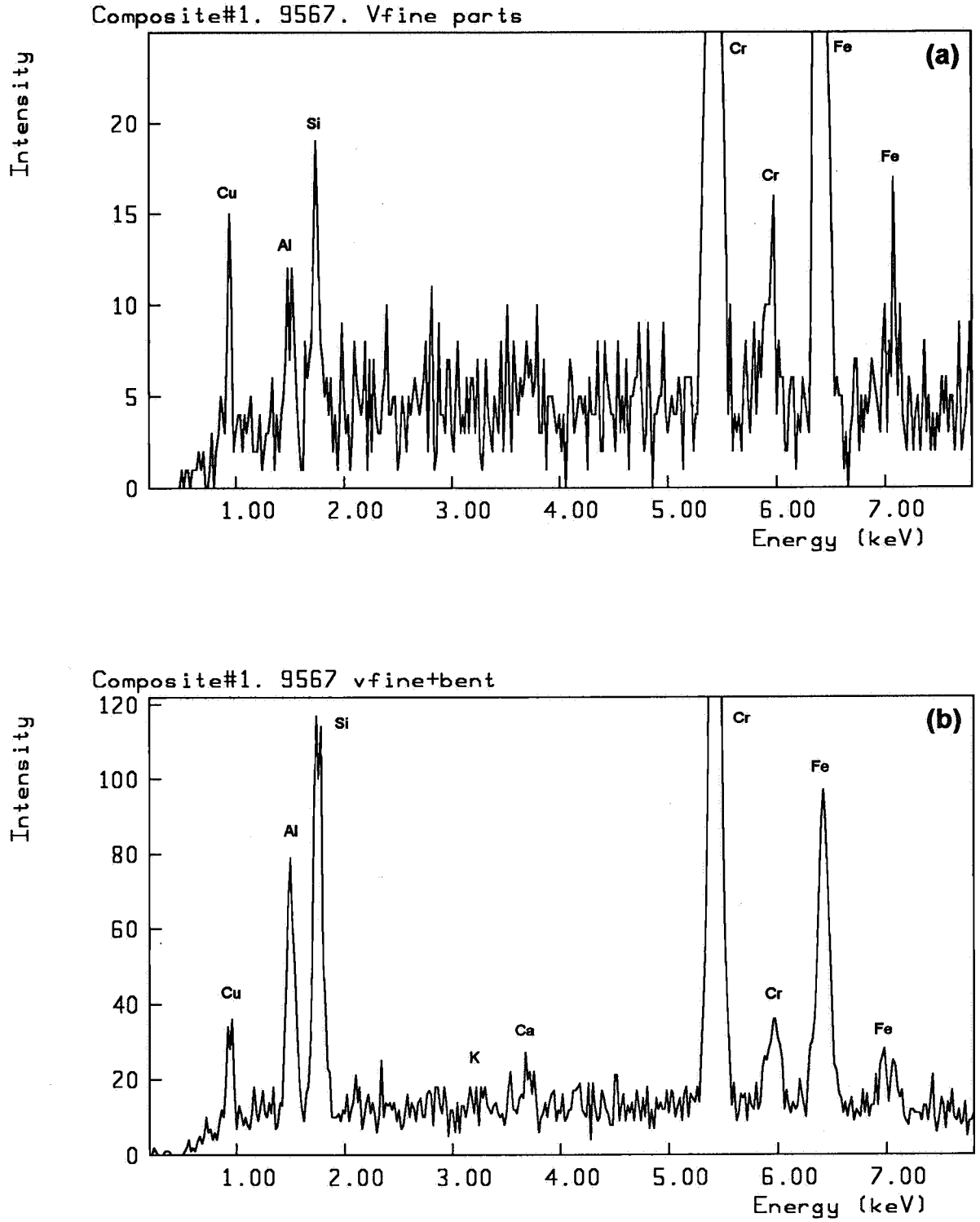


Fig. 17. EDX spectra of (a) particles marked A and (b) particle marked B in Fig. 16.

For comparison, a sample of Ca saturated Wyoming bentonite was also examined by TEM. The Wyoming bentonite consisted almost entirely of very thin (0.001μm to 0.002μm) plates that were often 1μm or more in extent (Fig. 18). The edges of the particles were irregular; the straight edges seen in Fig. 18 are from the particles folding back on themselves (presumably during drying). The totally random stacking of the particles on the carbon support film suggests that the bentonite has almost completely dispersed right down to individual smectite layers.

EDX analyses of Wyoming bentonite are similar to those of "Composite #1" excepting that Wyoming bentonite shows no presence of potassium (Fig. 19).

The differences in morphology of "Composite #1" and Wyoming bentonite suggest that the genesis of the two clays was somewhat different. "Composite #1" may have formed from weathering or alteration of a mica-like mineral and has inherited characteristics of mica, such as particle shape, and includes layers with an illite composition. Alternatively, this predominantly montmorillonite sediment has undergone diagenetic alteration with some random recrystallisation of montmorillonite to illite. Wyoming bentonite, on the other hand, has an irregular shape and shows no evidence of being influenced by the crystallography of a precursor mineral nor does it show any signs of recrystallisation.

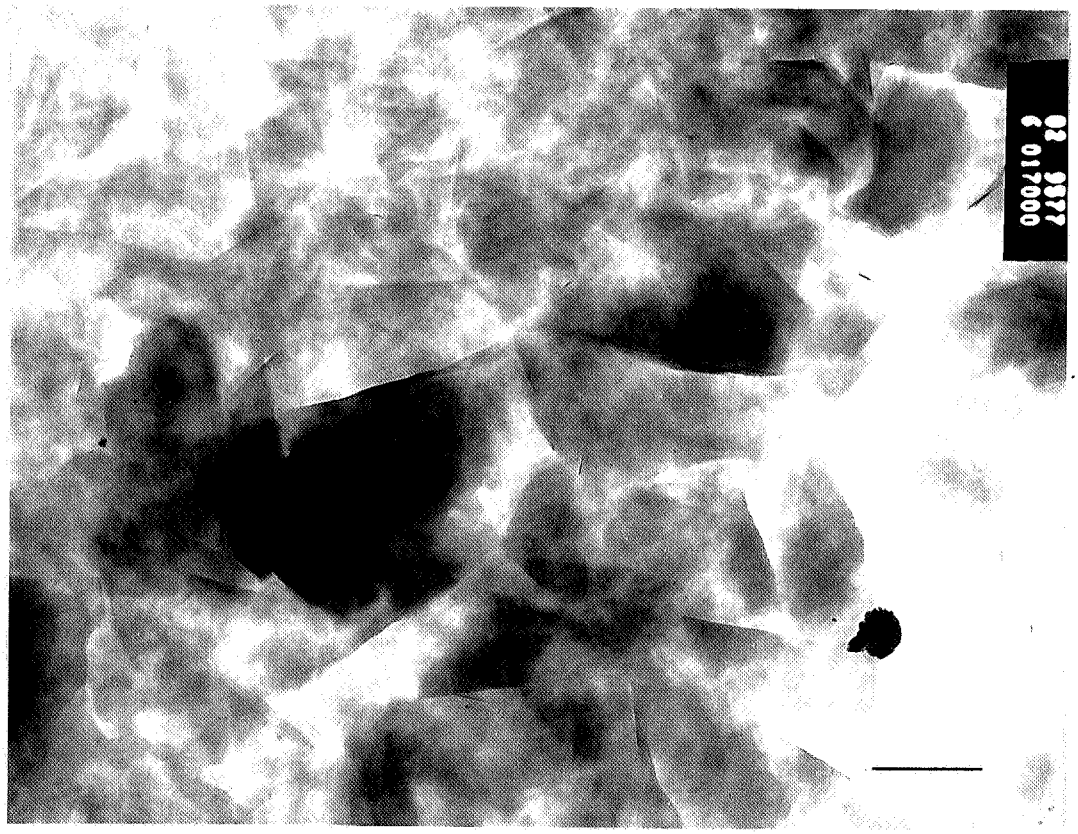


Fig. 18. ***Wyoming bentonite.*** **Transmission electron micrograph of bentonite as very thin flakes often 1μm or more in extent. Scale bar 0.5μm, photo. no. 9577.**

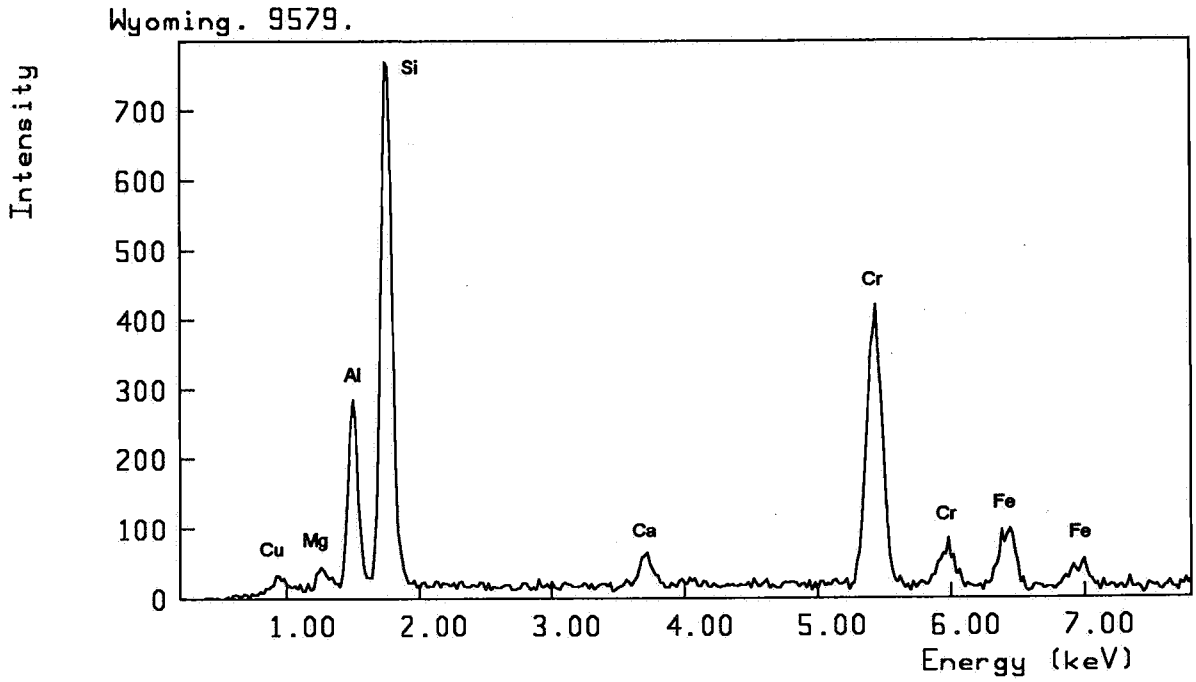


Fig. 19. EDX spectrum of Wyoming bentonite

DISPERSION OF CLAY LUMPS

Additional tests were done on sample #135011 +75μm from previous analyses (Raven *et al.*, 1992), to determine the effect of various cations on the dispersibility of the bentonite. Approximately 5g of sample was placed into each of three glass beakers with approximately 20 ml each of water, 1M NaCl and 1M LiCl respectively. The beakers were left overnight to allow the solutions to saturate the air dried samples. The samples were washed repeatedly to remove excess cations, followed by vigorous shaking with 20ml of water in a Spex shaker mill for 10 minutes. The <2μm fraction was extracted from each sample by successive centrifugation, oven dried (105°C) and carefully weighed to determine the amount of dispersed material.

Results of the dispersion tests on the +75μm sample indicated that when saturated with either LiCl or NaCl, the bentonite samples dispersed relatively easily. Percentages of >2μm fraction of 6.6% and 5.9% were recorded for NaCl and LiCl saturation respectively. Binocular microscopic inspection of the >2μm fraction showed clean, fine quartz grains indicating complete dispersion of the bentonite.

The water dispersed sample, however, contained 22.5% >2μm material. This comprised clay aggregates and clay-coated quartz grains confirming incomplete dispersion of clay.

DISCUSSION AND CONCLUSIONS

The 7 composite samples of clay examined all had a high smectite content with minor quartz and anatase. Composite #4 also contained 16% dolomite and <1% analcime. Composite #5 contained <1% dolomite. Chemical analyses supplied by CML showed all samples had a potassium content slightly higher than 1%. Additional tests on sample "Composite #1" showed that the potassium was not present as an exchangeable interlayer cation but was present as illite which was randomly interstratified with smectite. For "Composite #1", about 10% illite was present in the clay fraction. From an analysis of the clay fraction, a chemical formula was determined for the smectite component. The smectite was found to be a dioctahedral clay with a low tetrahedral charge and therefore classified as a **Wyoming-type** montmorillonite. A value of 0.39 magnesium in the octahedral site (based on 11 oxygens) is high for a **Wyoming-type** montmorillonite (Mg average of 0.19 octahedral positions) and would place this clay on the borderline between **Wyoming-type** and **Cheto-type** montmorillonite (Mg average of 0.55 octahedral positions) (Güven, 1988). Clays of the two types exhibit very different physical behaviour (Grim & Kulbicki, 1961).

At least some of the clay does not disperse readily in water and possible physical causes were examined using SEM and TEM. No non-clay mineral cements were detected but in comparison with Wyoming bentonite, there was a higher proportion of very fine-grained clay particles in the Arumpo montmorillomite. This resulted in very fine average pore space between clay microaggregates which may have acted to restrict fluid movement in clay lumps and also effectively increased the number of contact bonds between clay microaggregates, both of which are factors which could inhibit dispersibilty. Problems with dispersing certain Australian montmorillonite clay soils has been investigated previously and concluded to be due to high electrostatic interaction between clay sheets and to particle-particle, non-ionic bonds between clay microaggregates (Norrish & Tiller, 1976).

The effect of randomly interstratified illite on the disperibility of Arumpo montmorillonite is uncertain. The presence of illite quite likely reflects the natural process of diagenic alteration of montmorillonite to illite. This process requires an increase in the tetrahedral charge on the montmorillonite in order to fix potassium. This suggests that some of the montmorillonite, at least, may have a higher layer charge than indicated from chemical data and may be a contributing factor in the dispersion difficulties.

Using a combination of finer grinding, sodium or lithium saturation, followed by washing and vigorous shaking, it was possible to disperse the clay fraction of the >75μm fraction leaving a clean, fine quartz residue. Dispersion is therefore a function of the physical properties of the clay and not the result of any cementing agent.

27 October, 1992

REFERENCES

Brindley, G.W. and Brown, G. 1984. *Crystal Structures of Clay Minerals and their X-ray Indentification.* Mineralogical Society, London.

Grabowska-Olszewska, B., Osipov, V. and Sokolov, V., 1984. *Atlas of the microstructure of clay soils.* Panstwowe Wydawnictwo Naukowe, Warsaw.

Güven, N., 1988. Smectites. in Bailey, S.W. (ed) Hydrous Phyllosilicates. *Reviews in Mineralogy* V.19:497-559.

Grim, R.E. and Kulbicki, G., 1961. Montmorillonite. High-temperature reactions and classification. *American Mineralogist,* 46:1329-1369.

Norrish, K. and Tiller, K.G., 1976. Subplasticity in Australian soils. V Factors involved and techniques of dispersion. *Australian Journal of Soil Research,* 14:273-289.

Raven, M.D. (1990) XPLOT Version 3.2 - User Manual. Manipulation of X-ray Powder Diffraction Data. *CSIRO Division of Soils Technical Memorandum No.24/1990.* 26pp.

Raven, M.D., Keeling, J.L. and McClure, S.G. 1992. Mineralogical Analysis of Arumpo Bentonites and Bandar Palau Kaolin, *CSIRO Division of Soils Technical Memorandum No.50/1992.* 8pp.

Self, P.G. (1989) PC-PW1800 - User Manual. PC Based System for the Control of a Philips PW1800 X-ray Diffraction System. *CSIRO Division of Soils Technical Memorandum No. 1/1989.* 29pp.

000138

ABSORBENT CLAY PROJECT

INTERIM PROGRESS REPORT No.2 TO MINES AND ENERGY, SOUTH AUSTRALIA

RESULTS ON THE UPTAKE OF Ni, Cd, Cr, Pb AND BENZENE BY SELECTED CLAYS

P.G. Slade and R.W.L. Kimber

CSIRO
Division of Soils
Commonwealth of Australia

November, 1994

TABLE OF CONTENTS

INTRODUCTION	1
SORPTION BY CLAYS	1
Smectites	2
Kaolin	2
Palygorskite and Sepiolite	2
EXPERIMENTAL	3
Column Method	4
HPLC Method	4
RESULTS AND DISCUSSION	7
Heavy Metals	7
Benzene	9
CONCLUSIONS	10
REFERENCES	11

APPENDIX 1:
X-ray Fluorescence Analyses of heavy metal cations

APPENDIX 2:
Industrial minerals in soil sealants and waste dump linings

Introduction

The need to reduce environmental pollution presents major scientific, ecological and social problems both currently and for the future. Considering that comprehensive legislation and safety standards are now being introduced in Australia, the development of suitable methods to contain man-made pollutants is imperative. In this context it is expected that natural and modified clays will play a major role. The Absorbent Clay Project was initiated by Mines and Energy, South Australia (MESA) in January 1994 to examine potential new applications for South Australian clays in the containment of water borne contaminants, principally toxic heavy metals and organic substances.

In this investigation, various local clays were selected and characterised as reported in "Absorbent Clay Project - Progress Report No. 1" (Churchman *et al.*, 1994). The present report describes progress to date on comparative sorption studies from aqueous solutions of heavy metal cations of Ni, Cd, Cu and Pb, and the non-polar organic molecule benzene. Sorption studies on unmodified clays are continuing. However, results to hand allow some prediction as to a clay's performance and confirm the need to modify clays in order to retain non-polar organic molecules. Experimentation with modification therefore, will be integrated with future sorption testing of organics.

Progress has been slowed by the need to develop a convenient technique that will allow liquid to flow through a clay barrier without it losing its very fine clay particles. An elegant method in the form of a modified High Pressure Liquid Chromatograph (HPLC) was adopted, but this has required ongoing adaptation to overcome problems caused by variations in the physical properties of different clay minerals. In conjunction, sorption studies are being made using glass columns which we had constructed for the purpose. These have the advantage in being able to accommodate bulk clay materials but are somewhat slower and allow less control over possible losses when dealing with volatile organic molecules.

Sorption by Clays

In Churchman *et al.* (1994) general structural information was provided for smectite, kaolin, illite and palygorskite that was related to these clays acting as absorbents. The mechanisms for sorption by clays were not discussed. As a principal aim of the Absorbent Clay Project is to examine the capacity of a group of mainly South Australian clays to act as sorbents for organic and inorganic pollutants, it is relevant to briefly review these mechanisms.

Smectites

Clay minerals, especially smectites, in addition to acting as cation exchangers, can imbibe guest organic molecules in much the same way as zeolites can entrap molecules within the pore space of a crystal lattice. Unlike zeolites, which have fixed pore dimensions, intercalation between the negatively charged silicate layers of smectites often causes the crystals to swell in order to accommodate the absorbed species.

Swelling of clay minerals occurs because the parallel silicate layers in these materials are held together by electrostatic and van der Waals forces rather than by covalent bonding. The electrostatic bonding arises when the negative charge on the layers is neutralised by interlayer cations. The strength of the bonding increases with the density of negative charge on the layers and is at a maximum in the micas where the silicate layers come together as closely as allowed by the size of the interlayer cations. Hence, mica crystals show little tendency to swell, and as a consequence, neutral molecules cannot be intercalated and the exchange of interlayer cations is difficult and slow. By contrast, in smectites, the charge density on the silicate layers is low and therefore the interlayer cations occur in low concentrations and are hydrated to a variable extent. Crystals of smectites will swell readily to accommodate penetration by polar molecules. However, when smectites have been dehydrated or outgassed they do not normally have interlayer pore space; it is created by guest molecules and the consequent swelling. Non-polar molecules are generally not able to intercalate into anhydrous smectites. However, this can be overcome by permanently opening the interlayer regions of smectites that will allow ready sorption of non-polar guest molecules.

Kaolin

In kaolins, where the charge on the silicate layers is very low and where, except for halloysite, water does not exist between the layers, intercalation of guest species can still occur under special conditions. These conditions generally depend upon initiating intercalation at the edges of the host crystals.

Palygorskite and Sepiolite

In the fibrous clays, palygorskite and sepiolite, there are slit-shaped channels which run parallel to the fibre axes. The availability of these channels for sorption is somewhat open to question but previous experimental work points to them having only a limited ability to take up guest molecules after initial outgassing (Barrer & Mackenzie, 1954; Barrer *et al.*, 1954).

Sorption of most species, including nitrogen and non-polar molecules seems to be confined to the external surfaces of the crystallites or to sites near the channel entrances.

However, such sorption can be very substantial because of the fine fibrous habit of the crystals and consequently the large external surface areas. The sorption of various hydrocarbon chains has been explained in terms of corrugations on the surfaces of palygorskite fibres. The straight chain paraffins are adsorbed to a greater extent than branched ones because the former are better accommodated than the latter. The overall conclusion from many studies is that although the fibrous clays show good sorption capacities and some selectivity they do not function as true molecular sieves. The latter have molecular frameworks forming regular arrays of apertures into internal pores. The size of the apertures is such as to enable some molecules to enter the porous structure while others, on the basis of their larger effective size, are rejected.

Experimental

To test the uptake of the metal cations, and also in part the sorption of benzene, a set of percolation columns was locally custom made by Buxton Glasscraft at Marion. The design is illustrated in Fig. 1.

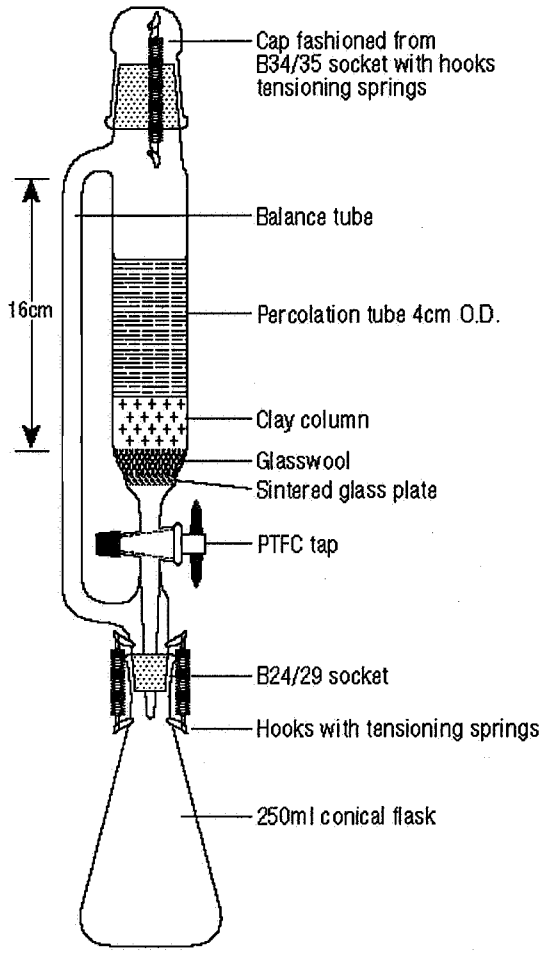


Fig. 1. Percolation column used in sorption studies.

Just above the sintered glass plates, the columns were packed with Merck glasswool to a depth of ~0.75 cm. On top of the glasswool, 15 gms of the air dried and lightly ground clay under test was carefully introduced with the help of a long stemmed glass funnel. The samples were then partially consolidated by gently shaking the columns. With the aid of a thistle funnel, 100 mls. of solution containing 1000 ppm of Ni, Cd, or Cr (as chlorides) or 1000 ppm Pb as nitrate were introduced into the columns. These were then capped and, in order to emulate the ponding of toxic liquids above barriers incorporating clays, allowed to stand for 4 days before the taps were opened. Except for Wyoming montmorillonite, which became swollen and rather impermeable, percolation through the clays took place in about an hour. Percolation through the Wyoming montmorillonite took up to 1 week.

After a series of calibration standards containing either 100 ppm or 500 ppm had been prepared by diluting the original stock solutions for each metal, X-ray fluorescent (XRF) spectroscopy was used to measure the concentrations of heavy metals in the percolated solutions. The XRF intensities from samples of the unknowns were compared with those of the relevant standards at the wavelengths of the Kα lines for Ni, Cd and Cr but at the Lβ line for Pb. Full details of the analytical method can be found in the CSIRO Division of Soils Technical Reports No. 37/1994 - 49/1994 and 41/1994 (Appendix 1).

Two methods were used to test for benzene sorption; one involved the use of glass columns and the second used a high performance liquid chromatograph (HPLC).

Column Method

To test for benzene sorption with the glass columns, a reference column was prepared with 15 gms of fine glass beads replacing the clay just above the glasswool. In order to minimise loss of the volatile organic, the QUICKFIT cone and socket joints were held tightly closed by the use of hooks and springs. Percolation of a 0.1% (1000 ppm) benzene/water solution through the clays and the reference column was carried out as described above. The amounts of benzene in the solutions which had percolated through the clays under test, or through the reference column containing the glass beads, were compared with that in the stock solution by ultra violet (UV) spectrophotometry using a Beckman model DU 640 Spectrophotometer.

HPLC Method

Analysis of the capacity of various clays for sorption of benzene was carried out by injecting 5 µl samples of a 0.1% benzene/water mixture into an HPLC (GBC Scientific Equipment, Plate 1, Fig. 2) fitted with automatic injector, pre-column stream splitter and UV detector. The solvent stream of 100% water could be passed alternately through small columns of fine glass beads and the clay. The aim was to use clay samples that had a

nominal particle size between 2 and 1 microns, but these were not always available with some samples also containing smaller particles. Attempts were also made to carry out sorption tests with these samples although they caused excessive HPLC pressures.

Cartridges (10 mm length by 4.3 mm diam.) with 2 micron pore size titanium frits at either end (Upchurch Scientific) were prepared by placing Millipore filters (0.1 µm) on either side of the frit, ie. inside and outside of the cartridge, on the outlet end. The small diameter Millipore filters were prepared from larger discs using a special punch manufactured in Adelaide. The clay to be tested (40 mg) was put into a cartridge and then loosely packed by light tamping. A 0.22 µm Millipore filter was placed on top of clay and then the column filled with fine glass beads. Finally the upper frit cap was fitted. The cartridge was then inserted into the stainless steel holder and attached to the HPLC (Figs 2 & 3). Peak areas reflected by UV absorption at 252 nm were used to compare the transport of the benzene through the clay sample compared to the glass beads. Relative reduction in peak area was taken to indicate relative sorption capacity of the clay.

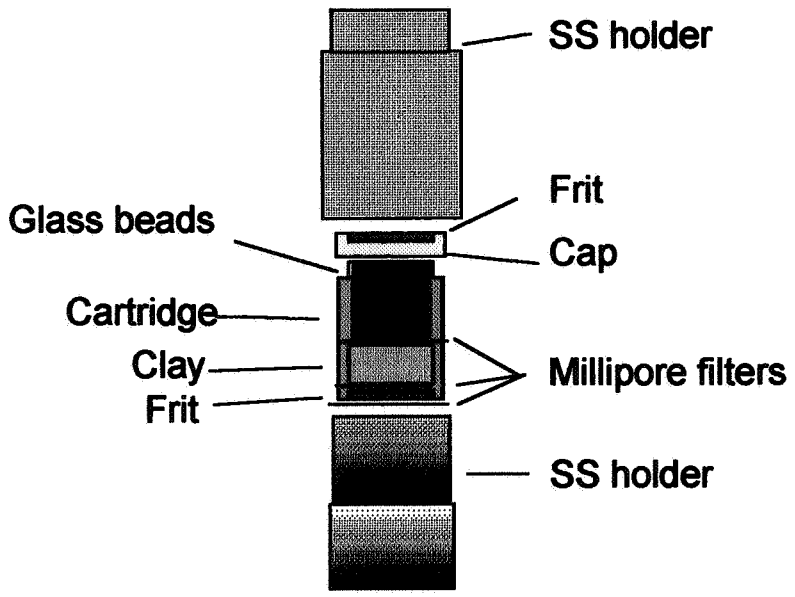


Fig. 3. Partially exploded and cutaway view of HPLC column and cartridge assembly.

As discussed above, very fine particles in the samples caused excessive HPLC pressures. However, we found that pressures up to ~30 KPa could generally be accommodated, although pressures around 20 KPa were more ideal and did not give problems with leaks. Sometimes a stabilisation period of some hours was required after installing a newly packed column as fines tended to be washed through the system. After some time a self-sealing process usually resulted in a stable baseline.



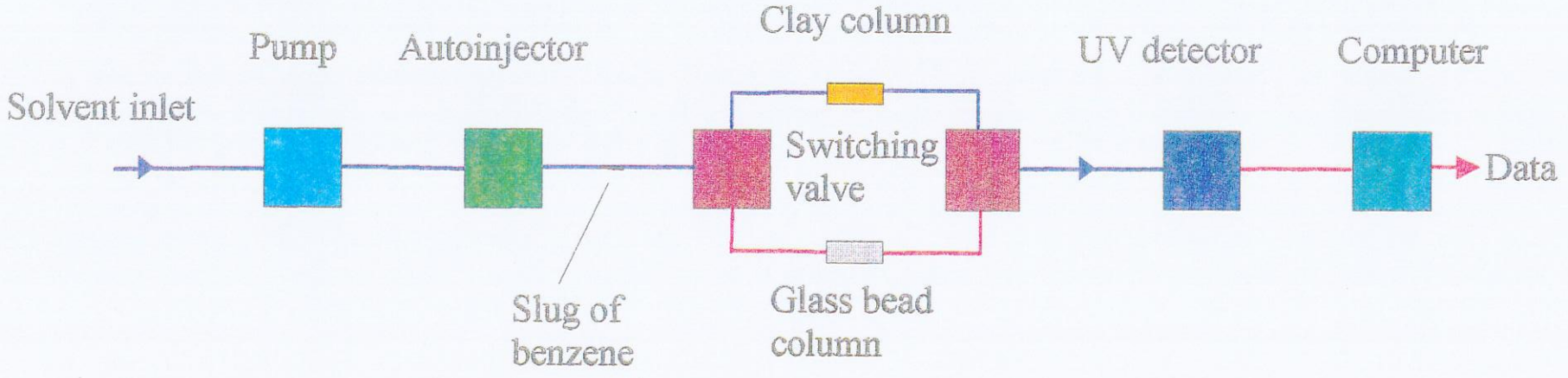


Plate 1 and Figure 2. Photo and diagrammatic representation of the HPLC system.

0001455

Results and Discussion

Heavy Metals

Table 1 shows the percentages of each element removed by the listed clays from the original 1000 ppm stock solutions of the heavy metals. Apart from those for Birdwood kaolinite, the results show that any of the clays examined could be used to remove metals from solutions containing them. However, and as might be expected, those clays which are smectitic or appreciably smectitic would be the most useful.

Table 1 Percentage uptake from 100 mls of 1000 ppm metal solutions by 15 gms of selected clays. 100% ≡ 7 gms/kg clay.

Clay	Metal			
	Ni	Cd	Cr	Pb
Commonwealth Law Court 5.5-9.1 m	78.6%	93.2%	80.5%	100.0%
Keswick Clay	95.6	98.5	85.6	100.0
Birdwood Kaolinite	6.2	15.0	6.6	37.6
Arumpo Bentonite TP-1 (M020593)	99.9	98.5	97.9	100.0
*Garford Palaeochannel P25 (5-9m composite)	98.0	100.0	79.3	100.0
Wyoming Bentonite (Na-saturated)	98.6	100.0	nd	nd
Muloorina Illite (Pit Sample)	61.2	31.3	73.0	100.0
Solution pH	5.28	4.70	2.85	4.15

* This sample is a mixture of auger cuttings taken at 1 metre intervals between 5 to 9 metres below the surface and comprises illite and palygorskite with minor halite. nd = not determined.

Muloorina illite is known to have a cation exchange capacity of only about 20% of that for Wyoming bentonite and, as a result, the illite does not take up the metal ions as well as the smectitic clays. However, it would appear that the very fine particle size of the illite (and consequently its large surface area) enables it to capture metals from solution reasonably well. Repeated percolations showed, however, that the concentrations of metals in solution rose after the initial pass, or in other words, the capacity of the illite to retain the heavy metals is more limited than for the smectitic clays. The concentration of metals in solutions percolated several times through the smectitic clays, changed little after the first pass.

Earlier work (Churchman et al., 1994, Table 3) showed that the Adelaide clays, represented here by the Keswick and the Commonwealth Law Court clays, contain high percentages (~50%) of particles below 1 μm. Consequently, one may expect that their large surface areas have contributed to their sorptive capacities.

Of particular note is the very strong sorption of Pb by all clays, including Birdwood kaolinite. Why the clays are showing such strong affinity for Pb is not clear at this stage.

The recommended upper limit for metals in soils are given jointly by the Agriculture and Resource Management Council of Australia and New Zealand and the Australian and New Zealand Environment and Conservation Council (1994) as 75 mg/kg (Ni), 3 mg/kg (Cd) and 250 mg/kg for Pb. Table 1 shows that any of the selected clays can, within the context of the experimental parameters, take up higher concentrations than the recommended upper limits, and therefore would seem to have potential for use in protective barriers. Such barriers, however, may be formed from mixtures of clays in order to achieve desirable combinations of mechanical and sorptive properties (Fiebiger & Schellhorn, 1994, reproduced as Appendix 2). In spite of their obvious advantages in having high cation exchange capacities, smectitic clays shrink and swell leading to the possible formation of cracks in barriers. Fiebiger and Schellhorn (1994) point to the benefits of incorporating kaolinite and illite in mixtures formulated as sealing barriers.

The pH values for the stock solutions of the heavy metals whose uptake is reported here are shown in Table 1; they are all acidic with the value for chromium solution being lowest. This is to be expected as a hydrolysis reaction takes place when chromic salts are dissolved in water. The reaction releases hydrogen ions so lowering the pH of the solution. Under acid conditions, cations are removed from the structures of the clay minerals and eventually silica remains (Granquist & Sumner, 1958; Churchman & Jackson, 1976). This process while decreasing permeability, will also reduce the cation retention properties of smectitic clays. Acid wastes will therefore present special problems for clay barriers.

Benzene

Table 2, which gives the results for 10 clay samples, shows that significant sorption of benzene under the experimental conditions described only occurred with sample P25 (~25 % palygorskite). On the other hand, Wyoming bentonite, which we have modified with dimethyl-dioctodecyl ammonium bromide (DMDOAB) removed 90% of benzene from the test solution. However, as previously mentioned some samples could not be tested properly because of the presence of very fine clay.

Table 2. Sorption of benzene on clays

Clay	Particle size range (μm)	Treatment	Sorption	Remarks
Smectite				
Wyoming Bentonite	1 - 2	nil	0	
Wyoming Bentonite (John C. Lane)	1 - 2	nil	0	
Wyoming Bentonite	1 - 2	dimethyl-dioctodecyl ammonium bromide	90%	
Arumpo TPI (M010893)	1 - 2	nil	-	clay too fine
Palygorskite				
Garford Palaeochannel P25 (5 - 9 m composite) (illite/paly* 60:25)	bulk	nil	30%	mixture
P35 (5 - 6 m) (dol/paly 75:20)	0.5 - 1	nil	0	
P35 (6 - 7 m) (dol/paly 90:5)	1 - 2	nil	0	
Mallina Attapulgite (paly/kao/ill 55:20:20)	0.5 - 1	nil	-	clay too fine
Kaolin				
Birdwood Kaolin	1 - 2	nil	0	
Illite				
Muloorina Illite	0.15 - 1	nil	-	clay too fine

*Abbreviations: dol - dolomite; paly - palygorskite; ill - illite, kao - kaolin

These preliminary results show that sorption of benzene on clays can be conveniently determined using HPLC equipment, although difficulties arise if a significant proportion of the clay particles are below 1 μm. The benefits of this method to evaluate hydrocarbon sorption on clays are:

- only small samples are needed - important for treated clays and those difficult to separate into the appropriate size fraction
- only very low amount of noxious chemicals need to be used in tests
- potential exists to easily determine rates of sorption of a given hydrocarbon on a particular clay by repeated injection.

The results of experiments carried out with benzene suggest that few unmodified natural clays will sorb significant amounts of petroleum hydrocarbons. The high degree of sorption achieved with the organically modified Wyoming Bentonite points to the effectiveness of such treatment. Future work will concentrate on making clays organophilic and will investigate their sorption of benzene, toluene, xylene and other hydrocarbons as appropriate.

Conclusions

Our investigations to date have shown that a range of locally available clays have appreciable sorption capacities for heavy metals. However, in their natural state, the clays, with the exception of the Garford P25 composite, do not show any appreciable sorption of benzene. Our results showed that, under test conditions, an organically modified sample of Wyoming Bentonite removed 90% of benzene from solution. Therefore we expect that with appropriate treatment, some clays can be modified to effectively take up targeted hydrocarbons. This will be the focus of the next stage of the project.

The results presented here should be taken as indicative only and in the event of a plan to use a specific material for pollution containment, further testing would be necessary to establish sorption limits.

References

Agriculture and Resource Management Council of Australia and New Zealand, Australian and New Zealand Environment and Conservation Council (1994) *National Water Quality Management Strategy Guidelines For Sewerage Systems 12.* Commonwealth of Australia.

Barrer, R.M. and Mackenzie, N. (1954) Sorption by attapulgite. Part I. Availability of intra-crystalline channels. *J. Phys. Chem.* **58**: 560-568.

Barrer, R.M., Mackenzie, N. and McLeod, D.M. (1954) Sorption by attapulgite. Part II. Selectivity shown by attapulgite, sepiolite and montmorillonite for n-paraffins. *J. Phys. Chem.* **58**: 568-572.

Churchman, G.J., Ferris, G.M., Keeling, J.L., McClure, S.G., Raven, M.D. Self, P.G. and Slade, P.G. (1994) Absorbent clay project: Progress report No.1 - Characterisation of the selected clays. CSIRO - Division of Soils, Report to Mines & Energy, South Australia, 109pp.

Churchman, G.J. and Jackson, M.L. (1976) Reaction of montmorillonite with acid aqueous solutions: solute activity control by a secondary phase. *Geochimica et Cosmochimica Acta* **40**: 1215-1259.

Fiebiger, W. and Schellhorn, M. (1994) Industrial minerals in soil sealants and waste dump linings. *Industrial Minerals* **317**: 41-47

Granquist, W.T. and Sumner, G.G. (1958) Acid dissolution of a Texas bentonite. In (Ed. A Swineford) *Clays Clay Minerals, Proceedings of the 6th National Clay Conference.* : 298-308.

APPENDIX 1

X-ray Fluorescence Analyses of heavy metal cations

CSIRO Division of Soils Technical Reports 37-39/1994 & 41/1994

P.G. Fazey

CSIRO Division of Soils Technical Report No. 37/1994

NOT FOR PUBLICATION.
The material contained herein has not been refereed. It may be quoted as a personal communication following the written consent of the authors.

An X-ray Fluorescence Method to Determine Nickel in Water Samples Containing $NiCl_2$ using a Philips PW1480 Spectrometer.

P G. Fazey

Introduction

A quick analytical technique to determine the concentration of nickel in an aqueous solution produced by adsorbance testing of clay materials has been developed. An X-ray fluorescence spectrometry liquid analysis technique was used to perform the analysis. The technique produced results in 30 seconds and the solution was totally recoverable enabling reuse in subsequent experiments.

Preparation of Standards

Deionised water and three solutions, 100 ppm Ni, 500 ppm Ni and 1000 ppm Ni respectively were prepared by Dr Phil Slade to be used as calibration standards. The standard solutions were prepared from $NiCl_2$. The same compound was used in the adsorbance experiments.

Program Assembly

The following data was assembled within the PW1480 XRF X40 control software in preparation for calibration. The channel data was stored to parameterbank SCMOFUSE.X48

Channel Assembly

The following channel was assembled to measure Ni Kα radiation.

Name	Line	kV	mA	Filter	Collimator	Xtal name	no.	ord.	Angle	+Off_ set	-Off_ set	Det.	Lower level	Upper level
Ni	KA	80	35	Out	Fine	LiF200	2	1	48.685	0.00	0.00	FL	30	70

Analytical Program

The following analytical program was developed to measure Ni in the aqueous solutions.

```
CSIRO Division of Soils                          19-AUG-94 16:37
 AP: NIWATER    Recal.:  NO  Created: 19-AUG-94 15:28  Revised: 19-AUG-94 15:55
 Ni in Water ScMo            Ch.Mask: SMALL            Req. data: none
 CP: NIWATER    Spinner:  IN  Delay:  0 s               Sum normalisation:   NO
 Monitors: NIWATER
```

Channel no	Reporting code	Print name	Print seq	Dec	Units	---Conc.limits--- lower	upper	Meas time	---Corrections-- drift	BKG	overl.
1	Ni	Ni	1	0	ppm			20	y		

Monitor Buffer

The following Monitor Buffer called NIWATER was assembled to measure monitor sample R8. This data will be used as a reference for the calibration. The data is used to correct for any instrumental changes which may have occurred in the spectrometer since the time of the calibration procedure.

```
                    CSIRO Division of Soils                    19-AUG-94 16:38
MB: NIWATER          Computed first: 19-AUG-94 15:31     Last:
For buffered DC                                          Monitor data: VALID

Correction for slope

                    Ni
Meas. time:         20
Drift factor:     1.0000
Background:       0.000

Monitor sample: R8
Measured first: 19-AUG-94 15:31  Last:
Delay:  0 seconds                Channel mask: SMALL     Status: NOT MEASURED
                    Ni

0 hour rate:      8.689
```

Measuring the Calibration Standards

5 mls of each of the known solutions were pipetted into 32mm plastic XRF liquid sample cups equipped with 1μm mylar windows. The liquid cups were placed into 32mm aluminium XRF sample holders and the standards measured at ambient air pressure on a Philips PW1480 X-ray fluorescence spectrometer energising a Sc/Mo X-ray tube anode. The analytical program used was NIWATER accessed through X40 version 4.0 control software.

Important Note

Liquid samples must only be run using ambient air pressure in the X-ray path. Samples run under vacuum will cause damage to the spectrometer.

Calibration Results

A simple calibration approach was chosen due to the simple matrix to be analysed. An alpha coefficient for Ni was calculated to correct for the matrix contribution of the chlorine in the standards. The calibration statistics appear below. Calibration data was stored to Calculation Program NIWATER. Figure 1 graphically shows the results of the calibration results.

Calibration Statistics

```
CSIRO Division of Soils                        19-AUG-94 16:38
 Ni              Used standards:      4  Calc. parameters:  2     19-AUG-94 16:38
 AP:    NIWATER  Conc. file:    NIWATER  Countrate file:    NIWATER   Unit: ppm
 RMS:   0.67810  K-factor:     0.00020  Error weighting: Sq. root( C + 1000.00 )
 Model: DJ                             E:    0.00048        D:  -0.00225

    Type      Factor  Corrections          Type      Factor  Corrections
 F Alpha    36.40374  C(Ni)
```

Chemical Concentrations versus XRF Results

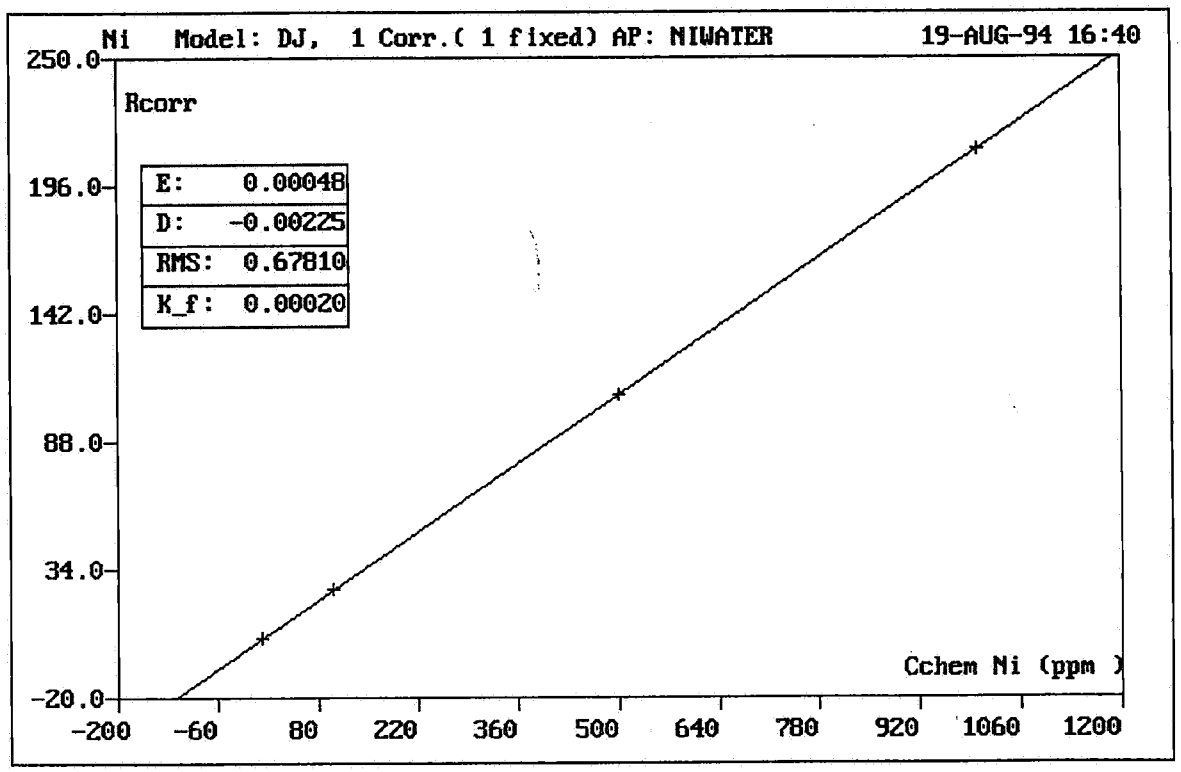
Below is a list of the calculated Ni values compared to the known chemical values.

CSIRO Division of Soils 19-AUG-94 16:39

No	St.	R(Ni) (kcps)	Concentrations (ppm) for Ni chemical	calc.	diff.	uncorr.	Matrix corr.	19-AUG-94 16:38 Identification
4		4.5500	0	-0	-0.48	-0	1.0000	WATER
3		25.3290	100	101	0.74	101	1.0036	100ppm
2		105.752	500	500	-0.37	500	1.0182	500ppm
1		203.474	1000	1000	0.11	1000	1.0364	1000ppm

The calibration data was stored to Calculation Program NIWATER within the X40 control software.

Figure 1 - Nickel as $NiCl_2$ in water calibration results (kcps vs conc)



Discussion

The above method is suitable to measure Ni in the ranges 1 ppm to 1000 ppm present as $NiCl_2$ in water. It is recommended that a pure water blank be measured during each unknown run to detect any background drift.

Summary of Analytical Data

Spectrometer:	Philips PW1480 XRF
X-ray tube anode:	Sc/Mo dual anode
Control software:	X40 version 4.0
Analytical program:	NIWATER
Monitor buffer:	NIWATER
Calculation program:	NIWATER
Parameterbank:	SCMOFUSE

CSIRO Division of Soils Technical Report No. 38/1994

NOT FOR PUBLICATION.
The material contained herein has not been refereed. It may be quoted as a personal communication following the written consent of the authors.

An X-ray Fluorescence Method to Determine Chromium in Water Samples Containing $CrCl_3$ using a Philips PW1480 Spectrometer.

P G. Fazey

Introduction

A quick analytical technique to determine the concentration of chromium in an aqueous solution produced by adsorbance testing of clay materials has been developed. An X-ray fluorescence spectrometry liquid analysis technique was used to perform the analysis. The technique produced results in 40 seconds and the solution was totally recoverable enabling reuse in subsequent experiments.

Preparation of Standards

Deionised water and three solutions,100 ppm Cr, 500 ppm Cr and 1000 ppm Cr respectively, were prepared by Dr Phil Slade to be used as calibration standards. The standard solutions were prepared from $CrCl_3$. The same compound was used in the adsorbance experiments.

Program Assembly

The following data was assembled within the PW1480 XRF X40 control software in preparation for calibration. The channel data was stored to parameterbank SCMOFUSE.X48

Channel Assembly

The following channel was assembled to measure Cr Kα radiation.

Name	Line	kV	mA	Filter	Collimator	Xtal name	no.	ord.	Angle	+Off_ set	-Off_ set	Det.	Lower level	Upper level
Cr3	KA	80	35	Out	Coarse	LiF200	2	1	69.35	0.00	0.00	FL	10	80

Analytical Program

The following analytical program was developed to measure Cr in the aqueous solutions.

```
CSIRO Division of Soils                          16-NOV-94 13:16
 AP: CRWATER     Recal.: YES  Created: 10-OCT-94 14:53  Revised:
 Cr in water                  Ch.Mask: SMALL            Req. data: none
 CP: CRWATER    Spinner:  IN  Delay:  0 s               Sum normalisation:   NO
 Monitors: CRWATER

 Channel Reporting  Print  Dec  Units   ---Conc.limits---  Meas ---Corrections--
 no code      name   seq                  lower    upper   time drift BKG overl.
  1 Cr3         Cr    1     0    ppm                         40   y
```

Monitor Buffer

The following Monitor Buffer called CRWATER was assembled to measure monitor sample R8. This data will be used as a reference for the calibration. The data is used to correct for any instrumental changes which may have occurred in the spectrometer since the time of the calibration procedure.

```
CSIRO Division of Soils                          16-NOV-94 13:16
 MB: CRWATER          Computed first: 10-OCT-94 14:56      Last: 31-OCT-94 11:27
 For buffered DC                                           Monitor data: VALID

 Correction for slope

                    Cr3
 Meas. time:         40
 Drift factor:    0.9749
 Background:      0.000

 Monitor sample: R8
 Measured first: 10-OCT-94 14:56  Last: 31-OCT-94 11:27
 Delay:  0 seconds                Channel mask: SMALL      Status: NOT MEASURED
                    Cr3

 0 hour rate:       3.839
 Last rate:         3.938
```

Measuring the Calibration Standards

5 mls of each of the known solutions were pipetted into 32mm plastic XRF liquid sample cups equipped with 1μm mylar windows. The liquid cups were placed into 32mm aluminium XRF sample holders and the standards measured at ambient air pressure on a Philips PW1480 X-ray fluorescence spectrometer energising a Sc/Mo X-ray tube anode. The analytical program used was CRWATER accessed through X40 version 4.0 control software.

Important Note

Liquid samples must only be run using ambient air pressure in the X-ray path. Samples run under vacuum will cause damage to the spectrometer.

Calibration Results

A simple calibration approach was chosen due to the simple matrix to be analysed. The calibration statistics appear below. Calibration data was stored to Calculation Program CRWATER. Figure 1 graphically shows the results of the calibration results.

Calibration Statistics

```
CSIRO Division of Soils                          16-NOV-94 12:48
 Cr3          Cr  Used standards:      4  Calc. parameters:  2     16-NOV-94 12:48
 AP:    CRWATER  Conc. file:    CRWATER  Countrate file:    149XRFB   Unit: ppm
 RMS:   0.98513  K-factor:     0.00070  Error weighting: Sq. root( C + 100.000 )
 Model: DJ                             E:    0.02068        D:  -0.00869

    Type       Factor  Corrections          Type       Factor  Corrections
 F Alpha    44.67165  C(Cr3)
```

Chemical Concentrations versus XRF Results

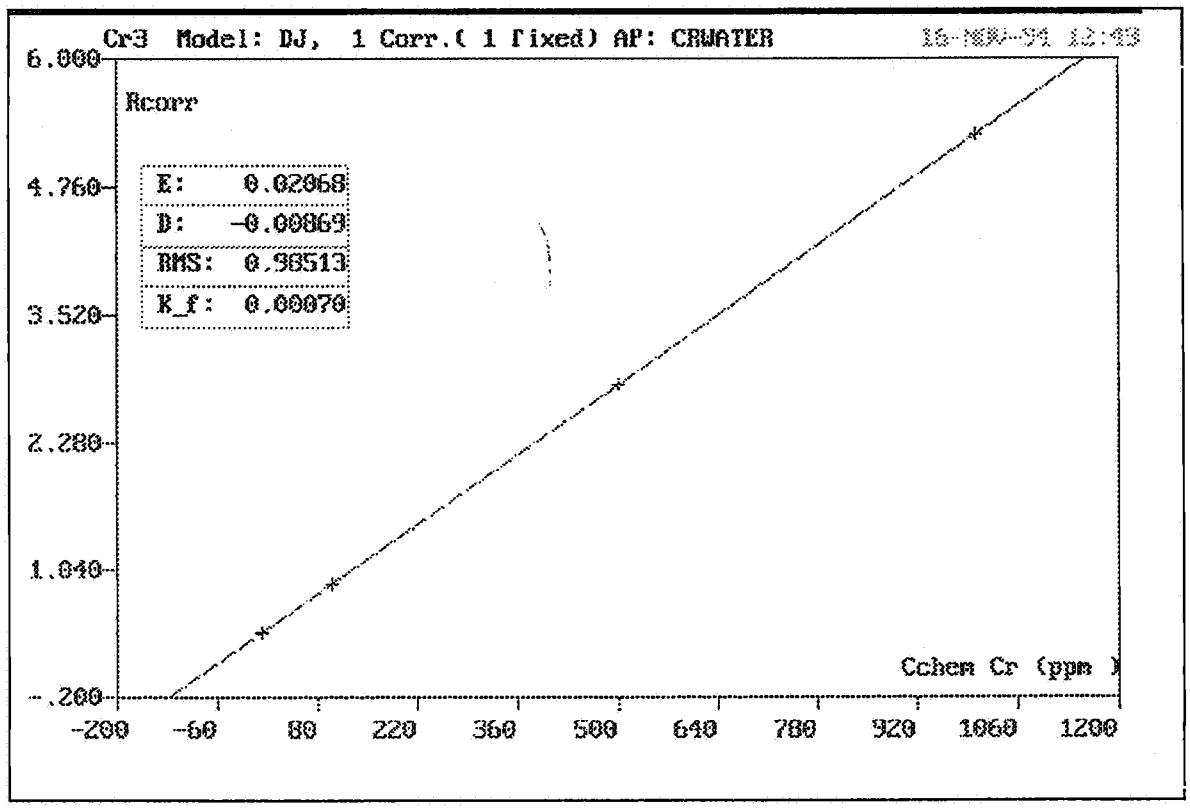
Below is a list of the calculated Cr values compared to the known chemical values.

CSIRO Division of Soils 16-NOV-94 12:48

No	St.	R(Cr3) (kcps)	Concentrations (ppm) for Cr chemical	calc.	diff.	Matrix uncorr.	corr.	16-NOV-94 12:48 Identification
1		0.4227	0	0	0.48	0	1.0000	WATER
2		0.8942	100	99	-1.18	99	1.0045	100PPM
3		2.7786	500	501	0.55	501	1.0223	500PPM
4		5.0315	1000	1000	0.13	1000	1.0447	1000PPM

The calibration data was stored to Calculation Program CRWATER within the X40 control software.

Figure 1 - Chromium as $CrCl_2$ in water calibration results (kcps vs conc)



Discussion

The above method is suitable to measure Cr in the ranges 1 ppm to 1000 ppm present as $CrCl_2$ in water. It is recommended that a pure water blank be measured during each unknown run to detect any background drift.

Summary of Analytical Data

Spectrometer:	Philips PW1480 XRF
X-ray tube anode:	Sc/Mo dual anode
Control software:	X40 version 4.0
Analytical program:	CRWATER
Monitor buffer:	CRWATER
Calculation program:	CRWATER
Parameterbank:	SCMOFUSE

CSIRO Division of Soils Technical Report No. 39/1994

NOT FOR PUBLICATION.
The material contained herein has not been refereed. It may be quoted as a personal communication following the written consent of the authors.

An X-ray Fluorescence Method to Determine Cadmium in Water Samples Containing $CdCl_2$ using a Philips PW1480 Spectrometer.

P G. Fazey

Introduction

A quick analytical technique to determine the concentration of cadmium in an aqueous solution produced by adsorbance testing of clay materials has been developed. An X-ray fluorescence spectrometry liquid analysis technique was used to perform the analysis. The technique produced results in 20 seconds and the solution was totally recoverable enabling reuse in subsequent experiments.

Preparation of Standards

Deionised water and three solutions, 100 ppm Cd, 500 ppm Cd and 1000 ppm Cd respectively, were prepared by Dr Phil Slade to be used as calibration standards. The standard solutions were prepared from $CdCl_2$. The same compound was used in the adsorbance experiments.

Program Assembly

The following data was assembled within the PW1480 XRF X40 control software in preparation for calibration. The channel data was stored to parameterbank SCMOFUSE.X48

Channel Assembly

The following channel was assembled to measure Cd Kα radiation.

Name	Line	kV	mA	Filter	Colli-mator	Xtal name	no.	Angle ord.		+Off_ set	-Off_ set	Det.	Lower level	Upper level
Cd2	KA	100	35	Out	Coarse	LiF200	2	1	15.245	0.00	0.00	SC	25	75

Analytical Program

The following analytical program was developed to measure Cd in the aqueous solutions.

```
CSIRO Division of Soils                          16-NOV-94 13:17
 AP: CDWATER    Recal.: YES  Created: 26-SEP-94 15:13  Revised: 27-SEP-94 14:49
 Cd in H2O                   Ch.Mask: SMALL           Req. data: none
 CP: CDWATER   Spinner:  IN  Delay:  0 s              Sum normalisation:   NO
 Monitors: CDWATER
```

Channel no	Reporting code	name	Print seq	Dec	Units	---Conc.limits--- lower	upper	Meas time	---Corrections-- drift	BKG	overl.
1	Cd2	Cd Ka	1	0	ppm			20	y		

Monitor Buffer

The following Monitor Buffer called CDWATER was assembled to measure monitor sample R8. This data will be used as a reference for the calibration. The data is used to correct for any instrumental changes which may have occurred in the spectrometer since the time of the calibration procedure.

```
CSIRO Division of Soils                          16-NOV-94 13:17
 MB: CDWATER          Computed first: 26-SEP-94 15:39     Last: 15-NOV-94 12:05
 For buffered DC                                          Monitor data: VALID

 Correction for slope

                    Cd2
 Meas. time:         20
 Drift factor:    1.1400
 Background:       0.000

 Monitor sample: R8
 Measured first: 26-SEP-94 15:38  Last: 15-NOV-94 12:05
 Delay:  0 seconds                Channel mask: SMALL     Status: NOT MEASURED
                    Cd2

 0 hour rate:     18.719
 Last rate:       16.420
```

Measuring the Calibration Standards

5 mls of each of the known solutions were pipetted into 32mm plastic XRF liquid sample cups equipped with 1μm mylar windows. The liquid cups were placed into 32mm aluminium XRF sample holders and the standards measured at ambient air pressure on a Philips PW1480 X-ray fluorescence spectrometer energising a Sc/Mo X-ray tube anode. The analytical program used was CDWATER accessed through X40 version 4.0 control software.

Important Note

Liquid samples must only be run using ambient air pressure in the X-ray path. Samples run under vacuum will cause damage to the spectrometer.

Calibration Results

A simple calibration approach was chosen due to the simple matrix to be analysed. The calibration statistics appear below. Calibration data was stored to Calculation Program CDWATER. Figure 1 graphically shows the results of the calibration results.

Calibration Statistics

```
CSIRO Division of Soils                          16-NOV-94 12:54
 Cd2      Cd Ka  Used standards:      4  Calc. parameters:  2     16-NOV-94 12:54
 AP:    CDWATER  Conc. file:    CDWATER  Countrate file:   146XRFB   Unit: ppm
 RMS:   1.17388  K-factor:     0.00084  Error weighting: Sq. root( C + 100.000 )
 Model: DJ                             E:   0.00343       D:  -0.04928
```

000160

Chemical Concentrations versus XRF Results

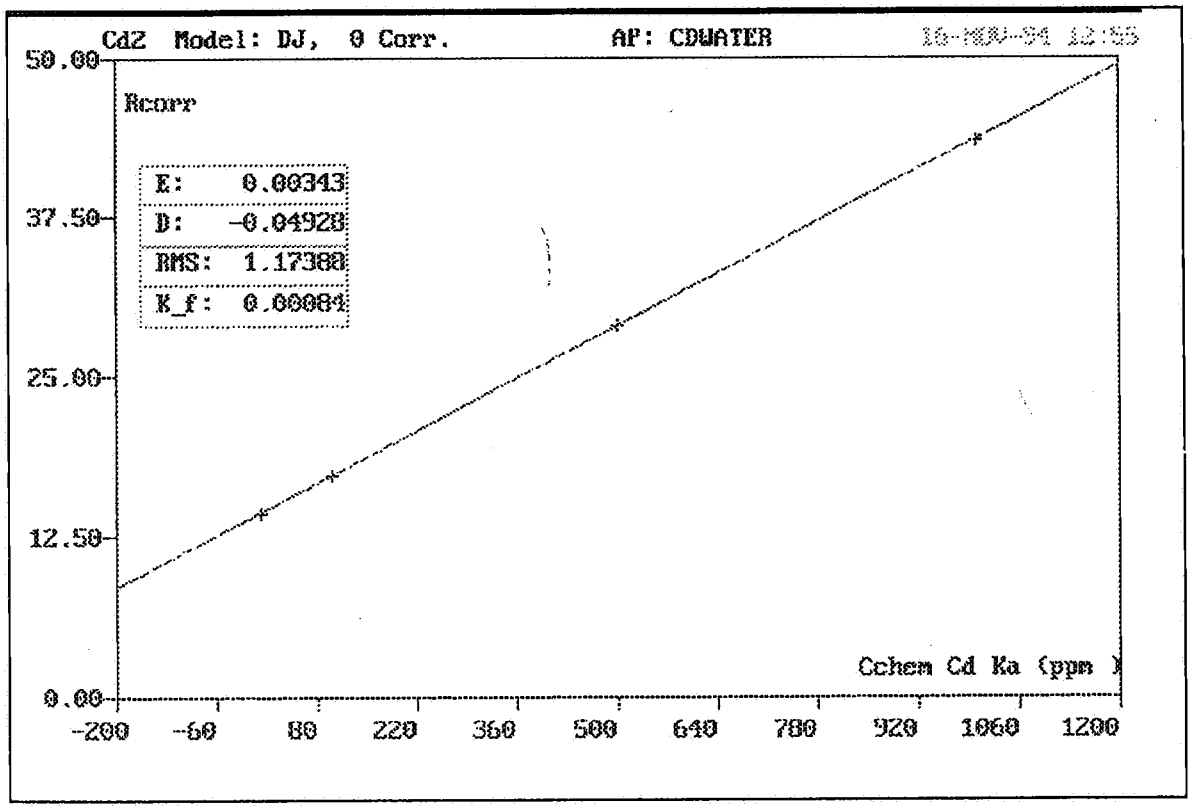
Below is a list of the calculated Cd values compared to the known chemical values.

CSIRO Division of Soils 16-NOV-94 12:54

No	St.	R(Cd2) (kcps)	Concentrations (ppm) for Cd Ka chemical	calc.	diff.	Matrix uncorr.	corr.	16-NOV-94 12:54 Identification
1		14.3813	0	1	0.58	1	1.0000	2107
4		17.2380	100	99	-1.41	99	1.0000	2110
3		28.9567	500	501	0.62	501	1.0000	2109
2		43.5182	1000	1000	0.19	1000	1.0000	2108

The calibration data was stored to Calculation Program CDWATER within the X40 control software.

Figure 1 - Cadmium as $CdCl_2$ in water calibration results (kcps vs conc)



Discussion

The above method is suitable to measure Cd in the ranges 1 ppm to 1000 ppm present as $CdCl_2$ in water. It is recommended that a pure water blank be measured during each unknown run to detect any background drift.

Summary of Analytical Data

Spectrometer:	Philips PW1480 XRF
X-ray tube anode:	Sc/Mo dual anode
Control software:	X40 version 4.0
Analytical program:	CDWATER
Monitor buffer:	CDWATER
Calculation program:	CDWATER
Parameterbank:	SCMOFUSE

CSIRO Division of Soils **Technical Report No. 41/1994**

NOT FOR PUBLICATION.
The material contained herein has not been refereed. It may be quoted as a personal communication following the written consent of the authors.

An X-ray Fluorescence Method to Determine Lead in Water Samples Containing $Pb(NO_3)_2$ using a Philips PW1480 Spectrometer.

P G. Fazey

Introduction

A quick analytical technique to determine the concentration of lead in an aqueous solution produced by adsorbance testing of clay materials has been developed. An X-ray fluorescence spectrometry liquid analysis technique was used to perform the analysis. The technique produced results in 40 seconds and the solution was totally recoverable enabling reuse in subsequent experiments.

Preparation of Standards

Deionised water and three solutions, 100 ppm Pb, 500 ppm Pb and 1000 ppm Pb respectively, were prepared by Dr Phil Slade to be used as calibration standards. The standard solutions were prepared from as $Pb(NO_3)_2$. The same compound which would be used in the adsorbance experiments.

Program Assembly

The following data was assembled within the PW1480 XRF X40 control software in preparation for calibration. The channel data was stored to parameterbank SCMOFUSE.X48

Channel Assembly

The following channel was assembled to measure Pb Kα radiation.

Name	Line	kV	mA	Filter	Collimator	Xtal name	no.	ord.	Angle	+Off_ set	-Off_ set	Det.	Lower level	Upper level
Pb1	KA	80	35	Out	Fine	LiF200	2	1	48.685	0.00	0.00	FL	30	70

Analytical Program

The following analytical program was developed to measure Pb in the aqueous solutions.

```
CSIRO Division of Soils                          16-NOV-94 13:15
 AP: PBWATER    Recal.: YES  Created:  1-NOV-94  9:52  Revised:  1-NOV-94 10:33
 Pb in Water                 Ch.Mask: SMALL           Req. data: none
 CP: PBWATER   Spinner:  IN  Delay:  0 s              Sum normalisation:   NO
 Monitors: PBWATER

 Channel Reporting  Print  Dec  Units  ---Conc.limits---  Meas ---Corrections--
 no code      name   seq                lower    upper   time drift BKG overl.
  1 Pb1         Pb    1     0    ppm                       40   y
```

Monitor Buffer

The following Monitor Buffer called PBWATER was assembled to measure monitor sample R8. This data will be used as a reference for the calibration. The data is used to correct for any instrumental changes which may have occurred in the spectrometer since the time of the calibration procedure.

```
CSIRO Division of Soils                          16-NOV-94 13:15
 MB: PBWATER          Computed first:  1-NOV-94 10:35      Last: 15-NOV-94 13:31
 For buffered DC                                           Monitor data: VALID

 Correction for slope

                    Pb1
 Meas. time:         40
 Drift factor:     1.1355
 Background:        0.000

 Monitor sample: R8
 Measured first:  1-NOV-94 10:35  Last: 15-NOV-94 13:31
 Delay:  0 seconds                Channel mask: SMALL      Status: NOT MEASURED
                    Pb1

 0 hour rate:      10.329
 Last rate:         9.097
```

Measuring the Calibration Standards

5 mls of each of the known solutions were pipetted into 32mm plastic XRF liquid sample cups equipped with 1μm mylar windows. The liquid cups were placed into 32mm aluminium XRF sample holders and the standards measured at ambient air pressure on a Philips PW1480 X-ray fluorescence spectrometer energising a Sc/Mo X-ray tube anode. The analytical program used was PBWATER accessed through X40 version 4.0 control software.

Important Note

Liquid samples must only be run using ambient air pressure in the X-ray path. Samples run under vacuum will cause damage to the spectrometer.

Calibration Results

A simple calibration approach was chosen due to the simple matrix to be analysed. The calibration statistics appear below. Calibration data was stored to Calculation Program PBWATER. Figure 1 graphically shows the results of the calibration results.

Calibration Statistics

```
CSIRO Division of Soils                          16-NOV-94 12:51
 Pb1          Pb  Used standards:      4  Calc. parameters:  2     16-NOV-94 12:51
 AP:    PBWATER   Conc. file:    PBWATER  Countrate file:    162XRFB   Unit: ppm
 RMS:   9.72193   K-factor:     0.00682  Error weighting: Sq. root( C + 100.000 )
 Model: DJ                               E:   0.00451        D:  -0.01530
```

Chemical Concentrations versus XRF Results

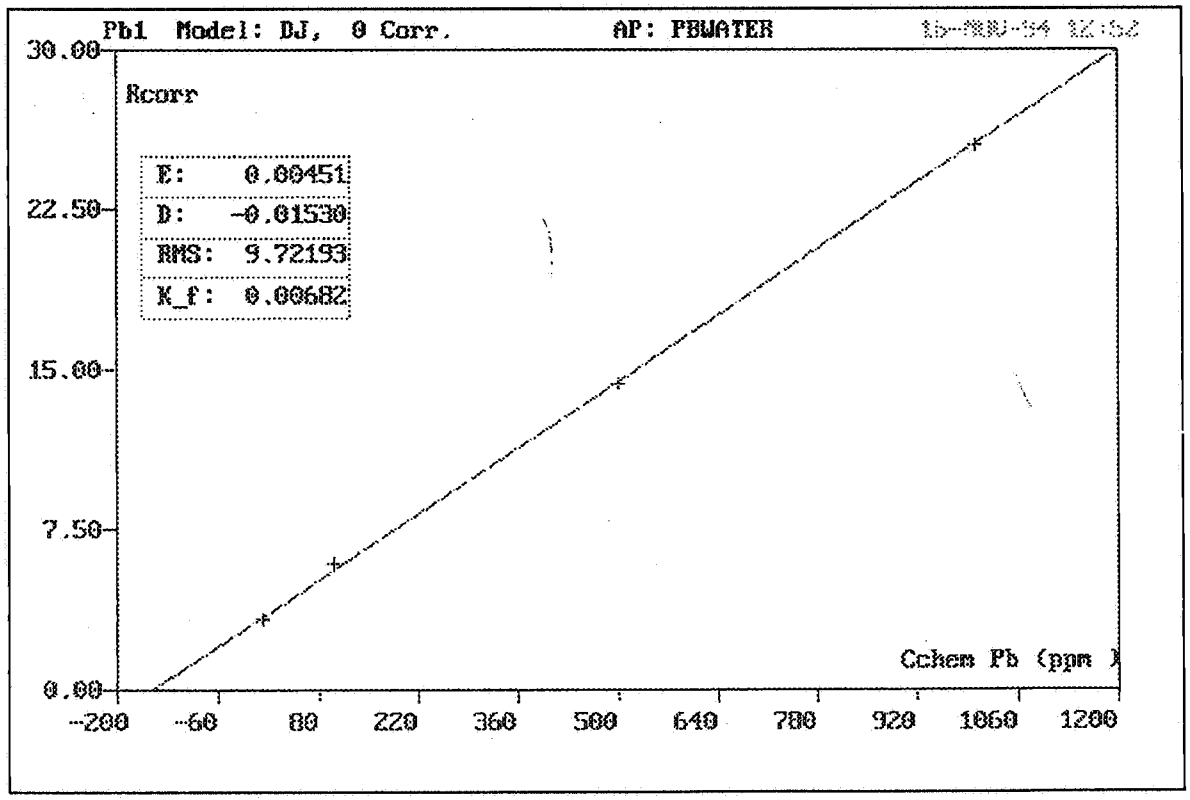
Below is a list of the calculated Pb values compared to the known chemical values.

CSIRO Division of Soils 16-NOV-94 12:52

No	St.	R(Pb1) (kcps)	Concentrations (ppm) for Pb chemical	calc.	diff.	Matrix uncorr.	corr.	16-NOV-94 12:51 Identification
1		3.2906	0	-5	-4.63	-5	1.0000	2198
2		5.8667	100	112	11.51	112	1.0000	2199
3		14.3633	500	495	-5.43	495	1.0000	2200
4		25.5213	1000	998	-2.38	998	1.0000	2201

The calibration data was stored to Calculation Program PBWATER within the X40 control software.

Figure 1 - Lead as $PbNO_4$ in water calibration results (kcps vs conc)



Discussion

The above method is suitable to measure Pb in the ranges 1 ppm to 1000 ppm present as $PbNO_4$ in water. It is recommended that a pure water blank be measured during each unknown run to detect any background drift.

Summary of Analytical Data

Spectrometer:	Philips PW1480 XRF
X-ray tube anode:	Sc/Mo dual anode
Control software:	X40 version 4.0
Analytical program:	PBWATER
Monitor buffer:	PBWATER
Calculation program:	PBWATER
Parameterbank:	SCMOFUSE

APPENDIX 2

Industrial minerals in soil sealants and waste dump linings

W. Fiebiger and M Schellhorn

(reproduced from *Industrial Minerals,* February 1994)

Industrial minerals in soil sealants & waste dump linings

by Werner Fiebiger and Matthias Schellhorn*

One of the major ecological and social problems both now and in the future is the production, treatment, and disposal of man-made wastes. Hazardous wastes with long-term toxicity need to be isolated from the biosphere. The long-term safety required of waste disposal sites can only be assured under specific geological and mineralogical conditions in specific parts of the lithosphere.

The handling of waste, the construction and maintenance of waste disposal units, as well as the rehabilitation of uncontrolled waste disposal areas is a multi-disciplinary task today, involving law makers, public and private environmental agencies and institutions, research organisations, federal, regional and local authorities, construction companies and — last but not least — all industries and private persons generating waste.

The construction and operation of waste disposal areas, apart from the technological safety problems, is becoming an ever increasing financial issue. Concepts have to be developed which guarantee the highest possible long-term safety of waste disposal sites at the lowest possible costs.

A wide range of techniques for the construction of disposal areas have been introduced, most of them involving natural raw materials as sealants. This article will discuss surface or near surface waste disposal areas excluding those for the deposition of radioactive substances.

Current status — the German example

In the mid-1980s the Federal Republic of Germany generated approximately 250m. tpa of solid wastes according to the following specifications:

- 45.2% construction waste and excavated ground
- 42.3% industrial waste
- 10.3% household and similar commercial wastes
- 1.2% sewage sludge
- 1.0% hazardous industrial waste

In 1984 about 86m. tonnes were disposed of by public plants, about 90% in dumps and 8.7% by incineration. The rest was composted, treated by chemico-physical processes, or stored in hazardous-waste dumps.

Even after the introduction of the "Dual System", eg. the sorting and separation of recyclable packing material in 1991 (which amounted to 11.6m. tonnes of recyclable waste in 1993), the total volume of waste to be disposed of in landfill dumps remains statistically at approximately 1 tpa per capita.

Currently this figure transforms into 2m. sq. metres of new waste disposal area per annum, assuming an average density of waste of about 1.3 tonnes per cu. metre and a maximum thickness of 30 metres of built-in waste layers.

*Stephan Schmidt Group, Dornburg, Germany

Considering that comprehensive legislation and safety standards for waste disposal have been introduced only in the seventies, the rehabilitation of old uncontrolled — and sometimes illegal — landfills is becoming an even more serious task in the future. The location and identification of hazardous areas is only a minor problem compared to the definition of feasible techniques to seal off these areas, bearing in mind that the locations may not be suitable for waste disposal because of their underground characteristics. In certain cases the installation of secondary linings may be an acceptable solution. In the worst scenario, however, the removal of toxic substances may become the only alternative. Legal aspects such as liability lead to questions regarding the financing of such projects.

State of the art

Quality and safety requirements with regard to waste disposal areas are principally defined by the characteristics of the waste. As a function of toxicity the following general classification of solid wastes has been introduced (except for radioactive waste):

- excavated ground (not contaminated)
- construction waste
- household and similar commercial waste
- industrial waste

It is obvious that uncontaminated, excavated ground bears a substantially lower risk to the environment than household and/or industrial wastes. The classification for other types is usually more complex. Construction waste may be classified as a completely harmless inert material: on the other hand it may be contaminated by highly toxic components such as lead pipes, asbestos, etc.

Additional criteria for the classification of waste with a view to its deposition are sorting effects and consistency. Well sorted waste types are much easier to characterise with regard to long term behaviour in waste disposal than unsorted substances of uncontrollable composition, such as household waste. Liquid and paste-like substances have to be compacted and hardened before disposal.

There is a wide range of technical options concerning how to deposit waste according to the imposed standards, and norms and how to rehabilitate leaking waste disposal sites to prevent contact between toxic substances and the biosphere.

According to current techniques, the following technical sealing elements may be identified:

- base linings
- surface linings
- sealing walls
- injected barriers

Base and surface linings follow similar construction criteria. Clay sealing agents, industrial sealing carpets with built-in clay or bentonite pockets, and heavy duty polyethylene foils (HDPE) are the principal components.

In the Federal Republic of Germany standards and norms for the construction of waste disposal sites are laid down in the "Technical instructions for household and similar commercial wastes" (TA Siedlungsabfall published 1 June 1993). According to the standard for the base lining of a waste disposal area, a combination of a mineral sealant and an HDPE foil is mandatory (*Figure 1*). On top of the sealing layer a drainage system is installed to capture filtering liquids in the central collecting unit. The surface lining follows the opposite principle since its objective is to prevent precipitation liquids from entering the waste deposit (*Figure 2*).

Sealing walls are vertical systems designed to protect the environment from toxic liquids which might penetrate into the surrounding ground. Ditches of 80cm width are excavated to a depth of more than 50 metres and filled with the sealing component.

The use of low viscosity sealants allows the immediate substitution of excavated material. The technique has been introduced as a **one phase sealing wall** and the mix is composed of slow binding cement with bentonite and ground clay plus smaller amounts of additives. The quantitative formulation is usually adapted in line with the specific requirements of impermeability, stability, and corrosion-resistance.

High duty sealing walls with extremely low permeability values are built as **two phase sealing walls**. After excavation a low viscosity support suspension — usually a bentonite base — is substituted by a high density sealing medium. The water content in such mixes can be as low as <10%. Resistance against corrosion

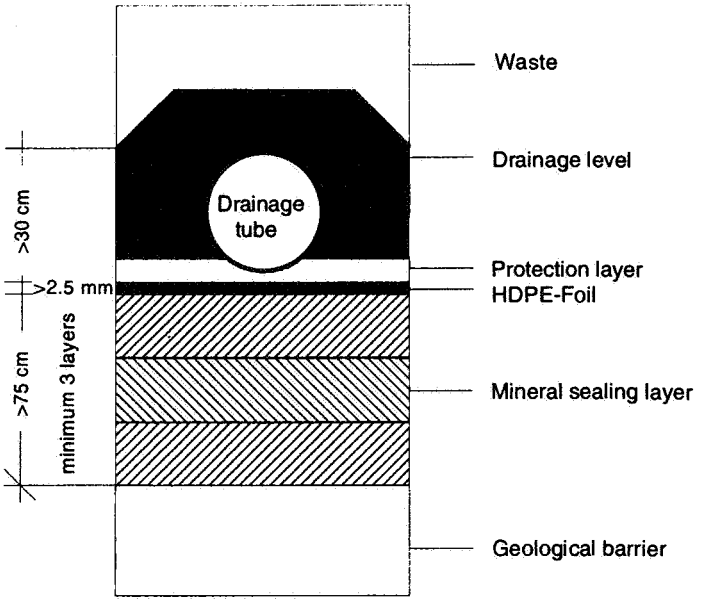


Figure 1. Schematic diagram of base lining
Source: TA Siedlungsabfall

Does your company feature in this issue of

INDUSTRIAL MINERALS?

Keep your name and activities to the forefront of your present and potential clients attention by using reprints of articles and advertisements from Industrial Minerals (and any other Metal Bulletin journal) to compliment your PR/Sales packages.

For further details contact:
Jackie Avison, Marketing Department,
Industrial Minerals, Park House,
Park Terrace, Worcester Park,
Surrey KT4 7HY, ENGLAND
Tel: (071) 827 9977 Fax: (081) 337 8943
Tlx: 21383 METBUL G

IM Industrial Minerals



SOCIETE KAOLINIERE ARMORICAINE
BP 417 - 22004 St-BRIEUC CEDEX 1 - FRANCE
TEL : (33) 96 33 21 55 - FAX : (33) 96 33 81 43

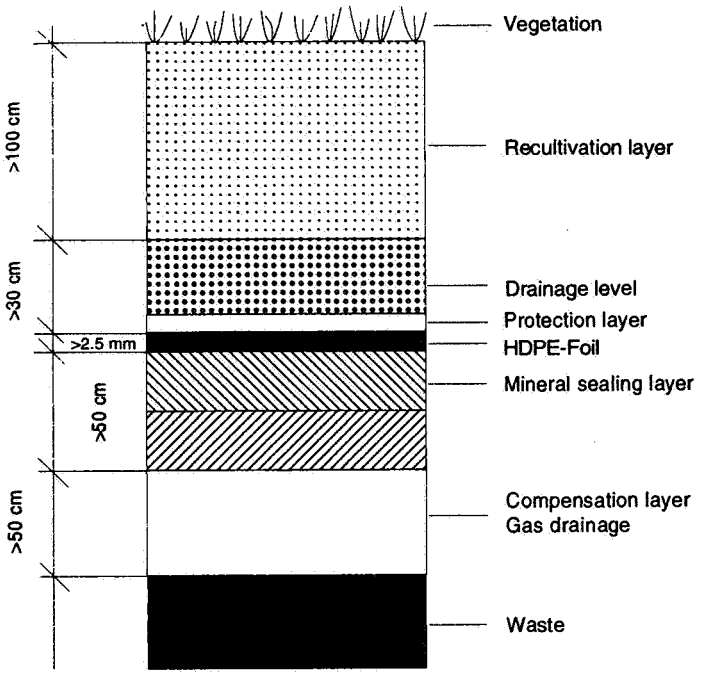


Figure 2. Schematic diagram of surface lining
Source: TA Siedlungsabfall

can be improved by cement-free systems with high clay contents. *Table 1* gives some batch formulation examples for sealing walls.

A further possibility for secondary sealing measures is the application of injection techniques. Injection torches are used to press low binding sealing and/or gel-generating mixes into permeable rock or soil layers. This rather recent technology in waste disposal construction is complex and costly. In general, for the time being, it is only being applied for small local leakages, such as soil contamination near fuel stations.

Construction of sealing systems

Two parameters are critical to achieve the lowest possible permeability in waste disposal sites:

- selection of the correct natural sealant
- correct utilisation of the natural sealant

In base and surface linings the compactability of clays is a function of their natural water content. The maximum compaction is reached when the material contains an optimum water level (Proctor-water content). This content has to be established and the moisture level of the material has to be controlled during construction.

To achieve the required density, the sealing material is spread in layers of 0.25 metres thickness and compacted by heavy duty vibrating rollers. After completion of one layer the surface is roughened with a rotary hoe to guarantee homogeneous contact with the next layer.

Where local soils are blended with clays, burnt lime, bentonite and coagulants, mixing plants are usually used to provide constant blend quality. The "mixed in plant" method has widely substituted the "mixed in place" technique, where the materials were blended by rotary hoes directly on the sealing layer.

Slurries for vertical sealing walls and injection are usually prepared in blending plants at the construction sites. Exceptions are dry mixes for one phase sealing systems and injection where the solid components are usually prepared in cement factories. Water is added and the suspension is stirred directly on site.

Table 1. Composition of vertical sealing wall slurries

	One phase sealing wall		*Two phase sealing wall*		
	A	*B*	*C*	*D*	*E*
Water	80.0	62.4	40.0	50.4	8.04
Cement	16.7	14.0	22.5	3.5	—
Clay	—	11.7	37.5	46.1	15.3
Sand	—	—	—	—	29.7
Gravel	—	—	—	—	45.0
Bentonite	3.3 (Na)	11.7 (Ca)	—	—	—
Silica gel	—	—	—	—	1.60
Additives	—	0.2	—	—	0.36
Density	1.2	1.31	1.64	1.41	2.23

A Conventional; B High density; C Conventional; D Low cement content; E Cement free

Mineral sealants for waste disposal construction

Quality specifications

To conform to the safety requirements of numerous standards and norms, minerals used in the construction of different types of waste disposal areas must adhere to criteria which affect the applicability of sealing elements. For base linings Germany has established a **multi barrier concept** where each of the single layers has its specific function (*Figure 1*).

One of the fundamental problems is the selection of a safe location. The site of a new waste disposal site should have a base with low permeability to, and filtration capacity for, toxic solution. Sediments with high clay mineral contents and good cation-exchange capacities are the most suitable formations for the geological barrier. Typical raw materials for this first sealing element are clayey soils and clays which show a certain amount of expandable smectitic minerals with a good cation-exchange capacity. Their chemical activity improves the filtration effect due to their capacity to adsorb toxic components from filtration waters. The percentage of smectitic clay minerals has to be controlled because they can exhibit some detrimental characteristics, such as shrinkage and instability in the presence of solutions with high electrolyte contents.

Typical requirements for the hydro-geological barrier are shown in *Table 2*. If the base at a selected site does not correspond to these parameters, the construction of an artificial geological

Table 2. Minimum requirements for geological and technical barriers*

Parameter	*Geological barrier*	*Mineral base sealing*
Thickness (metres)	>3	>0.75
Permeability (m/s)	$<10^{-7}$	$<5 \times 10^{-10}$
% <2μ fraction	—	>20
% clay mineral	—	>10
Cation exchange capacity	High	Low

*According to the German Standard for household waste disposal
Source: TA Siedlungsabfall

barrier is achieved by blending local soil with high quality standard clays and/or smectitic materials.

The base lining or technical barrier is the most critical element for the long term safety of a waste disposal site. To guarantee the retention of toxic fluids within the waste body, the quality of the natural sealants and type of construction have to be selected carefully. Because HDPE foils tend to deteriorate in time, only high quality mineral sealing elements provide long term protection of the biosphere. Consequently, base linings follow stringent safety regulations and only chemical resistant clays with a high content of <2μ fraction are allowed for construction. The minimum requirements according to German standards are listed in *Table 2.*

The principle of improving local materials by blending also prevails for base linings. To guarantee chemical inertness and resistance against secondary swelling and shrinkage, expandable minerals eg. smectites are permitted only in minor amounts in base linings. Kaolinitic and illitic clays proved to be ideal components.

In general, the requirements for surface linings are identical to those for the base linings. The use of additives such as burnt lime or coagulant-building agents may further improve the characteristics of horizontal sealing systems.

Burnt lime is used to reduce the water content of the sealing material to the required levels. Coagulants such as Hüls AG's "Dynagrout-Systems" substitute pore water with stable gels and reduce the permeability of the sealant.

Raw material requirements for vertical sealing walls and injection suspensions are more complex than those for horizontal systems. Two principal parameters for the successful application of natural raw materials derive from the safety standards of these sealing systems — low permeability and long term resistance against contaminated effluents.

On the other hand, some important installation criteria have to be observed:

- good movement of suspensions
- high supporting capacity
- low loss of filtrate water
- late solidification of suspension

Consequently, certain components are required to guarantee good workability of the slurry which might have adverse properties with regard to long term stability of the sealing wall. For example, sodium-activated bentonites provide a high supporting capacity in the one phase sealing wall but are critical in terms of their resistance to highly contaminated solutions derived from the waste. Also, in one phase sealing walls, the use of cement as a hydraulic binder is required but cement-aggressive effluents influence the long term stability.

Table 3. Typical inert clay for base lining and sealing wall applications

Application	*Sealing walls*	*Base & surface linings*	
Clay	Secursol 3101	Secursol 3301	Secursol 3060
% <2μ fraction	55-65	70-80	80-90
% clay minerals	50-60	50-60	80-90
kaolinite	≥ 60	≥ 65	≥ 75
illite	≤ 35	≤ 30	≤ 20
smectite	≤ 3	≤ 3	≤ 5
CEC (meq/100g)	≤ 20	≤ 20	≤ 20
Water adsorption capacity (after Enslin-Neff 16 min)	60-70	75-85	80-90

Source: Stephan Schmidt KG

Inert fillers such as kaolinitic clays are of major importance for the quality of the vertical sealing system. Coagulants may further improve stability.

The assessment of the risk potential of waste disposal is of fundamental importance for the selection of a safe sealing system. Whereas slightly contaminated effluents may be contained by comparatively simple measures, highly toxic solutions derived from household or certain industrial wastes, require complex systems.

Quantity requirements

Based on the assumption that the Federal Republic of Germany annually requires approximately 2m. sq. metres of new waste disposal area and that the total average thickness of lining amounts to about 1.25 metres (0.75 metre base linings and 0.5 metre surface linings), and that the average Proctor density would be 1.8 tonnes per cu. metre, a total of 4.5m. tpa of sealing material, eg. clays, would be needed.

This figure refers only to the technical barriers and does not consider hydro-geological barriers and vertical sealing or injection systems.

According to safety standards with regard to minimum raw material requirements, the use of local soils is becoming increasingly limited since most of the material does not conform to the quality specifications.

Consequently, high quality clays are shipped to the construction sites. In many cases, however, the distance and transport costs make the transportation of shredded and moist material prohibitive.

INDUSTRIAL MINERALS BY
PELETICO
OF CYPRUS

Processors of:
- BENTOCYP BENTONITE
  - Oil, gas & water well drilling mud (OCMA DFCP-4)
  - Civil Engineering
  - Cat Litter
  - Binder & Filler - Extender
- HIGHLY PURE GYPSUM
  - Cement Manufacture
  - Plaster
- PERLITE
  - Crude (crushed & graded) and expanded
  - Turnkey perlite expanding units

In recent years, a growing number of projects have been realised using mixes of local materials (sometimes on-site) with high quality fine ground clays to increase the capacity of the waste disposal site. In general, the addition of 5-10% of special clays to the product achieved the respective quality specifications.

In terms of long term stability problems of sealing systems there seems to be a trend to substitute smectitic clays and bentonites with chemically resistant products such as kaolinitic clays. Indications are that activated bentonites, with their notable cation-exchange capacities, tend to collapse and shrink once exposed to certain toxic effluents. Kaolinitic and illitic clays exhibit similar permeability levels without showing detrimental effects.

The increasing demand for standardised, quality controlled and tested products created a new market for fine ground non-smectitic clays with the following standard quality criteria:

- high content of kaolinitic minerals
- high percentage of minus 2μ fraction
- low smectite minerals content
- low soluble salts content
- low organic material content

Consequently, some of the major German clay producers are specialising in products for the construction of waste disposal sealing components such as "TDT-clays", "Securson" and "Depo-Mix", to name just a few typical products (*Table 3*).

For 1994 the German market is estimated to consume the following in waste disposal site construction projects:

- >100,000 tonnes of fine ground clays
- >100,000 tonnes of bentonitic products
- >1m. tonnes of shredded clays

Conclusions

The installation and operation of waste disposal sites constitutes a major hazard to the environment.

Safety standards to protect the biosphere against toxic effluent from waste disposal are becoming more and more stringent.

Major problems derive from old uncontrolled waste dumps and require measures to seal off sites, in some cases to prevent high ground water contamination risks.

The use of bentonitic clay in waste disposal linings has become a somewhat controversial issue with regard to its long term, resistance and stability against chemical reactions.

Major producers of kaolinitic clays have developed specific products that respond to the new market segment.

It is expected that quality standards will also become more stringent at the European level. The total demand for quality clays is estimated to reach several million tonnes per year in the near future.

References:

A.G. Herrmann & B. Knipping (1993) "Waste Disposal and Evaporites. Contributions to Long-Term Safety." Lecture Notes in Earth Science 45, Springer Vlg, Berlin, Germany

T.A. Siedlungsabfall (1993) "Technische Anleitung zur Verwertung, Behandlung und sonstiger Entsorgung von Siedlungsabflen." Bundesanzeiger, Köln, Germany■

000169

CMD

ceramic minerals consulting

– the best Place to start Quality –

WORKING FOR THE CERAMIC AGE

- Minerals Exploration
- Evaluation of Ceramic Raw Materials
- Complete Laboratory Services
- Development of Customer designed Ceramic Bodies and Slurries
- Mine Layout and Implementation
- Design of Mineral Dressing Facilities
- Feasibility and Market Studies
- Manpower Training
- Environmental Protection Services

ASSISTING RAW MATERIALS PRODUCERS, PLANT EQUIPMENT SUPPLIERS AND CERAMIC FACTORIES – WORLDWIDE

Ceramic products are as good as their raw materials – we improve both.

ceramic minerals consulting

D-65599 Dornburg-Langendernbach · Telex 4821612
Phone 06436/4044 · Fax 06436/60949

stephan schmidt gruppe

Env 8785
000170

ABSORBENT CLAY PROJECT

PROGRESS REPORT NO. 3 TO MINES AND ENERGY, SOUTH AUSTRALIA

CLAYS FOR THE UPTAKE OF POLLUTANTS: MODIFICATION, PROPERTIES AND ASSESSMENT TECHNIQUES

P.G. Slade, R.M. Taylor, M.D. Raven, G.J. Churchman, S. Fletcher, A.J. Urban, R.W. Kimber, J.L. Keeling, S.G. McClure and P.G. Self.

CSIRO

Division of Soils

Commonwealth of Australia

March, 1995

Mines & Energy SA
R96/01688
00135020

SUMMARY

Investigations in this stage of the Absorbent Clay Project were focussed primarily on modification of selected clays and improving their uptake of organic pollutants.

It has been shown that unmodified smectitic clays do not sorb aromatic hydrocarbons. Furthermore, smectitic clays do not show a capacity for the sorption of hydrocarbons when pillared with either alumina or with clusters of metallic copper. When modified with quaternary ammonium cations, however, smectitic clays sorb benzene and toluene from water. The sorption of non-ionic organic molecules takes place best when clays are rendered hydrophobic. Clays modified with an alkylammonium cation with alkyl radicals comprised of long straight carbon chains were more efficient sorbers of the aromatic hydrocarbons than were clays modified with an alkylammonium cation containing an aromatic radical but no alkyl chains.

Following its modification with alkylammonium cations, the smectitic Arumpo bentonite from New South Wales proved to be a very effective material for the uptake of aromatic hydrocarbons, but even a subsoil (Keswick clay from South Australia) when treated with an alkylammonium salt, showed substantial uptake of aromatic hydrocarbons.

It has been demonstrated that particles of magnetite can be attached to alkylammonium modified smectitic clays and that the resultant composite magnetite-organophilic clay particles retain a capacity for the sorption of aromatic hydrocarbons. Magnetite particles can also be attached to palygorskites. As a result of these associations, clays containing sorbed toxic organic compounds could be removed from water by magnetic forces.

Zeolites were produced from each of several kaolins from South Australia by a relatively simple chemical process. These zeolites have demonstrated a high capacity for the removal of cations such as heavy metals from solution.

Experiments aimed at increasing the sorption capacity of kaolins and illites, by leaching them with alkali and acid solutions, have begun.

Using gas sorption it has been shown that many of the clays being studied have a high concentration of pores of particular sizes. Arumpo bentonite has fine pores (diameter < 6nm). These pores become concentrated into even finer sizes (< 4nm) when this smectite is pillared with alumina. Muloorina illite and also an illite-rich South Australian clay containing palygorskite have a high concentration of medium-size pores (diameter < 20nm) as do halloysites from Western Australia and New Zealand. A palygorskite from South Australia has a significant concentration of even coarser pores (< 40nm). These various types of pore size distributions may enable the use of the clays as molecular sieves for either gases or liquids. Other samples studied, including both kaolinites and halloysites from South Australia, have few pores and also low surface areas. An allophanic soil from Mount Gambier, while having a high surface area, shows little porosity. For a smectite, Arumpo bentonite has an exceptionally high surface area.

A feasibility study was conducted to determine whether high performance liquid chromatography could be adapted to the routine measurement of the sorbing power of clays. Commercially-available technology was able to be configured into an appropriate form, but severe difficulties were encountered in the use of chromatography-type columns due to the swelling of the clays and the presence of colloidal-sized particles which tended to block the inlet and outlet filters. Notwithstanding these difficulties, some successful measurements were carried out using wide-bore guard columns, and it was shown that various metal ions (Pb, Cd, Zn, Cu, and Ni) could be absorbed on Arumpo Bentonite.

TABLE OF CONTENTS

INTRODUCTION 1

THE MODIFICATION OF SMECTITES AND THE SORPTION OF BENZENE AND TOLUENE 3

Principal researcher: P.G. Slade.

COATING ORGANOPHILIC CLAYS WITH SYNTHETIC MAGNETITE PARTICLES 19

Principal researcher: R.M. Taylor.

ZEOLITE 'A' SYNTHESIS FROM SOUTH AUSTRALIAN AND NEW ZEALAND KAOLINS 26

Principal researcher: M.D. Raven.

SIMPLE MODIFICATION OF KAOLINS AND ILLITES 41

Principal researcher: G.J. Churchman.

SURFACE AREA AND POROSITY OF CLAY MINERALS 44

Principal researcher: G.J. Churchman.

FEASIBILITY STUDY ON THE DEVELOPMENT OF AN APPARATUS FOR FLOW-THROUGH TESTING OF ADSORBING POWER OF CLAYS 65

Principal researchers: S. Fletcher and A.J. Urban.

ACKNOWLEDGMENTS 73

INTRODUCTION

This report describes the results of the third part of a project which has been carried out under a contract with Mines and Energy, South Australia during 1994 and early 1995. The aims of the project were to investigate possible environmental uses for South Australian clays although another promising Australian clay (a Na-Mg smectite from Arumpo NSW, mined by Browns Creek Gold N.L.) was also included. The project had 3 parts or phases:

1. Characterisation of the clays
2. Assessment of the ability of the unmodified clays to sorb pollutants, and
3. Modification of the clays and assessment of the ability of the modified clays to adsorb pollutants.

The results of Phase 1 were reported in Absorbent Clay Project, Progress Report No. 1, Characterisation of the Selected Clays (June 1994). Arising from this work, further characterisation of palygorskite clays from Garford Palaeochannel was pursued and will be reported separately. Additional characterisations of particular relevance to the interactions of clays with pollutants (notably surface area and porosity) were not available for inclusion in earlier reports and are reported herein. The results of Phase 2 were reported in Absorbent Clay Project, Progress Report No. 2, Results on the Uptake of Ni, Cd, Cr, Pb and Benzene by Selected Clays (November 1994). Results of some further studies of the sorption of heavy metals by clays are also reported herein because they provide validation of a new method, developed in this Project, using high-performance liquid chromatography (HPLC) for the investigation of sorption by clays.

The sorption work reported in Progress Report No. 2 was aimed at investigation of the uptake by the unmodified clays of heavy metals and also an aromatic hydrocarbon. Since several of the clays were shown to sorb heavy metals very efficiently but not to sorb the aromatic hydrocarbon, the main purpose of the present (third) phase of the study was to investigate methods for the modification of clays so that they might usefully sorb aromatic hydrocarbons.

In the course of this work, however, other possible environmental applications for clays were encountered and it was considered worthwhile to align the work to these other uses as well. They included the removal of pollutants from water for human and animal consumption.

Increasing contact with other researchers and clay users concerned with environmental pollution has led to an awareness of further actual and possible uses for clays such as the uptake of gases, the removal of dyes from dyeing plant effluents, the removal of algal toxins from river-derived water supplies, and as barriers against water and associated pollutants in landfills and mine tailings dams. Many of these uses would require prior modification of suitable clays.

The project is continuing and it is intended that further significant results will be reported subsequently.

1. THE MODIFICATION OF SMECTITES AND THE SORPTION OF BENZENE AND TOLUENE

Introduction

In order to consider smectites as possible sorbents for the common constituents of petroleum which enter groundwaters from leaking storage tanks, one needs to note that the aromatic hydrocarbons involved (benzene, ethylbenzene, xylene and toluene) do not readily penetrate between the lamellae of the natural, hydrated, inorganically exchanged, forms of the clay (Absorbent Clay Project, Progress Report No. 2, November 1994). However, by modifying smectites and increasing their hydrophobicity, this situation can be substantially improved.

Although a great variety of organic cations have been introduced into the interlamellar regions of smectites, only the long chain ion organo-clays have been found to imbibe both polar and non-polar guest molecules. In particular, smectites treated with quaternized cationic surfactants are markedly organophilic and have been shown to absorb a range of aromatic organic pollutants (Barrer and Kelsey, 1961).

The sorptive properties of the swelling clays (smectite) can be improved by incorporating surfactant molecules into their interlamellar regions. As a result, the interlamellar regions become hydrophobic and organic contaminants in water can be incorporated into the interlamellar complex. Factors which are likely to affect the uptake of the guest species include the size and configuration of the incorporated surfactant molecules and the ability of the surfactant molecules to interact with the guest species, perhaps via Van der Waals bonding.

In part, the following study contrasts the sorbency of *inorganically-pillared* clays which, although providing interlamellar porosity, are essentially organophobic, with those incorporating cationic organic molecules providing for associative relations between the host and guest species.

Other aspects, such as the extent of the hydrophobicity, are also exemplified in the following study of the uptake of benzene and toluene by modified and unmodified Arumpo bentonite, the partially-smectitic Keswick clay and Wyoming bentonite.

Methods

1. The preparation of alumina pillared montmorillonite

The first and most important step in pillaring smectites with metal oxides is to replace the resident interlayer cations with oligomeric hydroxy-metal cations. The latter are subsequently converted into metal oxide pillars by calcination.

The oligomeric cation used for the present work has the general formula:-

$$[Al_{13}\ O_4\ (OH)_{24+y}\ (H_2O)_{12-y}]^{(7-y)+}$$

and was prepared by titrating 0.1M NaOH at the rate of 1 drop/second into 0.1M $AlCl_3.6H_2O$. The temperature of the mixture was maintained at 60°C and methyl orange was used to indicate the final pH (near 4.0).

The final OH/Al molar ratio was 2.2; that is 88mls of 0.1M NaOH was added to each 40mls of 0.1M $AlCl_3.6H_2O$. At the end of the titration, the mixture was aged for 1 hour at 60°C, followed by further ageing for 24 hours at room temperature.

In order to actually prepare the alumina pillared clay, a 2% (wt) suspension of clay was stirred for 1 hour with the aged base-hydrolysed aluminium chloride (BHAlCl). A ratio of 5mmol of Al per gram of clay was used. The pillared clay product was washed until chloride free by using a combination of centrifugation and dialysis.

2. The preparation of montmorillonite pillared with metal clusters

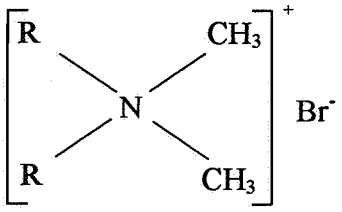
In metal-cluster intercalates, the clustered metal atoms prop the silicate layers apart as aluminium oxide does in alumina pillared clay. The method for preparing them involves saturating the clay with a transition metal cation, for example Cu^{2+}, and then reducing the ions to the neutral form, for example Cu^0, with ethylene glycol (Malla *et al.*, 1991).

In the present context, Na-saturated Wyoming montmorillonite was treated successively with 3 fresh aliquots of 0.5M $CuCl_2.2H_2O$ over a period of 36 hours. The Cu^{2+} saturated clay was washed by using centrifugation and dialysis until Cl^- ions were not detectable in the wash liquid.

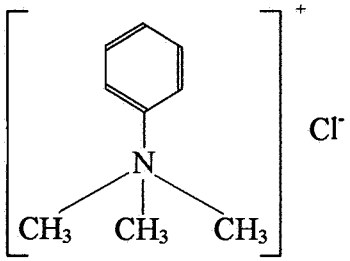
The reduction of the Cu^{2+} ions in the Cu^{2+}-saturated clay was then achieved by heating the material in ethylene glycol at 195°C under reflux. A constant stream of pure argon was passed through the mixture in order to displace air. After cooling, the product was repeatedly washed with methanol. Finally, in order to displace any residual interlamellar ethylene glycol, the Cu^0-clay was heated at 200°C for 2 hours under high vacuum.

3. The preparation of the organo-clays

Two contrasting quaternary ammonium compounds were selected as intercalates; dimethyldioctadecylammonium bromide (DMDOAB) and phenyltrimethyl-ammonium chloride (PTMAC). The first can be represented as



where R, the alkyl radical, has the following structure CH_3-$(CH_2)_{17}$-. The second intercalate can be represented as



DMDOAB and PTMAC were obtained from the SIGMA CHEMICAL CO. and the ALDRICH CHEMICAL CO. INC. respectively.

The organo clays were prepared by reacting 0.01M solutions of either DMDOAB or PTMAC with suspensions containing known weights of clay so that its exchange capacity was stoichiometrically satisfied. The reactants, while being stirred for between 16 and 24 hours, were maintained at 70°C. The organo-clays were then separated from the liquid by centrifugation, washed with warm distilled water followed by isopropyl alcohol and finally dried at 60°C.

4. Sorption testing

The uptake of benzene and toluene by the clays was measured using a batch method. 5ml aliquots of aqueous mixtures containing 1000ppm of either one or the other aromatic hydrocarbon were mixed in stoppered glass tubes (100mm x 13mm) with known amounts (generally 100mg) of clay to give suspensions containing 0.5-2.0% (wt/V) of clay. A "Vortex" mixer was initially used to agitate the samples but they were then mixed for 15 hours in an end-over-end shaker.

The suspensions were cleared by centrifugation at either 3000rpm for 15mins or 3500rpm for 10mins. Each run included both a water blank, and an aliquot of the stock solution without clay. The optical densities of the unknown solutions were compared with those of the stock solutions using a BECKMAN MODEL DU 640 SPECTROPHOTOMETER. Wavelength scans between 220 and 280nm and between 225 and 280nm for benzene and toluene respectively were employed. The final concentrations of the hydrocarbons in solution were obtained by comparing the optical densities of the unknowns with those of the standards. These comparisons were made at the wavelengths of the main absorption peaks, that is 252.2nm for benzene and 255nm for toluene.

Results

1. Alumina pillared clays

Powder X-ray diffraction patterns were obtained from both moist and calcined samples of oriented portions of pillared Arumpo Bentonite and Wyoming bentonite. Figs. 1.1, 1.2, 1.3 and 1.4 show the results. When moist, each pillared clay has a basal spacing between 2.2 and 2.3nm (Figs. 1.1 and 1.2). However, the pattern for Wyoming bentonite is sharper than that for Arumpo bentonite but this difference is almost certainly caused by interstratification with illite which affects the Arumpo clay and broadens its basal reflections.

After calcination at 500°C, each clay has a basal spacing of ~1.73nm (Figs. 1.3 and 1.4) but each pattern shows broader peaks than in the corresponding pattern for the uncalcined material. The spacings of the calcined clays, along with the known thickness of the silicate layers, enable the gallery heights within the pillared materials to be estimated as:- (1.73 - 0.96) = 0.77nm.

2. Cu^0-intercalated montmorillonite

Figure 1.5 shows the powder X-ray diffraction patterns of Wyoming bentonite treated with copper ions and ethylene glycol. As can be seen, the patterns for the heated and the unheated materials are very similar; indicating perhaps that any ethylene glycol fragments which may have been driven off did so via interlamellar galleries formed by the metal clusters. The gallery height for this copper cluster clay is 0.44nm and therefore differs from the value of 0.5nm given by Malla *et al.* (1991) for the material produced from the Tsukimino montmorillonite from Japan.

3. The organo-clays

(i) Fig. 1.6 shows the diffraction pattern of Na-saturated Arumpo bentonite after having been reacted with DMDOAB at 70°C for 24 hours. Reaction of the same materials, at the same temperature, for 16 hours produced a material with a similar diffraction pattern but having a basal spacing of 2.6nm so that the organo cations are

arranged in interlamellar spaces which are 1.64nm high. Apparently the longer reaction period allows the organic molecules to undergo some structural rearrangement within the interlamellar spaces. The material produced by the longer reaction was subsequently used to test the uptake of the aromatic hydrocarbons.

Although Keswick clay was also reacted with DMDOAB, a diffraction pattern was not recorded because the material had previously been shown to be heterogeneous (Absorbent Clay Project, Progress Report No. 1, June 1994).

ii) The diffraction patterns obtained from the organo-clay produced by reacting PTMAC and Arumpo bentonite are shown in Fig. 1.7. As can be seen, air drying causes the basal spacing to drop from 1.54 to 1.49nm in 24 hours. The organo cations are therefore arranged in interlamellar spaces which are 0.53nm high.

4. Sorption of the aromatic hydrocarbons

Table 1.1 shows, in percentages with respect to the 1000ppm stock solutions, the sorption of benzene and toluene by a range of modified and unmodified clays. The data show that modification of smectite containing materials with DMDOAB or PTMAC produces materials which have significant capacity to sorb the aromatic hydrocarbons benzene and toluene.

Furthermore, the sorption by the smectitic materials treated with DMDOAB is greater than for those treated with PTMAC. *Untreated clays, however, do not show any sorption capacity* and this can be seen not only for the smectitic materials but also for the palygorskites, kaolinites and the allophane containing soil (see Table 5.1).

Although the Keswick clay is a heterogeneous material, containing only 30% smectite, Table 1.1 shows that, after treatment with DMDOAB, it has an appreciable capacity to sorb toluene (58%).

Table 1.1 shows that the alumina pillared clays and Wyoming bentonite pillared with copper clusters do not sorb the hydrocarbons. The heights of the galleries

in the alumina-pillared material (0.77nm) especially, would appear to be sufficient to accommodate aromatic molecules on edge. For instance, Greene-Kelly (1955) has quoted 0.53nm as the perpendicular distance between adjacent silicate layer surfaces necessary to accommodate aromatic molecules oriented perpendicular and edge-on to the interlamellar surfaces. The width of the hexagonal aromatic structure, from Van der Waals dimensions, is 0.67nm and hence the alumina pillared materials would still seem to be able to accommodate either benzene or toluene. That they do not do so probably reflects the essentially hydrophilic, rather than organophilic, character of alumina-pillared clays.

The difference in the extent to which DMDOAB and PTMAC treated smectites sorb hydrocarbons, is a further reflection of the enhanced and important organophilic properties conferred upon the swelling clays when cations, such as $DMDOA^+$, with straight chain aliphatic radicals attached to the primary ammonium groups, are intercalated. In PTMAC, which has an aromatic ring attached to the primary ammonium group as well as only one cation length aliphatic chains, the organophilic character is considerably less and sorption of the aromatic hydrocarbons tested is also less.

Although the quaternary ammonium salts used in the current study were pure and for laboratory use, commercial grade salts are available. In these, the alkyl radicals are formed of chains with a range of carbon numbers. In a given set of circumstances, such variations may reduce the efficiency of organo-clays made by using commercial quaternary ammonium salts. However, in comparison with the poor performance of unmodified clays, the performance of organo equivalents made from commercial salts is still likely to be very superior.

References

Barrer, R.M. and Kelsey, K.E. (1961). Thermodynamics of interlamellar complexes. Part 2. - Sorption by dimethyldioctadecylammonium bentonite. *Trans. Faraday Soc.*, **57**, 625-640.

Greene-Kelly, R. (1955). Sorption of aromatic organic compounds by montmorillonite. *Trans. Faraday Soc.*, **51**, 412-424 and 425-430.

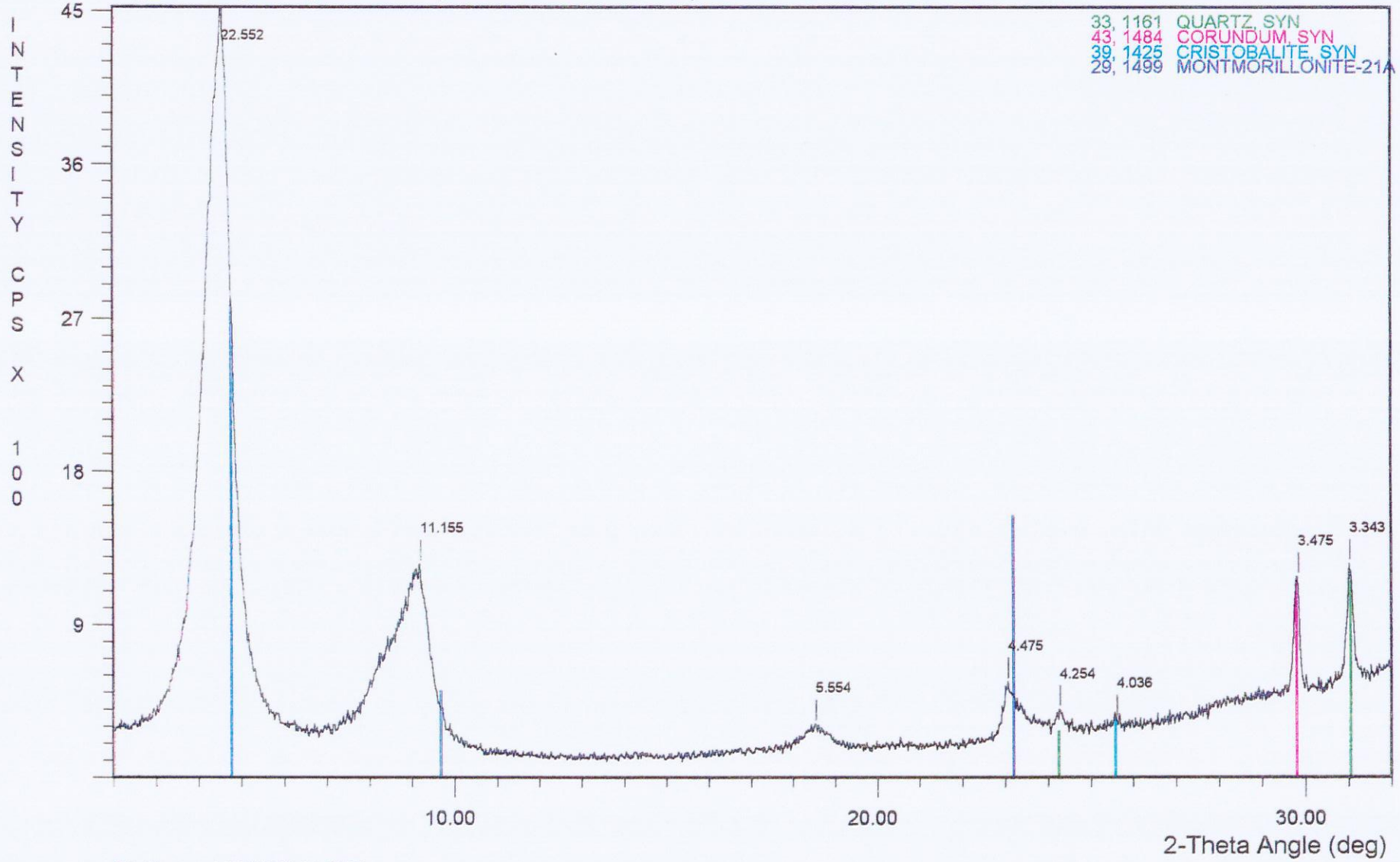
Malla, B., Ravindtanathan, P., Komarneni, S. and Roy, R. (1991). Intercalation of copper metal clusters in montmorillonite. *Nature*, **351**, 555-557.

Table 1.1. %Sorption from 1000ppm aqueous solution of hydrocarbon.

Sorbent Clay	Sorbate	
	Benzene	Toluene
Arumpo bentonite, not sized	0	nd
Arumpo bentonite, 1-2μm fraction	0	nd
Arumpo bentonite + DMDOAB	60	76
Arumpo bentonite + PTMAC	32	50
Keswick clay + DMDOAB (not sized)	nd	58
Keswick clay + PTMAC	nd	0
Al pillared Wyoming bentonite, < 2μm	0	0
Al pillared Arumpo bentonite, < 2μm	0	0
Cu-Wyoming bentonite	nd	0

nd = not determined.

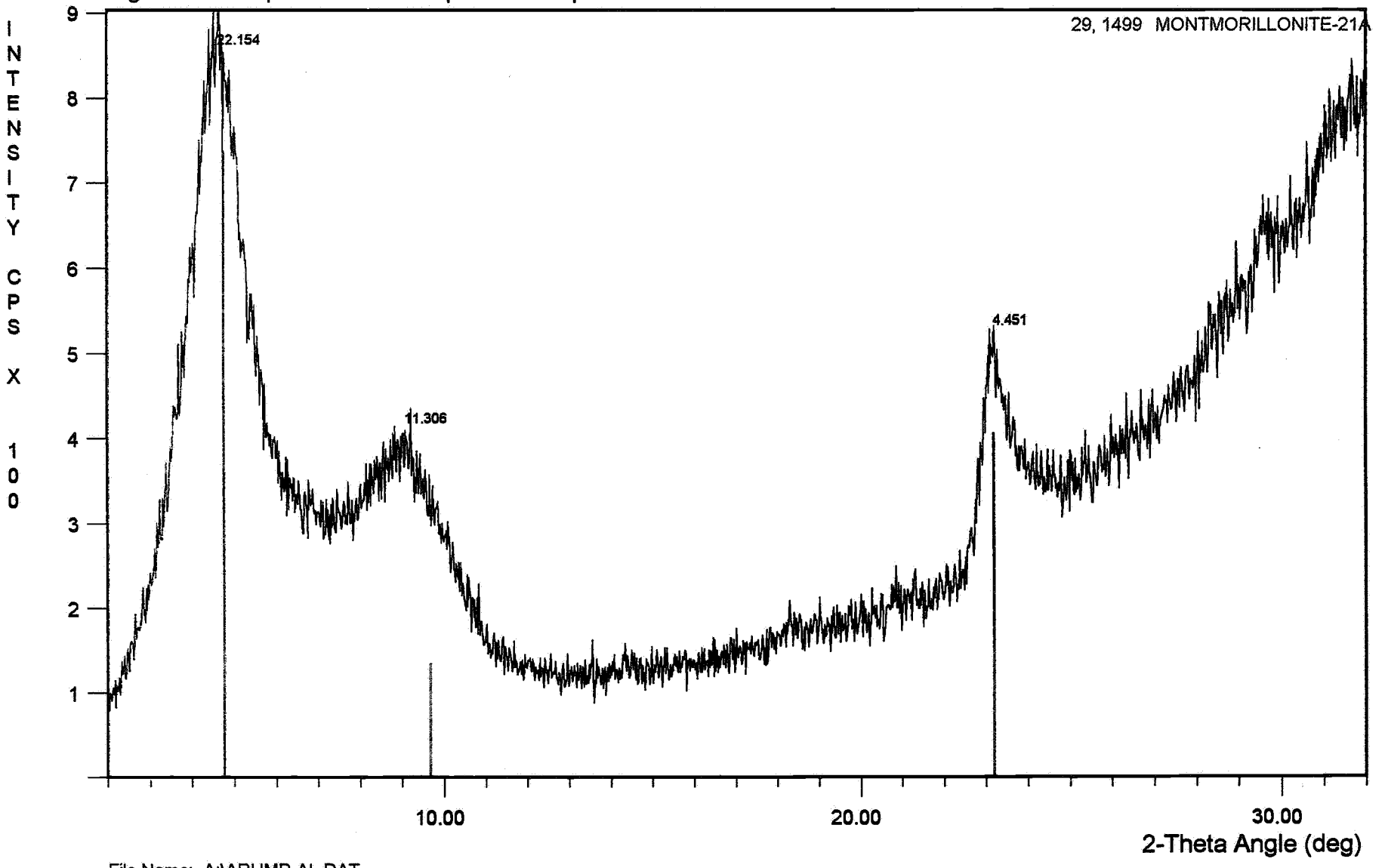
Fig. 1.1. Wyoming Bentonite pillared with BHAlCl at pH 4.1. Run moist. Co Ka radiation.



File Name: A:\WYOM-AL.DMP

0001185

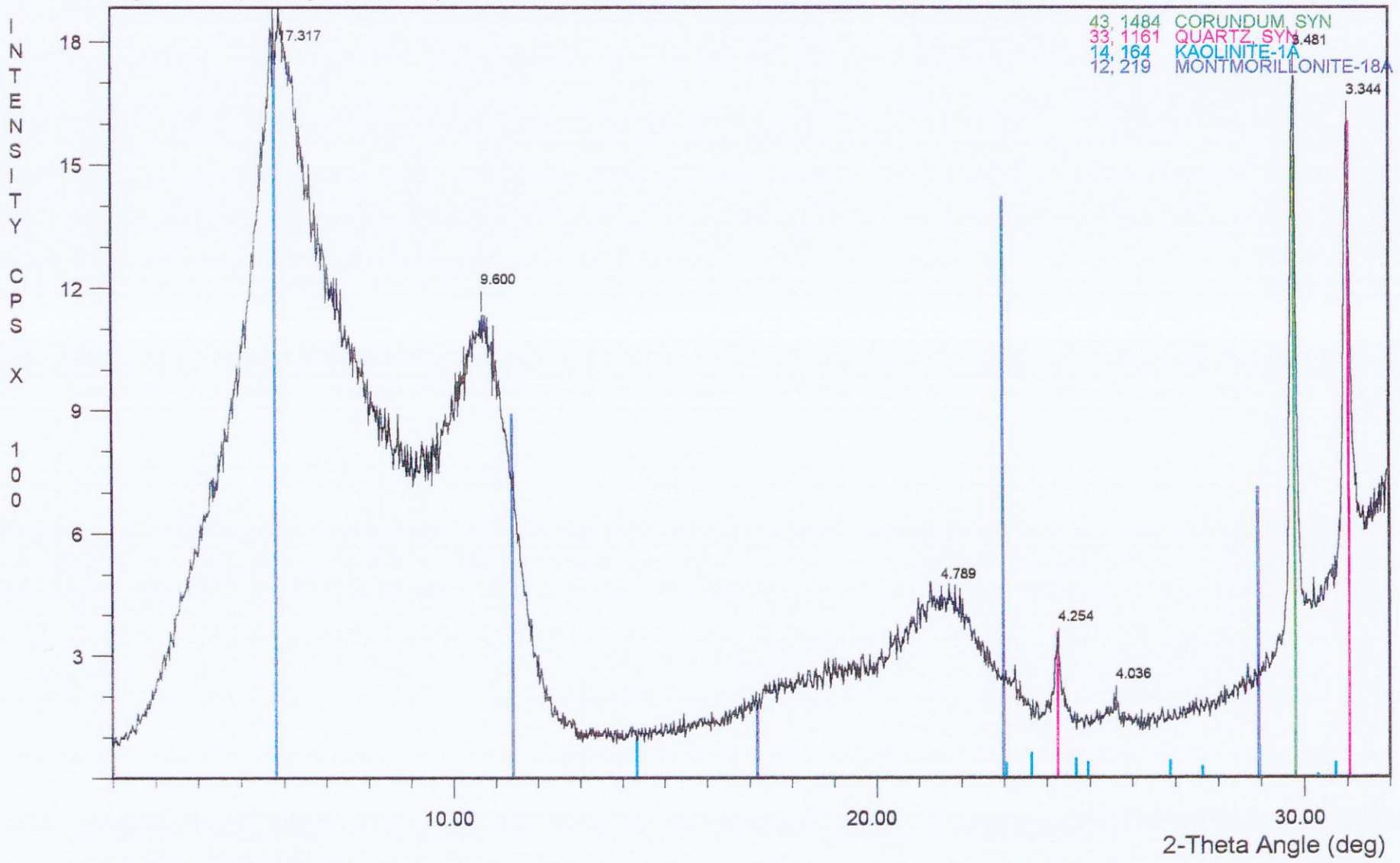
Fig. 1.2. Arumpo Bentonite 1-2µm fraction pillared with BHAlCl. Co Ka radiation.



File Name: A:\ARUMP-AL.DAT

000186
13

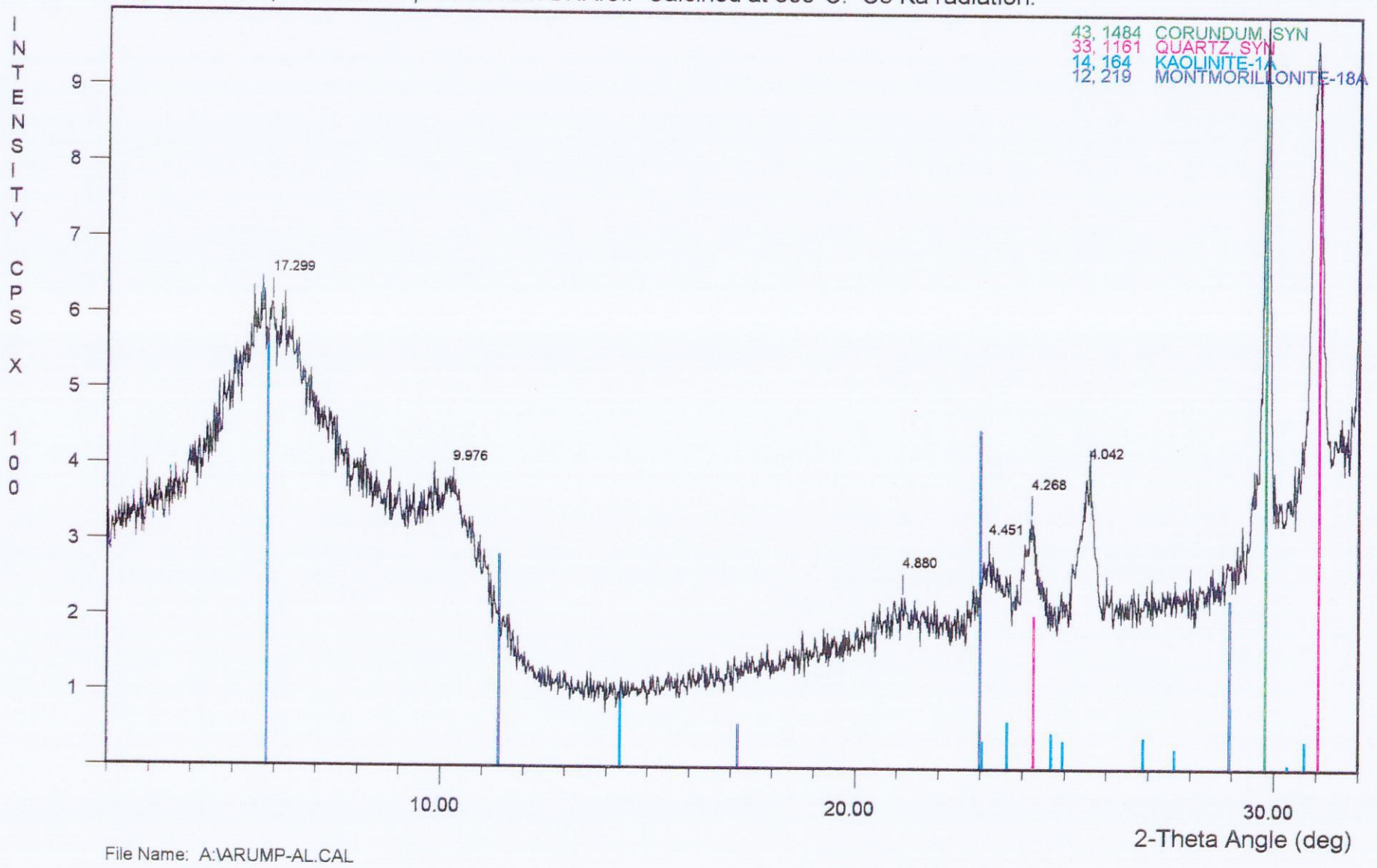
Fig. 1.3. Wyoming Bentonite pillared with BHAlCl. Calcined at 500°C. Co Ka radiation.



File Name: A:\WYOM-AL.500

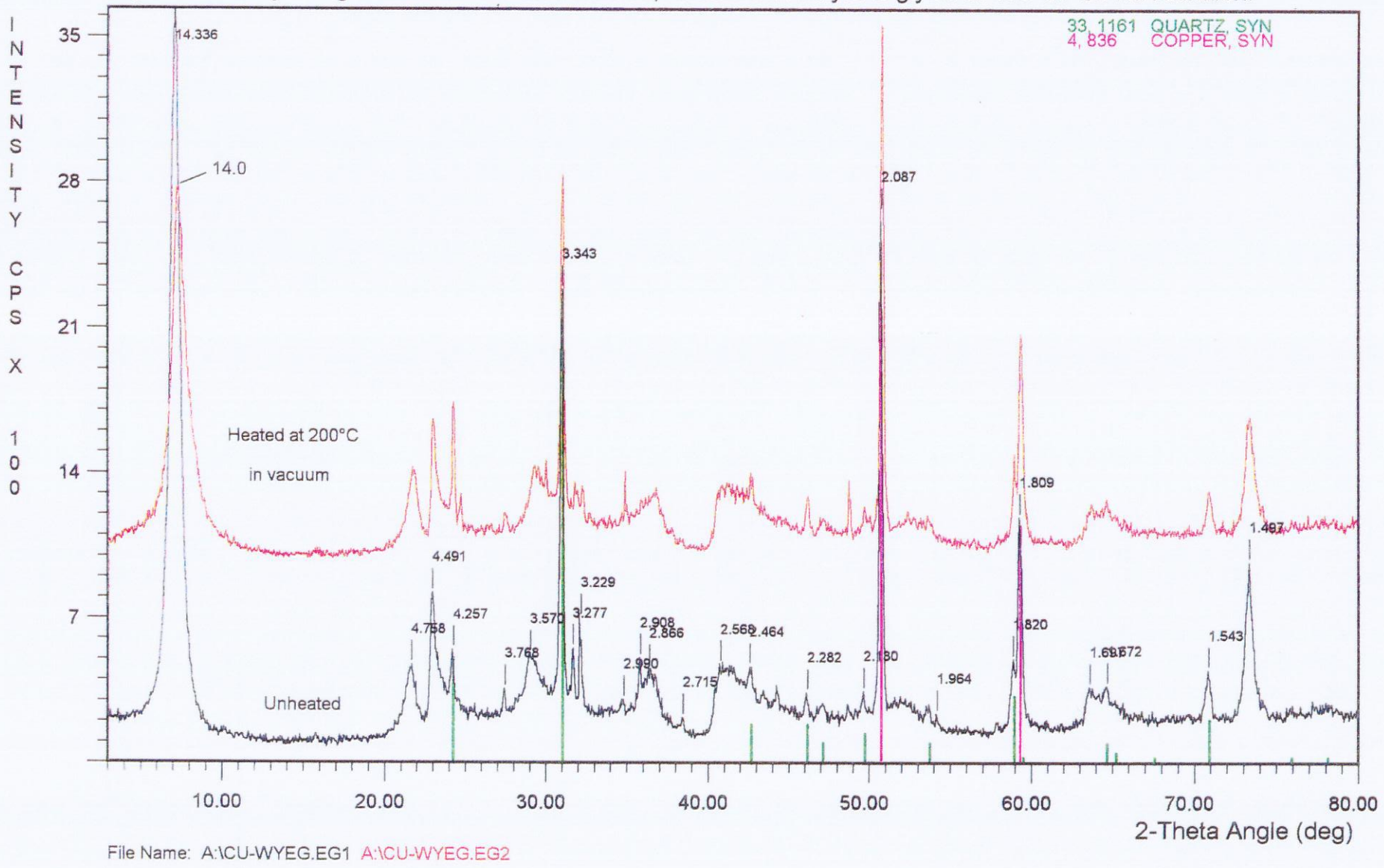
000187
14

Fig. 1.4. Arumpo Bentonite pillared with BHAlCl. Calcined at 500°C. Co Ka radiation.



0001188
15

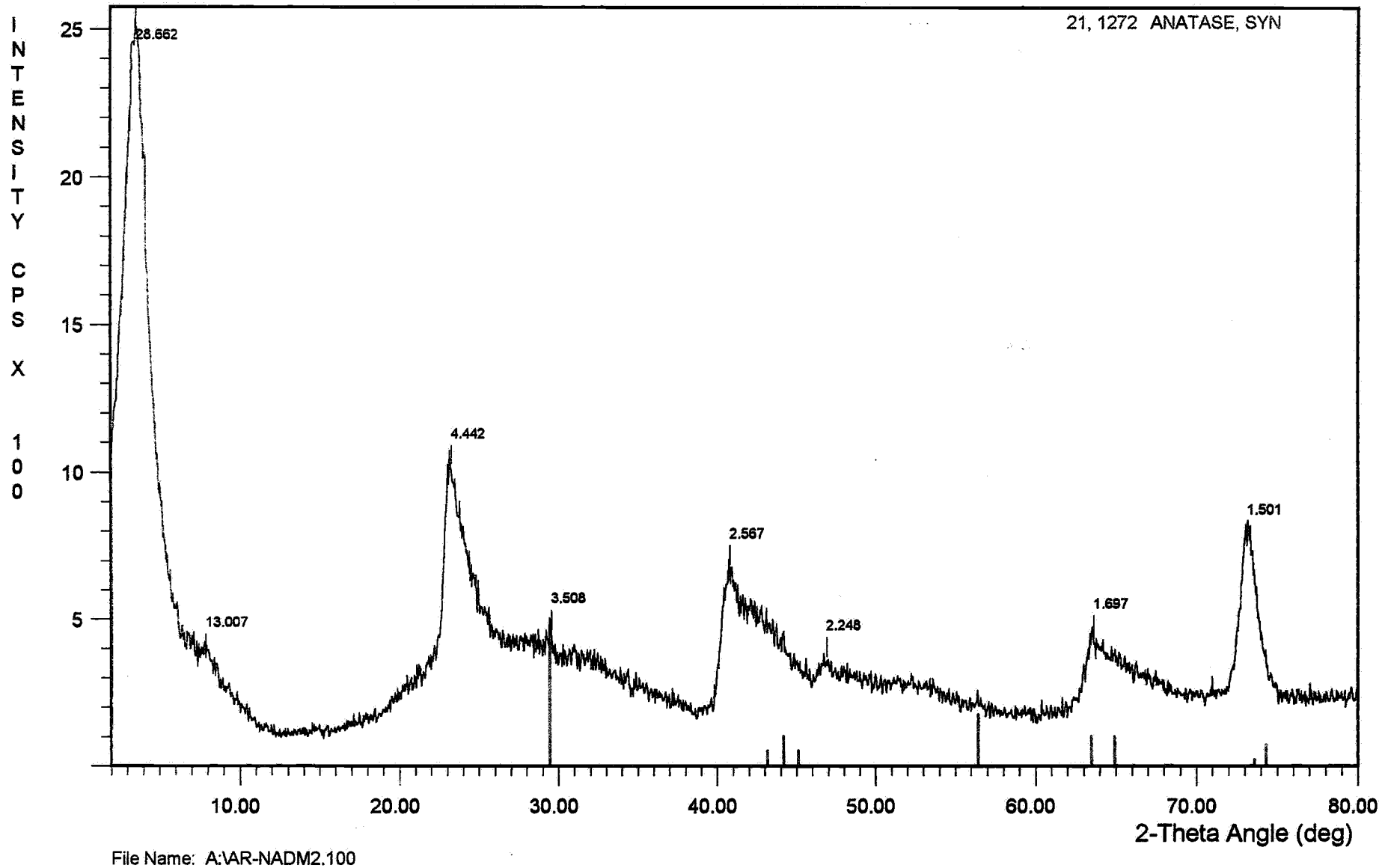
Fig. 1.5. Na Wyoming Bentonite saturated with Cu, heated with ethylene glycol at 195°C. Co Ka radiation.



File Name: A:\CU-WYEG.EG1 A:\CU-WYEG.EG2

0001891

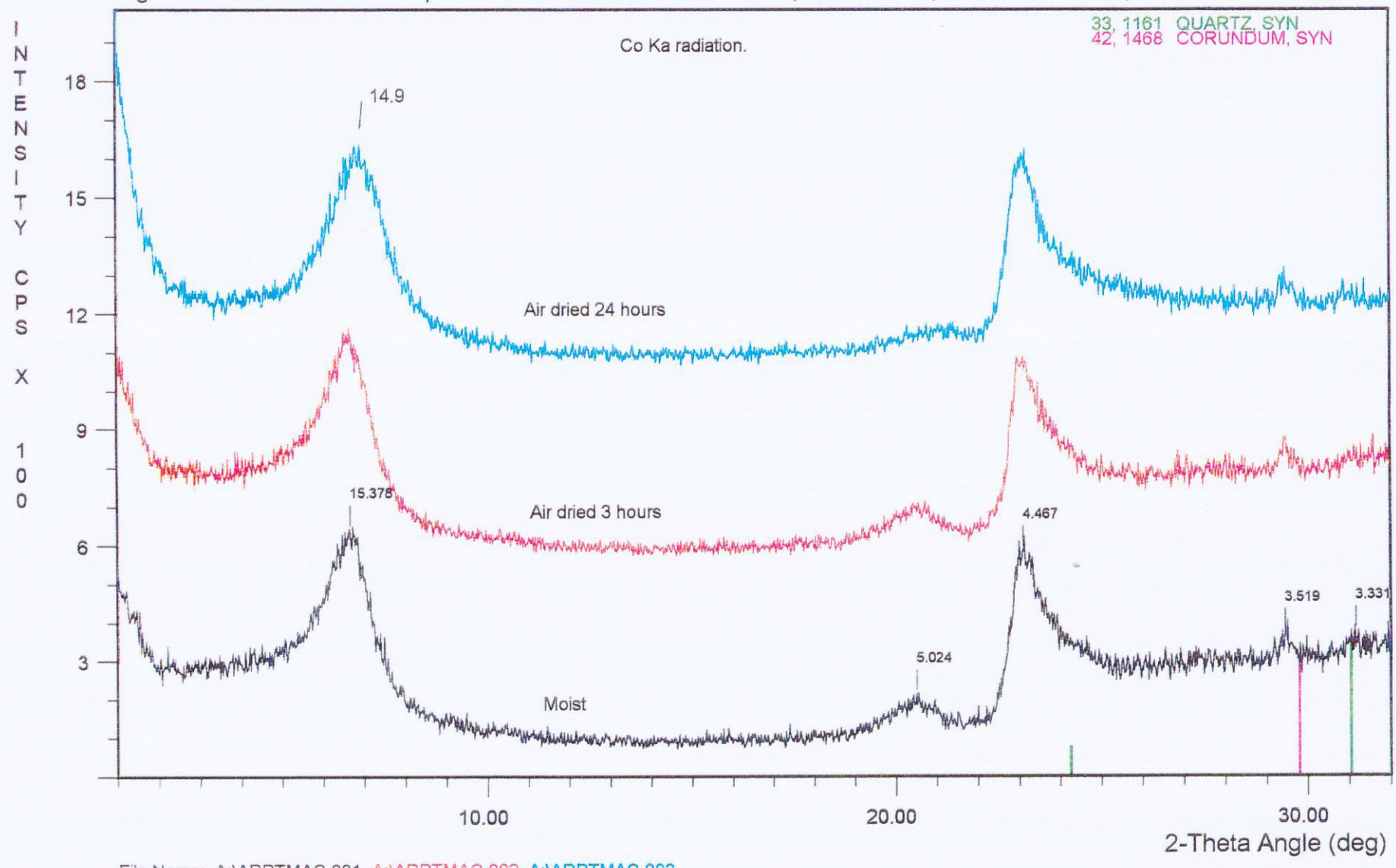
Fig. 1.6. Na-saturated Arumpo bentonite treated with DMDOAB at 70°C for 24 hours. Co Ka radiation.



File Name: A:\AR-NADM2.100

000190

Fig. 1.7. Na-saturated Arumpo bentonite reacted with PTMAC; water moist, air dried 3 hours, air dried 24 hours.



0001191

2. COATING ORGANOPHILIC CLAYS WITH SYNTHETIC MAGNETITE PARTICLES

In a very successful method of removing certain types of organic matter from water (the SIROFLOC process), organic matter is adsorbed onto fine-grained magnetite by electrostatic forces. The particles are then magnetically separated from the water and, by changing the pH from below to above the isoelectric point of magnetite, the organic matter removed. The cleaned magnetite is then reused. The success of this process is clearly reliant on the complete magnetic scavenging of organic coated magnetite from suspension.

The pH dependant sorption of magnetite particles is suitable for the removal of humic materials (which are largely anionic) but is not likely to be as effective for the removal of non-polar or cationic organic molecules. Non-polar compounds, such as the aromatic hydrocarbons that are common constituents of petroleum, are significant pollutants in water supplies. The aim of this research was to endow organophilic clays, such as those described in Section 1 of this Report, with "magnetic" properties so that they can be removed from suspension in a similar way to that used in the SIROFLOC process. As clays have no inherent magnetic properties, it is necessary to attach magnetic particles to them in order to achieve this aim.

The CSIRO Division of Soils has developed methods of synthesising very-fine-grained magnetite particles (Taylor *et al.*, 1987; Maher and Taylor, 1989). The magnetite produced by these techniques has been successfully used in an adaptation of the SIROFLOC process during laboratory trials at the University of Birmingham, UK. Clearly, if the synthesis techniques could be modified so that magnetite particles could be attached to the surfaces of clays, then our aim would be achieved.

Initially the possibility of incorporating magnetite into the interlayer positions of smectite clays was investigated. This was not successful because the Fe(III) required for the synthesis of magnetite is not stable in the interlayer sites of smectitic clays (Cardile and Slade, 1995). Consequently an investigation was carried out to see if magnetite could be attached to the external surfaces of (organophilic) clays by variation

of the magnetite synthesis technique. Thus smectite and palygorskite were introduced during the synthesis of magnetite.

The relevant clay samples were dispersed as well as possible in a small quantity of water and then added to a solution of iron compounds required for the synthesis of magnetite. Magnetite was then precipitated, onto the clay, from solution by a variation of the method described by Taylor *et al.* (1987) and Maher and Taylor (1989). The resultant composite material was separated magnetically, washed in water, ethanol and dried from acetone. Samples were examined by X-ray diffraction and, in some cases, transmission electron microscopy.

The important points observed in the preliminary trials were:-

1. the whole resultant sample was magnetic with the magnetic particles adhering to the clay surfaces (Figs. 2.1 and 2.2);

2. when a smectitic clay was used, X-ray diffraction showed that it still exhibited interlayer expansion when glycerol was applied to an oriented sample; and

3. when a pillared clay was coated with magnetite by these techniques the pillaring was not destroyed.

The first point shows that the synthesis technique does allow magnetite to attach to the clay surfaces. The magnetite particles attached to palygorskite (Fig. 2.2) are dispersed relatively well compared to the magnetite particles attached to smectite (Fig. 2.1). This suggests that the magnetite attaches more strongly to palygorskite than to smectite so that the magnetite particles are unable to aggregate by magnetic attraction. The difference in dispersion may be due to differences in the surface charges of palygorskite and smectite. However, for both the smectite and palygorskite preparations there are magnetite aggregates not attached to clay surfaces.

The second and third points show that the procedure for synthesising magnetite does not affect the interlayer exchange properties of smectites and therefore

should not adversely affect the organophilic properties of modified clays. In order to test this hypothesis, several smectite samples, intercalated with dimethyldioctadecyl ammonium ions (see Section 1 of this Report), were coated with magnetite as described above and their sorption capacities measured by the method described in Section 1 of this Report. The results of the sorption experiments are shown in a Table 2.1. The absorptive capacity of the modified smectites, although slightly reduced by coating with the fine-grained magnetite (compare with results shown in Table 1.1), are still sufficient for use in the removal of non-polar organic compounds from water.

The work to date on the coating of organophilic clays shows considerable promise for the treatment of contaminated water. However, further work needs to be carried out. In particular, the optimum conditions for the adhesion of magnetite to clay particles needs to be determined. Furthermore, the apparent differences in the adhesion of magnetite to palygorskite and smectite needs to be investigated.

References

Maher, B.A. and Taylor, R.M. (1989). Formation of ultrafine magnetite in soils. *Nature*, **336**, 368-370.

Cardile, C.M. and Slade, P.G. (1995). Interlayer cations in vermiculite. In: G.J. Churchman, R.W. Fitzpatrick and R.A. Eggleton (eds.) *Proceedings of the 10th International Clay Conference*. CSIRO, Melbourne.

Taylor, R.M., Maher, B.A. and Self, P.G. (1987). Magnetite in soils: 1. The synthesis of single-domain and superparamagnetic magnetite. *Clay Min.*, **22**, 411-422.

Table 2.1. %Sorption from 1000ppm aqueous solution of hydrocarbon.

Sorbent Clay	Sorbate	
	Benzene	Toluene
Arumpo bentonite + DMDOAB + magnetite coating (29 Nov.)	43	nd
Arumpo bentonite + DMDOAB + magnetite coating (6 Dec.)	39	nd

nd = not determined.

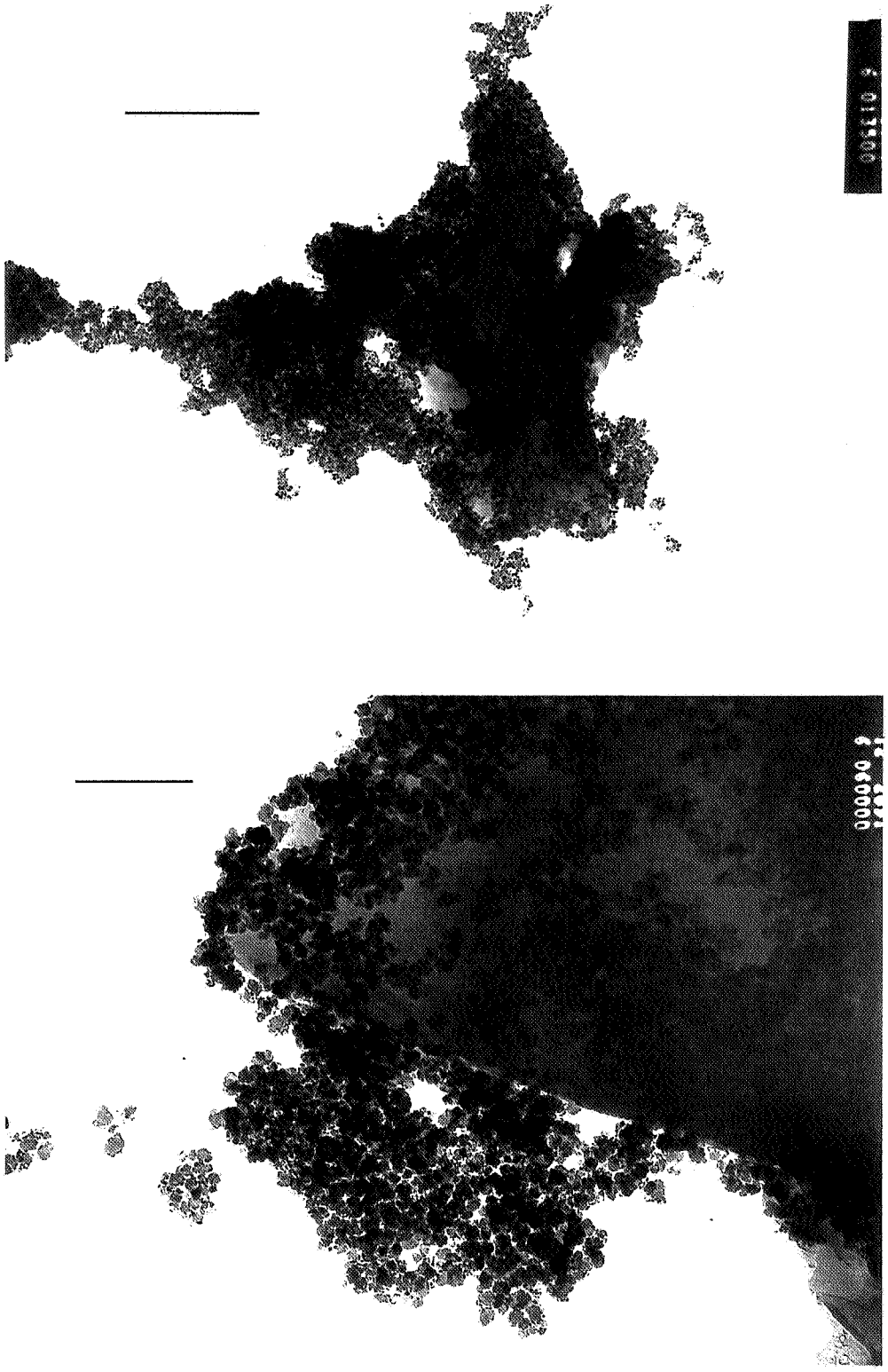


Fig. 2.1. Magnetite attached to Arumpo bentonite. Neg. Nos. 2090 and 2091. Scale bars 1μm (upper) and 0.2μm (lower).

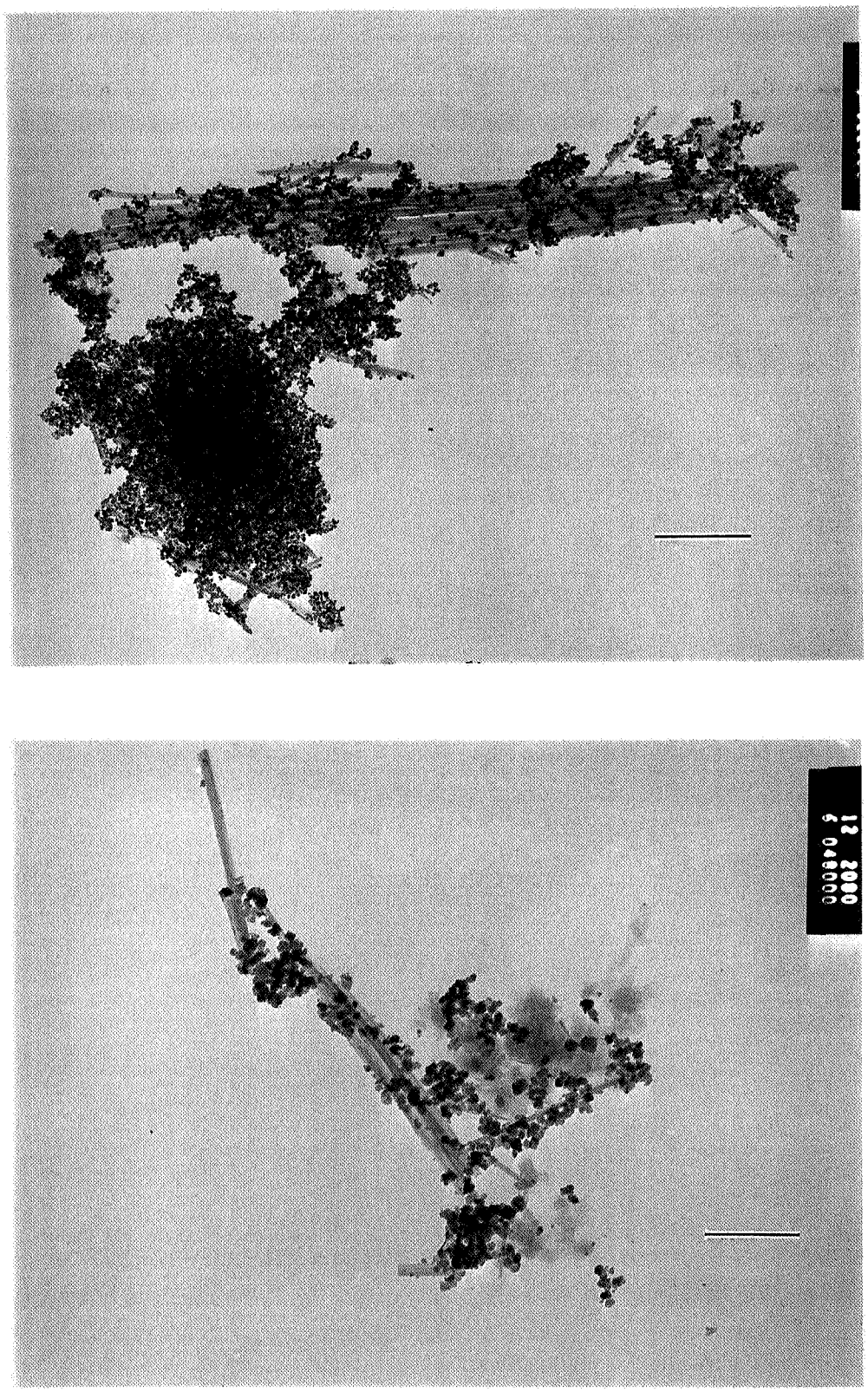


Fig. 2.2. Magnetite attached to palygorskite. Neg. Nos. 2081 and 2080. Scale bars 0.5μm (upper) and 0.2μm (lower).

3. ZEOLITE 'A' SYNTHESIS FROM SOUTH AUSTRALIAN AND NEW ZEALAND KAOLINS

Introduction

Zeolites are hydrated aluminosilicate minerals which carry a high net negative charge. Their structures are composed of linked tetrahedra in rings through which access to the source of the charge is via channels within the rings. These have limited sizes and only ions or molecules with smaller diameters can permeate the structural channels. As a result, zeolites are useful as ionic or molecular sieves. They are particularly useful for the uptake of simple cations such as those of heavy metals.

Zeolites can be synthesised from silica, alumina and metal cations in appropriate proportions. The starting materials for zeolite synthesis are commonly silica and alumina gels but clay minerals (generally kaolins) can be used after their prior disintegration (Breck, 1974; Murat *et al.*, 1992). A study of a number of South Australian kaolins and also a standard halloysite from New Zealand was carried out to determine their effectiveness as raw materials for the synthesis of a zeolite.

Methods

Four South Australian kaolins and one New Zealand kaolin were selected for modification to zeolite. These were:

Birdwood - well-crystalline kaolinite

Cromer 'C' - < 2μm fraction, moderately-crystalline kaolinite with halloysite

Imbitcha - halloysite with some alunite

Mount Hope Shaft - fine fraction, well crystalline kaolinite as large thin sheets with traces of quartz and anatase

New Zealand China Clays - halloysite product with trace quartz and cristobalite.

The Birdwood, Cromer 'C' and New Zealand China Clays samples are described in Absorbent Clay Project, Progress Report No. 1, June 1994. The Mount Hope shaft clay is described as sample MHS1 by Keeling *et al.* (1992). Imbitcha kaolin was not included

in earlier characterisation and an XRD pattern and scanning electron microscopy images of this material are given in Fig. 3.1 and Fig. 3.2 respectively.

Samples were calcined by heating to 900°C in a muffle furnace for 3 hours in order to "activate" the kaolins. 10ml of a solution of 11% NaOH was added to 1.85g of each of the calcined kaolins in a glass beaker. The mixture was then allowed to 'gel' at room temperature by continuous agitation with a magnetic stirrer for 24 hours. The 'gel' was then placed in a 105°C oven for 4 hours to crystallise into zeolite 'A'.

The samples were lightly ground in an agate mortar and pestle and the resulting powders pressed into aluminium holders for X-ray diffraction analysis (XRD). XRD patterns were recorded with a Philips PW1800 microprocessor-controlled diffractometer using CoKα radiation, variable divergence slit, and graphite monochromator. The diffraction patterns were recorded in steps of 0.05° 2θ with a 1.0 second counting time per step, and logged to permanent data files on an IBM-compatible PC for analysis.

Scanning electron microscopy (SEM) was used to display the crystal morphology of the processed samples. Small subsamples were dispersed in alcohol and deposited onto aluminium stubs before being coated with 10nm of gold. A Cambridge Instruments Stereoscan S250 was used in the backscattered electron mode to record the electron micrographs.

Sorption testing for Cr and for toluene by a synthetic product formed from Birdwood kaolin and by commercial zeolites (clinoptilolite from Zeolite Australia and Pivot) were carried out as described respectively in Absorbent Clay Project, Progress Report No. 2, November 1994 and in Section 1 of this Report.

Results

All kaolin samples were converted to very pure zeolite 'A' (> 90% conversion). Zeolite formation from the kaolin samples with other impurities was not inhibited by their presence. Figs. 3.3 to 3.7 show the diffraction patterns of the zeolite

produced from the Birdwood, Cromer, Imbitcha, Mt Hope and NZ China Clay samples respectively. The diffraction patterns show very sharp well crystalline materials that match the "standard" zeolite 'A' phase found in the ICDD (International Centre for Diffraction Data) database. Impurity phases were generally carried through the process without significant modification. Alunite in Imbitcha clay was absent in the processed sample.

Figs. 3.8 to 3.12 show the crystal morphology of the processed samples. All show dominant well formed cubes of uniform 2μm widths. Crystal twins are common, along with some finer irregularly shaped particles. The Imbitcha sample (Fig. 3.10) contains a greater abundance of finer particles and clumped crystal aggregates.

The results of sorption testing for Cr are shown in Table 3.1 and for toluene in Table 3.2. The Cr was taken up almost completely by the synthetic zeolite and to a lesser extent by the commercial zeolites. Neither the synthetic zeolite nor the commercial zeolite absorbed any toluene. These results are consistent with the notion that zeolites are unable to absorb large molecules and that their usefulness is restricted to simple cations.

References

Breck, D.W. (1974). *Zeolite Molecular Sieves. Structure, Chemistry and Uses.* John Wiley and Sons, New York.

Keeling, J.L., Self, P.G., McClure, S.G., Raven, M.D. and Milnes, A.R. (1992). Characterisation of kaolin samples from the Mount Hope deposit. *Mines and Energy Review, South Australia*, **158**, 21-26.

Murat, M., Amokrane, A., Bastide, J.P. and Montanaro, L. (1992). Synthesis of zeolites from thermally activated kaolinite. Some observations on nucleation and growth. *Clay Minerals*, **27**, 119-130.

Table 3.1. %Uptake from 100mls of 1000ppm Cr solution by 15gms of zeolite.

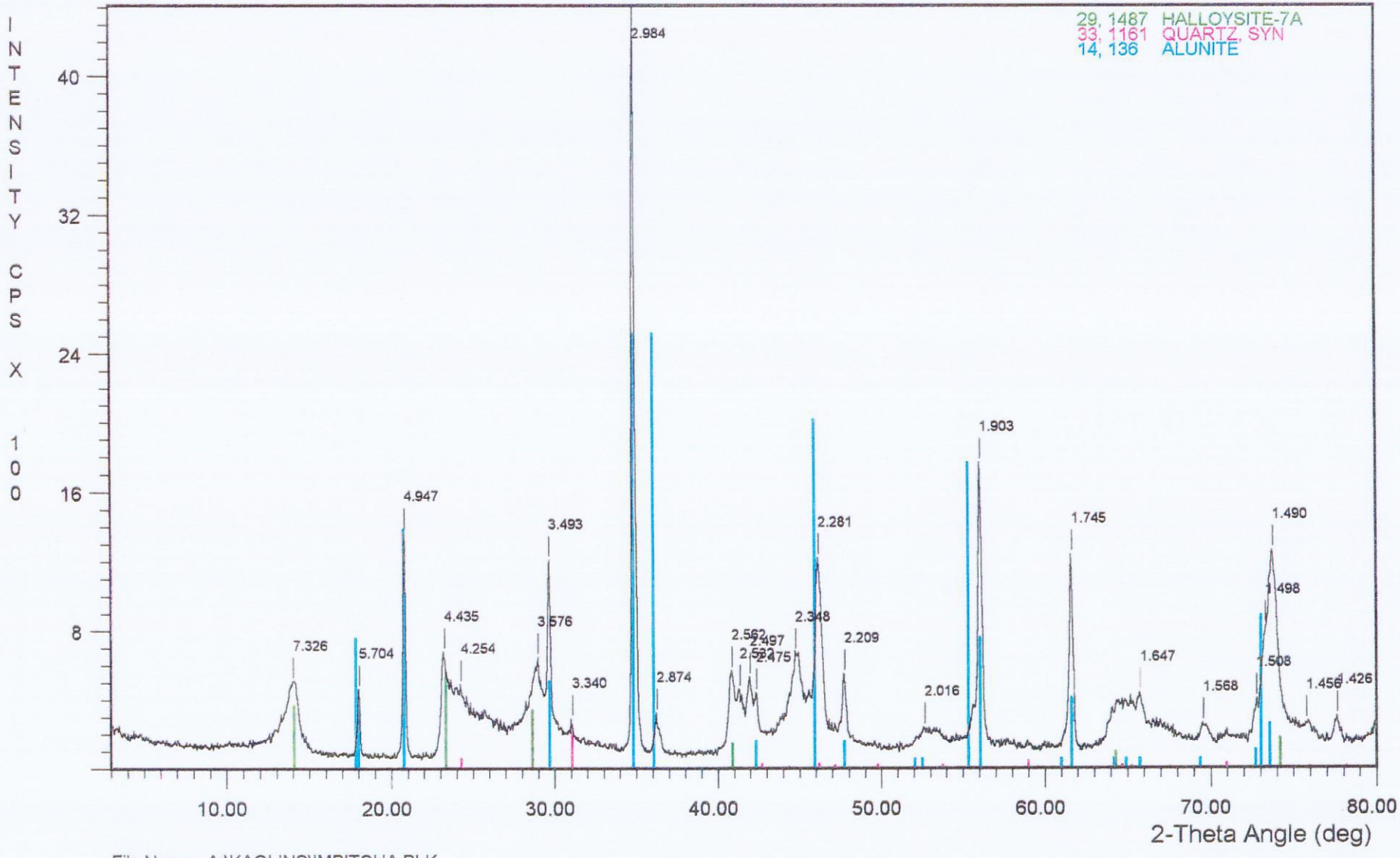
Sorbent	%Uptake of Cr
ZEOLITE AUSTRALIA clinoptilolite	40.2
PIVOT clinoptilolite	74.9
Synthetic zeolite 'A' (from Birdwood kaolinite)	99.5

Table 3.2. %Sorption from 1000ppm aqueous solution of hydrocarbon.

Sorbent	Sorbate	
	Benzene	Toluene
PIVOT clinoptilolite	nd	0
Synthetic zeolite 'A' (from Birdwood kaolinite)	nd	0

nd = not determined.

Fig. 3.1. Imbitcha bulk sample (Co Ka radiation).



File Name: A:\KAOLINS\IMBITCHA.BLK

0002047

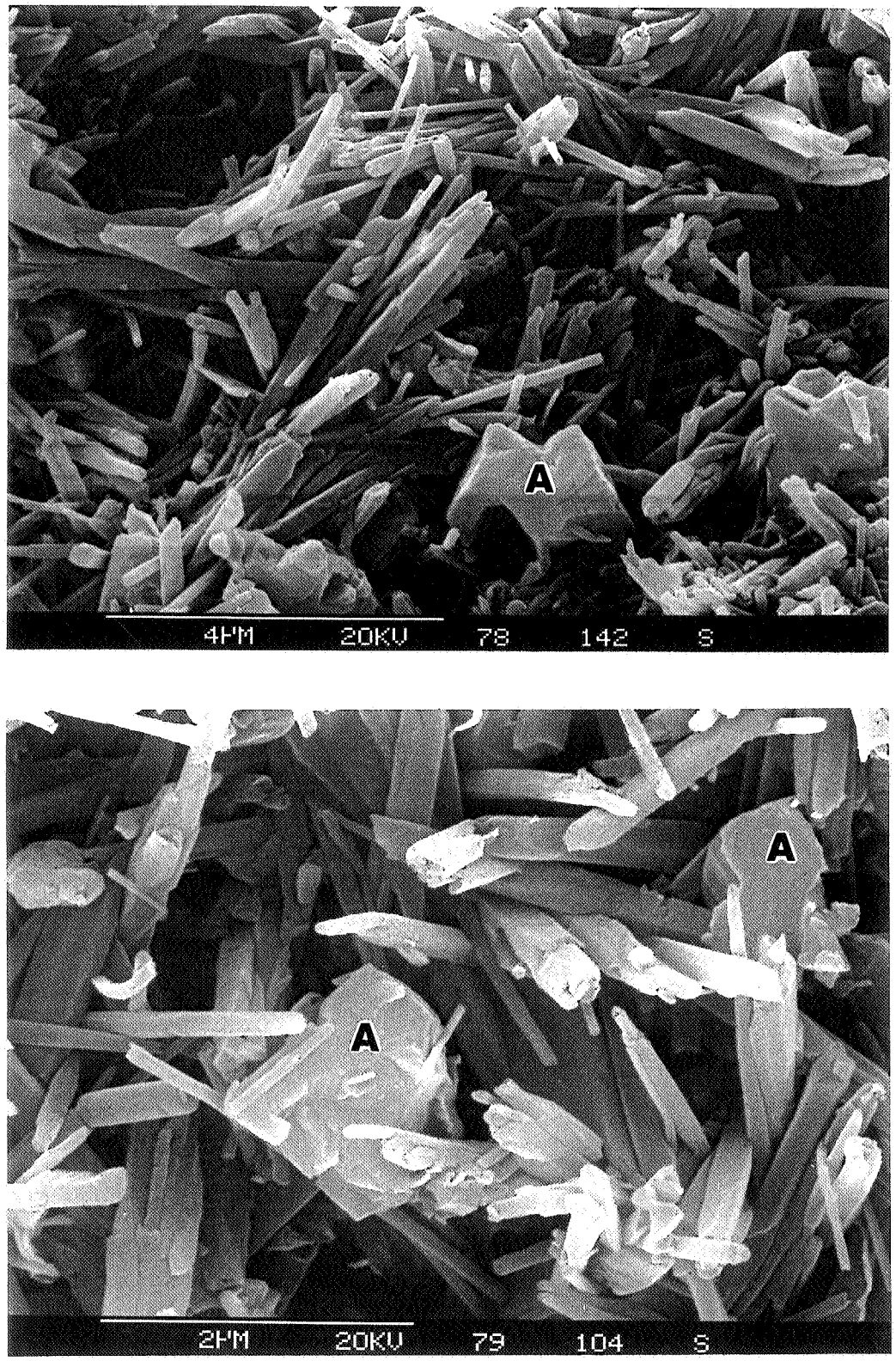
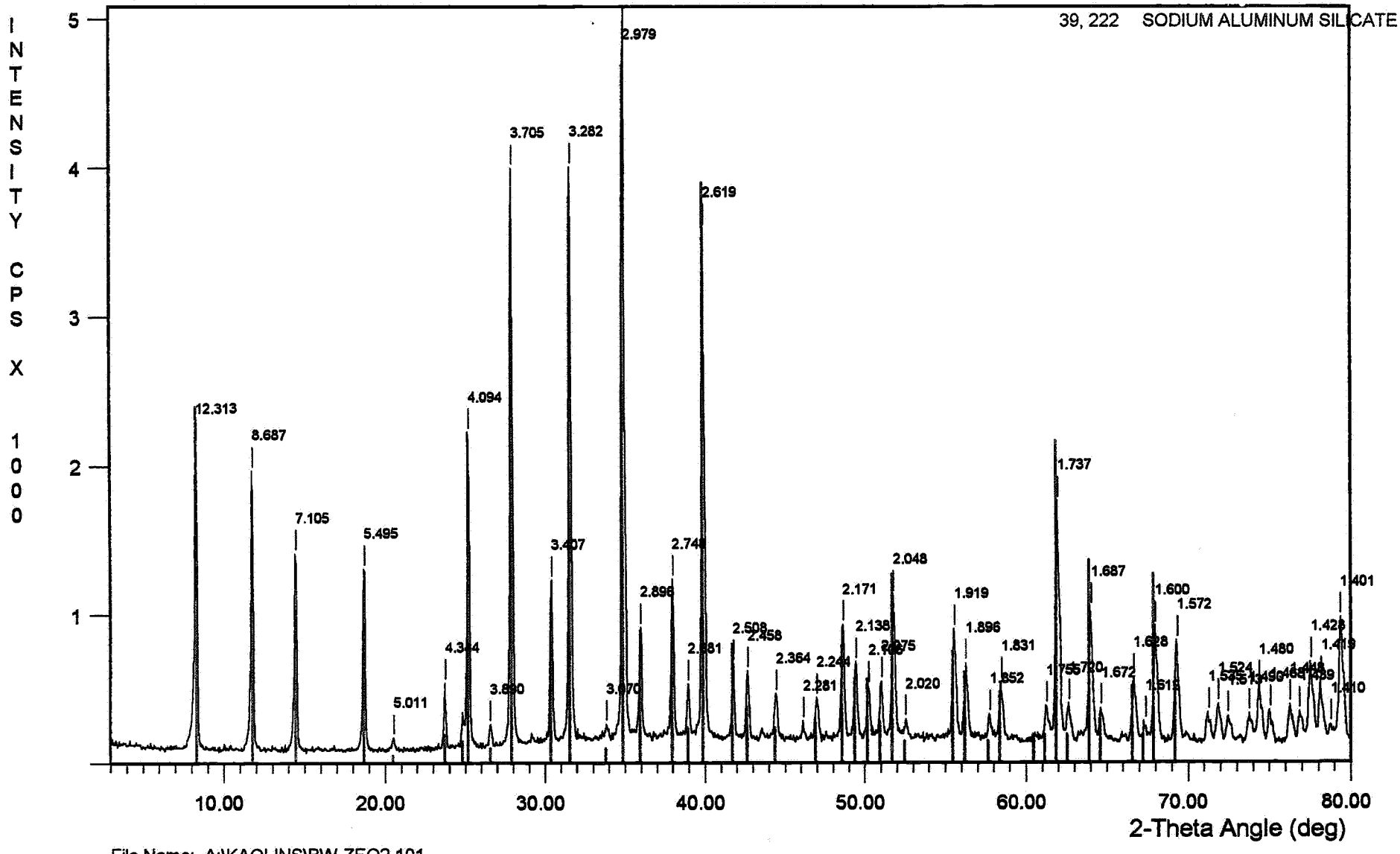


Fig. 3.2. Scanning electron micrographs of Imbitcha kaolin showing tubular halloysite and blocky alunite (A). Neg. Nos. 783142 and 793104.
Scale bars 4μm (upper) and 2μm (lower).

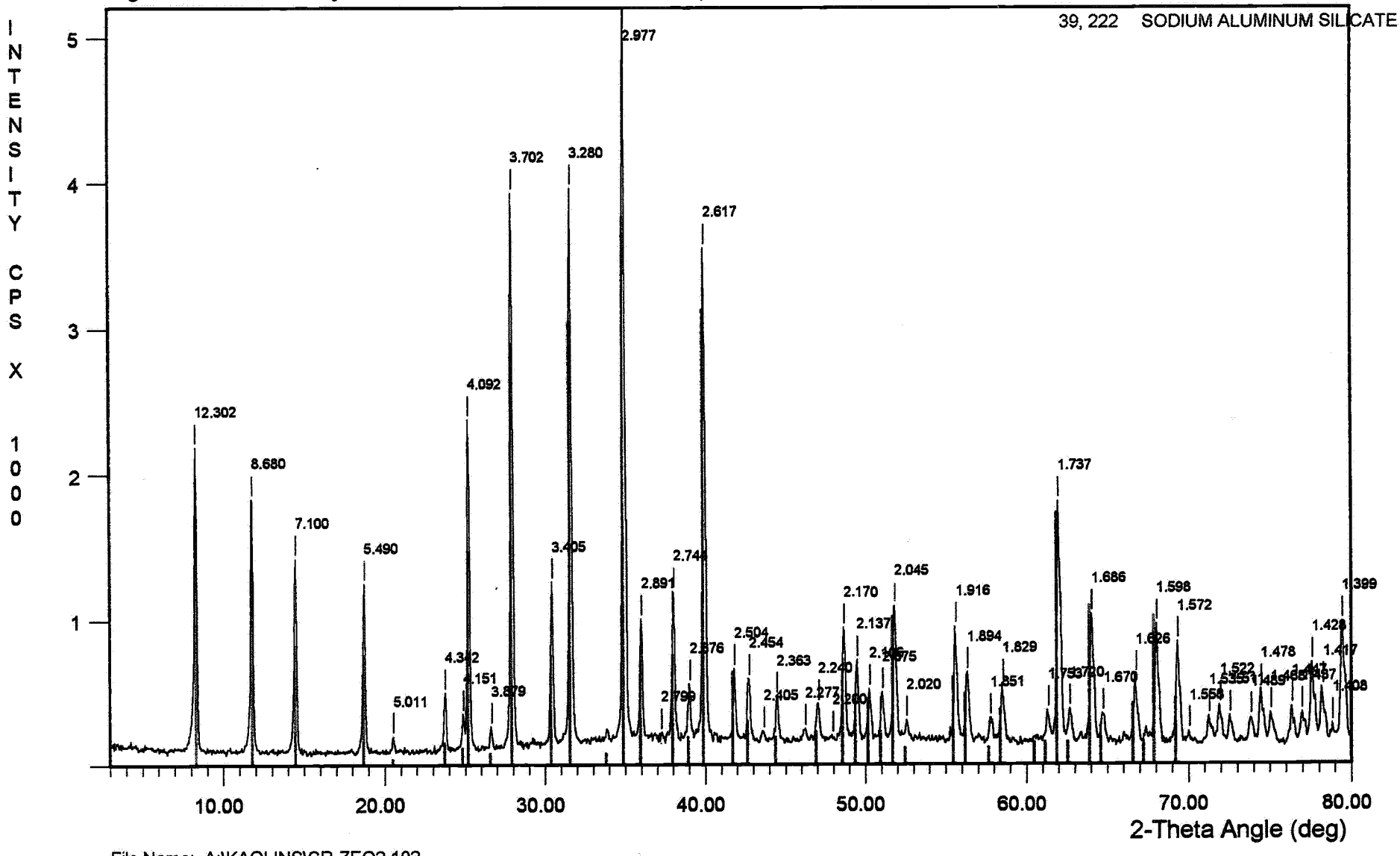
Fig. 3.3. Zeolite 'A' synthesised from Birdwood bulk kaolin (Co Ka radiation).



File Name: A:\KAOLINS\BW-ZEO2.101

000206

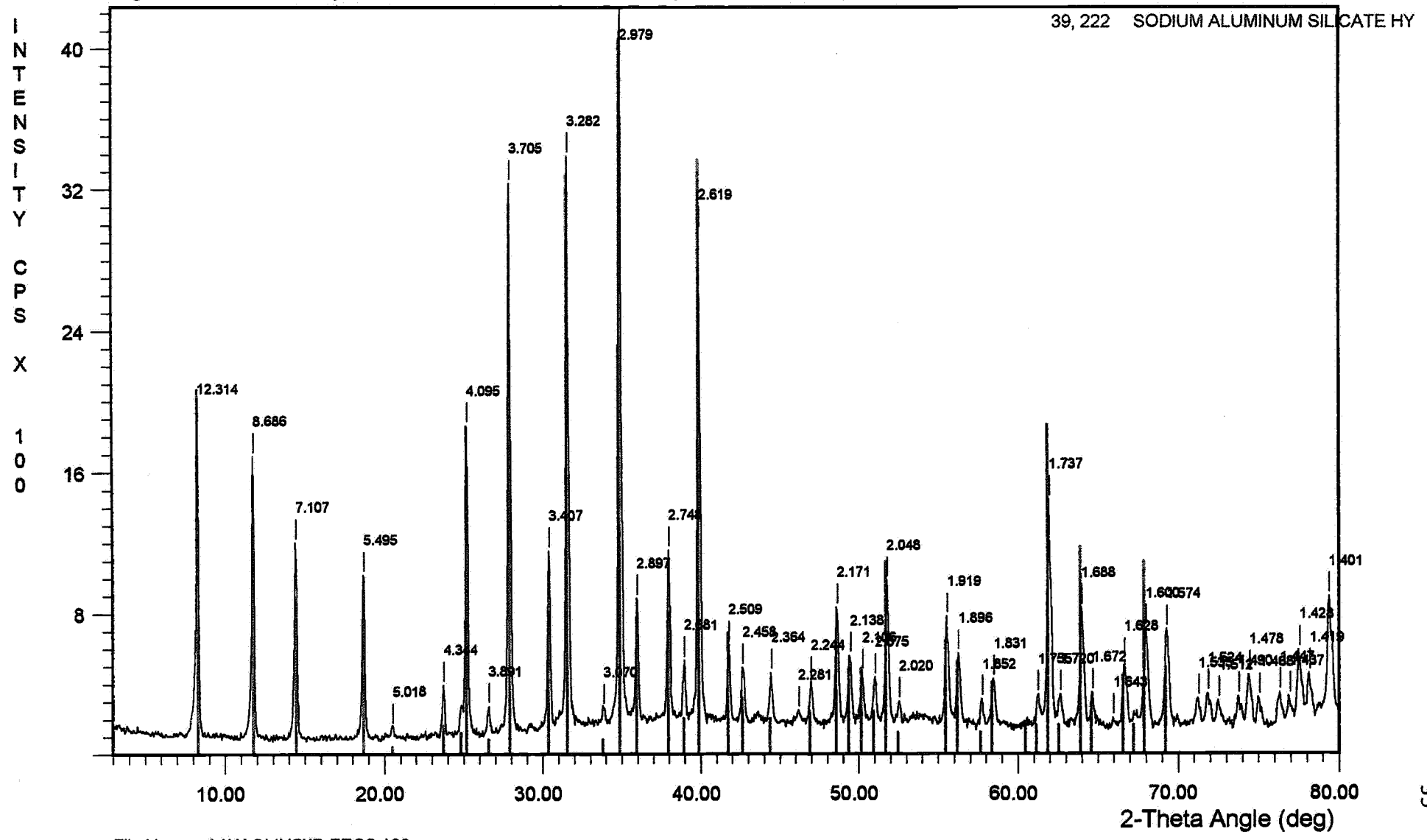
Fig. 3.4. Zeolite 'A' synthesised from Cromer 'C' kaolin (Co Ka radiation).



File Name: A:\KAOLINS\CR-ZEO2.102

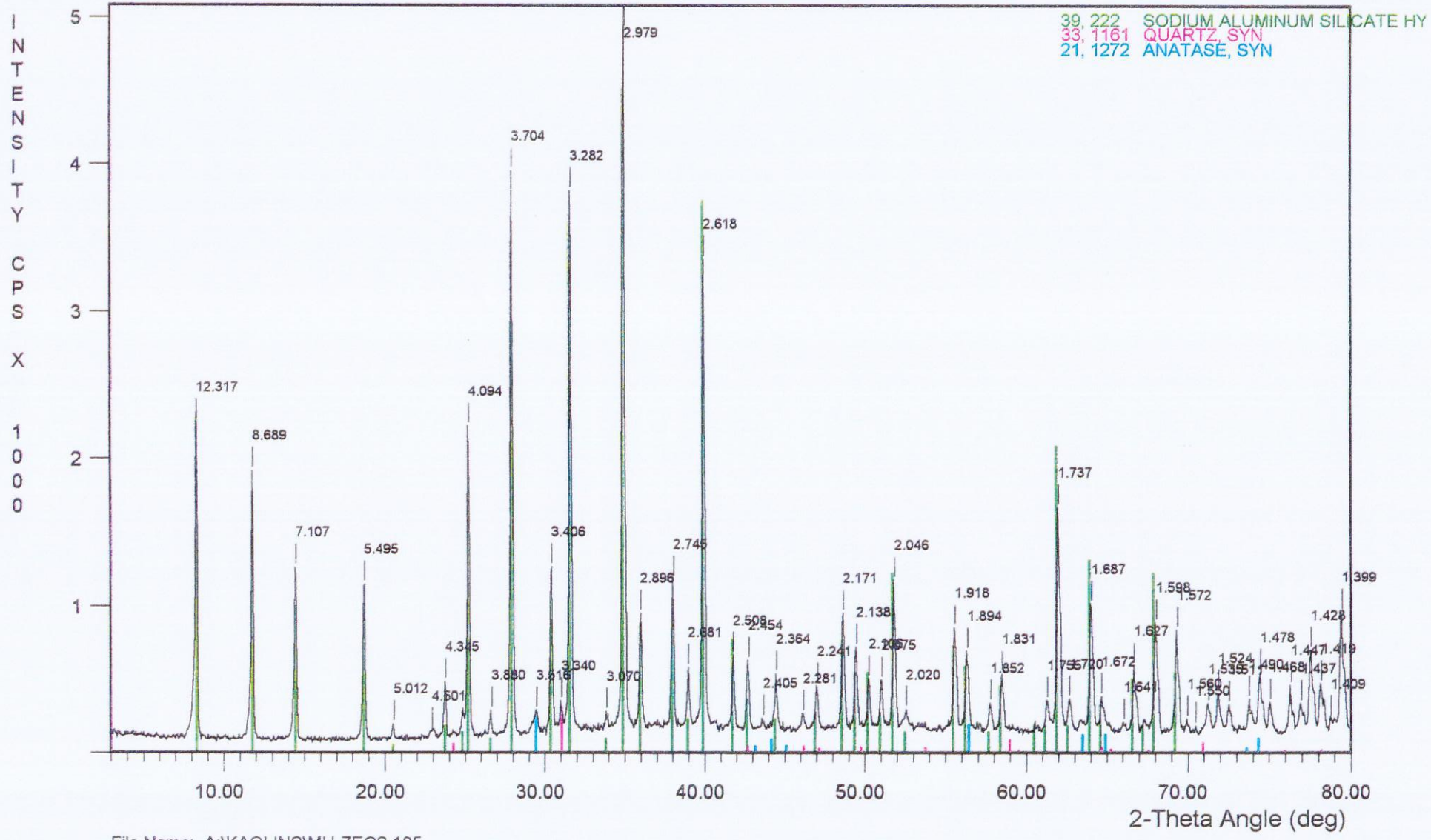
0002207

Fig. 3.5. Zeolite 'A' synthesised from Imbitcha kaolin (Co Ka radiation).



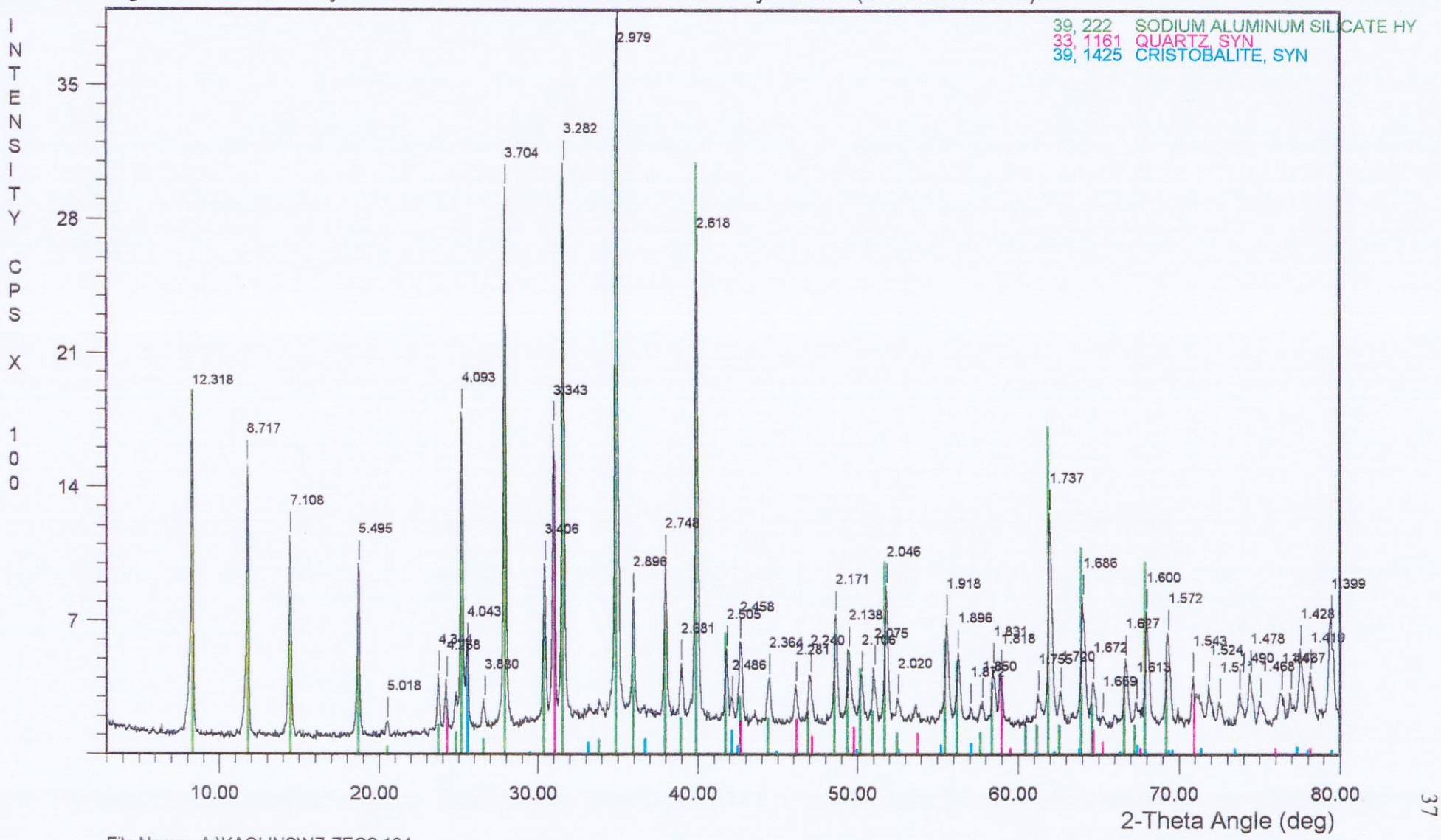
000208

Fig. 3.6. Zeolite 'A' synthesised from Mt Hope kaolin (Co Ka radiation).



File Name: A:\KAOLINS\MH-ZEO2.105

Fig. 3.7. Zeolite 'A' synthesised from New Zealand China Clays kaolin (Co Ka radiation).



File Name: A:\KAOLINS\NZ-ZEO2.104

000210

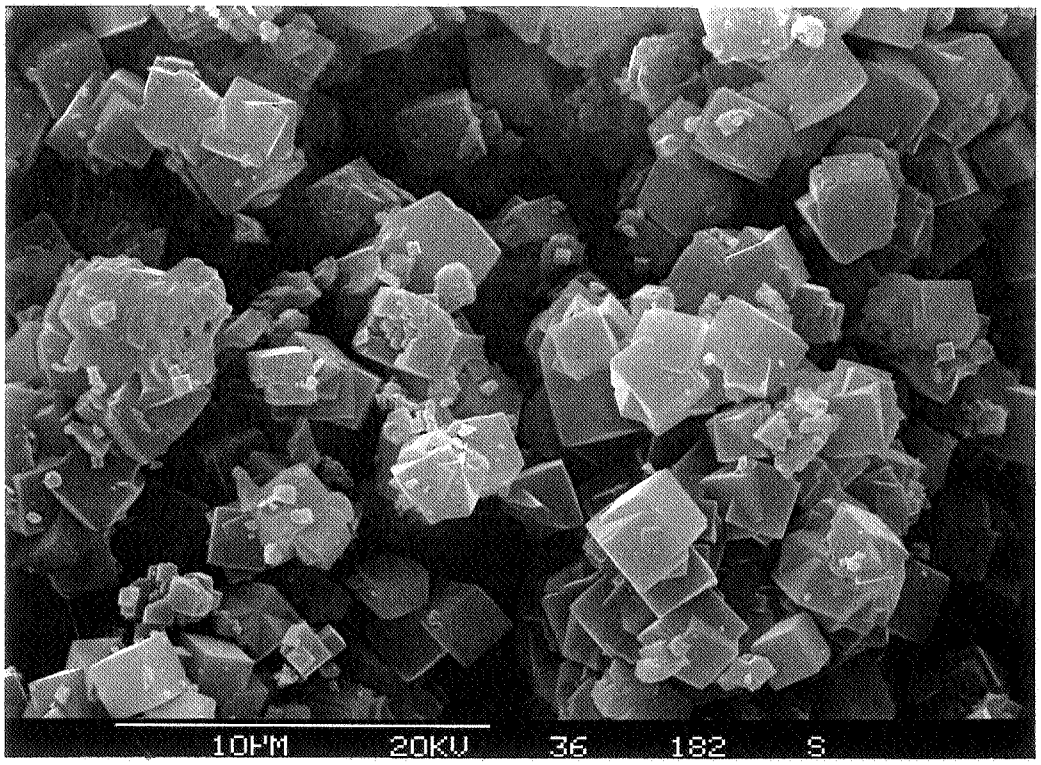


Fig. 3.8. Zeolite 'A' synthesised from Birdwood kaolin (bulk sample).

Neg. No. 363182. Scale bar 10μm.

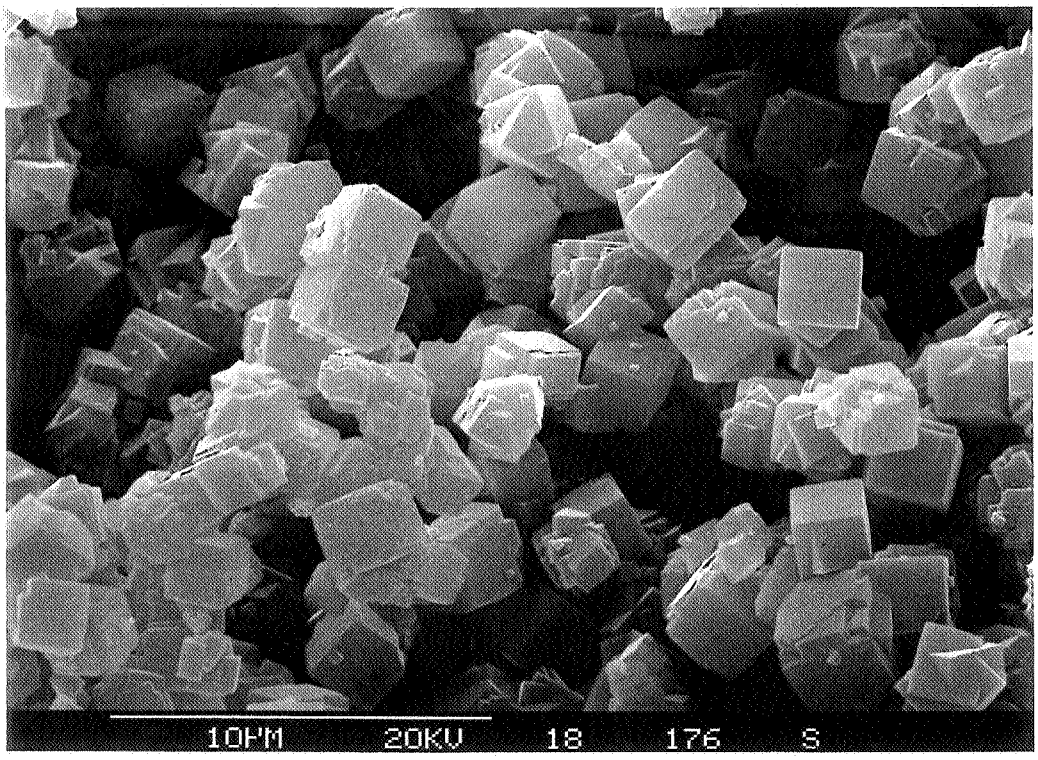


Fig. 3.9. Zeolite 'A' synthesised from Cromer 'C' kaolin.

Neg. No. 183176. Scale bar 10μm.

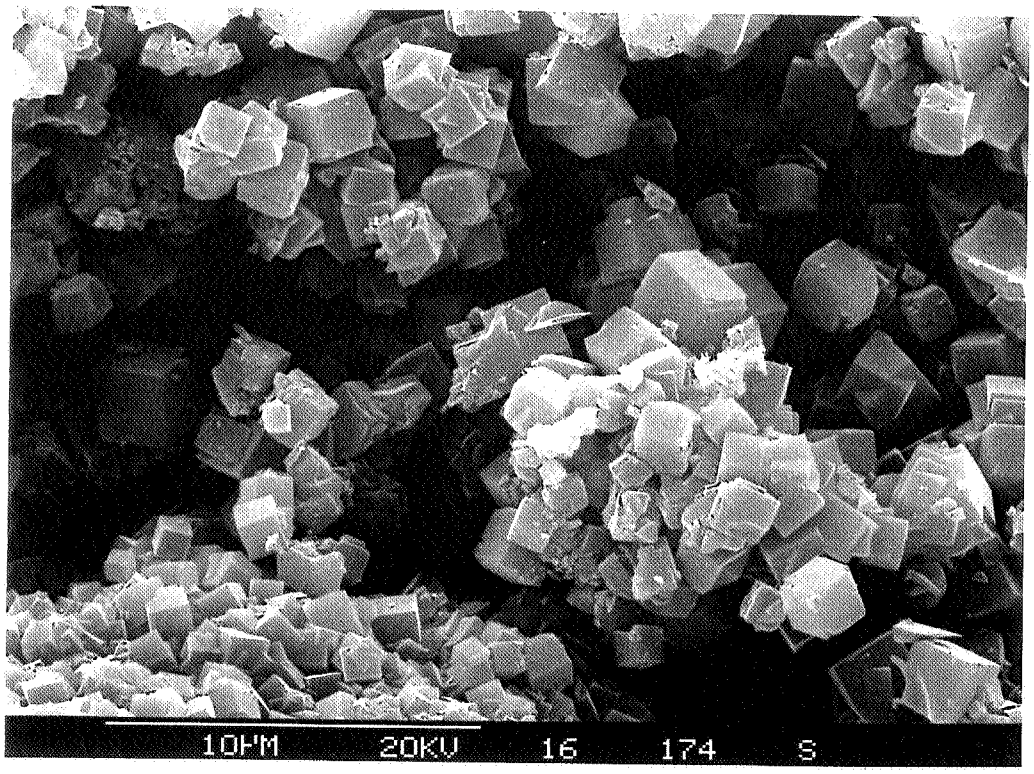


Fig. 3.10. Zeolite 'A' synthesised from Imbitcha' kaolin.

Neg. No. 163174. Scale bar 10µm.

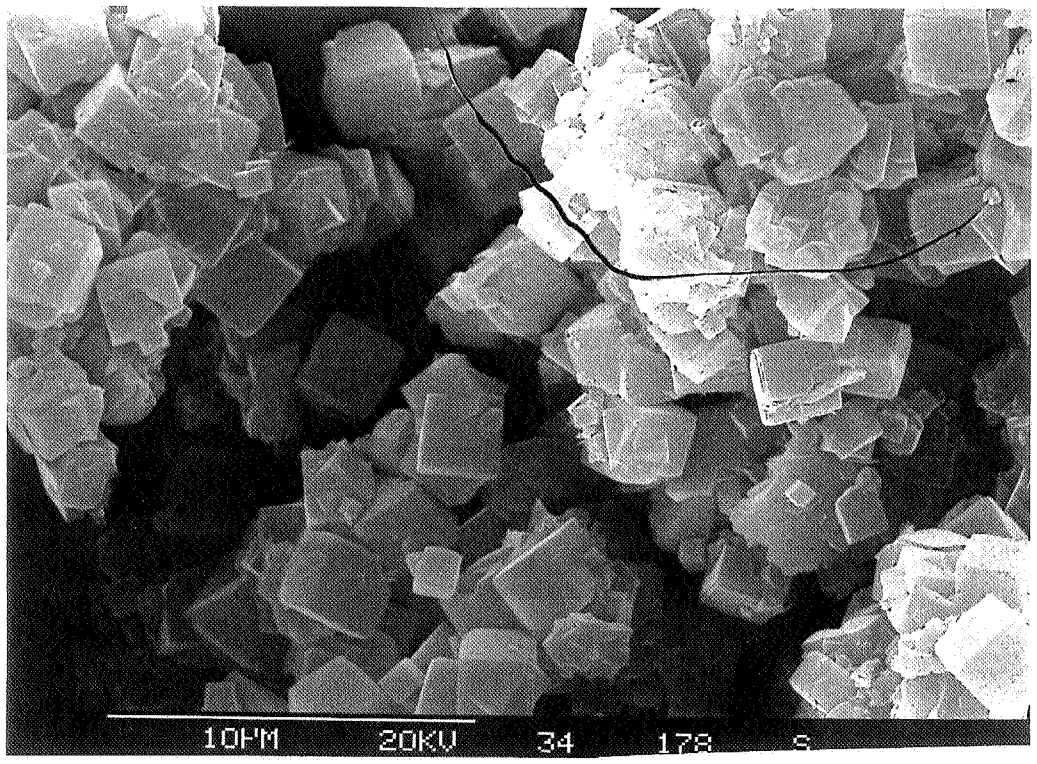


Fig. 3.11. Zeolite 'A' synthesised from Mount Hope Shaft sample.

Neg. No. 343178. Scale bar 10µm.

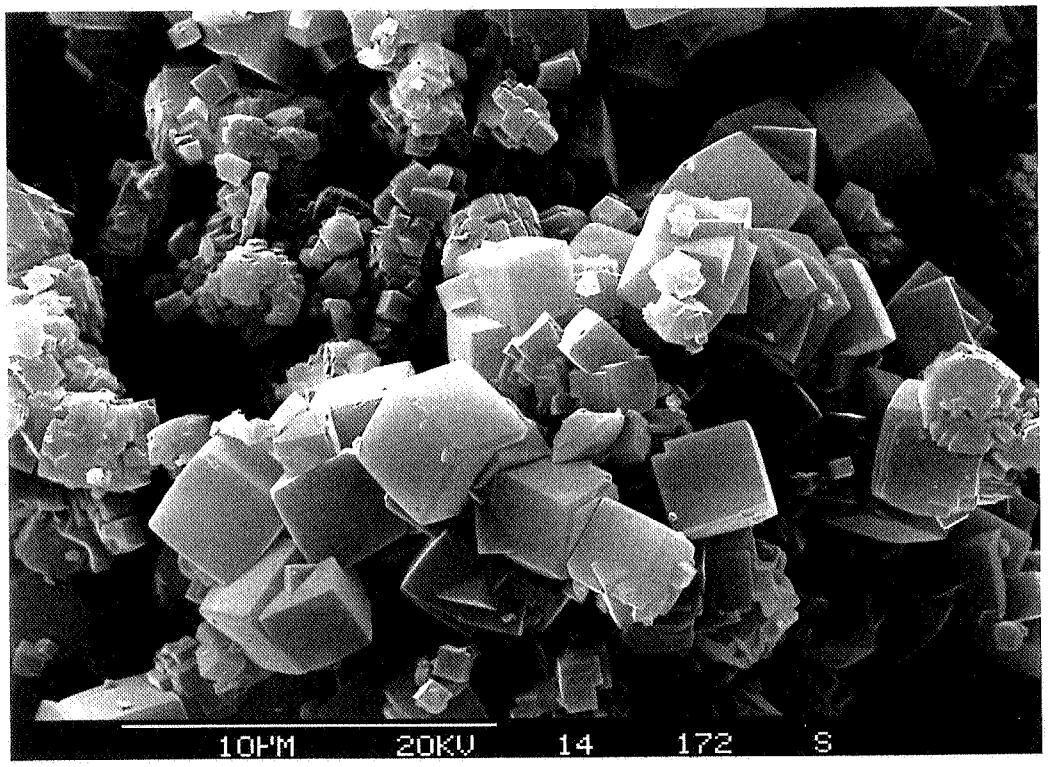


Fig. 3.12. Zeolite 'A' synthesised from New Zealand China Clays kaolin.

Neg. No. 143172. Scale bar 10µm.

4. SIMPLE MODIFICATION OF KAOLINS AND ILLITES

Like other clays, kaolins are not good absorbers of organic molecules (see Table 5.1). However, kaolins can be modified to increase their sorption capacity. For example, and as described Section 3 of this Report, kaolin minerals can be transformed into zeolites by chemical treatments. As a result, materials (zeolites) which are capable of selectively adsorbing small molecules and taking up heavy metal cations can be made from kaolins. However, zeolites are not capable of adsorbing large organic molecules.

It is apparent that the key to the successful uptake of organic materials by clays lies in the prior transformation of clay surfaces so that they become hydrophobic. Jaynes and Boyd (1991) have shown that non-expanding clay minerals such as illite and kaolinite can be transformed by reaction with an alkylammonium salt so that they adsorb non-ionic organic compounds. Lee *et al.* (1989) found that when soils which did not contain smectites, that is easily expandable minerals, were reacted with alkylammonium cations they also adsorbed non-ionic organic compounds. Adsorption depended on the amount of exchanged alkylammonium cation, which was usually a function of the CEC of the clay (Jaynes and Boyd, 1991).

An investigation has been begun into methods for increasing the CECs of clays with naturally low CECs in order to increase their efficacies for the adsorption of non-ionic compounds. Following the use of alkali during the transformation of (pre-heated) kaolin clays during their conversion to zeolites, alkali solutions are being used to attempt to bring about an increase in the CECs of kaolins. Treatment with mild alkali solutions has been shown to gradually release silica from montmorillonite (Grim, 1968). It is thought that the use of similar solutions might deplete silica from the aluminosilicate layers of kaolins, at least prior to the complete dissolution of the minerals, and hence lead to an increase in their CECs.

Acid is more likely than alkali to transform illites (Grim, 1968). Acids may modify illites by two different mechanisms: 1. the replacement of interlayer potassium by the hydrogen (or hydronium) ion, and 2. leaching aluminium and other cations from the

octahedral sheet of the aluminosilicate layer. Both routes would bring about an increase in the CEC of illites.

It may also be possible to increase the CECs of kaolins by leaching cations from their aluminosilicate layers with acids.

Accordingly, experiments have also begun to examine the changes in the CECs of both illites and kaolinites by treating them with acid. Citric acid is being used to ensure that aluminium released is complexed with citrate rather that being made available to occupy exchange sites of the modified clays. Aluminium can effectively "block" exchange sites on clays (Barnhisel and Bertsch, 1989).

Results of these experiments, which began in February 1995, will be reported later.

References

Barnhisel, R.I. and Bertsch, P.M. (1989). Chlorites and hydroxy-interlayered vermiculite and smectite. In: J.B. Dixon and S.B. Weed (eds.) *Minerals in Soil Environments*, 2nd edition. Soil Science Society of America, Madison, Wisconsin.

Grim, R.E. (1968). *Clay Mineralogy*. McGraw-Hill.

Jaynes, W.F. and Boyd, S.A. (1991). Clay mineral type and organic compound sorption by hexadecylammonium-exchanged clays. *Soil Science Society of America Journal*, **55**, 43-48.

Lee, J-F., Crum, J.R. and Boyd, S.A. (1989). Enhanced retention of organic contaminants by soils exchanged with organic cations. *Environmental Science and Technology*, **23**, 1365-1372.

5. SURFACE AREA AND POROSITY OF CLAY MINERALS

Introduction

High surface areas confer useful properties on clay minerals. As a result clays have a high capacity for the physical adsorption of materials. A proportion of the surface areas of many clay minerals may be associated with pores, which can be intracrystalline, resulting from the crystal morphology, or else intercrystalline, resulting from gaps in the arrangement of adjacent clay platelets or fibres.

The pores in clays may be used for the selective adsorption or entrapment of appropriate molecules, although modification of clay mineral surfaces could be necessary before these processes can take place. For example, it may be necessary to render surfaces hydrophobic in order to prevent water sorption by clays so as to enable the uptake of uncharged organic molecules from aqueous solutions.

The potential usefulness of pores in clay minerals for selective adsorption can be seen by drawing analogies with the well-established use of zeolites as molecular sieves. Zeolites, like clays, are crystalline aluminosilicates with a negative layer charge, but they differ from clays in that they have rigid open structures containing channels and cavities which have controlled molecular dimensions. Entry to the sites of adsorption and centres of charge within the zeolite frameworks is through "windows" which are restricted in size. The largest windows in stable zeolites are only 0.8nm in size. According to a recent analysis of the use of zeolites as molecular separators (Taylor, 1990), "the major problem in the zeolite area is an apparent restriction of pore size to less than 8Å". As a result, zeolites cannot be used for the adsorption of large or complex organic molecules. Clay minerals, by contrast, can provide larger intracrystalline pores, both in their natural state (Aylmore and Quirk, 1967; Diamond, 1970; Churchman and Payne, 1983; Churchman *et al.*, 1995) and also after modification by pillaring with interlamellar cations to hold layers apart (Barrer, 1990).

An investigation was carried out of the surface areas and the extent and sizes of pores in a number of South Australian clays. These were compared with the same

characteristics of natural clays from other sources in Australia and also New Zealand and also with a suitable Australian clay both before and after pillaring.

Clays

Kaolins

1. Golden Grove (South Australia). (Absorbent Clay Project, Progress Report No. 1, June 1994). Dominantly kaolinite, together with substantial mica (about 30%), and minor quartz (<5%), smectite and rutile. Comprises largely hexagonal or pseudo-hexagonal platy crystals with a range of sizes (*c.* 0.05-1μm).

2. Woodside (South Australia). (Absorbent Clay Project, Progress Report No. 1, June 1994). A mixture of kaolinite and dehydrated halloysite, together with minor quartz (*c.* 10%) and coarse mica (< 10%). Comprises platy crystals of *c.* 1-2μm with irregular edges intermixed with tubular particles, most of which are *c.* 1μm in length and *c.* 0.2μm in width.

3. Cromer (South Australia). (Absorbent Clay Project, Progress Report No. 1, June 1994). A mixture of dehydrated halloysite and kaolinite, together with only a trace (< 2%) of quartz. Comprises tubular particles, most of which are 2-4μm in length and 0.2-0.3μm in width although some are much smaller (i.e. ≤ 0.5μm long and *c.* 0.03μm wide), as well as platy crystals of *c.* 0.5μm or less, most of which have irregular edges.

4. Imbitcha (South Australia). A mixture of dehydrated halloysite and alunite, together with a trace of quartz. X-ray diffraction traces, and scanning and transmission electron micrographs are presented in Section 3 of this Report. The halloysite comprises tubular particles (*c.* 2μm by 0.1μm) while the alunite is made up of blocky particles with dimensions *c.* 1μm.

5. Patch clay (Western Australia). (Norrish, 1995). Pure halloysite with long but very narrow tubular particles, up to 30μm long and uniformly *c.* 0.03μm in width.

6. N.Z. China Clay (New Zealand). (Churchman and Theng, 1984; Absorbent Clay Project, Progress Report No. 1, June 1994). Largely halloysite, together with minor quartz and cristobalite. The halloysite occurs as large tubular particles, with an average length of 0.7μm and an average width of 0.2μm.

7. Hamilton soil (New Zealand). (Churchman *et al.*, 1995). Dominantly halloysite, together with cristobalite, quartz, goethite, allophane and ferrihydrite. The halloysite comprises small tubular particles with average lengths of 0.17μm and average widths of 0.07μm.

Illite

8. Muloorina illite (South Australia). (Absorbent Clay Project, Progress Report No. 1, June 1994). Dominantly illite, together with minor quartz and kaolinite. The illite particles are very small, < 0.1μm in length and *c.* 0.006μm thick.

Palygorskites

9. P33 0-1m palygorskite (South Australia). (Absorbent Clay Project, Supplementary Report, Mineralogical Characterisation of Garford Palaeochannel Clays, April 1995). Predominantly (90%) palygorskite, very minor halite, dolomite and quartz.

10. P25 5-7m composite sample (South Australia). (Absorbent Clay Project, Supplementary Report, April 1995). Illite (65%), palygorskite (20%), very minor quartz, halite and kaolin.

Allophane

11. DJL33 Mt Gambier soil (South Australia). (Lowe, 1992). Allophane, while only a minor component by weight (*c.* 16%) of the whole soil (from the 50-60cm depth), is its most active component.

Smectites

12. Arumpo bentonite. (Absorbent Clay Project, Progress Report No. 1, June 1994). Dominantly smectite, but contains approximately 10% illite interstratified with the smectitic layers, which are closely similar to Wyoming-type montmorillonite. The majority of the sample comprises very fine-grained, thin platelets, 0.02 to 0.3μm in diameter.

13. Alumina-pillared Arumpo bentonite (Section 1 of this Report).

Methods

Several of the samples were tested for sorption of toluene or benzene by the method given in Section 1 of this Report.

Between 0.1 and 1g of powdered sample was outgassed at 110°C for 16 hours at a pressure of $< 10^{-5}$torr. Isotherms for the adsorption and desorption of nitrogen at 77°K were measured using an Omnisorp 100 automated volumetric instrument.

Specific surface areas were determined via BET plots (Brunauer *et al.*, 1938; Gregg and Sing, 1982) over the linear range (0.02-0.15 p/p^o, where p/p^o is the relative pressure, that is the ratio of pressure of N_2 to its pressure at saturation). Pore size distributions were calculated from analyses of the desorption branches of the isotherms using the BJH method (Barrett *et al.*, 1951; Gregg and Sing, 1982).

Results

Sorption

Sorption results are shown in Table 5.1. None of the samples showed any affinity for the organic molecules.

Surface areas

The BET specific surface areas are shown in Table 5.2. Common values for the various mineral types (collated from the scientific literature by Churchman *et al.*, 1983) are shown in Table 5.3. Where values in Table 5.2 differ from these common values, the variations may be explicable by the influence of other phases present, which can lead to values that may be either higher or lower than common values, or to small crystals or particle sizes, which can lead to higher than expected values.

Isotherms

Isotherms are presented in 4 separate figures according to maximum extent of adsorption and, where possible, also like mineralogies. Fig. 5.1 presents the adsorption/desorption isotherms for four samples containing halloysites (Woodside, Cromer, N.Z. China Clay and Hamilton soil). Fig. 5.2 presents these isotherms for the Golden Grove kaolinitic sample, the Imbitcha kaolin and the allophanic soil. Those for the illite and the two forms of Arumpo bentonite are presented in Fig. 5.3, while Fig. 5.4 includes the isotherms for Patch halloysite and the two palygorskite samples.

The isotherms are of two types, according to conventional classification (Gregg and Sing, 1982). Type II isotherms, represented by Cromer, Woodside, Golden Grove and N.Z. China Clay kaolin samples, show little or no hysteresis. These samples are essentially non-porous. All other samples give type IV isotherms, with substantial hysteresis arising from the occurrence of mesopores with radii between 1 and 20nm (Gregg and Sing, 1982).

Pore size distributions

Pore size distributions are presented in two different ways. The first is by means of plots of cumulative pore volume against pore radius. Fig. 5.5 presents plots of this type corresponding to the isotherms in Fig. 5.1, while Fig. 5.6 and Fig 5.2 correspond in the same way to each other and Fig. 5.7 is a cumulative pore volume vs. pore radius plot which derives from the isotherms in Figs. 5.3 and 5.4.

When the distributions were compared, it became apparent that the various samples fell into four main groups according to their pore size distributions. These were:

1. Small pores (radii < 2nm) dominant. Mt Gambier soil (allophane); Arumpo bentonite; Alumina-pillared Arumpo bentonite.
2. Substantial medium size pores (most radii < 8nm). Muloorina illite; Hamilton soil (halloysite); Patch halloysite; Palygorskite composite (P25).
3. Coarse pores (radii > 8nm) present, but substantial proportion of fine and medium size pores. Woodside kaolin; Imbitcha kaolin; Palygorskite (P33).
4. Coarse pores (radii > 8nm) dominant. Cromer kaolin; N.Z. China Clay halloysite; Golden Grove kaolinite.

Histograms of pore size distributions into ranges (Figs. 5.8-5.11) are presented for the samples ordered into each of these groups (Fig. 5.8 for Group 1; Fig. 5.9 for Group 2; Fig. 5.10 for Group 3 ; Fig. 5.11 for Group 4).

Discussion

Except in the case of some halloysites (Churchman *et al.*, 1995), pores in the range examined largely arise from intercrystalline effects of the interleaving of particles (Aylmore and Quirk, 1967). The sizes of pores therefore reflect the sizes of particles while their concentration into particular ranges reflect a homogeneity in particle sizes. The high concentration of small size pores in Arumpo bentonite indicates that this clay has many small particles of a similar size. This is confirmed by the exceptionally high surface area of the material. Such a surface area could confer very useful properties on Arumpo bentonite. For example, preliminary studies at CSIRO Division of Chemicals and Polymers (Dr L. Kolarik, pers. comm.) have suggested that clays with high surface areas may be most useful, in association with polycationic flocculants, for the removal of anionic dyes from water.

Only those clays with a considerable volume of pores per gram and with pores concentrated toward the finer sizes are likely to be useful for the selective adsorption of organic molecules from solution, following suitable modification to render

surfaces hydrophobic. Nevertheless, the allophanic soil, while showing a high concentration of fine pores, has very little porosity (Fig. 5.8). On these grounds, the smectite (Arumpo) offers the best prospect for adsorbing relatively small molecules. Its selectivity is improved by pillaring with alumina. Although the bulk of its pores are smaller than those in the other clays investigated, this clay mineral offers the prospect of the adsorption of larger molecules than can be adsorbed by zeolites. The results in Section 1 of this Report confirm the effectiveness of the clay mineral, following appropriate modification, for the uptake of both benzene and toluene.

The Muloorina illite and the palygorskite composite (P25) both show the potential for selectively sorbing rather larger molecules. It is not surprising that these two samples group together, as the palygorskite composite (P25) comprises substantial illite with similar characteristics to Muloorina illite. The palygorskite sample (P33) itself has larger pores and hence would have a lower selectivity than the illite and composite samples. Apart from two of the samples included in the set for comparisons (Patch halloysite and Hamilton soil halloysite), the other clays lack promise as porous adsorbents because of both the large size and wide range of sizes of their pores.

The most porous clays may be particularly useful for the sorption of gases and different clays could be used as sieves for the separation of different gases by molecular size.

References

Aylmore, L.A.G. and Quirk, J.P. (1967). The micropore size distribution of clay mineral systems. *Journal of Soil Science*, **18**, 1-17.

Barrer, R.M. (1990). Expanded layered silicates. p. 55-65. In: I.V. Mitchell (ed.). *Pillared Layered Structures: Current Trends and Applications.* Elsevier, London.

Barrett, E.P., Joyner, L.G. and Halenda, P.H. (1951). The determination of pore volume and area distributions in porous substances. *J. Am. Chem. Soc.*, **73**, 373-380.

Brunauer S., Emmett P.H. and Teller E. (1938). Adsorption of gases in multimolecular layers. *J. Am. Chem. Soc.*, **60**, 309-310.

Churchman, G.J. and Payne, D. (1983). Mercury intrusion porosimetry of some New Zealand soils in relation to clay mineralogy and texture. *Journal of Soil Science*, **34**, 437-451.

Churchman, G.J., Skjemstad, J.O. and Oades, J.M. (1983). Influence of clay minerals and organic matter on effects of sodicity on soils. *Australian Journal of Soil Research*, **31,** 779-800.

Churchman, G.J., Davy, T.J., Aylmore, L.A.G. and Gilkes, R.J. (1995). Characteristics of fine pores in some halloysites. *Clay Minerals*, **30**, (in press).

Diamond, S. (1970). Pore size distribution in clays. *Clays and Clay Minerals*, **18**, 7-23.

Gregg S.J. and Sing, K.S.W. (1982). *Adsorption, Surface Area and Porosity.* 2nd Edition. Academic Press, London.

Lowe, D.J. (1992). Profile descriptions of Quaternary Basaltic Volcanogenic soils of the Mount Gambier area, southeast South Australia. *CSIRO Division of Soils Technical Report 9/1992.*

Norrish, K. (1995). An unusual fibrous halloysite. In: G.J. Churchman, R.W. Fitzpatrick and R.A. Eggleton (eds.) *Proceedings of the 10th International Clay Conference.* CSIRO, Melbourne.

Taylor, R.S. (1990). Molecular separators in industrial use present and future. p. 3-12 In: I.V. Mitchell (ed.) *Pillared Layered Structures: Current Trends and Applications.* Elsevier, London.

Table 5.1. %Sorption from 1000ppm aqueous solution of hydrocarbon.

Sorbent Clay	Sorbate	
	Benzene	Toluene
Golden Grove Kaolinite, 1-2μm fraction	nd	0
Woodside Kaolinite, 1-2μm fraction	nd	0
Cromer Kaolinite, 1-2μm fraction	nd	0
Palygorskite (Garford) P33 0-1m	0	nd
Palygorskite (Garford) P25 5-6m	0	nd
Palygorskite (Garford) P25 6-7m	0	nd
Allophanic soil (DJL33), S.E. South Aust.	nd	0

nd = not determined.

Table 5.2. BET specific surface areas for clay samples.

Sample[1]	BET Specific Surface Area (m^2/g)
Golden Grove kaolinite	12.5
Woodside kaolin	16.7
Cromer kaolin	22.2
Imbitcha kaolin	20.8
Patch halloysite	132
N.Z. China Clay halloysite	33.6
Hamilton soil halloysite	93.8
Muloorina illite	101
P33 palygorskite	135
P25 palygorskite composite	135
DJL33 Mt Gambier soil allophane	94.2
Arumpo bentonite	207
Alumina pillared Arumpo bentonite	261

[1] Named according to predominant mineral.

Table 5.3. Common values of BET specific surface areas for various mineral types.

Kaolinite	6-40 m^2/g
Halloysite	20-60 m^2/g
Illite	55-195 m^2/g
Palygorskite	140-190 m^2/g
Allophane	145-600 m^2/g
Smectite	15-160 m^2/g

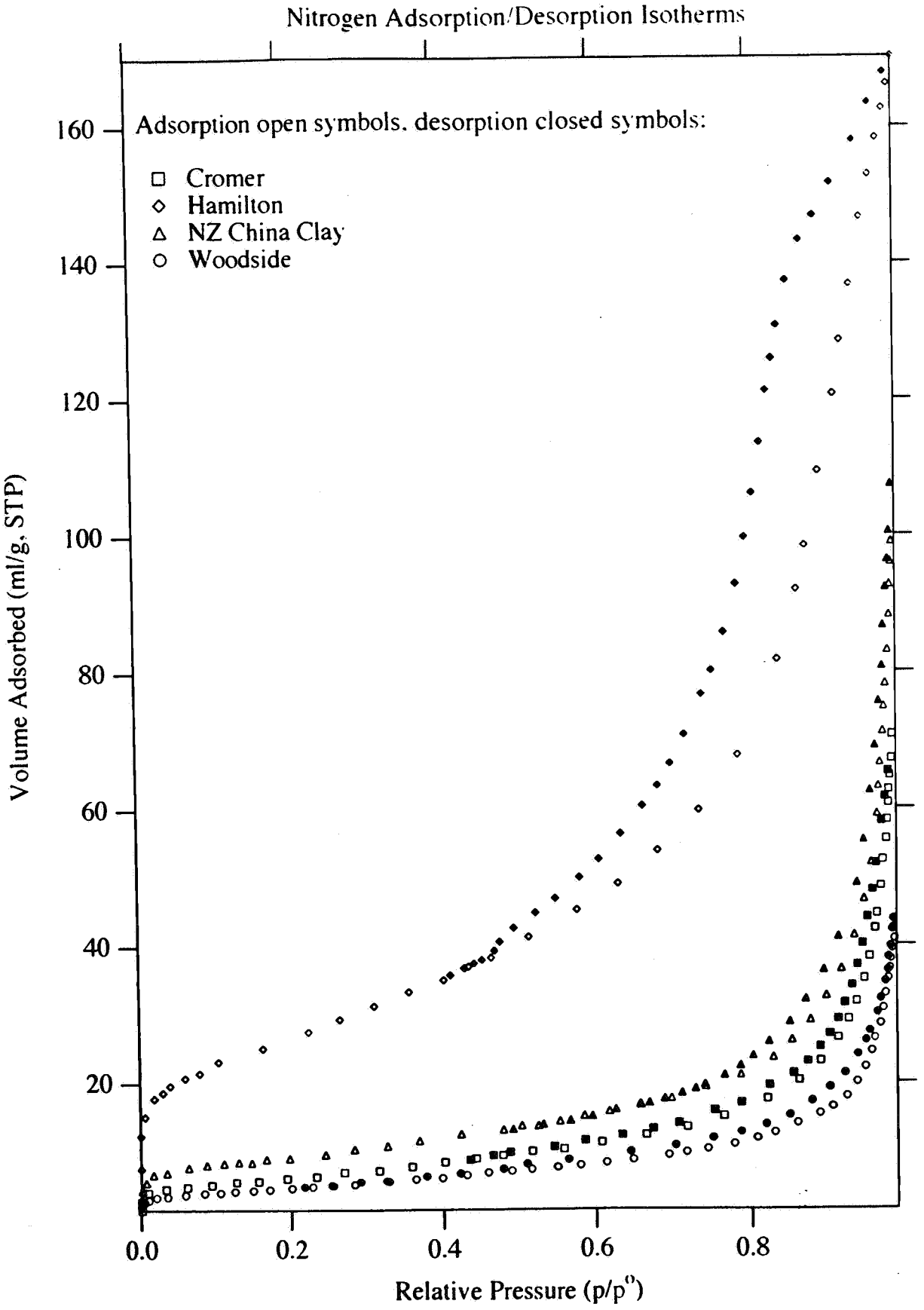

Nitrogen Adsorption/Desorption Isotherms
Adsorption open symbols. desorption closed symbols:
Cromer
Hamilton
NZ China Clay
Woodside
Volume Adsorbed (ml/g. STP)
160
140
120
100
80
60
40
20
0.0
0.2
0.4
0.6
0.8
Relative Pressure (p/p°)

Fig. 5.1.

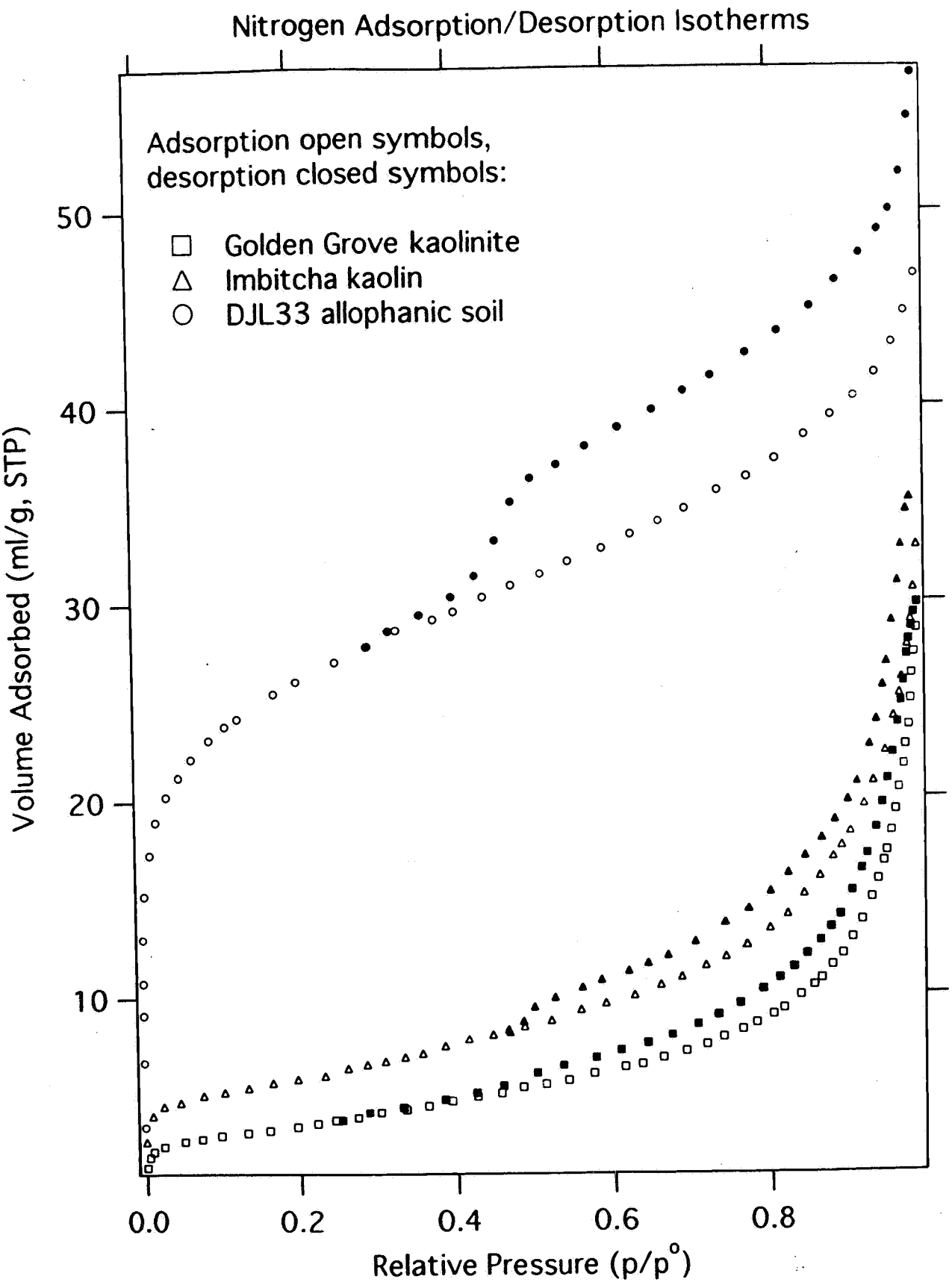

Nitrogen Adsorption/Desorption Isotherms
Adsorption open symbols,
desorption closed symbols:
Golden Grove kaolinite
Imbitcha kaolin
DJL33 allophanic soil
Volume Adsorbed (ml/g, STP)
50
40
30
20
10
0.0
0.2
0.4
0.6
0.8
Relative Pressure (p/p°)

Fig. 5.2.

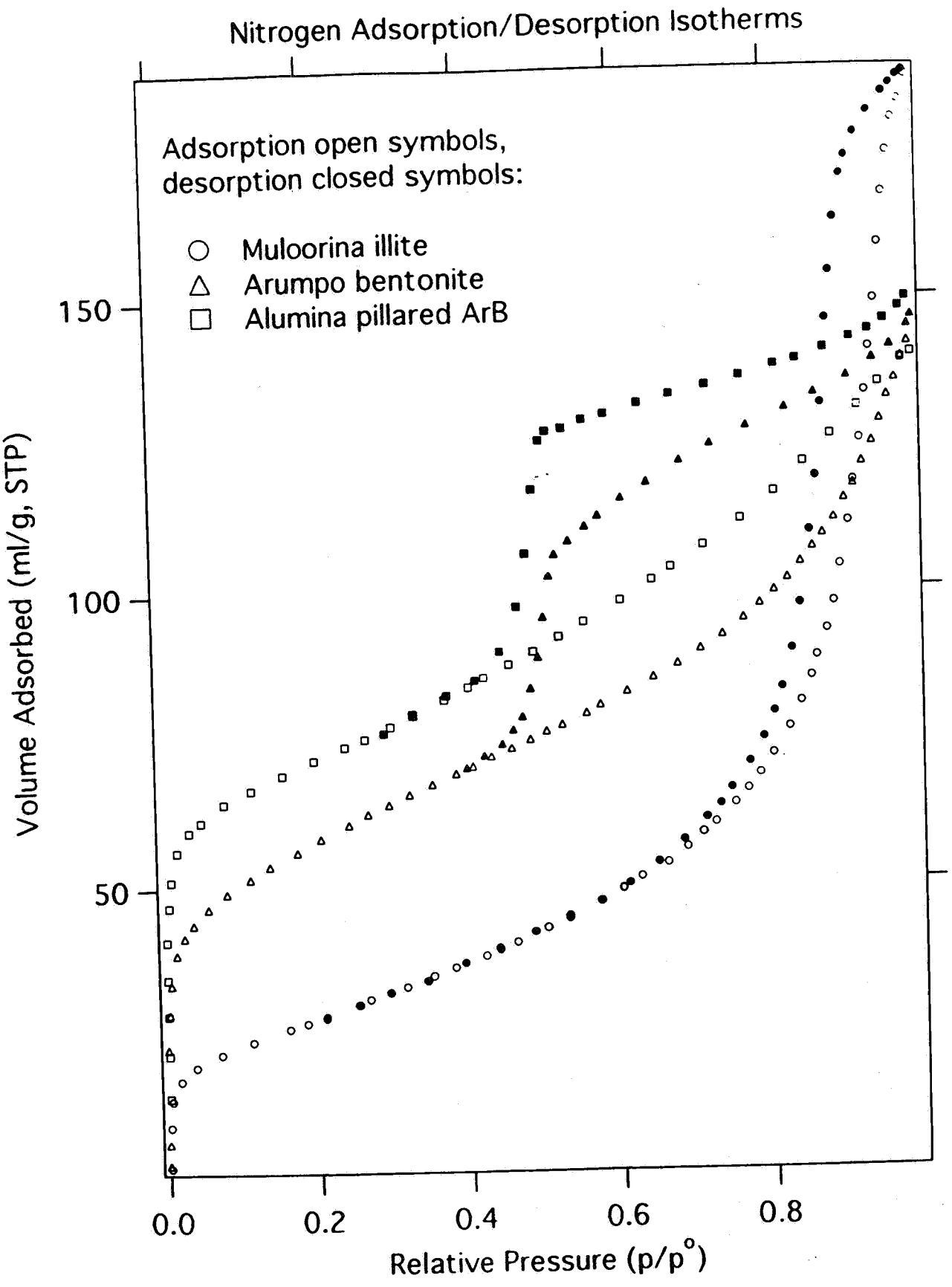

Nitrogen Adsorption/Desorption Isotherms
Adsorption open symbols,
desorption closed symbols:
Muloorina illite
Arumpo bentonite
Alumina pillared ArB
Volume Adsorbed (ml/g, STP)
150
100
50
0.0
0.2
0.4
0.6
0.8
Relative Pressure (p/p°)

Fig. 5.3.

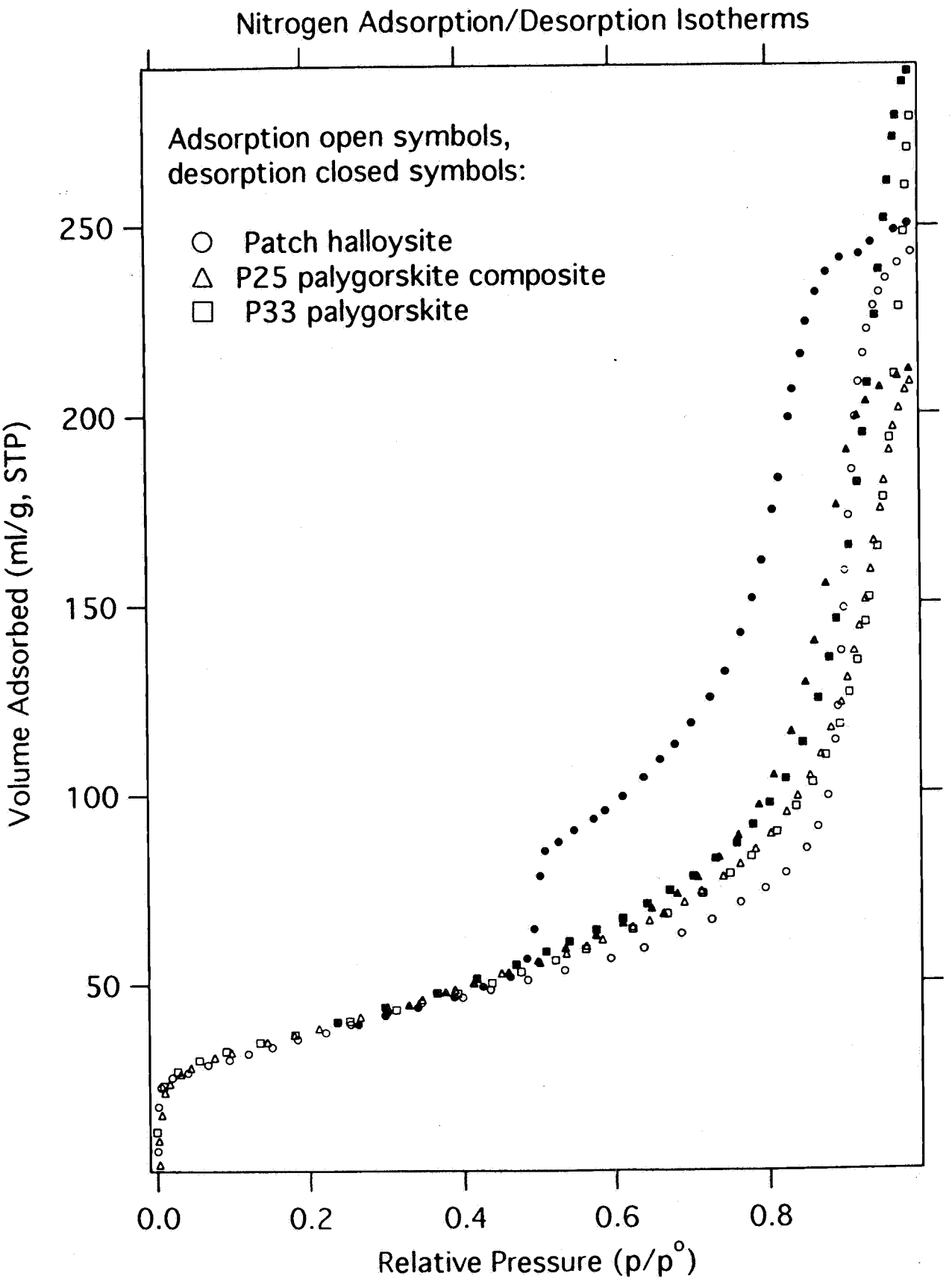

Nitrogen Adsorption/Desorption Isotherms
Adsorption open symbols,
desorption closed symbols:
Patch halloysite
P25 palygorskite composite
P33 palygorskite
Volume Adsorbed (ml/g, STP)
250
200
150
100
50
0.0
0.2
0.4
0.6
0.8
Relative Pressure (p/p°)

Fig. 5.4.

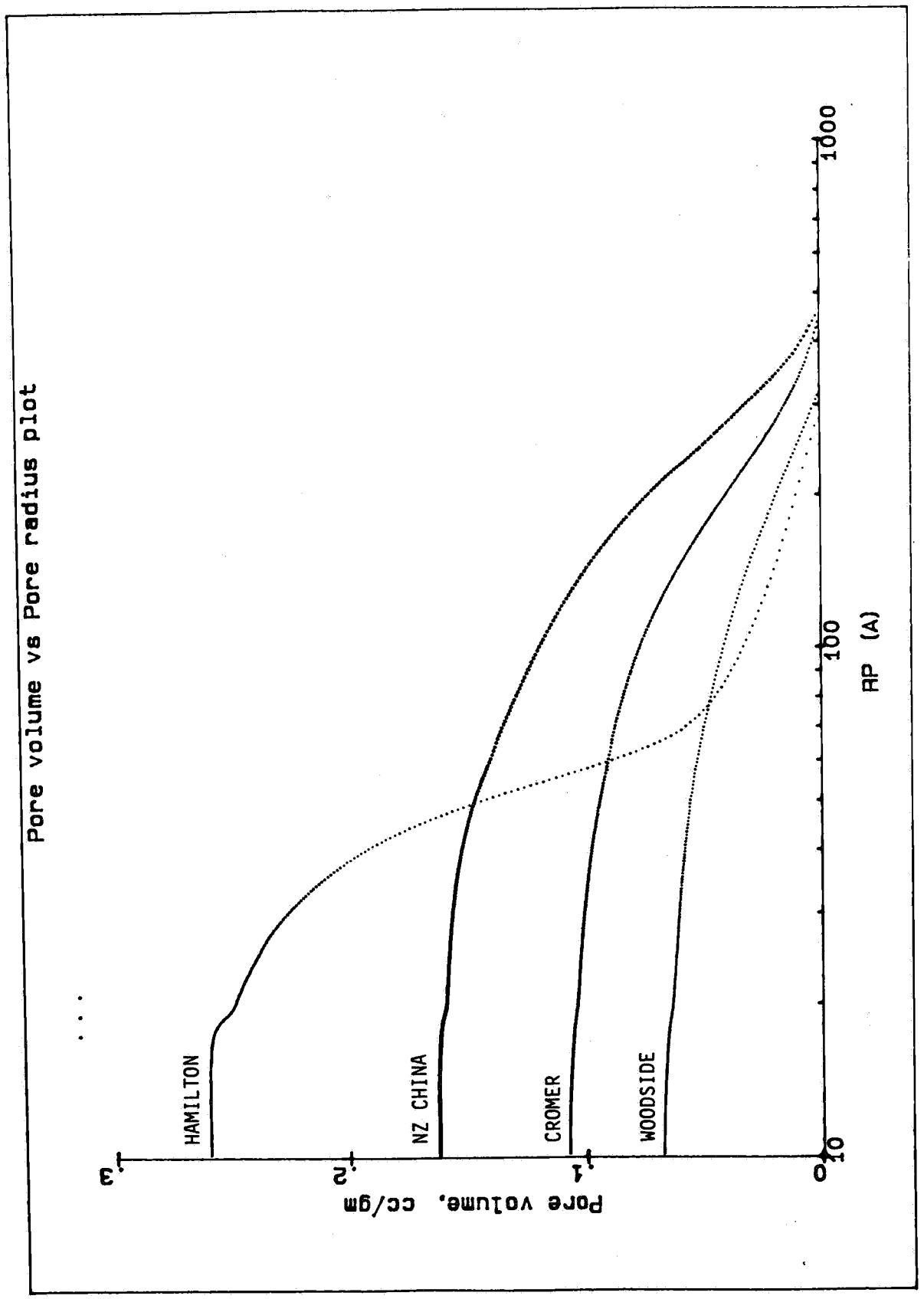

Pore volume vs Pore radius plot
Pore volume, cc/gm
0
1
2
3
10
100
1000
RP (A)
HAMILTON
NZ CHINA
CROMER
WOODSIDE

Fig. 5.5.

Fig. 5.6.

0002232

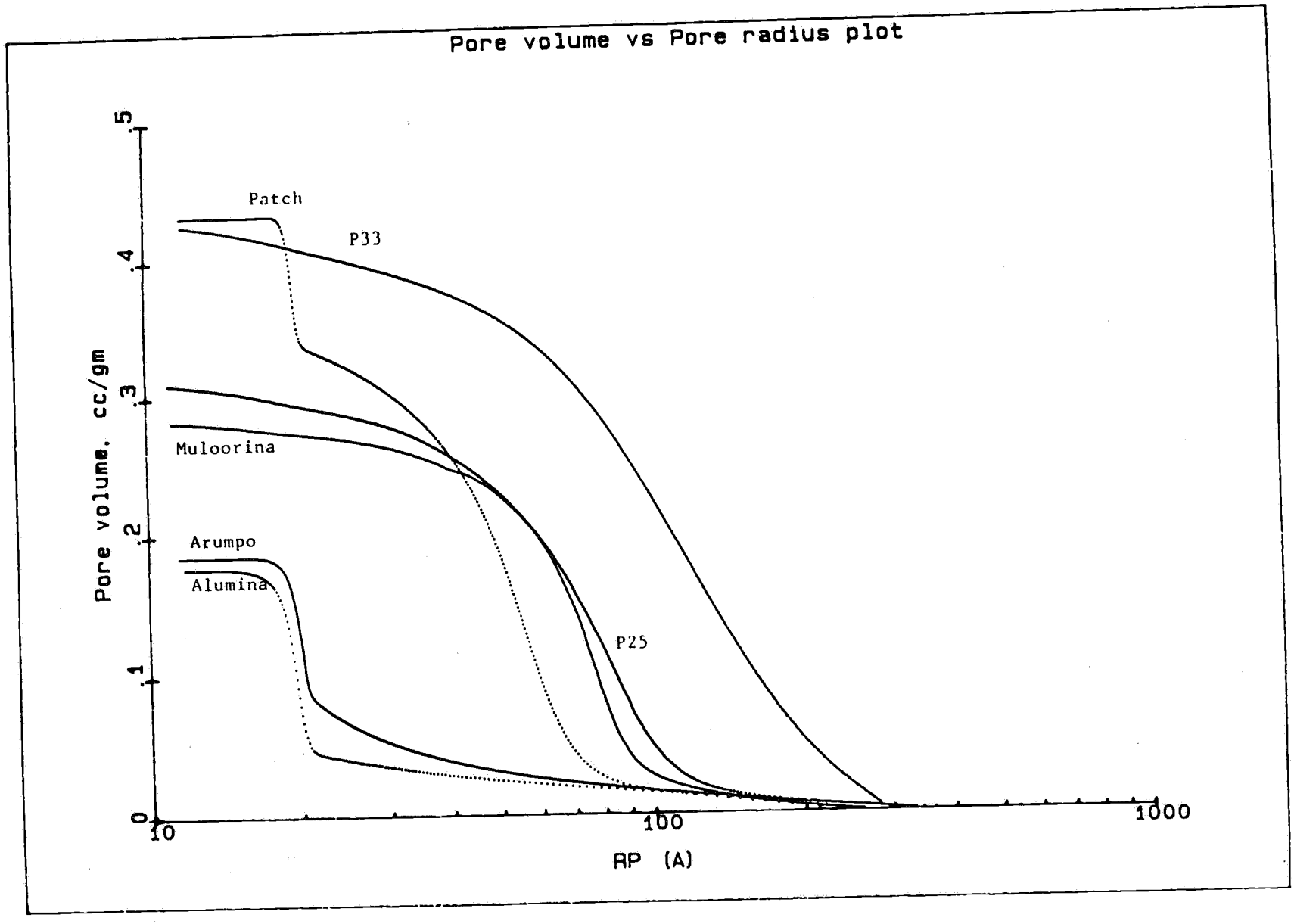
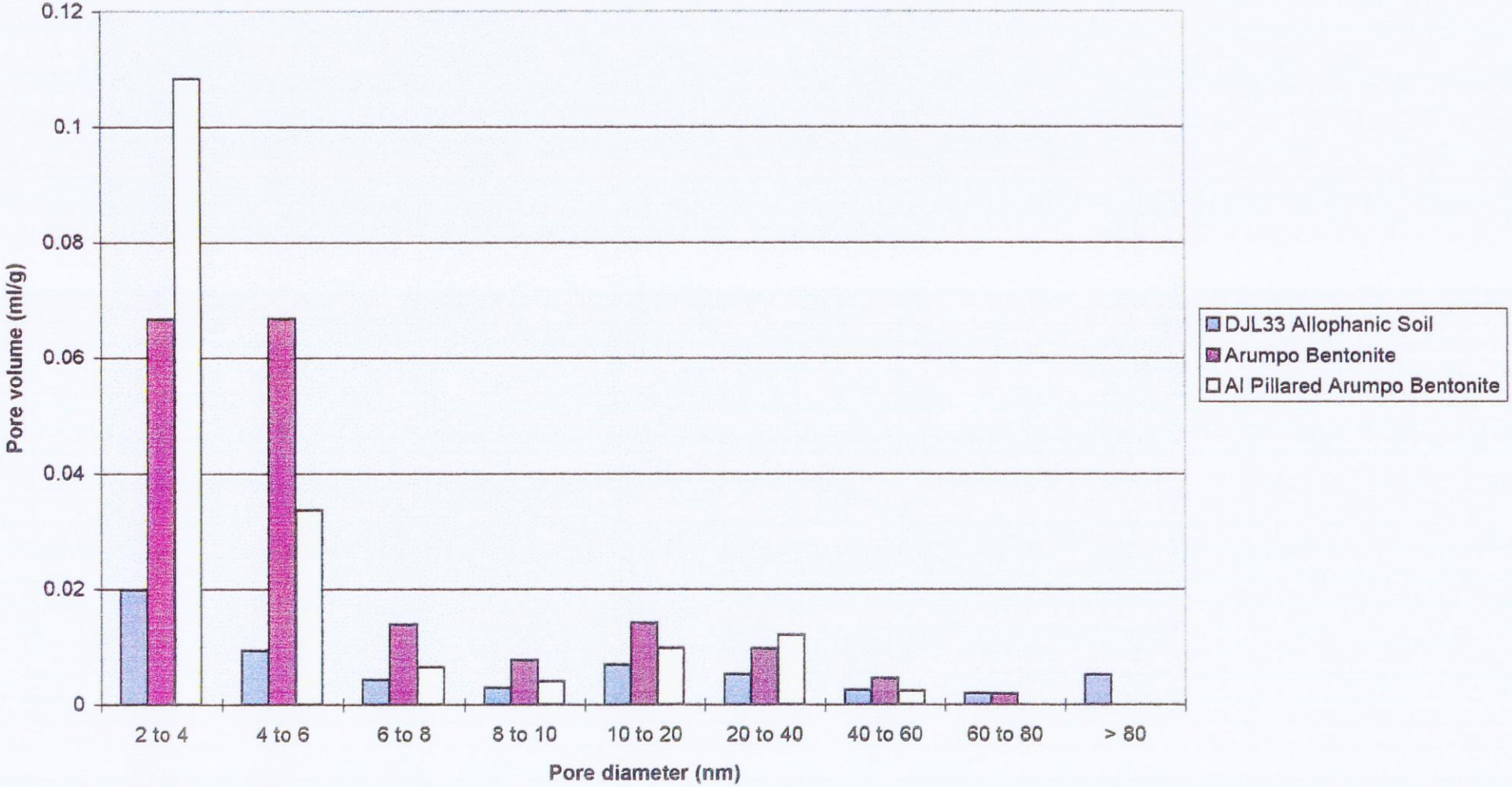


Fig. 5.7.

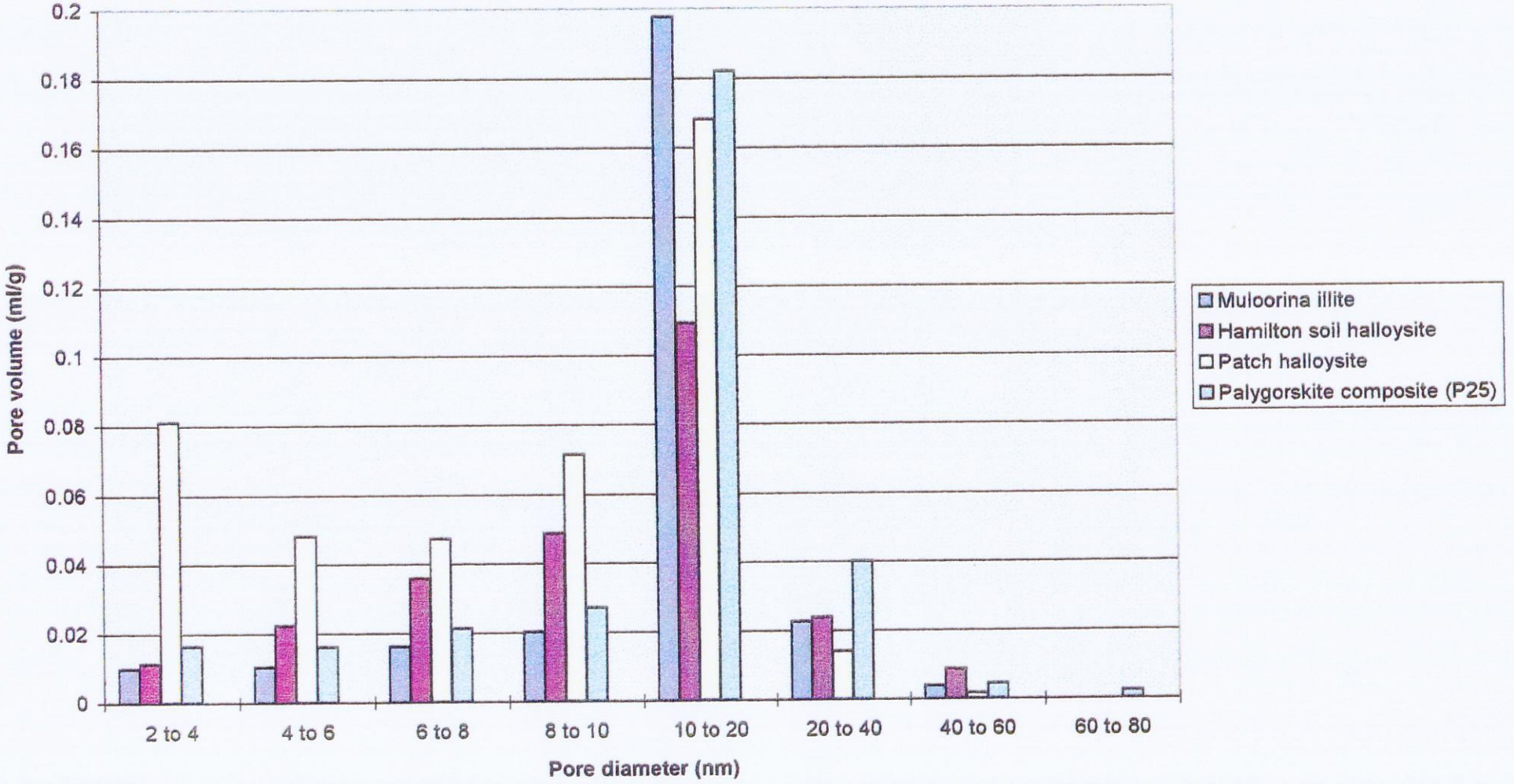
000233

Fig. 5.8 Pore size distribution of clays with dominant small pores



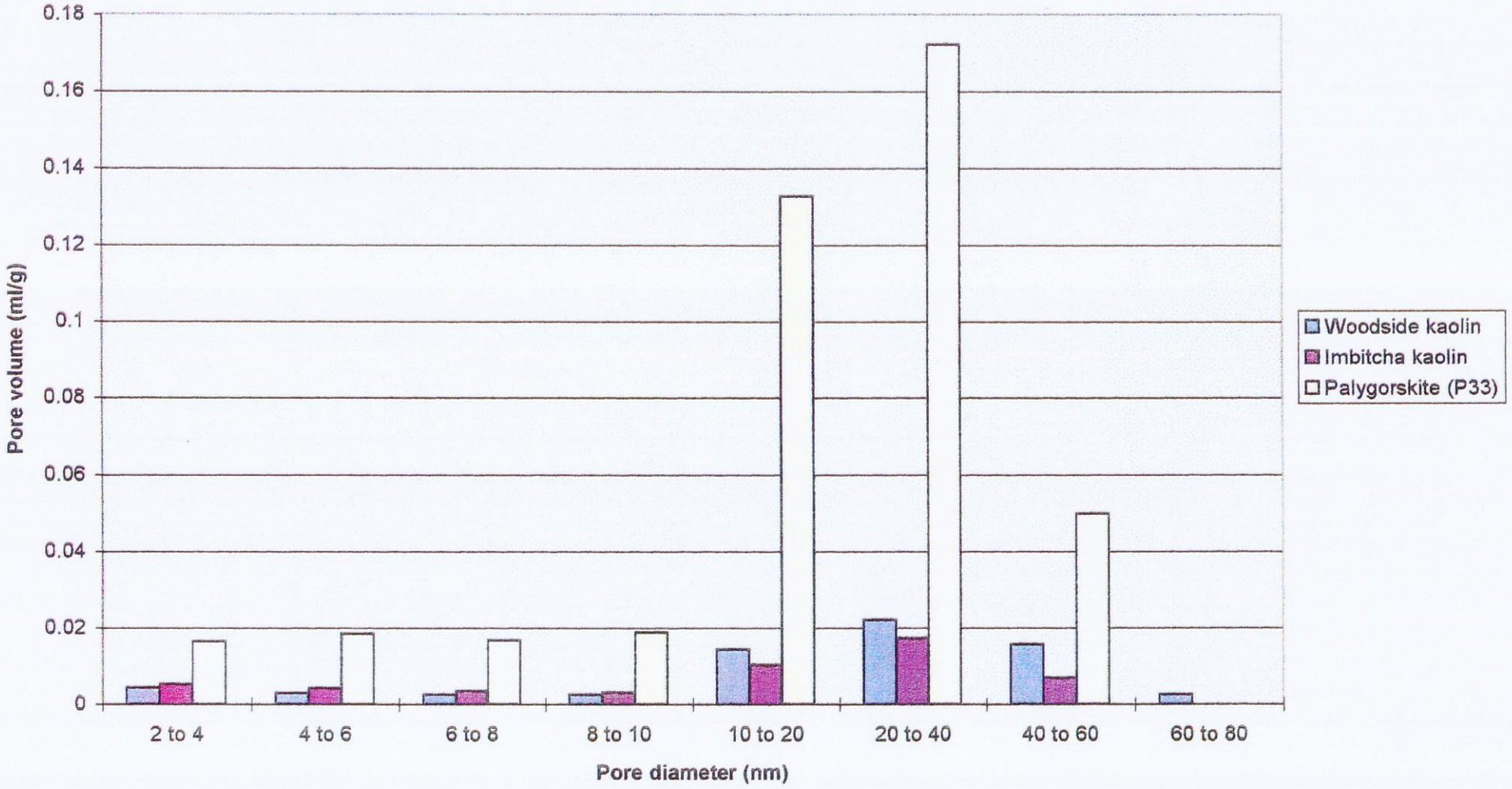
000234

Fig. 5.9 Pore size distribution of clays with substantial medium pores



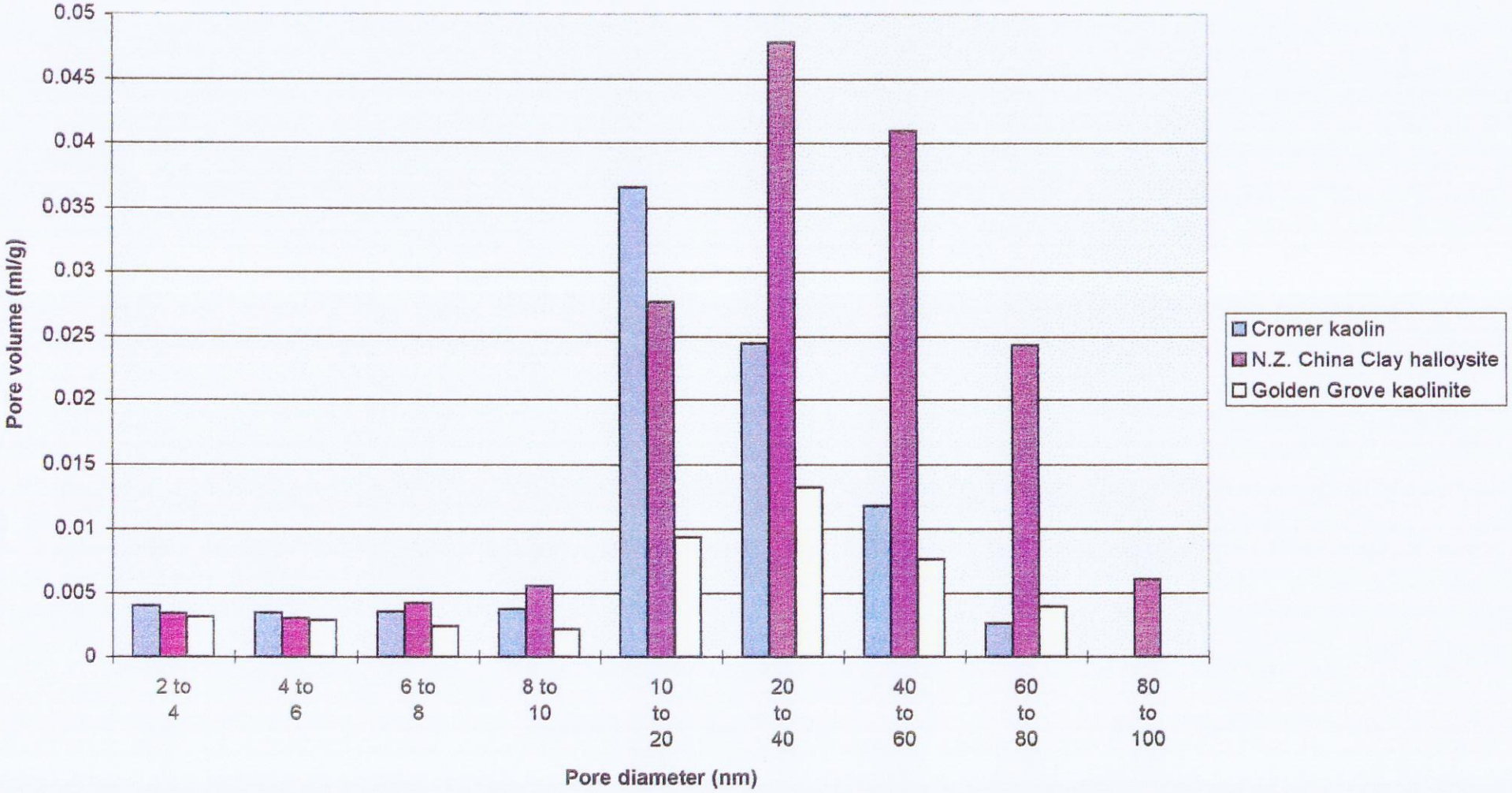
000235

Fig. 5.10 Pore size distribution of clays with wide range of pores



000236

Fig. 5.11 Pore size distribution of clays with dominant coarse pores



000237

6. FEASIBILITY STUDY ON THE DEVELOPMENT OF AN APPARATUS FOR FLOW-THROUGH TESTING OF ADSORBING POWER OF CLAYS

Introduction

The CSIRO concept of flow-through testing of the absorbing power of clays is summarised schematically in Fig. 6.1. Essentially the idea was to inject metal ions into a solution stream which would be pumped through a bed of clay in a chromatography column (Fig. 6.2). Displaced ions from the column could then be monitored using a conductivity detector. From conductivity/time plots the absorbing power of the clay could also be determined.

To allow experiments to be performed under a wide range of conditions, the apparatus was designed to allow for programming of the temperature of the test columns, and also had by-pass columns for the recording of baseline data. In addition, the entire apparatus was under computer control.

The apparatus that we constructed is shown in Fig. 6.3. The columns containing the clays were housed in Modules 5 and 6, solution degassing and solvent delivery were carried out in Module 2, and samples were injected, either directly or via a sample loop, in Module 3.

Originally, conventional chromatography guard columns (20mm long and 1mm diameter) were packed with clays using a dry-packing technique. However, it immediately became evident that the back pressures on these columns exceeded the compliance of the injection valves, which resulted in their destructive failure. Attempts were therefore made to switch to shorter columns having larger diameters. These new columns were 10mm long and 1mm diameter. Unfortunately, these also failed by leaking. Finally, we managed to procure some columns having the dimensions 10mm long by 4.6mm diameter and these allowed some successful experiments to be carried out.

Results

Examples of typical conductivity-time curves for Pb, Cd, Ni, Zn, and Cu injected into a clay-filled column are shown in Fig. 6.4. In these experiments 5μL of metal ions (approx. 10^{-4}M as nitrates) were injected into Arumpo bentonite with deionised water used as the eluent at a flow rate of 0.25ml/min and 25°C. Absorption was confirmed by spot tests. For example, in the case of nickel the outlet solution was collected and the following solutions were added: 1% dimethylglyoxime (DMG) solution, dilute perchloric acid (to oxidise the nickel), and dilute ammonia solution (to adjust the pH to 8-9). The presence of nickel would have been indicated by a rose-pink colour change. However, no nickel was found. The peak shown in Fig. 6.4 thus represents ions displaced by nickel, most likely Ca or Na ions. Table 6.1 lists details of all the other experiments.

Unfortunately, we were not able to absorb metal ions to saturation levels for any of the heavy metals tested because the swelling of clay particles eventually produced a back-pressure which was too high for our HPLC system to sustain. A maximum time of about 2-3 hours was permissible which was not long enough to determine the full extent of absorption.

Conclusions

The concept of flow-through testing of the absorbing power of clays has been successfully demonstrated. However, severe difficulties were encountered in the use of chromatography-type columns since these resulted in inordinately high back pressure. Any future work would therefore need to concentrate on wide-bore, short-length columns; or possibly inert diluents might be added with the clay to prevent column blockage.

The metal ions absorbed on Arumpo Bentonite apparently displace sodium or calcium ions whose conductivity can be detected downstream in a conductivity detector. Since these are environmentally benign there is at least preliminary evidence that Bentonite clays are a good choice for immobilising heavy metals.

Table 6.1. Summary of four series of heavy metal adsorption experiments with Arumpo bentonite clay.

Heavy Metal	Concentration* (M)	Volume (µl)	Eluent	Mass of Clay (g)	Experiment Type	Results
Pb	10^{-4}	5	deionised water	0.0126	Adsorption	System back-pressure was too high; sample mass needs to be decreased
Pb, Cd, Zn, Cu, Ni	10^{-4}	5	deionised water	0.0073	Adsorption	All heavy metals adsorbed
Ni	10^{-4}	-	Ni at 10^{-4}M	0.0085	Adsorption Capacity	Ni was adsorbed continuously for 83 minutes until high system backpressure (> 3000psi) forced experiment to be stopped. Capacity was not determined.
Ni	10^{-3}	-	Ni at 10^{-3}M	0.0068	Adsorption Capacity	At this higher concentration the detector was overwhelmed by excess nickel

* As nitrate solutions (AR grade) with exact concentrations (M) as follows: 0.97×10^{-4} Pb; 0.95×10^{-4} Cd; 1.05×10^{-4} Zn; 1.03×10^{-4} Cu; 1.02×10^{-4} Ni; and 1.03×10^{-3} Ni.

0000240

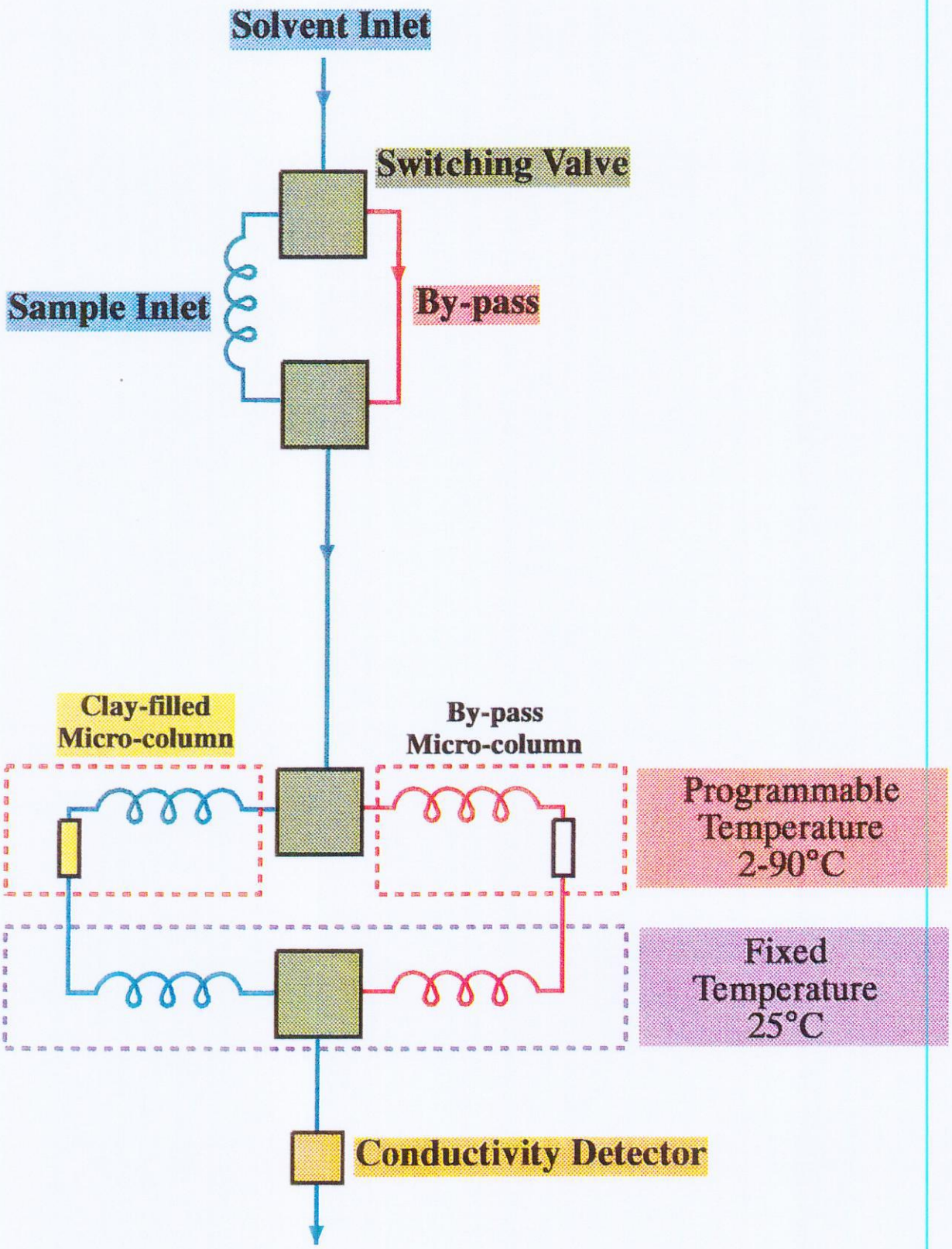

Solvent Inlet
Switching Valve
Sample Inlet
By-pass
Clay-filled
Micro-column
By-pass
Micro-column
Programmable
Temperature
2-90°C
Fixed
Temperature
25°C
Conductivity Detector

Fig. 6.1.

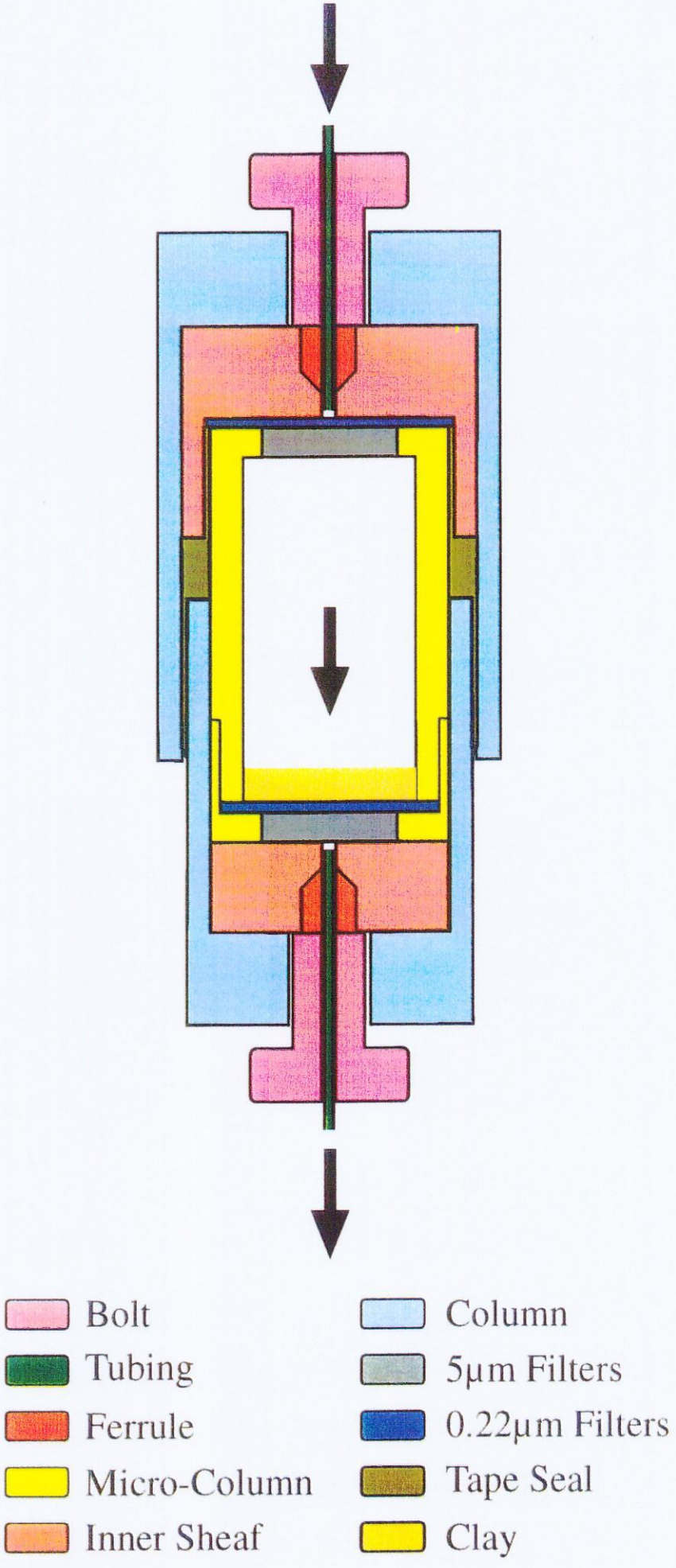
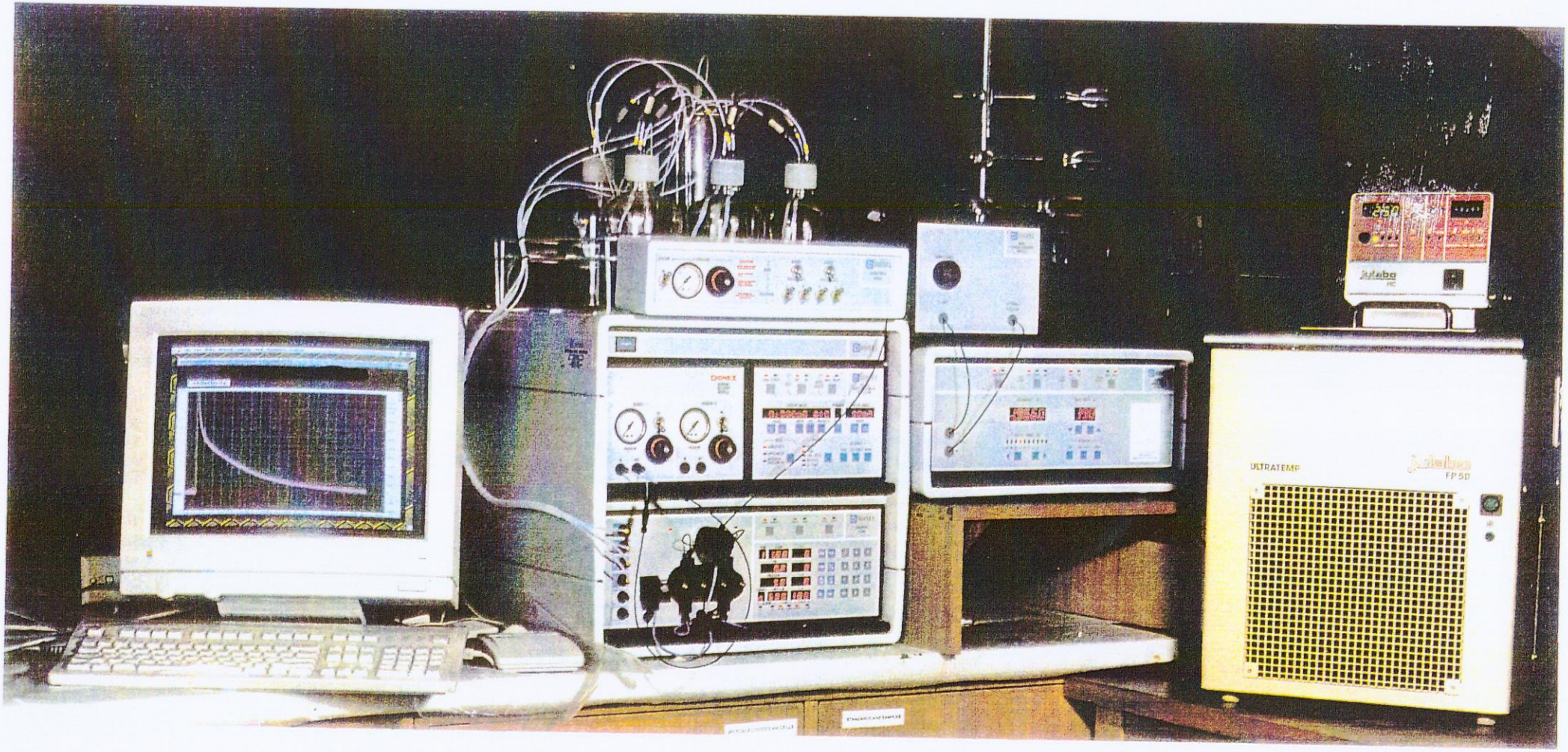

Bolt
Tubing
Ferrule
Micro-Column
Inner Sheaf
Column
5µm Filters
0.22µm Filters
Tape Seal
Clay

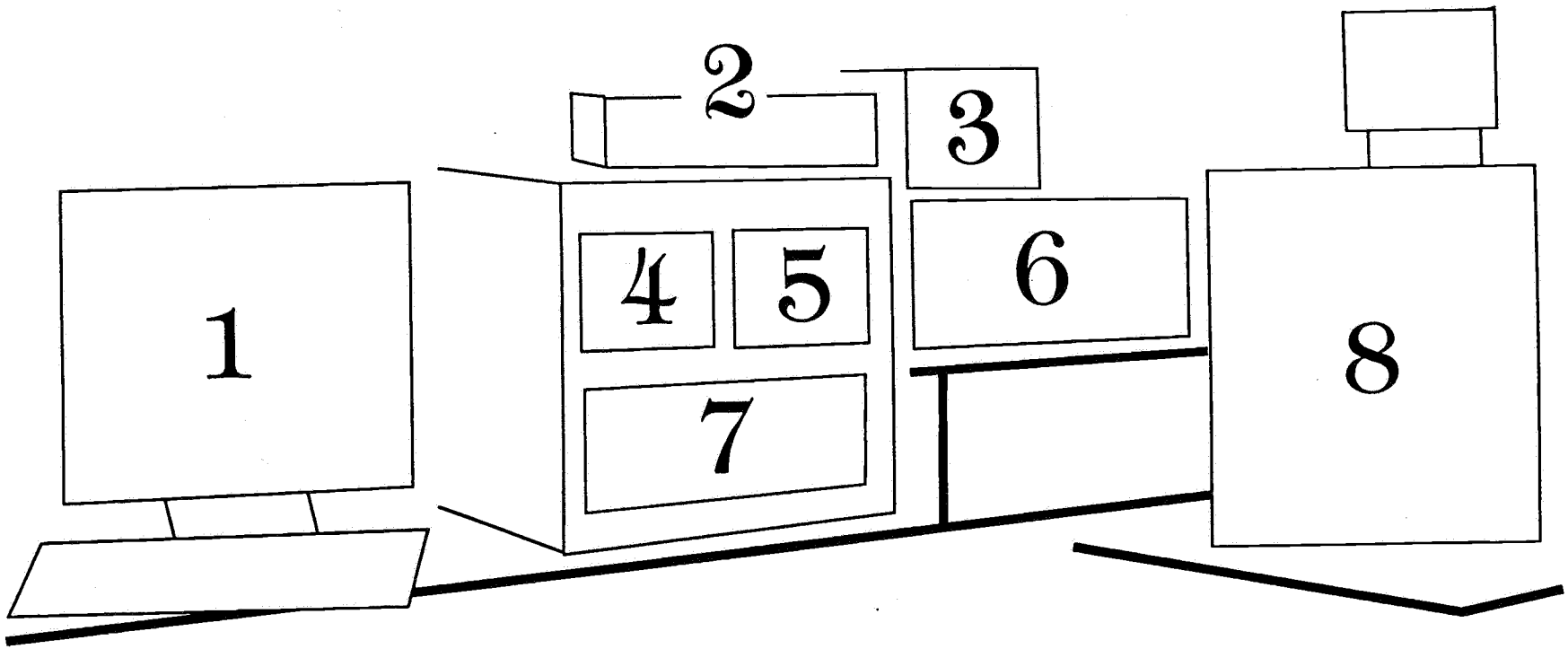
Fig. 6.2.



Apparatus for flow-through testing of adsorbing power of clays

Fig. 6.3a.

000243
70



1. Macintosh Computer
Data Acquisition and Instrument Control

2. Solution degassing and pressurization

3. Column and Sample Delivery

4. Post-column Reagent Delivery

5. Electrochemical and Conductivity Dectector

6. Ultraviolet/Visible Detector

7. Gradient Pump

8. Temperature Controller

Fig. 6.3b.

000244

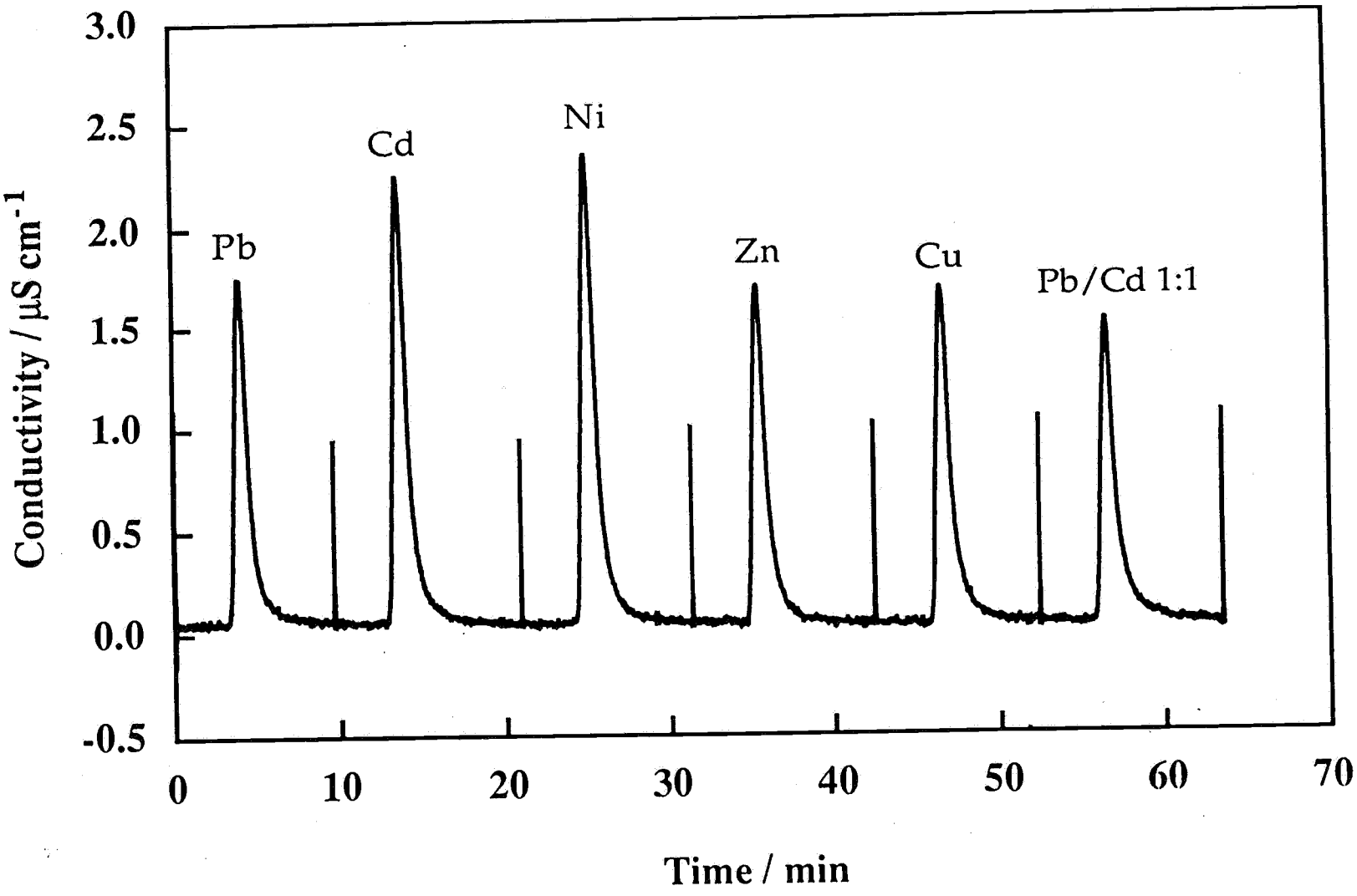


Fig. 6.4. Conductivity of Ca and/or Na ions measured downstream from a clay bed after displacement by different heavy metal ions (as indicated). Intermediate spikes represent start time for each heavy ion injection.

ACKNOWLEDGMENTS

The authors would like to thank Ms N. Delacy, Mr N. Abolins and Mr G. Ferris for assistance in specimen preparation, Mr J. Coppi for photographic processing and Mr P. Fazey for XRF analyses.

000247

ABSORBENT CLAY PROJECT

SUPPLEMENTARY REPORT TO MINES AND ENERGY SOUTH AUSTRALIA

MINERALOGICAL CHARACTERISATION OF GARFORD PALAEOCHANNEL CLAYS

M.D. Raven, N. Abolins, J.L. Keeling and P.G. Self.

CSIRO

Division of Soils

Commonwealth of Australia

RECEIVED
24 APR 1995
DEPT. MINES AND ENERGY SECURITY

April, 1995

Summary

Extensive mineralogical characterisation was carried out on samples obtained from Garford Formation clays taken during the 1991 MESA drilling programme. The characterisation included bulk sample mineralogy, particle size analysis, size-fraction mineralogy and particle morphology as determined by transmission electron microscopy. Two commercial attapulgite samples, from Lake Nerramyne, WA and Xuyi, China, were characterised in the same way for comparison purposes.

Palygorskite present in Garford Formation clay is generally mixed with either illite/smectite clay or with fine-grained dolomite. The nature and distribution of the clays suggest that they formed as lacustrine chemical sediments where mineralogy was controlled by changing chemical conditions in the lake waters. Within the area tested by drilling, the clay sequence shows a trend from illite-dominated clays near the base to dolomite-dominated sediments near the top. Palygorskite formation most closely correlates with increasing alkaline conditions marked by the onset of dolomite deposition. Samples typically comprise less than 60% palygorskite.

One sample, P33 0-1m, showed a very high palygorskite content (approximately 80%). This sample was mineralogically similar to commercial drilling mud (attapulgite) from China. Hole P33 is located in an area of the palaeochannel that has not been tested by drilling. Drilling is recommended to determine the extent of the palygorskite in this area and to collect additional samples for characterisation.

MINERALOGICAL CHARACTERISATION OF GARFORD PALAEOCHANNEL CLAYS

Introduction

The Garford palaeochannel is a major tributary of the Tallaringa palaeodrainage system that, during Tertiary times, drained a wide area to the west of Coober Pedy in northern South Australia. The Garford tributary was approximately 120 km long by 2 to 10 km wide and during Early to Mid-Tertiary times flowed from east to west, joining the Tallaringa channel some 25 km east of Wilkinson Lakes.

Possible uplift of the Garford block, south of the Karari Fault, and periods of aridity in the Late Tertiary were accompanied by decreased flow in the tributary and development of a chain of broad shallow lakes. Within the confines of the palaeochannel there was widespread deposition of Garford Formation clay of Late Miocene to Early Pliocene age.

Eroded sections of clay capped by windblown gypsum form the banks of present day playa lakes scattered along topographic depressions that mark sections of the former drainage system. The clays are uniformly fine grained and are up to 14 m thick (Pitt *et al.*, 1978). Stratigraphic and reconnaissance drilling (Pitt *et al.*, 1978; Robertson, 1984; Warne, 1987; and MESA in 1991) have shown that clays of between 6 to 10 m thickness occur over areas of many square kilometres.

The high palygorskite content of clays from the Garford palaeochannel make them of interest for a wide variety of industrial applications including filtration, sorption, drilling mud and gelling agents. This report provides detailed mineralogical data for clays collected during the 1991 MESA drilling programme and supplements or refines data given in Churchman *et al.* (1994).

Materials

The Garford palaeochannel clays for this investigation were taken from 19 gemco auger drill holes (P24-P28; P30-P43) and one cliff section (P29). The locations of sample sites are shown in Fig. 1. During the drilling programme, representative logging samples of auger cuttings were collected at 1 m intervals. For selected holes, 2 kg samples of clay were also taken at 1 m intervals for use in absorbency and heating trials (Keeling *et al.*, in preparation). For mineralogical investigations, sub-samples were taken preferentially from the 2 kg samples but, where these were not available, the smaller logging samples were used.

In addition, 2 reference palygorskite (attapulgite) samples, from Xuyi, Jiangsu Province China (Keeling, 1994) and from Lake Nerramyne (Mallina Minerals) WA (Rakich, 1990), were included for comparison.

Methods

The methods of mineralogical characterisation used in this study were essentially as described by Churchman *et al.* (1994) in the section on palygorskites.

X-ray Diffraction (XRD)

Samples for XRD examination were scanned either in the form of pressed powders or oriented films. For pressed powders a small portion of each sample was crushed in an agate mortar and pestle with the resulting powders pressed into aluminium sample holders for XRD analysis. For oriented films, samples were dispersed in water and drops of the resulting slurry allowed to dry on porous corundum plates that were under suction. XRD patterns were recorded with a Philips PW1800 microprocessor-controlled diffractometer using CoKα radiation, variable divergence slit and graphite monochromator. Diffraction patterns of pressed powders were recorded in steps of 0.05°2θ with a 1 second counting time per step. Diffraction patterns of oriented films were recorded in steps of 0.02°2θ with a 1 second counting time per step. The data were logged to permanent files on an IBM PC

for analysis. Abundances of the mineral components of each sample were determined by a combination of Rietveld analysis, calibration using standards and integrated peak intensities as described in Appendix 1.

Chemistry

The chemistry of selected samples was determined by x-ray fluorescence spectroscopy (XRF). Preparation of samples involved the "grab" weight method, which comprised accurately weighing 0.28 g of finely ground powders into glass vials with 1.5 g of Norrish/Hutton lithium tetraborate and lanthanum oxide flux. The mixture was then fused into a Pt-Au crucible over an oxy-propane flame at approximately 1050°C and the molten material quench-pressed into a glass disk between a graphite mould and an aluminium plunger. The resulting glass disks were analysed on a Philips PW1480 XRF system.

Size Separation

Selected samples, representative of the various mineralogical sub-groups found in Garford Palaeochannel clays, were separated into size fractions. To size fractionate these samples, 10 g portions of the each clay were dispersed in distilled water by shaking in a SPEX mill for 10 minutes. The resulting slurries were then poured into 400 ml beakers and approximately 150 mls of 1M NaCl added to each. They were left to stand for 2 hours and then, with the aid of centrifugation, repeatedly washed by redispersion and rinsing with deionised water until a stable (non-flocculating) suspension was obtained. The samples were then split into <0.2 μm, 0.2-0.5 μm, 0.5-1 μm, 1-2 μm and >2 μm fractions by centrifugation. The materials in each size fraction were then calcium saturated using $CaCl_2$, washed to remove the excess calcium, dried at 105°C and weighed.

Transmission Electron Microscopy (TEM)

Size fractionated samples were prepared for TEM examination by suspending a small amount of a clay in water and then allowing a drop of the suspension to dry on a carbon support film mounted on a Cu grid. The samples were examined using a Philips EM400 fitted with a Link Systems energy dispersive x-ray (EDX) analyser.

Results and Discussion

Auger-hole logs and mineralogy of bulk samples are shown in Table 1. The non-oriented (pressed powder) XRD patterns for these samples are shown in Figs. 2 to 17. For comparison, the mineralogy and XRD patterns of the commercial grade (reference) attapulgites are shown in Table 2 and Fig. 18.

The mineralogy of the bulk samples taken together with results of earlier stratigraphic drilling (Pitt *et al.*, 1978) show a similar pattern of mineralogical variation in Garford Formation clays throughout the palaeochannel. This is discussed below commencing with the stratigraphically lower and older part of the clay sequence and working through to the upper and younger units.

Few auger holes penetrated the full clay sequence, however there is sufficient drilling data to indicate that the lowermost clay units of the Garford Formation are dominantly kaolinite, interstratified kaolinite/smectite, interstratified illite/smectite or illite. Kaolinite is possibly more common near the margins of the channel or the edges of former lakes. The presence of relatively pure illite may correspond with deeper channel sections. This would be consistent with kaolinite entering the lakes as detrital particles from adjacent weathered Proterozoic bedrock while fine-grained illite was formed by chemical precipitation in deeper lake waters.

Some palygorskite is found precipitated along with illite. The proportion of palygorskite generally increases up the profile and probably reflects a higher content of Mg ions in lake waters and/or increasing alkalinity. The clays appear to have been precipitated together and show no evidence of transformation from one clay to the other. The proportion of palygorskite in association with illite in the Garford palaeochannel clays seldom exceeds 35%. Palygorskite content in these clays has been substantially overestimated in some previous XRD analyses because of overlap and shift of diagnostic x-ray reflections from the (001) crystal lattice planes. The spacing of the basal planes is similar for the two clay minerals and the presence of any randomly interstratified smectite in illite shifts the illite

peak in the direction of the palygorskite peak. The illitic clays are typically dark grey to greenish grey because of the high iron content of the illite.

Where palygorskite content exceeds 35%, dolomite rather than illite is generally the other dominant mineral phase. The clay becomes increasingly dolomitic toward the top of the unit and grades into overlying Millers Creek Dolomite Member which is widespread and extends onto areas marginal to the palaeochannel. Dolomite associated with palygorskite was chemically precipitated as subrounded fine particles 0.5 to 4 μm diameter. Palygorskite generally infills the voids between dolomite grains. Dolomitic clays are typically pale brown to pale yellow to white and it is difficult to determine, in hand specimen, those clays in which palygorskite is the dominant phase.

The main prospective zones for high concentrations of palygorskite appear to be the upper part of the illite-rich clays and within the dolomitic sequences. These zones were targeted in the 1991 drilling based on earlier results showing high values for water sorption. The mineralogy of this part of the clay sequence is dominated by palygorskite, dolomite and illite. A triangular diagram of the relative concentrations of these three minerals in each of the bulk samples examined is shown in Fig. 19. Samples with higher than 55 wt% palygorskite are rare. The samples tend to comprise mixtures of dolomite and palygorskite or illite and palygorskite so that samples with roughly equal amounts of all three minerals are uncommon. Where this does occur (e.g. P35 7-8 m) the sample interval crosses a transitional boundary and the mineralogy is a composite of separate sedimentary layers. Samples containing high amounts of both dolomite and illite do not occur.

The change from illite-dominated clays to dolomitic clay is generally associated with a marked colour change that can be either abrupt from greenish grey to pale greyish yellow or may be gradational with layers of alternating colour over several metres. The change in mineralogy reflects increasing alkalinity in the lakes in the palaeochannel and a change in chemical conditions that was largely incompatible with illite formation. Under these conditions, lakes with high concentrations of Mg cations relative to Ca cations could be expected to deposit more palygorskite and less dolomite.

Areas with low prospectivity for palygorskite include playa lakes along sections of the palaeochannel where erosion of Garford Formation clays has exposed either the lower clay units of dominantly illitic or interstratified clay, or underlying older Tertiary sandy clay.

Of the 86 Garford samples analysed, only one (P33 0-1m) was relatively pure palygorskite (90%). This was from an area of the palaeochannel that is virtually untested by drilling. Other samples with high palygorskite were P24 1-3m (55-60%) and P41 4-4.5m (50%).

Comparison with the two reference samples shows that, in general, the XRD peaks for palygorskite from the Garford palaeochannel samples are more like those of the West Australian Lake Nerramyne attapulgite. These differ from the Chinese attapulgite which shows relatively sharp and intense diffraction peaks for palygorskite, indicative of longer fibre length. An exception is the sample from P33 0-1m which shows similarities to the Chinese attapulgite (Fig. 18).

Samples Selected for Further Study

The grouping of the mineralogy of the Garford palaeochannel clays is such that it is possible to choose a subset of samples that is representative of the whole suite. More extensive analysis on this subset can be used to characterise all samples. The subset of samples chosen as being representative of the Garford palaeochannel clays and therefore selected for further mineralogical analysis is shown in Table 3. Also included in the set are the two reference attapulgites. The particle size distribution of the samples is shown in Table 4. The XRF analysis and illite content (see Appendix 2) for the smallest sized fraction of these samples is shown in Table 5. The mineralogy of the samples is shown in Table 6. The non-oriented (pressed powder) and oriented XRD patterns for the samples are shown in Figs. 20 to 29. TEM images of the sized fractions (where there was sufficient quantity) of the samples are shown in Plates 1 to 33.

For samples containing predominantly illite (i.e. P25), particles are predominantly in the <0.2 μm size range. For samples containing predominantly dolomite and/or palygorskite the particle sizes are more broadly distributed. For these samples it is interesting to note that, with the exception of sample P35, illite is evenly distributed amongst all size fractions.

TEM images show that although the illite particles are small (approximately 0.03 μm) they tend to remain entrapped within mats of palygorskite and so do not separate into the <0.2 μm size fraction as would be expected from their observed size. Whether this entrapment is purely mechanical or involves some chemical bonding is unclear but the uniform content of illite throughout all size fractions would suggest the latter.

TEM shows that dolomite exists as relatively large particles (approximately 1 μm). In this case, TEM images indicate that the large dolomite particles become entangled in mats of palygorskite (e.g. Plate 22). This results in palygorskite remaining in coarser size fractions than would be expected based on observed fibre size.

The overlap of the illite (001) and palygorskite (110) XRD peaks makes it difficult to determine the abundances of these minerals by XRD. This is especially the case when illite is randomly interstratified with smectite or kaolin (e.g. sample P25, Fig. 3). Slow XRD scanning of the region of peak overlap using oriented clay particles can largely overcome this problem. This is because of the increased peak to background ratio of basal reflections in XRD patterns obtained from oriented clay particles. As such, the mineralogy of the sized fractions, which was determined by using both oriented films and non-oriented powders (see Appendix 1), are more accurate than the mineralogy determined for the bulk samples. The results in Table 6 suggest that, in almost all cases, the palygorskite contents given in Table 1 are overestimated. Similarly, when samples have a low illite content relative to palygorskite content, the illite component of the sample can be overlooked (e.g. Chines attapulgite, Tables 2 and 6). If necessary, TEM can be used to check the mineralogical content of samples.

TEM confirms that Garford palaeochannel palygorskite has a very similar morphology to Lake Nerramyne attapulgite (e.g. compare Plate 8 with Plate 31). The dispersion of palygorskite on TEM grids (as shown in the TEM images) indicates that matting of palygorskite fibres does not occur when the palygorskite content of the sample is too low. For example, compare Plate 11 (73% palygorskite) with Plate 13 (53% palygorskite). TEM images indicate that a sample must contain at least 50% palygorskite if significant matting of fibres is to occur. This effect would be of consequence if a clay was to be used for filtration purposes or as a drilling mud. It is interesting to note that TEM images of the Chinese

attapulgite (Plates 26 to 29) show a stronger matting of palygorskite fibres than is shown in images of Lake Nerramyne attapulgite (Plates 30 to 33). Confirmation of this qualitative TEM observation would require rheological testing of appropriate palygorskite-water mixes.

Conclusions

Mineralogical variation in Garford Formation clays of Late Miocene to Early Pliocene age was studied for gemco auger drill hole samples from the 1991 MESA drilling programme in the Garford palaeochannel. The bulk mineralogy of 86 samples was determined by XRD of pressed powders using Rietveld analysis to quantify the mineral phases present. Eight samples were selected for closer examination using particle size separation, XRD of oriented samples, and quantitative mineralogy by a combination of analytical techniques.

The results show a general variation in clay mineralogy that reflects changing chemical conditions during deposition of the Garford Formation.

- Initial deposition was dominantly kaolinite, interstratified kaolinite/smectite, interstratified illite/smectite or illite. The kaolinite component was probably detrital.
- This was followed by a period of chemical precipitation of dominantly fine-grained illite with variable lesser amounts of palygorskite. There is no evidence of transformation of illite to palygorskite or vice versa.
- Probable increasing alkaline conditions resulted in chemical precipitation of dolomite and palygorskite and cessation of illite formation. Clays become more dolomitic toward the top of the formation.

The most prospective zones for high palygorskite clay are in the transition to more alkaline conditions shown by decreasing illite content in the presence of palygorskite and at levels favourable to dolomite precipitation but where the supply of Ca cations may have been restricted.

Quantitative determination of palygorskite in the presence of illite and interstratified clays can be misleading when testing bulk samples using XRD techniques. Size separation of clay particles combined with chemical analysis and XRD of oriented sized fractions provides a

more reliable method. Results presented in this report indicate that for Garford palaeochannel clays, the presence of significant amounts of illite usually means that palygorskite content will be less than 35%. Samples with apparent high palygorskite content should be confirmed by TEM examination.

Comparison with commercial attapulgite from Xuyi, China and Lake Nerramyne, WA indicate that the Garford palygorskite is in general similar to the Lake Nerramyne sample but may also contain areas of palygorskite comparable with that from Xuyi.

Further drilling is required to locate areas with relatively pure palygorskite clays that have greater commercial potential. The physical properties of these could then be assessed and related to their mineralogical characteristics.

References

Churchman, G.J., Ferris, G.M., Keeling, J.L., McClure, S.G., Raven, M.D., Self, P.G. and Slade, P.G. (1994). Absorbent Clay Project. Characterisation of the selected clays. Progress Report No. 1 to Mines and Energy, South Australia, June 1994. South Australian Department of Mines and Energy, Envelope 8785 (unpublished).

Keeling, J.L. (1994). Report on mission to China to explore collaborative research opportunities on modification of clay minerals for industrial and environmental uses. South Australian Department of Mines and Energy, Report Book 94/37.

Pitt, G.M., Benbow, M.C., Barnes, L.C., Harris, W.K. and Lindsay, J.M. (1978). Report on Tallaringa Palaeodrainage System - 1976. South Australian Department of Mines and Energy, Report Book 78/38.

Rakich, P.B. (1990). Development of the attapulgite industry in Australia. Proceedings of the 9th Industrial Minerals International Congress, Sydney 1990. Metal Bulletin PLC, London.

Robertson, R.S. (1984). Reconnaissance sampling of palygorskite clay, Garford Palaeochannel - Coober Pedy. South Australian Department of Mines and Energy, Report Book 84/52.

Warne, S.B. (1987). Roebuck Resources N.L. Report for the period 19th September 1986 to 18th December 1987, Sandstone, EL 1371, South Australia. Roebuck Resources N.L., Technical report No. 81. South Australian Department of Mines and Energy, Open File Envelope 6809 (unpublished).

TABLES

Table 1. Garford Palaeochannel auger hole logs and mineralogy of bulk samples

Hole No	Sample interval (m)	Description	Mineralogy	
P24	0.0 - 1.0	**CLAY**, white to very pale yellow with minor orange coloured spots and infilling cracks (root casts ?).	Dol 75%, Qtz 2%, Celes 1%	Paly 15%, Halite 5%,
	1.0 - 1.5	**CLAY**, pale grey to pale yellow with patchy orange staining, moist.	Dol 20%, Illite 7%, Halite 6%,	Paly 60%, Qtz 5%, Gypsum 2%
	1.5 - 2.0	**CLAY**, greyish yellow to yellowish green, slightly SANDY (VF-F), moist, plastic.		
	2.0 - 3.0	**CLAY**, dark greenish grey, slightly SANDY (VF-M). Some orange brown Fe staining, moist, plastic.	Dol 7%, Illite 25%, Halite 6%	Paly 55%, Qtz 4%,
		EOH 3.0m. Logged JLK 19 March 1991.		
P25	0.0 - 1.0	**CLAY**, white to pale yellow, minor yellow brown staining. Hard at surface but soft and slightly moist below 0.2m. Greyish patches at 1.0m.	Dol 90%, Qtz 2%,	Paly 7%, Halite 2%
	1.0 - 2.0	**CLAY**, white to pale yellow to pale orange, salty, rare quartz grains, minor yellow brown Fe oxides.	Dol 80%, Qtz 5%,	Paly 15%, Halite 2%
	2.0 - 3.0	**CLAY**, greenish grey and yellow, some darker grey patches, moist, moderately plastic, salty.	Dol 10%, Illite 45%, Halite 5%	Paly 35%, Qtz 5%,
	3.0 - 4.0	**CLAY**, dark greenish grey, moderately - very plastic, trace of quartz sand (M). Colour less patchy than above.	Dol 9%, Illite 40%, Halite 7%	Paly 35%, Qtz 9%,
	4.0 - 5.0	**CLAY**, dark greenish grey with rare black patches ~2mm across, shiny and magnetic. Very rare quartz grains (M-C).	Dol 2%, Illite 55%, Halite 4%	Paly 35%, Qtz 6%,
	5.0 - 6.0	**CLAY**, dark greenish grey smooth, wet, very stiff. WATER CUT at ~5.8m. Even colour and texture, minor quartz grains. Pliable and waxy, soapy feel when wet, dark greyish green to grey. Pulled rods and cleaned off.	Dol <1%, Illite 60%, Halite 4%	Paly 25%, Qtz 8%,
	6.0 - 7.0	**CLAY**, dark grey to greenish grey with yellow brown and red brown Fe oxide staining, wet.	Dol <1%, Illite 65%, Halite 4%,	Paly 20%, Qtz 4%, Kaolin 4%
	7.0 - 9.0	**CLAY**, dark olive green to grey, very plastic, cracks on drying.	Dol <1%, Illite 50%, Halite 5%,	Paly 25%, Qtz 9%, Kaolin 8%
		EOH 9.0m. Logged JLK 20 March 1991.		

Hole No	Sample interval (m)	Description	Mineralogy
P26	0.0 - 1.0	**CLAY**, white to pale yellow, dry easily crumbled.	Dol 80%, Paly 15%, Qtz 4%, Halite 3%, Celes <1%
	1.0 - 2.0	**CLAY**, white to pale yellow brown, dry becoming moist below 1.5m.	Dol 65%, Paly 25%, Illite 6%, Qtz 1%, Halite 2%, Tr Celes, Kaolin
	2.0 - 3.0	**CLAY**, white to very pale yellow brown, some orange bands or patches, moist plastic.	Dol 65%, Paly 25%, Illite 2%, Qtz 1%, Halite 2%, Tr Celes Kaolin
	3.0 - 4.0	**CLAY**, white to pale yellow with minor orange specking.	Dol 60%, Paly 35%, Qtz 1%, Halite 2%, Tr Celes
	4.0 - 5.0	**CLAY**, white to very pale yellow with minor orange Fe oxide patches, moist, plastic.	Dol 80%, Paly 15%, Qtz 1%, Halite 3%, Tr Celes, Kaolin
	5.0 - 6.0	**CLAY**, white to pale grey with rare grey quartz (C-VC) moist, plastic.	Dol 80%, Paly 15%, Halite 3%, Tr Qtz, Celes, Kaolin
	6.0 - 6.5	**CLAY**, greyish green to yellowish green, even grained, smooth, plastic.	Paly 10%, Illite 20%, Qtz 15%, Halite 5%, Kaolin/interstratified kaolin-smectite 45%, Tr Anatase, Kaolin
		EOH 6.5m. Logged JLK 20 March 1991.	
P27	0.0 - 1.0	**SAND** (VF-F), moderately **CLAYEY**, with some nodules of silicified clay up to 50mm across. White to pale yellow grey.	
	1.0 - 2.0	**SAND** (VF-F), mod.- very **CLAYEY**, moist, pale red brown to brownish grey.	
	2.0 - 3.0	**SAND** (VF-F), mod.- very **CLAYEY**, pale to dark grey.	
	3.0 - 4.5	**SAND** as above, dark grey to greenish grey, wet.	
		EOH 4.5m. Logged JLK 20 March 1991.	
P28	0.0 - 1.0	**SILT**, mod. **SANDY** (VF), dark brown.	
	1.0 - 2.0	**SILT**, mod. **CLAYEY** dark brown.	
	2.0 - 3.0	**CLAY**, very **SILTY**, dark brown to black (organic matter).	
	3.0 - 4.5	**SAND** (VF-F), mod. **CLAYEY**, black and organic rich. WATER CUT at 3.0m.	
		EOH 4.5m. Logged JLK 20 March 1991.	

Hole No	Sample interval (m)	Description	Mineralogy
P29 (cliff section, true vertical thickness)	0.0 - 1.3	**GYPCRETE**, massive blocky, white to pale greyish green and pale orange brown.	
	1.3 - 2.1	**GYPCRETE**, rubbly, pale greenish grey to white and pale orange brown. Weathered vughy with hard platelets and nodules.	
	2.1 - 4.4	**GYPSUM** sand (F-VC), slightly to mod. SILTY, orange brown, free flowing with some hard patches.	
	4.4 - 4.9	**GYPCRETE**, massive to rubbly, pale orange brown with white patches.	
	4.9 - 6.9	**GYPSUM** sand (F-M), mod. to very SILTY, dark orange brown.	
	6.9 - 9.0	**GARFORD FORMATION: CLAY** white to very pale yellow with minor black and orange brown spidery patches. Salt encrusted on the surface and white.	Dol 85%, Paly 10%, Qtz 1%, Halite 1%, Gypsum 1%
	9.0	**LAKE FLOOR**: gypsum silt.	
		True height 9m. Logged JLK 21 March 1991.	
P30	0.0 - 1.0	**CLAY**, white to pale grey with minor orange brown to yellow Fe staining, dry.	Dol 65%, Paly 7%, Illite 10%, Qtz 15%, Halite 2%
	1.0 - 2.0	**CLAY**, white to pale grey, moist. Rare scattered quartz grains (C), black patches (organic or Mn) and minor Fe patches that appear to infill root holes or burrows.	Dol 85%, Paly 15%, Qtz<1%, Halite 2%
	2.0 - 3.0	**CLAY**, white to very pale grey, even colour, moist.	Dol 85%, Paly 15%, Qtz 1%, Halite 2%
	3.0 - 4.0	**CLAY**, very pale grey, moist, plastic, smooth. WATER CUT.	Dol 50%, Paly 30%, Illite 20%, Qtz<1%, Halite 3%
	4.0 - 6.0	**CLAY**, dark greenish grey with minor yellow brown Fe patches, smooth stiff, good sample return.	Dol 45%, Paly 7%, Qtz 3%, Halite 3%, Celes 2%, Illite/interstratified illite-smectite 40%
		EOH 6.0m. Logged JLK 21 March 1991	

Hole No	Sample interval (m)	Description	Mineralogy
P31	0.0 - 1.3	**GYPSUM** sand (F-M), yellow brown to red brown with minor quartz sand (C). Colour greenish yellow to yellow brown below 0.7m.	
	1.3 - 2.0	**CLAY**, white to very pale grey, crumbly with low moisture, minor yellow brown staining.	
	2.0 - 3.5	**CLAY**, calcareous, white to very pale grey, moist.	Dol 90%, Paly 10%, Qtz 1%, Halite 1%
	3.5 - 5.0	**CLAY**, very pale yellowish grey, moist plastic smooth with some small yellowish patches.	Dol 90%, Paly 8%, Qtz 2%, Halite 1%
	5.0 - 6.0	**CLAY,** very pale grey, smooth, plastic. WATER CUT. Flights pulled and cleaned.	Dol 80%, Paly 20%, Qtz 1%, Halite 1%
	6.0 - 7.0	**CLAY**, grey green to grey with minor yellow orange patches, smooth, plastic.	Halite 6%, Illite/interstratified illite-smectite 90%, Tr Kaolin
	7.0 - 7.5	**CLAY**, dark grey green, smooth plastic with yellow orange to orange Fe oxide patches.	
		EOH 7.5m. Logged JLK 21 March 1991.	
P32	0.0 - 1.0	**SILT**, orange brown to white gypsum with quartz SAND (M-C).	
	1.0 - 2.0	**SAND** (VF-M), very CLAYEY, white to very pale grey.	
	2.0 - 3.0	**SAND** (VF-M), slightly to mod. CLAYEY, pale grey.	
	3.0 - 4.0	**SAND** (VF-M), mod. CLAYEY, pale grey, moist.	
	4.0 - 6.0	**CLAY**, mod. SANDY (VF), grey. WATER CUT at 5.5m.	
		EOH 6.0m. Logged JLK 21 March 1991.	
P33	0.0 - 0.2	**CLAY**, white with orange brown Fe staining.	Dol 3%, Paly 90%, Qtz 2%, Halite 4%, Tr Kaolin, Amphibole
	0.2 - 1.5	**CLAY**, greenish grey with occasional hard bands.	Dol 3%, Paly 90%, Qtz 2%, Halite 4%, Tr Kaolin, Amphibole
	1.5 - 2.0	**CLAY**, white to pale grey, dry powdery.	Dol 75%, Paly 20%, Qtz 2%, Halite 2%
	2.0 - 3.0	**CLAY**, greenish grey, waxy, mod. plastic but with some hard bands. WATER CUT.	Dol 60%, Paly 30%, Qtz 5%, Halite 5%, Tr Kaolin
		EOH 3.0m. Logged JLK 21 March 1991.	

Hole No	Sample interval (m)	Description	Mineralogy	
P34	0.0 - 0.4	**GYPSUM** sand (F-M), mod CLAYEY, pale orange brown.		
	0.4 - 1.0	**CLAY,** white, dry, with minor yellow brown Fe oxide staining.		
	1.0 - 2.0	**CLAY**, white to very pale grey, to very pale yellow, dry, becoming slightly moist at 2.0m.	Dol 65%, Halite 2%	Paly 30%,
	2.0 - 3.0	**CLAY**, white to very pale grey, moist.	Dol 75%, Qtz 2%,	Paly 20%, Halite 1%
	3.0 - 4.0	**CLAY**, very pale greenish yellow, moist, slightly plastic. WATER CUT at ~3.8m.	Dol 65%, Qtz 1%,	Paly 35%, Halite 2%
	4.0 - 5.0	**CLAY**, white to very pale yellow, becoming pale greenish grey below 4.5m, mod. plastic.	Dol 70%, Qtz 1%,	Paly 25%, Halite 2%
	5.0 - 6.0	**CLAY**, very pale greenish yellow to very pale yellow, moist, plastic.	Dol 75%%, Halite 2%	Paly 25%,
	6.0 - 6.5	**CLAY**, dark greenish grey with some orange brown patches, moist.	Dol 85%, Halite 2%	Paly 10%,
	6.5 - 7.5	**CLAY**, very pale yellow grey to pale pink, mod. plastic.		
		EOH 7.5m. Logged JLK 24 March 1991.		
P35	0.0 - 1.5	**SILT**, mod. SANDY (VF-M), gypsum orange brown.		
	1.5 - 2.0	**CLAY**, very pale orange brown, with minor quartz grains (M) and some coarse clear gypsum crystals.		
	2.0 - 3.0	**CLAY**, white to very pale grey, dry and hard with some quartz grains (M-VC).	Dol 65%, Qtz<1%	Paly 30%, Halite 1%
	3.0 - 4.0	**CLAY**, white to very pale yellow, dry, clean.	Dol 65%, Qtz 1%,	Paly 35%, Halite 1%
	4.0 - 5.0	**CLAY**, pale grey green, dry to moist with pale yellow clay interbeds.	Dol 65%, Qtz<1%,	Paly 35%, Halite 1%
	5.0 - 6.0	**CLAY**, white to pale brown with thin dark grey green bands, moist.	Dol 70%, Qtz 1%,	Paly 30%, Halite<1%
	6.0 - 7.0	**CLAY**, white to pale yellowish grey with minor thin greyish bands, very moist, plastic. WATER CUT at ~6.0m.	Dol 45%, Qtz<1%,	Paly 50%, Halite 5%
	7.0 - 8.0	**CLAY**, white to pale greyish yellow with bands of dark greenish grey clay, moist, plastic.	Dol 30%, Illite 30%, Halite 4%	Paly 35%, Qtz<1%,
	8.0 - 9.0	CLAY, white with pale yellow to orange brown patches of Fe oxides, plastic , stiff.	Dol 60%, Illite 15%, Halite 3%	Paly 20%, Qtz<1%,
		EOH 9.0m. Logged JLK 24 March 1991.		

Hole No	Sample interval (m)	Description	Mineralogy
P36	0.0 - 1.0	**SILT**, gypsum, very pale orange brown with 10-20% quartz GRAVEL (F) and SAND (VC).	
	1.0 - 2.0	**SILT**, mod. SANDY (VF-F) pale orange brown gypsum.	
	2.0 - 3.0	**SILT**, mod. CLAYEY with sand sized gypsum crystals.	Dol 65%, Paly 30%, Halite 3%
	3.0 - 4.0	**CLAY**, pale grey to orange brown, minor quartz grains.	Dol 40%, Paly 15%, Qtz 20%, Halite 3%, Gypsum/Bassanite 25%
	4.0 - 5.0	**CLAY**, white to very pale grey, smooth with minor quartz sand (M-C), difficult sample return, water added.	Dol 65%, Paly 25%, Qtz 9%, Halite 1%, Tr Gypsum, Bassanite
	5.0 - 6.0	**CLAY**, white to very pale grey, slightly SANDY (F-C), mod. plastic.	Dol 65%, Paly 25%, Qtz 7%, Halite 2%, Gypsum 1%
	6.0 - 8.0	**CLAY**, white to very pale grey, slightly SANDY (F-C), mod. plastic, some grey-green bands.	Dol 60%, Paly 30%, Qtz 7%, Halite 2%
	8.0 - 9.0	**CLAY**, white to very pale yellow, mod. plastic with minor sandy interbeds.	Dol 55%, Paly 35%, Qtz 7%, Halite 2%
		EOH 9.0m. Logged JLK 24 March 1991.	
P37	0.0 - 1.0	**CLAY**, white to very pale greyish yellow, dry.	Dol 65%, Paly 30%, Qtz 3%, Halite 3%
	1.0 - 2.0	**CLAY**, very pale yellow, dry and powdery.	Dol 55%, Paly 35%, Qtz 6%, Halite 1%, Celes 1%
	2.0 - 3.0	**CLAY**, very pale yellow, grey and white, dry to slightly moist.	Dol 45%, Paly 45%, Qtz 2%, Halite 5%, Tr Celes
	3.0 - 4.0	**CLAY**, white, plastic, stiff, minor quartz sand (M-C). WATER CUT at ~3.0m.	Dol 50%, Paly 45%, Qtz 2, Halite 5%, Tr Celes
	4.0 - 5.0	**CLAY**, greenish grey, plastic smooth.	Dol 60%, Paly 20%, Illite 15%, Qtz 2%, Halite 7%, Tr Celes
	5.0 - 6.0	**CLAY**, white to very pale grey with greenish grey bands.	Dol 60%, Paly 15%, Illite 15%, Qtz 2%, Halite 6%, Tr Celes
	6.0 - 7.5	**CLAY**, greenish grey becoming red brown with depth, smooth, plastic, no grit.	Dol 10%, Paly 15%, Illite 60%, Qtz<1%, Halite 7%
		EOH 7.5m. Logged JLK 24 March 1991.	

Hole No	Sample interval (m)	Description	Mineralogy	
P38	0.0 - 1.0	**CLAY**, white to pale greenish grey, dry and powdery.		
	1.0 - 2.0	**CLAY**, white to very pale yellow with gypsum crystals, dry.	Dol 55%, Qtz 1%,	Paly 45%, Halite 2%
	2.0 - 3.0	**CLAY**, white to very pale greenish grey, moist smooth and mod. plastic. Very minor yellow brown patches.		
	3.0 - 4.0	**CLAY**, white to very pale yellowish grey, mod. plastic.	Dol 45%, Illite 15%, Halite 3%,	Paly 30%, Qtz<1%, Celes 5%
	4.0 - 5.0	**CLAY**, white to very pale greenish yellow with minor yellow brown patches.	Dol 55%, Illite 15%, Halite 3%	Paly 25%, Qtz<1%,
	5.0 - 5.5	**CLAY**, pale greenish grey.	Dol 55%, Illite 10%, Halite 3%, Celes	Paly 25%, Qtz<1%, Tr Kaolin,
	5.5 - 6.3	**CLAY**, pale yellow grey to dark greenish grey.		
		EOH 6.3m. Logged JLK 24 March 1991.		
P39	0.0 - 0.2	**SAND** (F-C), gypsum with some quartz grains. Gypsum crystals on the surface.		
	0.2 - 1.0	**CLAY**, white to very pale grey, dry powdery, low density.		
	1.0 - 2.4	**CLAY**, white, slightly SANDY (VF-F), in bands, elsewhere white to very pale grey, moist.		
	2.4 - 3.0	**CLAY**, slightly GRAVELLY (F) quartz, white to very pale yellow.		
	3.0 - 4.5	**CLAY**, slightly GRAVELLY (F) angular grey quartz. Clay white to very pale grey, slightly micaceous (possible kaolinized bedrock).		
		EOH 4.5m. Logged JLK 25 March 1991.		

Hole No	Sample interval (m)	Description	Mineralogy	
P40	0.0 - 1.0	**CLAY**, pale grey with minor orange and yellow brown patches, spots and dendrites.	Dol 75%, Qtz<1%, Gypsum 1%	Paly 20%, Halite 5%,
	1.0 - 2.0	**CLAY**, pale grey, slightly SILTY.	Dol 85%, Qtz<1%,	Paly 15%, Halite 2%
	2.0 - 3.0	**CLAY,** white to pale grey, slightly SILTY, dry.	Dol 75%, Halite 3%,	Paly 20%, Tr Illite
	3.0 - 4.0	**CLAY**, very pale greenish grey, smooth and moist.	Dol 60%, Qtz 1%, Celes 1%	Paly 30%, Halite 7%,
	4.0 - 5.0	**CLAY**, pale brown to pale greenish grey, plastic. WATER CUT at ~4.0m.	Dol 70%, Qtz 5%, Celes<1%	Paly 20%, Halite 5%,
	5.0 - 6.0	**CLAY**, pale greenish grey to dark greenish grey, moist, plastic.	Dol 60%, Illite 10%, Halite 8%,	Paly 20%, Qtz<1%, Gypsum 1%
	6.0 - 7.5	**CLAY**, dark greenish grey to grey with orange brown slightly SANDY (VF-F), plastic, very stiff.	Dol 15%, Illite 45%, Halite 15%,	Paly 10%, Qtz 6%, Celes 1%
		EOH 7.5m. Logged JLK 25 March 1991.		
P41	0.0 - 0.3	**SAND** (VF-M), mod. SILTY gypseous.		
	0.3 - 1.0	**CLAY**, white, dry powdery to slightly moist with yellow brown to black patches.	Dol 65%, Qtz 10%,	Paly 20%, Halite 2%
	1.0 - 2.0	**CLAY**, white, dry and powdery, trace of quartz grains.	Dol 70%, Qtz 2%,	Paly 25%, Halite 3%
	2.0 - 3.0	**CLAY**, white to very pale grey, slightly moist.	Dol 55%, Illite 5%, Halite 5%	Paly 30%, Qtz 1%,
	3.0 - 4.0	**CLAY**, pale greenish grey to dark grey to pale yellow, stiff, moist, plastic with trace of quartz sand (M). WATER CUT just below 3m.	Dol 60%, Illite 7%, Halite 6%	Paly 20%, Qtz<1%,
	4.0 - 4.5	**CLAY**, pale greenish grey to pale greyish brown with patches and veinlets of yellow Fe oxides.	Dol 20%, Illite 10%, Halite 15%,	Paly 50%, Qtz 2%,
		EOH 4.5m. Logged JLK 25 March 1991.		

Hole No	Sample interval (m)	Description	Mineralogy
P42	0.0 - 0.3	**SAND** (F-M), gypsum, orange brown to red brown.	
	0.3 - 1.0	**CLAY**, white to very pale yellowish grey, dry.	Dol 50%, Paly 50%, Qtz 5%, Halite 6%
	1.0 - 2.0	**CLAY**, white to very pale grey, dry and crumbly or slightly moist. Fe oxides as yellow orange stringers.	Dol 55%, Paly 35%, Qtz 3%, Halite 4%
	2.0 - 3.0	**CLAY**, very pale grey, slightly moist, crumbly.	Dol 50%, Paly 30%, Qtz 15%, Halite 7%, Tr Celes
	3.0 - 5.0	**CLAY**, pale yellowish grey, moist, mod. plastic with rare quartz grains (C).	Dol 50%, Paly 30%, Illite 8%, Qtz 2%, Halite 8%, Tr Celes
	5.0 - 6.0	**CLAY**, very pale yellowish grey to very pale greenish grey, soft, smooth and plastic but very sticky. WATER CUT.	Dol 50%, Paly 15%, Illite 15%, Qtz 3%, Halite 9%, Kaolin/interstratified kaolin-smectite 7%, Tr Celes
	6.0 - 7.0	**CLAY**, dark greenish grey with some orange brown patches, plastic.	Dol 40%, Paly 20%, Illite 25%, Qtz 3%, Halite 9%, Tr Celes
	7.0 - 8.0	**CLAY**, greenish grey, becoming dark grey with depth, stiff, plastic.	Dol 15%, Paly 5%, Illite 15%, Qtz 5%, Halite 8%, Kaolin/interstratified kaolin-smectite/ interstratified illite-smectite 45%, Tr Anatase
	8.0 - 9.0	**CLAY**, dark grey, smooth and plastic, very stiff.	Dol 6%, Paly<1%, Illite 5%, Qtz 40%, Halite 5%, Kaolin/interstratified kaolin-smectite/ interstratified illite-smectite 40%, Tr Anatase

EOH 9.0m. Logged JLK 25 March 1991.

Hole No	Sample interval (m)	Description	Mineralogy
P43	0.0 - 0.1	**SAND**, gypsum, pale brown to white. Coarse white gypsum crystals on the surface.	
	0.1 - 1.0	**CLAY**, slightly SILTY, dry and powdery.	Dol 70%, Paly 25%, Halite 5%, Qtz<1%
	1.0 - 1.5	**CLAY**, white, smooth, trace of sand (M).	Dol 60%, Paly 30%, Halite 7%, Qtz<1%, Tr Celes
	1.5 - 2.5	**CLAY**, very pale grey, dry to slightly moist.	Dol 65%, Paly 25%, Illite 4%, Halite 7%, Qtz 1%, Tr Celes
	2.5 - 3.0	**CLAY**, grey to greyish brown, moist, plastic with some orange brown staining.	Dol 30%, Paly 40%, Illite 8% Qtz<1%, Halite 15%, Kaolin/interstratified kaolin-smectite 5%
		EOH 3.0m. Logged JLK 25 March 1991.	

Celes = celestine; Dol = dolomite; Kaolin = kaolinite/halloysite; Paly = palygorskite; Qtz = quartz; Tr = trace.
EOH = end of hole; JLK = John L. Keeling.
Mineralogy accuracy ≈ ±10% (relative).

Table 2. Mineralogy of standard specimens.

Chinese attapulgite	Dolomite <1%, palygorskite 70%, quartz 10%, smectite 15%
Lake Nerramyne attapulgite	Dolomite 5%, palygorskite 60%, quartz 10%, kaolin 20%

Table 3. Samples selected for further investigation. A summary of the mineralogy data from Table 1 is also given.

P25 5-6m	Illite - D	Palygorskite - SD	Dolomite - Tr
P25 6-7m	Illite - D	Palygorskite - SD	Dolomite - Tr
P31 2-3m	Dolomite - D	Palygorskite - M	
P33 0-1m	Palygorskite - D	Dolomite - Tr	
P35 5-6m	Dolomite - D	Palygorskite - SD	
P35 6-7m	Dolomite - CD	Palygorskite - CD	
P42 3-4m	Dolomite - D	Palygorskite - SD	Illite - M
P42 4-5m	Dolomite - D	Palygorskite - SD	Illite - M
Chinese attapulgite	Palygorskite - D	Smectite - SD	
Lake Nerramyne attapulgite	Palygorskite - D	Kaolin - SD	

D = dominant, SD = sub-dominant, CD = co-dominant, M = minor, Tr = trace.

Table 4. Particle size distribution for the selected samples.

Sample	Size range (μm)	Proportion (wt%) <0.2	0.2-0.5	0.5-1	1-2	>2
P25 5-6m		84	5	11 (>0.5μm)		
P25 6-7m		85	8	1	0.3	6
P31 2-3m		0	<0.1	20	18	62
P33 0-1m		8	<0.2	5	82	5
P35 5-6m		3	23	45	12	17
P35 6-7m		4	48	28	4	17
P42 3-4m			45	24	11	19
P42 4-5m			14	78	8 (>1μm)	
Chinese attapulgite		31	3	41	15	10
Lake Nerramyne attapulgite		64	11	4	4	18

Table 5. X-ray Fluorescence Analysis and Illite content (based on the composition of Muloorina Illite) of sized fractions of the selected samples.

Sample	SiO_2 %	TiO_2 %	Al_2O_3 %	Fe_2O_3 %	MnO %	MgO %	CaO %	Na_2O %	K_2O %	P_2O_5 %	SO_3 %	ZrO_2 %	Sr %	Sum %	Illite wt%
P25 5-6m <0.2μm	54.2	0.51	19.01	7.21	0.011	4.26	1.13	0.10	5.11	0.029	0.013	0.020	0	91.6	69
P25 6-7m <0.2μm	50.6	0.46	20.81	7.47	0.011	2.75	2.06	0.08	3.39	0.018	0.010	0.018	0	87.7	46
P31 2-3m 0.5-1μm	19.6	0.19	4.03	1.96	0.175	17.3	22.1	0.22	0.46	0.042	0.112	0.003	0.022	66.2	6
P33 0-1m 1-2μm	59.6	0.57	9.60	4.76	0.021	11.6	0.56	0.07	1.17	0.027	0.013	0.023	0.002	88.0	16
P35 5-6m <0.2μm	52.2	0.55	14.68	6.64	0.015	7.4	0.87	0.41	3.50	0	0.016	0.016	0	86.3	47
P35 6-7m <0.2μm	53.6	0.65	15.29	6.06	0.009	6.9	0.89	0.18	3.56	0.015	0.024	0.013	0	87.1	48
P42 3-4m <0.5μm	35.8	0.43	8.69	2.76	0.103	13.7	12.03	0.18	1.04	0.029	0.138	0.006	0.016	75.0	14
P42 4-5m <0.5μm	27.4	0.39	7.57	2.35	0.142	14.5	15.12	0.23	0.96	0.024	0.128	0.001	0.027	68.8	13
Chinese attapulgite <0.2μm	54.1	0.32	10.41	5.90	0.029	10.9	2.31	<0.03	0.74	0.024	0.007	0.005	0	84.8	10
Lake Nerramyne attapulgite <0.2μm	55.9	0.48	15.89	6.47	0.010	6.5	1.54	0.08	1.89	0.018	0.010	0.008	0	88.8	26

Table 6. Mineralogy of sized fractions of the selected samples.

Sample	Size µm	% sample	Dolomite wt%	Palygorskite wt%	Illite wt%	Quartz wt%	Kaolin wt%	Smectite wt%	Calcite wt%
P25 5-6m	<0.2	84	-	8	69(90)[1]	-	1	-	-
	0.2-0.5	5	-	-	80[1]	-	20	-	-
P25 6-7m	<0.2	85	-	-	46(80)[1]	-	20[2]	-	-
	0.2-0.5	8	-	-	37	4	59	-	-
P31 2-3m	0.2-0.5	<0.1	20	45	30	-	2	-	-
	0.5-1	20	84	10	6	-	Trace	-	-
	1-2	18	96	4	-	-	-	-	-
P33 0-1m	<0.2	8	-	73	27	-	-	-	-
	0.2-0.5	<0.2	-	73	27	-	Trace	-	-
	0.5-1	5	2	73	24	Trace	1	-	-
	1-2	82	2	73	16	7	2	-	-
P35 5-6m	<0.2	3	-	53	47	-	-	-	-
	0.2-0.5	23	53	41	5	1	-	-	-
	0.5-1	45	75	21	3	1	-	-	-
	1-2	12	89	7	1	3	-	-	-
P35 6-7m	<0.2	4	-	44	48	-	3	-	-
	0.2-0.5	48	53	39	4	1	3	-	-
	0.5-1	28	63	29	4	1	3	-	-
	1-2	4	89	6	1[3]	3	1	-	-
P42 3-4m	<0.5	45	46	30	14	1	7	-	-
	0.5-1	24	73	13	8	2	3	-	-
	1-2	11	88	5	2[3]	3	2	-	-
P42 4-5m	<0.5	14	54	22	13	1	10	-	-
	0.5-1	78	73	12	7	1	6	-	-

Sample	Size	%	Dolomite	Palygorskite	Illite	Quartz	Kaolin	Smectite	Calcite
	µm	sample	wt%	wt%	wt%	wt%	wt%	wt%	wt%
Chinese attapulgite	<0.2	31	-	80	10	-	-	10	Trace
	0.2-0.5	3	-	60	15[3]	15	Trace	10	Trace
	0.5-1	41	-	60	15[3]	15	-	10	Trace
	1-2	15	-	55	10[3]	30	-	5	Trace
Lake Nerramyne attapulgite	<0.2	64	-	64	26	-	10	Trace	-
	0.2-0.5	11	-	42	17[3]	1	40	Trace	-
	0.5-1	4	-	52	21[3]	7	20	-	-
	1-2	4	-	54	22[3]	14	10	-	-

[1] Randomly interstratified illite/smectite. Where shown the first figure represents the illite content determined by using the K_2O content of the sample; the figure in brackets represents the total content of randomly interstratified material.

[2] Randomly interstratified kaolin - illite/smectite.

[3] Mica (rather than illite).

FIGURES

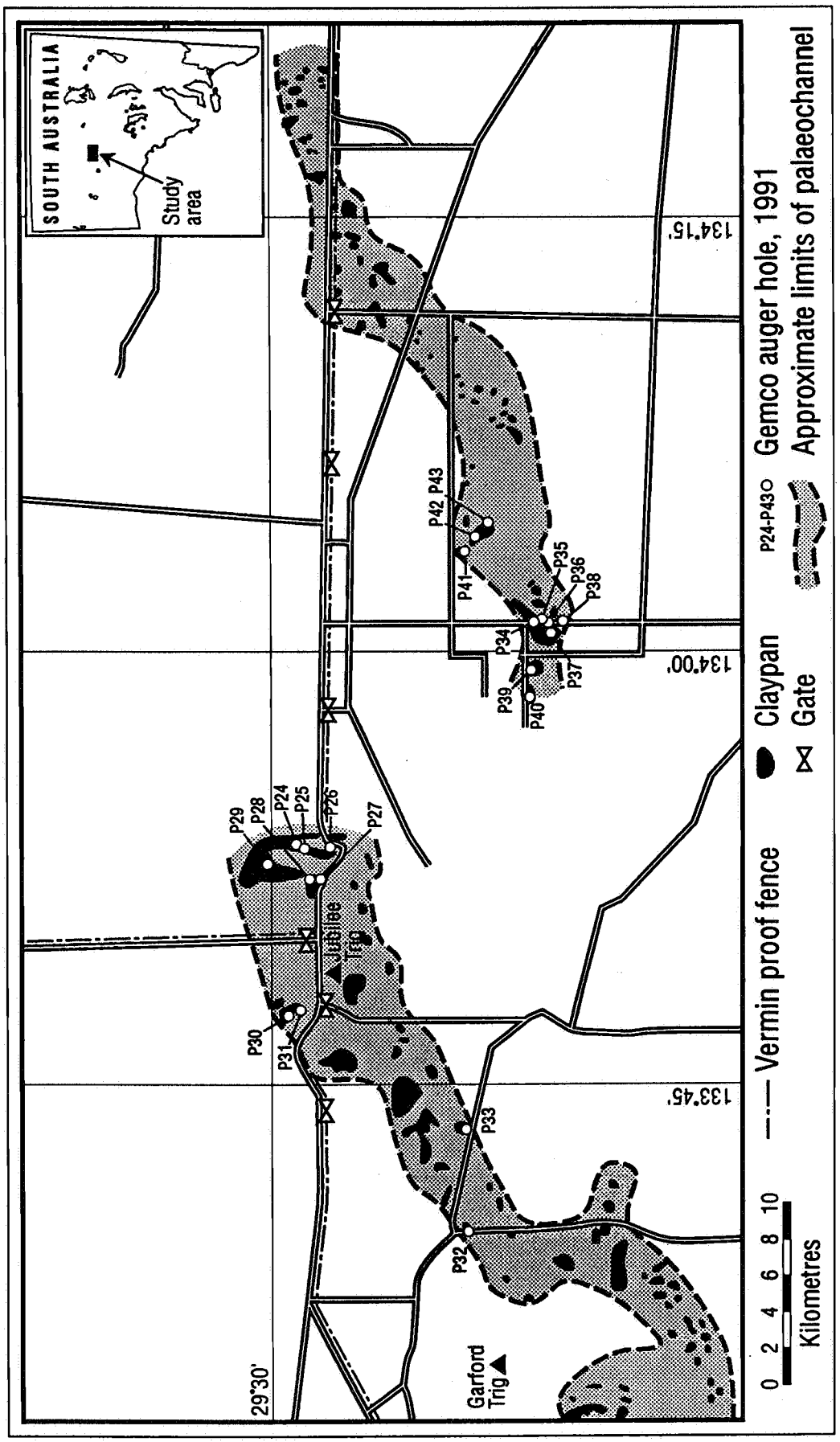
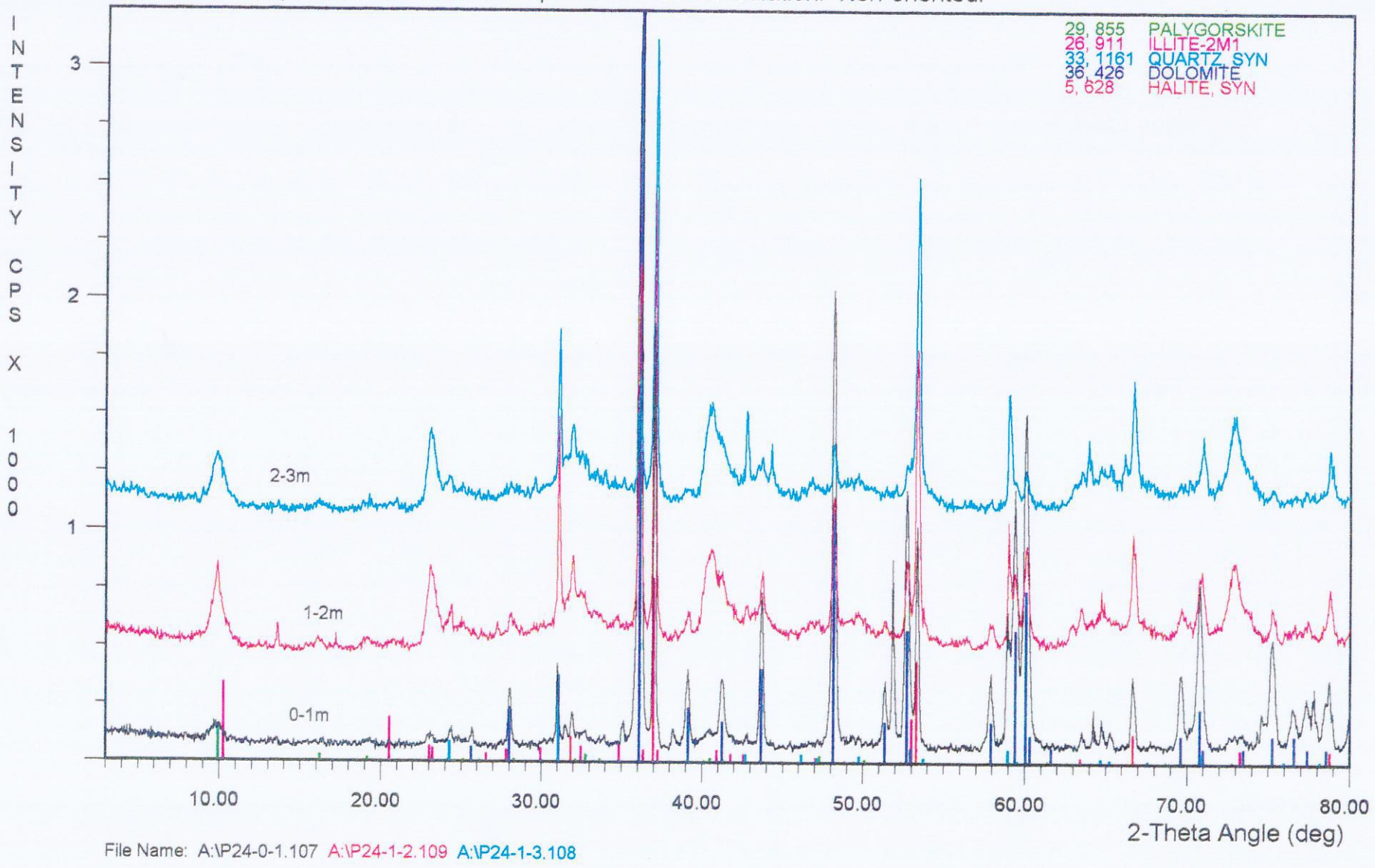


Fig. 1. Location of auger holes (P24-28; P30-P43) and cliff section (P29).

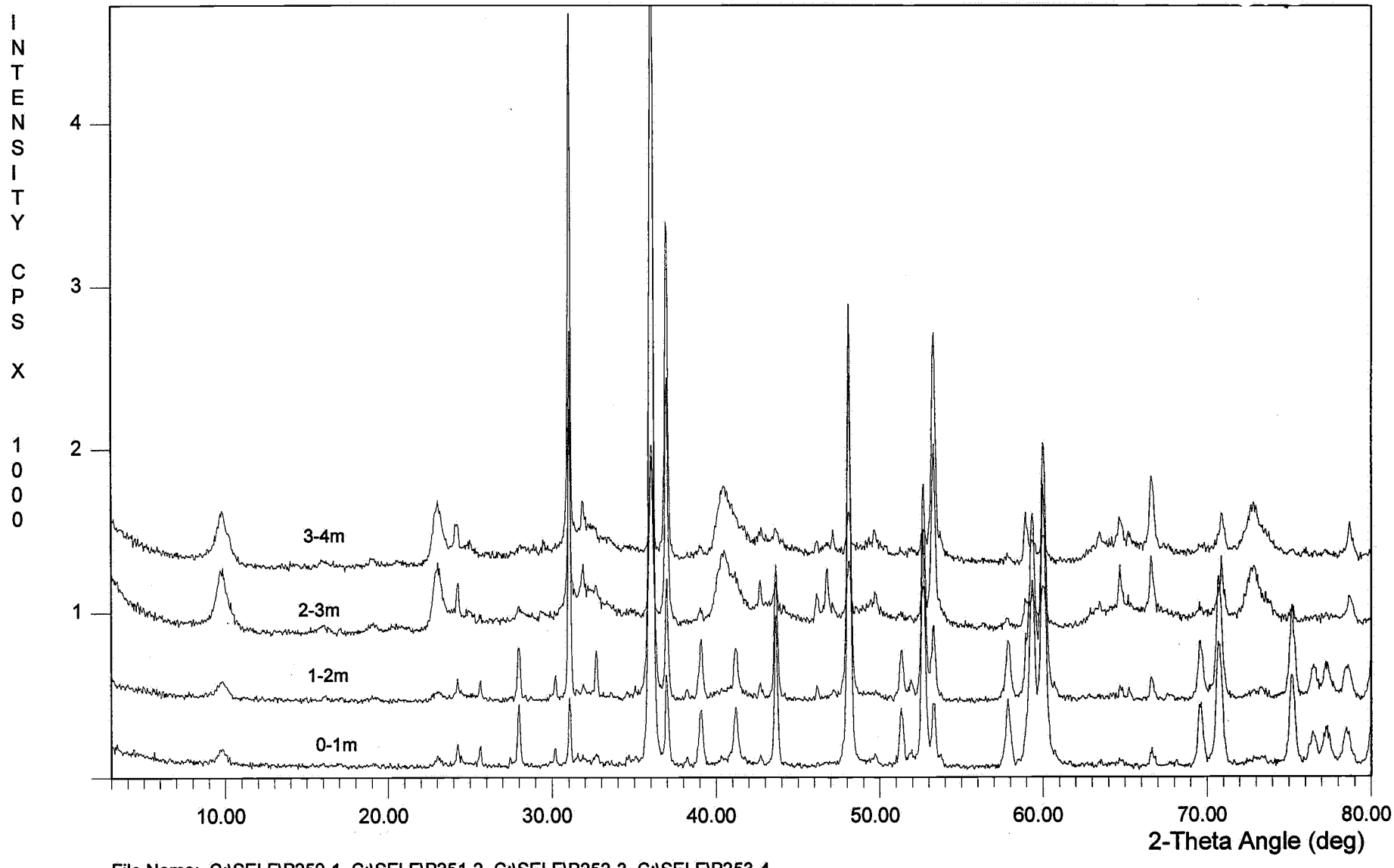
Fig. 2. Garford palaeochannel bulk samples P24. Co Ka radiation. Non-oriented.



File Name: A:\P24-0-1.107 A:\P24-1-2.109 A:\P24-1-3.108

000278
32

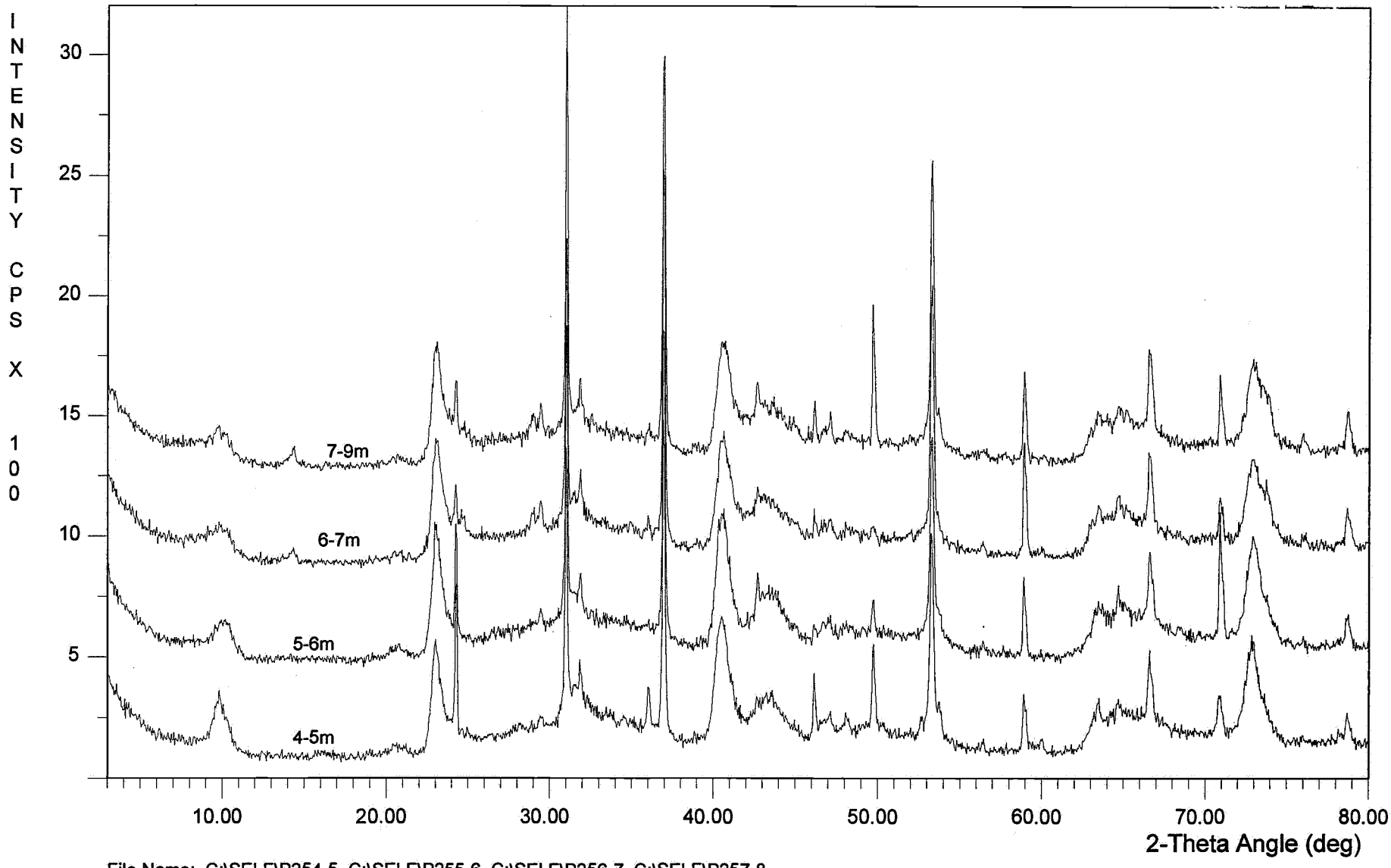
Fig. 3a. Garford palaeochannel bulk samples P25 (upper). Co Ka radiation. Non-oriented.



File Name: C:\SELF\P250-1 C:\SELF\P251-2 C:\SELF\P252-3 C:\SELF\P253-4

0002179

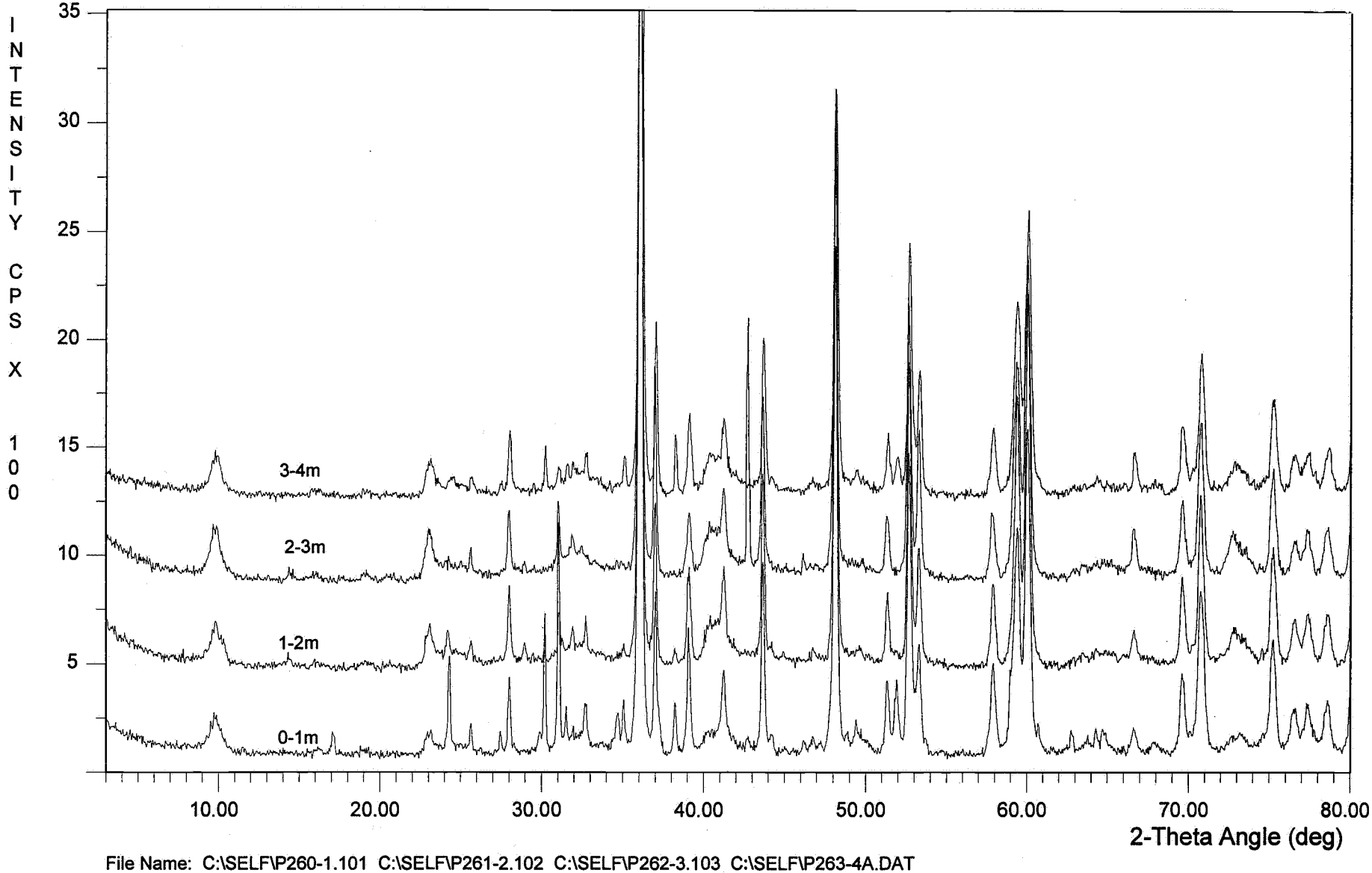
Fig. 3b. Garford palaeochannel bulk samples P25 (lower). Co Ka radiation. Non-oriented.



File Name: C:\SELF\P254-5 C:\SELF\P255-6 C:\SELF\P256-7 C:\SELF\P257-8

0002280

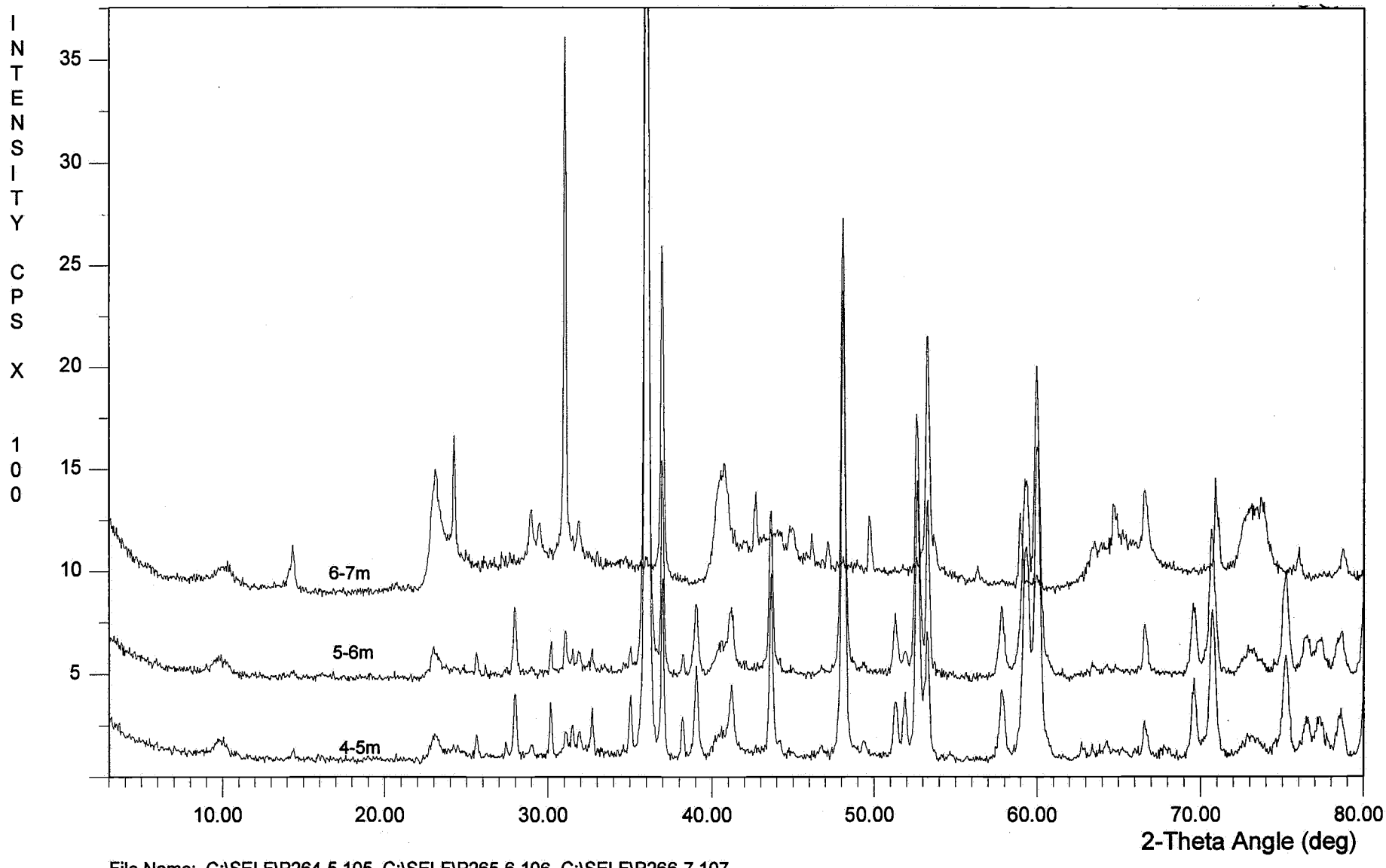
Fig. 4a. Garford palaeochannel bulk samples P26 (upper). Co Ka radiation. Non-oriented.



File Name: C:\SELF\P260-1.101 C:\SELF\P261-2.102 C:\SELF\P262-3.103 C:\SELF\P263-4A.DAT

000281
35

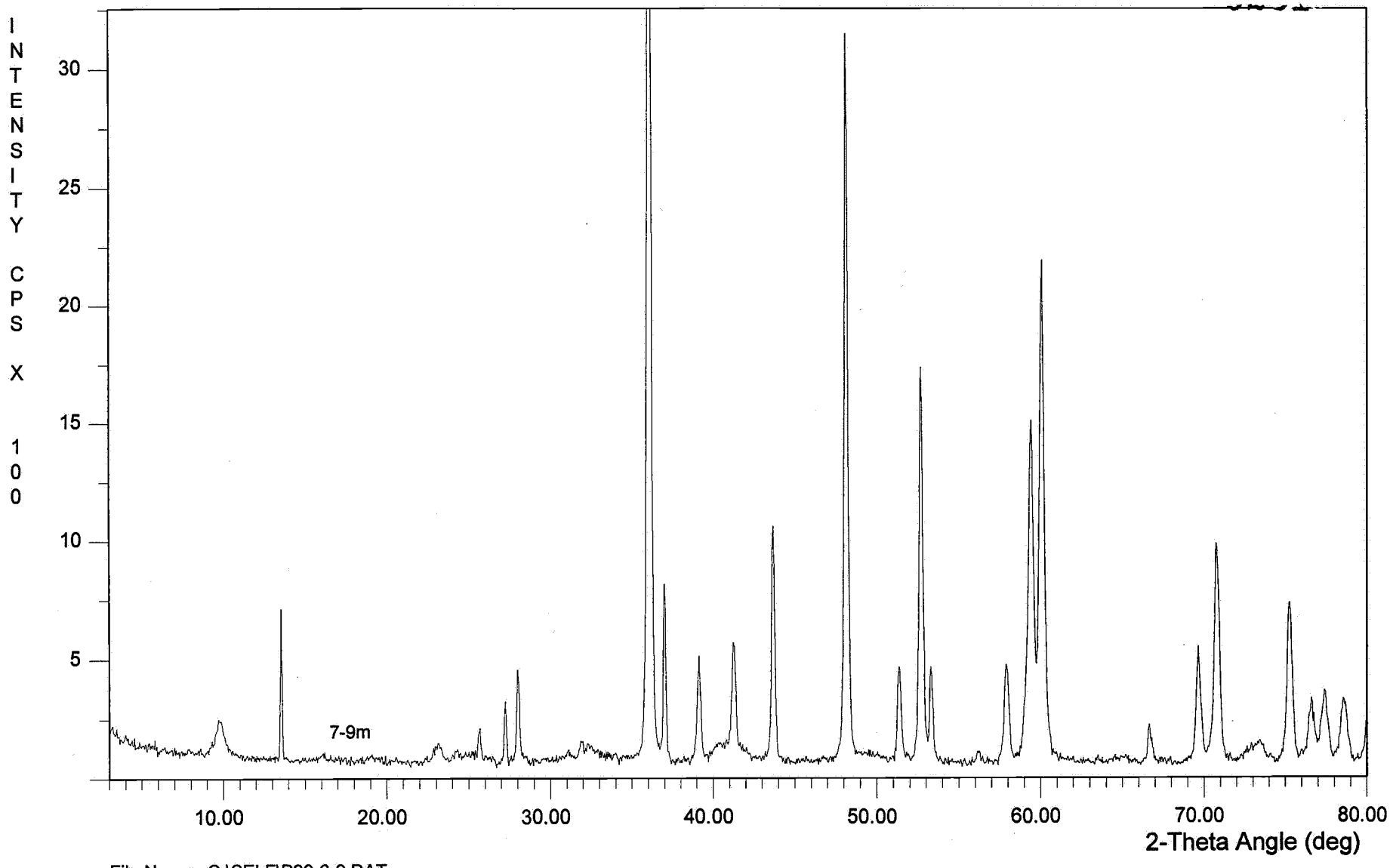
Fig. 4b. Garford palaeochannel bulk samples P26 (lower). Co Ka radiation. Non-oriented.



File Name: C:\SELF\P264-5.105 C:\SELF\P265-6.106 C:\SELF\P266-7.107

000282
36

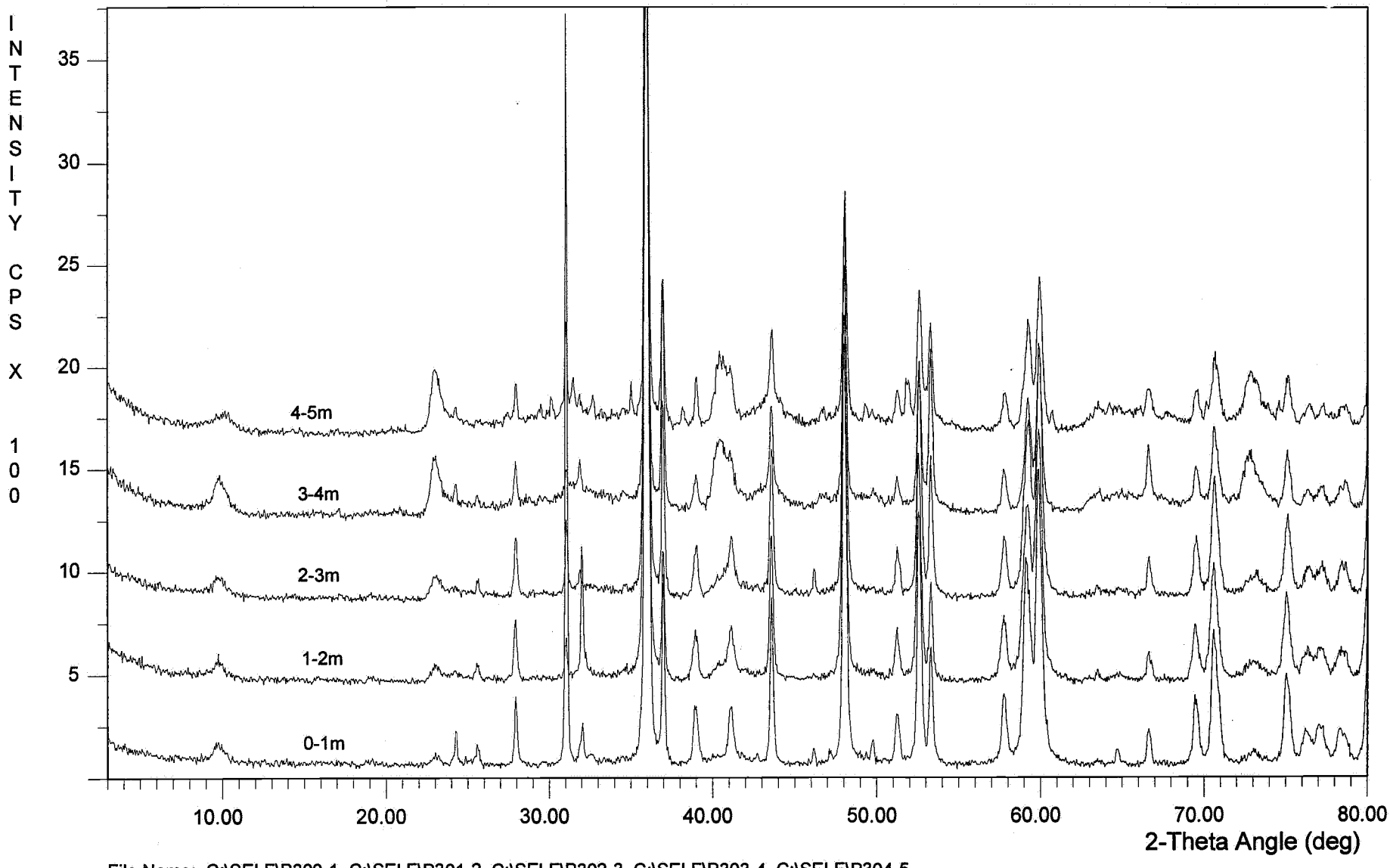
Fig. 5. Garford palaeochannel bulk sample P29. Co Ka radiation. Non-oriented.



File Name: C:\SELF\P29-6-9.DAT

000283
37

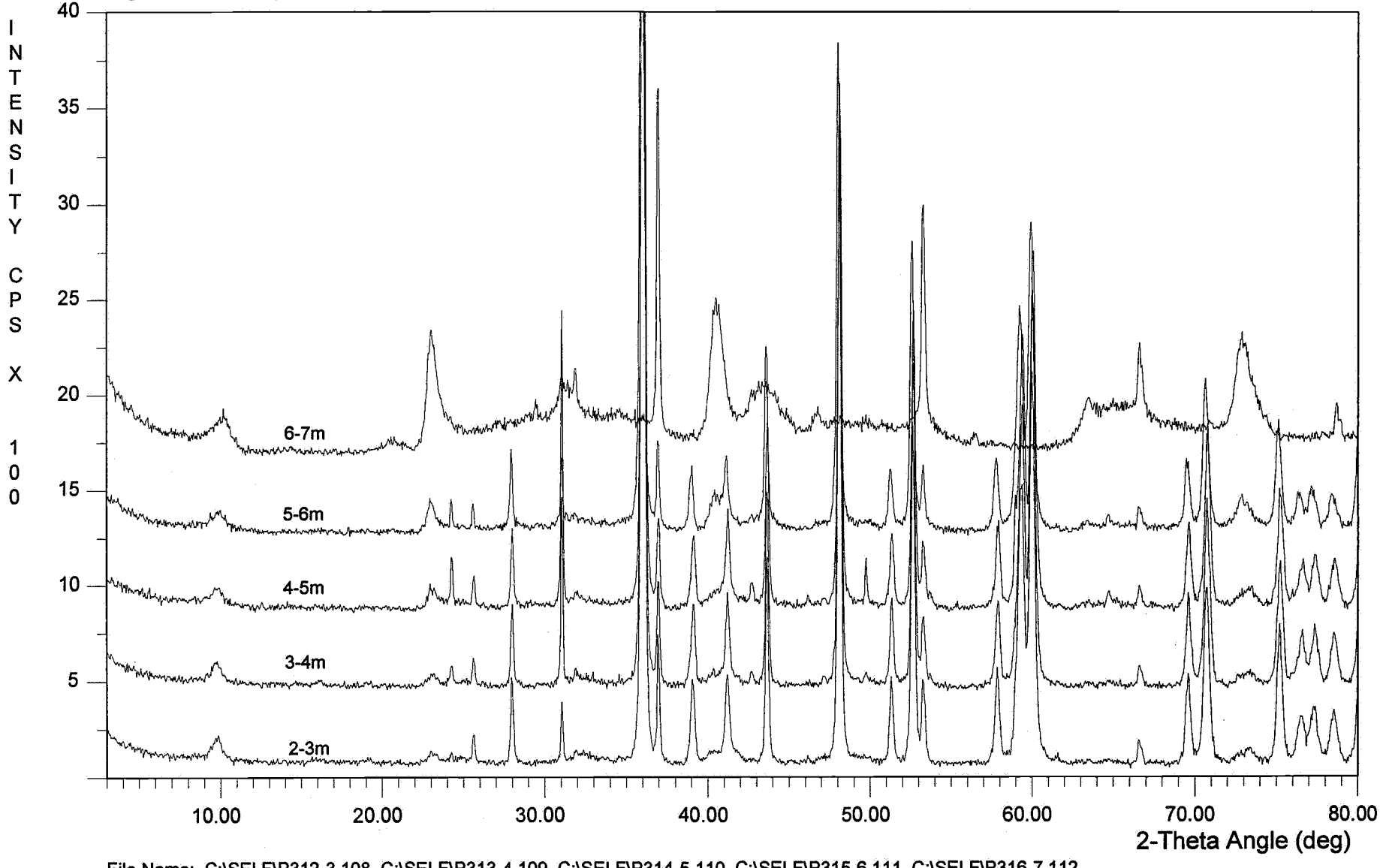
Fig. 6. Garford palaeochannel bulk samples P30. Co Ka radiation. Non-oriented.



File Name: C:\SELF\P300-1 C:\SELF\P301-2 C:\SELF\P302-3 C:\SELF\P303-4 C:\SELF\P304-5

000284
38

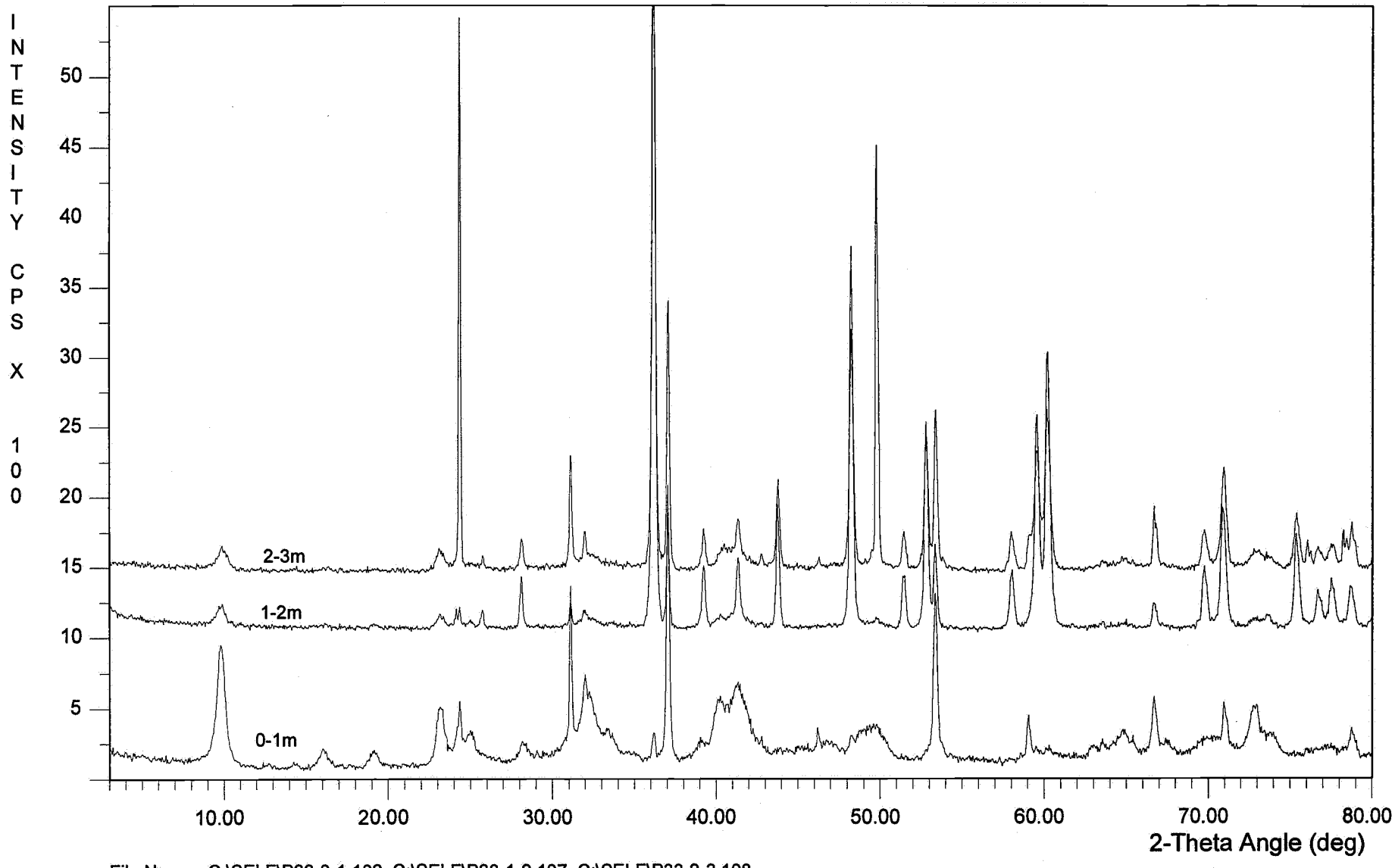
Fig. 7. Garford palaeochannel bulk samples P31. Co Ka radiation. Non-oriented.



File Name: C:\SELF\P312-3.108 C:\SELF\P313-4.109 C:\SELF\P314-5.110 C:\SELF\P315-6.111 C:\SELF\P316-7.112

000285
39

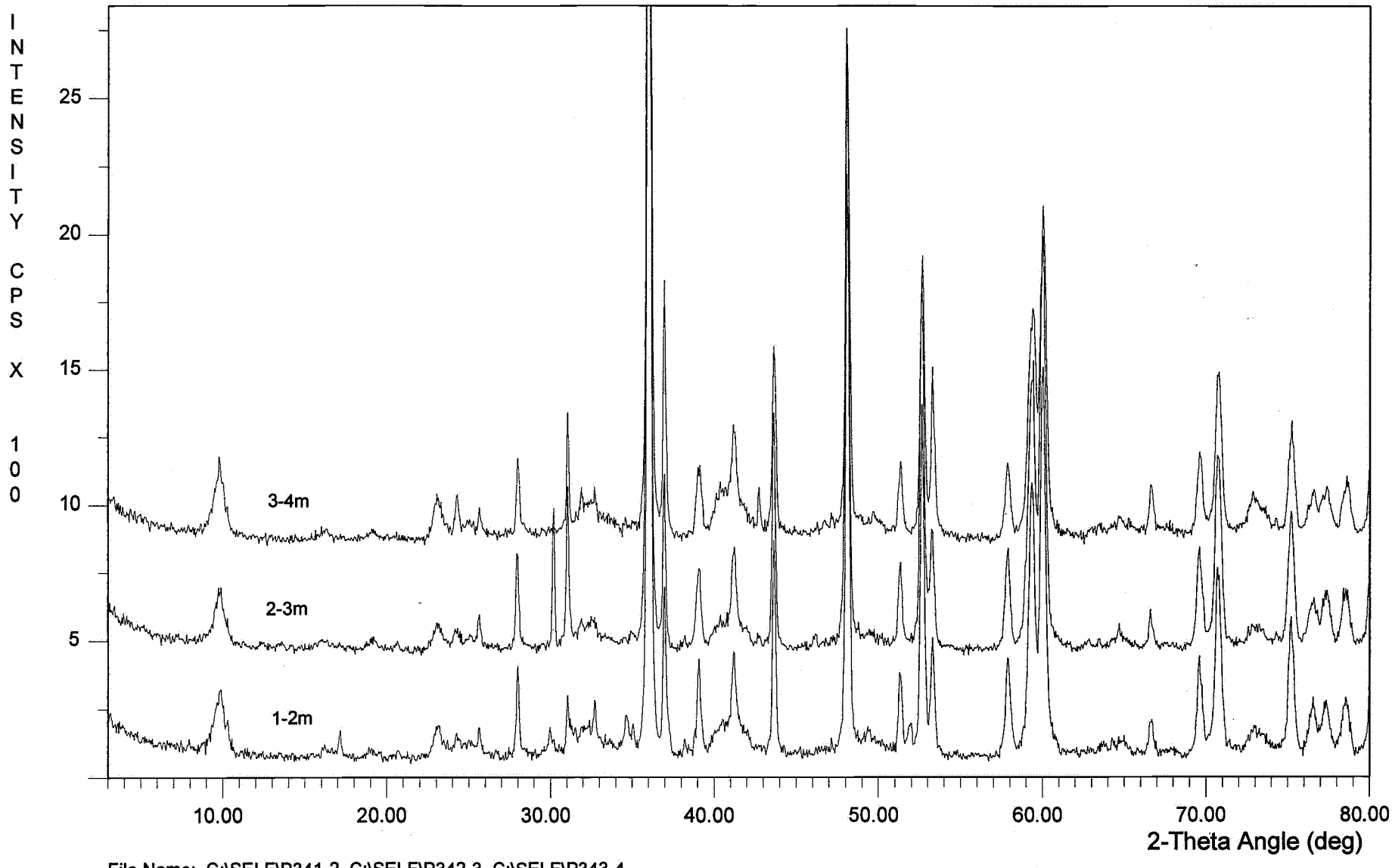
Fig. 8. Garford palaeochannel bulk samples P33. Co Ka radiation. Non-oriented.



File Name: C:\SELF\P33-0-1.106 C:\SELF\P33-1-2.107 C:\SELF\P33-2-3.108

000286
40

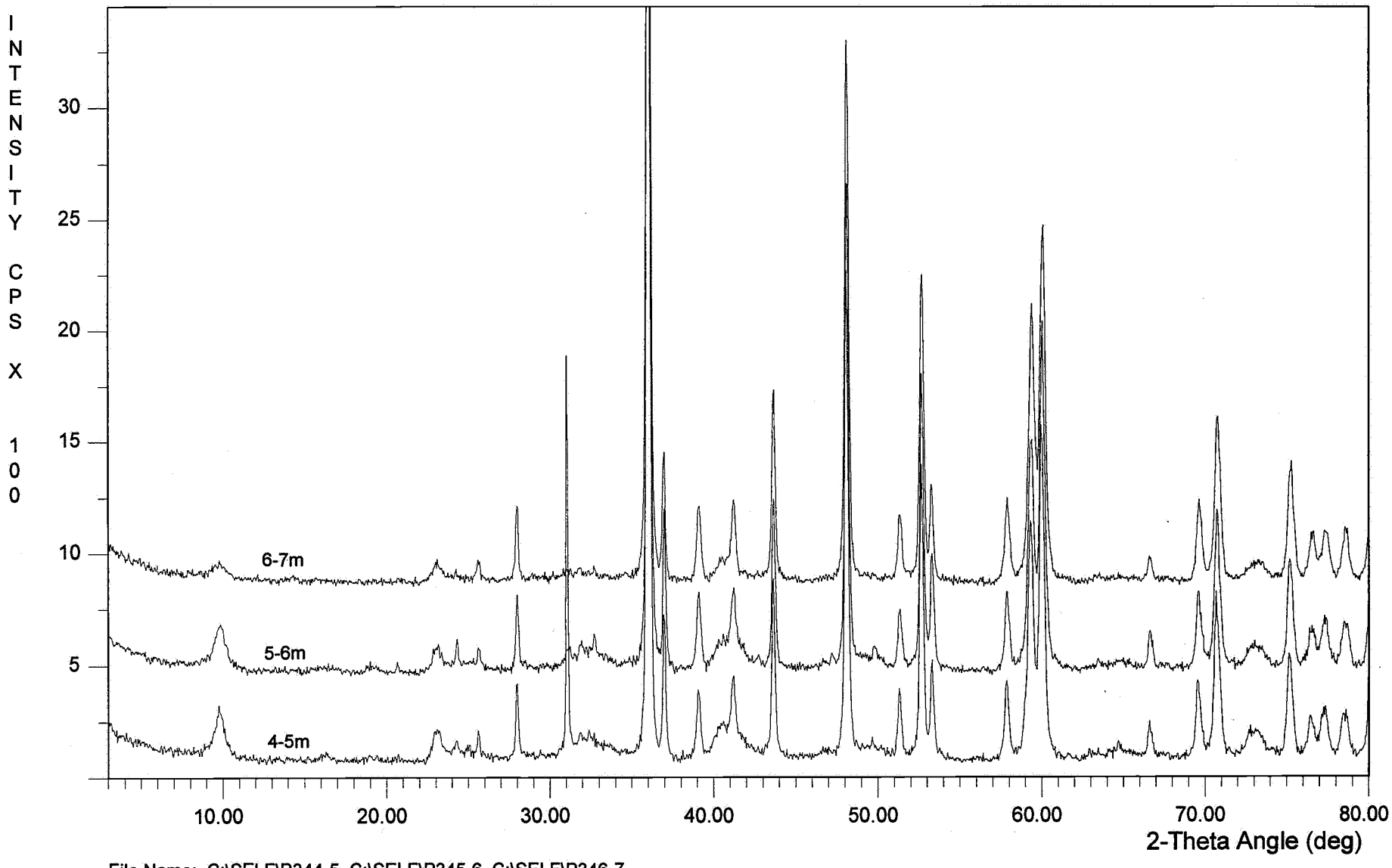
Fig. 9a. Garford palaeochannel bulk samples P34 (upper). Co Ka radiation. Non-oriented.



File Name: C:\SELF\P341-2 C:\SELF\P342-3 C:\SELF\P343-4

000287

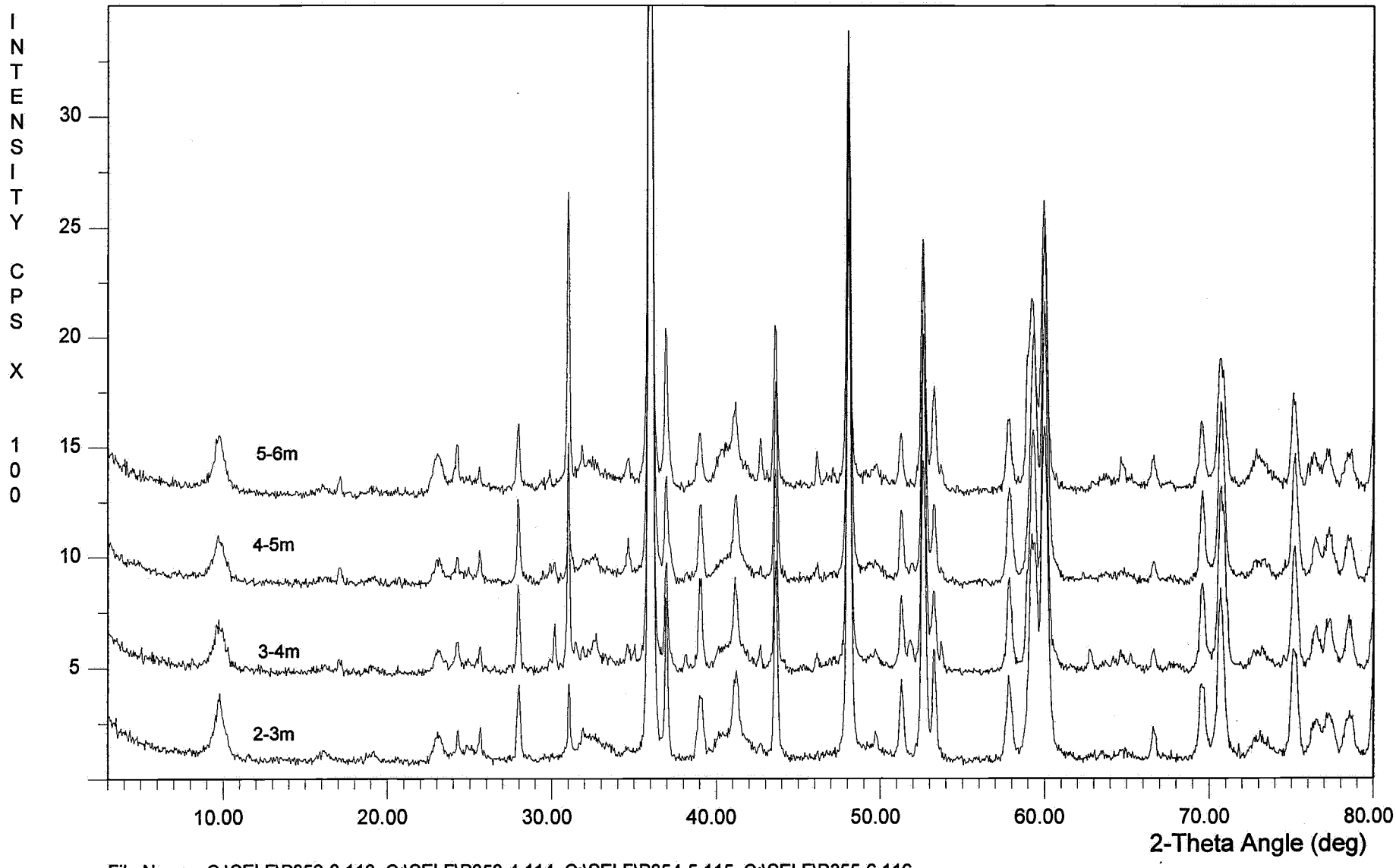
Fig. 9b. Garford palaeochannel bulk samples P34 (lower). Co Ka radiation. Non-oriented.



File Name: C:\SELF\P344-5 C:\SELF\P345-6 C:\SELF\P346-7

000288
42

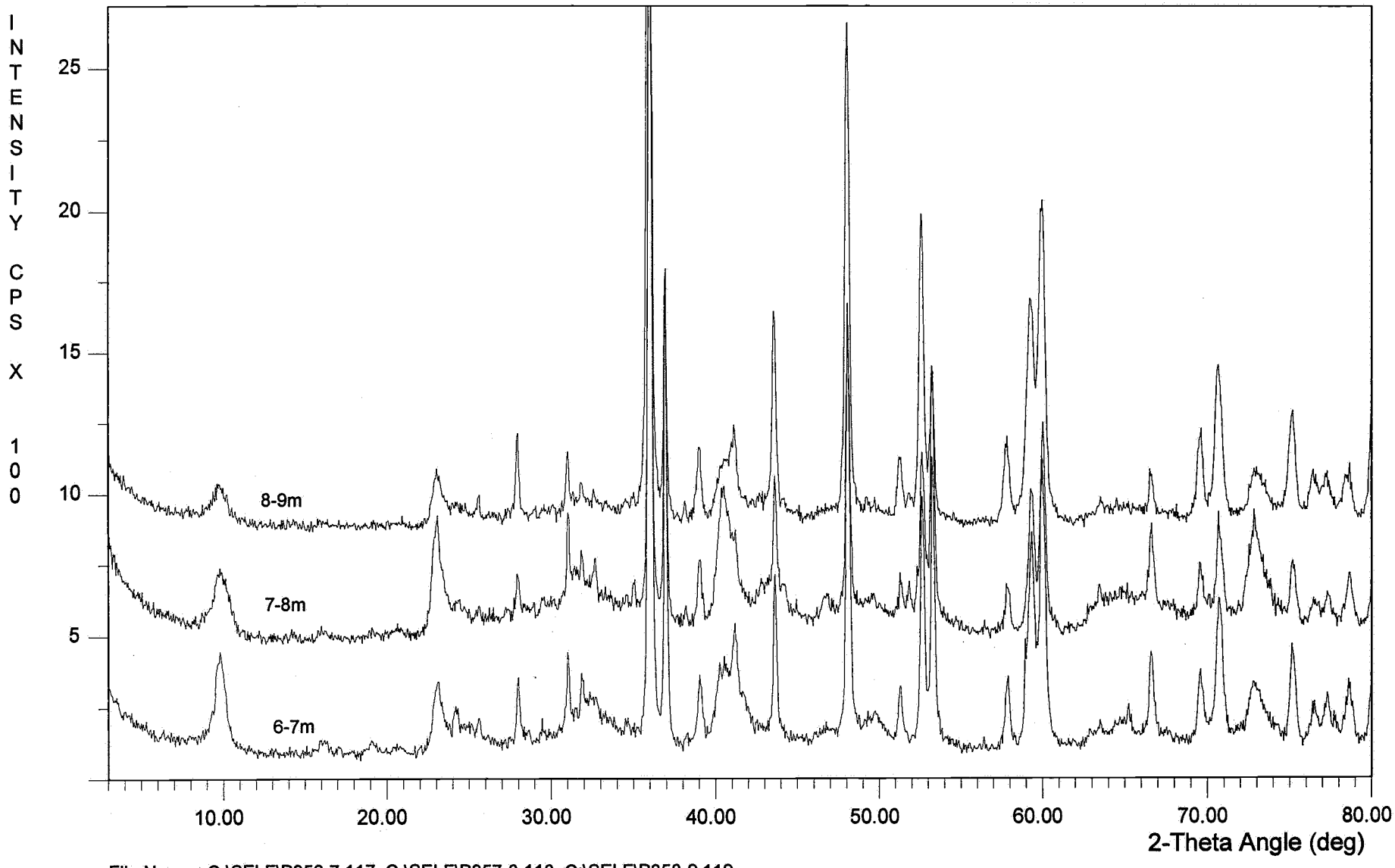
Fig. 10a. Garford palaeochannel bulk samples P35 (upper). Co Ka radiation. Non-oriented.



File Name: C:\SELF\P352-3.113 C:\SELF\P353-4.114 C:\SELF\P354-5.115 C:\SELF\P355-6.116

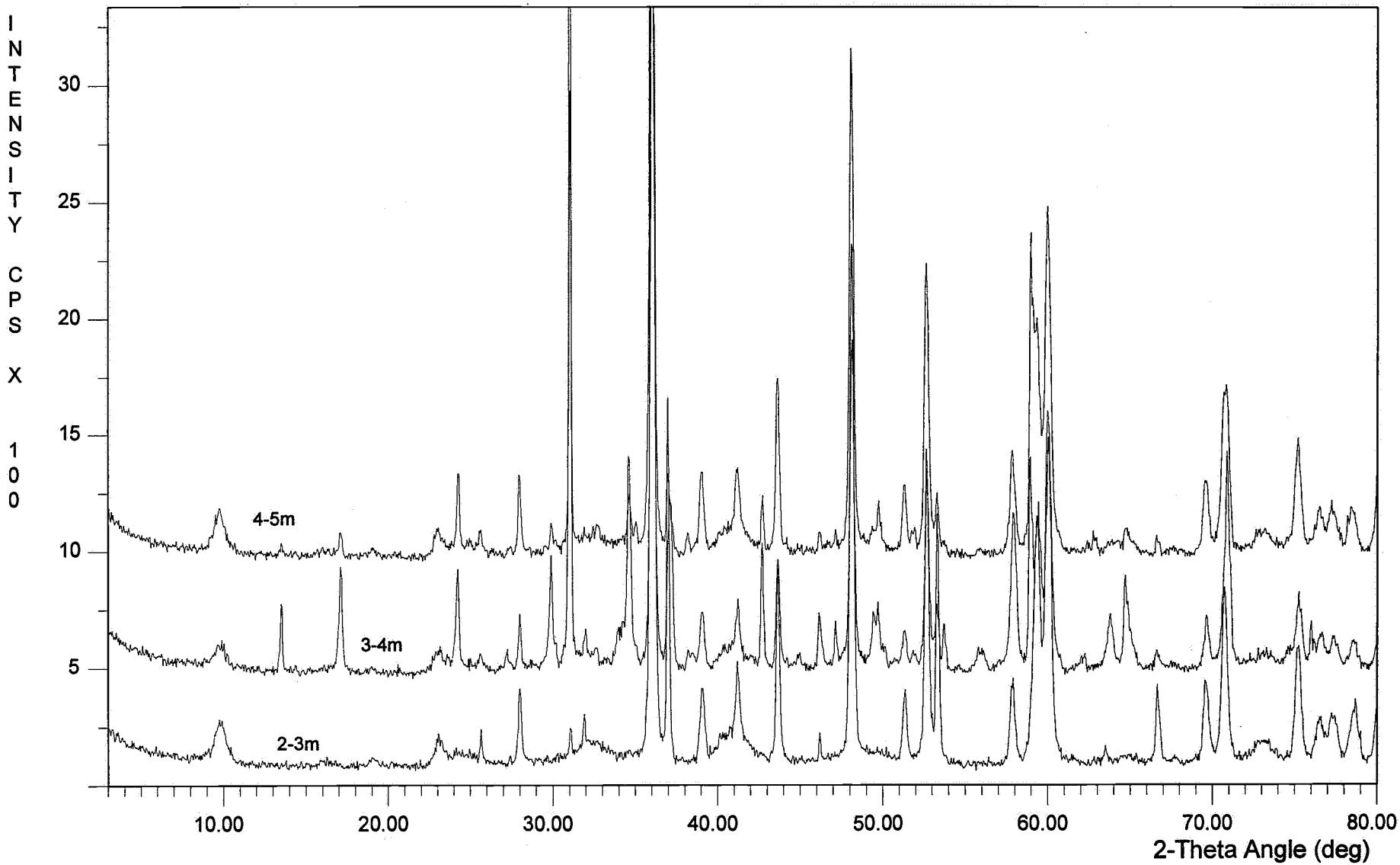
000289
43

Fig. 10b. Garford palaeochannel bulk samples P35 (lower). Co Ka radiation. Non-oriented.



File Name: C:\SELF\P356-7.117 C:\SELF\P357-8.118 C:\SELF\P358-9.119

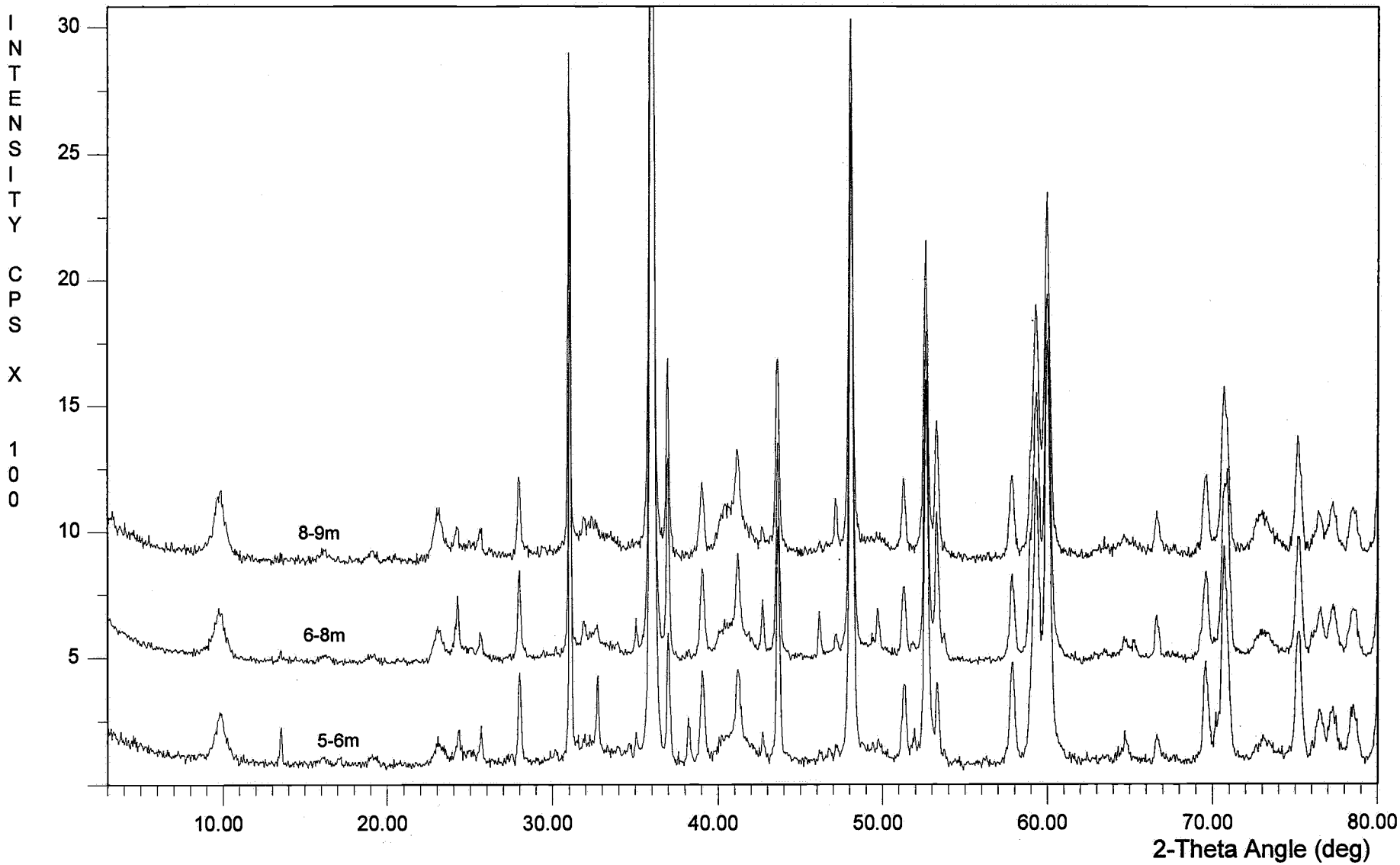
Fig. 11a. Garford palaeochannel bulk samples P36 (upper). Co Ka radiation. Non-oriented.



File Name: C:\SELF\P362-3.101 C:\SELF\P363-4.102 C:\SELF\P364-5.103

0002914

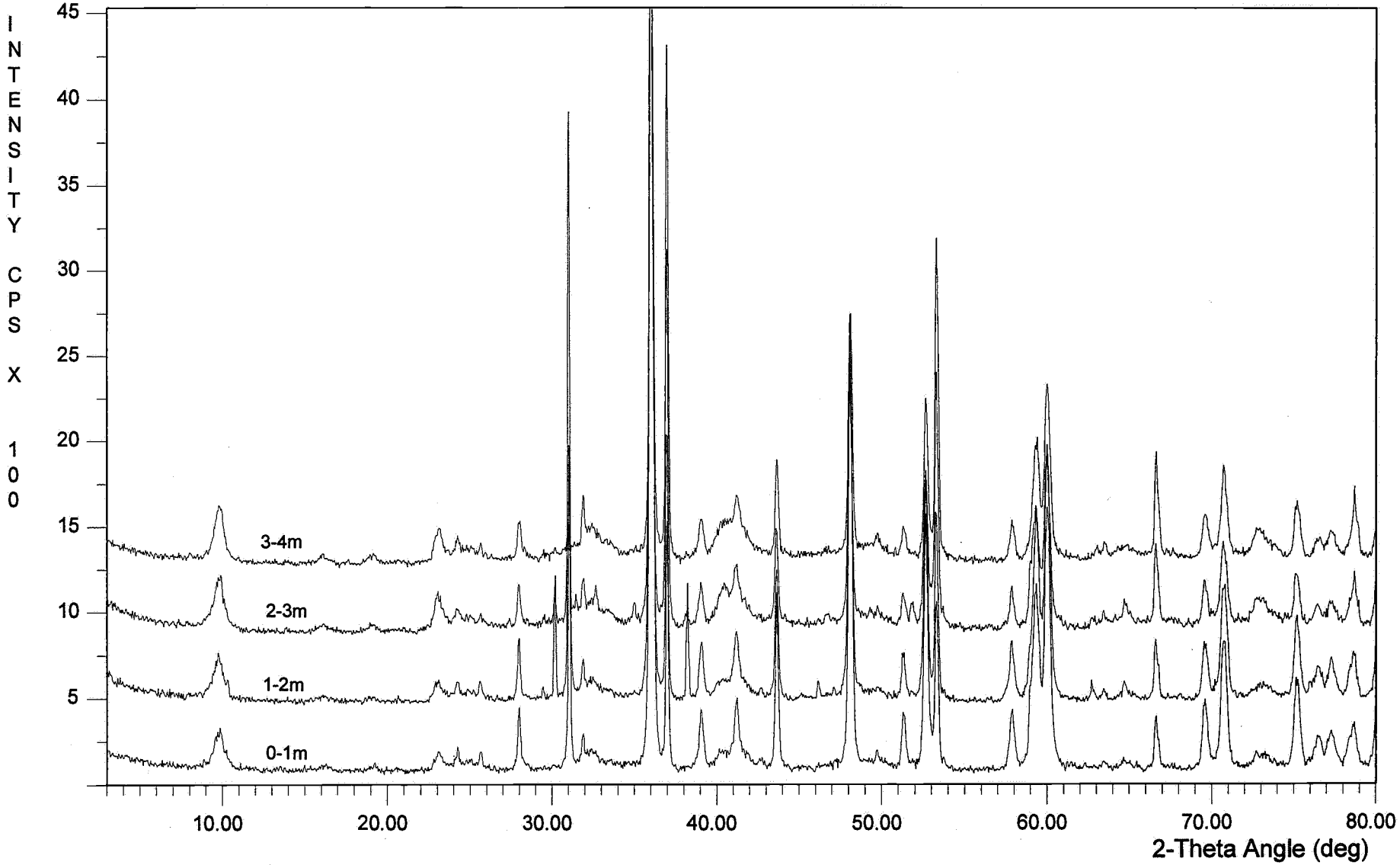
Fig. 11b. Garford palaeochannel bulk samples P36 (lower). Co Ka radiation. Non-oriented.



File Name: C:\SELF\P365-6.104 C:\SELF\P366-8.DAT C:\SELF\P368-9.107

000292

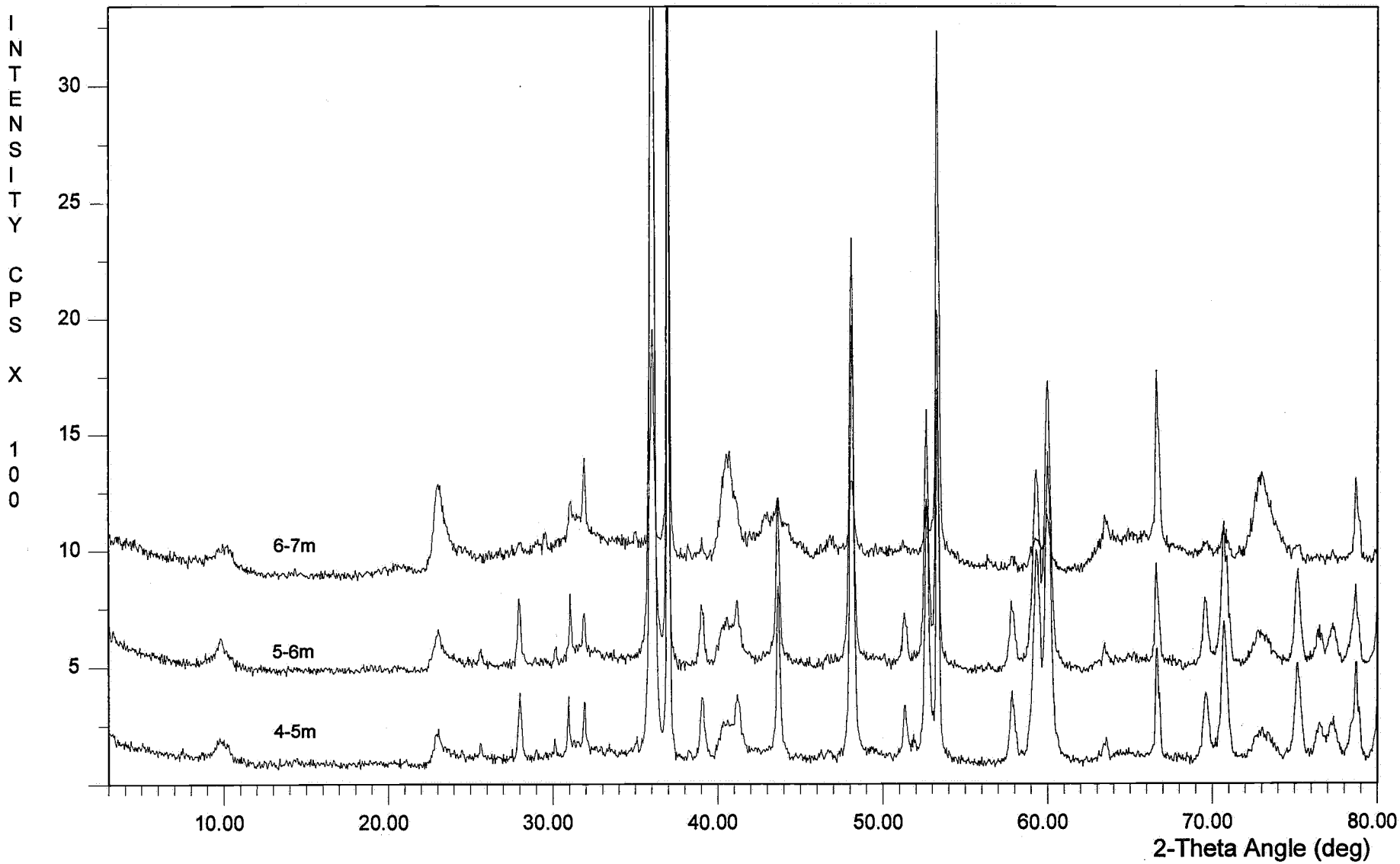
Fig. 12a. Garford palaeochannel bulk samples P37 (upper). Co Ka radiation. Non-oriented.



File Name: C:\SELF\P370-1.108 C:\SELF\P371-2.109 C:\SELF\P372-3.110 C:\SELF\P373-4.111

0002934
47

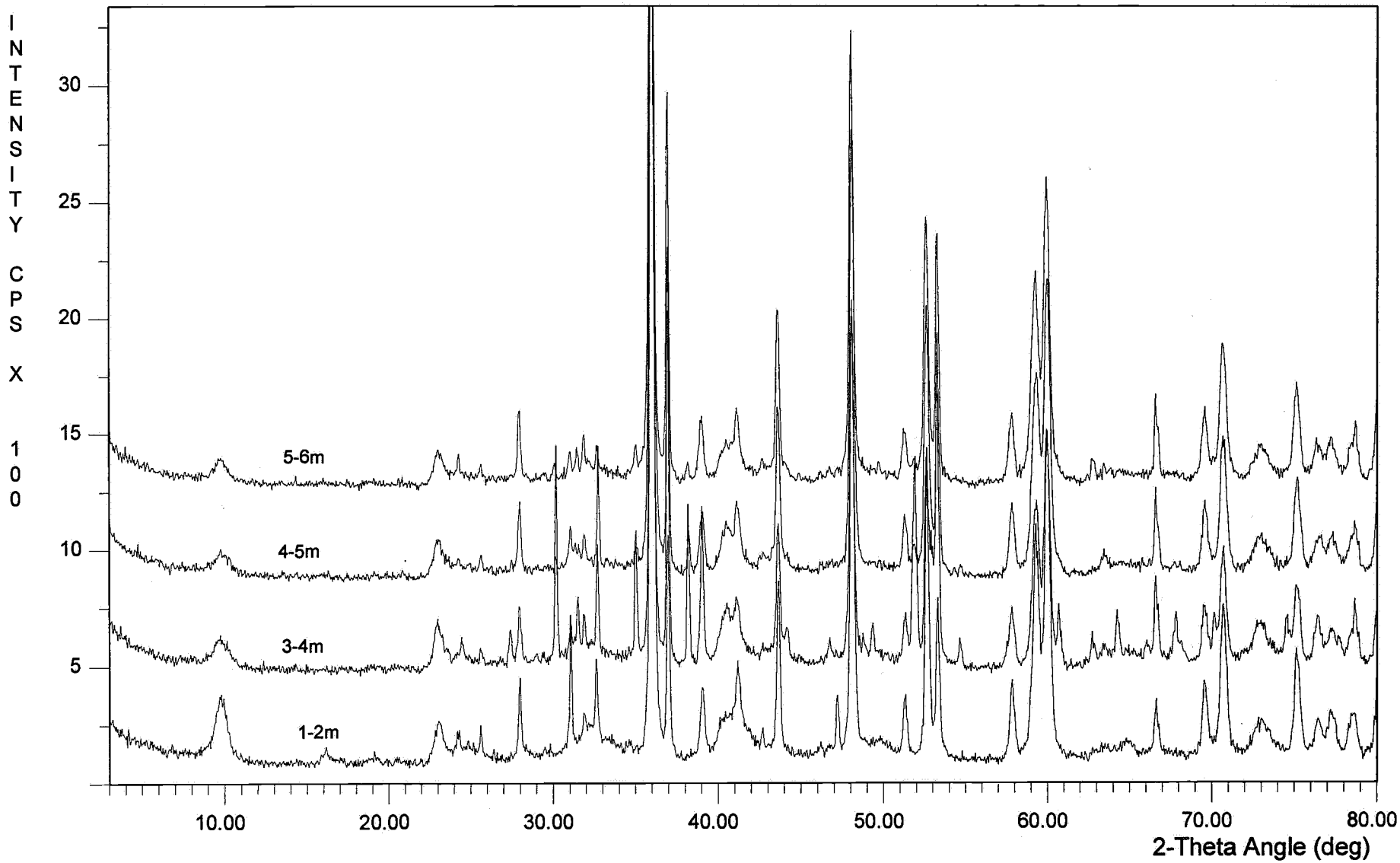
Fig. 12b. Garford palaeochannel bulk samples P37 (lower). Co Ka radiation. Non-oriented.



File Name: C:\SELF\P374-5.112 C:\SELF\P375-6.113 C:\SELF\P376-7.114

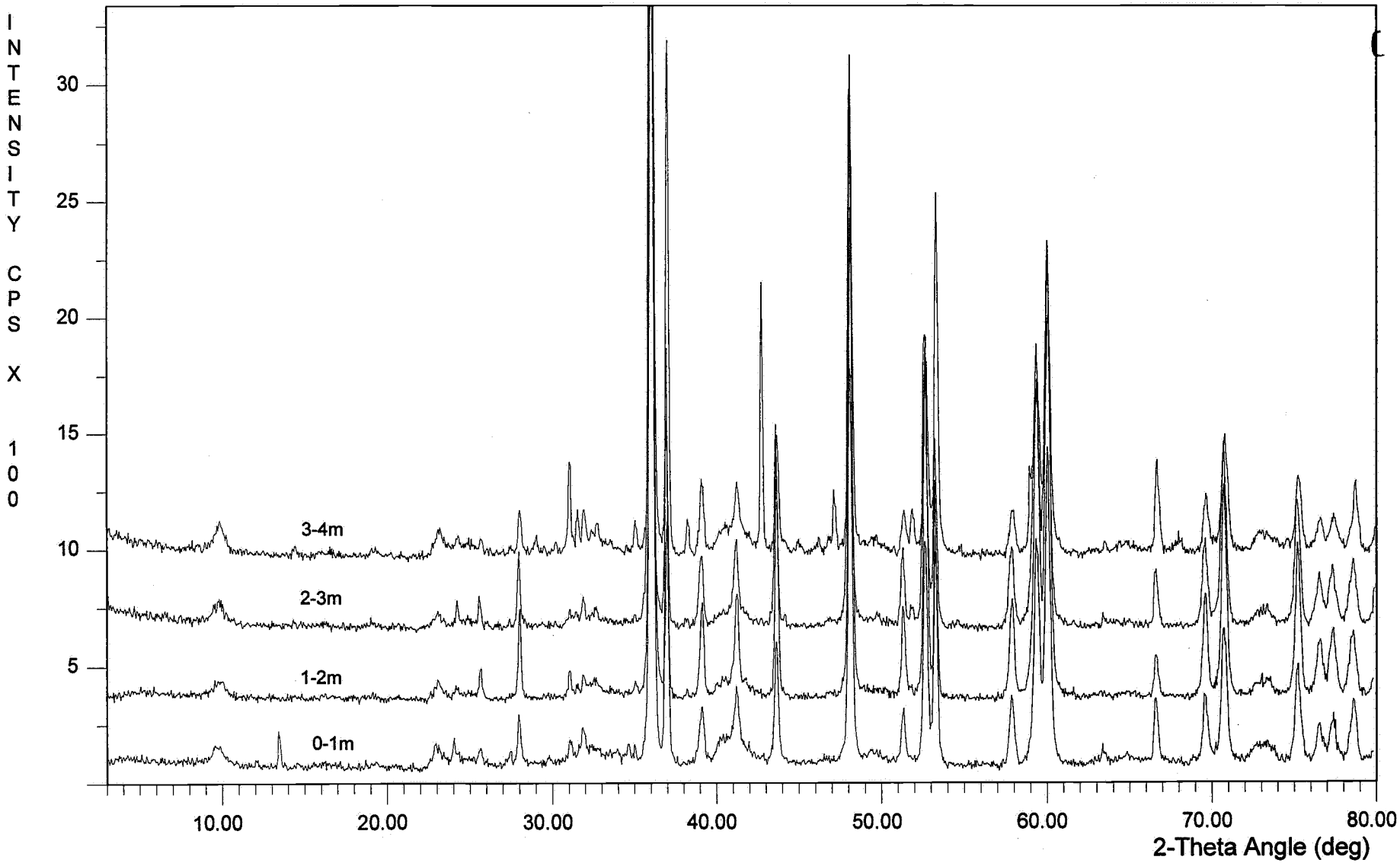
000294

Fig. 13. Garford palaeochannel bulk samples P38. Co Ka radiation. Non-oriented.



File Name: C:\SELF\P381-2.115 C:\SELF\P383-4.116 C:\SELF\P384-5.117 C:\SELF\P385-6.118

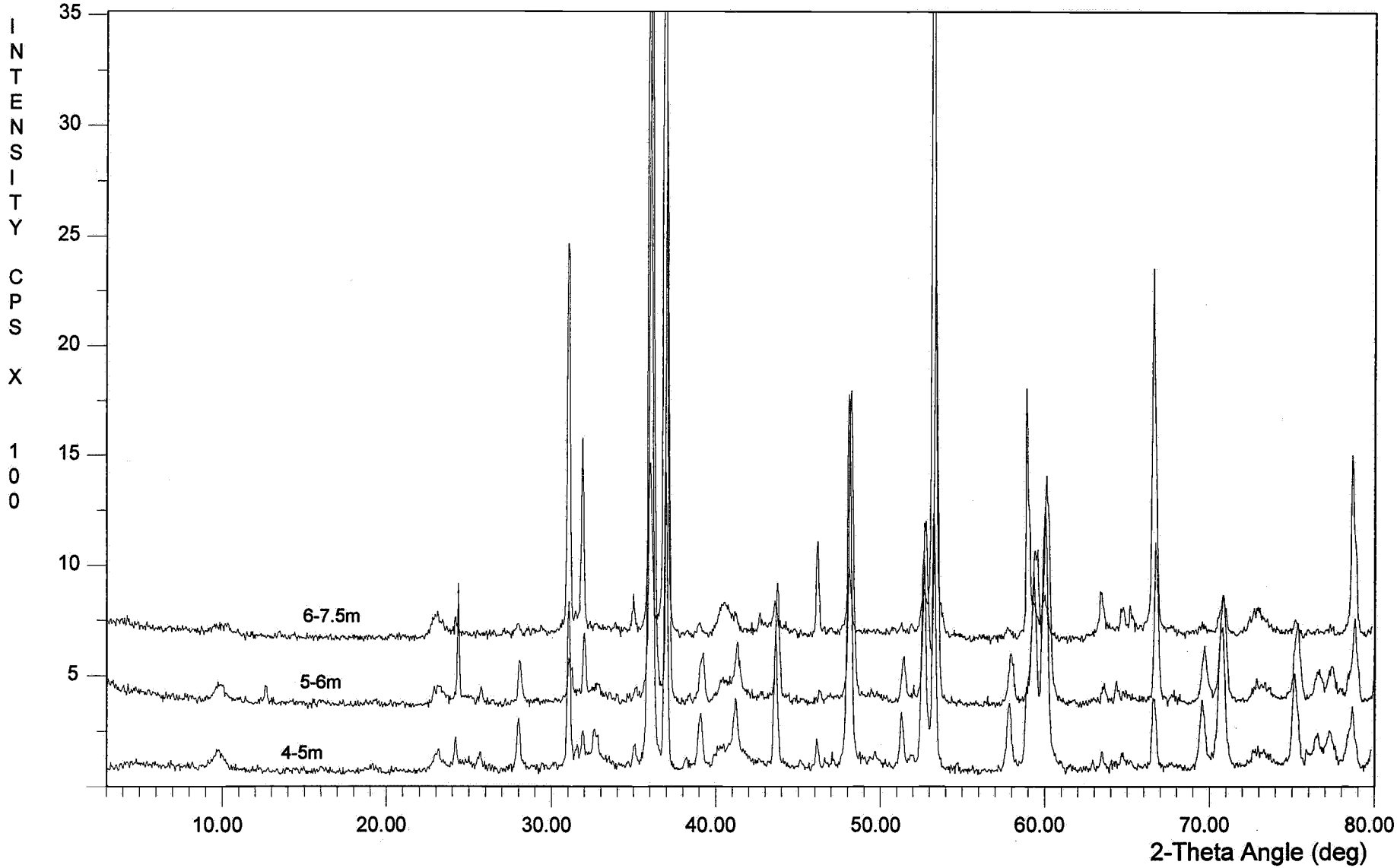
Fig. 14a. Garford palaeochannel bulk samples P40 (upper). Co Ka radiation. Non-oriented.



File Name: C:\SELF\P40-0-1.201 C:\SELF\P40-1-2.202 C:\SELF\P40-2-3.203 C:\SELF\P40-3-4.204

000296
50

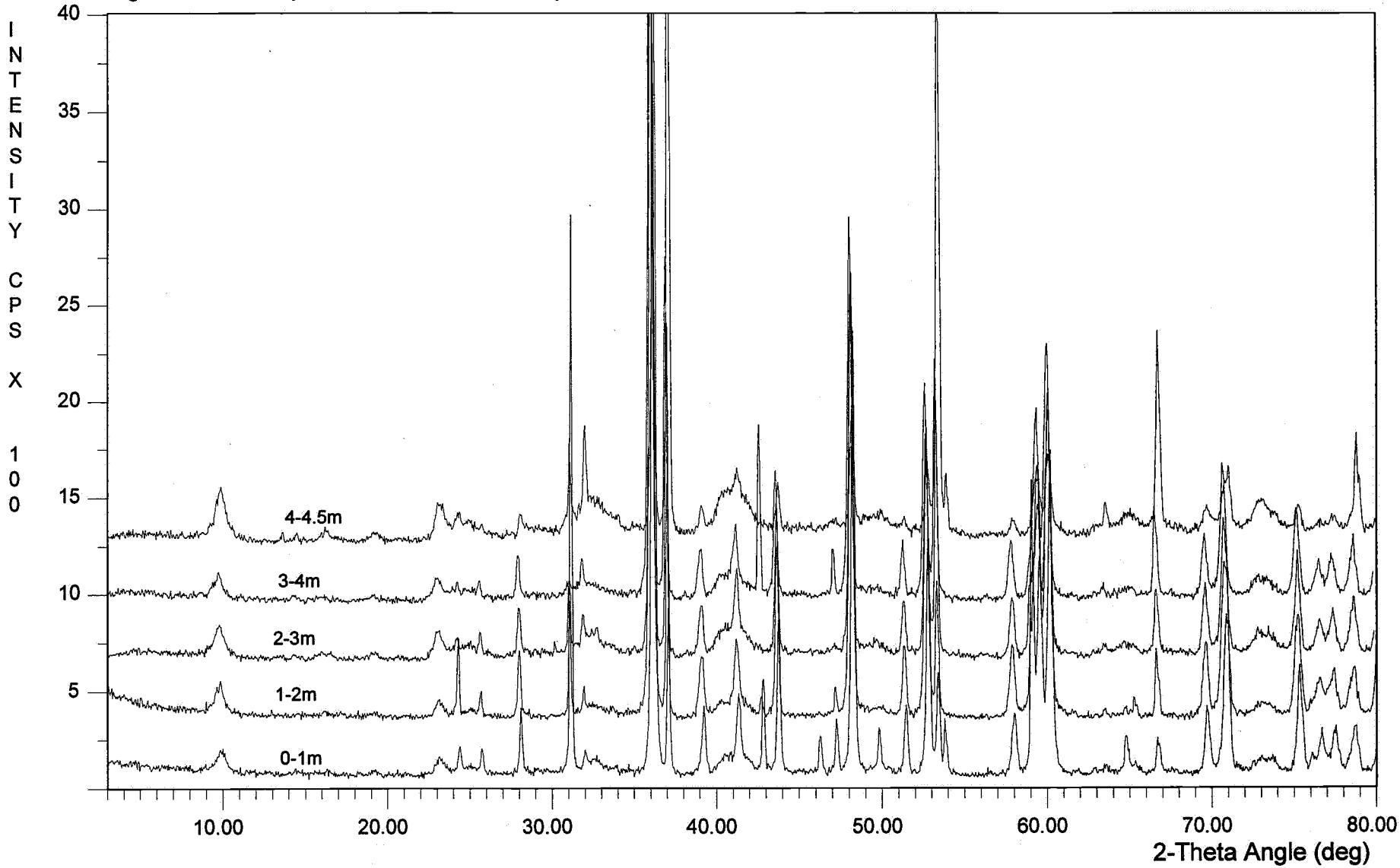
Fig. 14b. Garford palaeochannel bulk samples P40 (lower). Co Ka radiation. Non-oriented.



File Name: C:\SELF\P40-4-5.205 C:\SELF\P40-5-6.206 C:\SELF\P40-6-7~.207

0002997

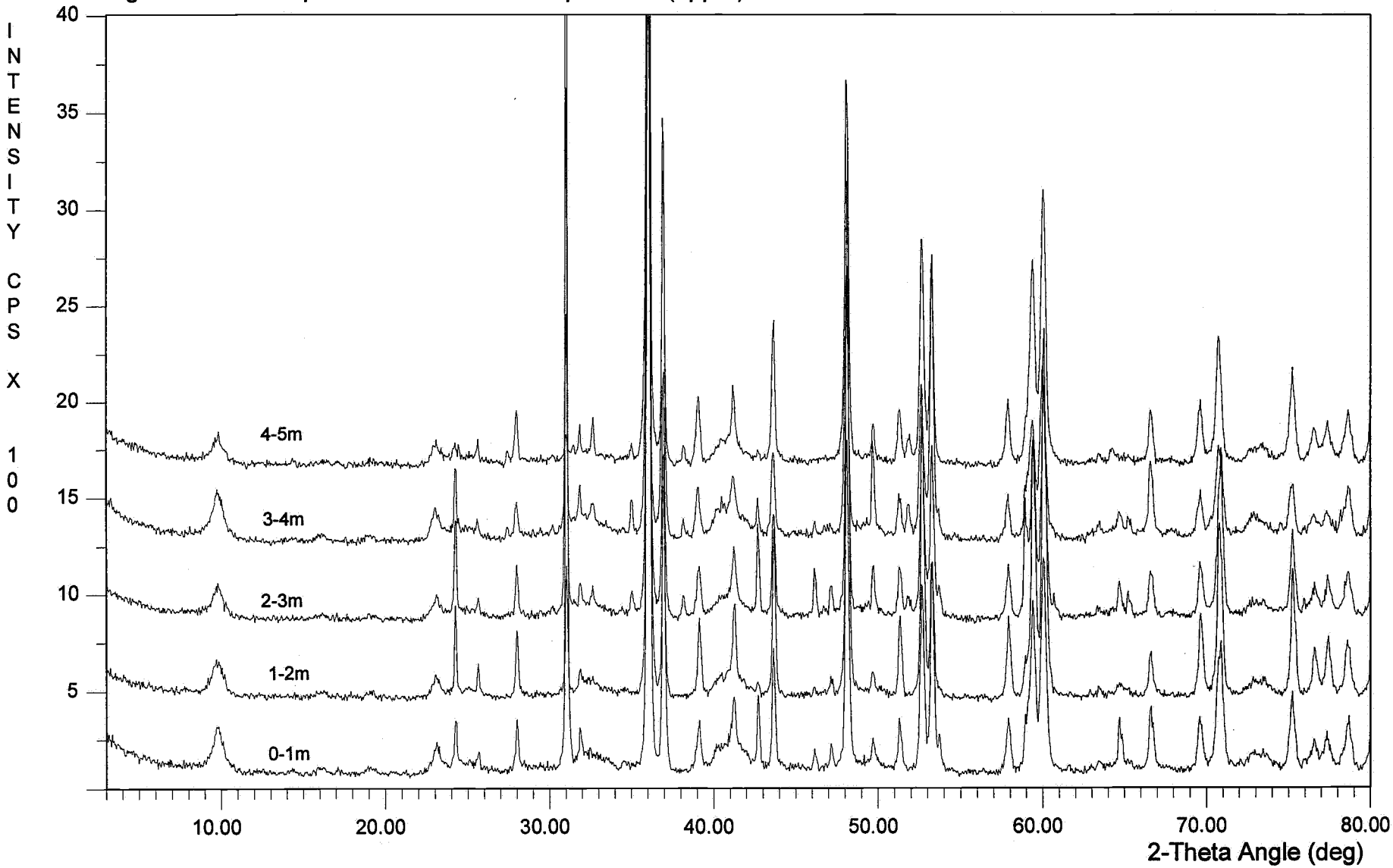
Fig. 15. Garford palaeochannel bulk samples P41. Co Ka radiation. Non-oriented.



File Name: C:\SELF\P41-0-1.301 C:\SELF\P41-1-2.302 C:\SELF\P41-2-3.303 C:\SELF\P41-3-4.304 C:\SELF\P41-4-4~.305

000298

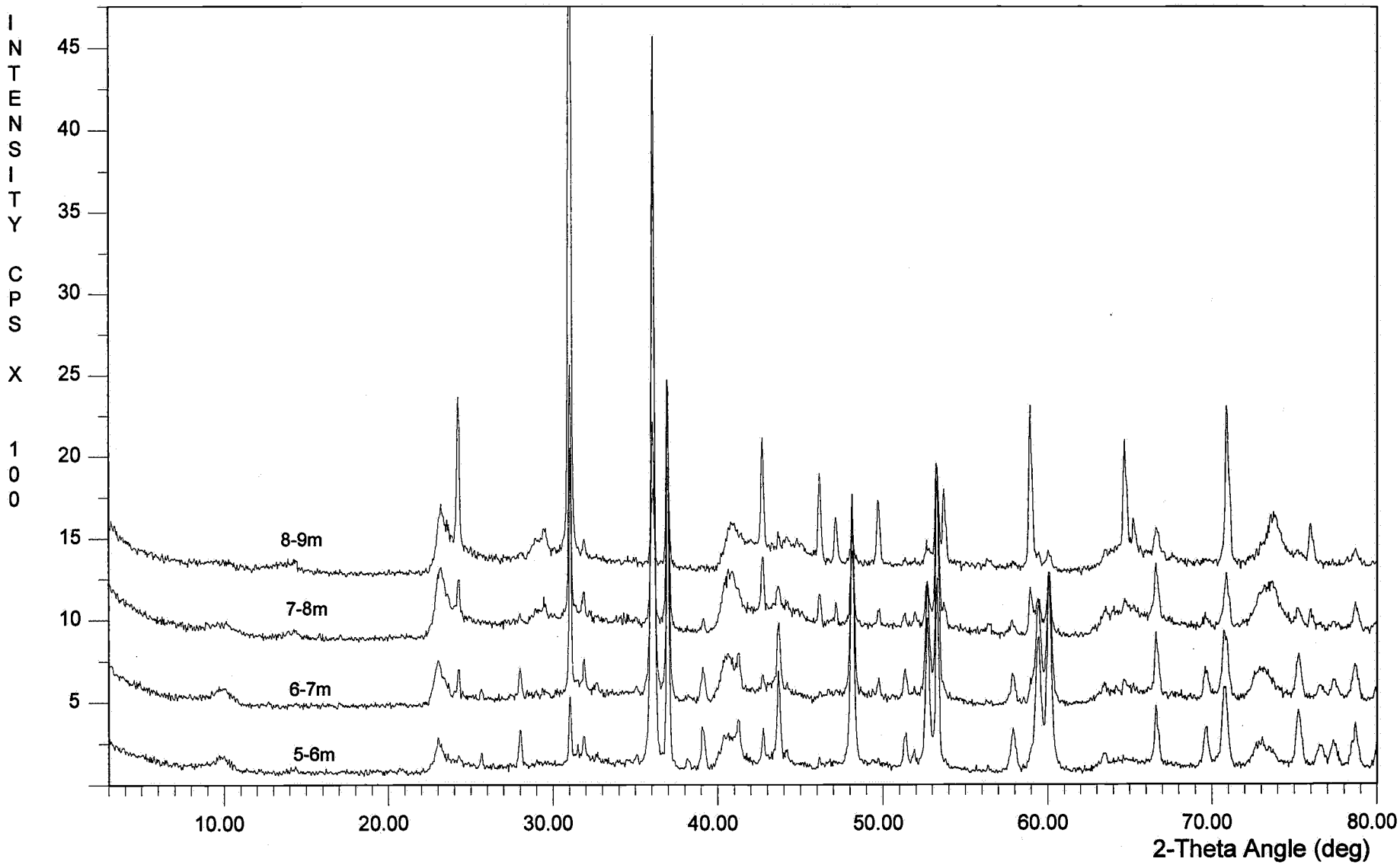
Fig. 16a. Garford palaeochannel bulk samples P42 (upper). Co Ka radiation. Non-oriented.



File Name: C:\SELF\P420-1 C:\SELF\P421-2 C:\SELF\P422-3 C:\SELF\P423-4 C:\SELF\P424-5

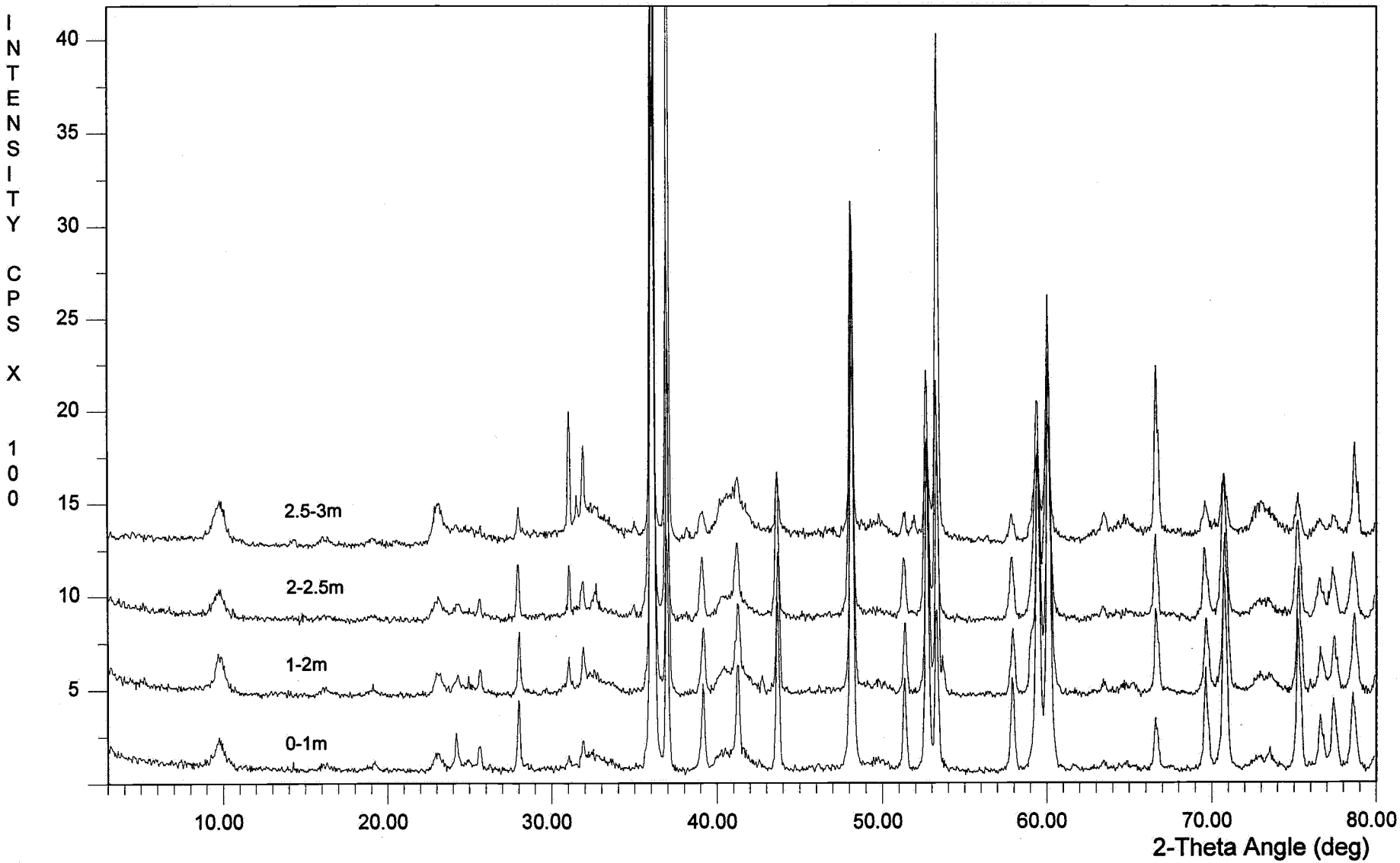
000299
53

Fig. 16b. Garford palaeochannel bulk samples P42 (lower). Co Ka radiation. Non-oriented.



File Name: C:\SELF\P425-6 C:\SELF\P426-7 C:\SELF\P427-8 C:\SELF\P428-9

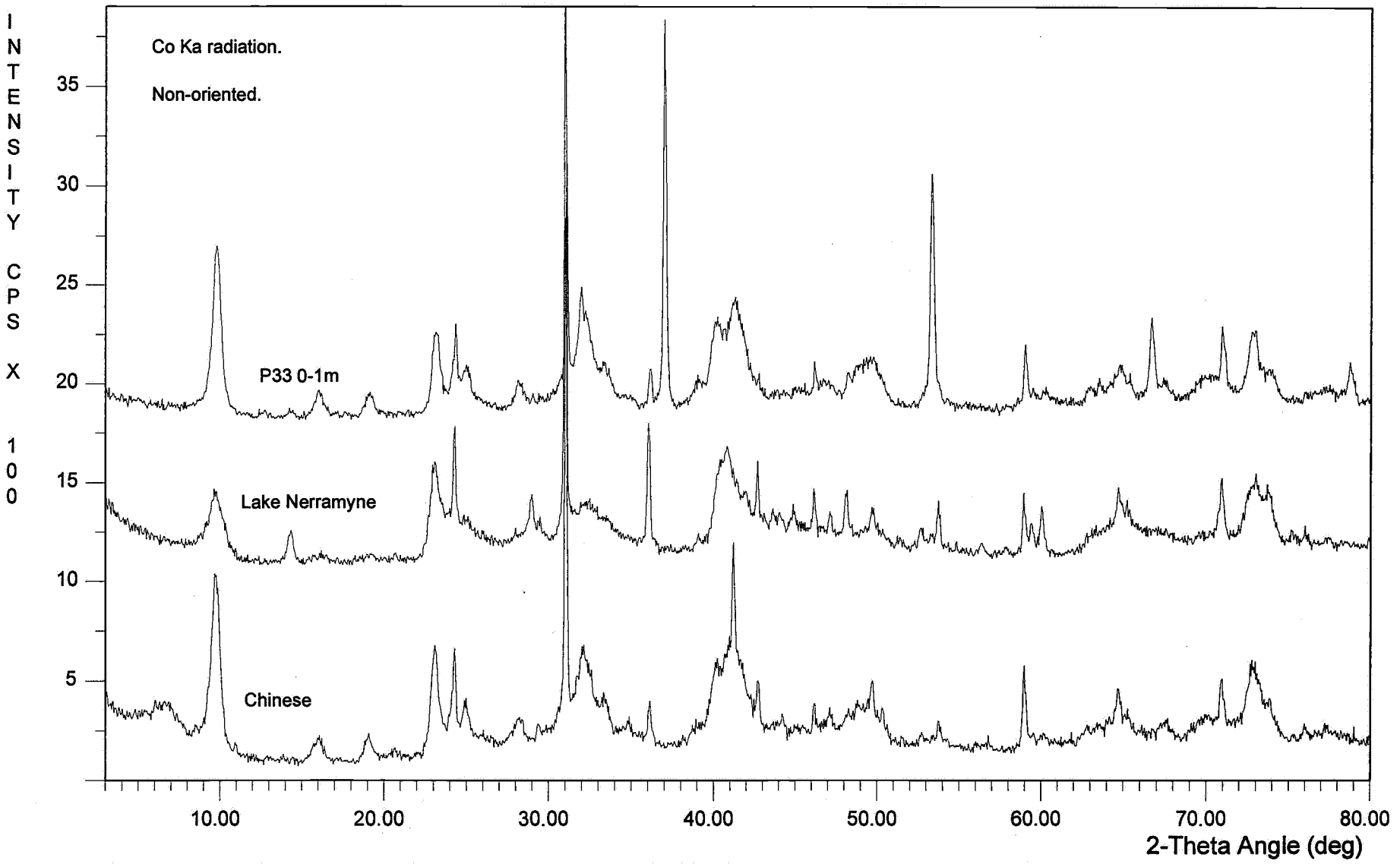
Fig. 17. Garford palaeochannel bulk samples P43. Co Ka radiation. Non-oriented.



File Name: C:\SELF\P43-0-1.101 C:\SELF\P43-1-2.102 C:\SELF\P43-2-2~.103 C:\SELF\P43-2~5-.104

000301
55

Fig. 18. Chinese attapulgite, Lake Nerramyne attapulgite and Garford palaeochannel sample P33 0-1m.



File Name: C:\SELF\CA-ASB.CAL C:\SELF\MALLINA.100 C:\SELF\P33-0-1.106

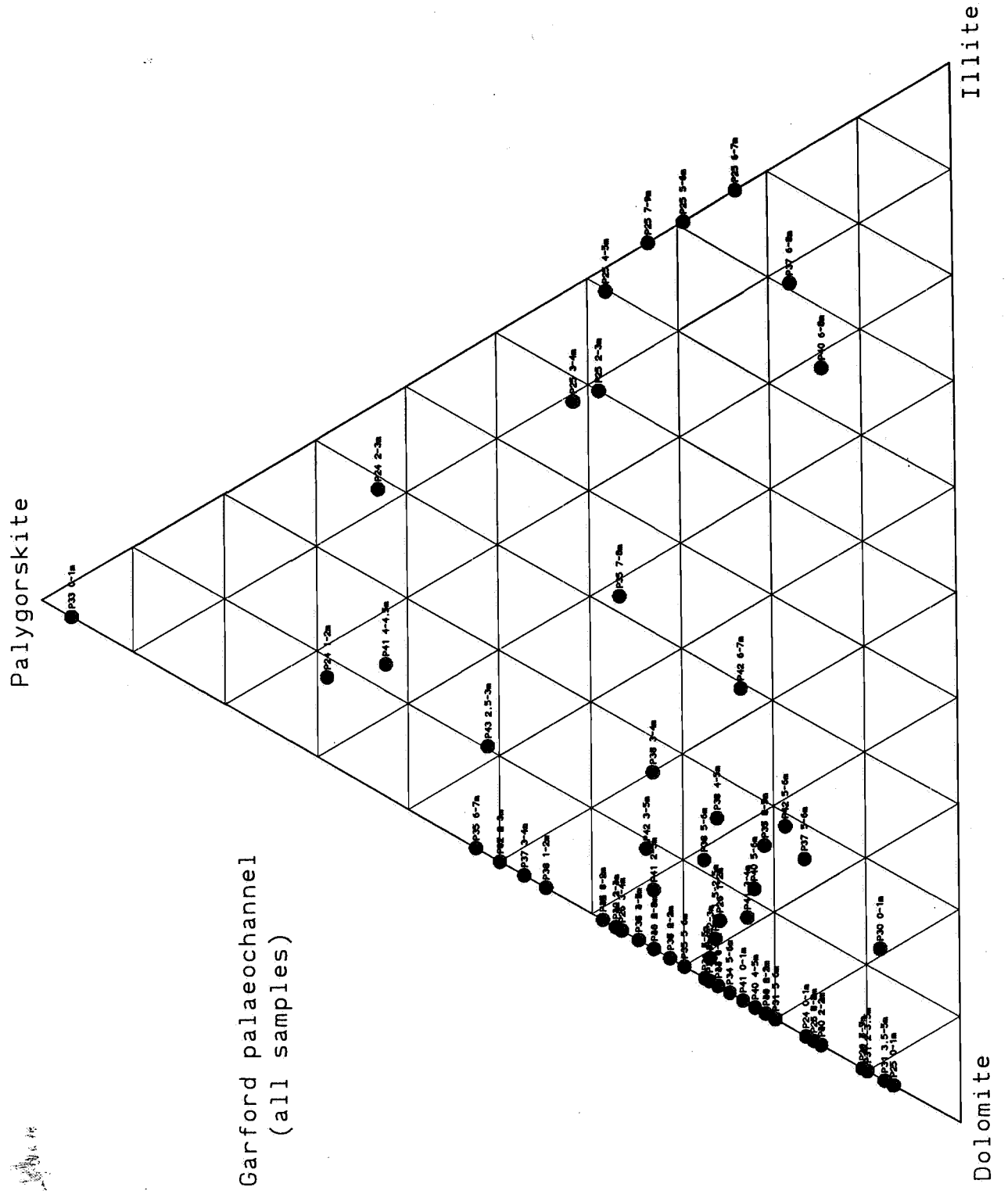
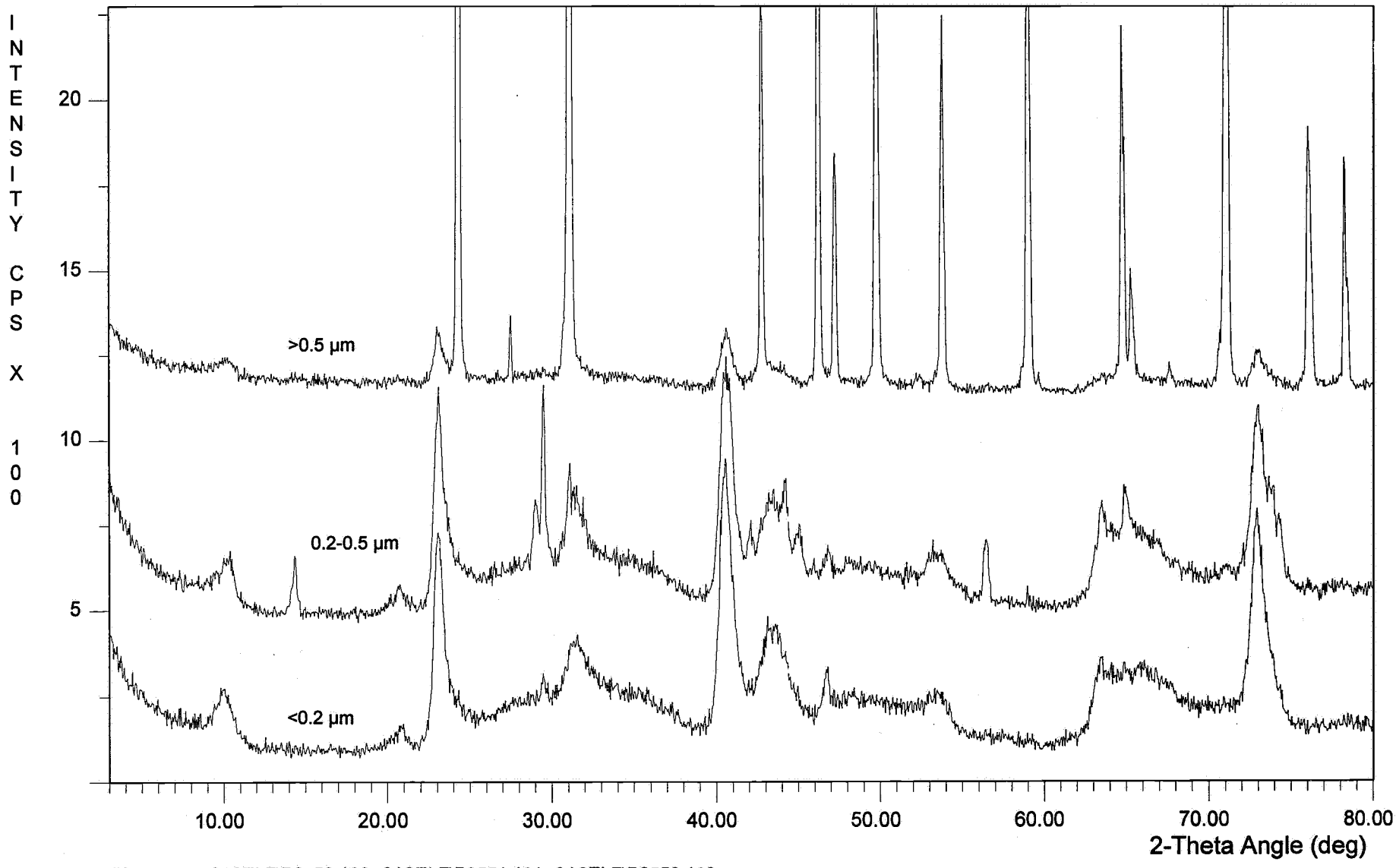


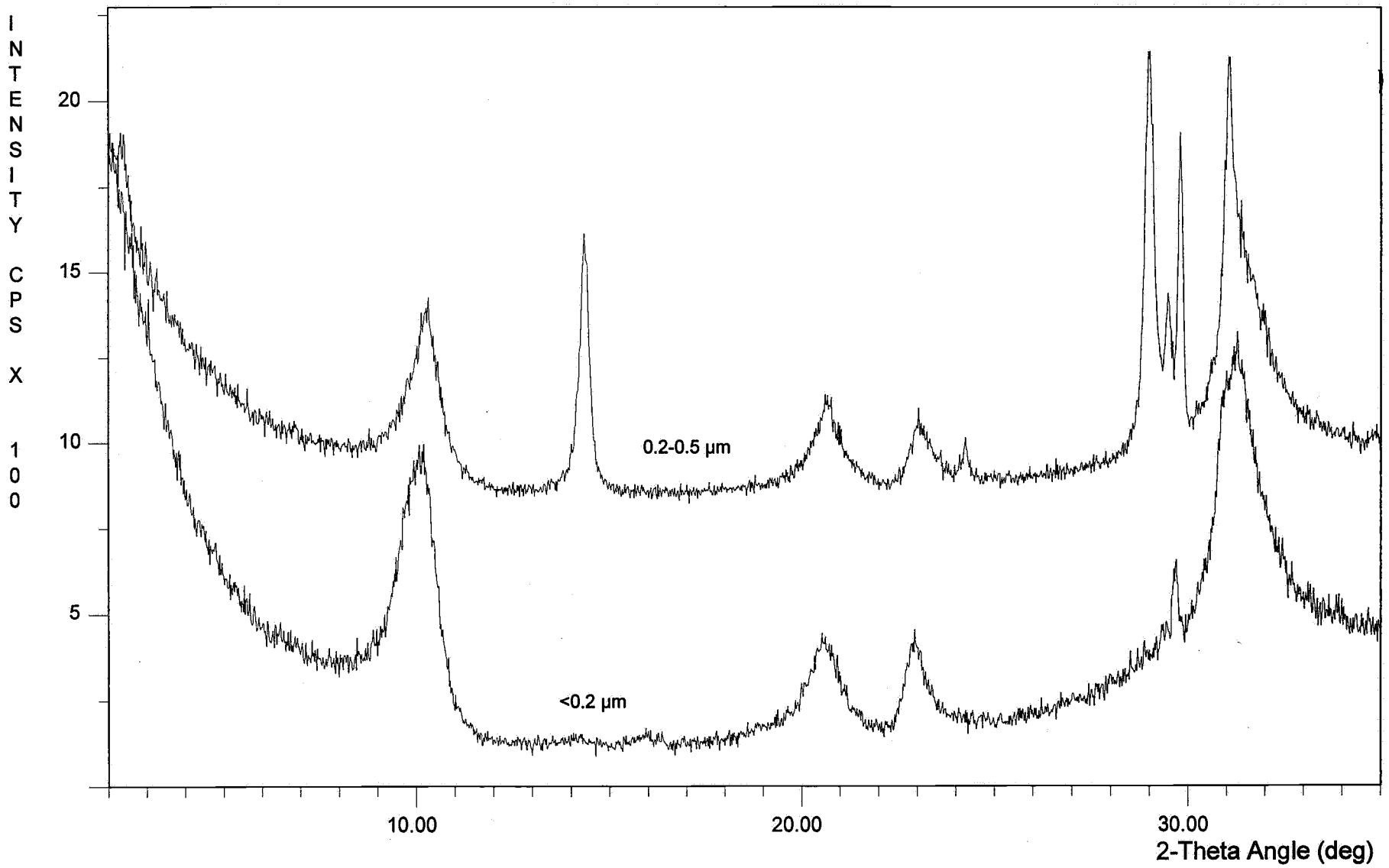
Fig. 19. Normalised palygorskite-dolomite-illite distribution of Garford palaeochannel bulk samples.

Fig. 20a. Garford palaeochannel sample P25 5-6m, sized fractions. Co Ka radiation. Non-oriented.



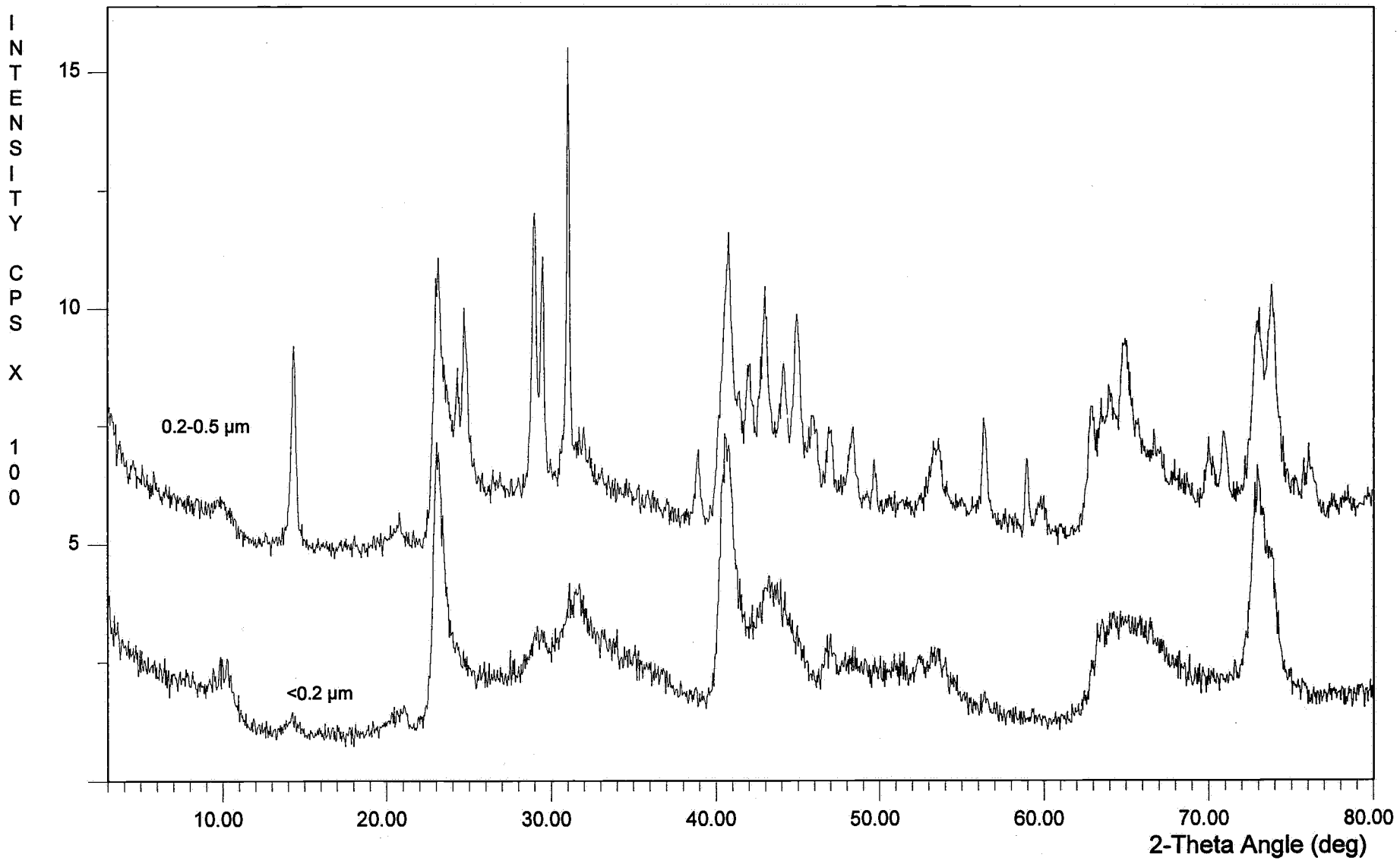
File Name: C:\SELF\P2552.102 C:\SELF\P2551.101 C:\SELF\P2553.103

Fig. 20b. Garford palaeochannel sample P25 5-6m, sized fractions. Co Ka radiation. Oriented.



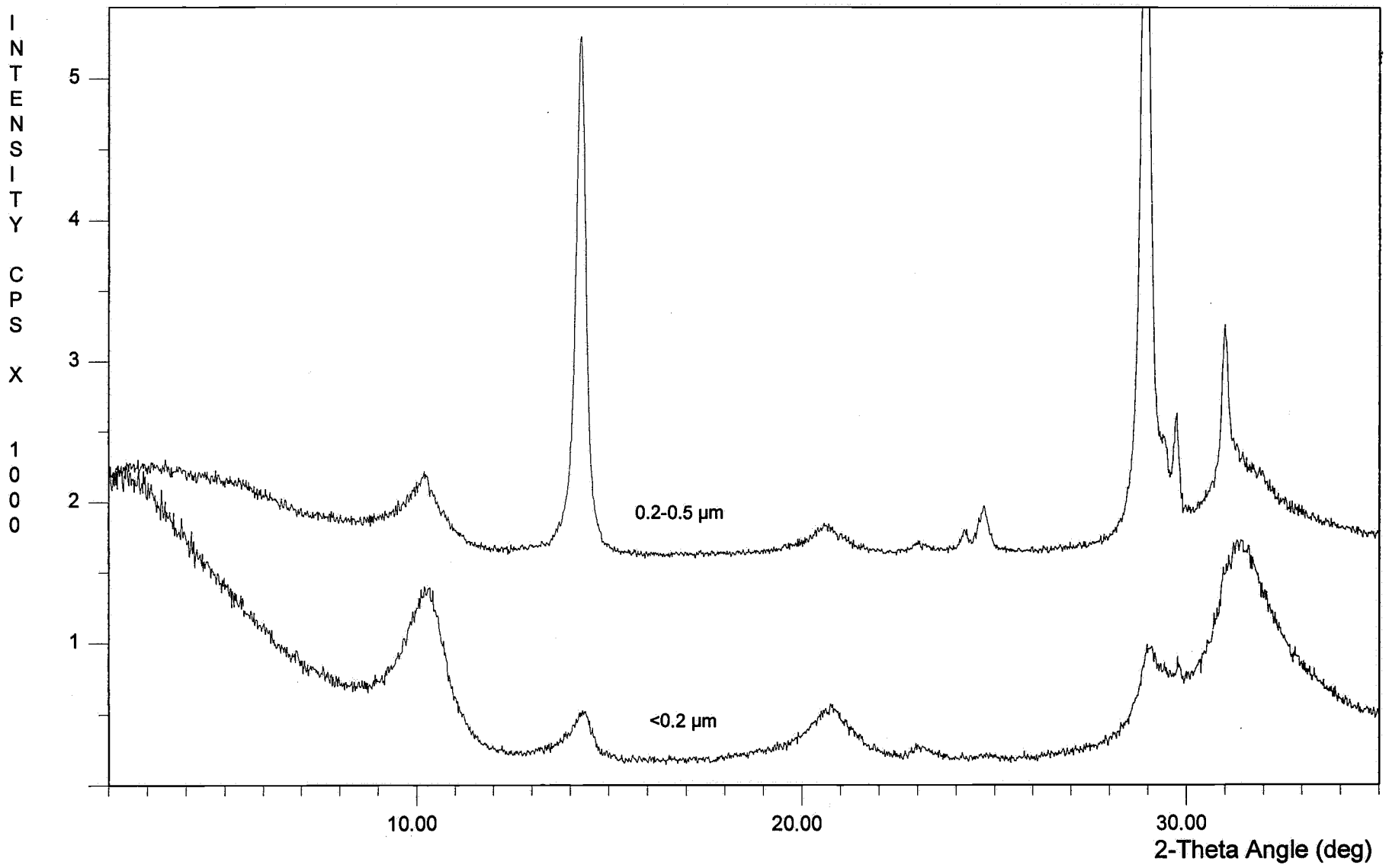
File Name: C:\SELF\OP2552.111 C:\SELF\OP2551.112

Fig. 21a. Garford palaeochannel sample P25 6-7m, sized fractions. Co Ka radiation. Non-oriented.



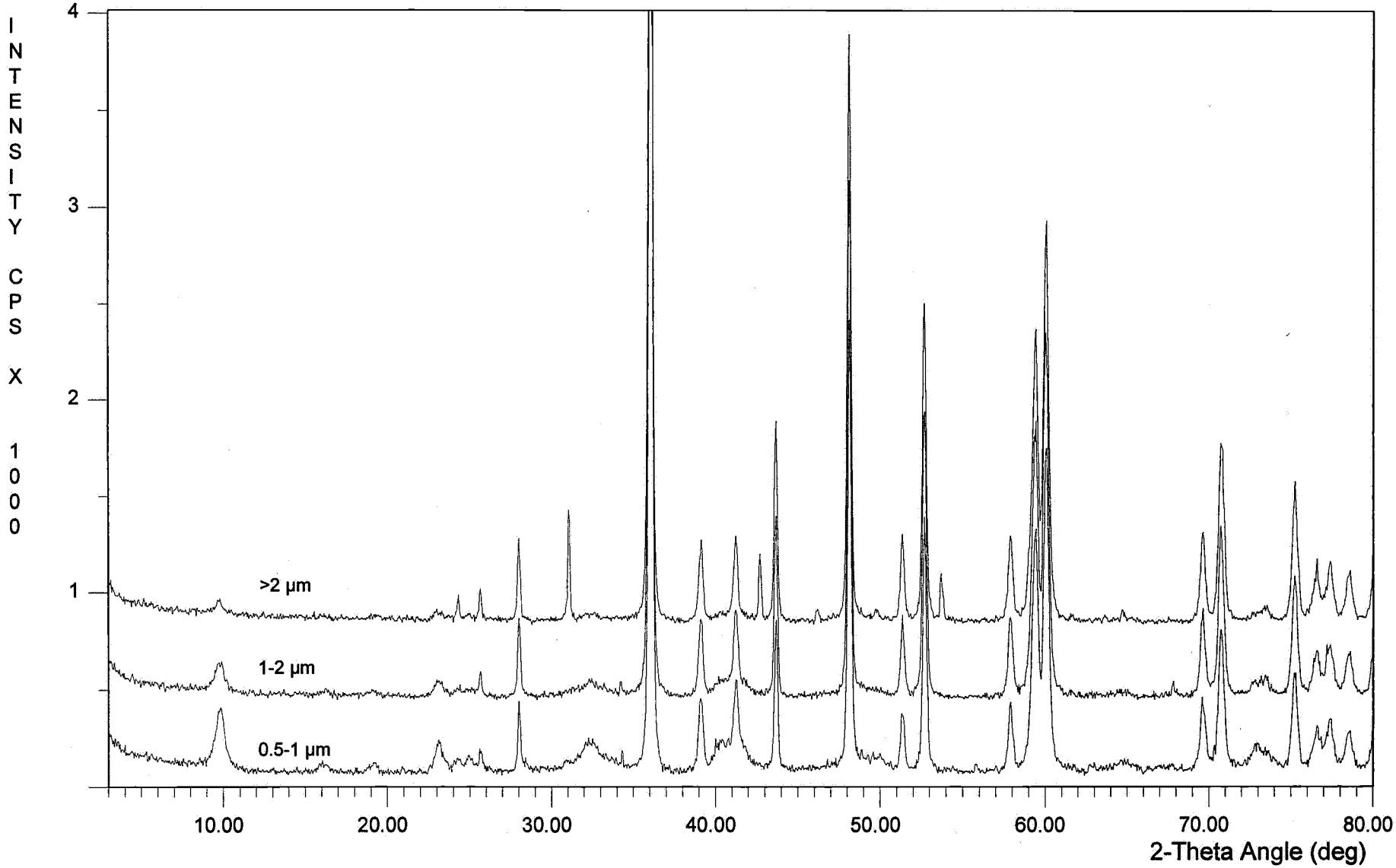
File Name: C:\SELF\P2561.104 C:\SELF\P2562.105

Fig. 21b. Garford palaeochannel sample P25 6-7m, sized fractions. Co Ka radiation. Oriented.



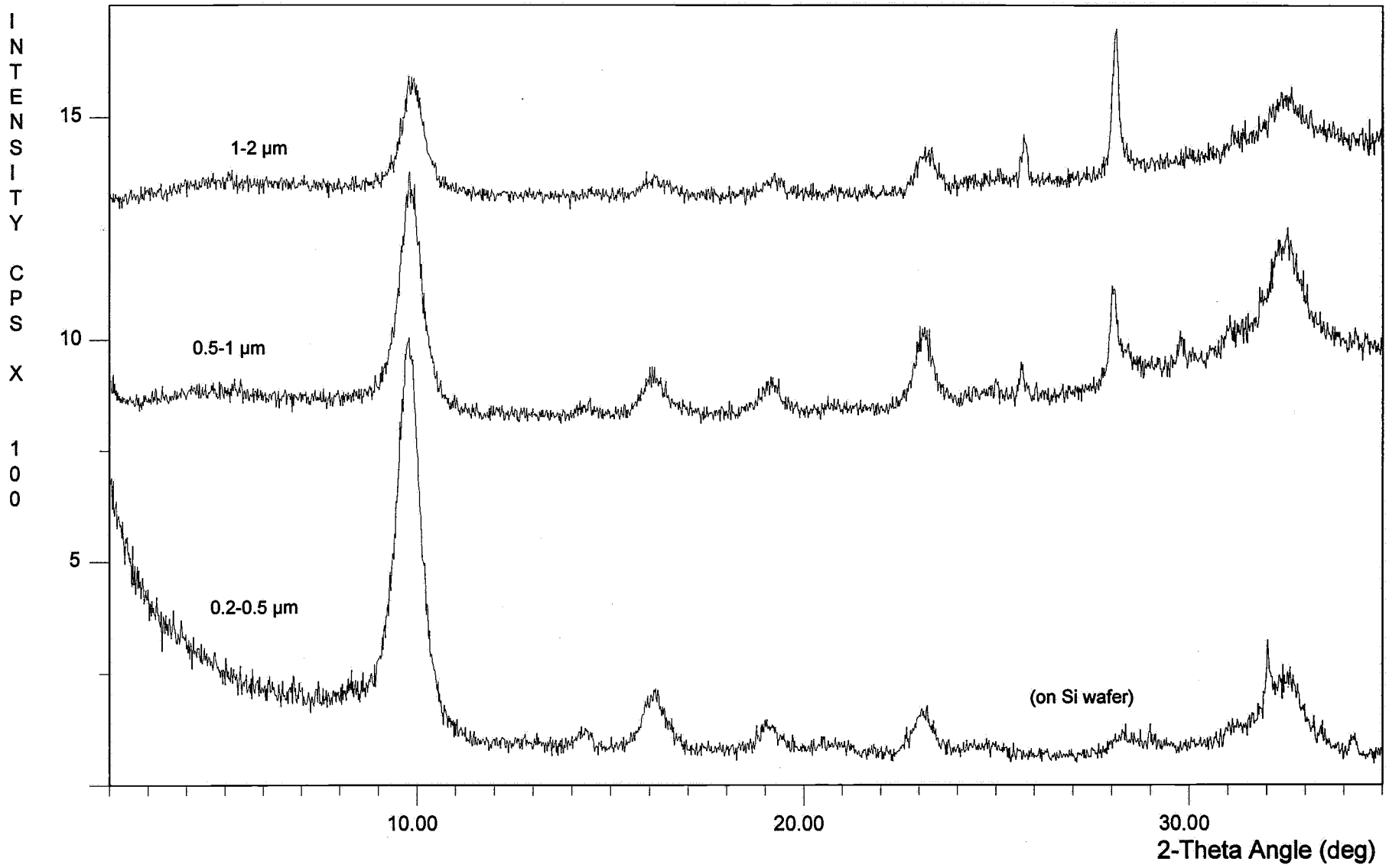
File Name: C:\SELF\OP2561.113 C:\SELF\OP2562.114

Fig. 22a. Garford palaeochannel sample P31 2-3m, sized fractions. Co Ka radiation. Non-oriented.



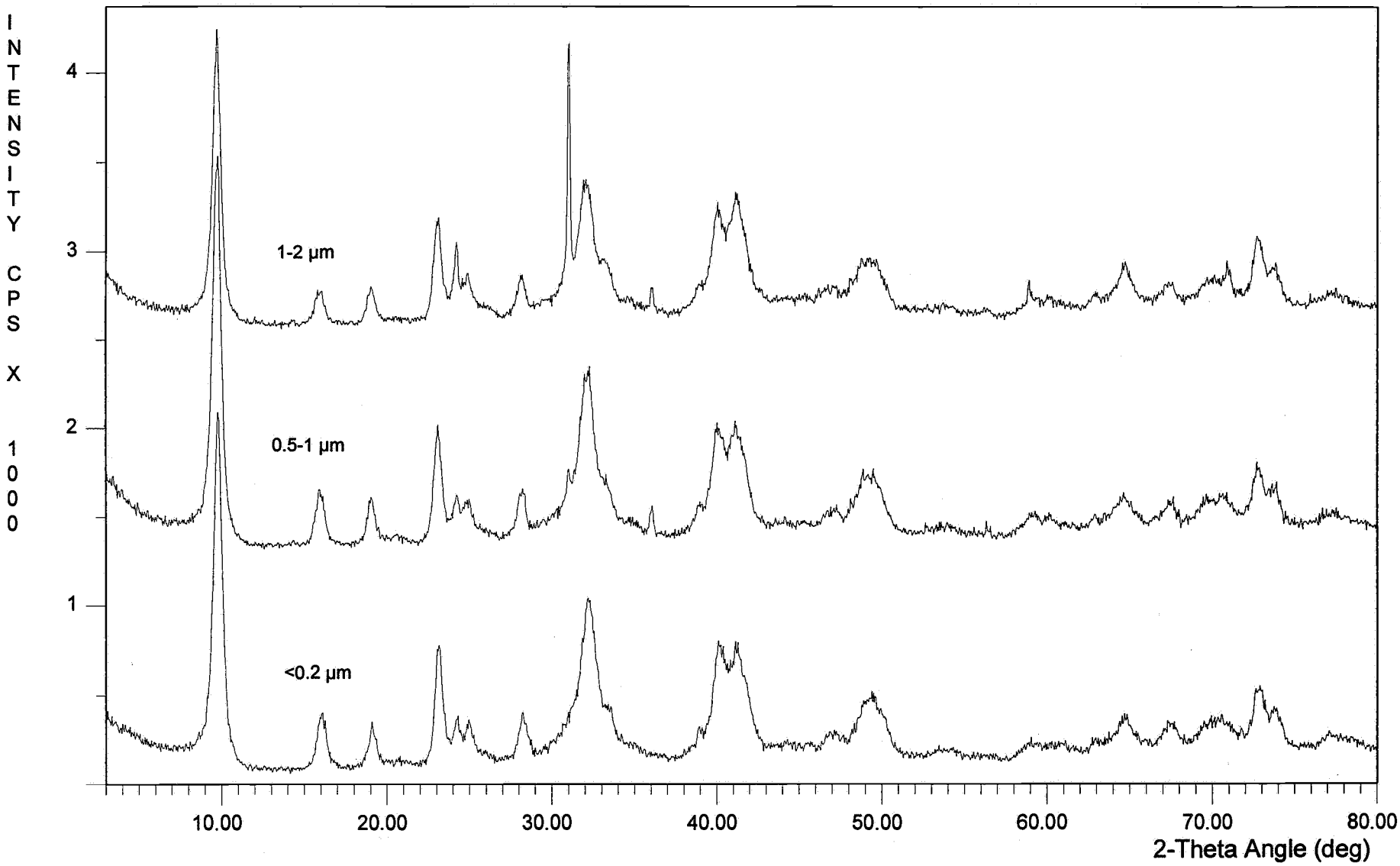
File Name: C:\SELF\P312351.DAT C:\SELF\P312312.DAT C:\SELF\P3123G2.DAT

Fig. 22b. Garford palaeochannel sample P31 2-3m, sized fractions. Co Ka radiation. Oriented.



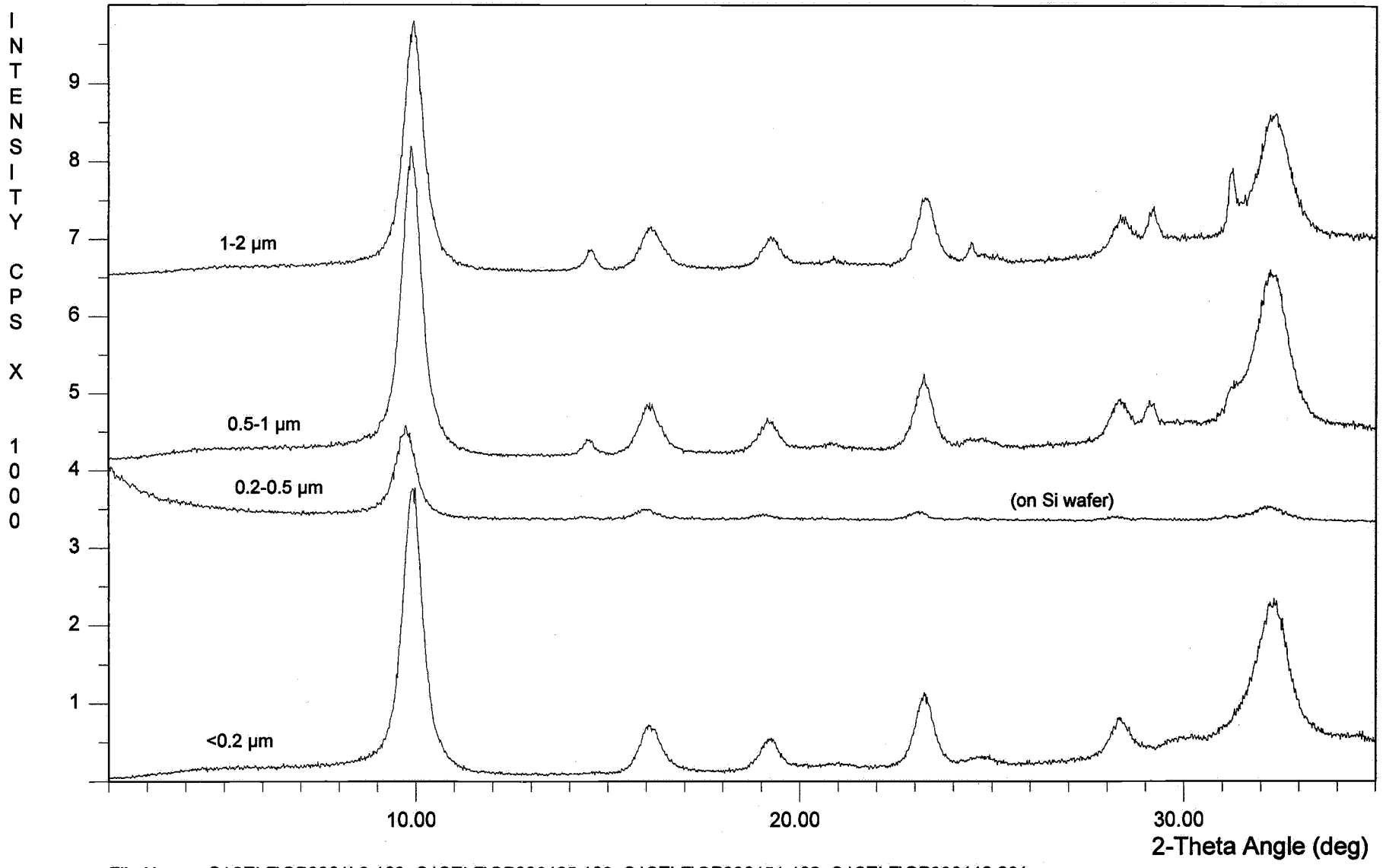
File Name: C:\SELF\OP312325.107 C:\SELF\OP312351.106 C:\SELF\OP312312.105

Fig. 23a. Garford palaeochannel sample P33 0-1m, sized fractions. Co Ka radiation. Non-oriented.



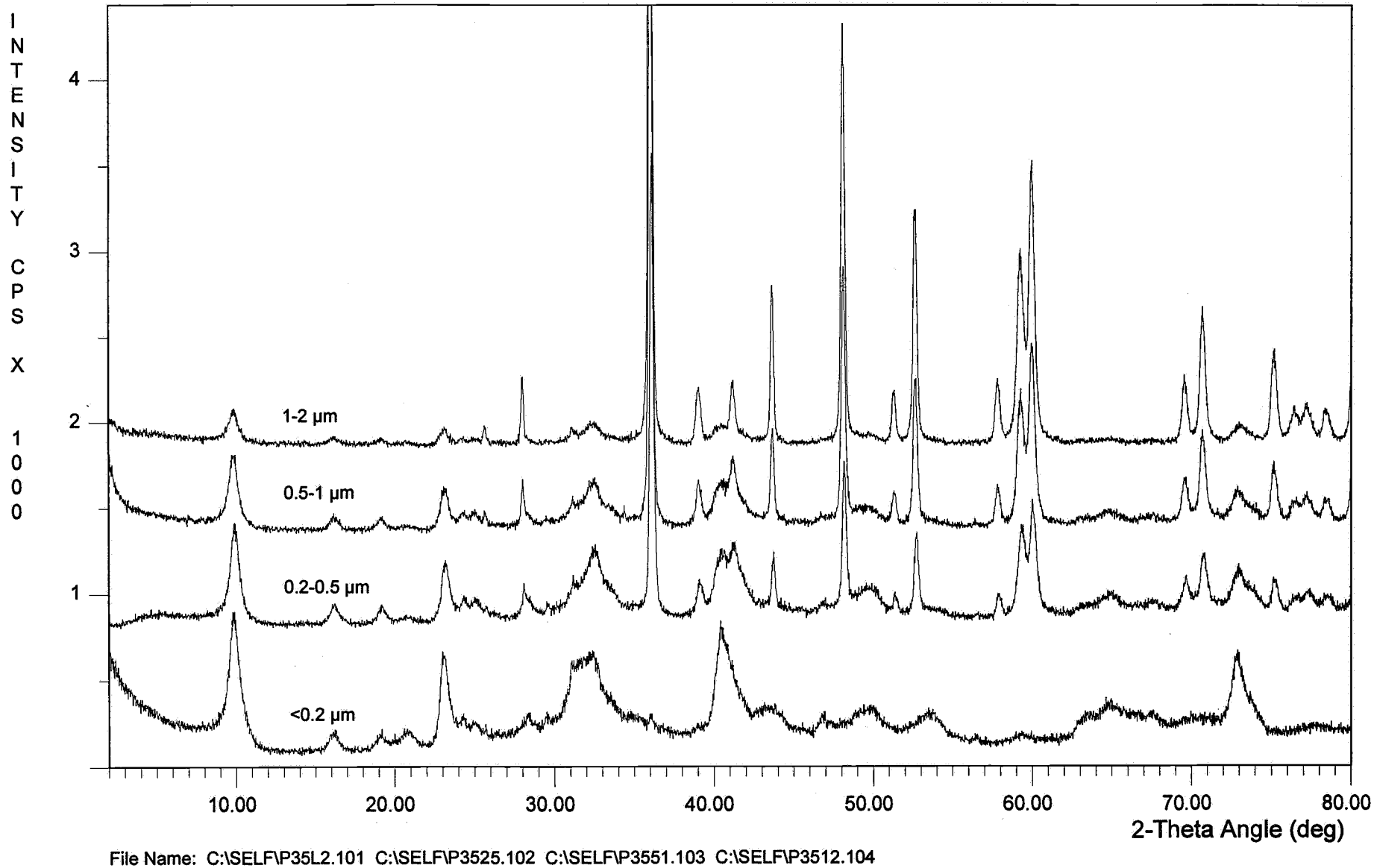
File Name: C:\SELF\P3301L2.DAT C:\SELF\P330151.DAT C:\SELF\P330112.DAT

Fig. 23b. Garford palaeochannel sample P33 0-1m, sized fractions. Co Ka radiation. Oriented.



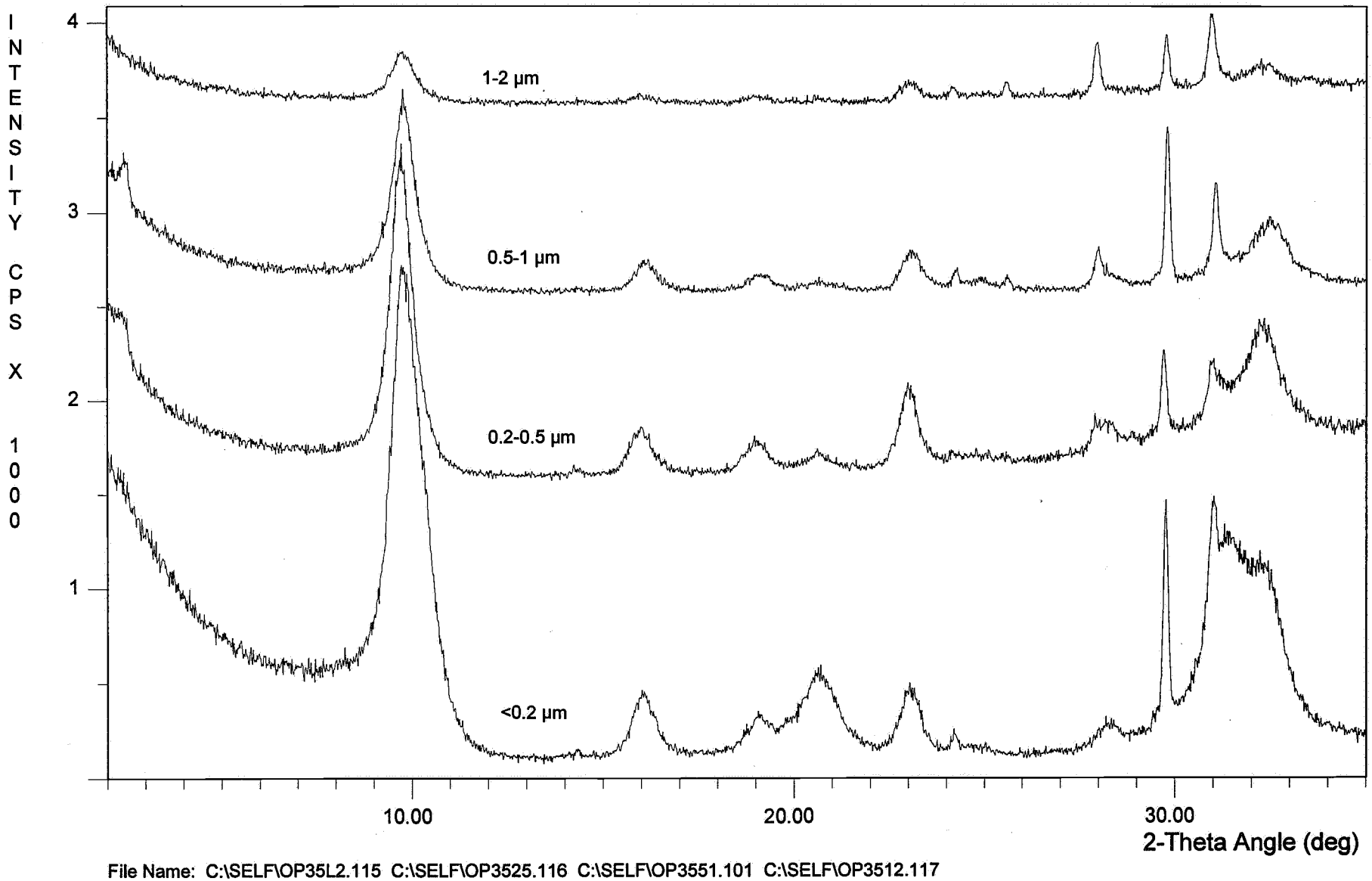
File Name: C:\SELF\OP3301L2.103 C:\SELF\OP330125.108 C:\SELF\OP330151.102 C:\SELF\OP330112.201

Fig. 24a. Garford palaeochannel sample P35 5-6m, sized fractions. Co Ka radiation. Non-oriented.



File Name: C:\SELF\P35L2.101 C:\SELF\P3525.102 C:\SELF\P3551.103 C:\SELF\P3512.104

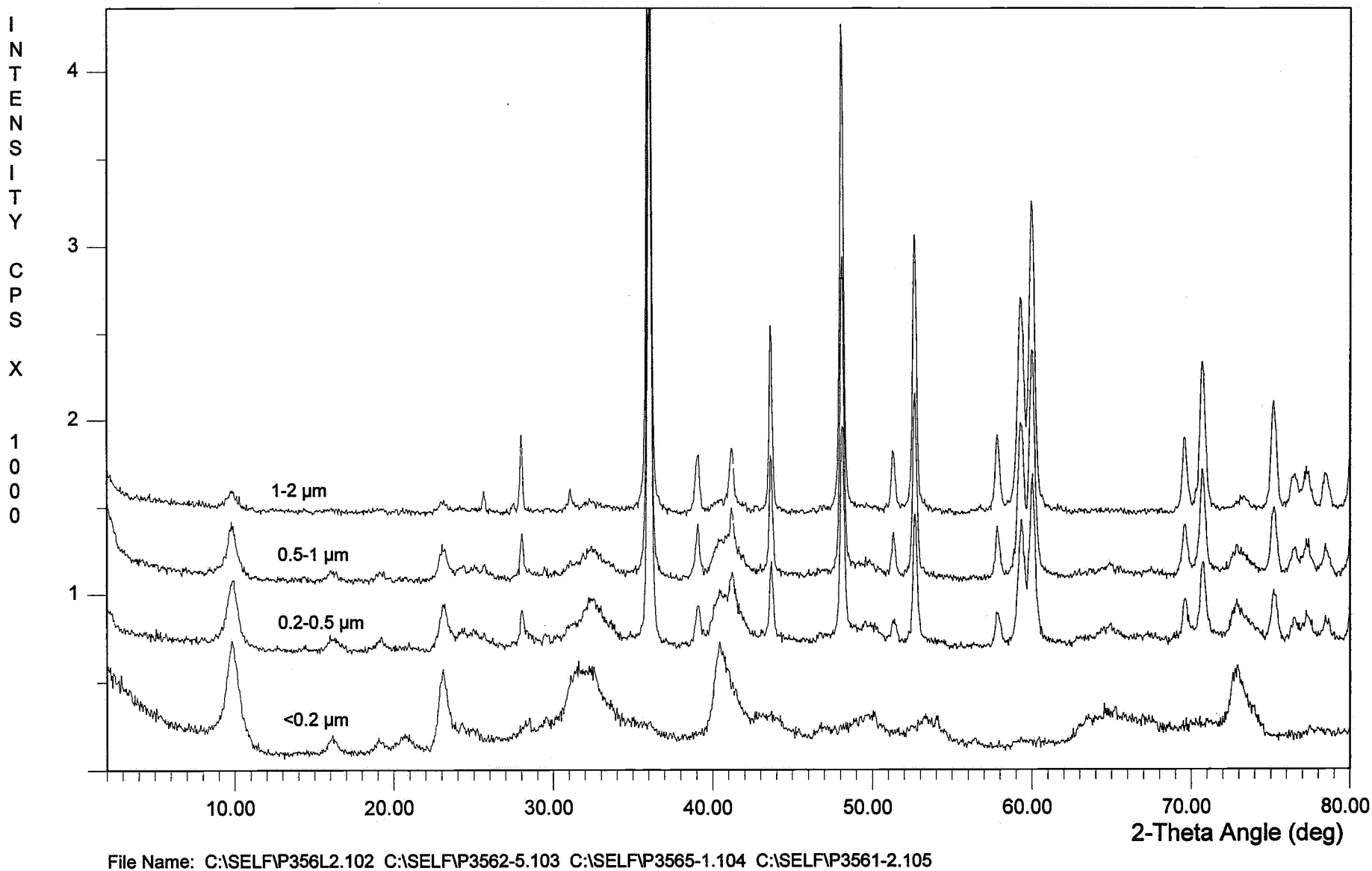
Fig. 24b. Garford palaeochannel sample P35 5-6m, sized fractions. Co Ka radiation. Oriented.



File Name: C:\SELF\OP35L2.115 C:\SELF\OP3525.116 C:\SELF\OP3551.101 C:\SELF\OP3512.117

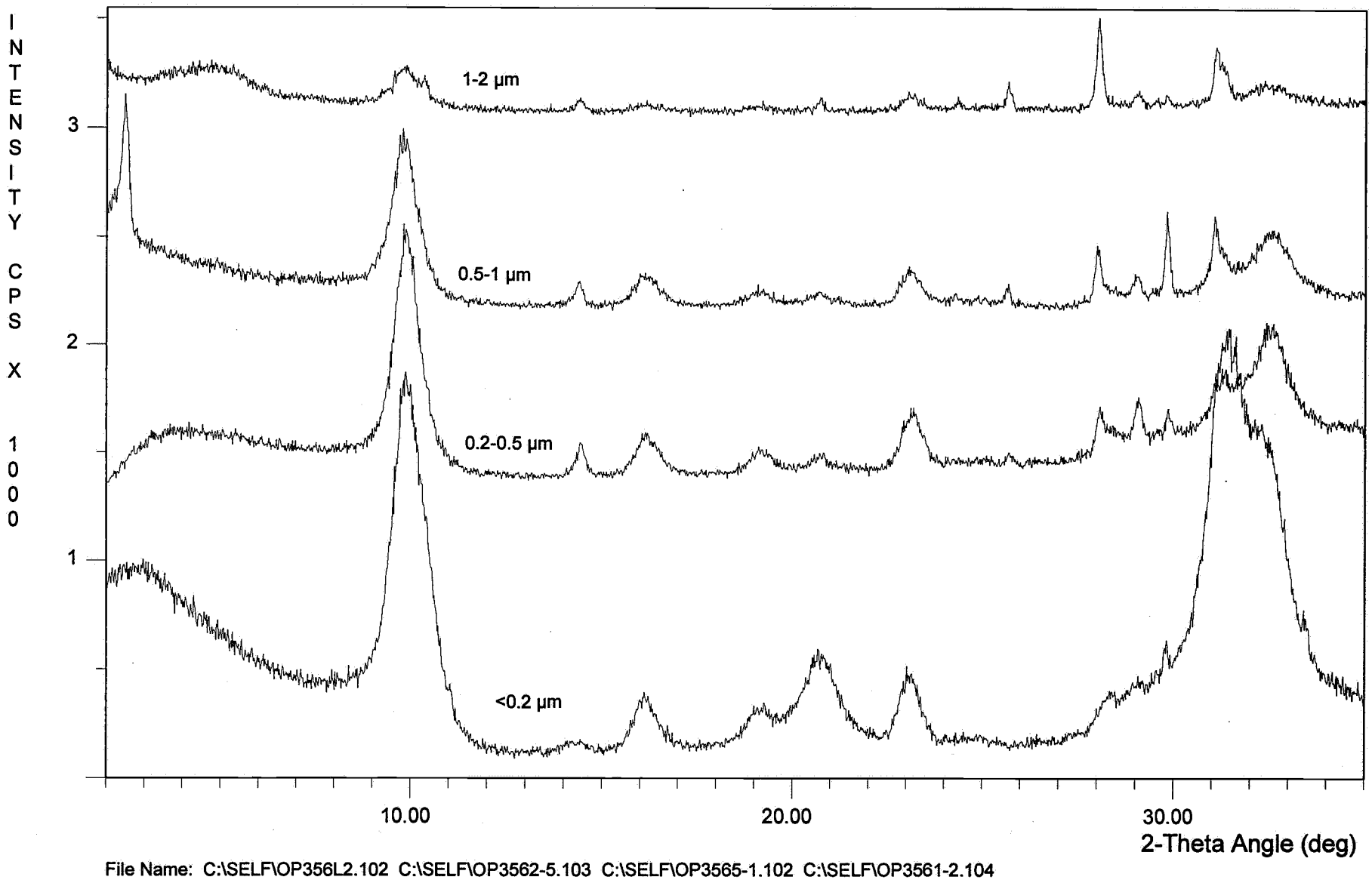
0003313
67

Fig. 25a. Garford palaeochannel sample P35 6-7m, sized fractions. Co Ka radiation. Non-oriented.



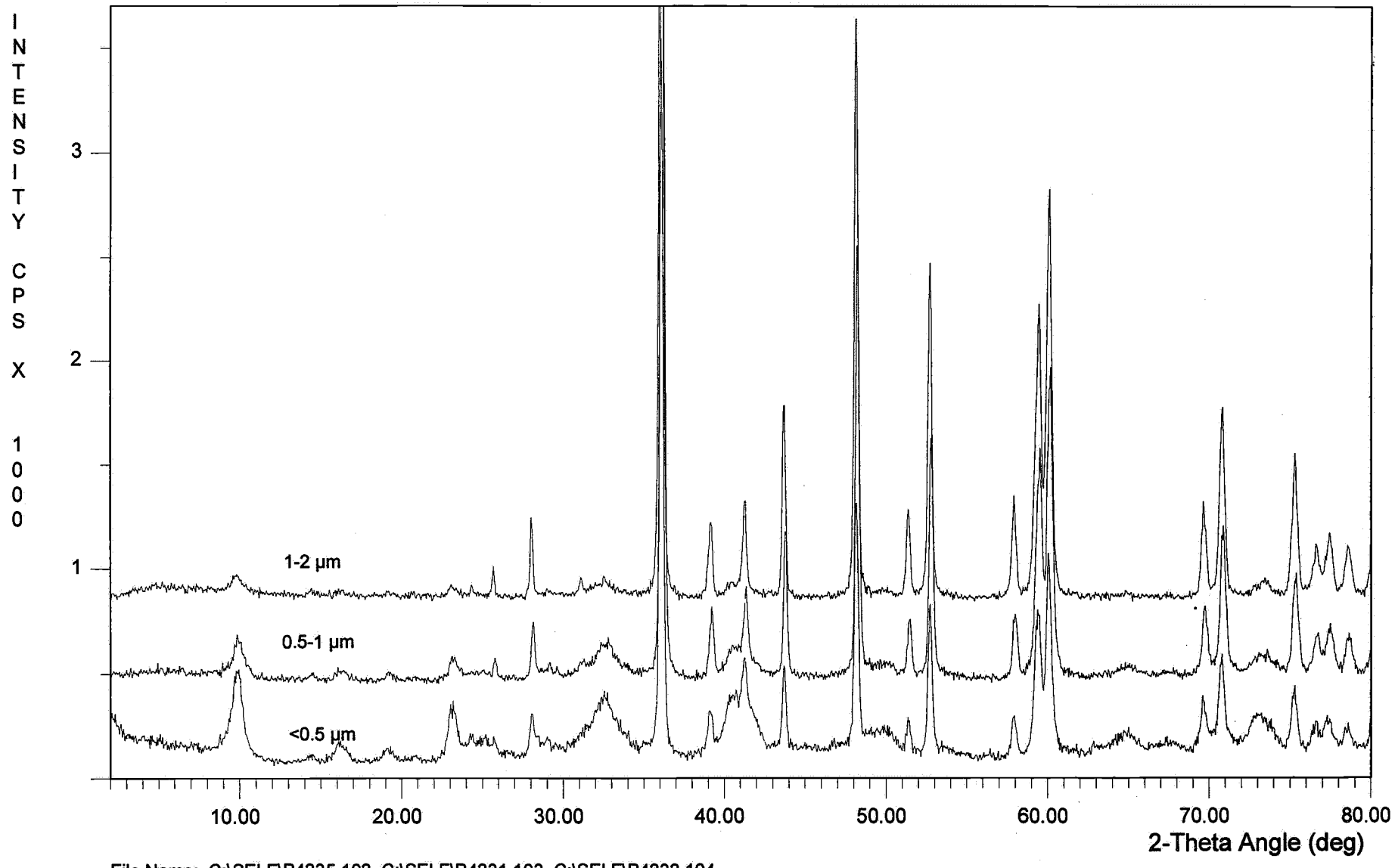
File Name: C:\SELF\P356L2.102 C:\SELF\P3562-5.103 C:\SELF\P3565-1.104 C:\SELF\P3561-2.105

Fig. 25b. Garford palaeochannel sample P35 6-7m, sized fractions. Co Ka radiation. Oriented.



File Name: C:\SELF\OP356L2.102 C:\SELF\OP3562-5.103 C:\SELF\OP3565-1.102 C:\SELF\OP3561-2.104

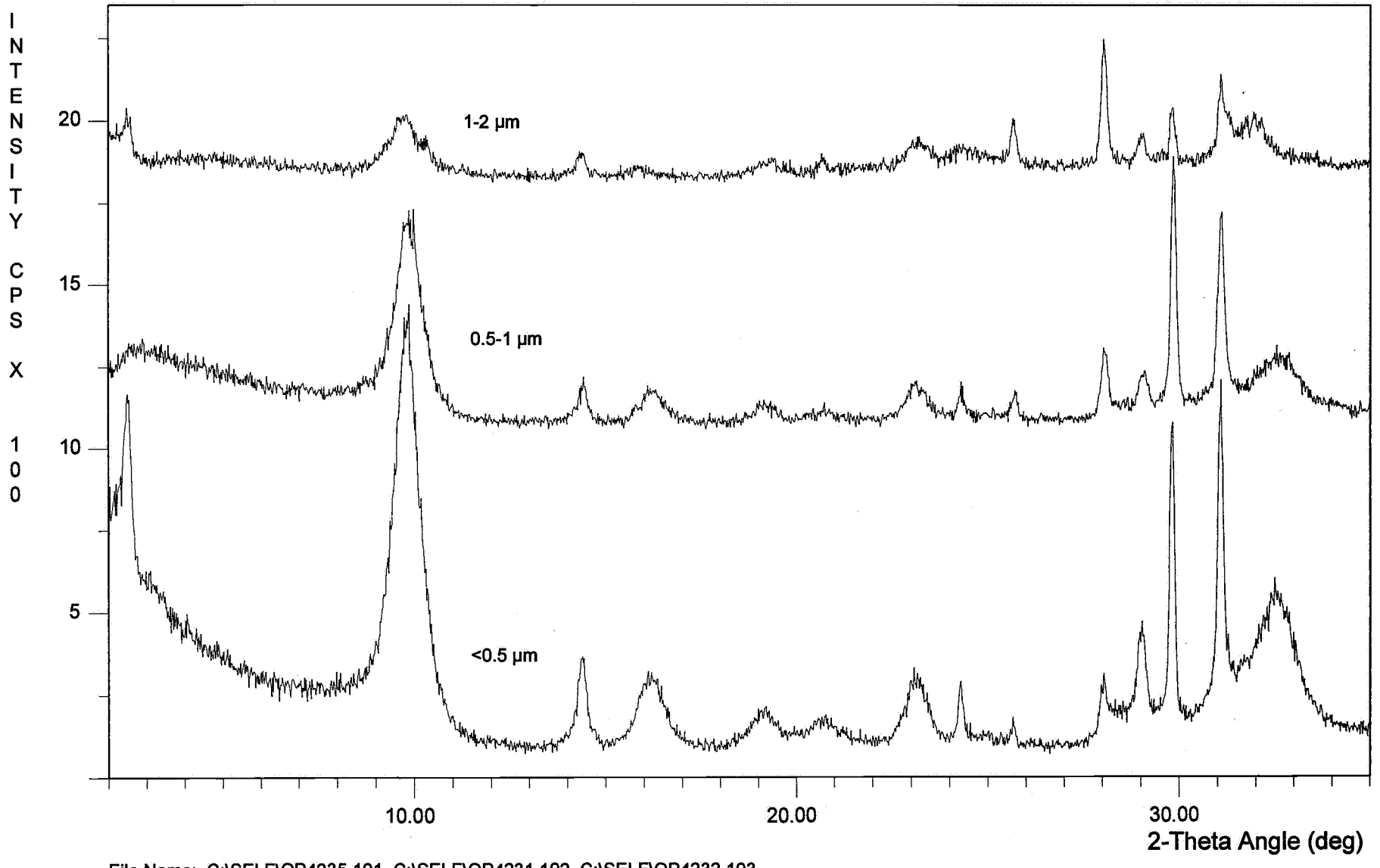
Fig. 26a. Garford palaeochannel sample P42 3-4m, sized fractions. Co Ka radiation. Non-oriented.



File Name: C:\SELF\P4235.102 C:\SELF\P4231.103 C:\SELF\P4232.104

000316

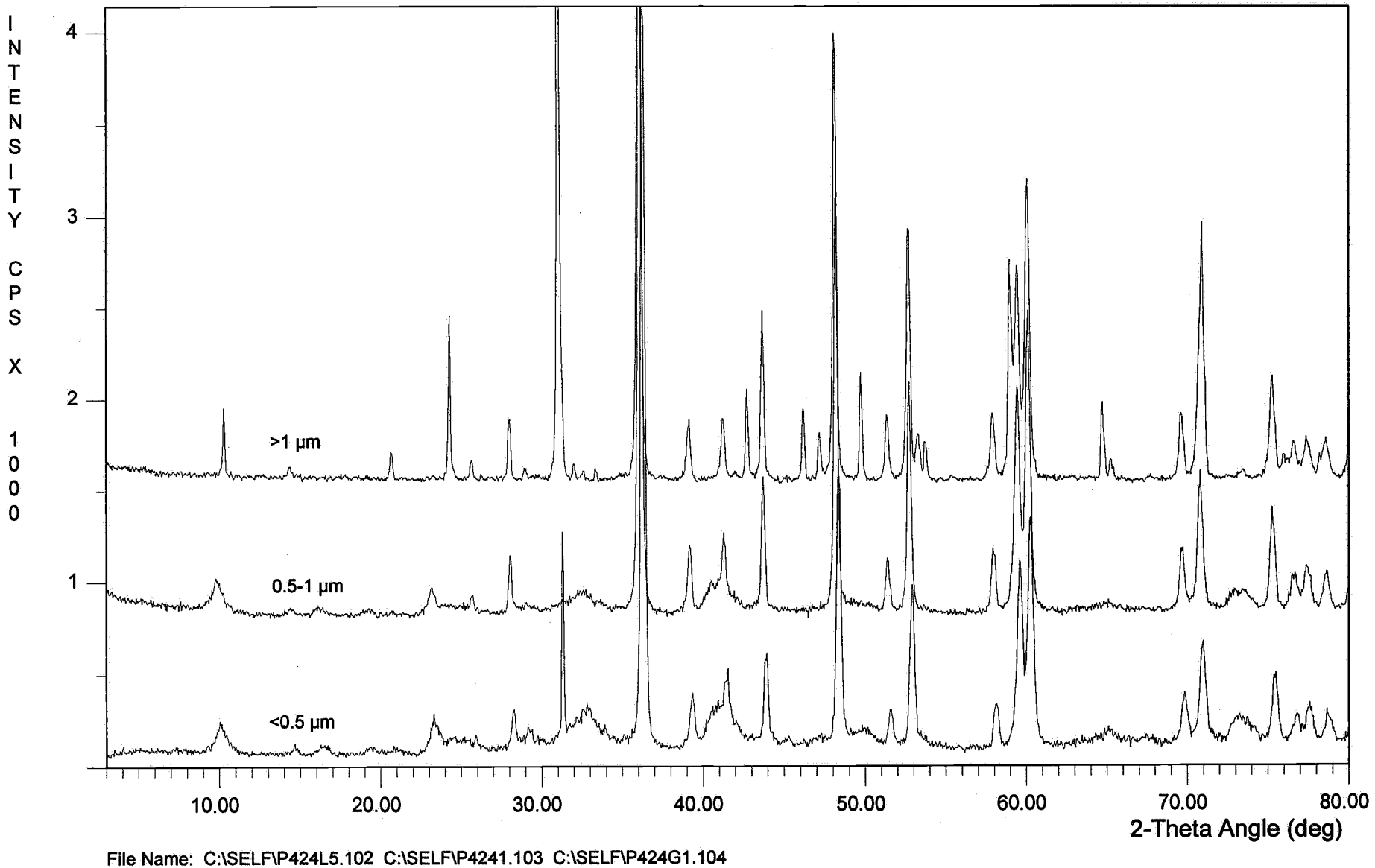
Fig. 26b. Garford palaeochannel sample P42 3-4m, sized fractions. Co Ka radiation. Oriented.



File Name: C:\SELF\OP4235.101 C:\SELF\OP4231.102 C:\SELF\OP4232.103

0003117

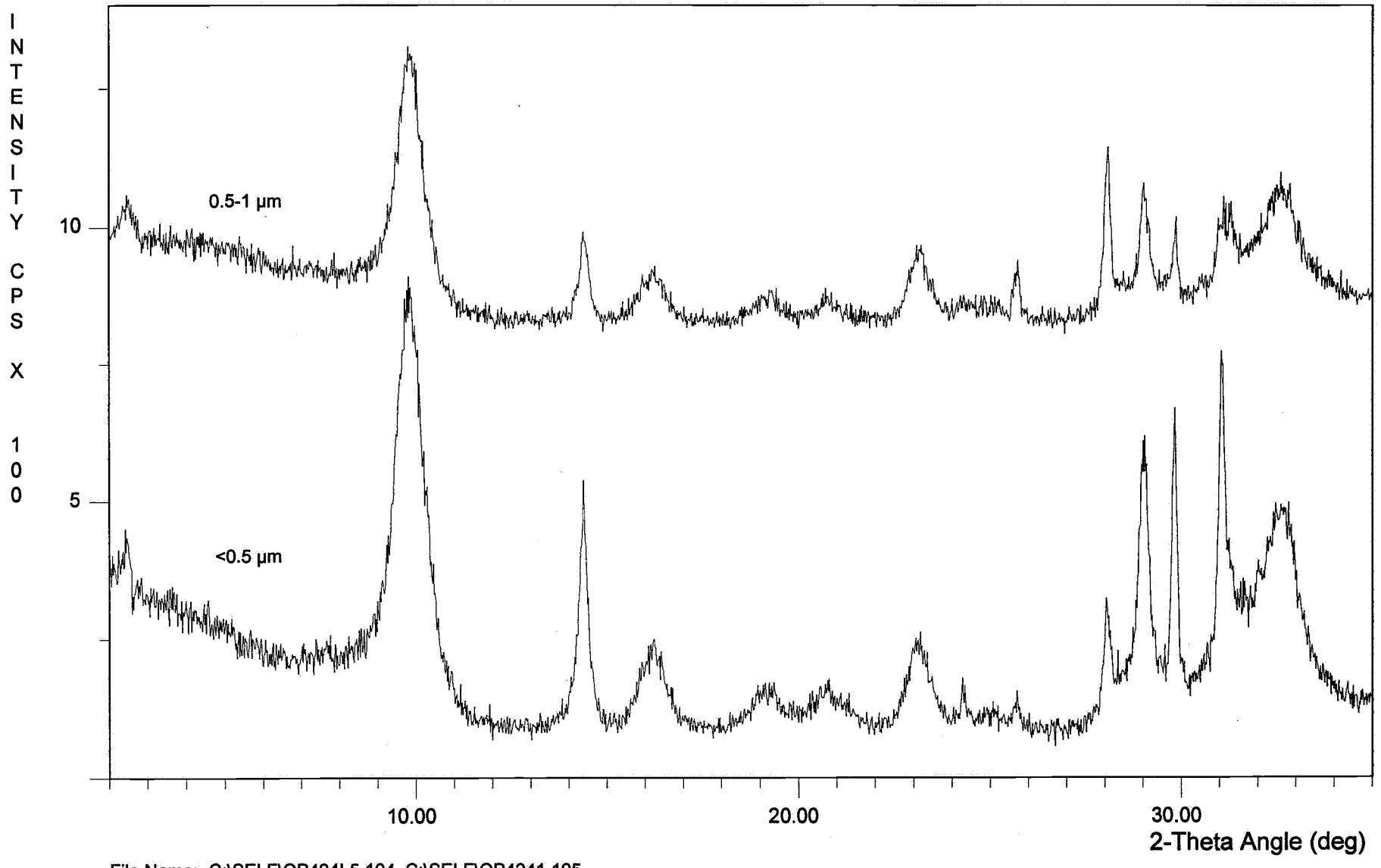
Fig. 27a. Garford palaeochannel sample P42 4-5m, sized fractions. Co Ka radiation. Non-oriented.



File Name: C:\SELF\P424L5.102 C:\SELF\P4241.103 C:\SELF\P424G1.104

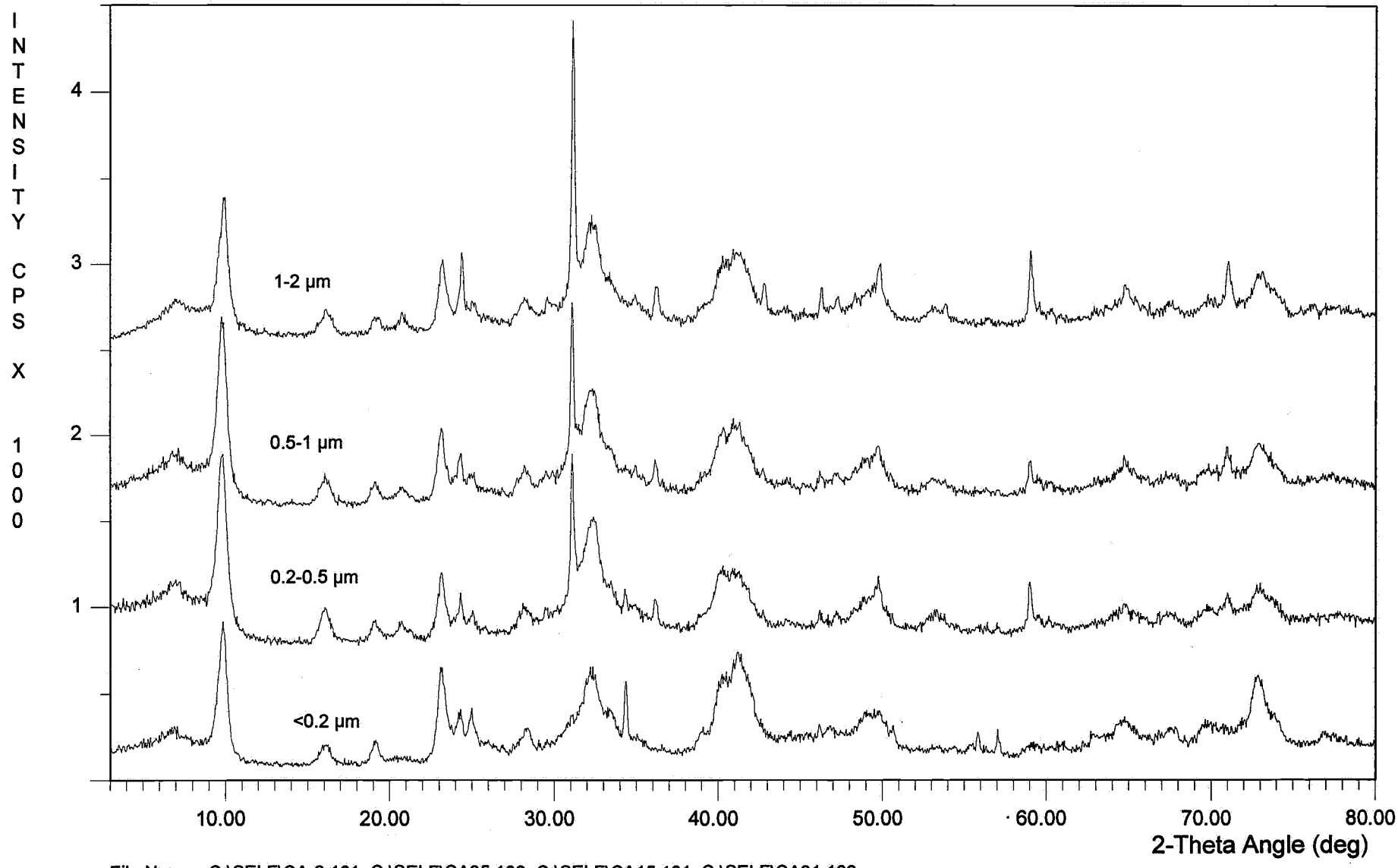
000318

Fig. 27b. Garford palaeochannel sample P42 4-5m, sized fractions. Co Ka radiation. Oriented.



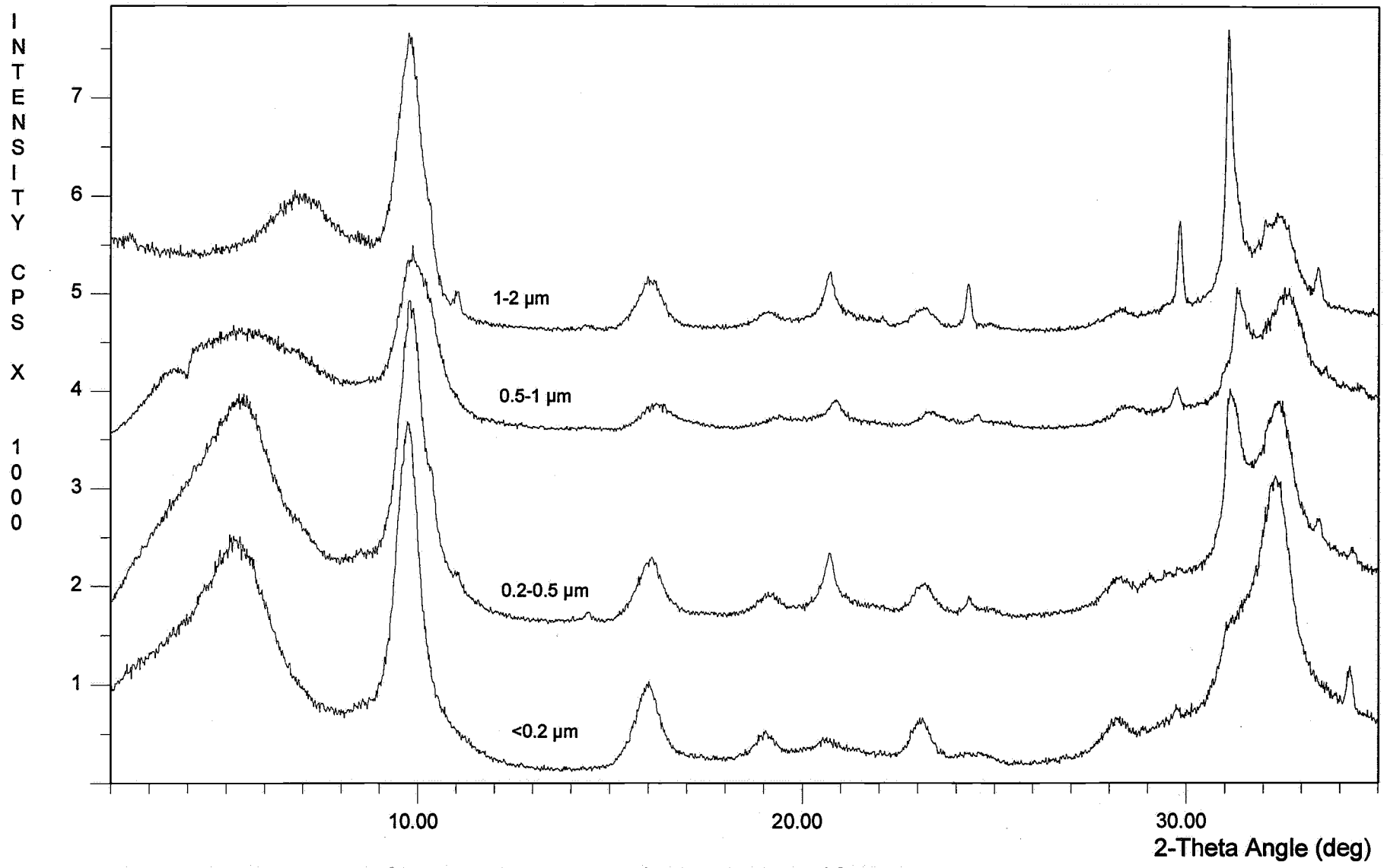
File Name: C:\SELF\OP424L5.104 C:\SELF\OP4241.105

Fig. 28a. Chinese attapulgite (antisalt bentonite), sized fractions. Co Ka radiation. Non-oriented.



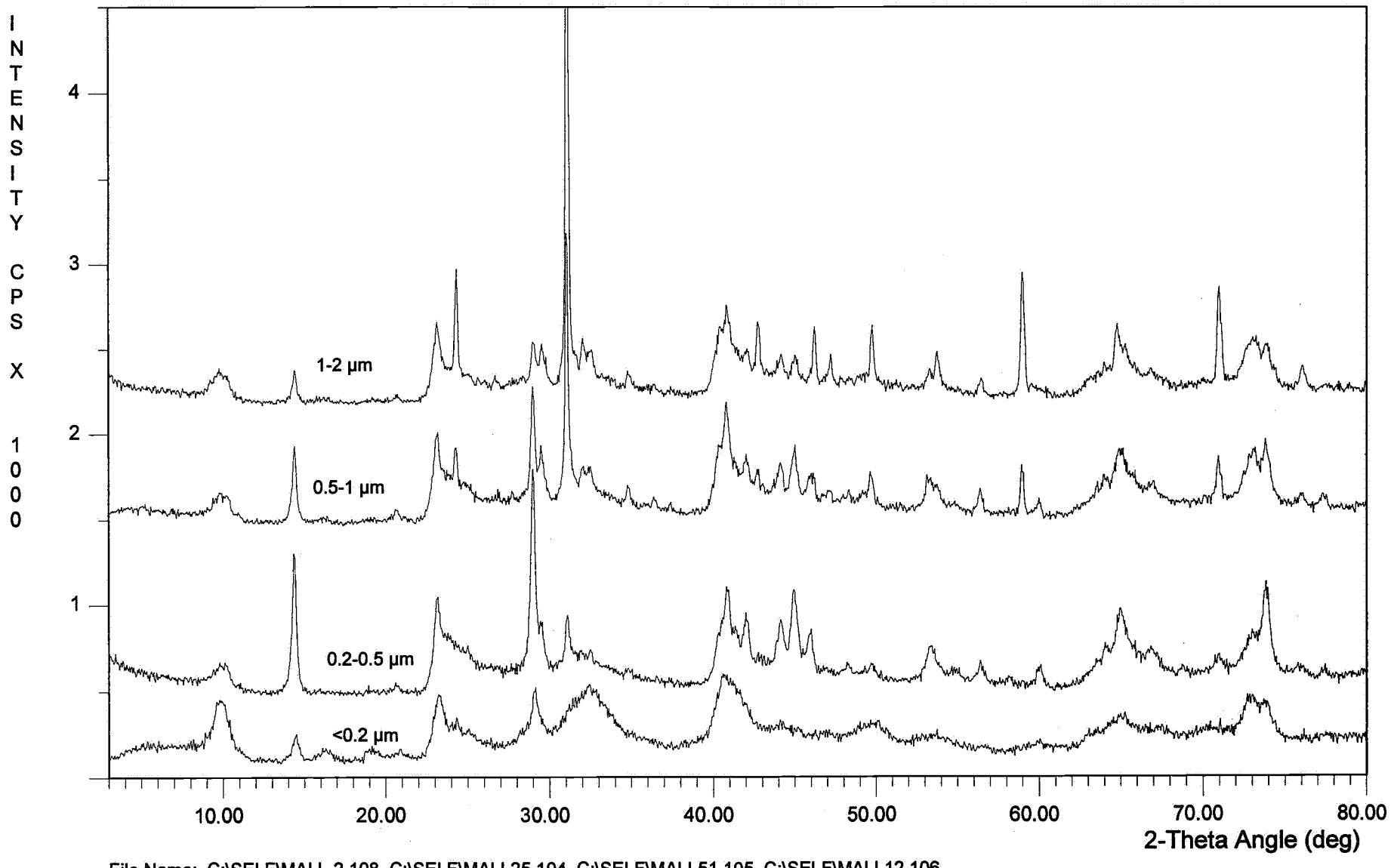
File Name: C:\SELF\CA-2.101 C:\SELF\CA25.103 C:\SELF\CA15.101 C:\SELF\CA21.102

Fig. 28b. Chinese attapulgite (antisalt bentonite), sized fractions. Co Ka radiation. Oriented.



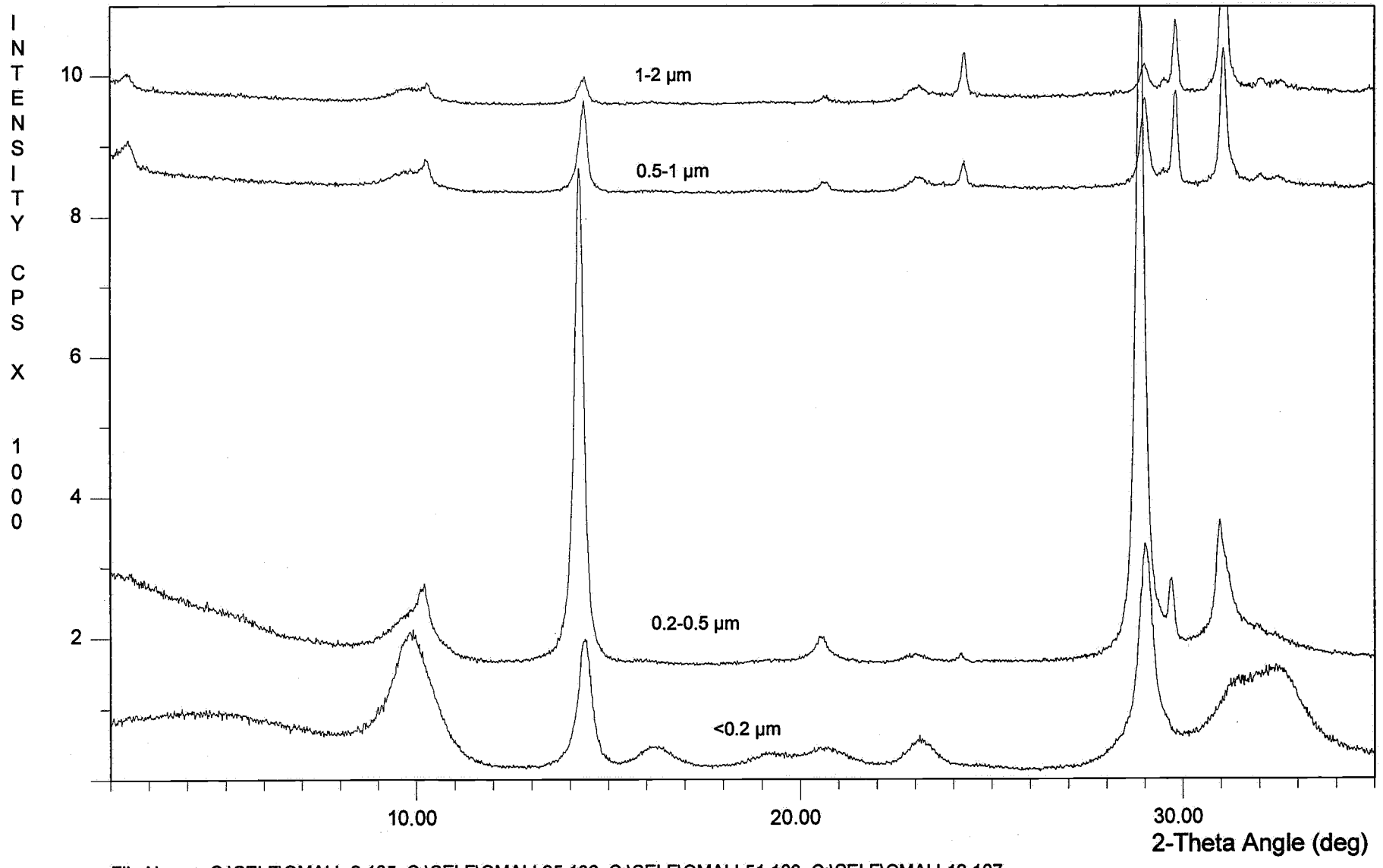
File Name: C:\SELF\OCA-2.108 C:\SELF\OCA25.109 C:\SELF\OCA21.110 C:\SELF\OCA12.104

Fig. 29a. Lake Nerramyne attapulgite, sized fractions. Co Ka radiation. Non-oriented.



File Name: C:\SELF\MALL-2.108 C:\SELF\MALL25.104 C:\SELF\MALL51.105 C:\SELF\MALL12.106

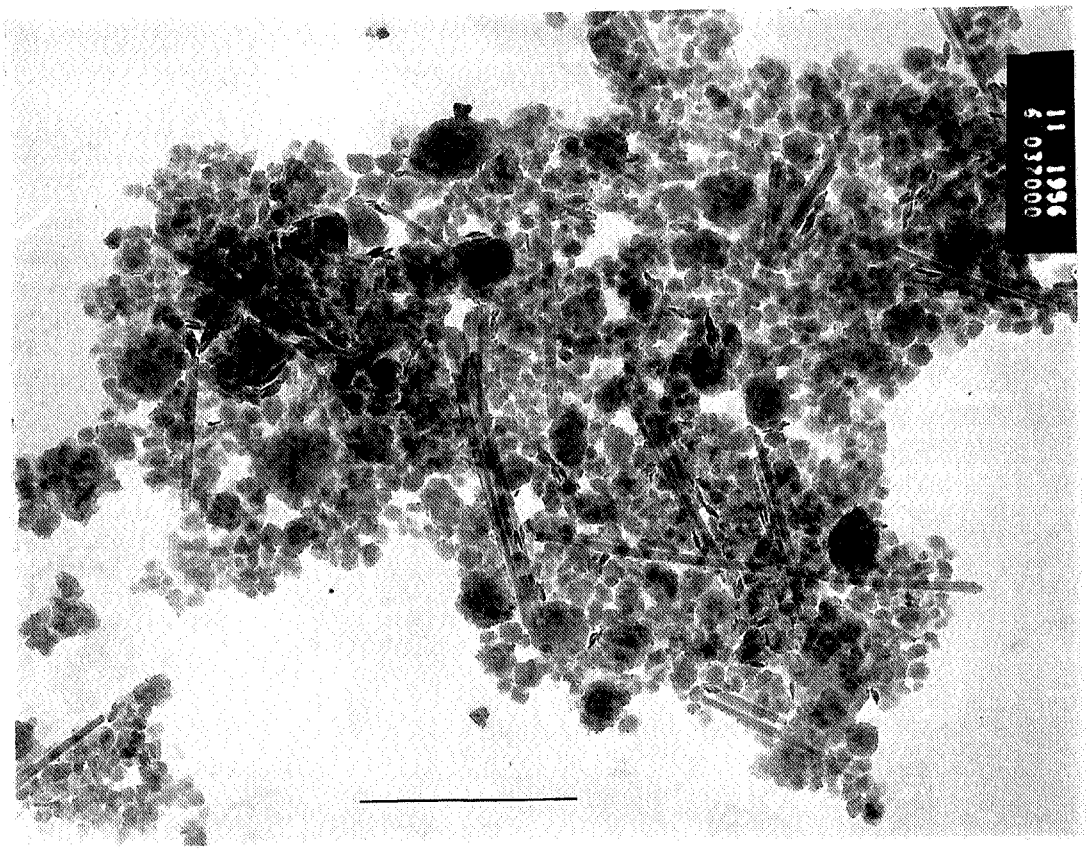
Fig. 29b. Lake Nerramyne attapulgite, sized fractions. Co Ka radiation. Oriented.



File Name: C:\SELF\OMALL-2.105 C:\SELF\OMALL25.106 C:\SELF\OMALL51.103 C:\SELF\OMALL12.107

000323

PLATES



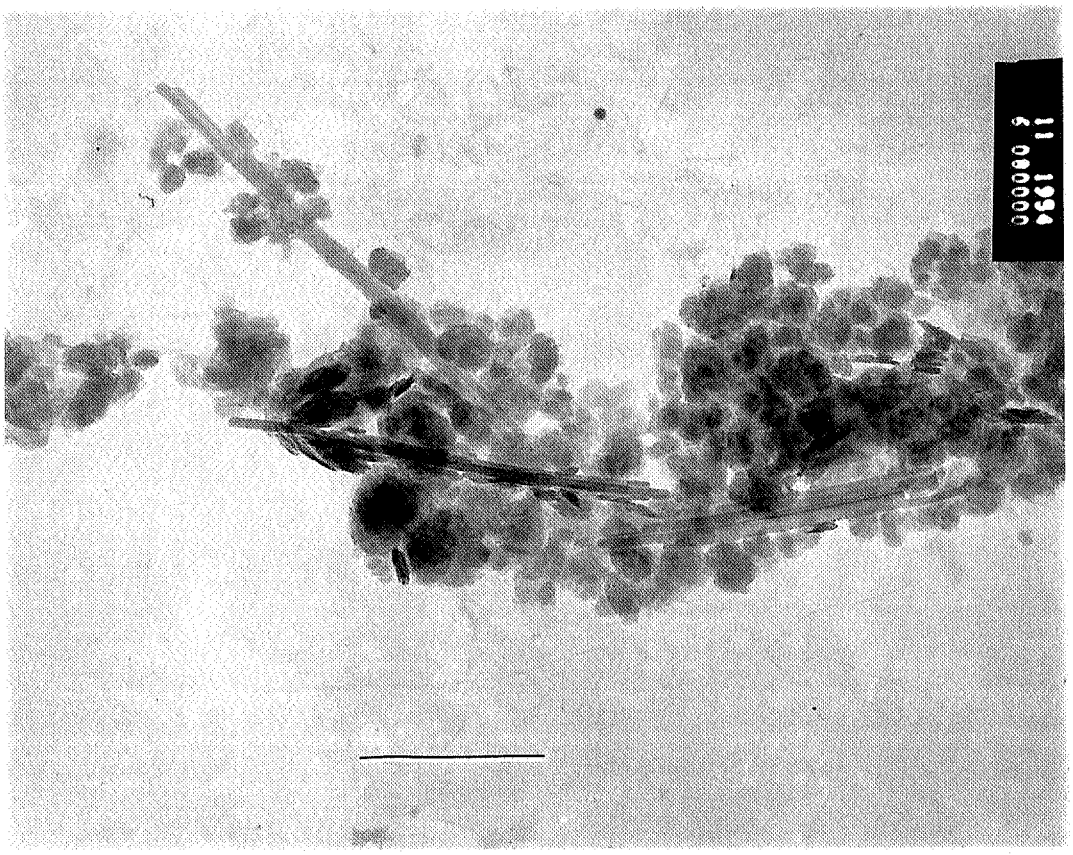


Plate 1. Garford palaeochannel sample P25 5-6m, <0.2 μm.

Illite and palygorskite. Negs. 021956 and 021954.

Scale bars: 0.5 μm (upper) and 0.2 μm (lower).

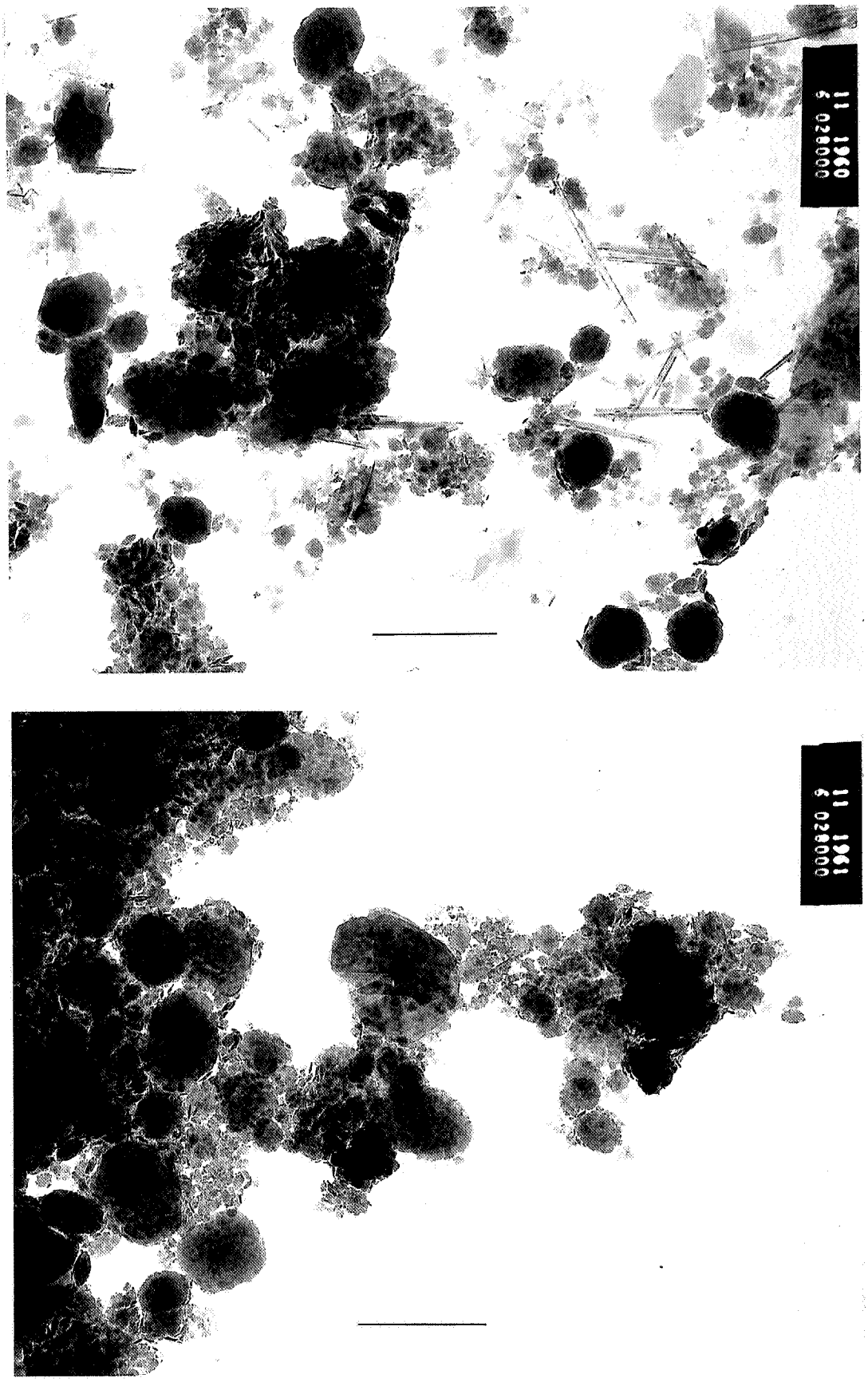


Plate 2. Garford palaeochannel sample P25 5-6m, 0.2 to 0.5 μm.
Illite with minor palygorskite. Negs. 021960 and 021961.
Scale bars: 0.5 μm (upper and lower).



Plate 3. Garford palaeochannel sample P25 5-6m, >0.5 µm.

Illite and quartz. Neg. 0315.

Scale bar: 2 µm.

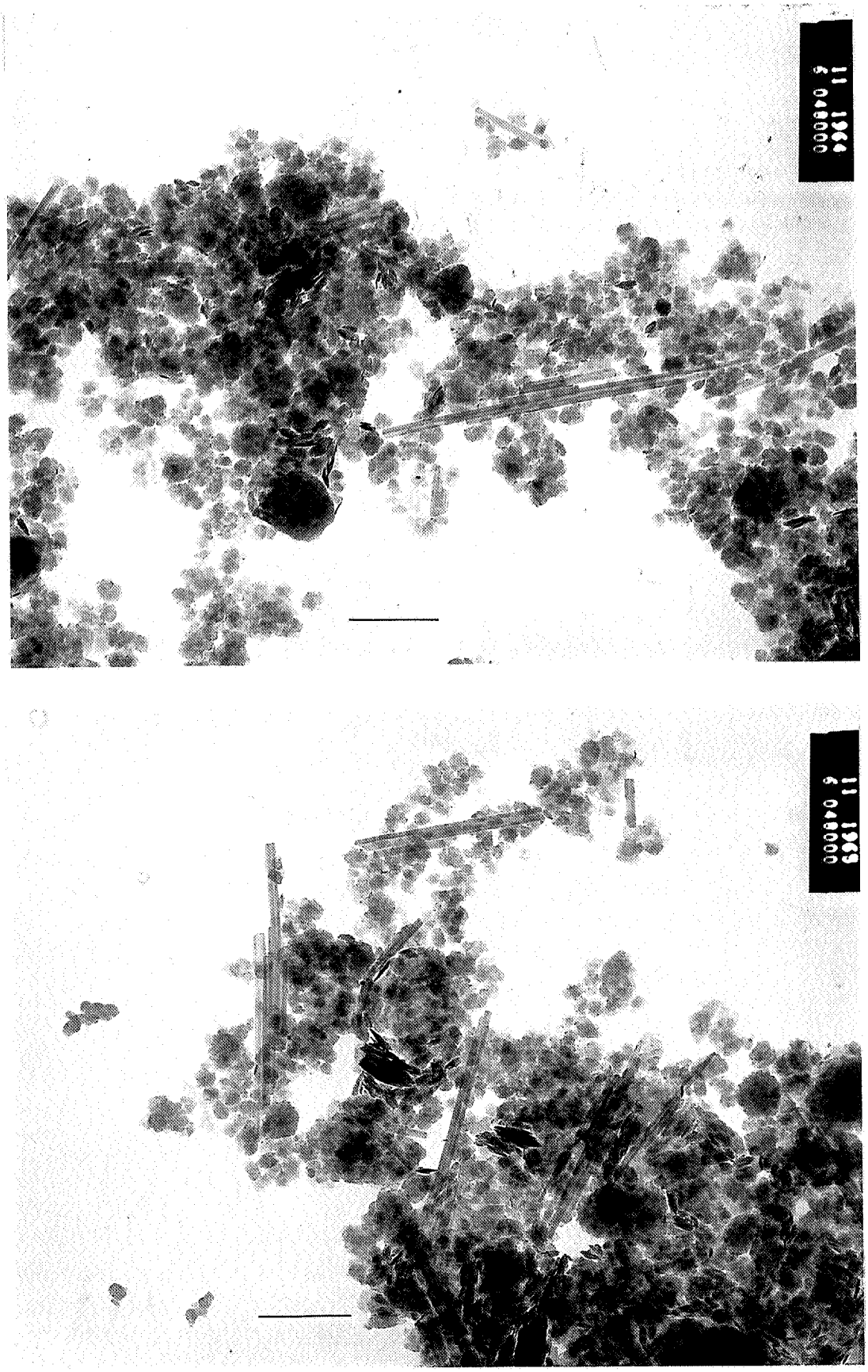


Plate 4. Garford palaeochannel sample P25 6-7m, <0.2 µm.

Illite and palygorskite. Negs. 021964 and 021965.

Scale bars: 0.2 µm (upper and lower).

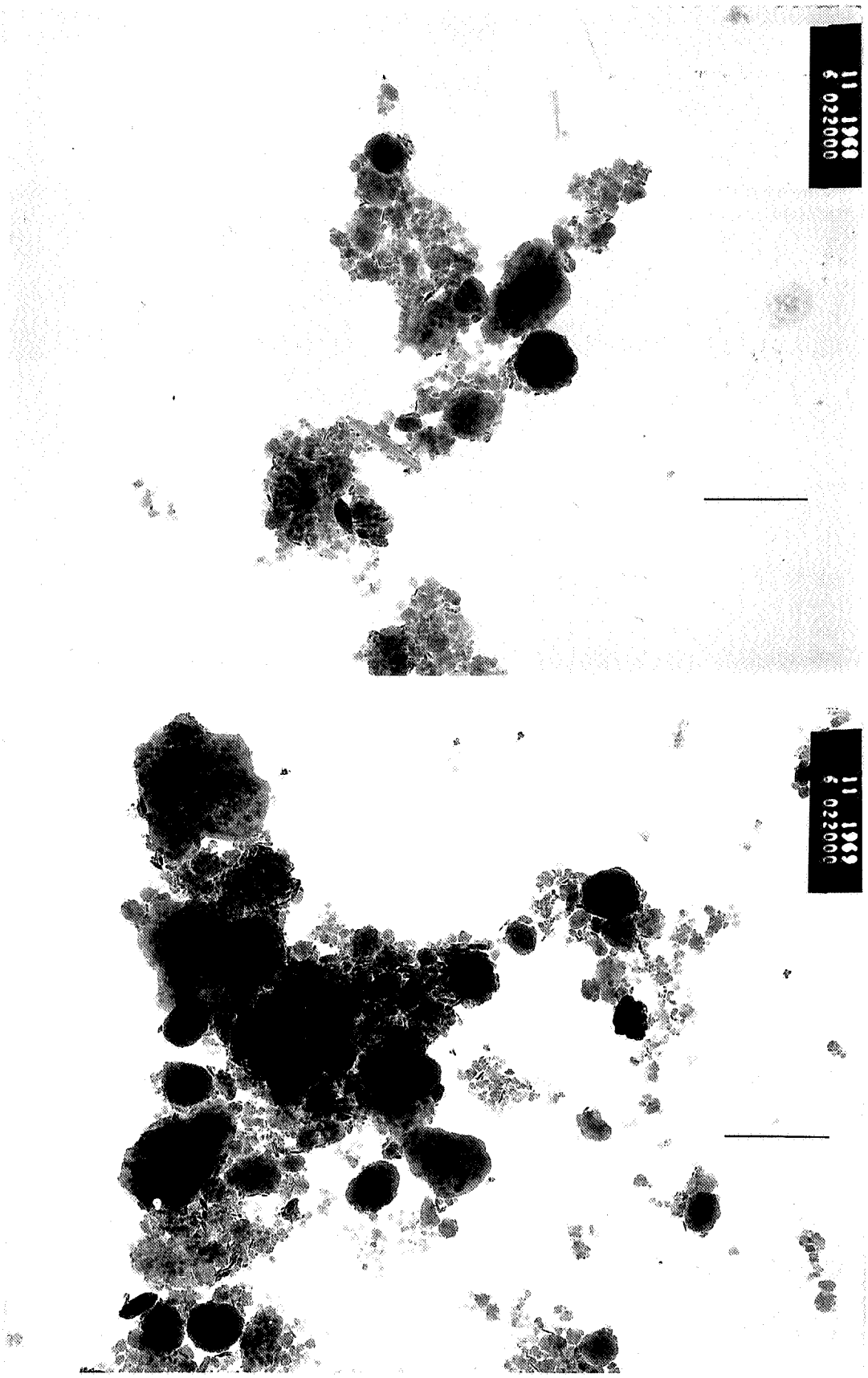


Plate 5. Garford palaeochannel sample P25 6-7m, 0.2 to 0.5 µm.

Kaolinite, illite and minor palygorskite. Negs. 021968 and 021969.

Scale bars: 0.5 µm (upper and lower).

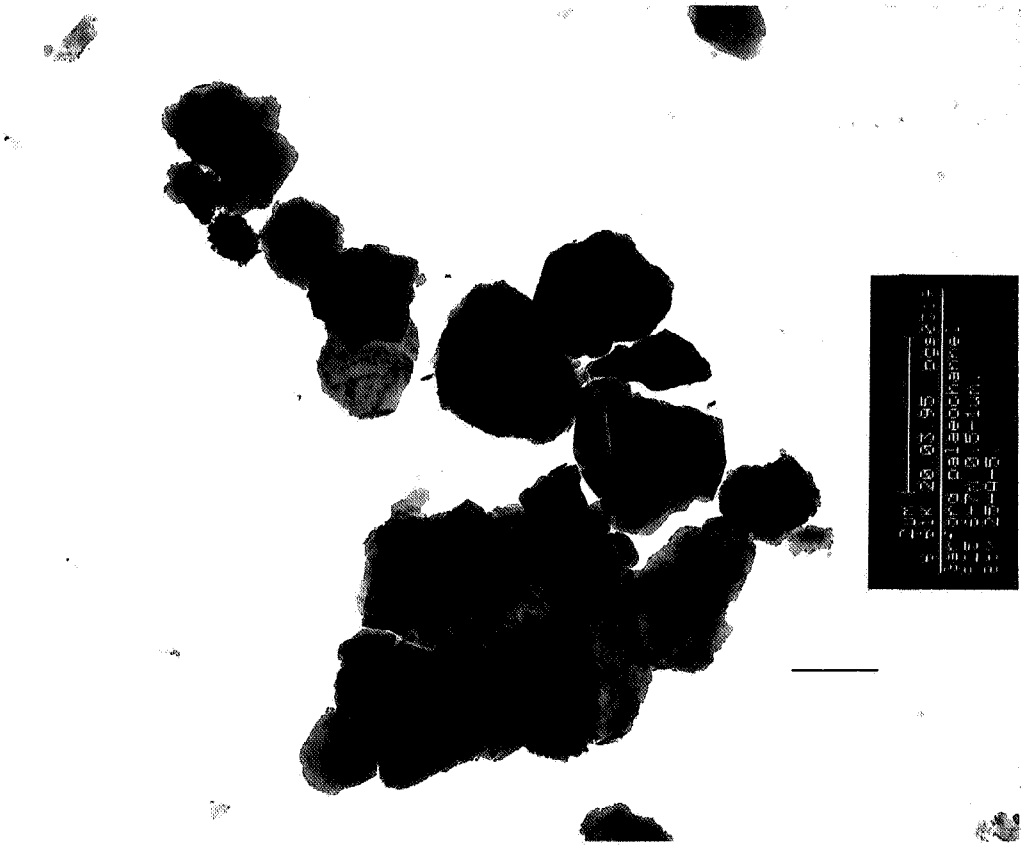


Plate 6. Garford palaeochannel sample P25 6-7m, 0.5 to 1 μm.

Kaolinite, illite and quartz. Neg. 0319.

Scale bar: 1 μm.



Plate 7. Garford palaeochannel sample P25 6-7m, 1 to 2 μm.

Kaolinite, illite and minor palygorskite. Neg. 0321.

Scale bar: 2 μm.

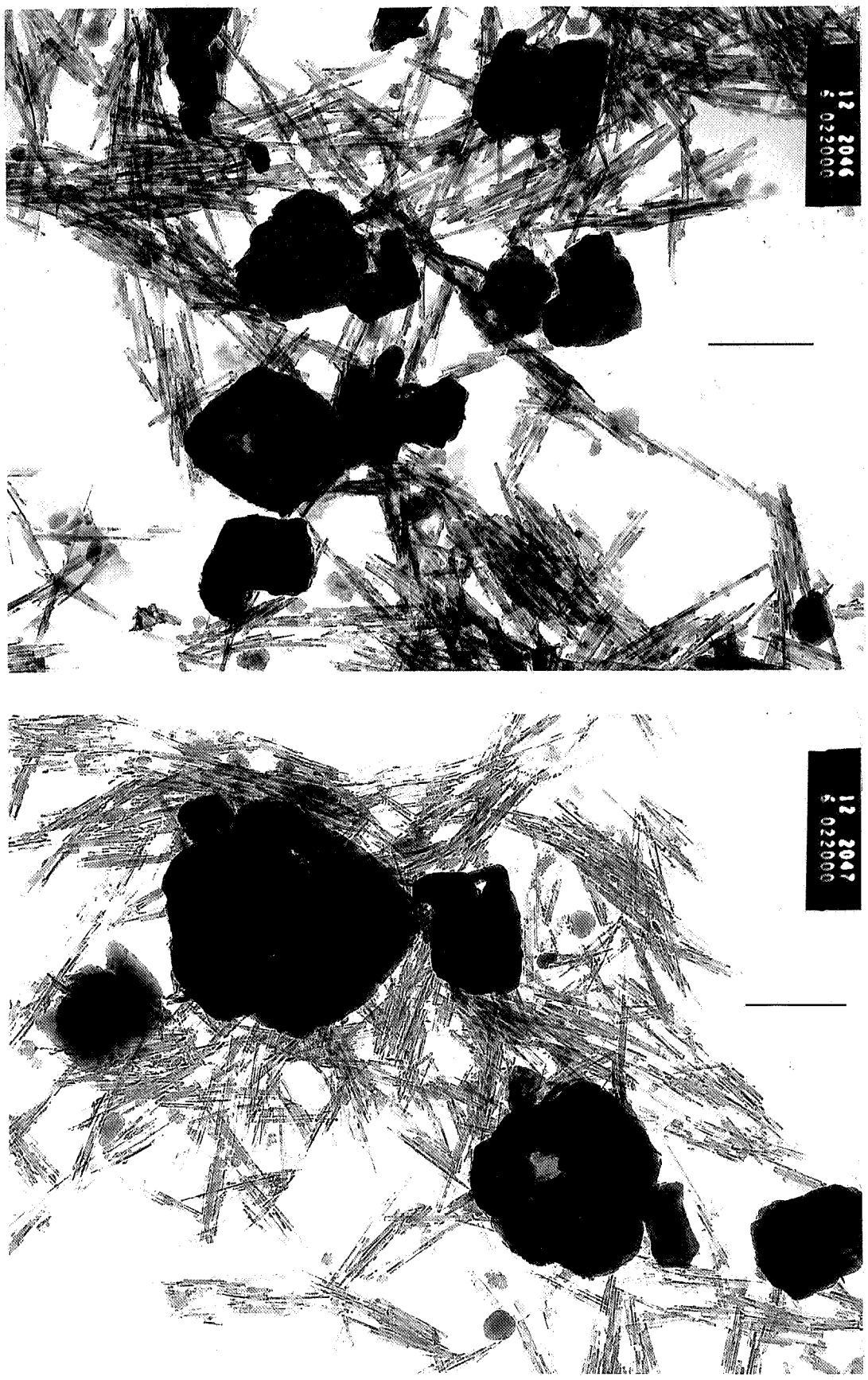


Plate 8. Garford palaeochannel sample P31 2-3m, 0.5 to 1 μm.

Dolomite, palygorskite, illite and celestine. Negs. 022046 and 022047.

Scale bars: 0.5 μm (upper and lower).

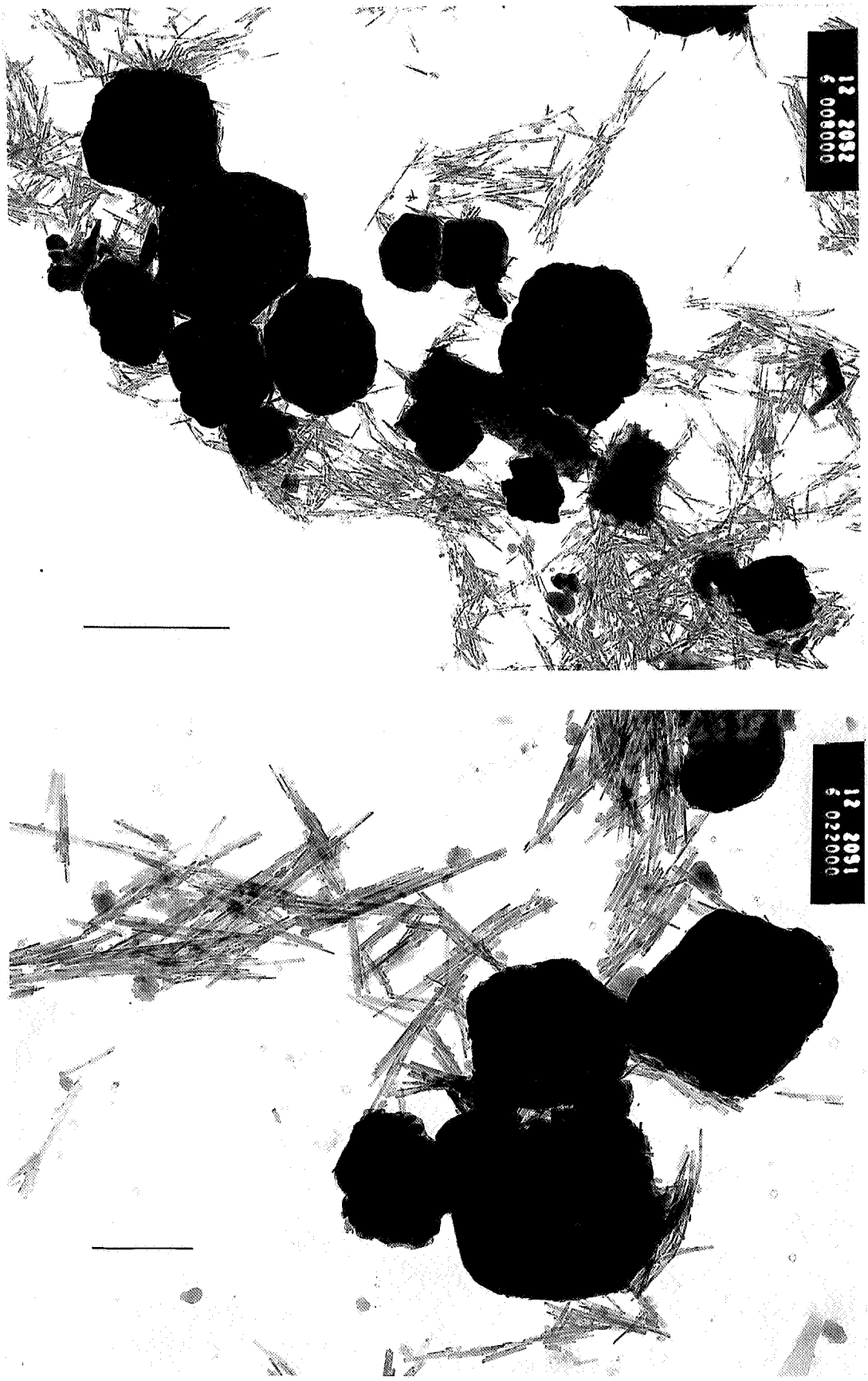


Plate 9. Garford palaeochannel sample P31 2-3m, 1 to 2 μm.

Dolomite, palygorskite and illite. Negs. 022052 and 022051.

Scale bars: 2 μm (upper) and 0.5 μm (lower).

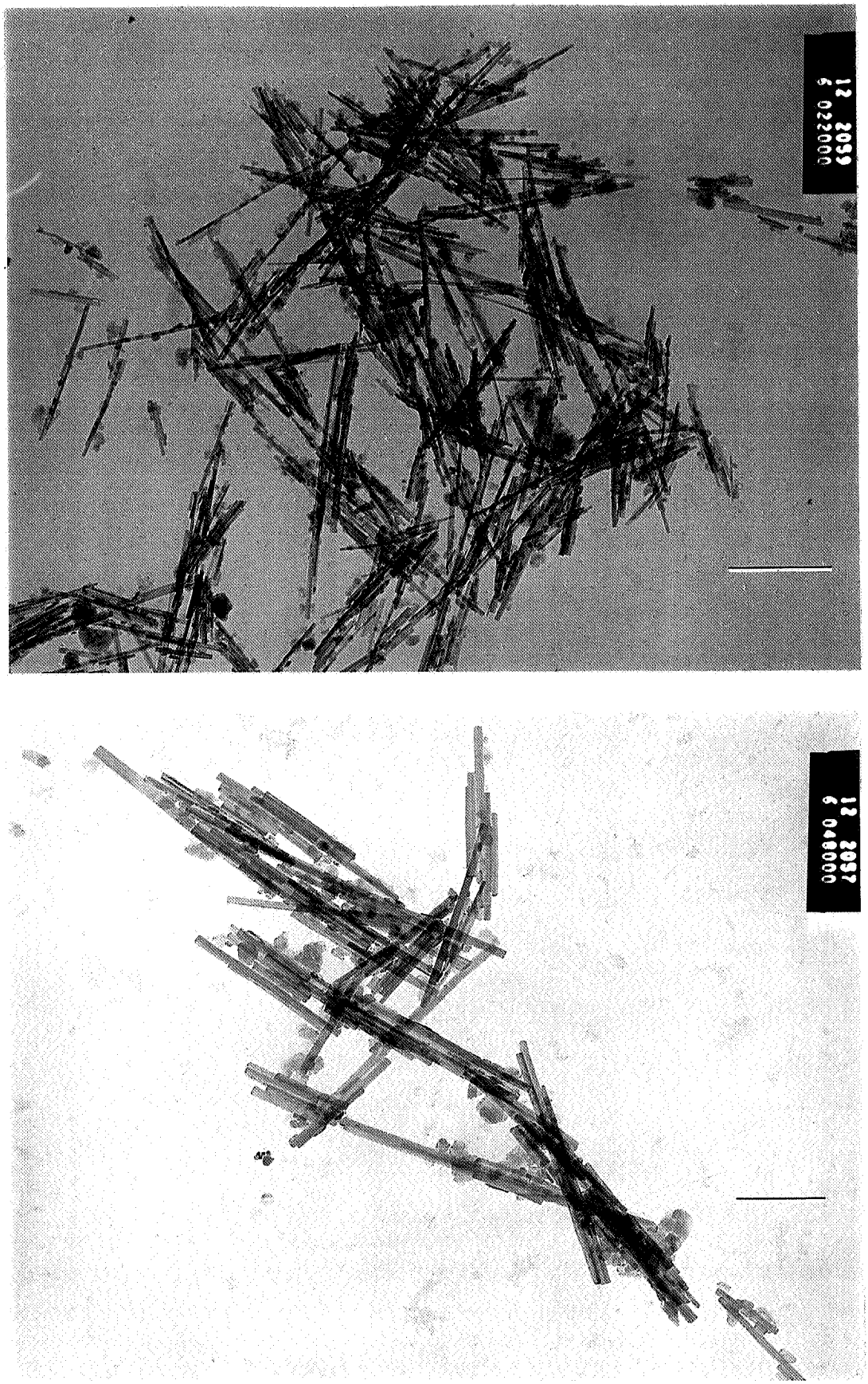


Plate 10. Garford palaeochannel sample P33 0-1m, <0.2 μm.

Palygorskite and illite. Negs. 022059 and 022057.

Scale bars: 0.5 μm (upper) and 0.2 μm (lower).

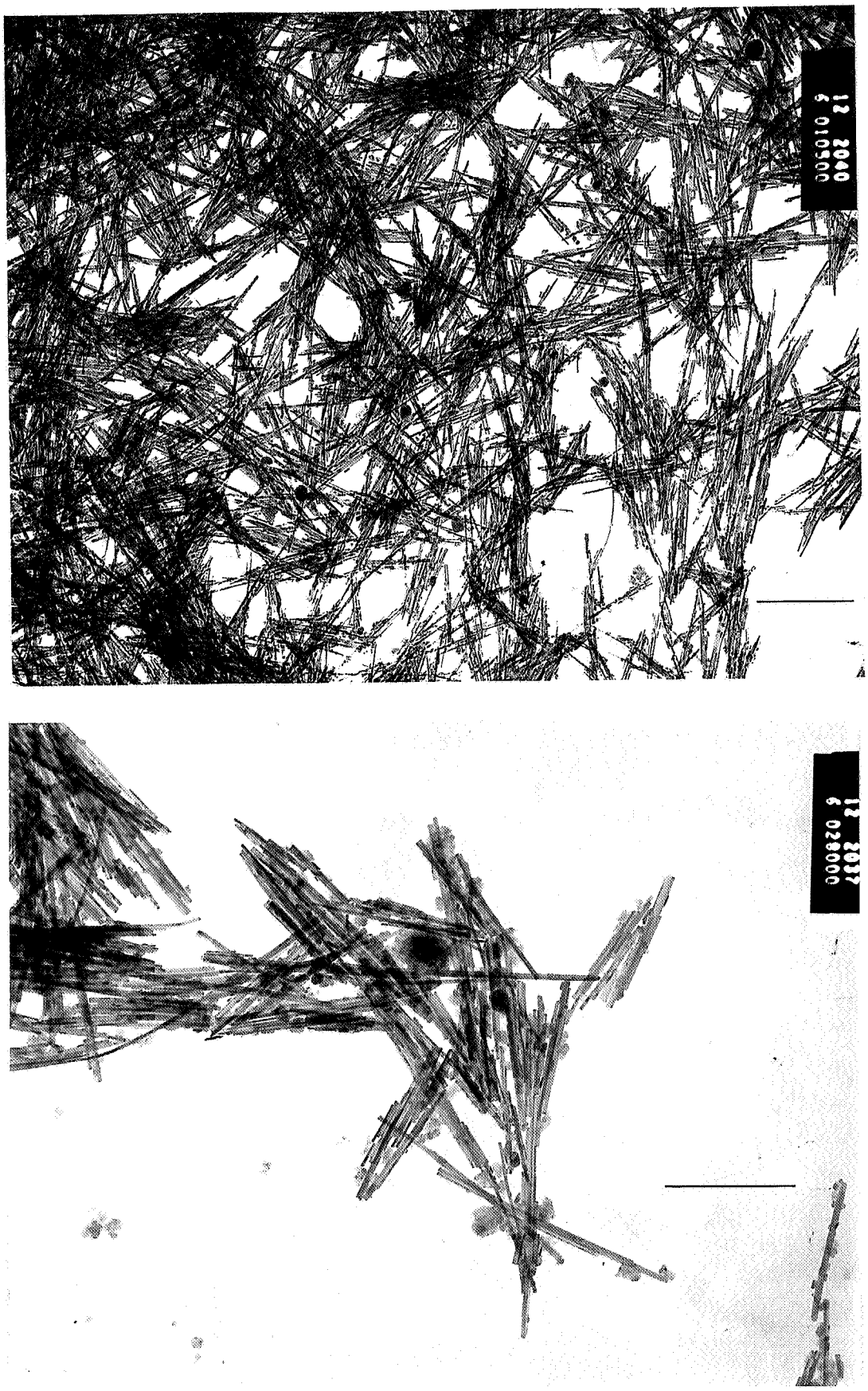


Plate 11. Garford palaeochannel sample P33 0-1m, 0.5 to 1 μm.

Palygorskite and illite. Negs. 022040 and 022037.

Scale bars: 1 μm (upper) and 0.5 μm (lower).

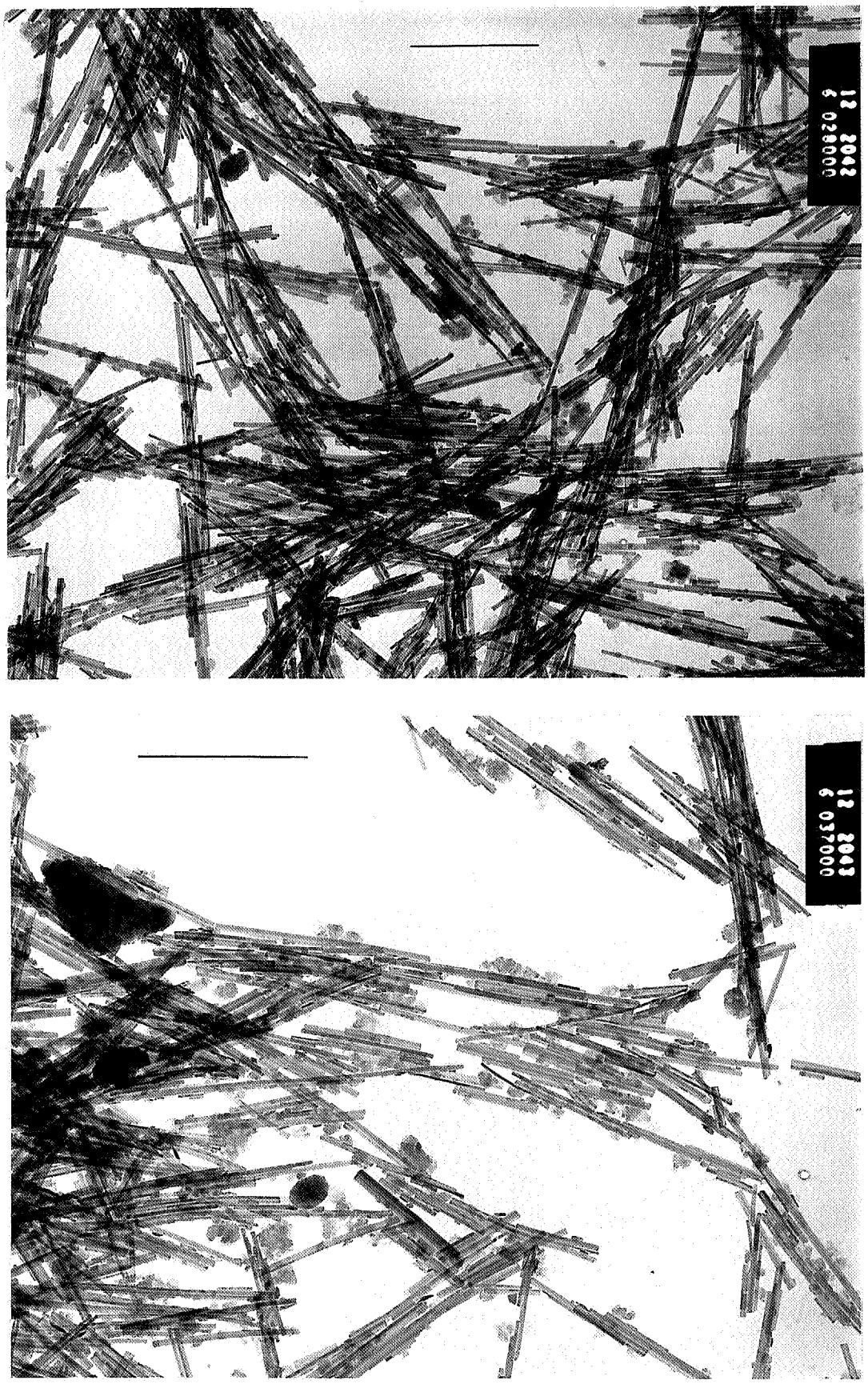


Plate 12. Garford palaeochannel sample P33 0-1m, 1 to 2 μm.

Palygorskite and illite. Negs. 022042 and 022043.

Scale bars: 0.5 μm (upper and lower).

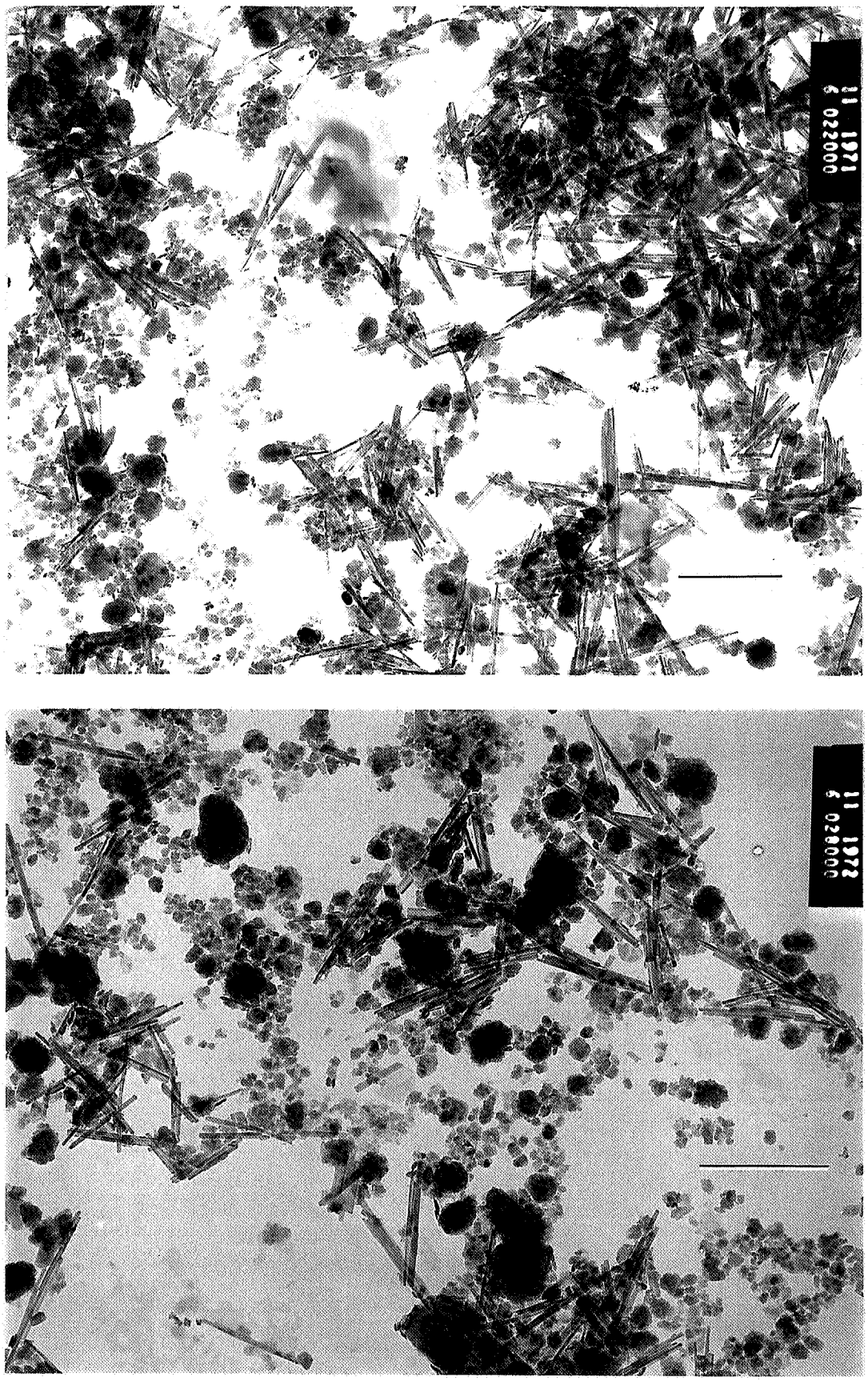


Plate 13. Garford palaeochannel sample P35 5-6m, <0.2 µm.

Illite and palygorskite. Negs. 021971 and 021972.

Scale bars: 0.5 µm (upper and lower).

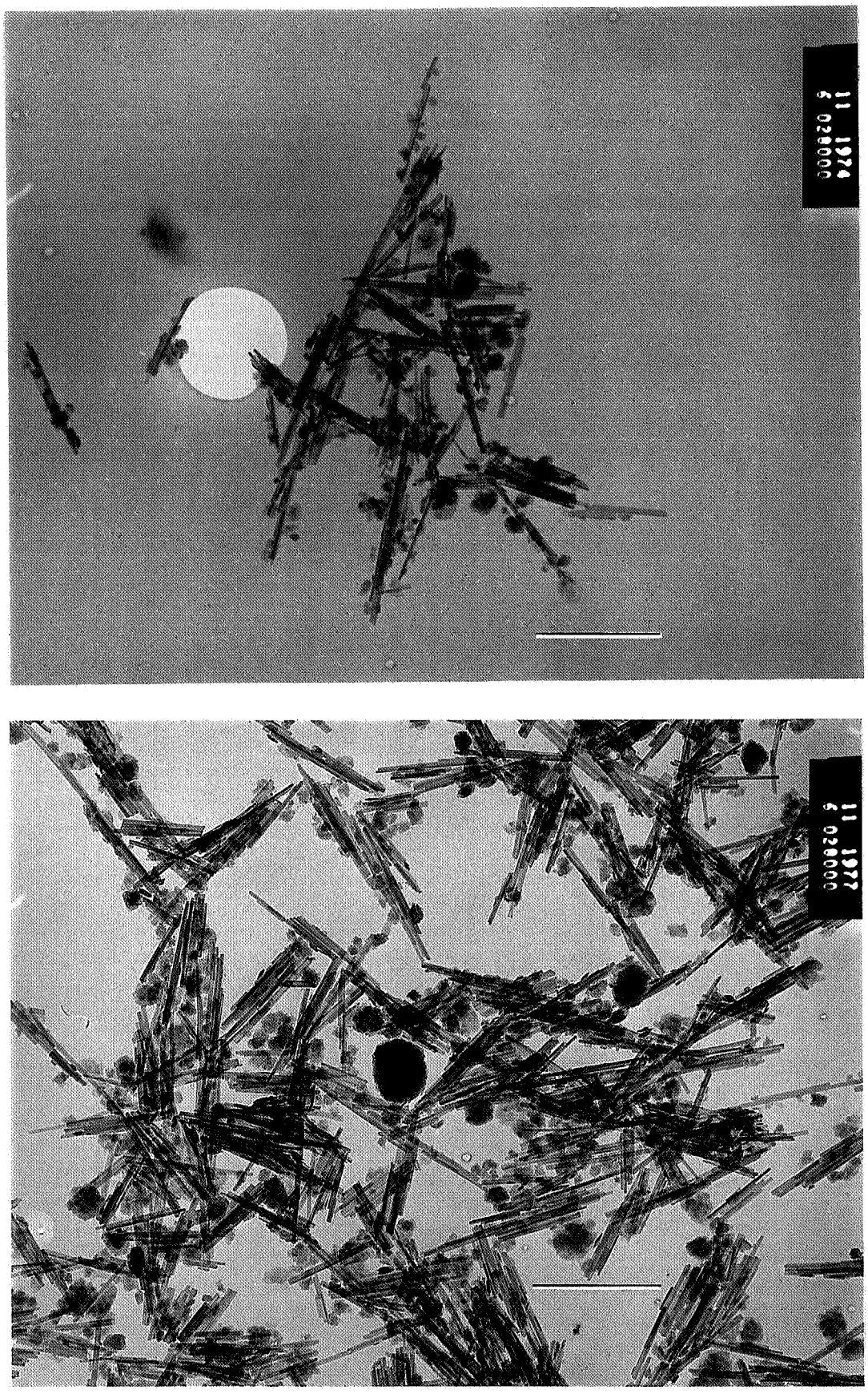


Plate 14. Garford palaeochannel sample P35 5-6m, 0.2 to 0.5 μm.

Palygorskite and illite. Negs. 021974 and 021977.

Scale bars: 0.5 μm (upper and lower).

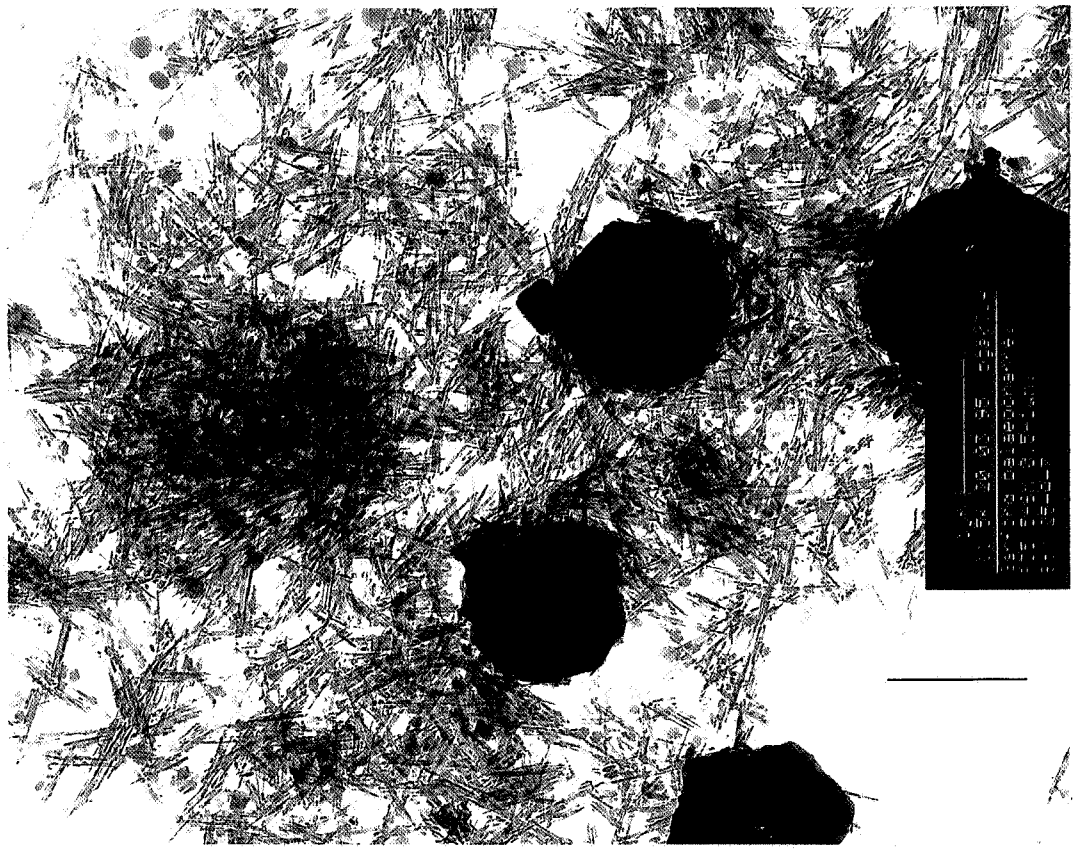


Plate 15. Garford palaeochannel sample P35 5-6m, 0.5 to 1 μm.

Dolomite, palygorskite and illite. Neg. 0324.

Scale bar: 1 μm.

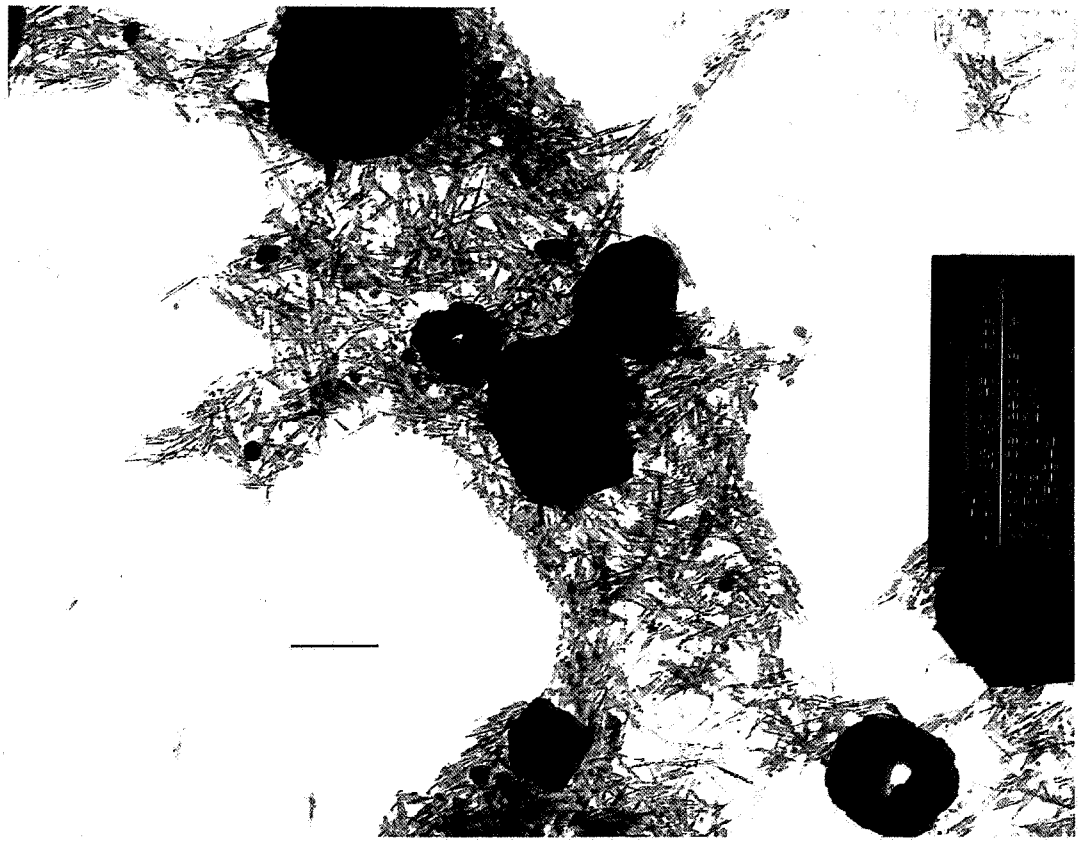


Plate 16. Garford palaeochannel sample P35 5-6m, 1 to 2 μm.

Dolomite and palygorskite. Neg. 0325.

Scale bar: 1 μm.



Plate 17. Garford palaeochannel sample P35 6-7m, <0.2 µm.

Palygorskite and illite. Negs. 021978 and 021979.

Scale bars: 0.5 µm (upper and lower).

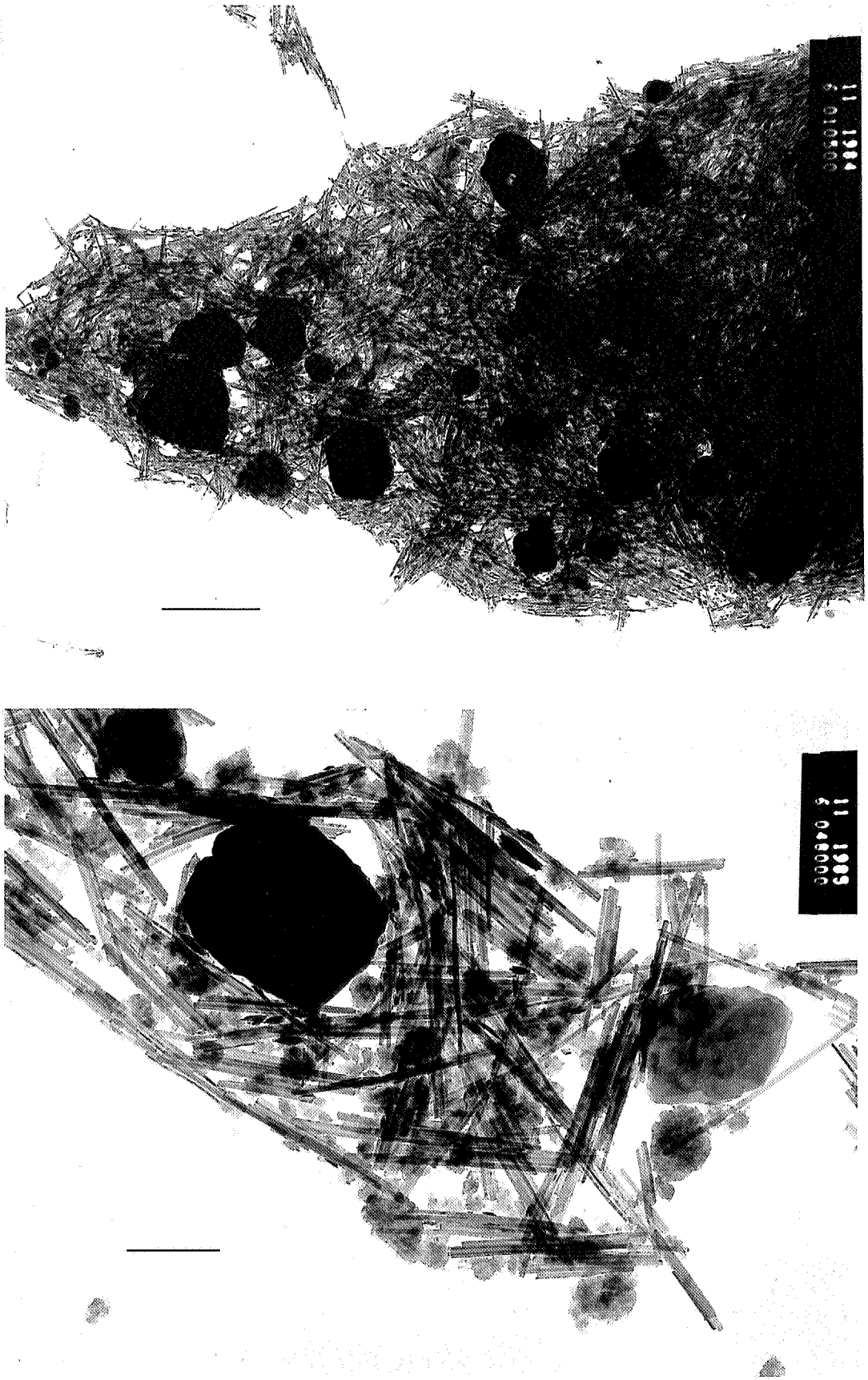


Plate 18. Garford palaeochannel sample P35 6-7m, 0.2 to 0.5 μm.
Dolomite, palygorskite and illite. Negs. 021984 and 0221985.
Scale bars: 1 μm (upper) and 0.2 μm (lower).

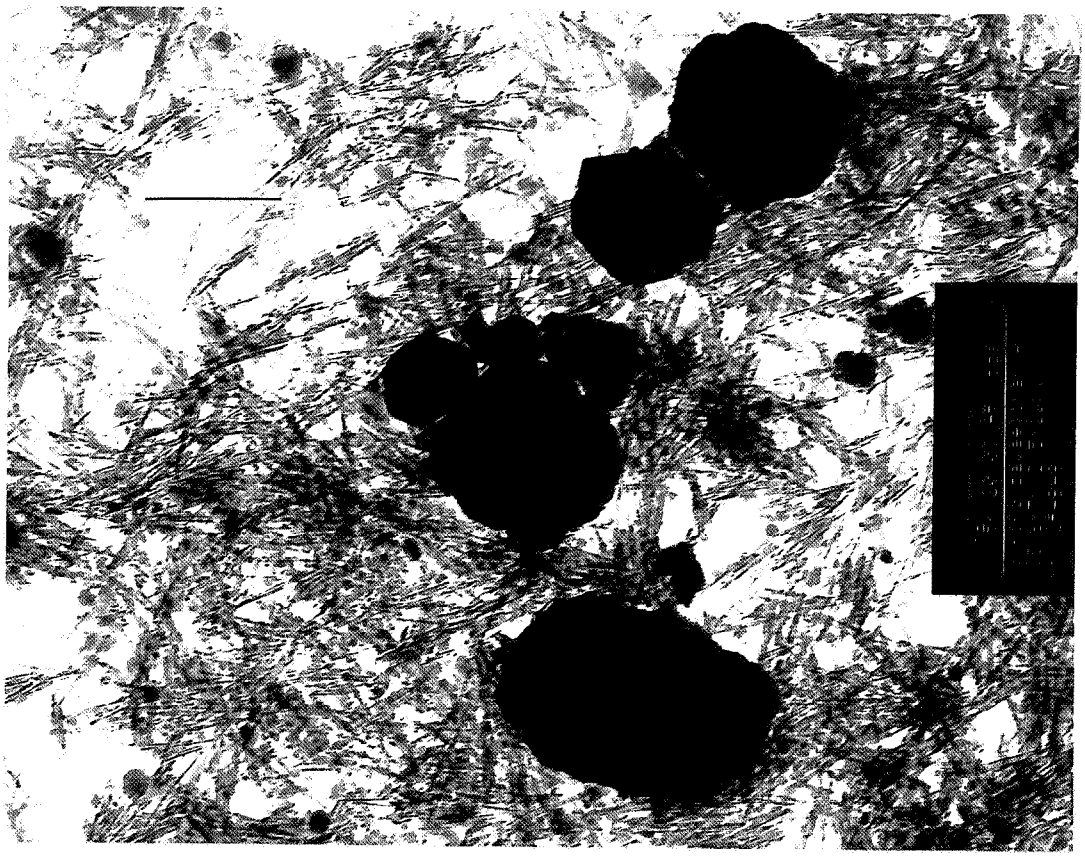


Plate 19. Garford palaeochannel sample P35 6-7m, 0.5 to 1 μm.

Dolomite and palygorskite. Neg. 0328.

Scale bar: 1 μm.



Plate 20. Garford palaeochannel sample P35 6-7m, 1 to 2 μm.

Dolomite and palygorskite. Neg. 0330.

Scale bar: 1 μm.

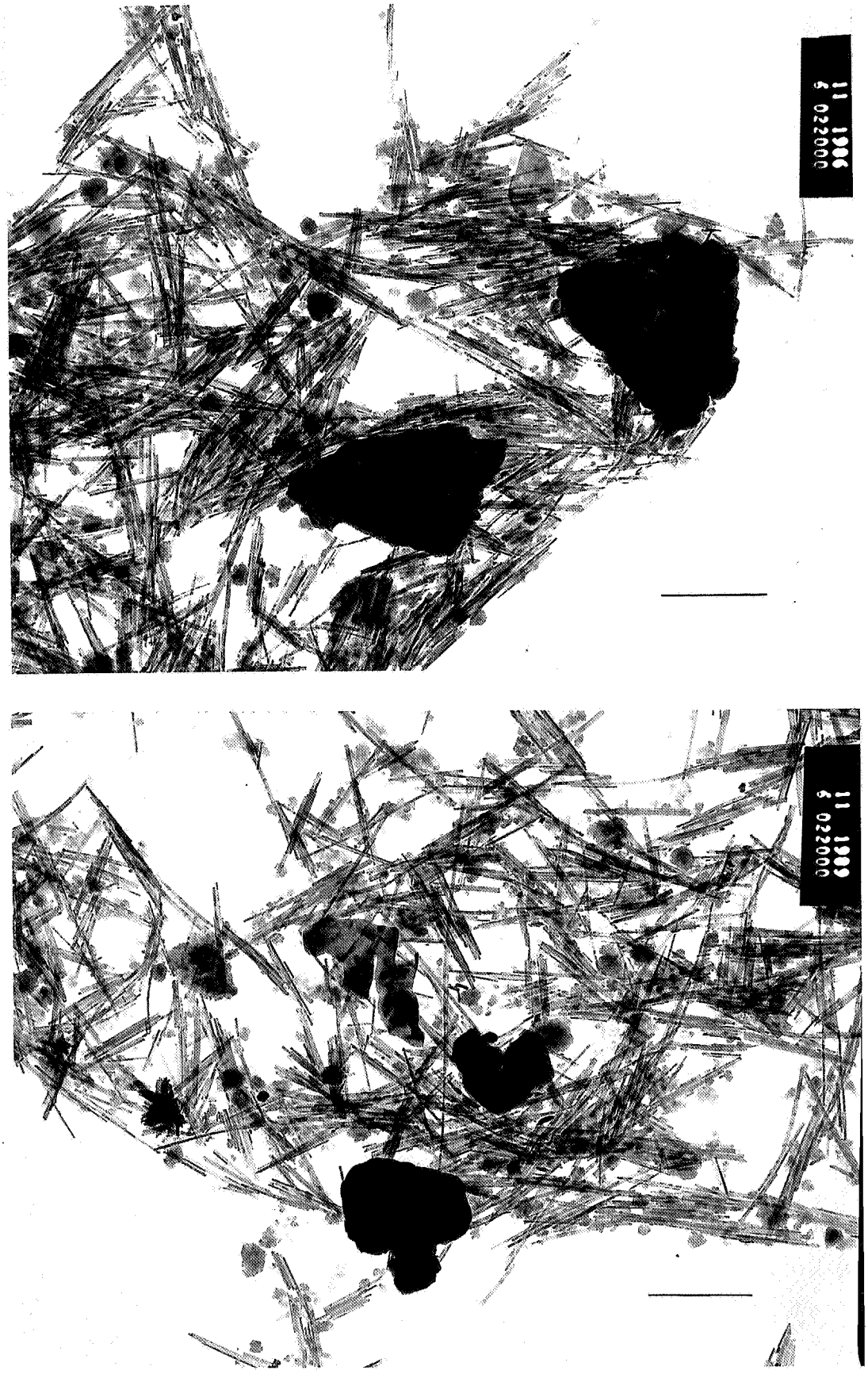


Plate 21. Garford palaeochannel sample P42 3-4m, <0.5 μm.

Dolomite, palygorskite, illite and kaolinite. Negs. 021986 and 021989.

Scale bars: 0.5 μm (upper and lower).

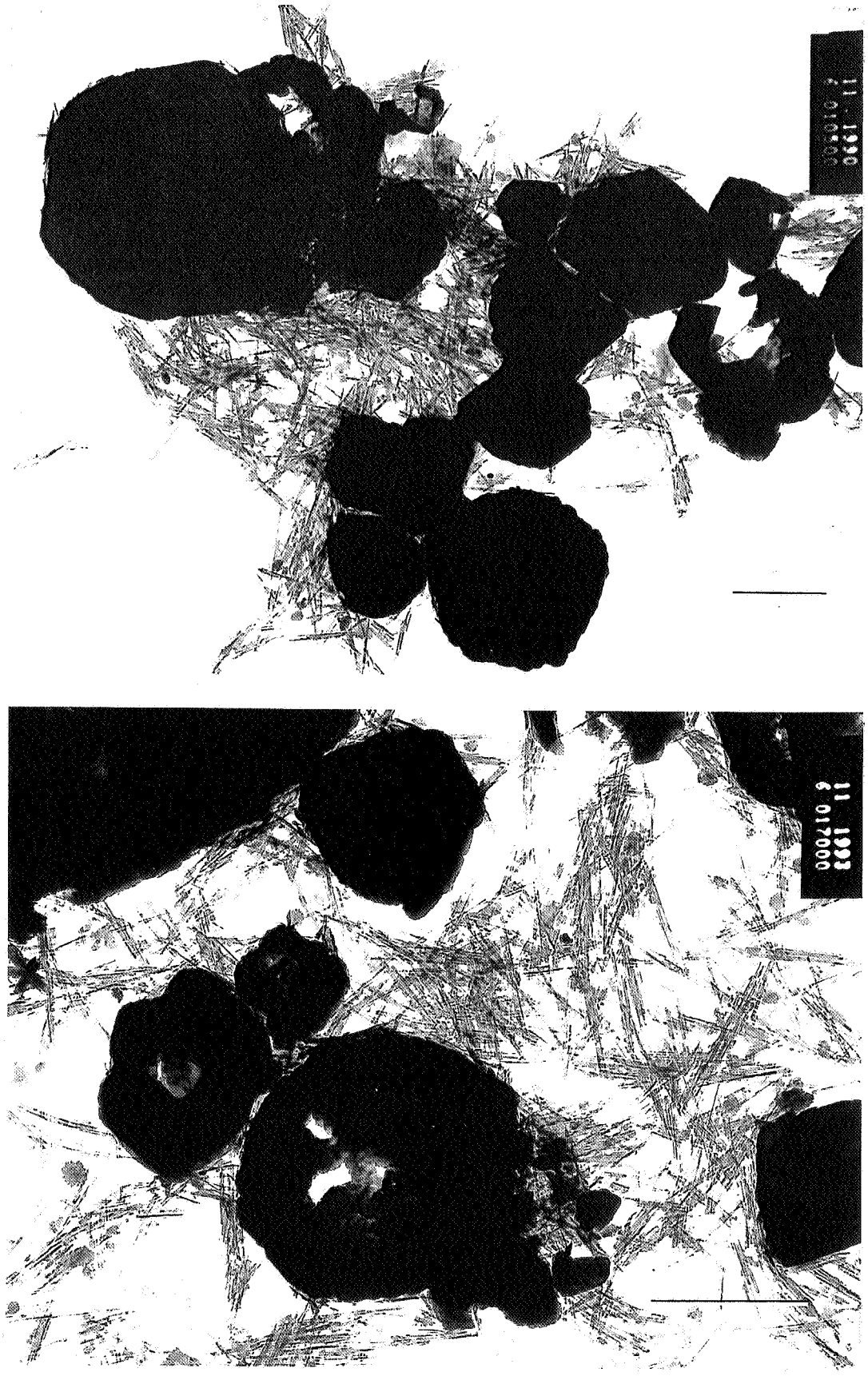


Plate 22. Garford palaeochannel sample P42 3-4m, 0.5 to 1 μm.

Dolomite, palygorskite and illite. Negs. 021990 and 021993.

Scale bars: 1 μm (upper and lower).

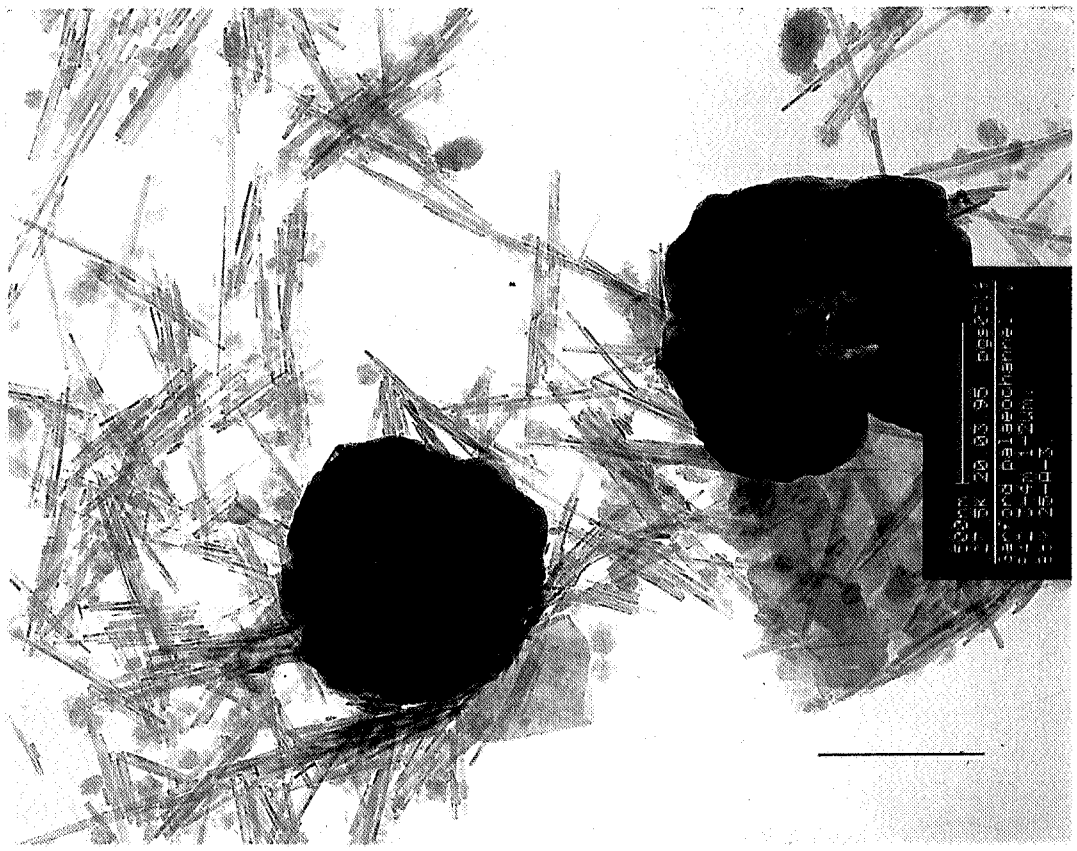


Plate 23. Garford palaeochannel sample P42 3-4m, 1 to 2 μm.

Dolomite, palygorskite and illite. Neg. 0318.

Scale bar: 0.5 μm.



Plate 24. Garford palaeochannel sample P42 4-5m, <0.5 μm.

Dolomite, palygorskite and illite. Negs. 021997 and 021996.

Scale bars: 1 μm (upper) and 0.5 μm (lower).

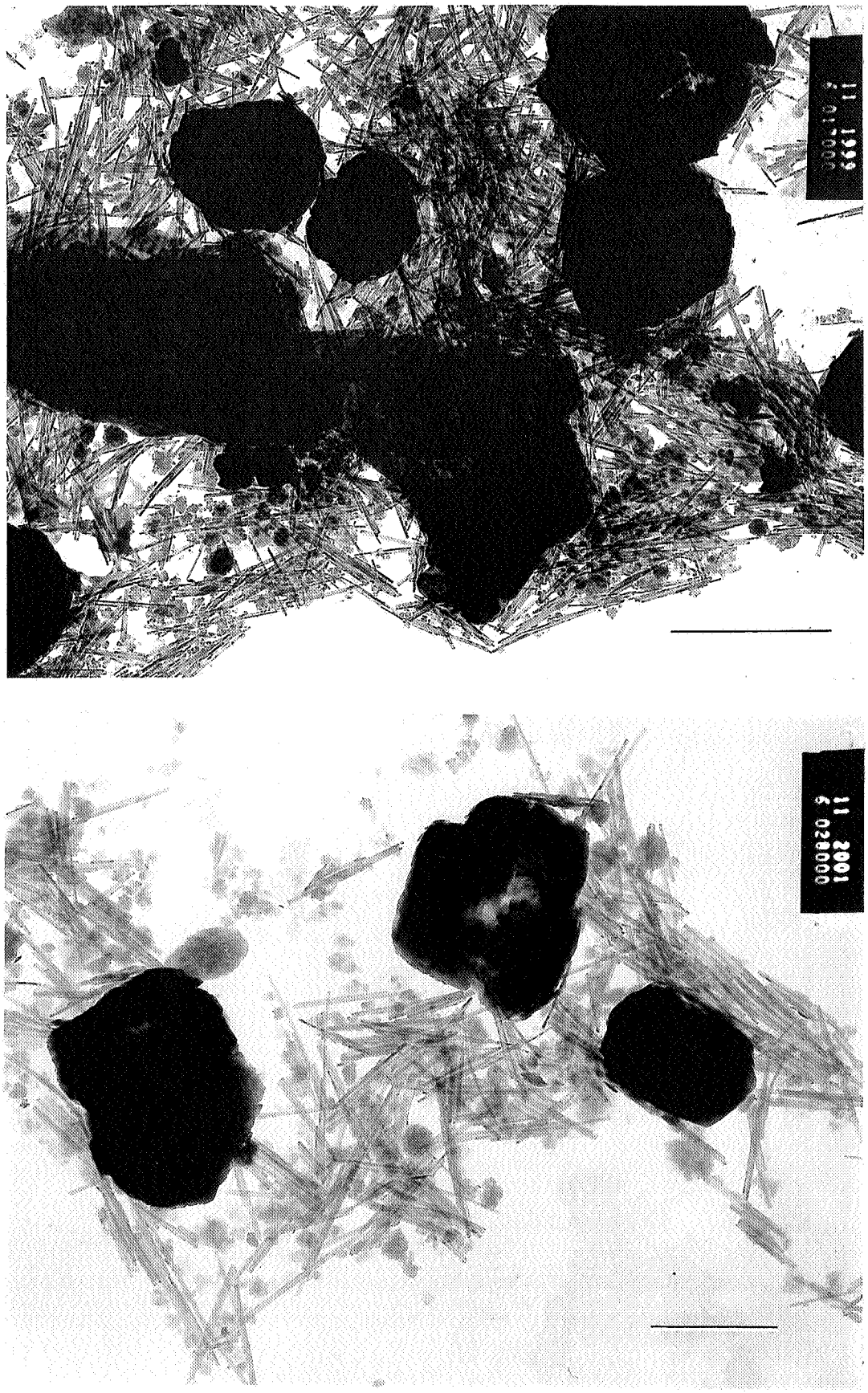


Plate 25. Garford palaeochannel sample P42 4-5m, 0.5 to 1 µm.

Dolomite, palygorskite and illite. Negs. 021999 and 02001.

Scale bars: 1 µm (upper) and 0.5 µm (lower).

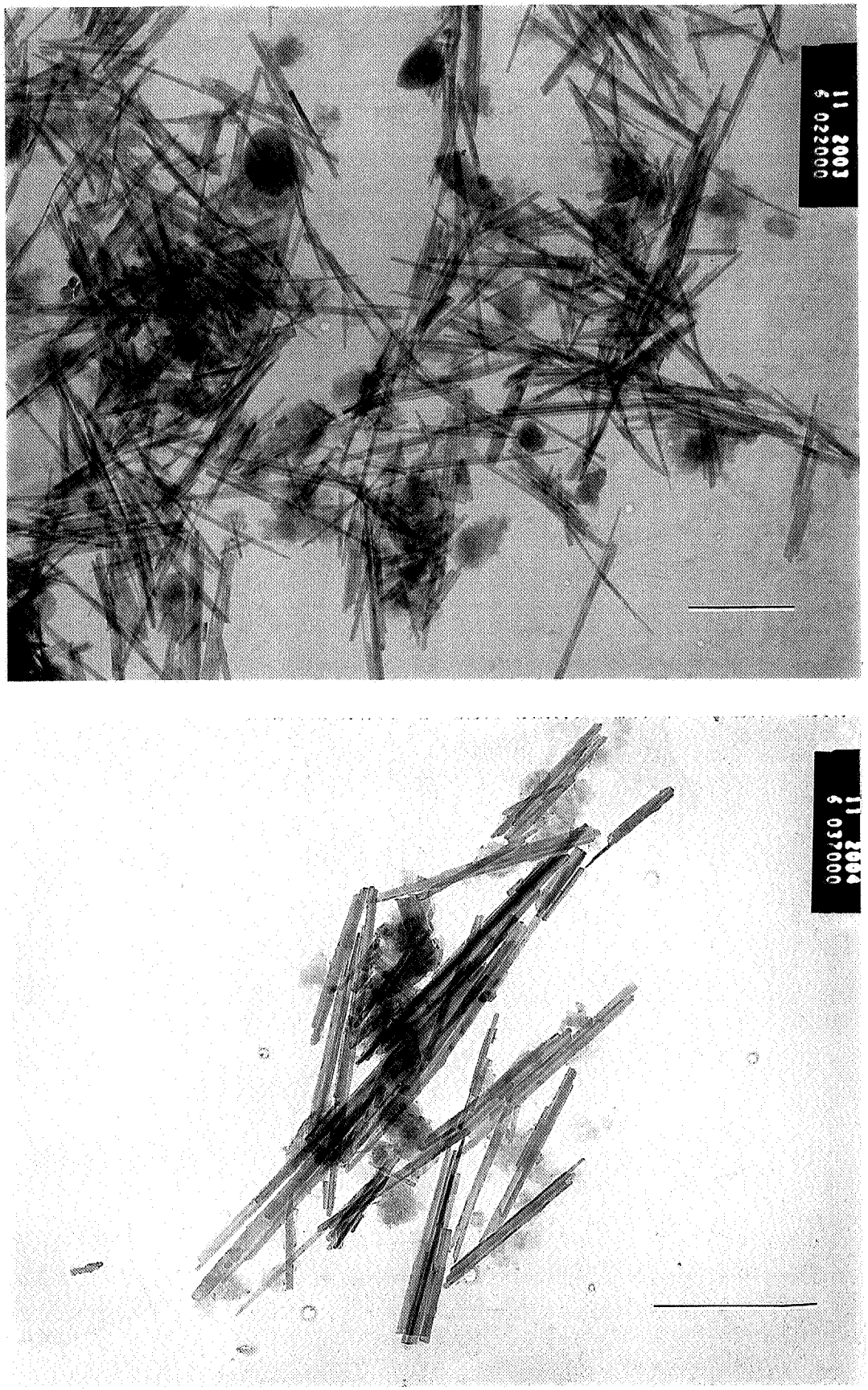


Plate 26. Chinese attapulgite - anti-salt bentonite, <0.2 µm.

Palygorskite, illite and smectite. Negs. 022003 and 022004.

Scale bars: 0.5 µm (upper and lower).

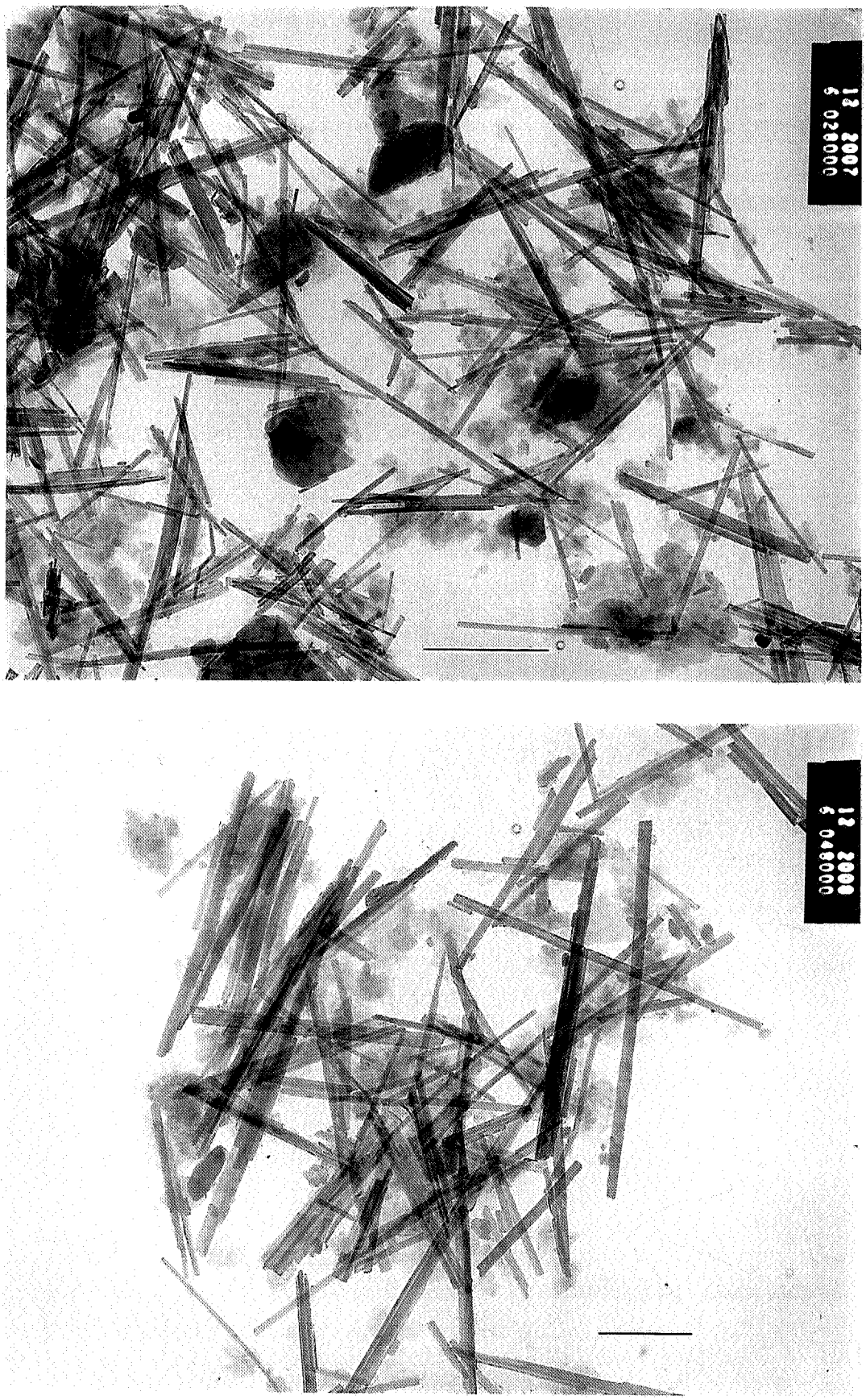


Plate 27. Chinese attapulgite - anti-salt bentonite, 0.2 to 0.5 μm.
Palygorskite, illite and smectite. Negs. 022007 and 022008.
Scale bars: 0.5 μm (upper) and 0.2 μm (lower).

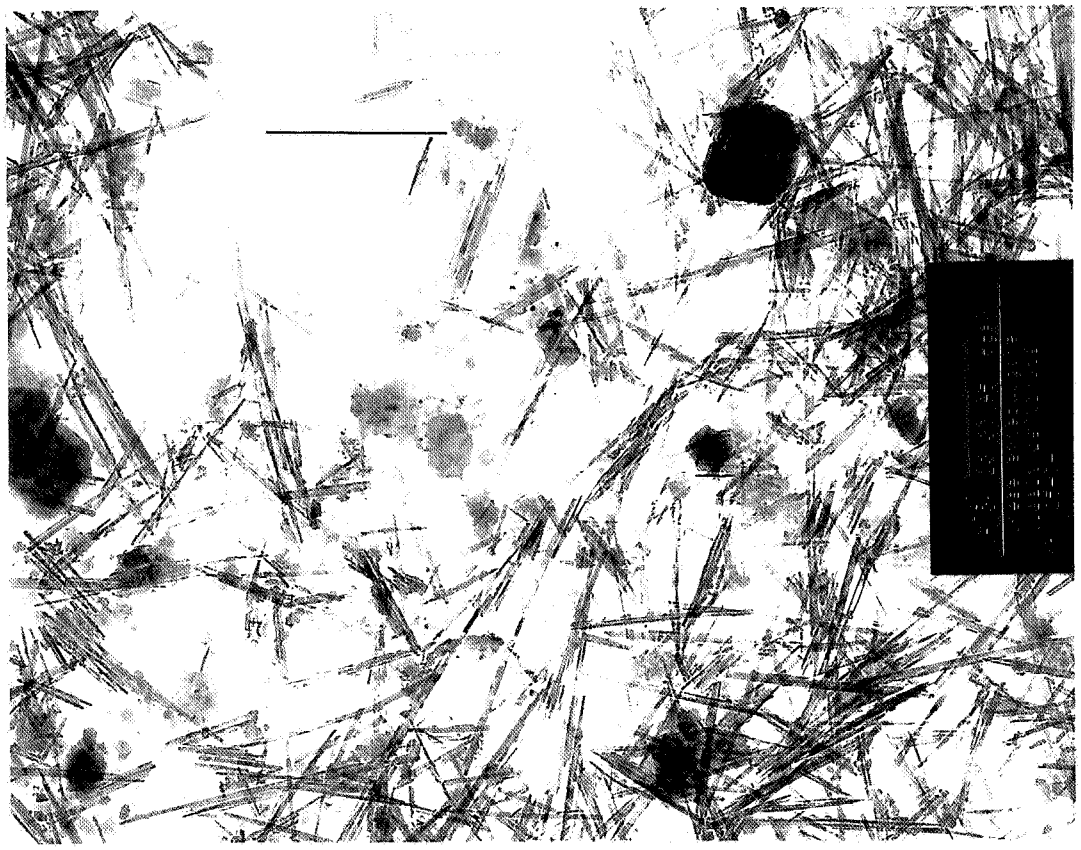


Plate 28. Chinese attapulgite - anti-salt bentonite, 0.5 to 1 µm.

Palygorskite, illite and smectite. Neg. 0331.

Scale bar: 1 µm.

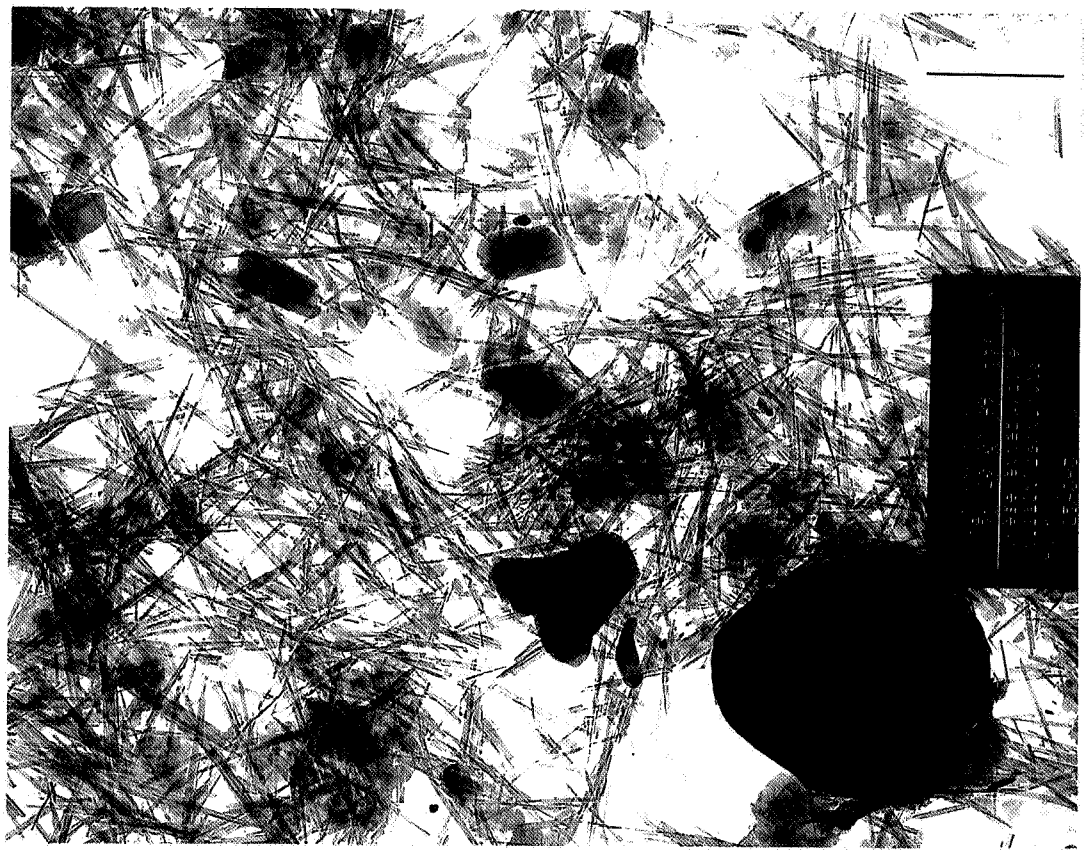


Plate 29. Chinese attapulgite - anti-salt bentonite, 1 to 2 μm.

Palygorskite, illite and smectite. Neg. 0334.

Scale bar: 1 μm.

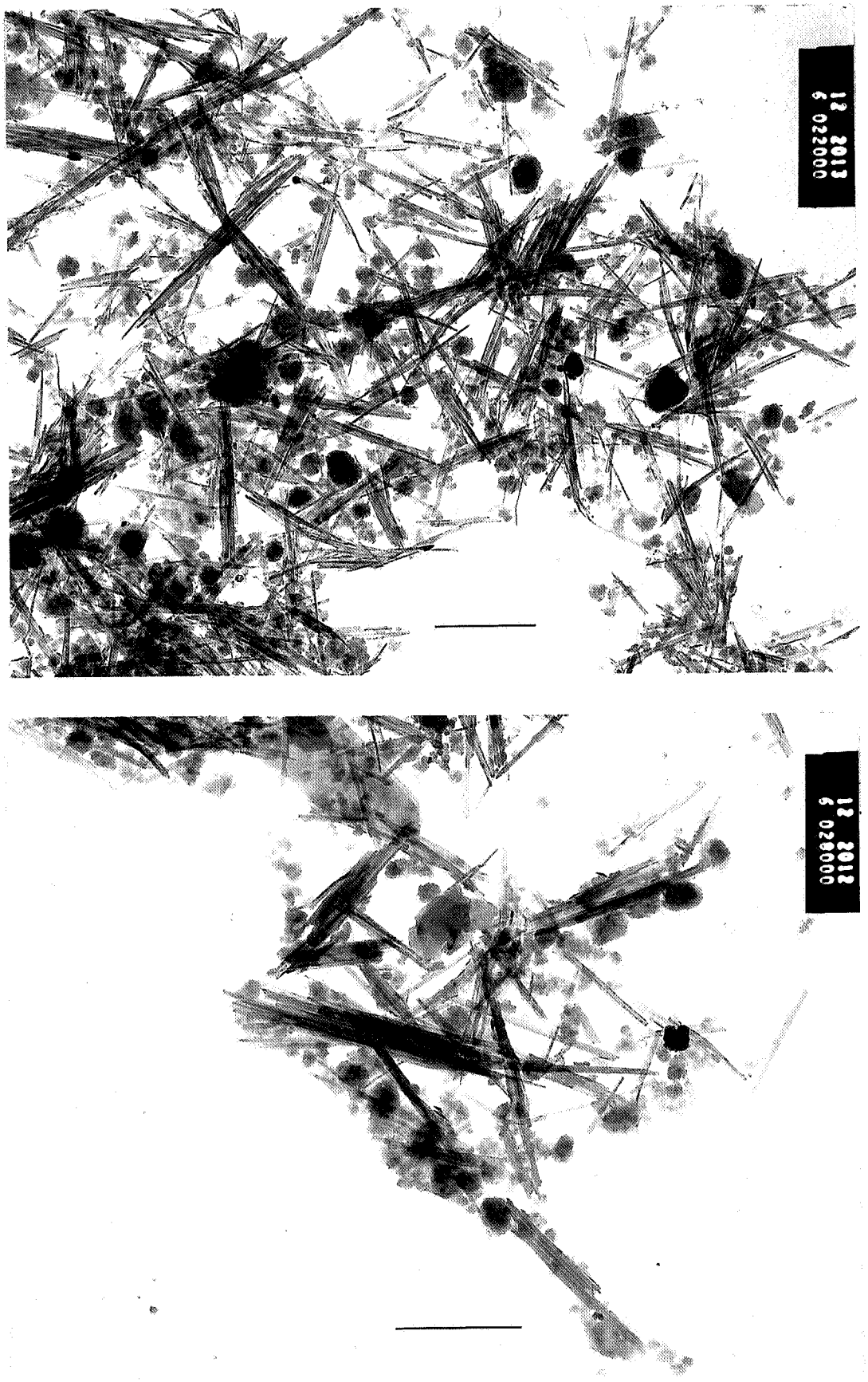


Plate 30. Lake Nerramyne attapulgite, <0.2 μm.

Palygorskite, illite and kaolinite. Negs. 022013 and 022012.

Scale bars: 0.5 μm (upper and lower).

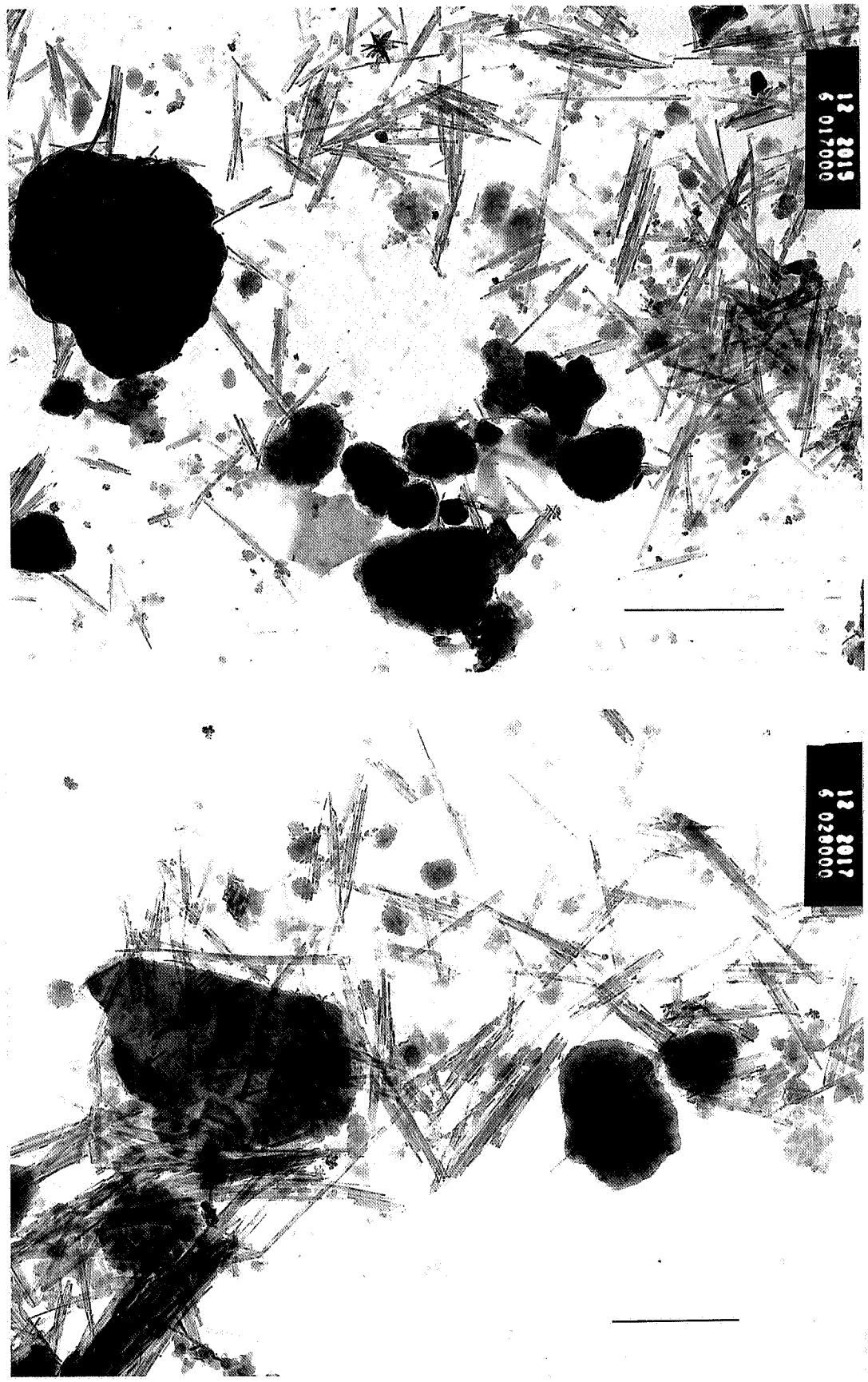


Plate 31. Lake Nerramyne attapulgite, 0.2 to 0.5 μm.

Palygorskite, illite and kaolinite. Negs. 022015 and 022017.

Scale bars: 1 μm (upper) and 0.5 μm (lower).

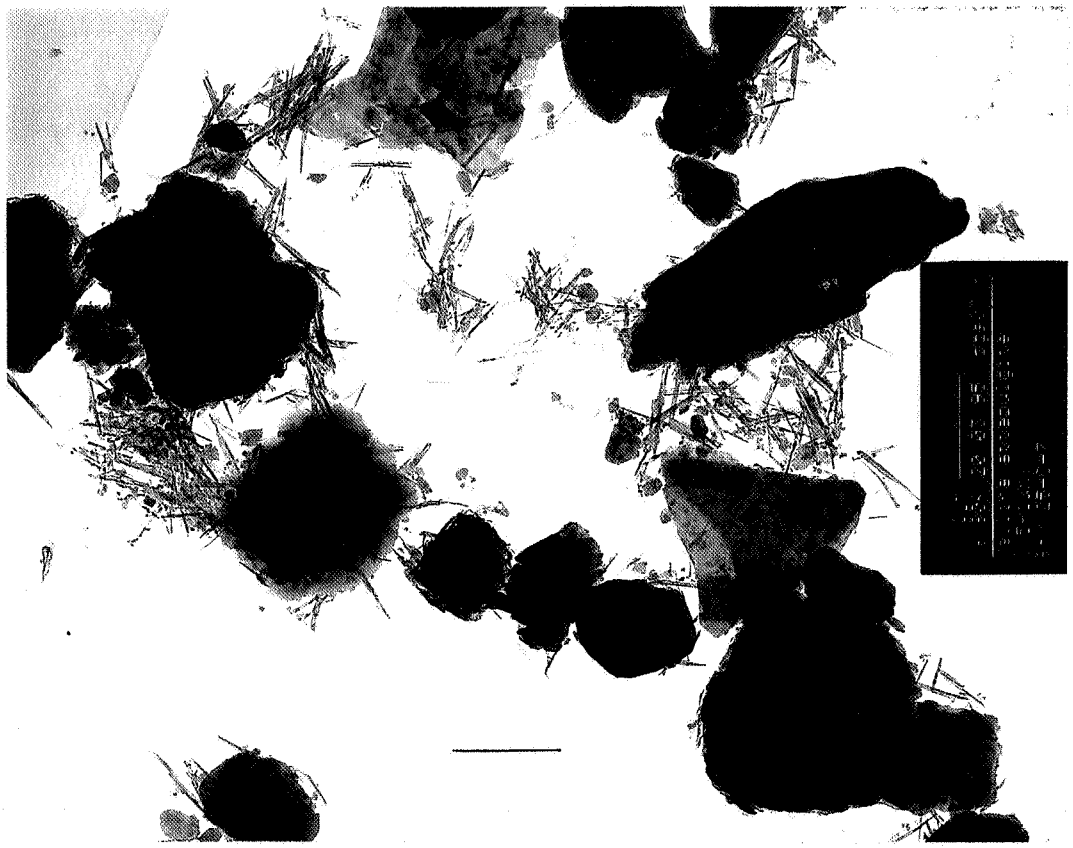


Plate 32. Lake Nerramyne attapulgite, 0.5 to 1 μm.

Palygorskite, illite and kaolinite. Neg. 0335.

Scale bar: 1 μm.

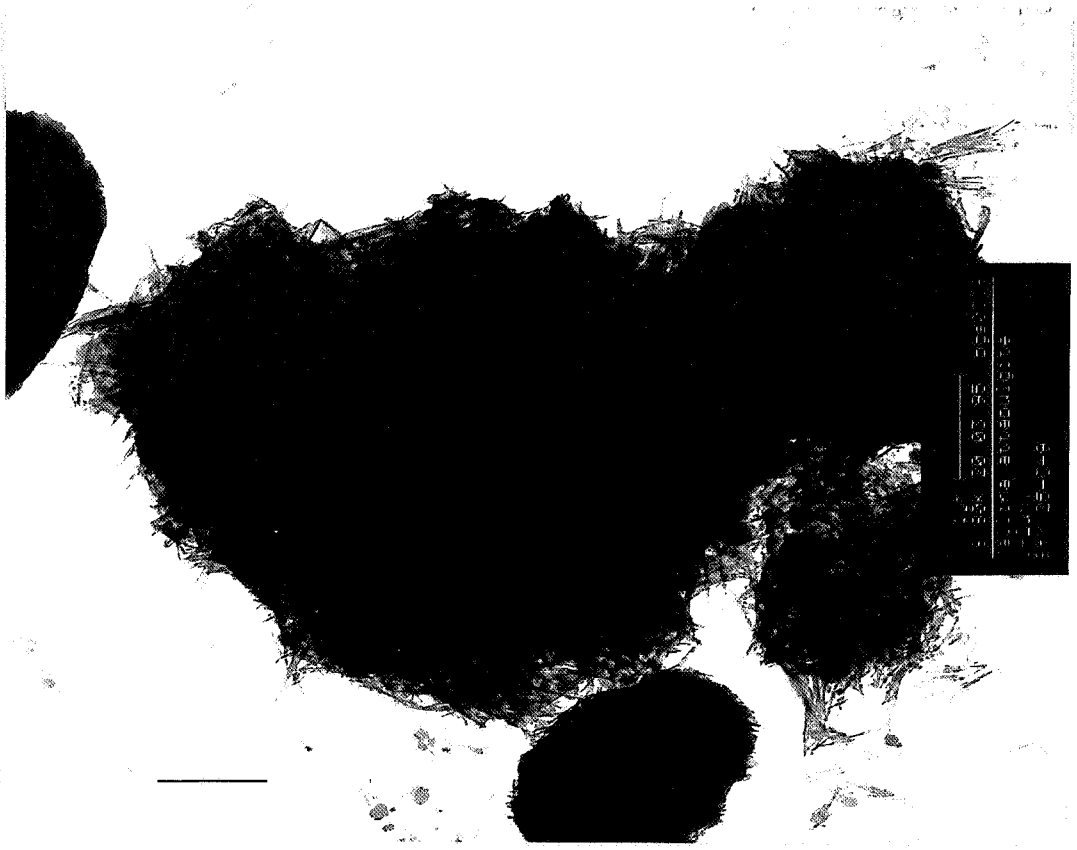


Plate 33. Lake Nerramyne attapulgite, 1 to 2 μm.

Palygorskite, illite and kaolinite. Neg. 0338.

Scale bar: 1 μm.

APPENDIX 1: Mineralogical analysis.

To determine the relative abundances of minerals in each sample the XRD system was calibrated using a sample whose illite concentration was determined by XRF (see Appendix 2) and whose palygorskite, dolomite, quartz and halite content was determined by Rietveld analysis (M. Raven, personal communication). The XRD peaks for the minerals in this calibration sample were fitted to Lorenzian curves with allowance made for α_1 and α_2 peak splitting. The areas of the fitted α_1 peaks were used to specify a proportionality constant for determining absolute mineral abundances in the bulk samples. As many as possible peaks characteristic of a mineral were used in the calibration. The concentrations of minerals not included in the calibration set were determined by difference. Wherever possible the peak areas of minerals whose concentration was determined by difference were used to define a calibration for these minerals that could then be used for samples containing a mixture of minerals with minor concentrations.

The calibration was also improved (i.e. the accuracy was increased) by cross-correlating from one sample to another the concentrations and peak areas of various minerals. This cross-correlation also was used to validate the use of a linear relation between peak intensity and mineral concentration. The calibration constants for determining mineral concentrations are given in Table A1.1. It should be noted that these values only apply for an integrated intensity of the quartz (101) CoKα_1 peak from an Arkansas stone standard of 4010 cps.deg 2θ. The calibrations need to be linearly adjusted for variations in this integrated intensity.

Overall this method of calibration allowed mineral concentrations (wt%) to be determined to an accuracy of 1½ significant figures.

A very similar approach was used to determine the mineral abundances for the sized samples. In this case, however, the calibration was improved by determining the illite concentration (see Appendix 2) by XRF for one size fraction in each of the samples. In addition, determination of clay concentrations (i.e. palygorskite, illite, kaolinite etc.) were supplemented by the use of XRD patterns from oriented samples. For oriented samples it is

only possible to determine relative concentrations but, because of the increased peak height, accuracy is improved over pressed powders. The calibration constants for the relative abundance of minerals is given in Table A1.2.

In summary, the best way (in terms of overall accuracy) to determine concentrations is illite by XRF, crystalline materials by Rietveld analysis and poorly- or non-crystalline materials by difference. It should be noted that XRF cannot be easily used on bulk samples and is best carried out on the <2 μm fraction. The second best method is to use Rietveld analysis for all crystalline materials including illite if possible. Finally, the third best method is to us a calibration set as has been done for this report. The advantage of the third method is that it requires much less analysis time and specimen preparation than the first two methods.

Table A1.1. Calibration constants for absolute concentrations of minerals. Pressed powders.

Concentration (wt%) = R x Integrated intensity (cps.deg 2θ)

Mineral	Characteristic peak		R
	2θ (Co $K\alpha_1$)	(hkl)	
Quartz	31.1	101	0.032 ± 0.009
Halite	37.0	200	0.016 ± 0.002
Dolomite	36.1	104	0.056 ± 0.008
Palygorskite	9.8	110	0.19 ± 0.07
	16.0	200	0.91 ± 0.33
	19.1	-130	1.2 ± 0.5
Illite	10.0	001	0.91 ± 0.58
	20.6	002	0.53 ± 0.28
Kaolin	14.4	001	0.20 ± 0.06
Gypsum	13.5	020	0.04 ± 0.02

Table A1.2. Calibration constants for relative concentrations of minerals. Oriented samples.

$$C_1/C_2 = V \times I_1/I_2$$

where

C_1 = concentration (wt%) of mineral 1.

C_2 = concentration (wt%) of mineral 2.

I_1 = integrated intensity of CoKα_1 peak for mineral 1 (cps.deg 2θ).

I_2 = integrated intensity of CoKα_1 peak for mineral 2 (cps.deg 2θ).

V = proportionality constant (tabulated below).

Mineral 1 / Mineral 2	Illite (10)	Illite (20)	Paly (9.8)	Paly (16)	Paly (19)	Kaol (14)
Illite (10)	1	2.2 ± 3.1	3.2 ± 1.5	0.45 ± 0.22	0.31 ± 0.1	4.2 ± 4.3
Illite (20)		1	2.29 ± 0.45	0.40 ± 0.02	0.22 ± 0.03	2.2 ± 1.3
Paly (9.8)			1	0.16 ± 0.05	0.10 ± 0.02	0.49 ± 0.19
Paly (16)				1	0.55 ± 0.08	2.2 ± 0.7
Paly (19)					1	4.4 ± 1.5

The figure shown in brackets with the mineral name is the approximate angle (deg 2θ, CoKα) for the relevant characteristic peak.

Shaded values are the most accurate and therefore indicate which peaks should be used in determining relative abundances.

APPENDIX 2: Potassium content of illite and the determination of illite concentrations.

In this report and Churchman *et al.* (1994) it is assumed that the illite contained in Garford palaeochannel clays has the same K concentration (wt%) as Muloorina illite. This is because the geological environment in which Muloorina illite is found (i.e. Lake Eyre, SA) is very similar to the geological environment of the Garford palaeochannel. By using this assumption the concentration of illite in Garford palaeochannel clays can be determined by XRF which gives the K content of the whole clay. In order to check the validity of this assumption, a Garford palaeochannel illite (P25 5-6m) was analysed in the TEM by EDX spectroscopy. A typical EDX spectrum from the illite is shown in Fig. A2.1.

EDX analysis gives the relative abundances of the elements in this sample. For the illite from the Garford palaeochannel the relative concentrations (at%) are

$$Si : K : Al : Mg : Fe = 1 : 0.178 : 0.354 : 0.077 : 0.164$$

The atomic formula for the illite can be derived from these relative concentrations using the following equations

$Al_t + Si = 8$ (number of tetrahedral cations)

$Al_t + Al_o = Al$ (total Al concentration)

$-Al_t + (3Al_o + 3Fe + 2Mg - 12) = -K$

(tetrahedral charge + octahedral charge = interlayer charge)

where Al, Fe, Mg, K and Si are the concentrations of the respective elements. The concentrations for Al, Fe, Mg and K can be replaced in the equations by the Si concentration multiplied by the ratio determined by EDX. Al_t and Al_o are the tetrahedral and octahedral Al concentrations respectively. These 3 equations and the atomic ratios determined by EDX give a formula of

$$(K_{1.33})(Al_{2.13}Fe_{1.23}Mg_{0.58})(Si_{7.48}Al_{0.52})O_{20}(OH)_4$$

for illite from the Garford palaeochannel. This formula then gives the concentration (wt%) of oxides as

	Fe_2O_3	K_2O	SiO_2	Al_2O_3	MgO	Sum
P25	12.2	7.8	55.9	16.8	2.9	95.6

The corresponding concentrations (wt%) for Muloorina illite are

	Fe_2O_3	K_2O	SiO_2	Al_2O_3	MgO	TiO_2	CaO	Sum
Muloorina	13	7.4	52	17	4.1	0.5	0.5	94.5

Given the measurement errors in EDX analysis (approximately 5%) the use of Muloorina illite as a standard for illite concentrations is justified. The concentration of illite in a sample is therefore the K_2O content determined by XRF multiplied by 100/7.4.

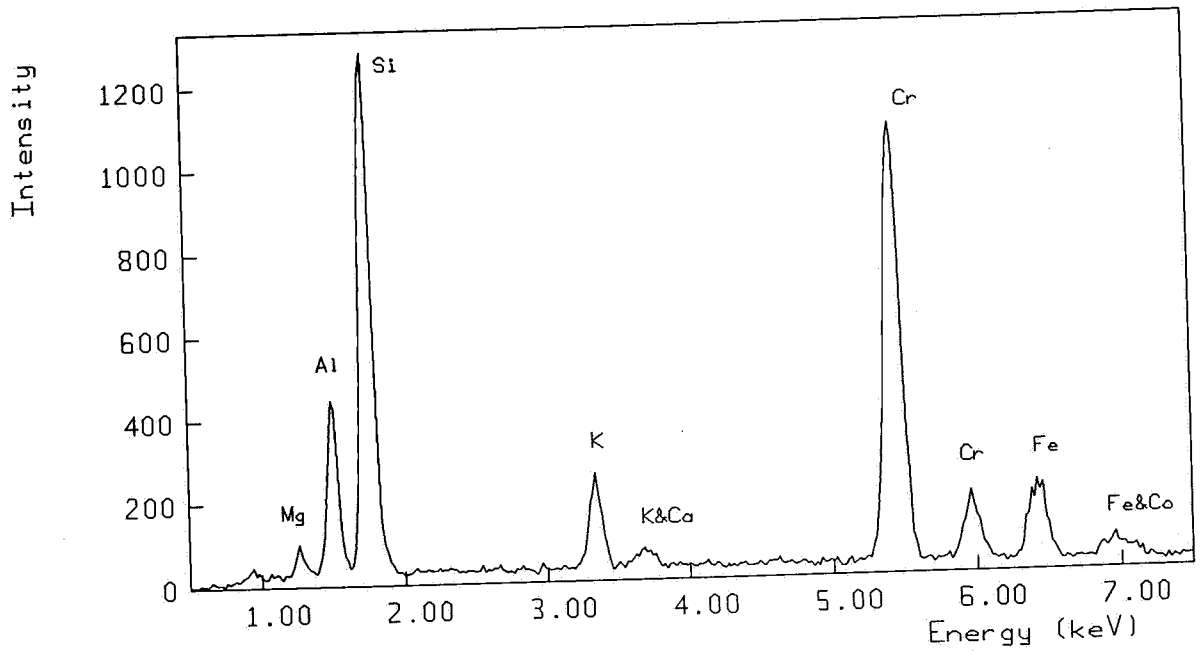


Fig. A2.1. EDX spectrum of illite in sample P25 5-6m (<0.2 μm). The Cr and Co peaks are from the TEM specimen holder and not from the illite. (Spectrum P2556-21.SP).

Acknowledgments

The authors would like to thank Mr G. Ferris for assistance in specimen preparation, Mr P. Fazey for XRF analyses, Mr J. Coppi for photographic processing and Mr G. Rinder for assistance with figure preparation.

000365

ABSORBENT CLAY PROJECT

ADDITIONAL REPORT TO MINES AND ENERGY, SOUTH AUSTRALIA

MINERALOGY AND PHYSICAL PROPERTIES OF SAMPLES CONTAINING PALYGORSKITE COLLECTED DURING THE MESA 1995 DRILLING PROGRAMME IN THE GARFORD PALAEOCHANNEL, SOUTH AUSTRALIA.

P.G. Self, J.L. Keeling, and M.D. Raven.

CSIRO

Division of Soils

Commonwealth of Australia

January, 1996

RECEIVED 29 FEB 1996 DEPT MINES AND ENERGY SECURITY

MINERALOGY AND PHYSICAL PROPERTIES OF SAMPLES CONTAINING PALYGORSKITE COLLECTED DURING THE MESA 1995 DRILLING PROGRAMME IN THE GARFORD PALAEOCHANNEL, SOUTH AUSTRALIA.

P.G. Self, J.L. Keeling, and M.D. Raven.

This Report was prepared exclusively for Mines and Energy, South Australia (MESA) and CSIRO, Division of Soils. The Report or any part of the Report should not be quoted without the written permission of the authors. The Report is not intended for, nor does CSIRO or MESA accept any responsibility for its, use by any third party. CSIRO and MESA have not made and hereby excludes all warranties, terms, conditions or undertakings, whether express or implied, written or oral, statutory or otherwise including any implied warranty of merchanatability or of fitness for a particular purpose in respect of the Services. To the full extent permitted by the laws of the Commonwealth of Australia or of any State or Territory of Australia having jurisdiction, all conditions or warranties imposed by such legislation are hereby excluded. In so far as liability under or pursuant to such legislation may not be excluded, such liability is limited, at the option of CSIRO and MESA, to:

(i) the re-performance of the Service; or

(ii) the payment of the cost of having the Service performed again.

CSIRO and MESA shall retain ownership and exclusive rights to use of all research expertise, research skills and research techniques developed in the preparation of results for this Report.

CSIRO and MESA give no warranty and makes no representation, whether express or implied that this Report is error free. CSIRO and MESA will accept no responsibility for any interpretation, opinion or conclusion that any person may form as a result of examining this Report.

Summary

During 1995, Mines and Energy, South Australia (MESA) completed a reverse circulation drilling and auger sampling programme in the Garford palaeochannel. The objective was to follow up a reported intersection of high-grade palygorskite clay and to outline areas of the palaeochannel with potential for commercial grades of palygorskite. Field identification of clays was made by infra-red analysis and from these data, samples were selected for more detailed investigations as reported herein.

Principal mineral components of Garford palaeochannel clays are dolomite, palygorskite, illite, quartz and halite. Quantitative mineralogy of 110 samples was determined from x-ray diffraction data by calculating the average ratio of integrated peak areas of a mineral phase and its pure standard and deriving concentration from empirically determined calibration curves. Where necessary, standard mineral phases were obtained by purifying selected palaeochannel samples.

Mixed dolomite and palygorskite is a widespread mineral association in the palaeochannel clays. A method of removal of dolomite by acid dissolution is given.

Characteristics of the major minerals associated with palygorskite, except for the soluble mineral halite, are outlined in the report. Palygorskite is characterised in more detail with reports on colloidal, thermal, compositional and exchange properties. Particular attention is given to the rheological and absorption properties of Garford palygorskite.

Two areas within the palaeochannel are identified where palygorskite is the dominant clay mineral (70-90 wt.% palygorskite). These high-grade palygorskite intersections also contain significant amounts of sand-sized quartz grains (10-45 wt.% quartz) and variable minor amounts of halite. Removal of quartz grains, in particular, is required to produce a palygorskite product with low grit content for rheological applications.

After beneficiation to remove sand-sized quartz and halite, palygorskite-bearing clays from the Garford palaeochannel have rheological and sorption properties that compare favourably to commercial attapulgites and bentonites.

TABLE OF CONTENTS

Introduction 1

References 2

Chapter 1: Mineralogy of drill hole samples 3

Mineral content 3
Particle size distribution (size fractionation) 4
Discussion 5
References 7
Tables 8
Figures 21

Chapter 2: Dolomite removal by dissolution in acid 66

Introduction 66
Experimental method 66
Results and discussion 67
Method for removal of dolomite from Garford palaeochannel clays 69
References 70
Figures 71

Chapter 3: Physico-chemical properties of clays and minerals from the Garford palaeochannel 78

Introduction 78
Quartz 78
Illite 78
Dolomite 79
Palygorskite 80
Dispersion and colloidal properties 80
Composition and cation exchange behaviour 83
Absorption and organic carbon 85
Thermal characteristics 86
Genesis of palygorskite 88
References 90
Tables 91
Figures 94

Chapter 4: Rheology of selected samples from the Garford palaeochannel 104

Methods 104
Results and discussion 105
Garford palaeochannel clays 105
Commercial attapulgites (palygorskites) 108
Bentonites 108
Conclusions 111
References 113
Table 114
Figures 115

Chapter 5: Absorption properties of selected samples 137

Absorption of dyes 137
Specific absorption of cations 140
References 143
Tables 144
Figures 146

Chapter 6: Water sorption by Garford palaeochannel clays 149

Methods 149
Results and discussion 149
Tables 152
Figures 154

Acknowledgments 156

Appendix 1: Quantification of mineral content by x-ray diffraction 157

Dolomite 158
Halite 158
Quartz 159
Illite 159
Using the calibration 161
Tables 162
Figures 164

Appendix 2: Mineralogy of all samples from the Garford palaeochannel 175

Tables 176

Appendix 3: Laboratory method for separation of quartz and dolomite from the Garford palaeochannel clay samples 190

Appendix 4: Analyses of reference samples 191

Tables 192
Figures 193

Appendix 5: Water sorption by Westinghouse method 202

Sample requirements 202
Apparatus 202
Method 202
Results 202
Figure 203

MINERALOGY AND PHYSICAL PROPERTIES OF SAMPLES CONTAINING PALYGORSKITE COLLECTED DURING THE MESA 1995 DRILLING PROGRAMME IN THE GARFORD PALAEOCHANNEL, SOUTH AUSTRALIA.

Introduction

Several investigations have been reported on clays from the Garford palaeochannel (Pitt *et al.*, 1978; Robertson, 1984; Warne, 1987; Churchman *et al.*, 1994; Raven *et al.*, 1995). These investigations showed the presence of palygorskite-bearing clays in the Miocene sediments in the palaeochannel. The clays can be high in palygorskite with one sample containing 70% to 90% palygorskite (Raven *et al.*, 1995). However, the majority of the samples studied contained high amounts of dolomite and illite. The 1995 RC drilling programme and associated pre-programme reconnaissance study were carried out to locate and characterise areas in the Garford palaeochannel where clays have a high palygorskite content. The geological significance of the samples obtained in the programme is discussed by Keeling *et al.* (1995).

Estimates of palygorskite content of samples was determined using short-wavelength infra-red analysis (Keeling *et al.*, 1995) calibrated on samples from earlier investigations (Raven *et al.*, 1995). For this study, a selection of field samples was taken for detailed determination of mineralogy and for characterisation of the principal minerals present in the samples.

The major uses of palygorskite clays are as drilling mud or adsorbents. Consequently the properties of the Garford palaeochannel clays presented in this Report are biased towards an understanding of the rheological and adsorbent properties of the clays.

References

Churchman, G.J., Ferris, G.M., Keeling, J.L., McClure S.G., Raven, M.D., Self, P.G. and Slade, P.G. (1994). Absorbent Clay Project. Characterisation of the selected clays. Progress Report No. 1 to Mines and Energy, South Australia, June 1994. South Australian Department of Mines and Energy, Envelope 8785 (unpublished).

Keeling, J.L., Ferris, G.M. and Statham-Lee, L. (1995). Palygorskite clay investigation, Garford palaeochannel, South Australia: Results of drilling April-May, 1995. Mines and Energy, South Australia, Report Book 95/48.

Pitt, G.M., Benbow, M.C., Barnes, L.C., Harris, W.K. and Lindsay, J.M. (1978). Report on Tallaringa palaeodrainage system - 1976. South Australian Department of Mines and Energy, Report Book 78/38.

Raven, M.D., Abolins, N., Keeling, J.L. and Self, P.G. (1995). Absorbent Clay Project. Mineralogical characterisation of Garford palaeochannel clays. Supplementary Report to Mines and Energy, South Australia, April 1995. South Australian Department of Mines and Energy, Envelope 8785 (unpublished).

Robertson, R.S. (1984). Reconnaissance sampling of palygorskitic clay, Garford Palaeochannel - Coober Pedy. South Australia. South Australian Department of Mines and Energy, Report Book 84/52.

Warne, S.B. (1987). Roebuck Resources N.L. Report for the period 19th September 1986 to 18th December 1987, Sandstone EL 1371, South Australia. South Australian Department of Mines and Energy, Open File Envelope, 6809 (unpublished).

CHAPTER 1. MINERALOGY OF DRILL HOLE SAMPLES.

The location of reverse circulation (RC) drill holes and shallow auger sample sites from which samples were taken for investigation are shown in Fig. 1.1. These locations are a subset of those sampled during the 1995 MESA drilling programme. Full details on all drillholes and sampling methods are given by Keeling *et al.* (1995).

Mineral content

The mineral content of the Garford palaeochannel samples was determined for sub-samples prepared for field characterisation by short-wavelength infrared spectroscopy (Keeling *et al.*, 1995). The as-received samples were hand ground with a mortar and pestle before being examined by powder x-ray diffraction (XRD). Mineral content was determined by comparing XRD traces from the samples with those from standard mixtures of minerals. The full details of this method are given in Appendix 1.

The method used in this study for quantitative mineralogical analysis differed in two ways from the method used in the study conducted by Raven *et al.* (1995). The first difference is that all of the sample was used in XRD analyses whereas some coarse, sand-sized fraction was rejected during preparation of samples used by Raven *et al.* (1995). The second difference is that a suite of standard mixtures of clays was specifically prepared and used in this study for calibration rather than a limited number of as-received samples as was used by Raven *et al.* (1995). Improved precision in the calibration because of the use of standard mixtures provides a more accurate analysis of the samples than previously reported.

The XRD patterns of samples are shown in Figs. 1.2 to 1.33 and colour overlays are provided inside the back cover to aid in the identification of minerals from the XRD patterns. The results of the quantitative analyses are given in Table 1.1. These results should be compared with the results of the field quantisation method by near infra-red spectroscopy as given by Keeling *et al.* (1995). The mineral contents of all Garford palaeochannel clays examined in the course of the Absorbent Clay Project are given in Appendix 2. However, care should be taken when comparing the analyses of samples

from previous studies (i.e. P24 to P43) with those from the present study because of the differences in the method of analysis as outlined above.

The mineralogy of the 1995 RC drilling programme and auger samples is essentially the same as that previously reported for samples from the Garford palaeochannel (Raven *et al.*, 1995). That is, the predominant minerals are palygorskite, illite, dolomite, halite and quartz. In general, however, the samples from the 1995 drilling programme have a higher quartz content than in previously reported samples. Encouragingly, there is also more samples containing high amounts of palygorskite and low amounts of dolomite and illite than previously reported (see samples marked with an asterisk in Table 1.1).

Particle size distribution (size fractionation)

The particle size distribution of selected, high-palygorskite samples and some reference clays were determined. The samples were divided into 4 fractions: >53μm, <53μm->2μm, <2μm->0.2μm and <0.2μm. To obtain these fractions, bulk samples were dried at 105°C and known amounts of each sample were dispersed in reverse osmosis (RO) water using a Waring laboratory blender. The >53μm fraction was obtained by wet sieving, the <53μm->2μm and <2μm->0.2μm fractions were obtained by centrifugation while the <0.2μm fraction was obtained by difference. All fractions were dried at 105°C. As a result of the method used the <0.2μm fraction also includes soluble salts. Results are shown in Table 1.2.

The major minerals in samples from the Garford palaeochannel are, to some extent, separated by particle size fractionation. Quartz is predominantly in the >53μm fraction whereas palygorskite and illite are in the <2μm. This separation is particularly apparent in the high-palygorskite, low dolomite samples (e.g. P86 0-0.63m and P88 0.4-2m). Dolomite is contained within the <53μm->0.2μm particle size range.

The particle size distribution of high-palygorskite, low-dolomite samples is essentially bimodal with quartz being >53μm in size and the remaining minerals being <2μm in size. This makes separation of quartz from the sample relatively easy. A simple laboratory method for the removal of quartz is described in Appendix 3. As the method

of separation involves dispersion in RO water, soluble salts (e.g. halite) are also removed from the sample.

The ease with which quartz and soluble salts can be removed from samples means that it is reasonable to re-examine the mineral content of the samples excluding quartz and halite as shown in Table 1.3. This table lists the samples from the 1995 drilling programme in order of decreasing palygorskite content. A similar table for all samples examined in the course of the Absorbent Clay Project is given in Appendix 2. These tables show that many samples are high in palygorskite (9 samples with 70wt.% or greater palygorskite content) and low in dolomite and therefore should have good rheological and absorbent qualities. The validity of the renormalised mineral content was confirmed by XRD examination of a number of samples beneficiated in the way described in Appendix 3.

Comparison of the results given in Table 1.2 for reference samples (e.g. Lake Nerramyne) with those given for the same samples by Raven *et al.* (1995) shows significant differences in the particle size distributions. This is a result of the different methods of dispersion used in this and the Raven *et al.* (1995) study. The method used by Raven *et al.* (1995) was one of repeated washing, ultrasonification and centrifugation. This method clearly breaks up aggregates to a greater extent than when only a laboratory blender is used. The results show the sensitivity of particle sizing techniques to the method of dispersing the particles.

Discussion

Mineralogical characterisation of samples from the 1995 drilling programme shows that there are at least two areas in the Garford palaeochannel where there are clays with high palygorskite contents. These two areas are in proximity to sites P33 (P85-P88) and P84. These areas warrant further study in order to determine the size of the clay resource.

The process of size fractionation of high-palygorskite content samples from the Garford palaeochannel (Table 1.2) revealed some interesting properties of these clays. The content of both sand-sized (>53μm) quartz and halite is higher than previously reported.

The Garford palaeochannel samples dispersed readily and self flocculated in RO water (approximately neutral pH). The colloidal properties of the samples and the variation of these properties with pH is discussed in Chapter 3.

Senegal, Attagel and Xuyi attapulgites (i.e. commercial attapulgites) show similar behaviour to the Garford palaeochannel samples in that they self flocculated in RO water. However, it was apparent that the concentration of palygorskite in flocculated gels of Senegal, Attagel and Xuyi attapulgites were lower than in flocculated gels of Garford palaeochannel samples. This is consistent with the longer fibre length of Senegal palygorskite, Xuyi palygorskite and Attagel relative to the fibre length of Garford palaeochannel palygorskite (Raven *et al.*, 1995). Lake Nerramyne attapulgite was considerably harder to disperse than both Garford palaeochannel clays and the commercial attapulgites (Senegal attapulgite, Xuyi attapulgite and Attagel 50).

Fine-grained dolomite is present in many of the Garford palaeochannel samples and a straight forward process of separation of dolomite from a sample would significantly increase the yield of high-grade palygorskite. During the centrifugation of the <2μm fraction of the Garford palaeochannel clays it was noticed that dolomite concentrated at the bottom of the centrifuge tubes and could be separated from the sample by scraping the dried centrifuge slugs. This behaviour was not seen in sedimentation. Therefore it would seem that by carefully controlling centrifugation conditions it may be possible to separate dolomite from palygorskite. An alternative is to use acid dissolution as discussed in the next Chapter.

References

Keeling, J.L., Ferris, G.M. and Statham-Lee, L. (1995). Palygorskite clay investigation, Garford palaeochannel, South Australia: Results of drilling April-May, 1995. Mines and Energy, South Australia, Report Book 95/48.

Raven, M.D., Abolins, N., Keeling, J.L. and Self, P.G. (1995). Absorbent Clay Project. Mineralogical characterisation of Garford palaeochannel clays. Supplementary Report to Mines and Energy, South Australia, April 1995. South Australian Department of Mines and Energy, Envelope 8785 (unpublished).

Table 1.1. Mineralogical analysis (wt. %) of selected, as-received, drill programme samples from the Garford Palaeochannel.

Sample	XRD File	Palygorskite	Illite	Dolomite	Halite	Quartz	Smectite[1]	Kaolin	Calcite	Gypsum	Celestine	Anatase
Quartz Boulder	3249-BLK.101	-	~3	-	~6	~15	0-5	~75	-	-	-	-
P33												
Upper	3250-BLK.102	0-3	-	94-98	1-3	<1	-	-	-	-	-	-
Middle	3251-BLK.103	5-8	-	80-85	4-6	2-4	-	-	-	1-3	-	-
*Lake Floor	3252-BLK.104	33-38	4-6	-	15-19	40-45	-	-	-	-	-	-
P44												
0-1m	3253-BLK.105	Tr	-	92-98	4-6	-	-	-	-	-	-	-
0.2-1m	3254-BLK.106	2-6	-	73-79	4-6	12-18	-	-	-	-	-	-
P45												
0-1m	3255-BLK.107	0-3	-	90-95	4-6	0-1	-	-	-	-	-	-
1-1.5m	3256-BLK.108	0-1	-	92-96	3-5	1-2	-	-	-	-	-	-
1.5-1.7m	3257-BLK.109	3-7	1-3	82-87	4-6	1-2	-	-	-	-	-	-
P46												
0-0.6m	3258-BLK.110	3-6	0-2	87-93	3-5	0-1	-	-	-	-	-	-
P47												
0-1m	3259-BLK.111	-	-	92-96	3-5	<1	0-2	-	-	Tr	-	-
P48												
Green clay	3260-BLK.112	-	8-12	-	2-4	62-68	5-10	5-10	-	Tr Microcline ~ 5	-	Tr Albite ~ 3
0-1m	3261-BLK.113	0-2	-	94-98	1-3	<1	-	-	-	-	-	-
1-1.7m	3262-BLK.114	0-3	-	94-98	1-2	1-2	-	-	-	-	-	-

0003728

Table 1.1 (continued).

Sample	XRD File	Palygorskite	Illite	Dolomite	Halite	Quartz	Smectite[1]	Kaolin	Calcite	Gypsum	Celestine	Anatase
P49												
0-0.2m	3263-BLK.115	4-8	4-8	0-1	2-4	72-78	5-10	5-10	-	-	-	-
											Microcline - Tr	
Black nodule	3264-BLK.116	-	-	-	-	12-18	-	-	~85	-	-	-
											Microcline - Tr	
P50												
0-0.7m	3265-BLK.117	-	-	94-98	1-3	1-3	-	-	-	-	-	-
P51												
0-1m	3266-BLK.118	0-3	-	86-92	2-4	5-7	-	-	-	-	-	-
P52												
0-1m	3267-BLK.119	7-10	<1	76-82	4-6	2-4	-	-	-	3-6	-	Tr
											Barite - Tr	
P53												
0.6-1m	3269-BLK.201	9-13	1-4	76-82	4-6	2-4	-	-	-	-	-	Tr
1-1.5m	3268-BLK.120	20-24	3-6	55-59	7-10	5-8	-	-	-	1-2	-	-

0003796

Table 1.1 (continued).

Sample	XRD File	Palygorskite	Illite	Dolomite	Halite	Quartz	Smectite[1]	Kaolin	Calcite	Gypsum	Celestine	Anatase
P54												
0.1-0.6m	3270-BLK.202	13-16	2-4	70-74	7-10	1-3	-	-	-	-	-	-
P55												
Upper grey clay	3271-BLK.203	3-7	3-7	-	6-10	38-42	15-20	1-5	1-2	~20	-	Tr
0-0.7m	3272-BLK.204	2-4	-	82-88	3-5	0-1	5-10	-	-	Tr	-	-
P56												
0.3-0.6m	3273-BLK.205	4-7	<1	86-92	2-4	2-3	-	-	-	-	-	-
P57												
0.1-0.6m	3274-BLK.206	19-23	4-6	58-62	7-10	5-7	-	-	-	-	-	-
P61												
6-8m	3375-BLK.101	5-10	20-30	1-5	1-3	20-30	5-10	20-30	1-5	-	-	Tr
8-10m	3376-BLK.102	5-10	20-30	15-25	1-4	15-25	5-10	10-20	1-3	-	-	Tr
10-11m	3377-BLK.103	33-38	20-22	18-20	5-7	18-20	-	-	-	-	-	-
11-12m	3378-BLK.104	23-28	12-15	11-13	4-6	42-48	-	-	Tr	-	-	-
12-13m	3379-BLK.105	36-40	10-12	9-11	3-5	36-39	-	-	Tr	-	-	-
13-14m	3380-BLK.106	23-28	55-60	2-5	5-7	5-10	-	-	-	-	-	-
14-15m	3381-BLK.107	15-20	60-65	1-4	<1	16-20	-	-	-	-	-	-

000380

Table 1.1 (continued).

Sample	XRD File	Palygorskite	Illite	Dolomite	Halite	Quartz	Smectite[1]	Kaolin	Calcite	Gypsum	Celestine	Anatase
P65												
6-7m	3382-BLK.108	11-15	0-2	80-85	1-3	2-5	-	-	-	-	-	-
7-8m	3383-BLK.109	1-3	<1	93-98	0-1	1-3	-	-	-	-	-	-
8-9m	3384-BLK.110	1-3	<1	93-98	1-2	1-2	-	-	-	-	-	-
9-10m	3385-BLK.111	39-43	6-8	31-35	5-7	11-15	-	-	-	-	-	-
10-11m	3386-BLK.112	39-43	23-28	2-3	5-7	20-25	1-5	-	-	-	-	-
11-12m	3387-BLK.101	31-34	23-28	1-2	5-7	20-25	10-15	-	-	-	-	Tr
12-13m	3388-BLK.102	39-43	9-13	31-35	3-5	7-9	1-5	-	-	-	-	Tr
13-14m	3389-BLK.103	42-46	23-28	1-2	5-7	8-11	10-15	-	-	-	-	Tr
14-15m	3390-BLK.104	5-10	35-40	0-1	2-3	30-35	15-20	-	-	-	-	Tr
15-16m	3391-BLK.105	4-7	55-60	<1	3-5	12-16	15-20	-	-	-	-	Tr
16-17.5m	3392-BLK.106	5-10	55-60	<1	4-6	11-15	15-20	-	-	-	-	Tr
P66												
14-15m	3393-BLK.107	9-13	0-2	80-85	1-3	3-6	-	-	-	-	-	-
15-16m	3394-BLK.108	24-28	4-6	50-55	2-5	11-15	-	-	-	-	-	-
16-17m	3395-BLK.109	42-47	6-10	25-28	5-9	4-6	5-10	-	-	-	-	Tr
17-18m	3396-BLK.110	9-13	8-12	6-10	4-6	55-60	7-12	-	-	-	-	Tr
18-19m	3397-BLK.111	7-10	45-55	1-2	3-5	17-20	15-20	-	-	-	-	Tr
19-20m	3398-BLK.112	2-5	65-75	0-1	4-6	4-7	15-20	-	-	-	-	-
P67												
14-15m	3399-BLK.100	30-35	8-12	39-43	5-9	5-10	0-5	-	-	-	-	-
15-16m	3400-BLK.101	22-27	19-23	37-41	4-6	5-10	0-5	-	-	-	-	-
16-17m	3401-BLK.102	35-40	25-30	2-4	6-9	15-20	5-10	-	-	-	-	-
P68												
11-12m	3402-BLK.104	27-33	30-35	15-19	3-5	7-11	5-10	-	-	-	-	-
12-13m	3403-BLK.105	11-15	8-12	67-73	1-3	1-3	0-5	-	-	-	-	-
13-14m	3404-BLK.106	10-14	8-12	62-67	1-3	7-12	0-5	-	-	-	-	-

000381

Table 1.1 (continued).

Sample	XRD File	Palygorskite	Illite	Dolomite	Halite	Quartz	Smectite[1]	Kaolin	Calcite	Gypsum	Celestine	Anatase
P69												
9-10m	3405-BLK.107	22-26	17-21	20-25	1-3	27-33	0-5	-	-	-	Tr	-
10-11m	3406-BLK.108	13-16	9-11	45-50	1-3	20-24	-	-	-	-	2-5	-
P70												
9-10m	3407-BLK.109	22-26	7-10	7-9	1-3	52-58	0-5	-	-	-	-	-
P74												
10-11m	3408-BLK.110	2-6	0-1	87-93	0-2	3-7	-	-	-	-	-	-
11-12m	3409-BLK.111	3-7	0-1	87-93	0-2	3-7	-	-	-	-	-	-
P76												
6-7m	3410-BLK.112	3-7	0-1	73-79	1-2	16-20	-	-	-	-	-	-
7-8m	3411-BLK.101	25-30	1-3	57-63	3-5	2-5	0-5	-	-	0-1	-	-
8-9m	3412-BLK.102	10-13	1-2	75-80	2-4	5-7	-	0-1	-	-	-	-
9-10m	3413-BLK.103	15-18	1-3	60-65	3-7	10-13	0-5	-	-	-	-	-
10-11m	3414-BLK.104	29-33	1-3	36-42	4-8	18-22	0-5	-	-	-	-	-
11-12m	3415-BLK.105	8-12	<1	68-74	2-4	4-7	8-12	-	-	-	-	-
12-13m	3416-BLK.106	7-11	<1	70-75	2-4	3-6	8-12	-	-	-	-	-
13-14m	3417-BLK.107	3-7	<1	80-85	1-3	2-5	5-10	-	-	-	-	-
14-15m	3418-BLK.108	15-20	2-4	69-73	4-8	0-1	0-5	-	-	-	-	-
15-16m	3419-BLK.109	37-41	17-21	17-21	4-6	9-11	5-10	-	-	-	-	-
16-17m	3420-BLK.110	15-20	3-7	60-65	3-5	1-3	5-10	-	-	-	-	-

Table 1.1 (continued).

Sample	XRD File	Palygorskite	Illite	Dolomite	Halite	Quartz	Smectite[1]	Kaolin	Calcite	Gypsum	Celestine	Anatase
P77												
4-5m	3421-BLK.111	13-17	1-2	57-63	1-4	9-13	5-10	-	-	2-5	-	-
5-6m	3422-BLK.112	33-36	5-9	22-26	4-6	8-12	15-20	-	-	1-3	-	-
6-7m	3423-BLK.101	33-36	9-12	3-4	5-9	27-33	15-20	-	-	-	-	-
7-8m	3424-BLK.102	45-50	9-12	1-2	8-12	11-15	15-20	-	-	-	-	-
8-9m	3425-BLK.103	35-39	10-14	30-34	4-6	10-14	5-10	-	-	-	-	-
9-10m	3426-BLK.104	15-20	2-4	56-60	4-6	8-10	5-10	-	-	-	-	-
10-11m	3427-BLK.105	13-17	1-2	57-63	1-4	9-13	5-10	-	-	-	-	-
11-12m	3428-BLK.106	43-46	11-15	19-23	5-7	1-3	10-15	-	-	-	-	-
12-13m	3429-BLK.107	8-12	8-12	57-63	1-4	6-10	5-10	-	-	-	-	-
13-14m	3430-BLK.108	14-18	2-4	53-57	6-8	7-9	6-11	-	-	1-3	-	-
14-15m	3431-BLK.109	1-5	13-17	22-27	5-7	30-35	15-20	-	-	1-2	-	-
P79												
9-10m	3432-BLK.110	10-14	1-2	77-81	1-3	5-7	-	-	-	-	-	-
10-11m	3433-BLK.111	10-14	1-2	77-81	1-3	3-5	-	-	-	-	-	-
11-12m	3434-BLK.112	25-30	4-6	58-62	1-3	4-6	-	-	-	-	-	-
12-13m	3435-BLK.101	27-31	27-31	37-41	1-3	0-1	-	-	-	-	-	-
13-14m	3436-BLK.102	10-14	2-4	76-80	1-3	2-4	0-5	-	-	-	-	-
14-15m	3437-BLK.103	9-12	2-4	77-81	1-2	4-6	0-5	-	-	-	-	-
15-16m	3438-BLK.104	8-11	3-5	77-81	1-2	3-5	0-5	-	-	-	-	-
16-17m	3439-BLK.105	-	16-20	35-40	1-3	3-5	35-40	-	-	-	-	-

Table 1.1 (continued).

Sample	XRD File	Palygorskite	Illite	Dolomite	Halite	Quartz	Smectite[1]	Kaolin	Calcite	Gypsum	Celestine	Anatase
P84												
6-7m	3440-BLK.106	1-2	2-4	0-2	-	65-70	5-15	15-20	-	-	-	Tr
7-8m	3441-BLK.107	5-9	3-5	-	0-1	70-75	5-15	1-5	-	-	-	Tr
* 8-9m	3442-BLK.108	55-61	7-10	5-7	1-3	20-25	0-5	-	-	-	-	Tr
9-10m	3443-BLK.109	17-20	4-7	70-75	1-2	1-5	-	-	-	-	-	-
10-11m	3444-BLK.110	4-8	1-3	87-93	0-1	1-2	-	-	-	-	-	-
11-12m	3445-BLK.111	34-38	2-5	34-38	2-3	20-23	-	-	-	-	-	-
* 12-13m	3446-BLK.112	44-48	5-9	6-10	2-5	34-37	-	-	-	-	-	-
13-14m	3447-BLK.101	42-46	6-10	10-14	3-5	30-34	-	-	-	-	-	-
14-15m	3448-BLK.102	10-13	1-3	42-48	1-2	35-39	0-5	-	-	-	-	-
* 15-16m	3449-BLK.103	50-55	6-10	5-7	3-5	24-28	0-5	-	-	-	-	-
16-17m	3450-BLK.104	37-42	10-14	14-18	2-3	26-30	0-5	-	-	-	-	-
P85												
*0.3-1.08m	3451-BLK.105	55-60	5-7	-	26-30	6-10	-	-	-	-	-	-
1.08-1.1m	3452-BLK.106	15-20	<1	67-73	3-7	6-8	-	-	-	-	-	-
P86												
*0.03-0.63m	3453-BLK.107	57-63	2-4	1-2	16-20	16-19	-	-	-	Tr	-	Tr
P87												
0-0.6m	3454-BLK.108	2-4	<1	87-93	3-5	1-3	-	-	-	-	-	-
P88												
* 0.4-1m	3455-BLK.109	37-41	2-4	1-2	12-15	40-45	-	-	-	-	-	-
* 1-2m	3456-BLK.110	40-45	7-10	-	12-15	33-37	-	-	-	-	-	Tr
* 2-3m	3457-BLK.111	35-40	14-18	-	12-15	31-35	-	-	-	-	-	Tr
3-4m	3458-BLK.112	-	-	-	12-15	42-47	40-45	-	-	-	-	Tr

* High-palygorskite, low-dolomite samples.

[1] Includes randomly interstratified and very-poorly crystalline material.

Tr = trace.

Table 1.2. Size fractions (wt.%) of selected, as-received samples from the Garford palaeochannel and some reference clays.

Sample	>53μm	<53μm->2μm	<2μm->0.2μm	<0.2μm[1]	Comments
P33 Lake Floor	29 quartz	53 palygorskite Colour = 5YR 7/1		18	Initial water content 33%. Contains large-grained goethite. Disperses readily but self-flocculates in RO water.
P84 7-10m	37 quartz, dolomite	34 dolomite, palygorskite, quartz	22 palygorskite, dolomite	7	Dolomite and palygorskite separate on centrifugation (dolomite settles more readily) but the same separation is not apparent on sedimentation. Does not disperse as readily as low dolomite samples. Some self-flocculation in RO water.
P84 12-14m	23 quartz	4.2 dolomite	68.3 palgorskite, dolomite	4.9	Dolomite and palygorskite separate on centrifugation (dolomite settles more readily) but the same separation is not apparent on sedimentation. Some self-flocculation in RO water.
P84 14-16m	24 quartz	23 dolomite	47 palygorskite, dolomite	4.5	Dolomite and palygorskite separate on centrifugation (dolomite settles more readily) but the same separation is not apparent on sedimentation. Some self-flocculation in RO water.
P86 0-0.63m	23 quartz	0.4 quartz	55 palygorskite	21	Disperses readily but self-flocculates in RO water.
P88 0.4-2m	25 quartz	0.3 quartz	52 palygorskite	23	Disperses readily but self-flocculates in RO water.
P88 2-3m	31 quartz	4.4 quartz	53 palygorskite	12	Disperses readily but self-flocculates in RO water.

000385

Table 1.2 (continued).

Sample	>53μm	<53μm->2μm	<2μm->0.2μm	<0.2μm[1]	Comments
Lake Nerramyne[2]	57 palygorskite, kaolin, quartz	27 palygorskite, kaolin, quartz	7 palygorskite, kaolin, quartz Colour = 5Y 8/1	9	Does not disperse readily. Does not self-flocculate in RO water. Supernatant does not clear after centrifugation (6000rpm for 10min).
Senegal Ore[2]	4.9 quartz, palygorskite	1.6 quartz, palygorskite	84 palygorskite Colour = 5Y 8/1	9.7	Relatively difficult to diperse. Self-flocculates in RO water. Large flocs. Sediments down to a lower density (i.e. more dispersed) than Garford palaeochannel samples. <2μm fraction is yellowy white while crushed ore and processed sample is light-brown in colour.
Xuyi attapulgite[2] No. 1 deposit, "wet".	11 quartz, palygorskite	4.4 palygorskite, quartz	76 palygorskite Colour = white	9.3	Disperses readily but self-flocculates in RO water. Slightly more difficult to disperse than Garford samples.
Arumpo Bentonite TP1[2].	20 quartz, smectite	21 smectite	46 smectite	12	Difficult to disperse. Does not self-flocculate in RO water.

[1] Also includes soluble salts.
[2] Further data on reference samples is given in Appendix 4.

000386

Table 1.3. Renormalised mineralogy (wt.%) of drill programme samples.

Paly	Ill	Dol	Sample	XRD File	Paly	Ill	Dol	Hal	Qtz	Smt	Kaol	Cal	Gyp	Cel	An	Other
93	5	2	P86 0.03-0.63m	3453-BLK.107	57-63	2-4	1-2	16-20	16-19	-	-	-	Tr	-	Tr	
91	9	0	P85 0.3-1.08m	3451-BLK.105	55-60	5-7	-	26-30	6-10	-	-	-	-	-	-	
90	7	3	P88 0.4-1m	3455-BLK.109	37-41	2-4	1-2	12-15	40-45	-	-	-	-	-	-	
88	12	0	P33 Lake Floor	3252-BLK.104	33-38	4-6	-	15-19	40-45	-	-	-	-	-	-	
83	17	0	P88 1-2m	3456-BLK.110	40-45	7-10	-	12-15	33-37	-	-	-	-	-	Tr	
77	15	8	P84 8-9m	3442-BLK.108	55-61	7-10	5-7	1-3	20-25	0-5	-	-	-	-	Tr	
76	15	9	P84 15-16m	3449-BLK.103	50-55	6-10	5-7	3-5	24-28	0-5	-	-	-	-	-	
75	11	13	P84 12-13m	3446-BLK.112	44-48	5-9	6-10	2-5	34-37	-	-	-	-	-	-	
70	30	0	P88 2-3m	3457-BLK.111	35-40	14-18	-	12-15	31-35	-	-	-	-	-	Tr	
69	13	19	P84 13-14m	3447-BLK.101	42-46	6-10	10-14	3-5	30-34	-	-	-	-	-	-	
64	19	17	P61 12-13m	3379-BLK.105	36-40	10-12	9-11	3-5	36-39	-	-	Tr	-	-	-	
62	36	2	P77 7-8m	3424-BLK.102	45-50	9-12	1-2	8-12	11-15	15-20	-	-	-	-	-	
57	40	3	P65 10-11m	3386-BLK.112	39-43	23-28	2-3	5-7	20-25	1-5	-	-	-	-	-	
56	21	23	P84 16-17m	3450-BLK.104	37-42	10-14	14-18	2-3	26-30	0-5	-	-	-	-	-	
56	26	19	P70 9-10m	3407-BLK.109	22-26	7-10	7-9	1-3	52-58	0-5	-	-	-	-	-	
53	46	2	P65 13-14m	3389-BLK.103	42-46	23-28	1-2	5-7	8-11	10-15	-	-	-	-	Tr	
52	42	5	P77 6-7m	3423-BLK.101	33-36	9-12	3-4	5-9	27-33	15-20	-	-	-	-	-	
51	18	31	P66 16-17m	3395-BLK.109	42-47	6-10	25-28	5-9	4-6	5-10	-	-	-	-	Tr	
51	9	41	P65 9-10m	3385-BLK.111	39-43	6-8	31-35	5-7	11-15	-	-	-	-	-	-	
50	26	24	P61 11-12m	3378-BLK.104	23-28	12-15	11-13	4-6	42-48	-	-	Tr	-	-	-	
50	46	4	P67 16-17m	3401-BLK.102	35-40	25-30	2-4	6-9	15-20	5-10	-	-	-	-	-	
49	28	23	P77 11-12m	3428-BLK.106	43-46	11-15	19-23	5-7	1-3	10-15	-	-	-	-	-	
48	5	48	P84 11-12m	3445-BLK.111	34-38	2-5	34-38	2-3	20-23	-	-	-	-	-	-	
47	28	25	P61 10-11m	3377-BLK.103	33-38	20-22	18-20	5-7	18-20	-	-	-	-	-	-	
47	16	38	P65 12-13m	3388-BLK.102	39-43	9-13	31-35	3-5	7-9	1-5	-	-	-	-	Tr	
46	31	22	P76 15-16m	3419-BLK.109	37-41	17-21	17-21	4-6	9-11	5-10	-	-	-	-	-	
45	53	2	P65 11-12m	3387-BLK.101	31-34	23-28	1-2	5-7	20-25	10-15	-	-	-	-	Tr	
42	30	29	P77 5-6m	3422-BLK.112	33-36	5-9	22-26	4-6	8-12	15-20	-	-	1-3	-	-	
42	22	36	P77 8-9m	3425-BLK.103	35-39	10-14	30-34	4-6	10-14	5-10	-	-	-	-	-	
42	6	52	P76 10-11m	3414-BLK.104	29-33	1-3	36-42	4-8	18-22	0-5	-	-	-	-	-	

0003887

Table 1.3 (continued).

Paly	Ill	Dol	Sample	XRD File	Paly	Ill	Dol	Hal	Qtz	Smt	Kaol	Cal	Gyp	Cel	An	Other
38	15	48	P67 14-15m	3399-BLK.100	30-35	8-12	39-43	5-9	5-10	0-5	-	-	-	-	-	
35	32	33	P69 9-10m	3405-BLK.107	22-26	17-21	20-25	1-3	27-33	0-5	-	-	-	Tr	-	
34	46	20	P68 11-12m	3402-BLK.104	27-33	30-35	15-19	3-5	7-11	5-10	-	-	-	-	-	
31	6	63	P66 15-16m	3394-BLK.108	24-28	4-6	50-55	2-5	11-15	-	-	-	-	-	-	
30	30	40	P79 12-13m	3435-BLK.101	27-31	27-31	37-41	1-3	0-1	-	-	-	-	-	-	
30	5	65	P76 7-8m	3411-BLK.101	25-30	1-3	57-63	3-5	2-5	0-5	-	-	0-1	-	-	
30	5	65	P79 11-12m	3434-BLK.112	25-30	4-6	58-62	1-3	4-6	-	-	-	-	-	-	
29	71	0	P84 7-8m	3441-BLK.107	5-9	3-5	-	0-1	70-75	5-15	1-5	-	-	-	Tr	
29	66	4	P61 13-14m	3380-BLK.106	23-28	55-60	2-5	5-7	5-10	-	-	-	-	-	-	
29	51	21	P66 17-18m	3396-BLK.110	9-13	8-12	6-10	4-6	55-60	7-12	-	-	-	-	Tr	
28	27	45	P67 15-16m	3400-BLK.101	22-27	19-23	37-41	4-6	5-10	0-5	-	-	-	-	-	
26	5	68	P53 1-1.5m	3268-BLK.120	20-24	3-6	55-59	7-10	5-8	-	-	-	1-2	-	-	
24	6	70	P57 0.1-0.6m	3274-BLK.206	19-23	4-6	58-62	7-10	5-7	-	-	-	-	-	-	
22	76	2	P49 0-0.2m	3263-BLK.115	4-8	4-8	0-1	2-4	72-78	5-10	5-10	-	-	-	-	Microcline - Tr
21	76	3	P61 14-15m	3381-BLK.107	15-20	60-65	1-4	<1	16-20	-	-	-	-	-	-	
20	14	66	P69 10-11m	3406-BLK.108	13-16	9-11	45-50	1-3	20-24	-	-	-	-	2-5	-	
20	12	67	P77 9-10m	3426-BLK.104	15-20	2-4	56-60	4-6	8-10	5-10	-	-	-	-	-	
20	5	75	P76 9-10m	3413-BLK.103	15-18	1-3	60-65	3-7	10-13	0-5	-	-	-	-	-	
20	0	80	P85 1.08-1.1m	3452-BLK.106	15-20	<1	67-73	3-7	6-8	-	-	-	-	-	-	
19	14	67	P77 13-14m	3430-BLK.108	14-18	2-4	53-57	6-8	7-9	6-11	-	-	1-3	-	-	
19	14	68	P76 16-17m	3420-BLK.110	15-20	3-7	60-65	3-5	1-3	5-10	-	-	-	-	-	
19	7	74	P84 14-15m	3448-BLK.102	10-13	1-3	42-48	1-2	35-39	0-5	-	-	-	-	-	
19	6	75	P84 9-10m	3443-BLK.109	17-20	4-7	70-75	1-2	1-5	-	-	-	-	-	-	
19	6	76	P76 14-15m	3418-BLK.108	15-20	2-4	69-73	4-8	0-1	0-5	-	-	-	-	-	
18	11	71	P77 4-5m	3421-BLK.111	13-17	1-2	57-63	1-4	9-13	5-10	-	-	2-5	-	-	
18	11	71	P77 10-11m	3427-BLK.105	13-17	1-2	57-63	1-4	9-13	5-10	-	-	-	-	-	
16	80	5	P55 Upper grey clay	3271-BLK.203	3-7	3-7	-	6-10	38-42	15-20	1-5	1-2	~20	-	Tr	
16	3	80	P54 0.1-0.6m	3270-BLK.202	13-16	2-4	70-74	7-10	1-3	-	-	-	-	-	-	
14	13	73	P68 12-13m	3403-BLK.105	11-15	8-12	67-73	1-3	1-3	0-5	-	-	-	-	-	

000388

Table 1.3 (continued).

Paly	Ill	Dol	Sample	XRD File	Paly	Ill	Dol	Hal	Qtz	Smt	Kaol	Cal	Gyp	Cel	An	Other
13	14	72	P68 13-14m	3404-BLK.106	10-14	8-12	62-67	1-3	7-12	0-5	-	-	-	-	-	
13	1	85	P65 6-7m	3382-BLK.108	11-15	0-2	80-85	1-3	2-5	-	-	-	-	-	-	
13	2	85	P79 9-10m	3432-BLK.110	10-14	1-2	77-81	1-3	5-7	-	-	-	-	-	-	
13	2	85	P7910-11m	3433-BLK.111	10-14	1-2	77-81	1-3	3-5	-	-	-	-	-	-	
13	2	85	P76 8-9m	3412-BLK.102	10-13	1-2	75-80	2-4	5-7	-	0-1	-	-	-	-	
13	6	82	P79 13-14m	3436-BLK.102	10-14	2-4	76-80	1-3	2-4	0-5	-	-	-	-	-	
12	87	1	P65 14-15m	3390-BLK.104	5-10	35-40	0-1	2-3	30-35	15-20	-	-	-	-	Tr	
12	3	85	P53 0.6-1m	3269-BLK.201	9-13	1-4	76-82	4-6	2-4	-	-	-	-	-	Tr	
12	1	87	P66 14-15m	3393-BLK.107	9-13	0-2	80-85	1-3	3-6	-	-	-	-	-	-	
11	87	2	P66 18-19m	3397-BLK.111	7-10	45-55	1-2	3-5	17-20	15-20	-	-	-	-	Tr	
11	81	8	P61 6-8m	3375-BLK.101	5-10	20-30	1-5	1-3	20-30	5-10	20-30	1-5	-	-	Tr	
11	20	69	P77 12-13m	3429-BLK.107	8-12	8-12	57-63	1-4	6-10	5-10	-	-	-	-	-	
11	11	78	P76 11-12m	3415-BLK.105	8-12	<1	68-74	2-4	4-7	8-12	-	-	-	-	-	
11	6	83	P79 14-15m	3437-BLK.103	9-12	2-4	77-81	1-2	4-6	0-5	-	-	-	-	-	
10	62	29	P61 8-10m	3376-BLK.102	5-10	20-30	15-25	1-4	15-25	5-10	10-20	1-3	-	-	Tr	
10	11	79	P76 12-13m	3416-BLK.106	7-11	<1	70-75	2-4	3-6	8-12	-	-	-	-	-	
10	7	83	P79 15-16m	3438-BLK.104	8-11	3-5	77-81	1-2	3-5	0-5	-	-	-	-	-	
10	0	90	P52 0-1m	3267-BLK.119	7-10	<1	76-82	4-6	2-4	-	-	-	3-6	-	Tr	Barite - Tr
9	91	0	P65 16-17.5m	3392-BLK.106	5-10	55-60	<1	4-6	11-15	15-20	-	-	-	-	Tr	
7	93	0	P65 15-16m	3391-BLK.105	4-7	55-60	<1	3-5	12-16	15-20	-	-	-	-	Tr	
7	0	93	P33 Middle	3251-BLK.103	5-8	-	80-85	4-6	2-4	-	-	-	1-3	-	-	
6	2	92	P84 10-11m	3444-BLK.110	4-8	1-3	87-93	0-1	1-2	-	-	-	-	-	-	
6	1	93	P76 6-7m	3410-BLK.112	3-7	0-1	73-79	1-2	16-20	-	-	-	-	-	-	
6	0	94	P56 0.3-0.6m	3273-BLK.205	4-7	<1	86-92	2-4	2-3	-	-	-	-	-	-	
5	92	3	P84 6-7m	3440-BLK.106	1-2	2-4	0-2	-	65-70	5-15	15-20	-	-	-	Tr	
5	54	41	P77 14-15m	3431-BLK.109	1-5	13-17	22-27	5-7	30-35	15-20	-	-	1-2	-	-	
5	8	87	P76 13-14m	3417-BLK.107	3-7	<1	80-85	1-3	2-5	5-10	-	-	-	-	-	
5	2	92	P45 1.5-1.7m	3257-BLK.109	3-7	1-3	82-87	4-6	1-2	-	-	-	-	-	-	
5	1	94	P74 11-12m	3409-BLK.111	3-7	0-1	87-93	0-2	3-7	-	-	-	-	-	-	
5	1	94	P46 0-0.6m	3258-BLK.110	3-6	0-2	87-93	3-5	0-1	-	-	-	-	-	-	
5	0	95	P44 0.2-1m	3254-BLK.106	2-6	-	73-79	4-6	12-18	-	-	-	-	-	-	

000389

Table 1.3 (continued).

Paly	Ill	Dol	Sample	XRD File	Paly	Ill	Dol	Hal	Qtz	Smt	Kaol	Cal	Gyp	Cel	An	Other
4	96	1	P66 19-20m	3398-BLK.112	2-5	65-75	0-1	4-6	4-7	15-20	-	-	-	-	-	
4	1	95	P74 10-11m	3408-BLK.110	2-6	0-1	87-93	0-2	3-7	-	-	-	-	-	-	
3	8	89	P55 0-0.7m	3272-BLK.204	2-4	-	82-88	3-5	0-1	5-10	-	-	Tr	-	-	
3	0	97	P87 0-0.6m	3454-BLK.108	2-4	<1	87-93	3-5	1-3	-	-	-	-	-	-	
2	0	98	P65 7-8m	3383-BLK.109	1-3	<1	93-98	0-1	1-3	-	-	-	-	-	-	
2	0	98	P65 8-9m	3384-BLK.110	1-3	<1	93-98	1-2	1-2	-	-	-	-	-	-	
2	0	98	P51 0-1m	3266-BLK.118	0-3	-	86-92	2-4	5-7	-	-	-	-	-	-	
2	0	98	P45 0-1m	3255-BLK.107	0-3	-	90-95	4-6	0-1	-	-	-	-	-	-	
2	0	98	P33 Upper	3250-BLK.102	0-3	-	94-98	1-3	<1	-	-	-	-	-	-	
2	0	98	P48 1-1.7m	3262-BLK.114	0-3	-	94-98	1-2	1-2	-	-	-	-	-	-	
1	0	99	P48 0-1m	3261-BLK.113	0-2	-	94-98	1-3	<1	-	-	-	-	-	-	
1	0	99	P45 1-1.5m	3256-BLK.108	0-1	-	92-96	3-5	1-2	-	-	-	-	-	-	
0	100	0	P88 3-4m	3458-BLK.112	-	-	-	12-15	42-47	40-45	-	-	-	-	Tr	
0	100	0	Quartz Boulder	3249-BLK.101	-	~3	-	~6	~15	0-5	~75	-	-	-	-	
0	100	0	P48 Green clay	3260-BLK.112	-	8-12	-	2-4	62-68	5-10	5-10	-	Tr	-	Tr	Microcline ~ 5 Albite ~ 3
0	60	40	P79 16-17m	3439-BLK.105	-	16-20	35-40	1-3	3-5	35-40	-	-	-	-	-	
0	1	99	P47 0-1m	3259-BLK.111	-	-	92-96	3-5	<1	0-2	-	-	Tr	-	-	
0	0	100	P44 0-1m	3253-BLK.105	Tr	-	92-98	4-6	-	-	-	-	-	-	-	
0	0	100	P49 Black nodule	3264-BLK.116	-	-	-	-	12-18	-	-	~85	-	-	-	Microcline - Tr
0	0	100	P50 0-0.7m	3265-BLK.117	-	-	94-98	1-3	1-3	-	-	-	-	-	-	

Paly = palygorskite; Ill = illite; Dol = dolomite; Hal = halite; Qtz = quartz;
Smt = smectite (includes randomly interstratified and very-poorly crystalline material);
Kaol = kaolinite; Cal = calcite; Gyp = gypsum; Cel = celestine; An = anatase.
Tr = trace.

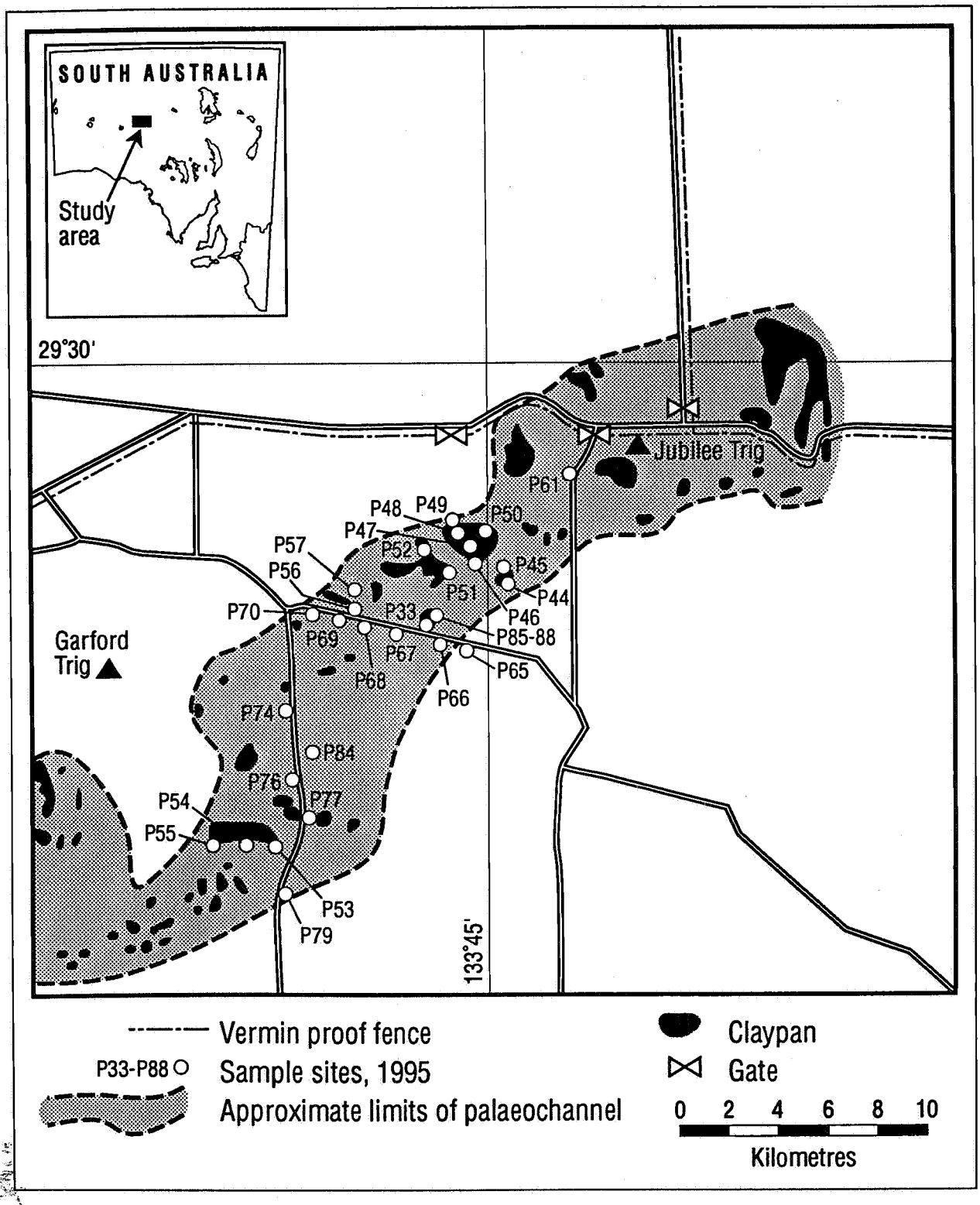


Fig. 1.1. Sketch map of Garford palaeochannel sampling locations.

(Drawing reference "Self map. D106/GER".)

Fig. 1.2. Garford Paleochannel Samples - Quartz Boulder.

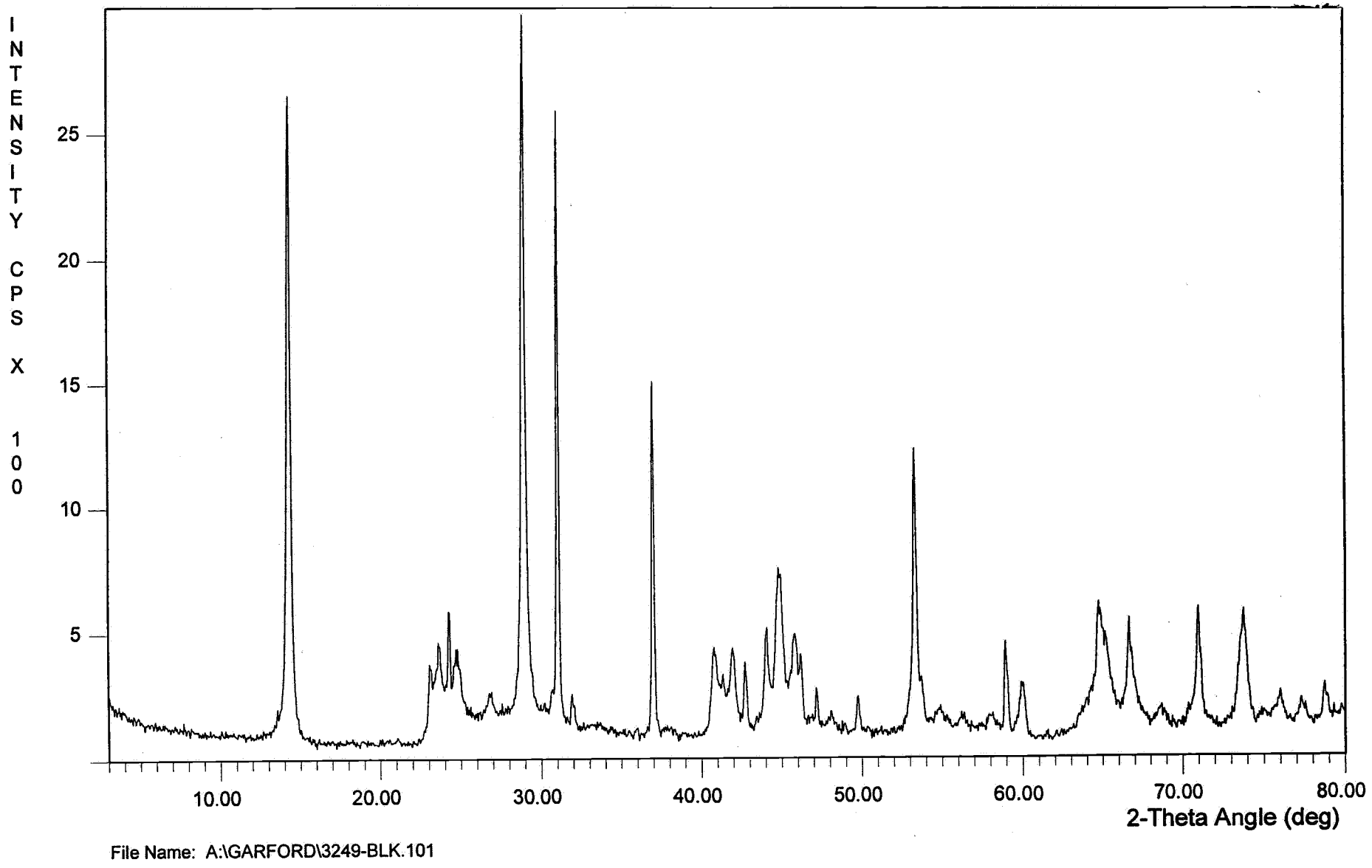


Fig. 1.2. XRD spectrum (Co Kα radiation, back pressed) of Garford palaeochannel quartz boulder sample.

Fig. 1.3a. Garford Paleochannel Samples - P33 Lake Floor.

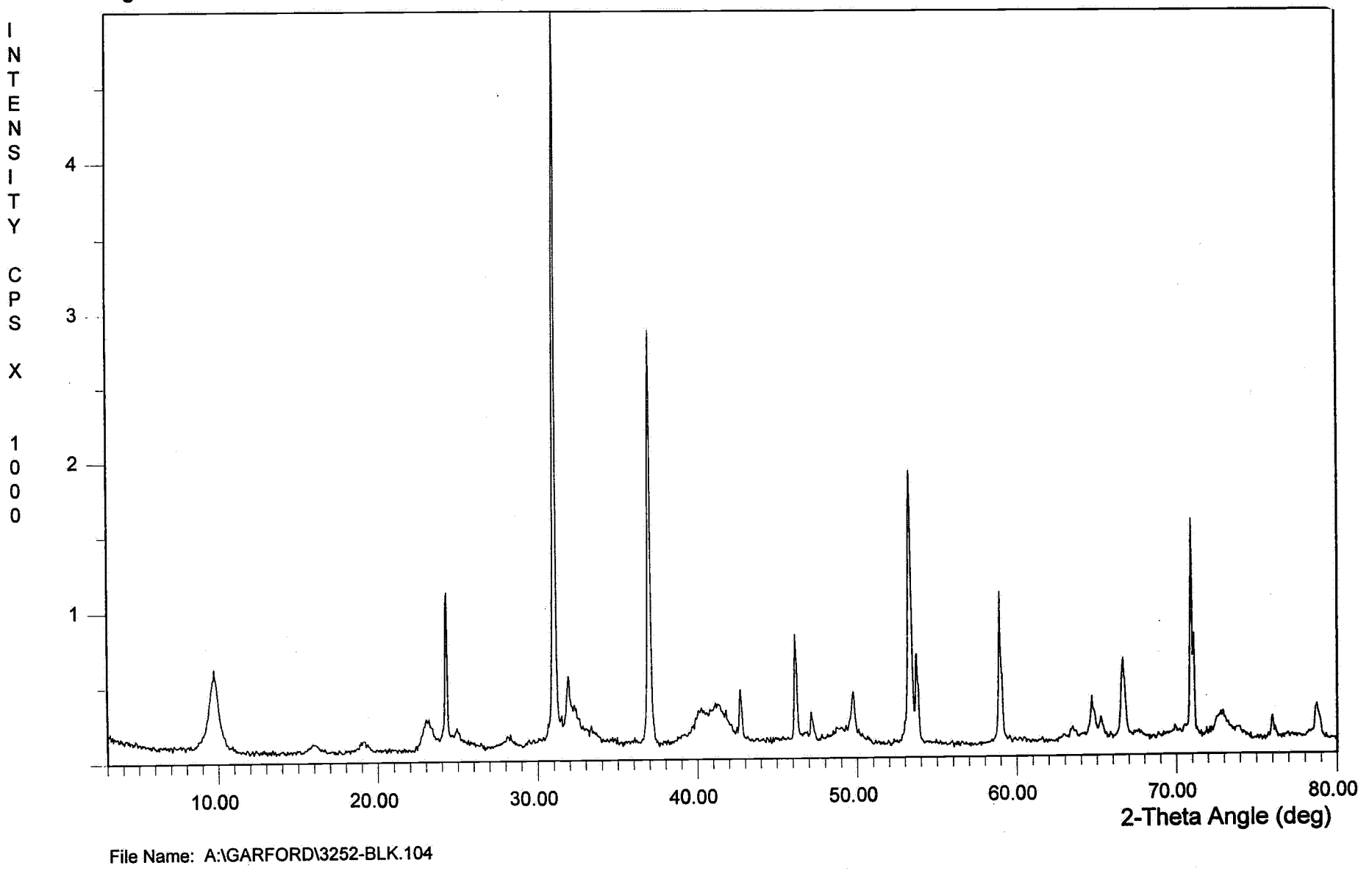


Fig. 1.3a. XRD spectrum (Co Kα radiation, back pressed) of Garford palaeochannel sample P33 Lake Floor.

Fig. 1.3b. Garford Paleochannel Samples - P33.

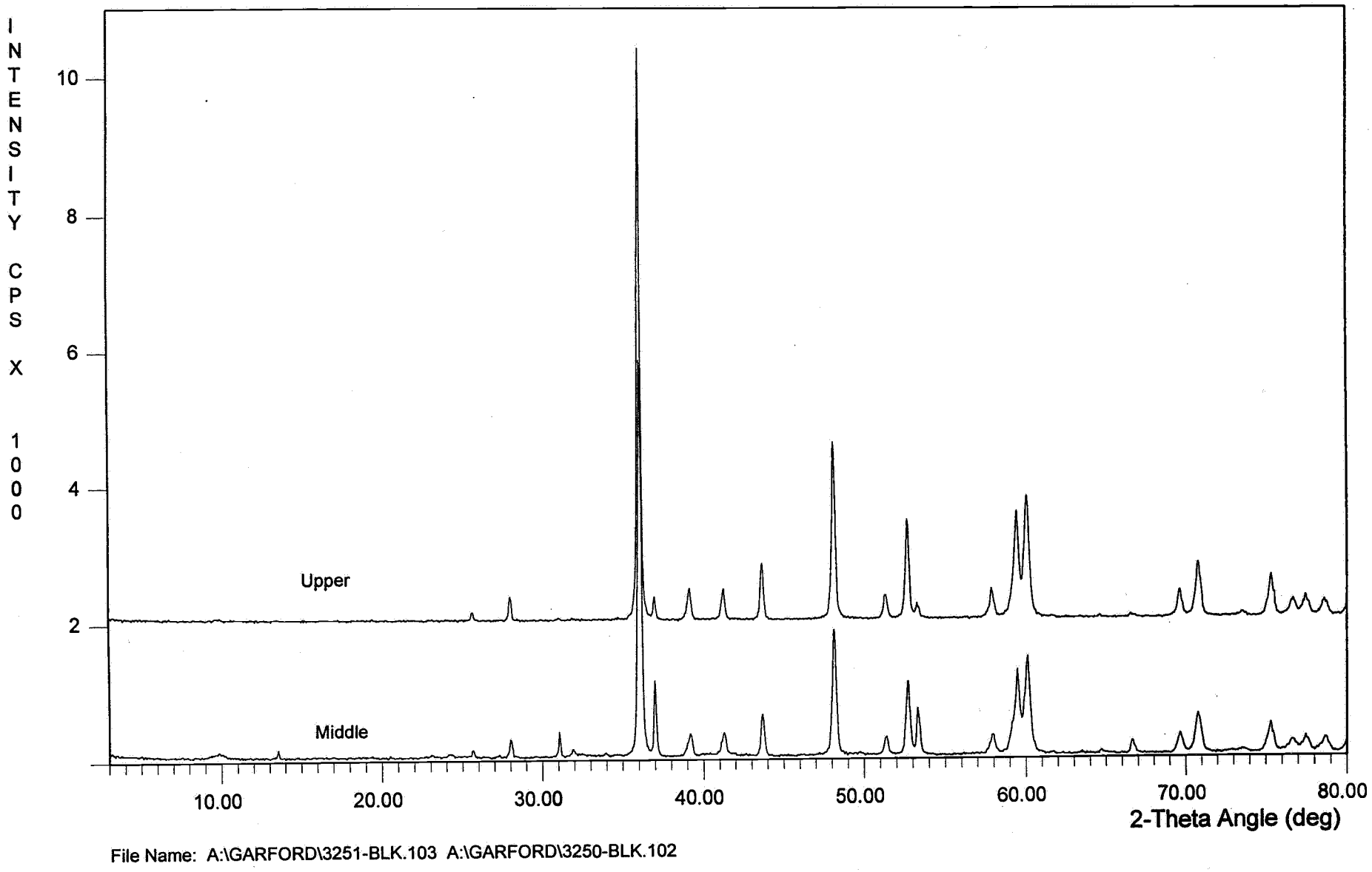


Fig. 1.3b. XRD spectrum (Co Kα radiation, back pressed) of Garford palaeochannel samples P33.

Fig. 1.4. Garford Paleochannel Samples - P44.

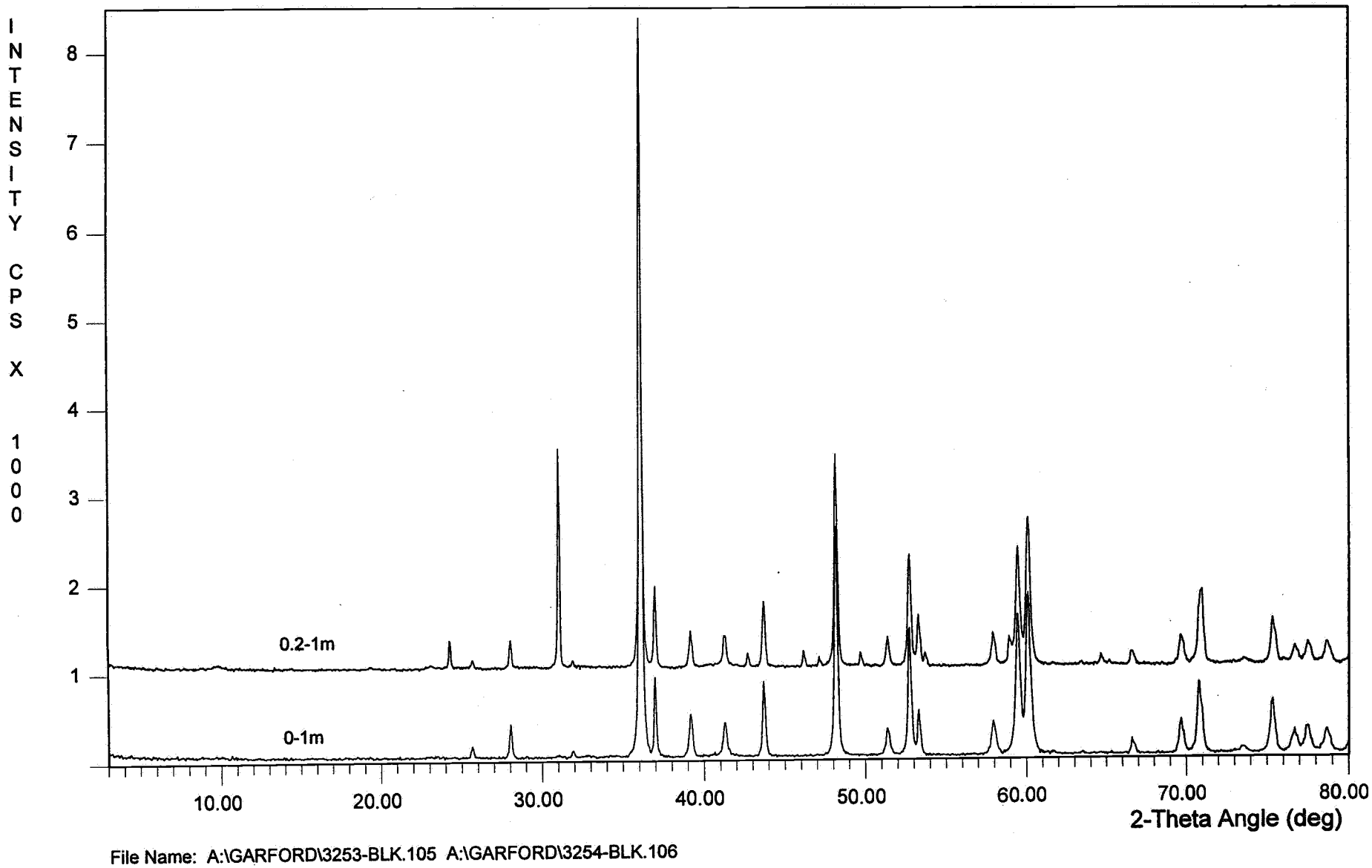


Fig. 1.4. XRD spectrum (Co Kα radiation, back pressed) of Garford palaeochannel samples P44.

0003955

Fig. 1.5. Garford Paleochannel Samples - P45.

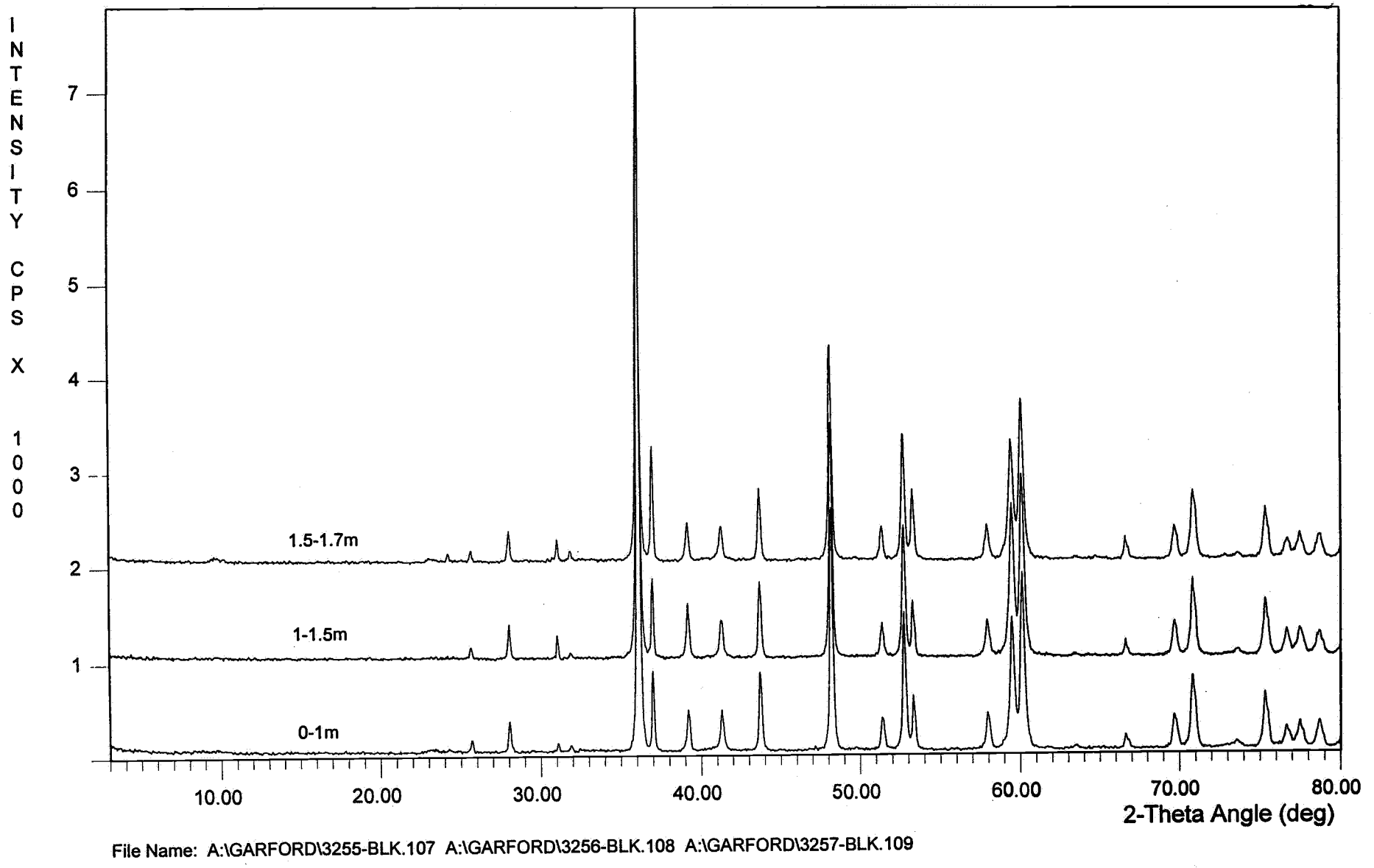


Fig. 1.5. XRD spectrum (Co Kα radiation, back pressed) of Garford palaeochannel samples P45.

Fig. 1.6. Garford Paleochannel Samples - P46 0-0.6m.

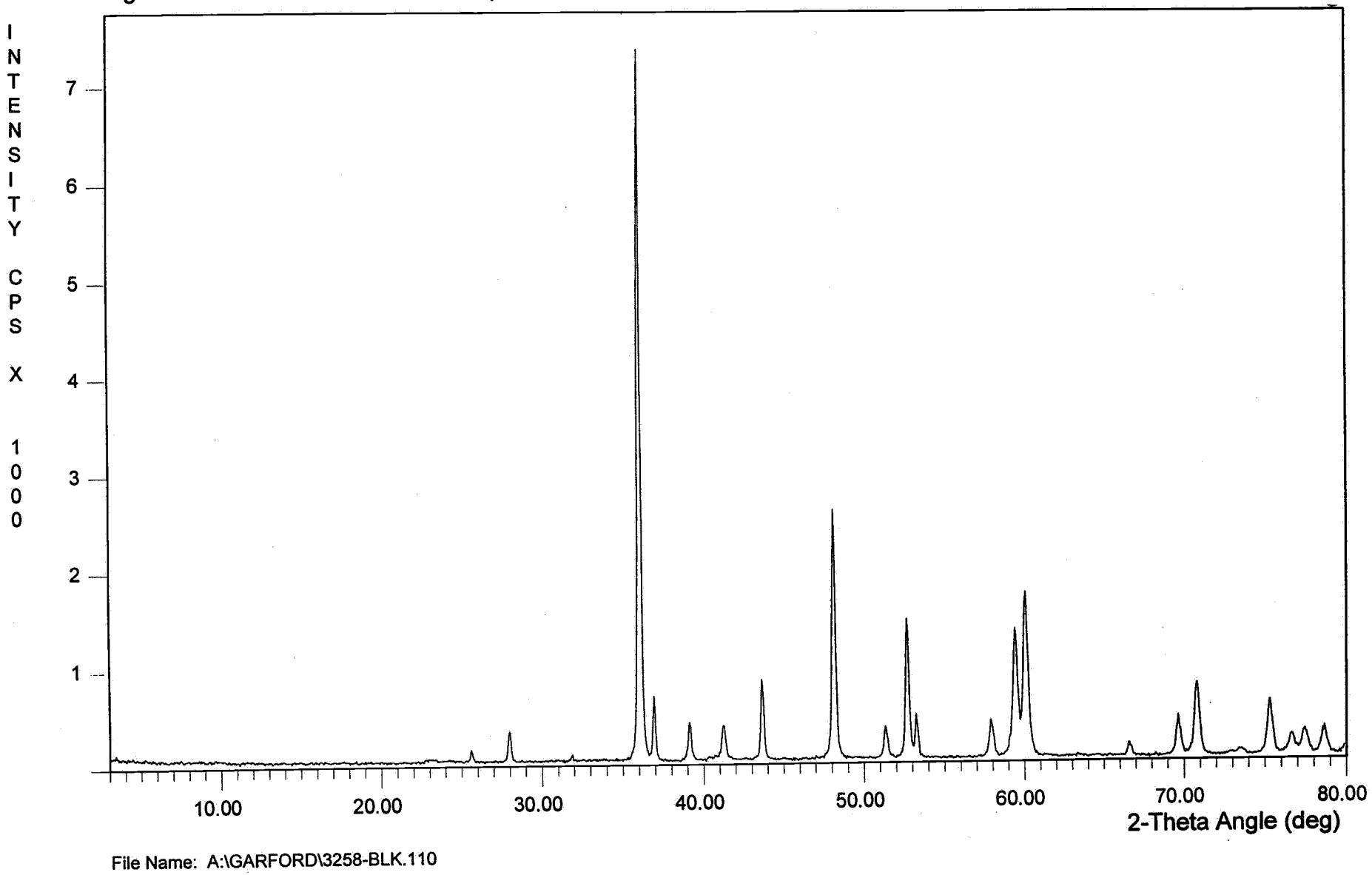


Fig. 1.6. XRD spectrum (Co Kα radiation, back pressed) of Garford palaeochannel sample P46 0-0.6m.

0003997
27

Fig. 1.7. Garford Paleochannel Samples - P47 0-1m.

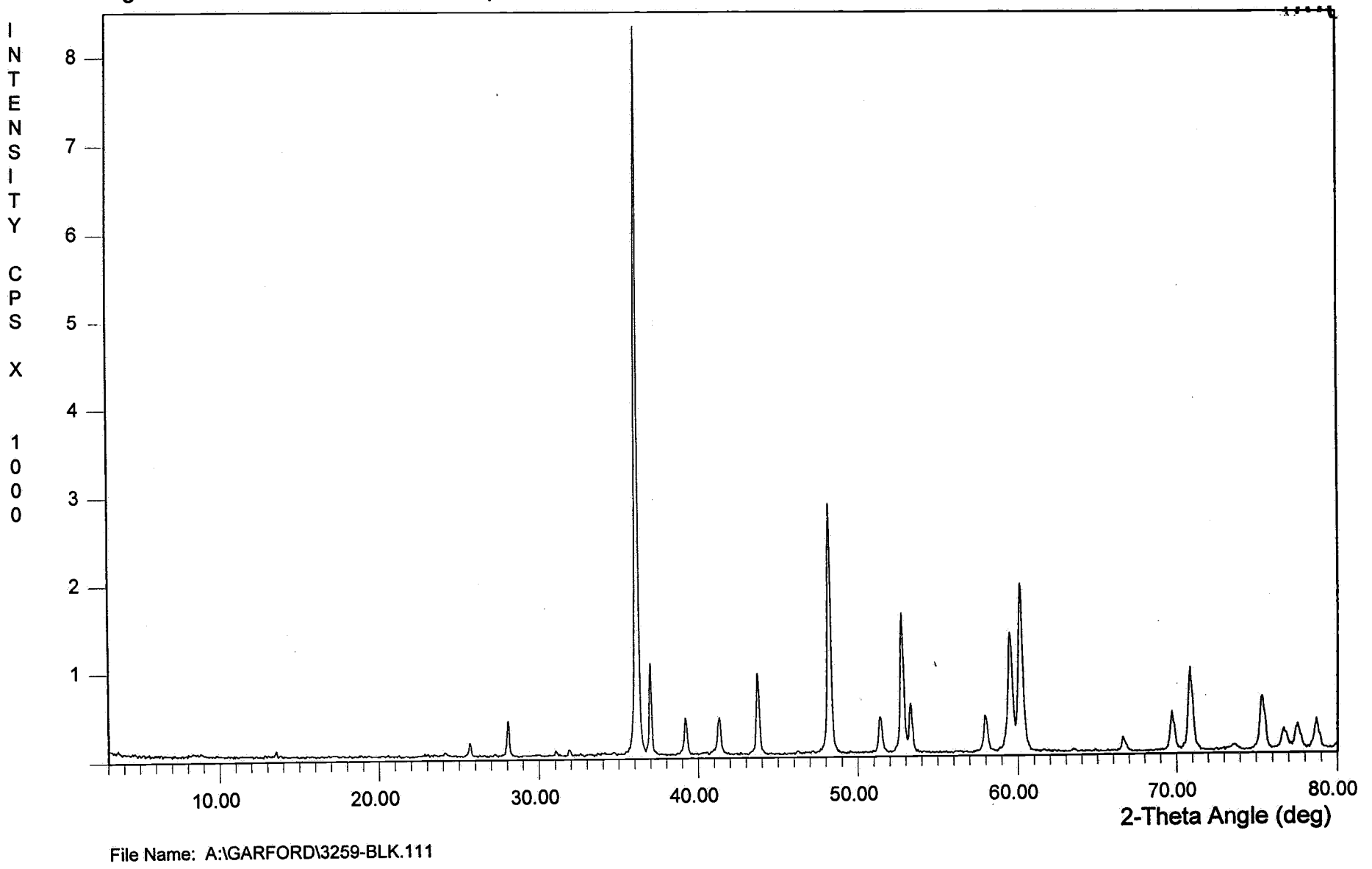


Fig. 1.7. XRD spectrum (Co Kα radiation, back pressed) of Garford palaeochannel sample P47 0-1m.

000398

Fig. 1.8. Garford Paleochannel Samples - P48.

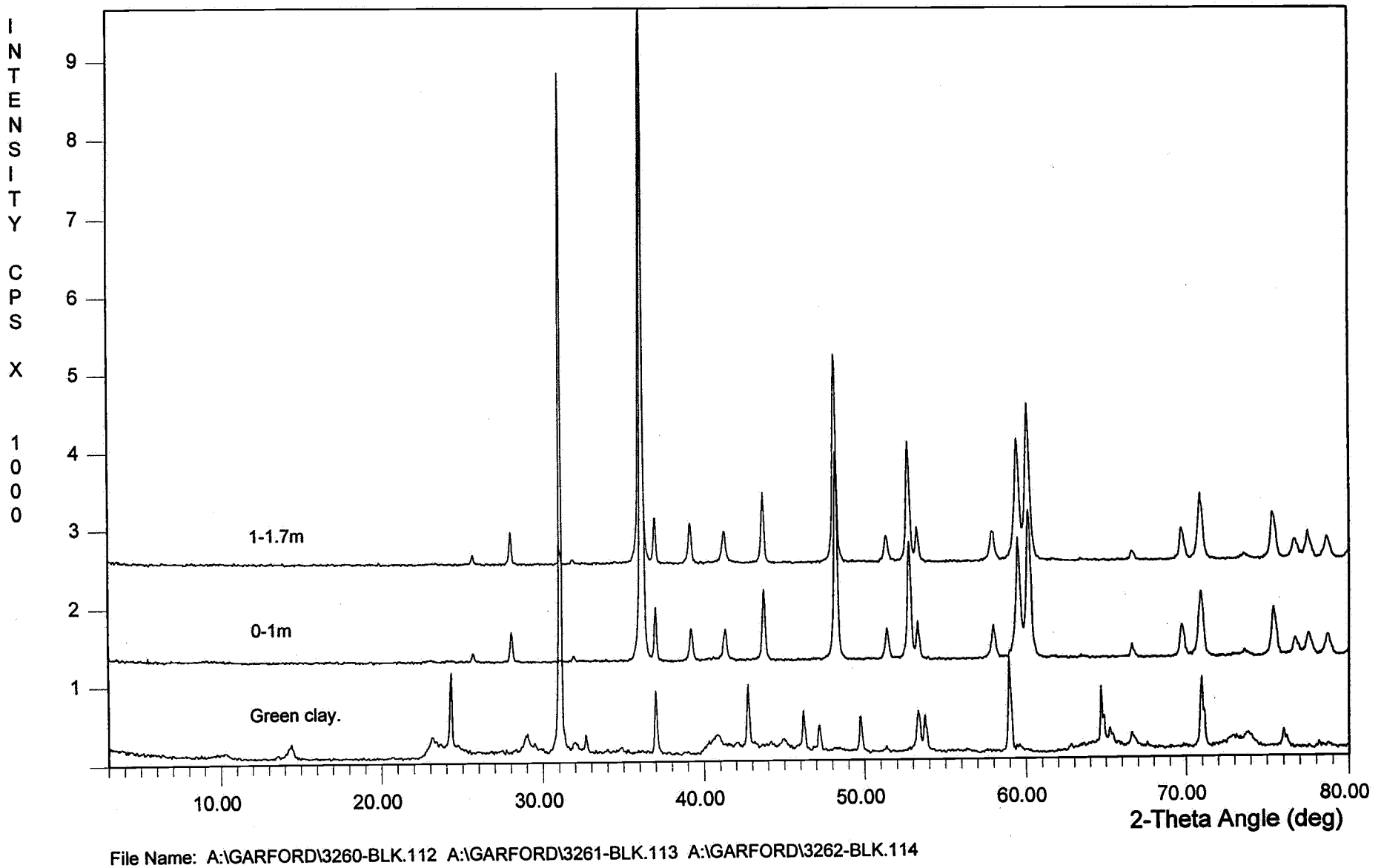


Fig. 1.8. XRD spectrum (Co Kα radiation, back pressed) of Garford palaeochannel samples P48.

0000399
29

Fig. 1.9. Garford Paleochannel Samples - P49.

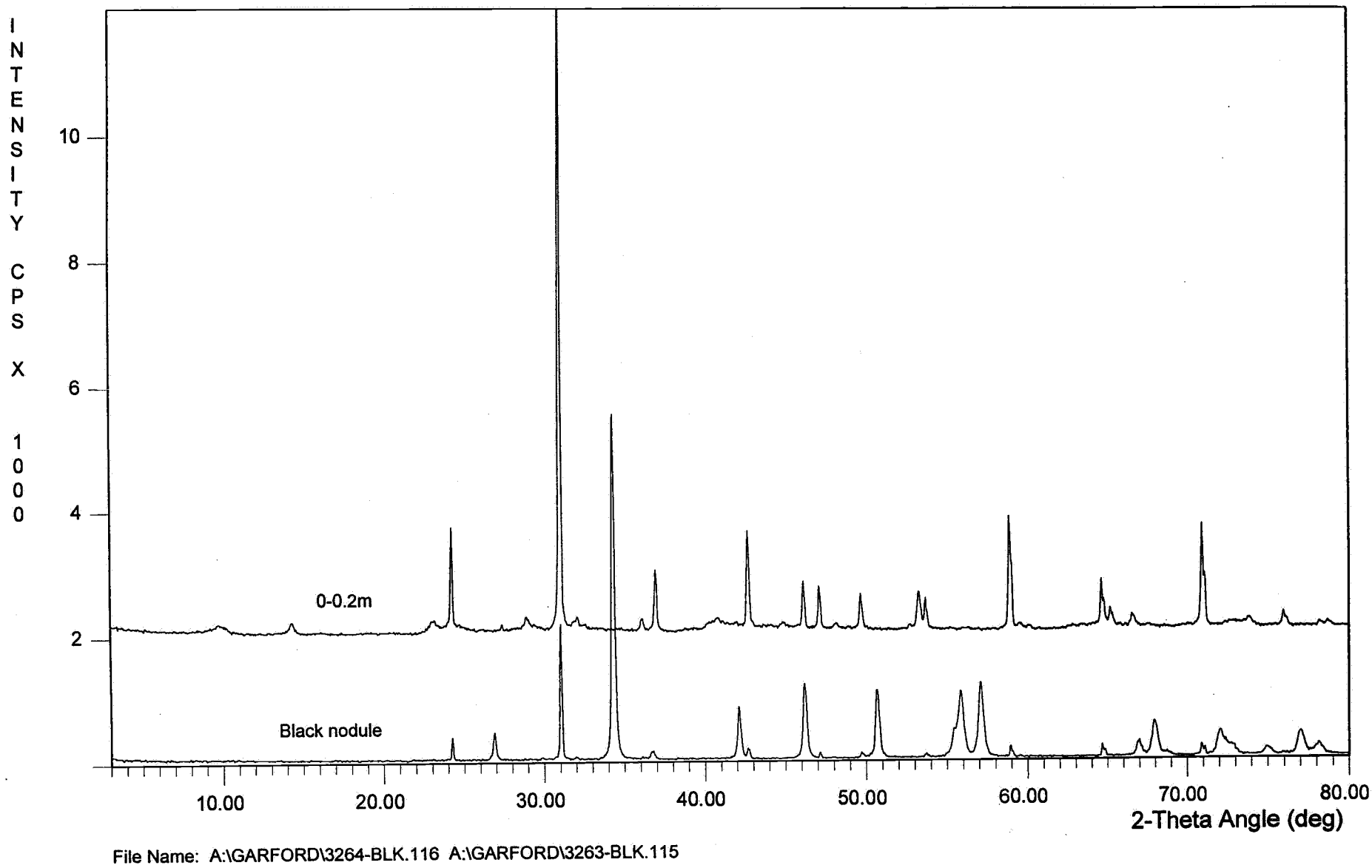


Fig. 1.9. XRD spectrum (Co Kα radiation, back pressed) of Garford palaeochannel samples P49.

Fig. 1.10. Garford Paleochannel Samples - P50 0-0.7m.

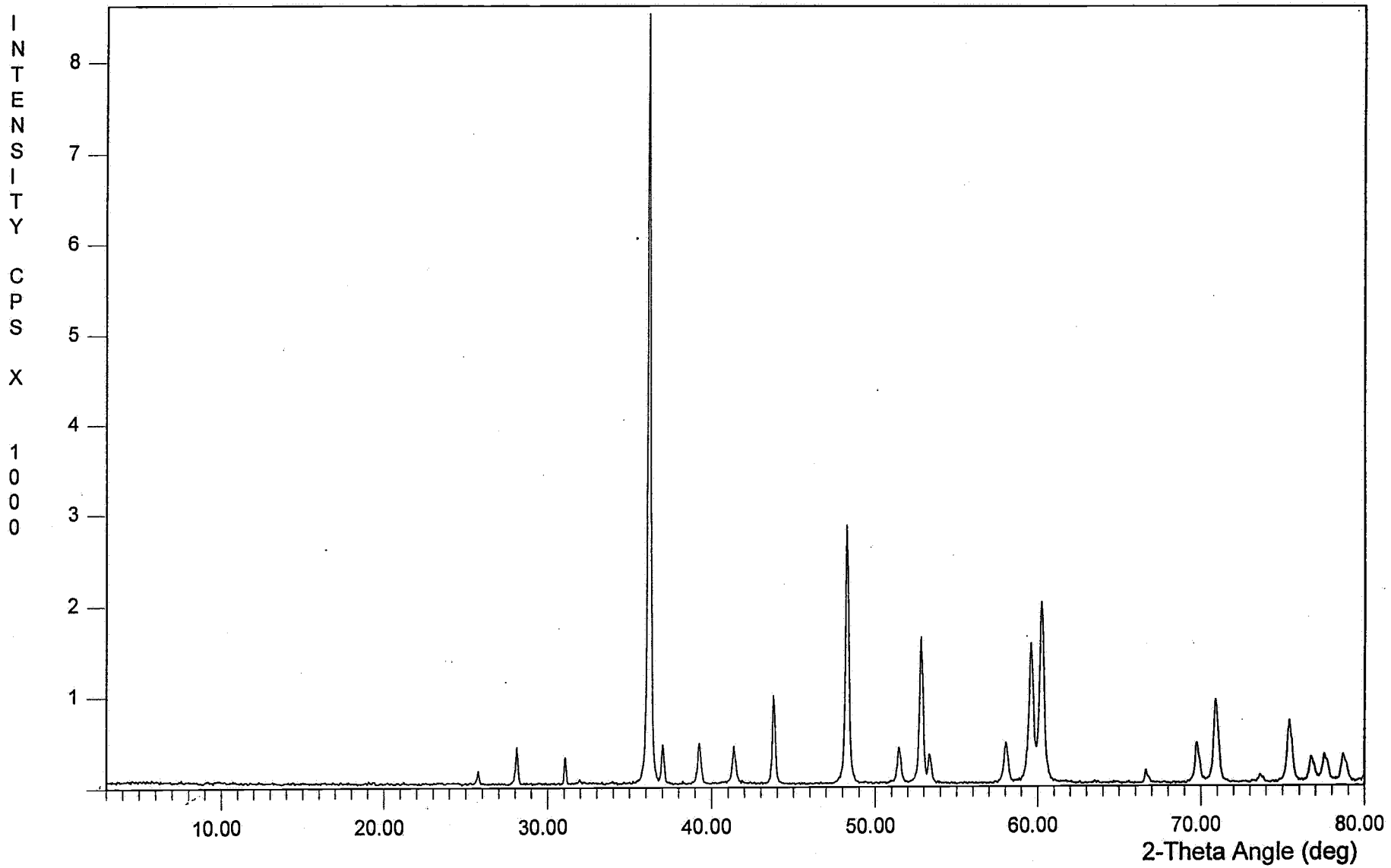


Fig. 1.10. XRD spectrum (Co Kα radiation, back pressed) of Garford palaeochannel sample P50 0-0.7m.

Fig. 1.11. Garford Paleochannel Samples - P51 0-1m.

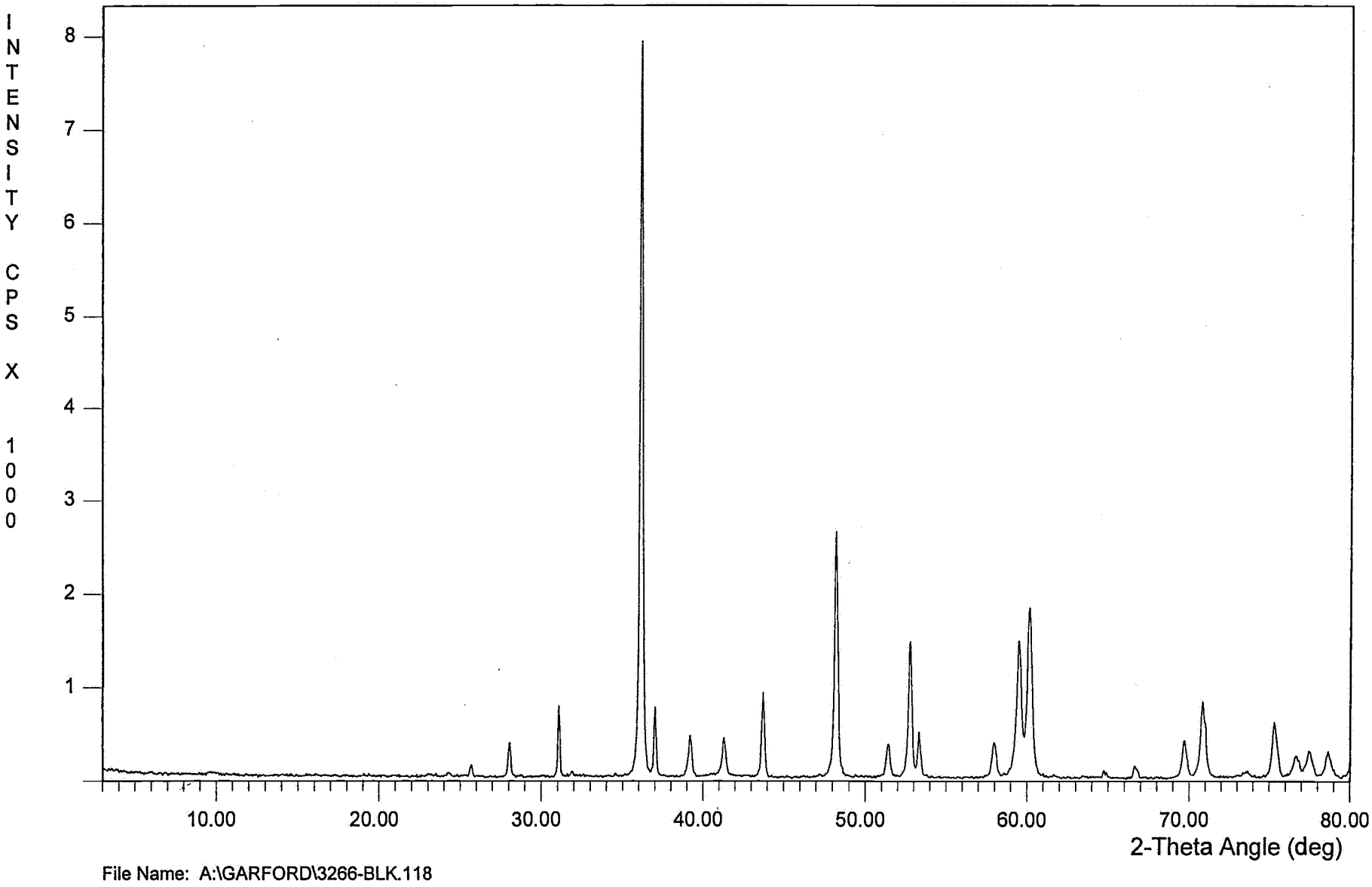


Fig. 1.11. XRD spectrum (Co Kα radiation, back pressed) of Garford palaeochannel sample P51 0-1m.

0004402
32

Fig. 1.12. Garford Paleochannel Samples - P52 0-1m.

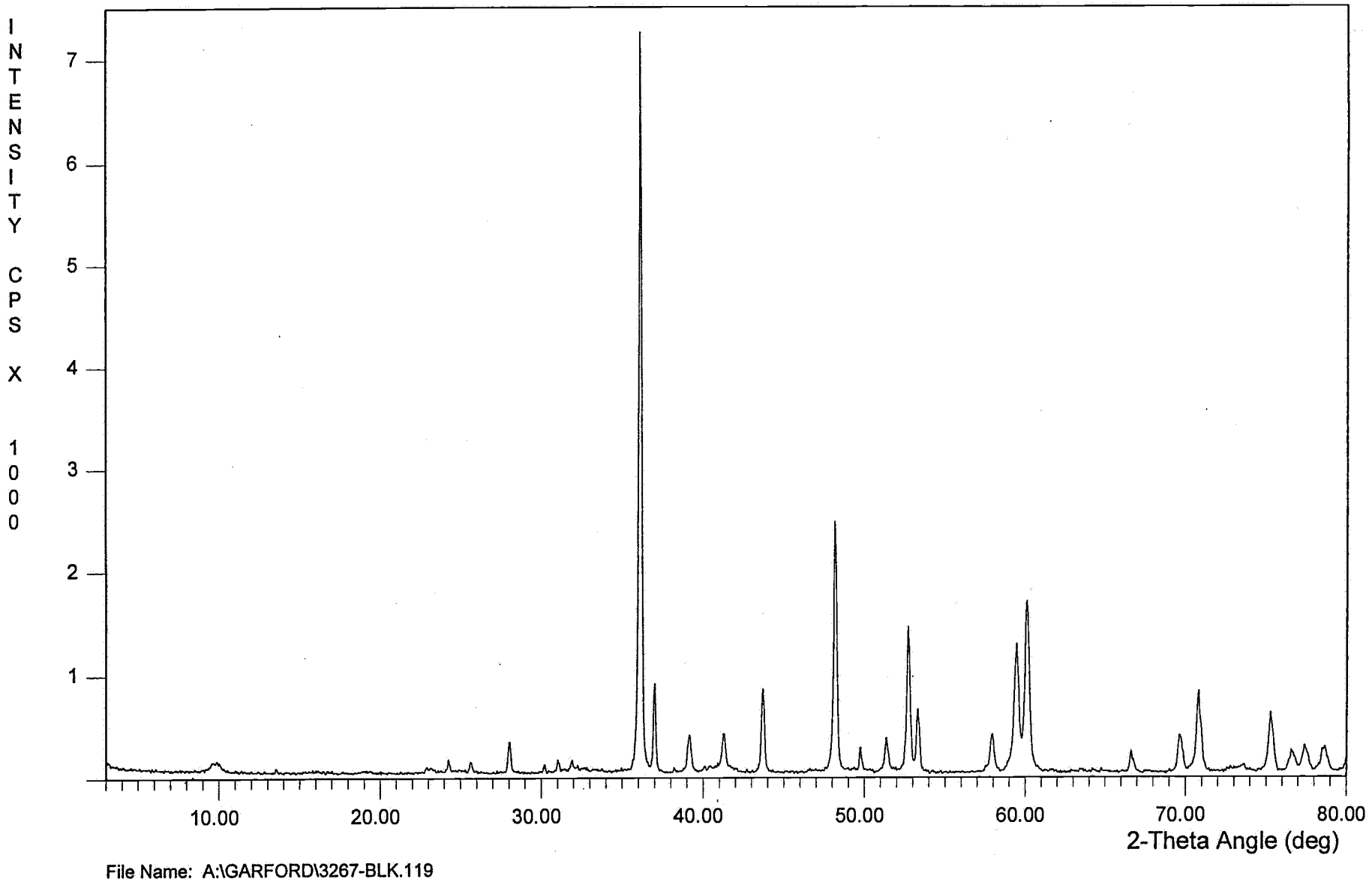


Fig. 1.12. XRD spectrum (Co Kα radiation, back pressed) of Garford palaeochannel sample P52 0-1m.

Fig. 1.13. Garford Paleochannel Samples - P53.

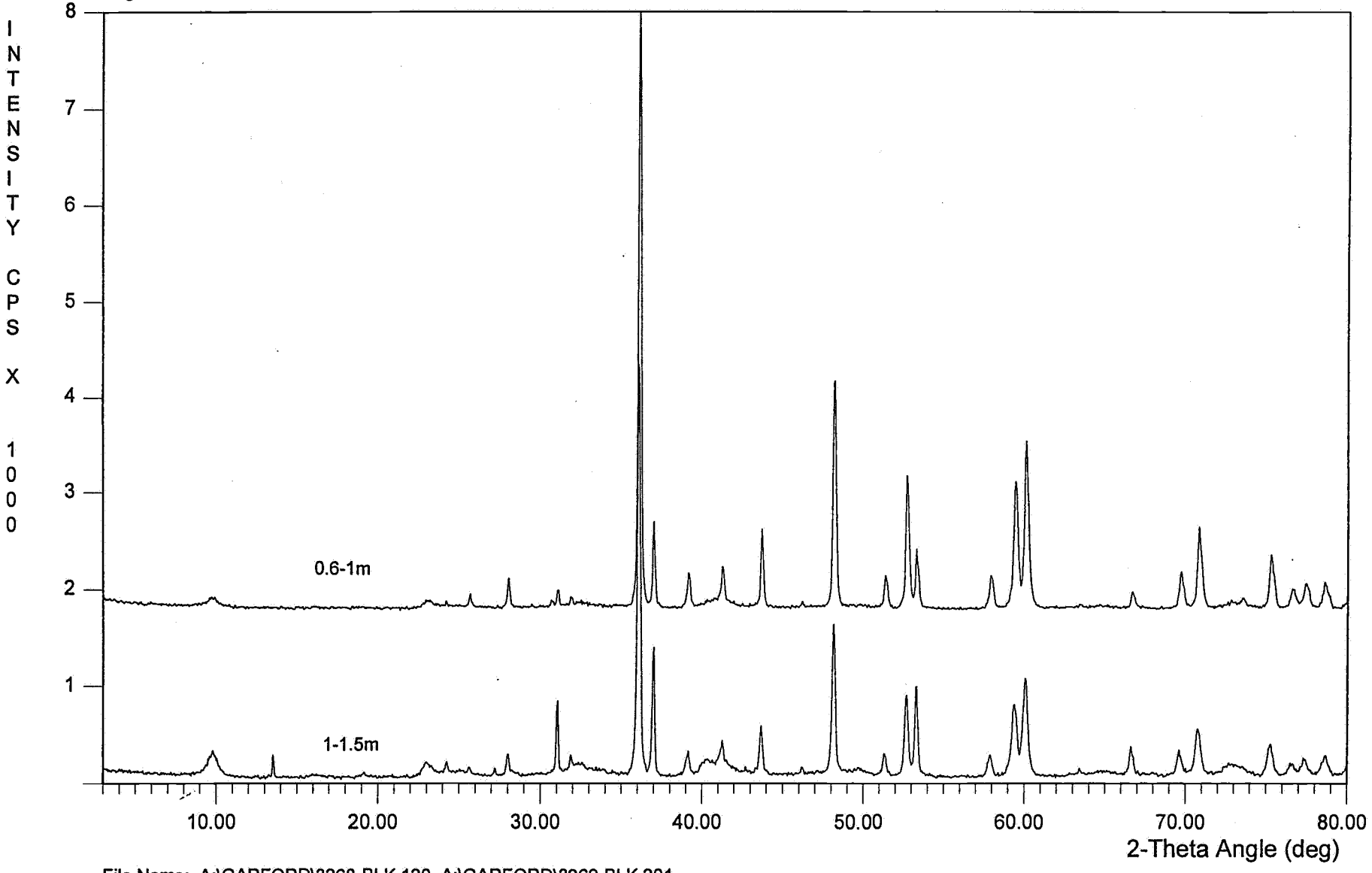


Fig. 1.13. XRD spectrum (Co Kα radiation, back pressed) of Garford palaeochannel samples P53.

000404

Fig. 1.14. Garford Paleochannel Samples - P54 0.1-0.6m.

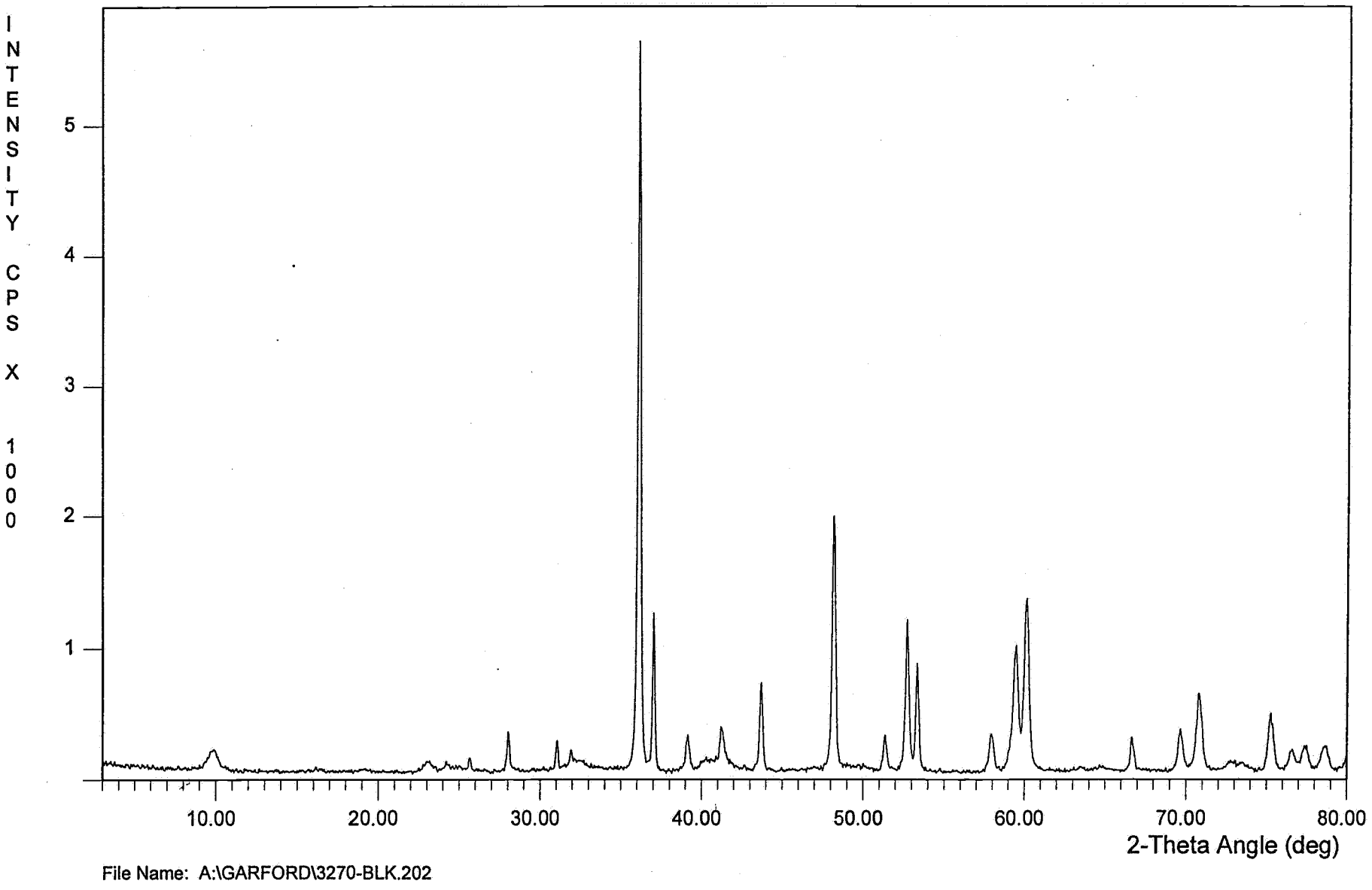


Fig. 1.14. XRD spectrum (Co Kα radiation, back pressed) of Garford palaeochannel sample P54 0.1-0.6m.

000405

Fig. 1.15. Garford Paleochannel Samples - P55.

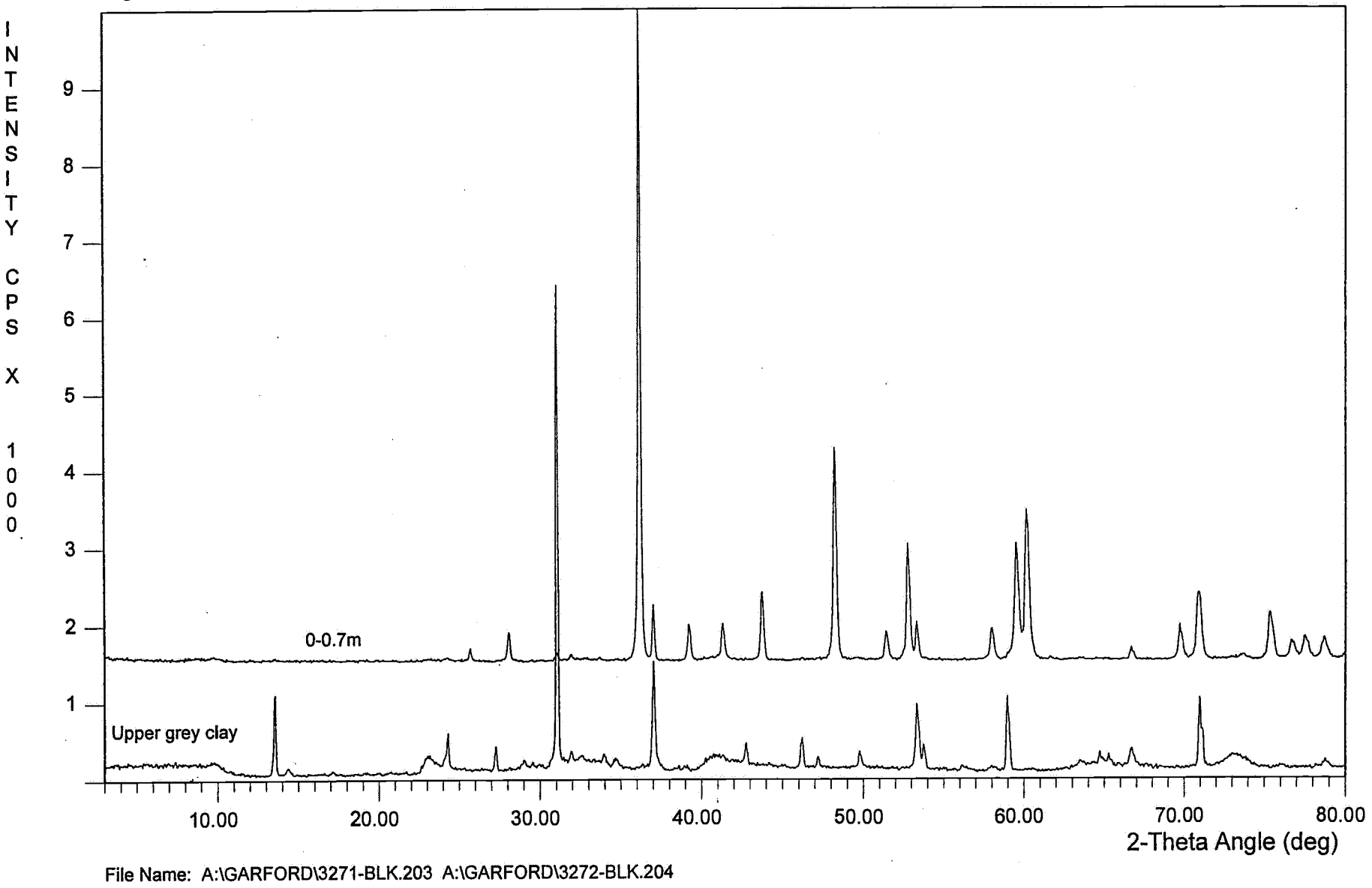


Fig. 1.15. XRD spectrum (Co Kα radiation, back pressed) of Garford palaeochannel samples P55.

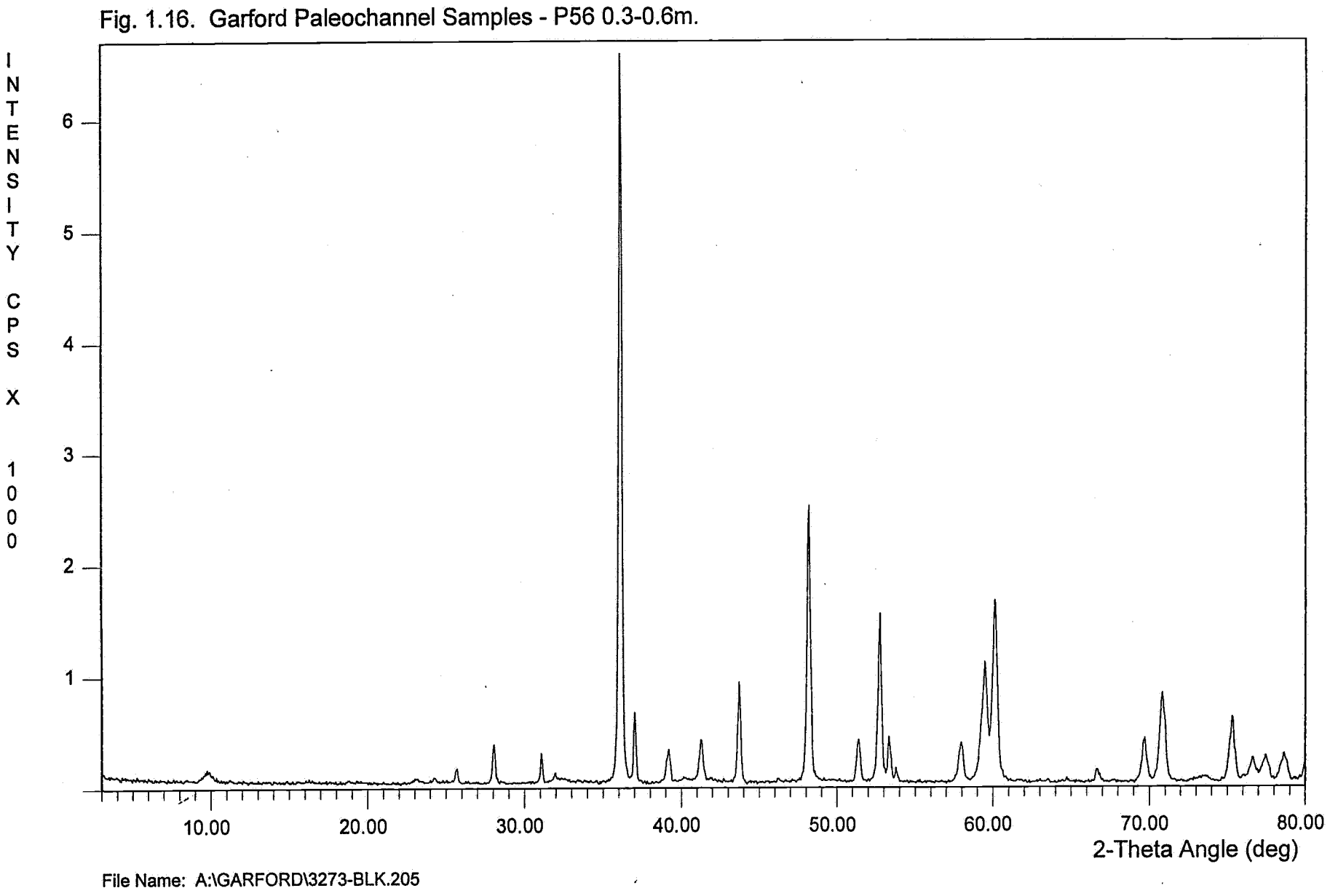


Fig. 1.16. XRD spectrum (Co Kα radiation, back pressed) of Garford palaeochannel sample P56 0.3-0.6m.

0004037

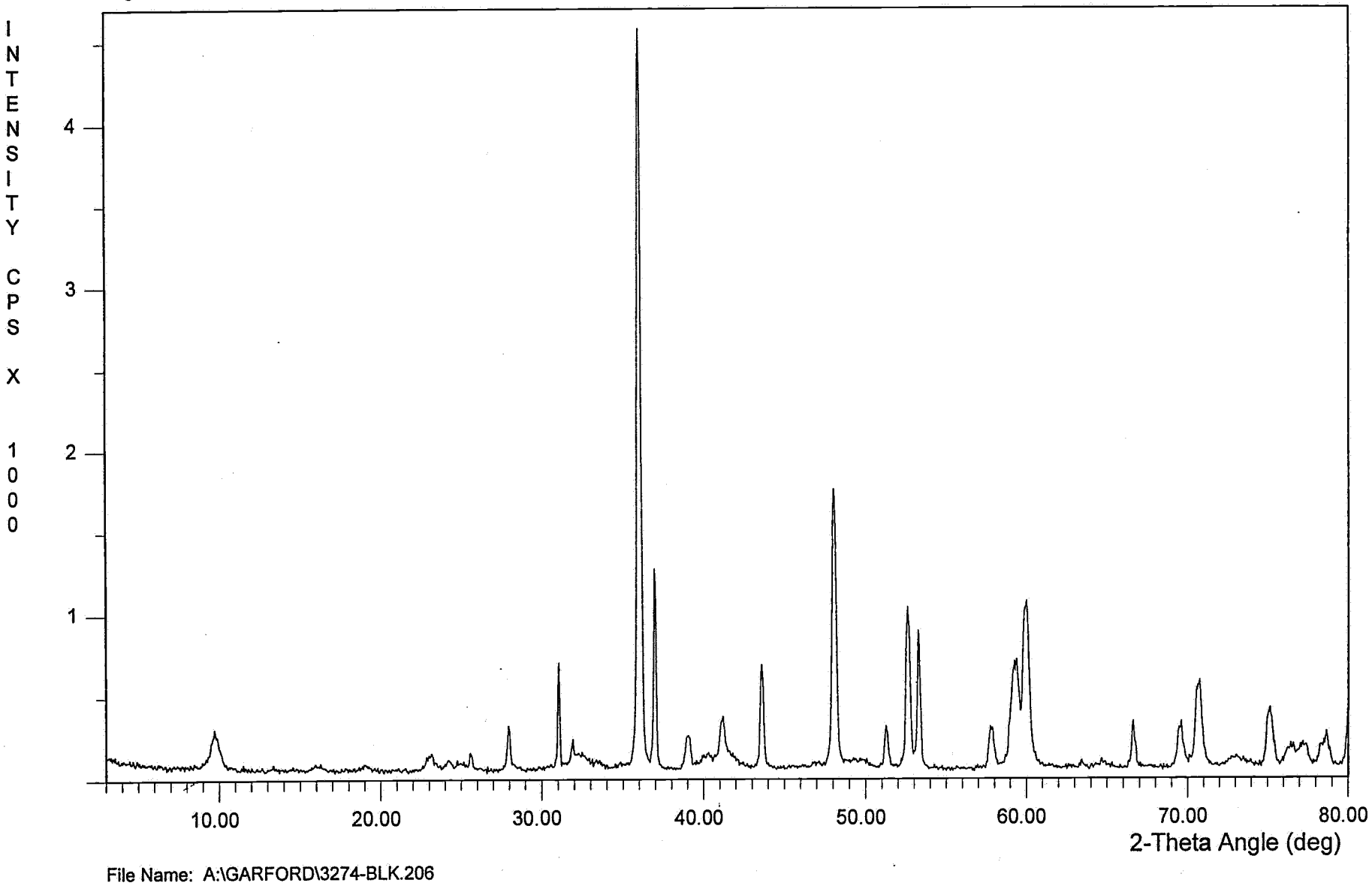


Fig. 1.17. XRD spectrum (Co Kα radiation, back pressed) of Garford palaeochannel sample P57 0.1-0.6m.

Fig. 1.18a. Garford Paleochannel Samples - P61.

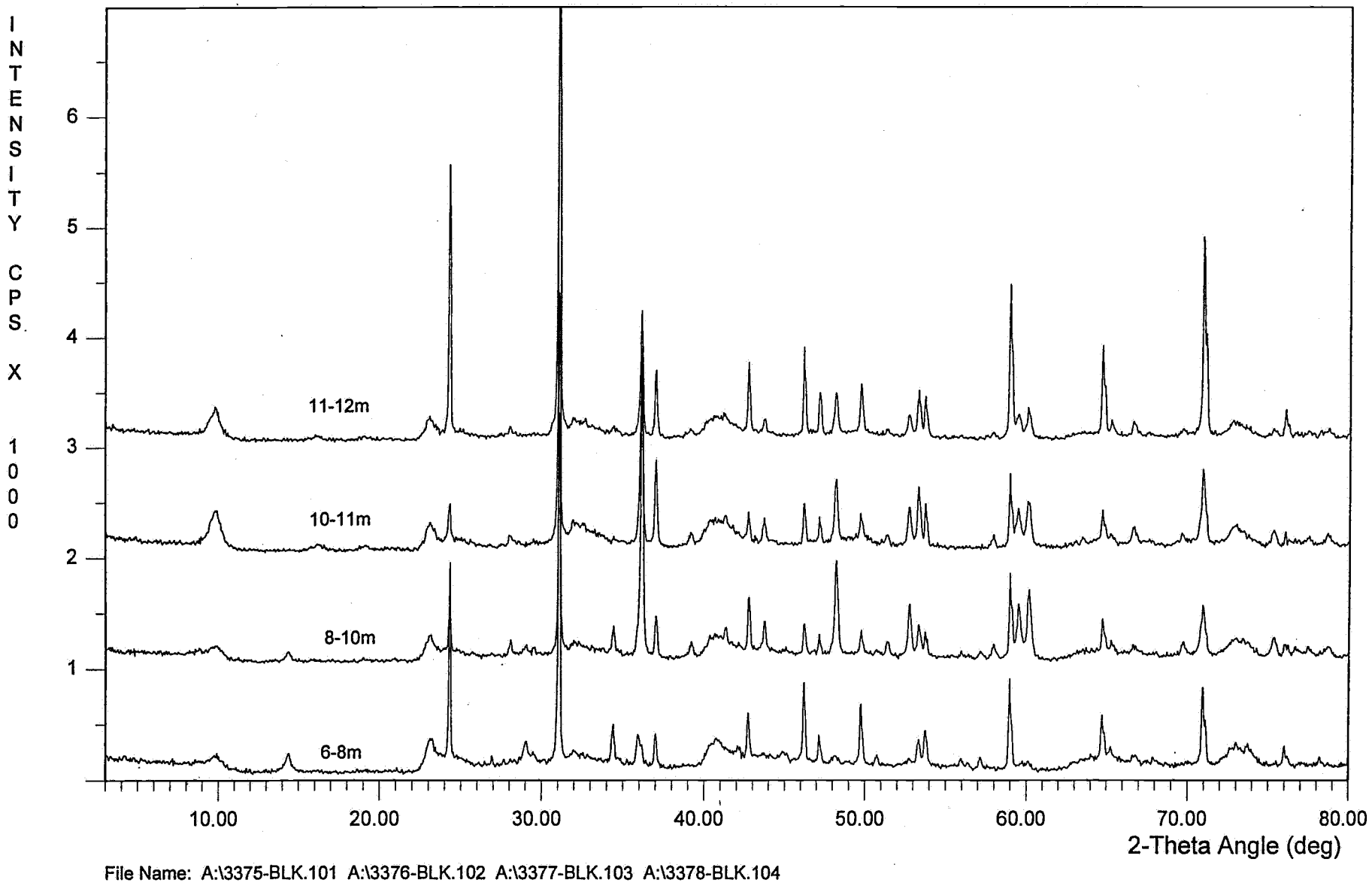


Fig. 1.18a. XRD spectrum (Co Kα radiation, back pressed) of Garford palaeochannel samples P61.

Fig. 1.18b. Garford Paleochannel Samples - P61.

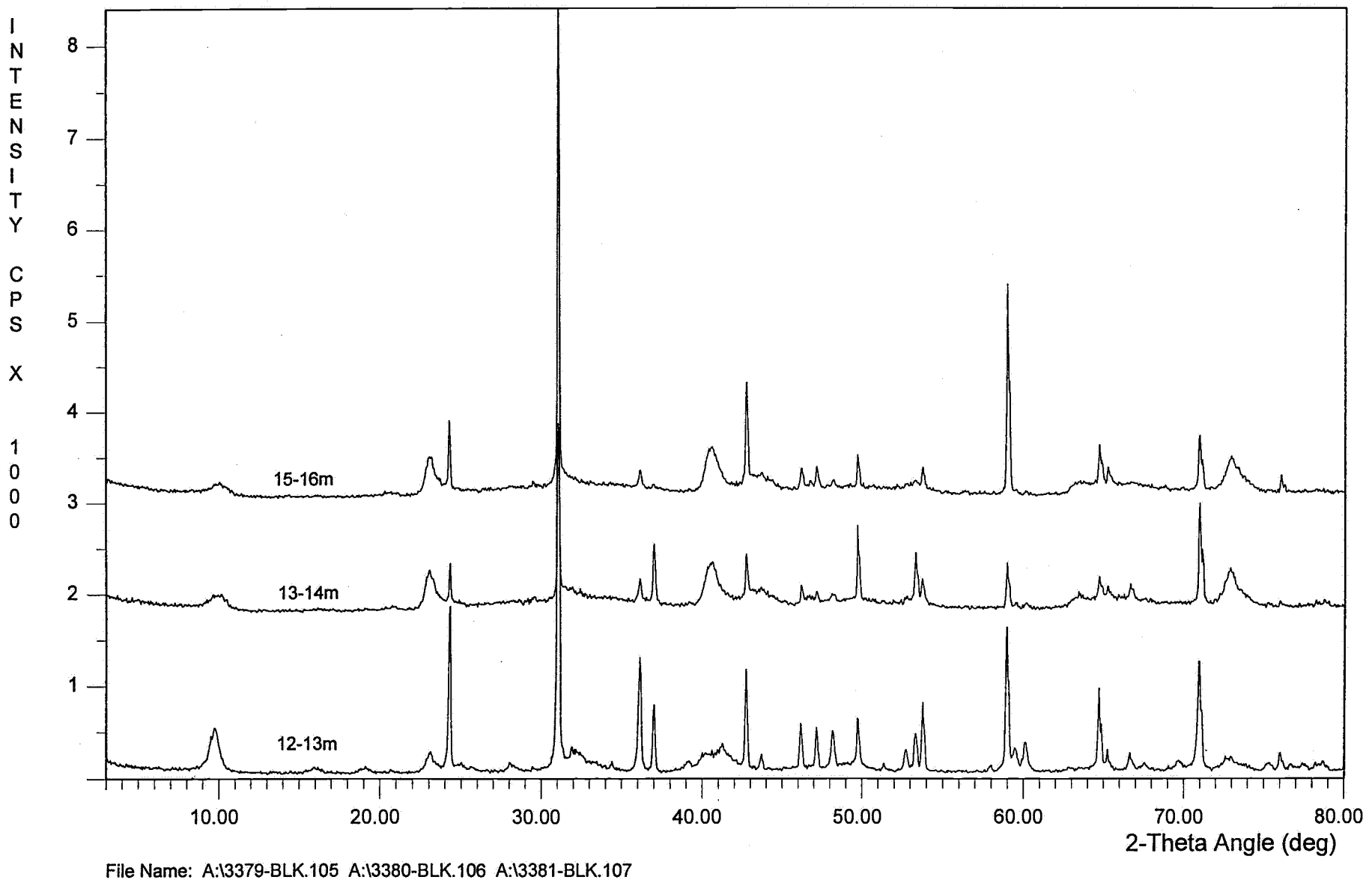


Fig. 1.18b. XRD spectrum (Co Kα radiation, back pressed) of Garford palaeochannel samples P61.

Fig. 1.19a. Garford Paleochannel Samples - P65.

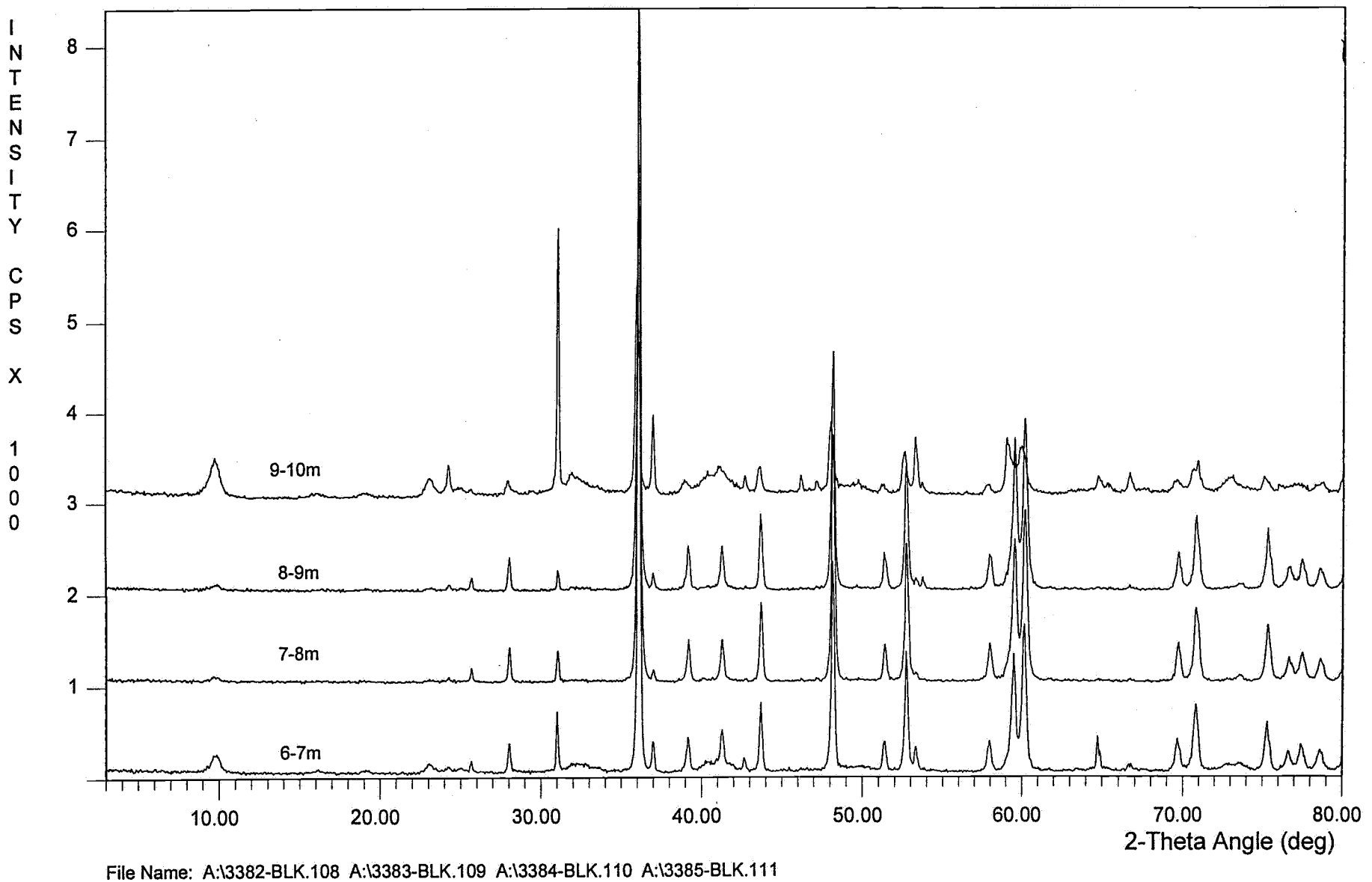


Fig. 1.19a. XRD spectrum (Co Kα radiation, back pressed) of Garford palaeochannel samples P65.

Fig. 1.19b. Garford Paleochannel Samples - P65.

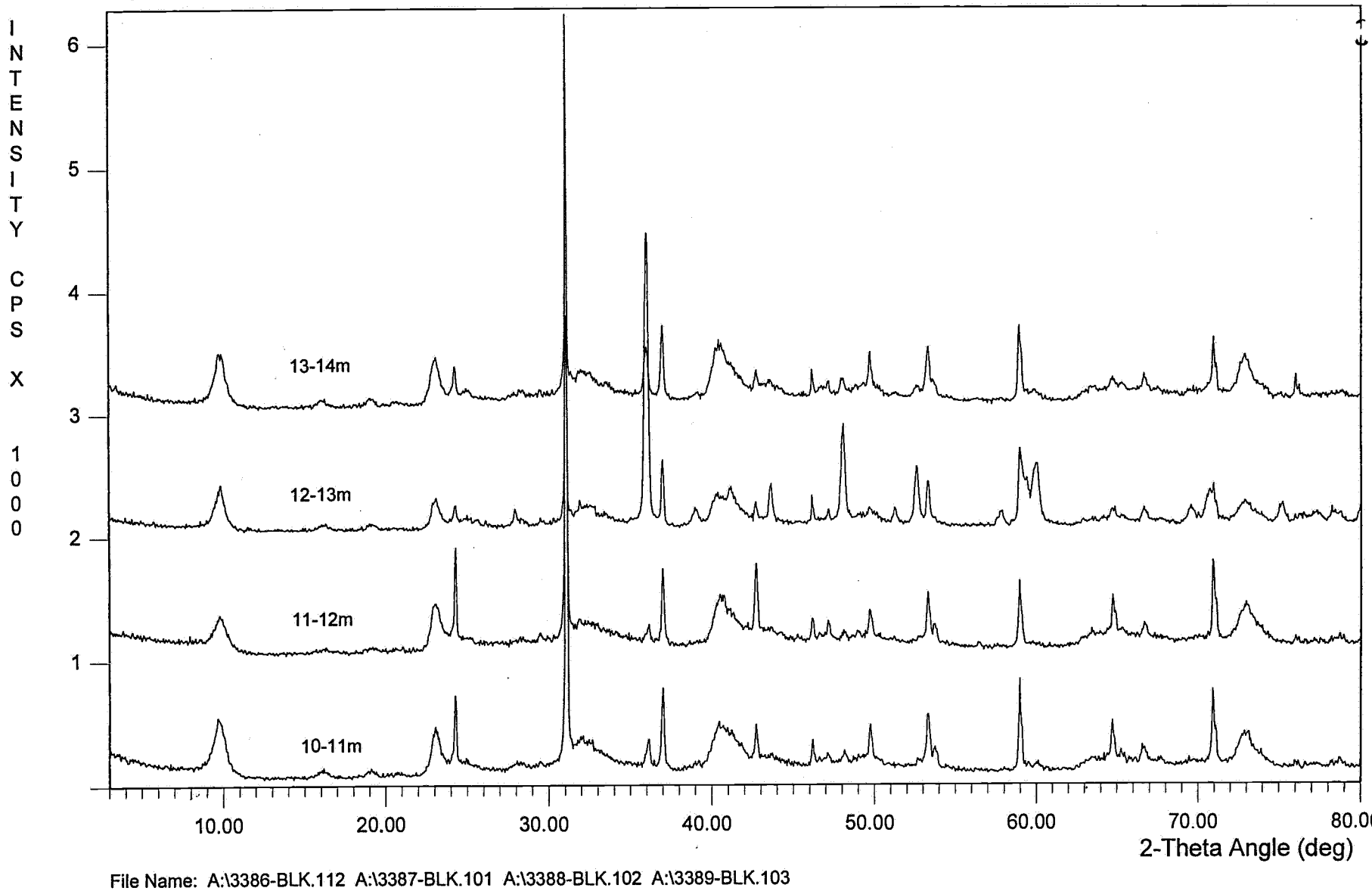


Fig. 1.19b. XRD spectrum (Co Kα radiation, back pressed) of Garford palaeochannel samples P65.

0004112

Fig. 1.19c. Garford Paleochannel Samples - P65.

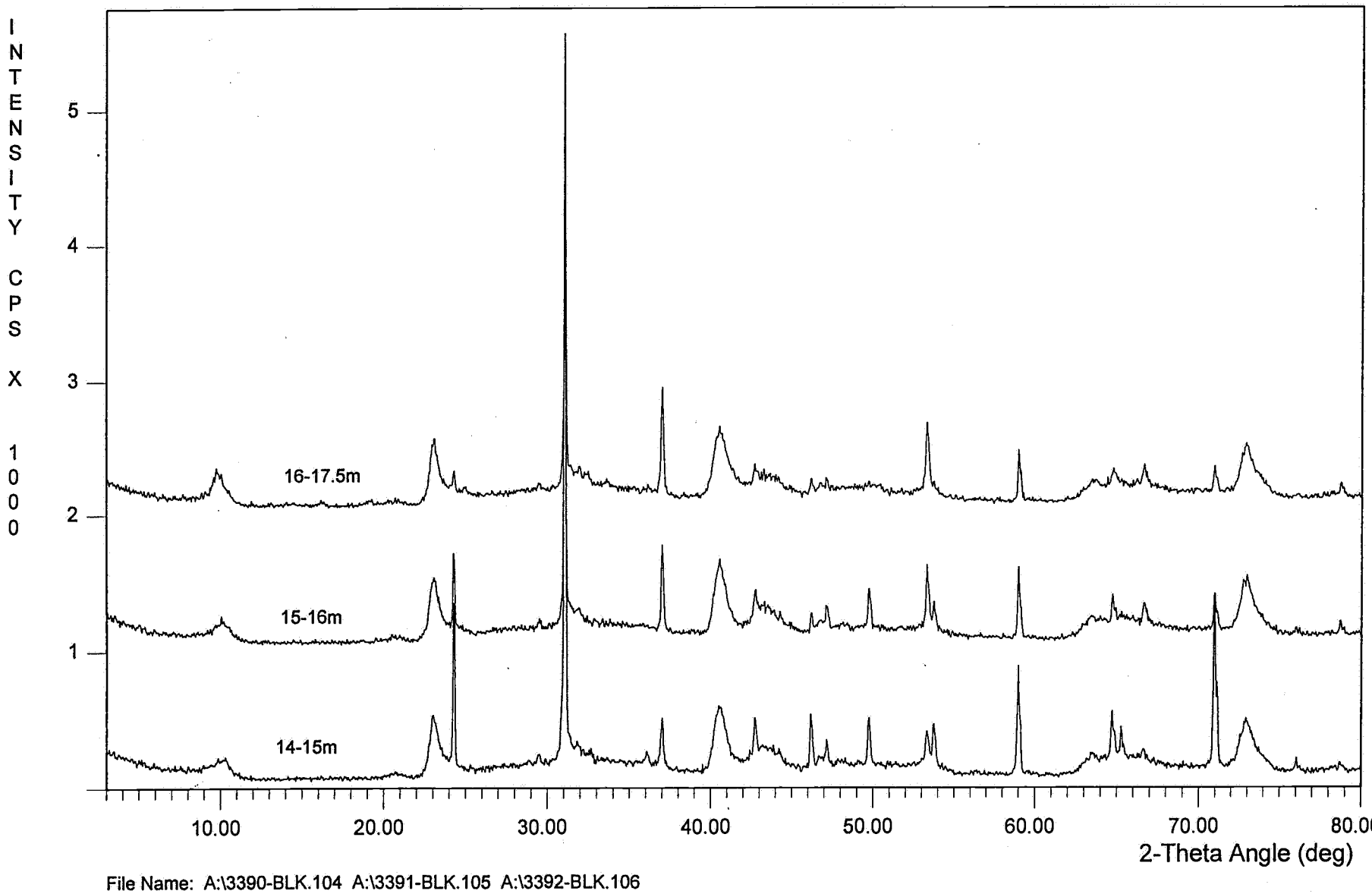


Fig. 1.19c. XRD spectrum (Co Kα radiation, back pressed) of Garford palaeochannel samples P65.

0004413

Fig. 1.20a. Garford Paleochannel Samples - P66.

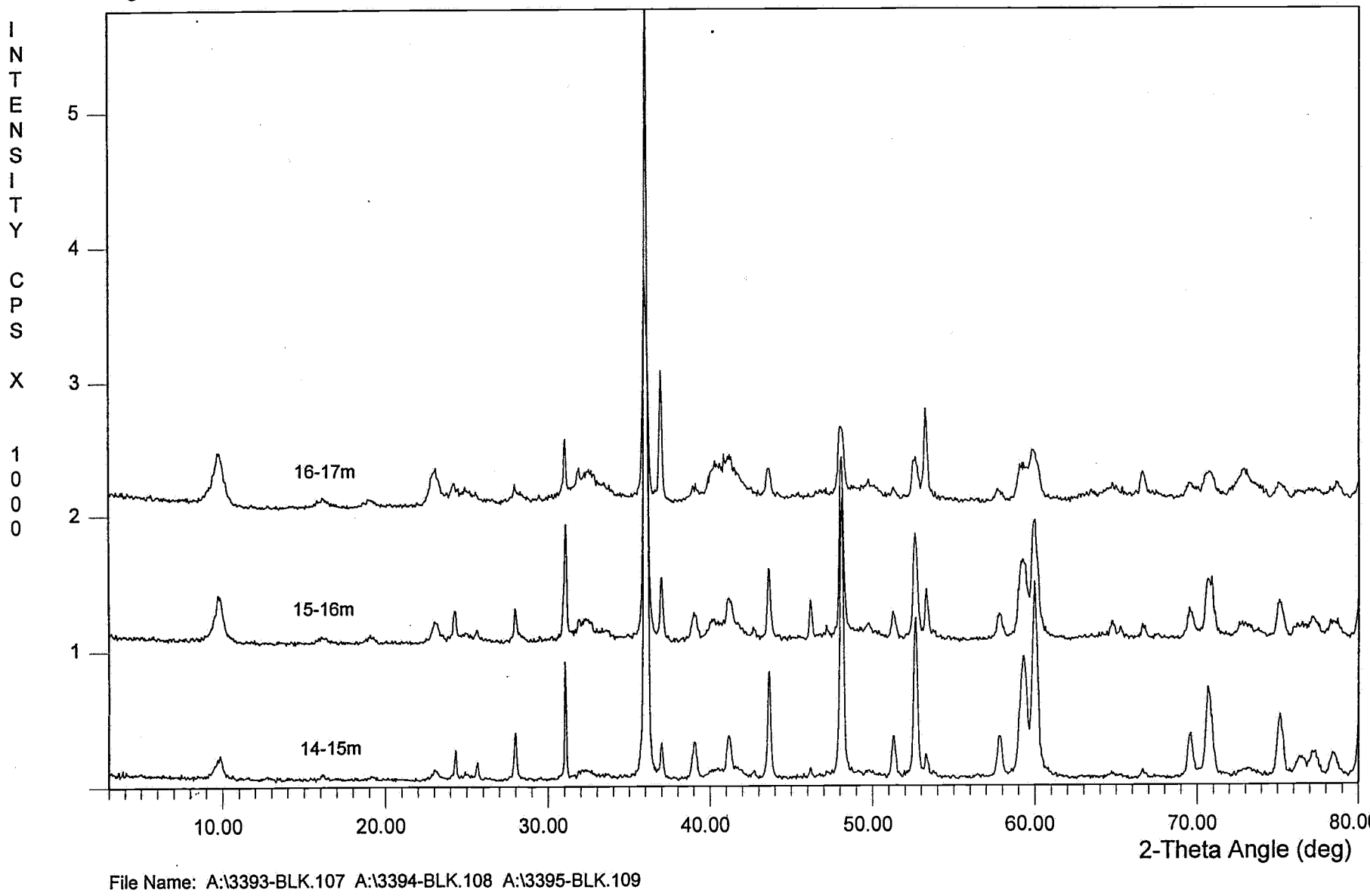


Fig. 1.20a. XRD spectrum (Co Kα radiation, back pressed) of Garford palaeochannel samples P66

Fig. 1.20b. Garford Paleochannel Samples - P66.

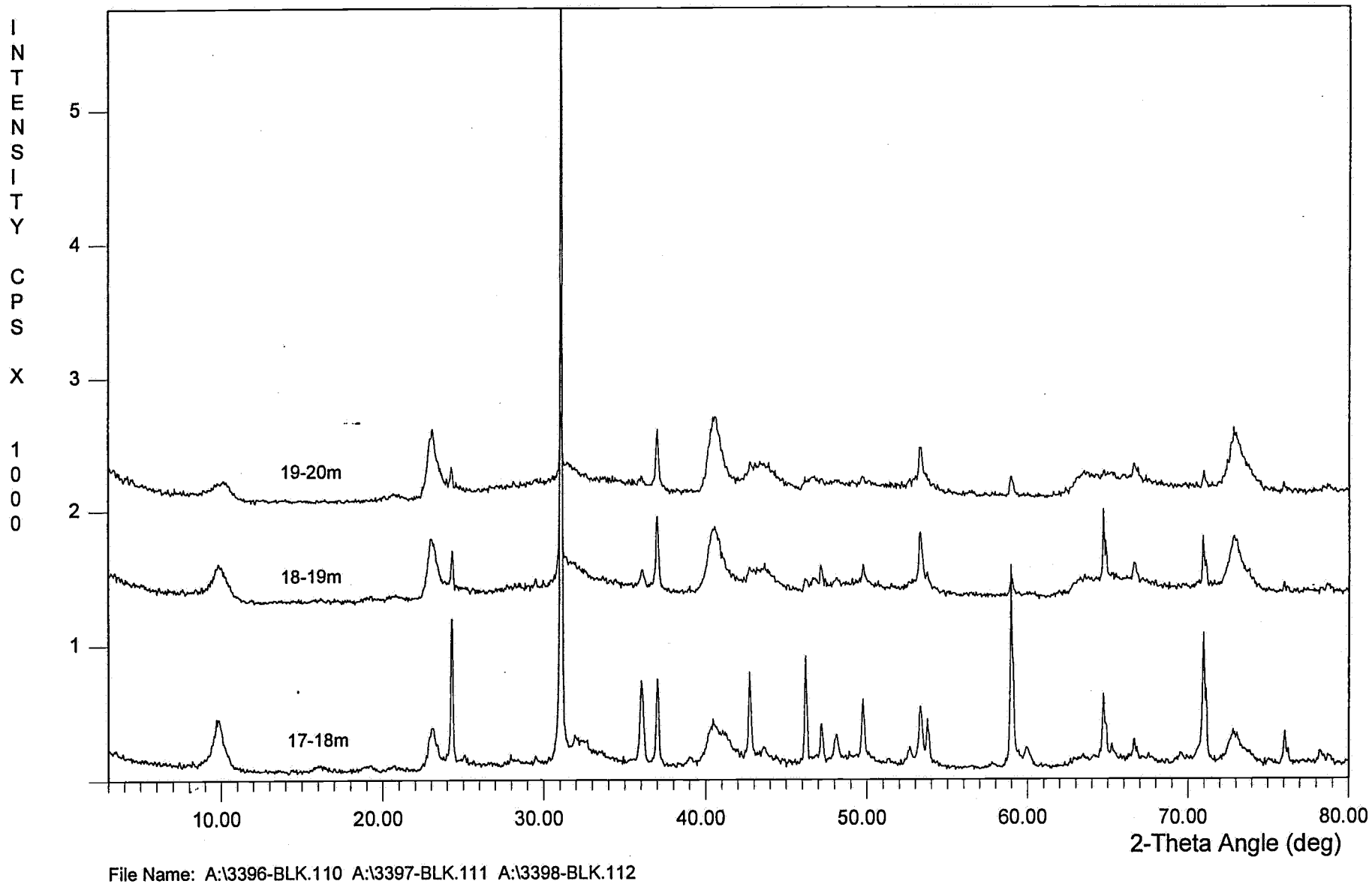


Fig. 1.20b. XRD spectrum (Co Kα radiation, back pressed) of Garford palaeochannel samples P66.

0004115

Fig. 1.21. Garford Paleochannel Samples - P67.

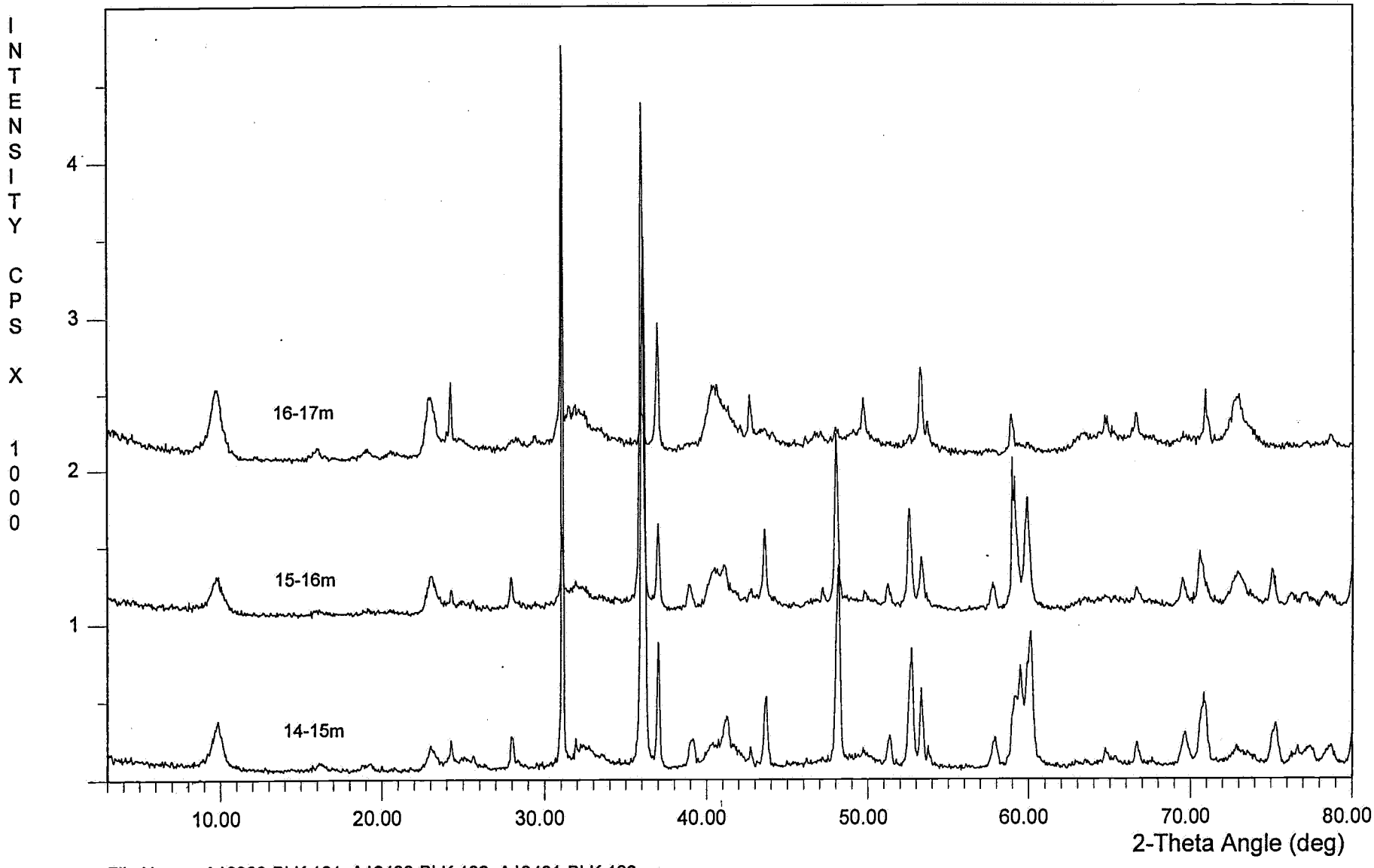


Fig. 1.21. XRD spectrum (Co Kα radiation, back pressed) of Garford palaeochannel samples P67.

000416

Fig. 1.22. Garford Paleochannel Samples - P68.

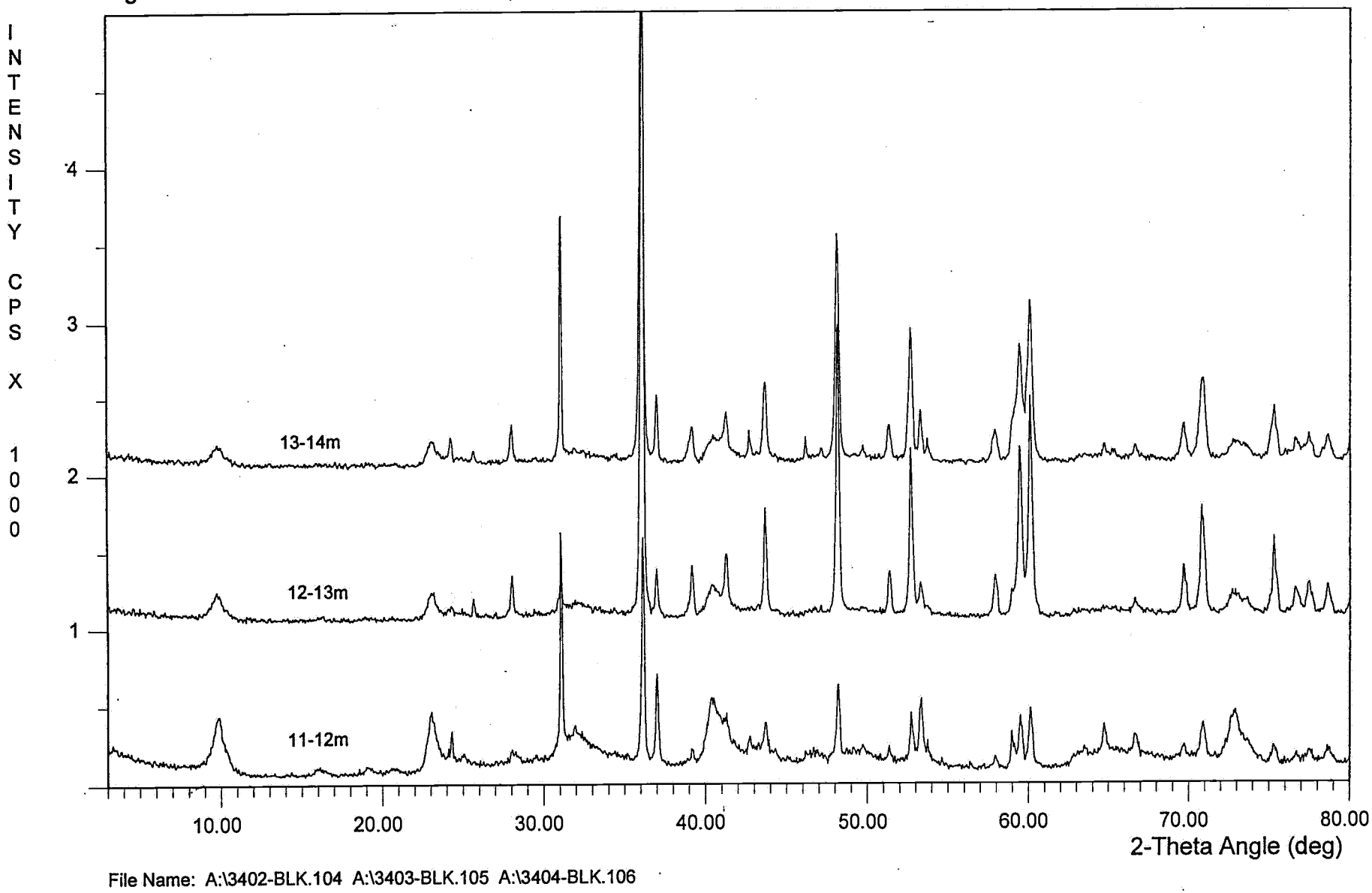


Fig. 1.22. XRD spectrum (Co Kα radiation, back pressed) of Garford palaeochannel samples P68.

0004117

Fig. 1.23. Garford Paleochannel Samples - P69.

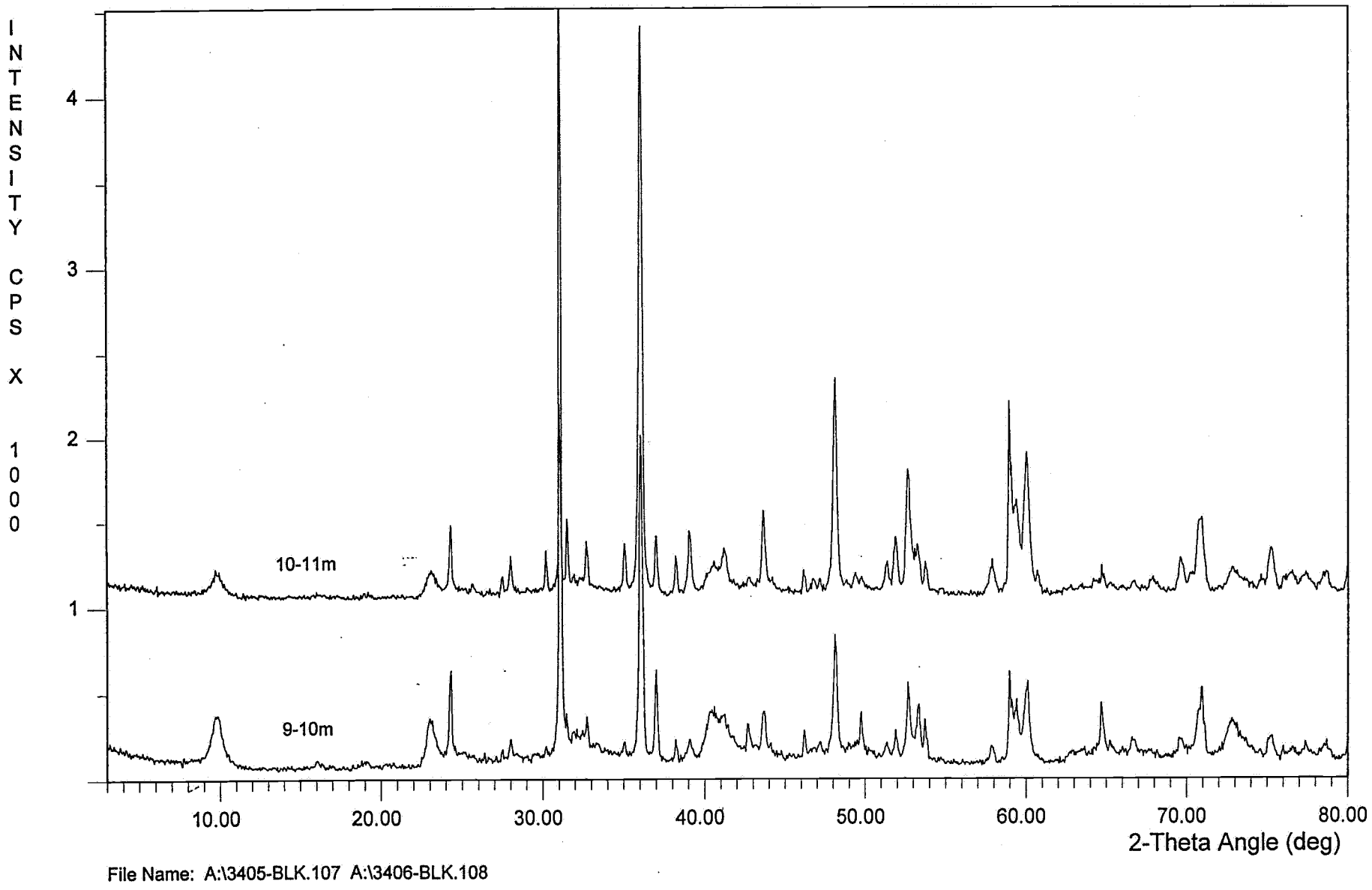


Fig. 1.23. XRD spectrum (Co Kα radiation, back pressed) of Garford palaeochannel samples P69.

0004418

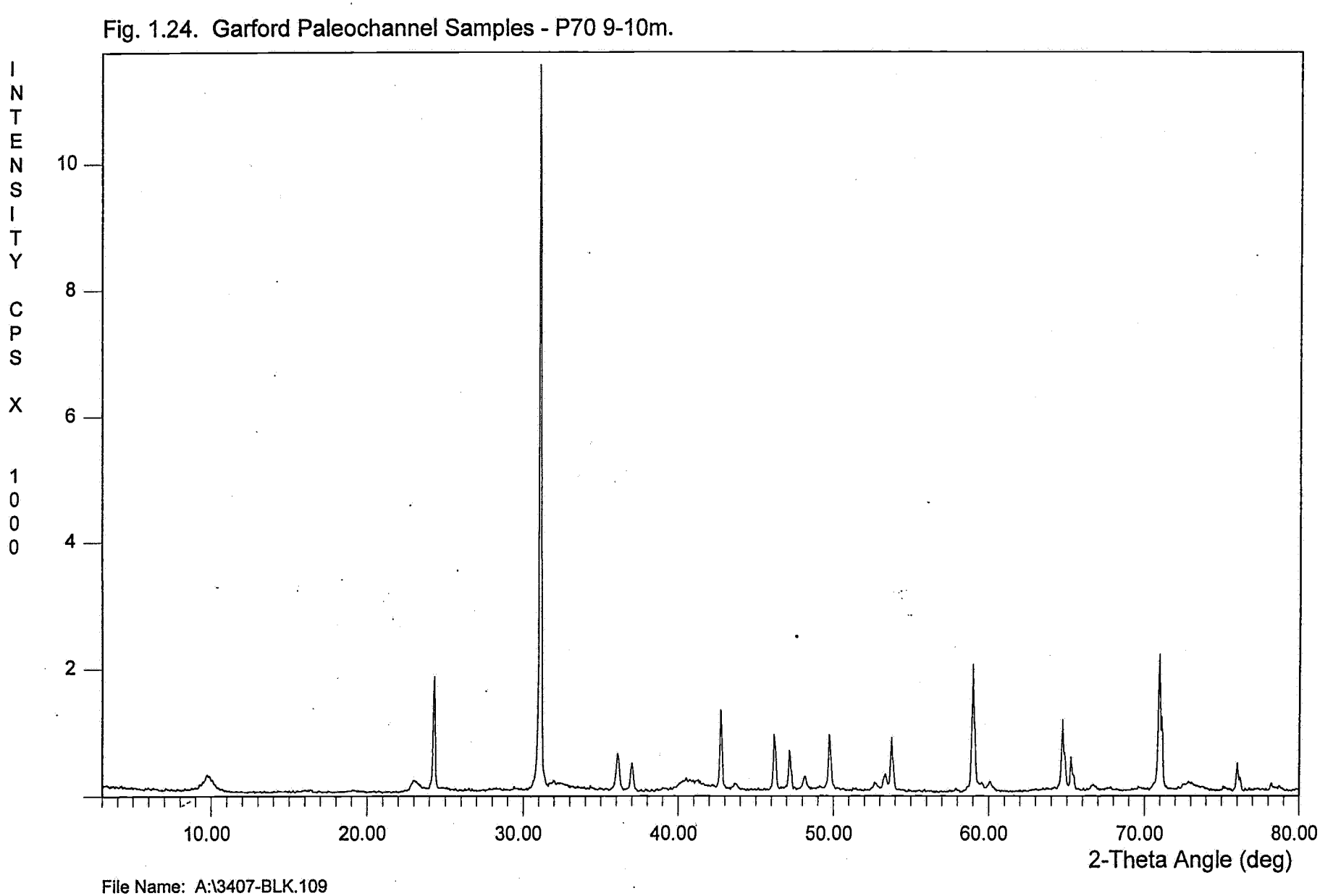


Fig. 1.24. XRD spectrum (Co Kα radiation, back pressed) of Garford palaeochannel sample P70 9-10m.

0004119

Fig. 1.25. Garford Paleochannel Samples - P74.

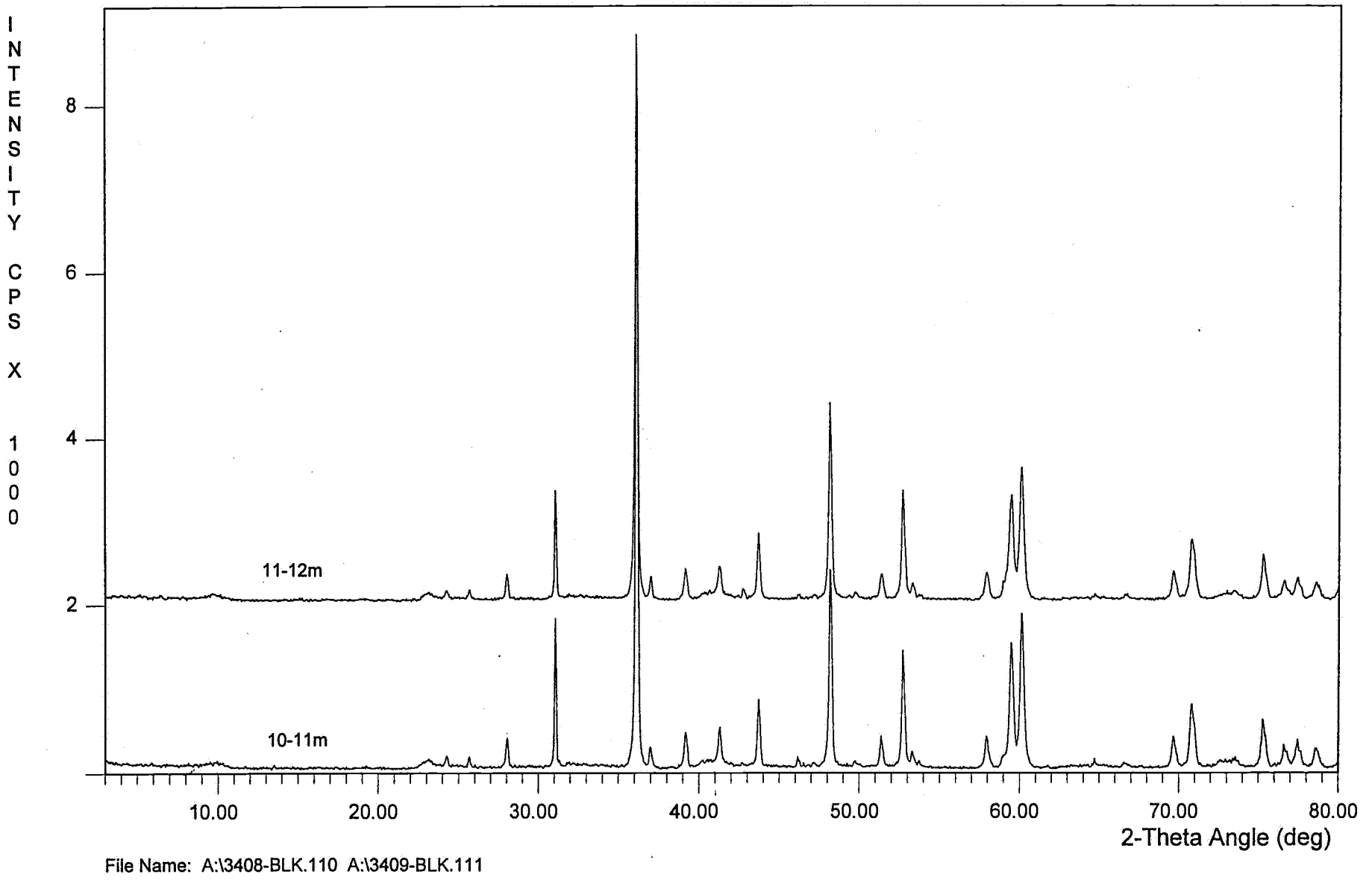


Fig. 1.25. XRD spectrum (Co Kα radiation, back pressed) of Garford palaeochannel samples P74.

0004420
50

Fig. 1.26a. Garford Paleochannel Samples - P76.

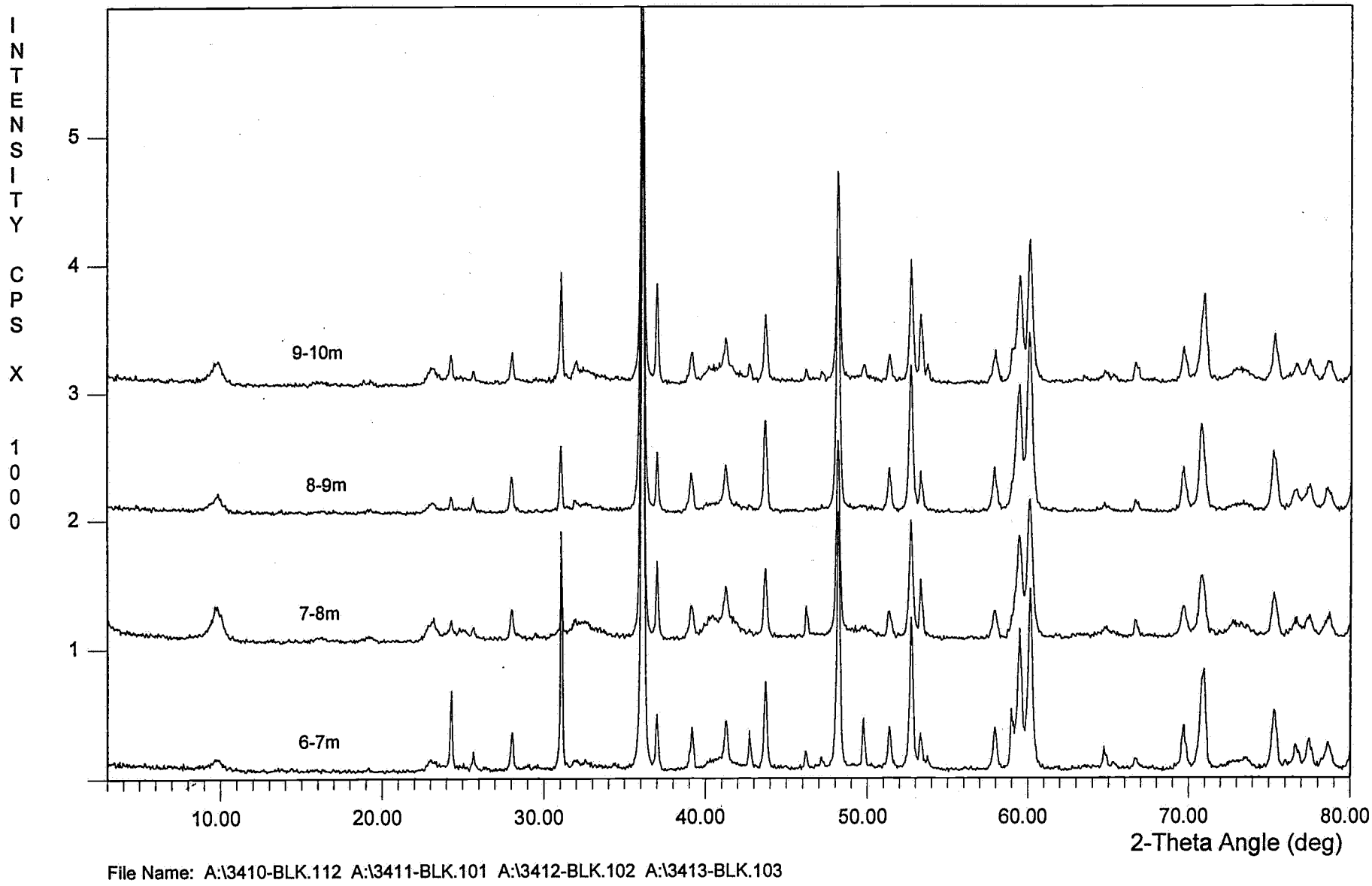


Fig. 1.26a. XRD spectrum (Co Kα radiation, back pressed) of Garford palaeochannel samples P76.

Fig. 1.26b. Garford Paleochannel Samples - P76.

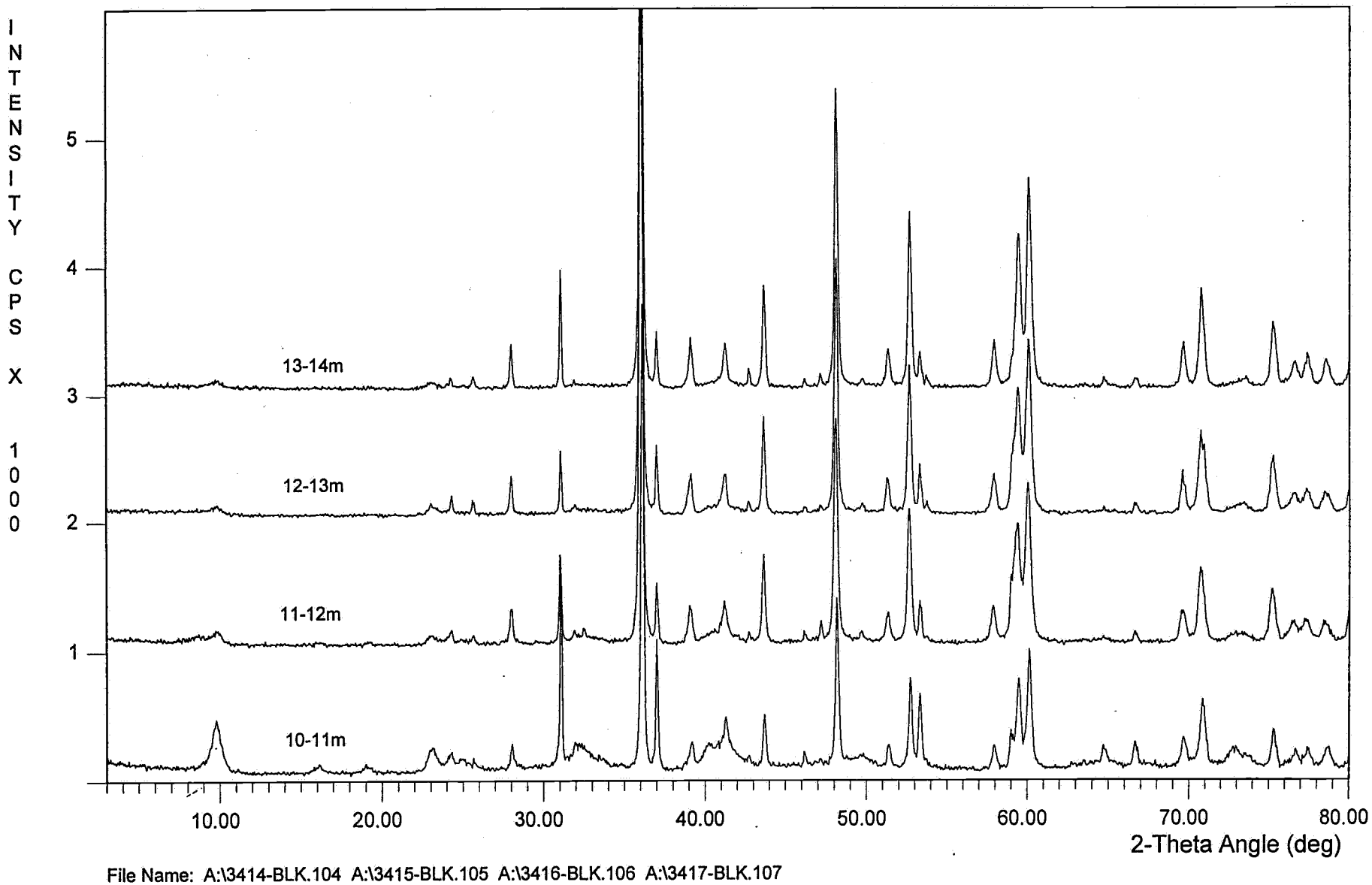


Fig. 1.26b. XRD spectrum (Co Kα radiation, back pressed) of Garford palaeochannel samples P76.

0004422

Fig.1.26c. Garford Paleochannel Samples - P76.

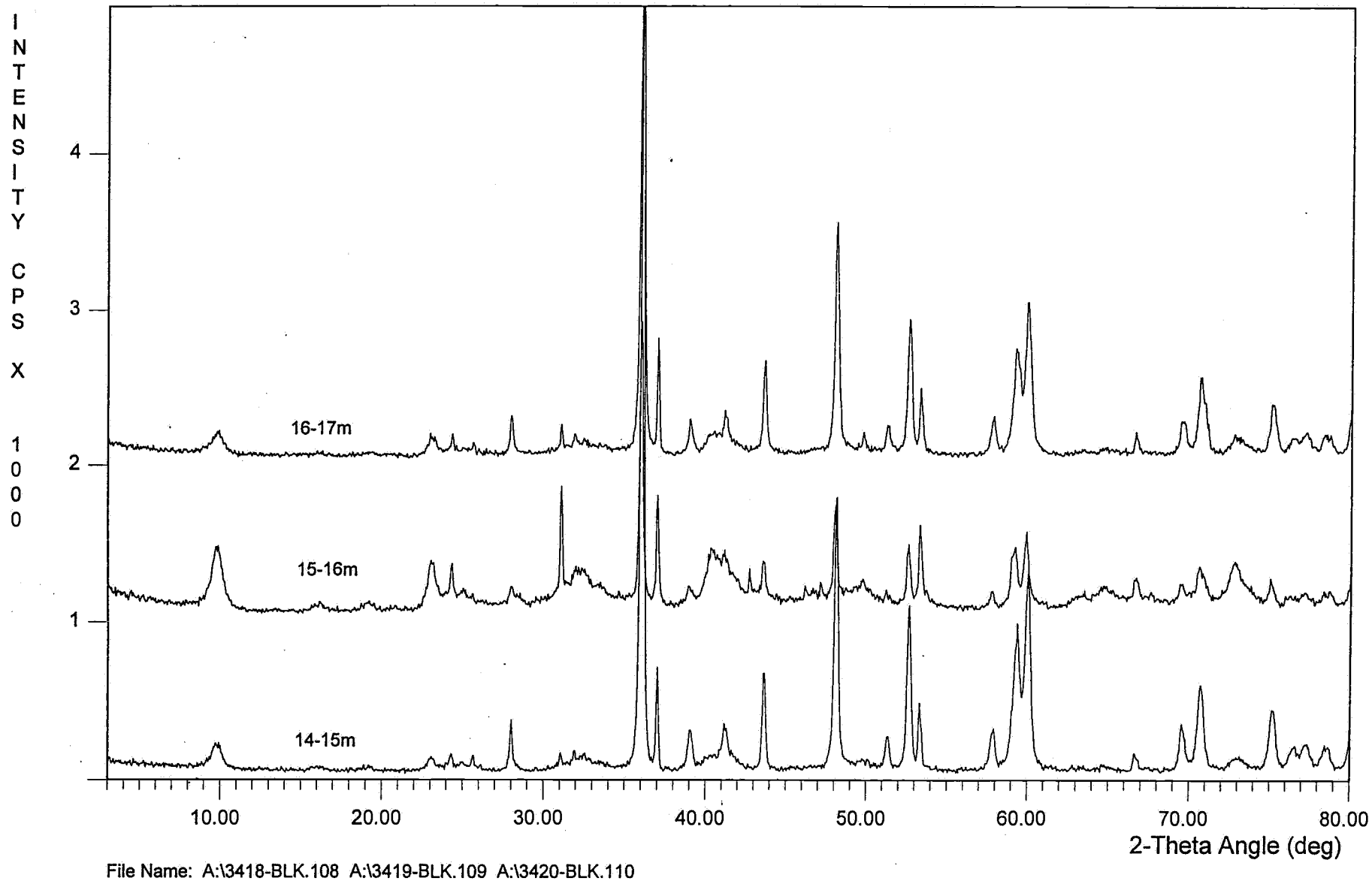


Fig. 1.26c. XRD spectrum (Co Kα radiation, back pressed) of Garford palaeochannel samples P76.

000423

Fig. 1.27a. Garford Paleochannel Samples - P77.

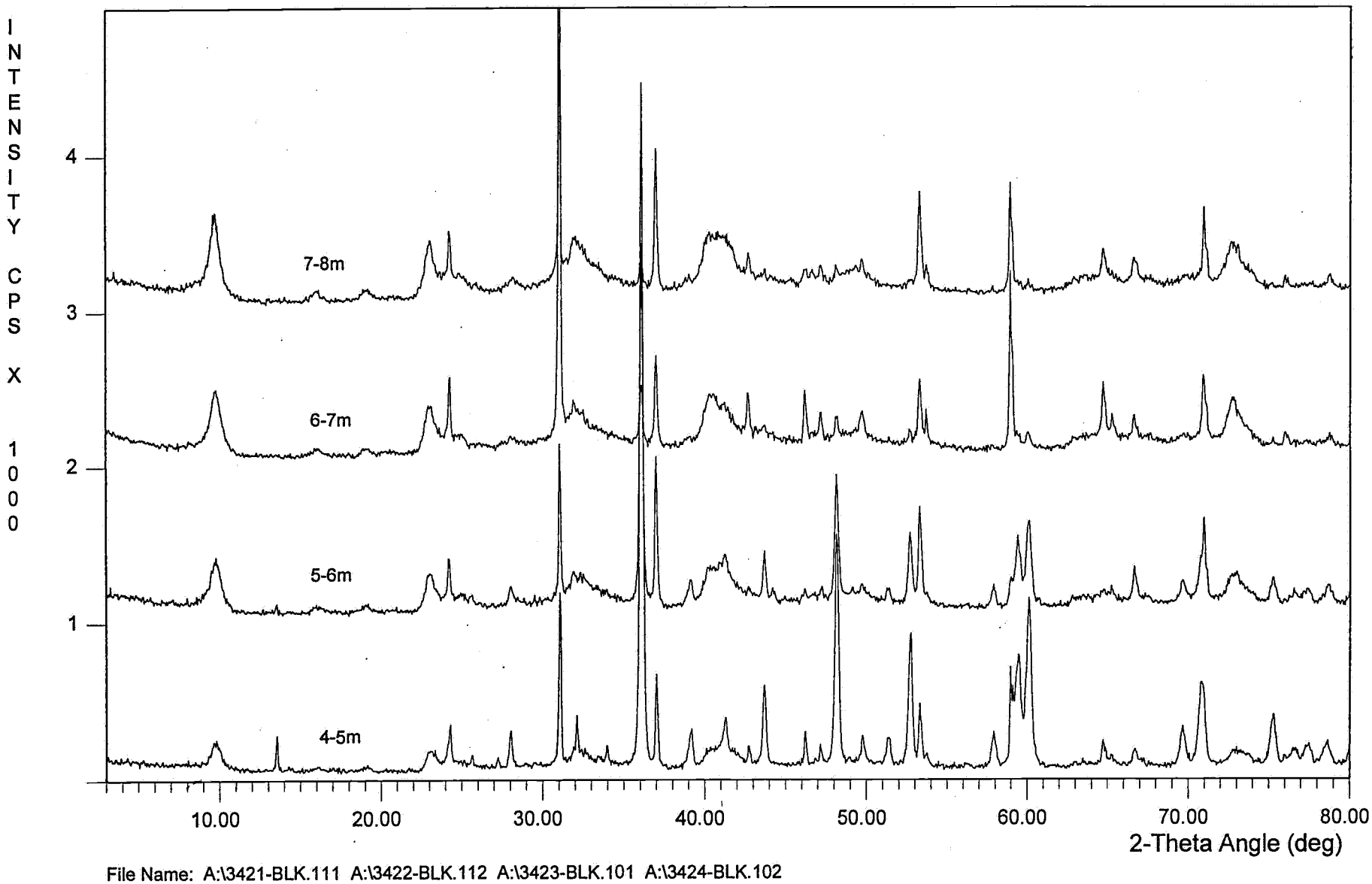


Fig. 1.27a. XRD spectrum (Co Kα radiation, back pressed) of Garford palaeochannel samples P77.

0004424
54

Fig. 1.27b. Garford Paleochannel Samples - P77.

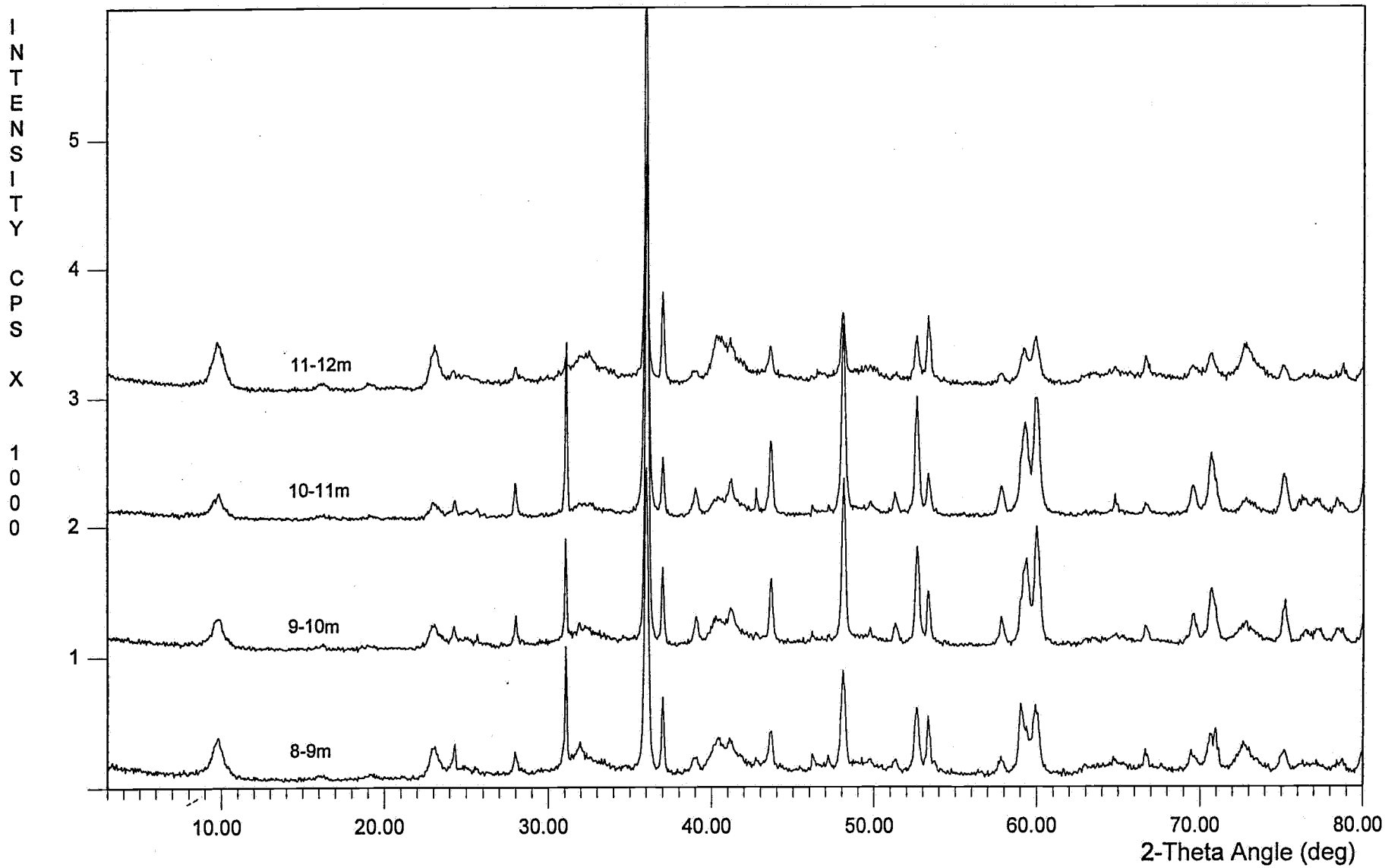


Fig. 1.27b. XRD spectrum (Co Kα radiation, back pressed) of Garford palaeochannel samples P77.

000425

Fig. 1.27c. Garford Paleochannel Samples - P77.

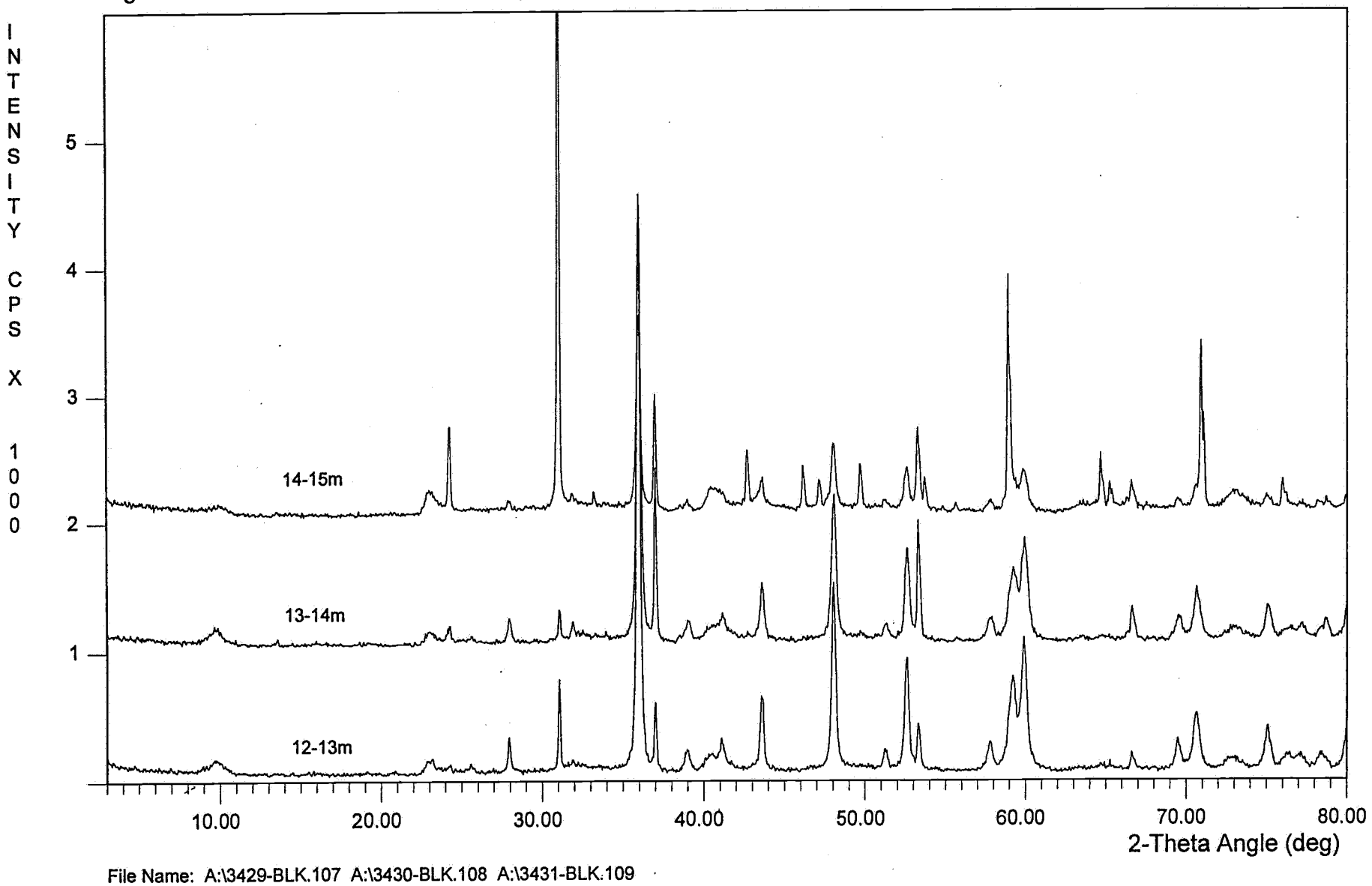


Fig. 1.27c. XRD spectrum (Co Kα radiation, back pressed) of Garford palaeochannel samples P77.

000426

Fig. 1.28a. Garford Paleochannel Samples - P79.

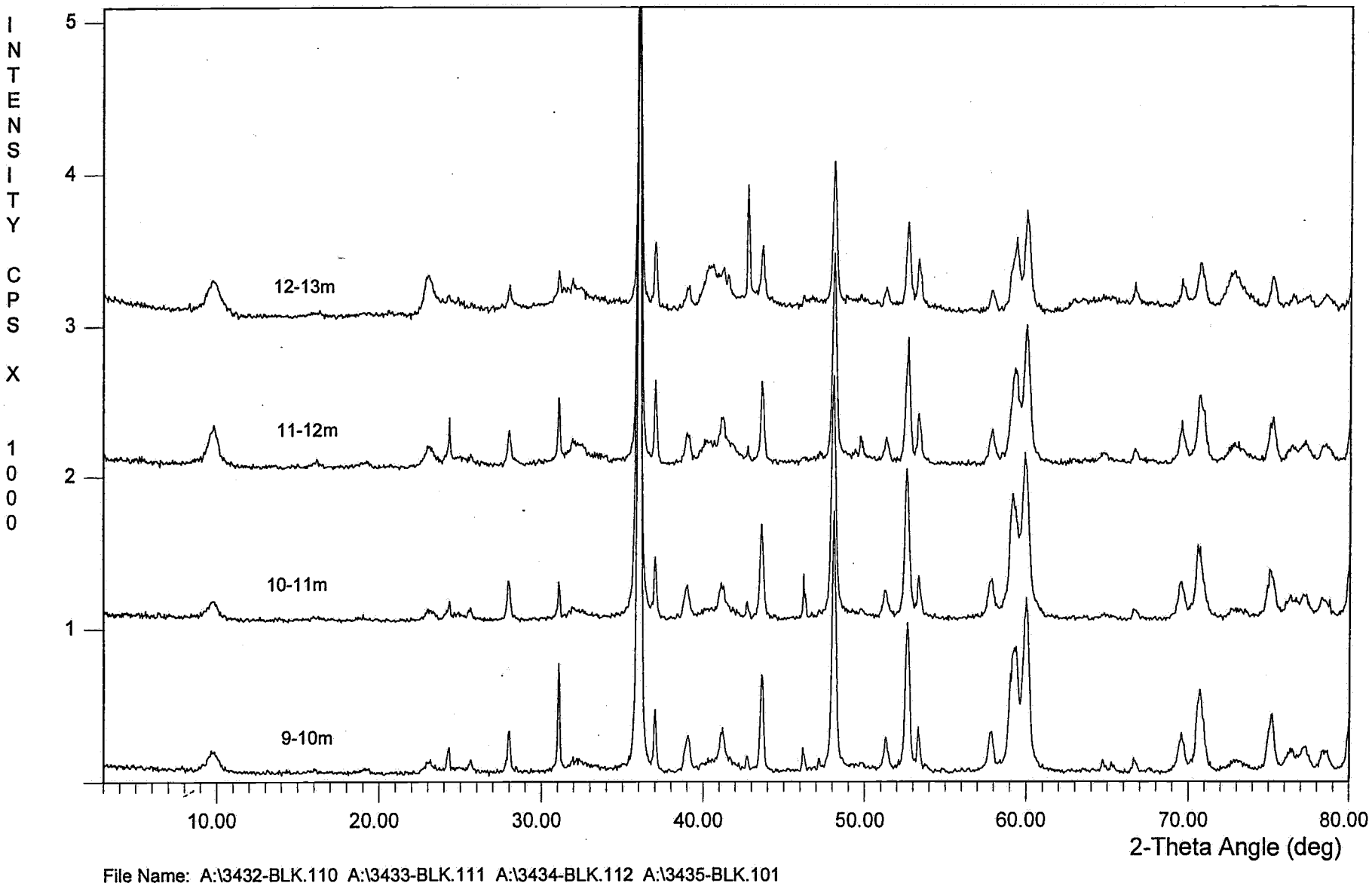


Fig. 1.28a. XRD spectrum (Co Kα radiation, back pressed) of Garford palaeochannel samples P79.

0004277

Fig. 1.28b. Garford Paleochannel Samples - P79.

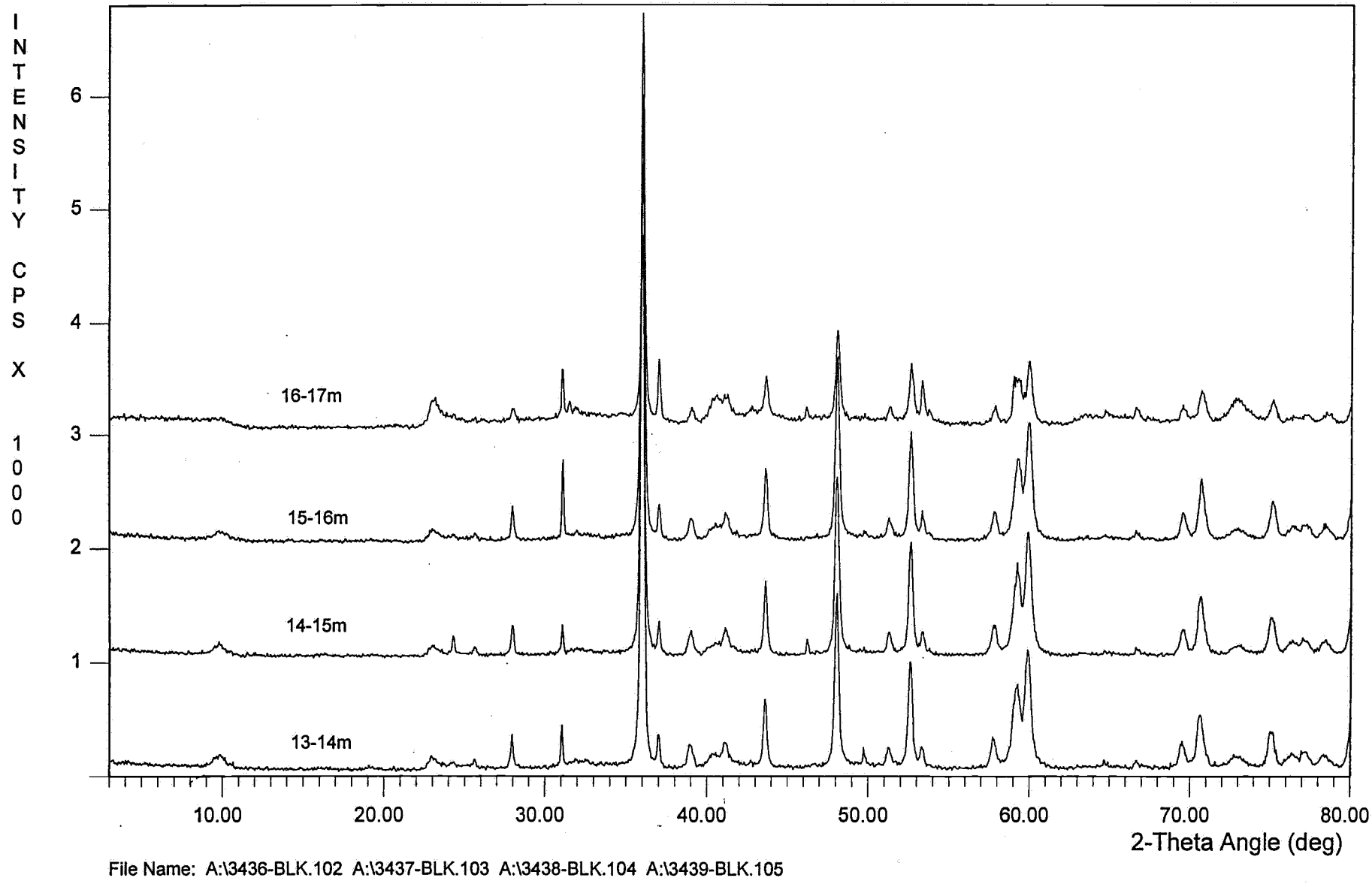


Fig. 1.28b. XRD spectrum (Co Kα radiation, back pressed) of Garford palaeochannel samples P79.

000428
58

Fig. 1.29a. Garford Paleochannel Samples - P84.

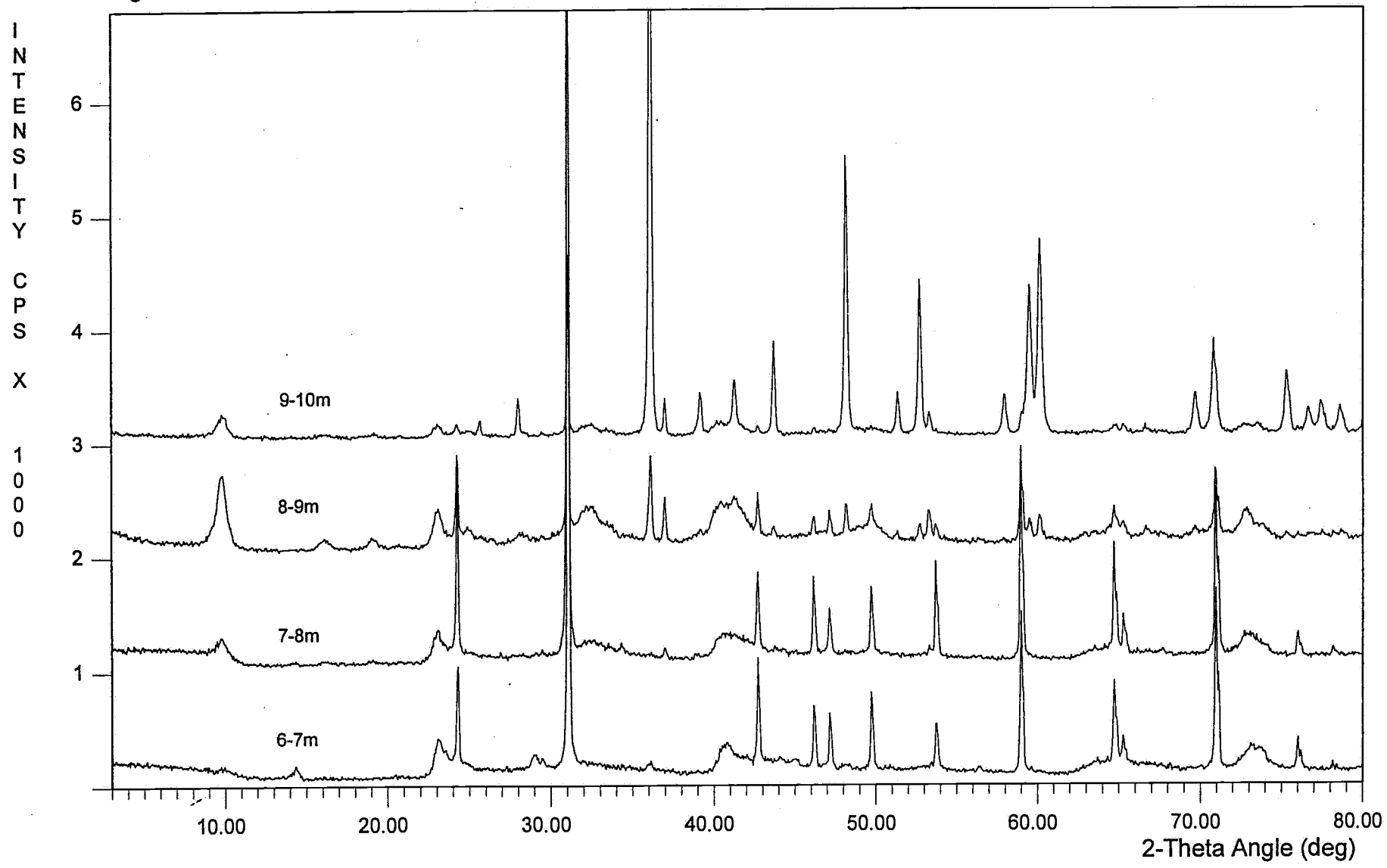


Fig. 1.29a. XRD spectrum (Co Kα radiation, back pressed) of Garford palaeochannel samples P84.

000429

Fig. 1.29b. Garford Paleochannel Sample - P84.

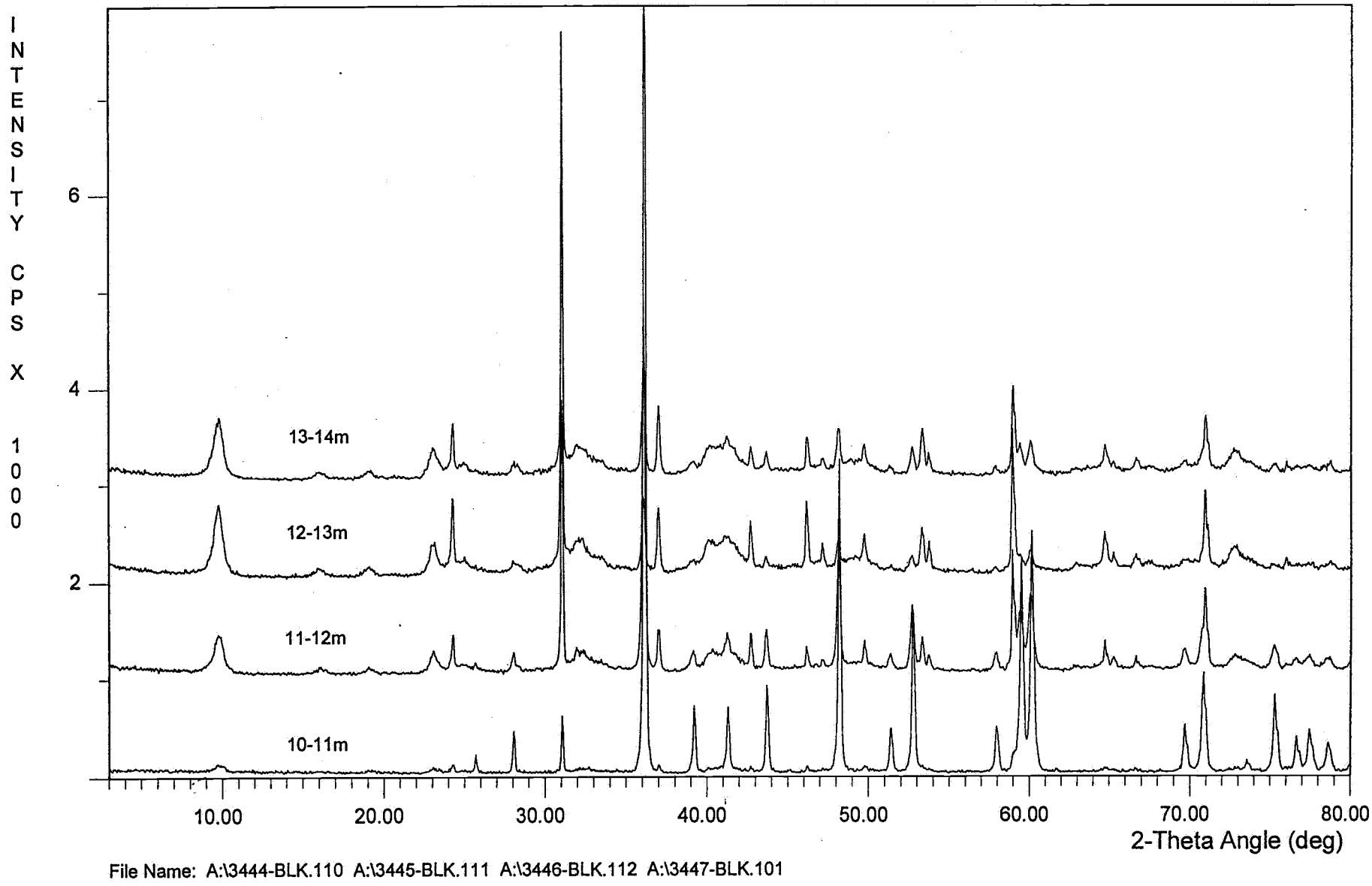


Fig. 1.29b. XRD spectrum (Co Kα radiation, back pressed) of Garford palaeochannel samples P84.

000430
60

Fig. 1.29c. Garford Paleochannel Sample - P84.

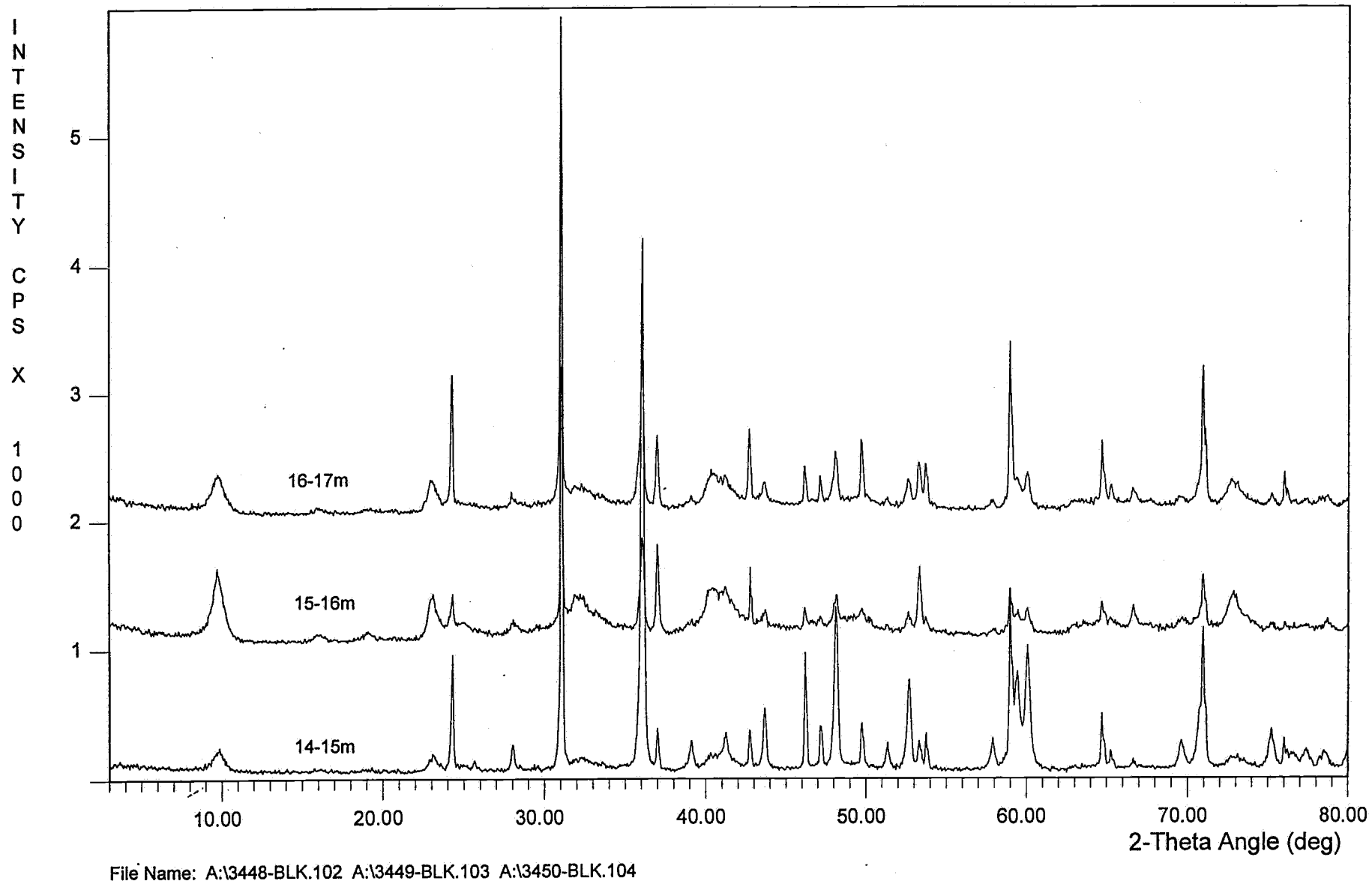


Fig. 1.29c. XRD spectrum (Co Kα radiation, back pressed) of Garford palaeochannel samples P84.

Fig. 1.30. Garford Paleochannel Samples - P85.

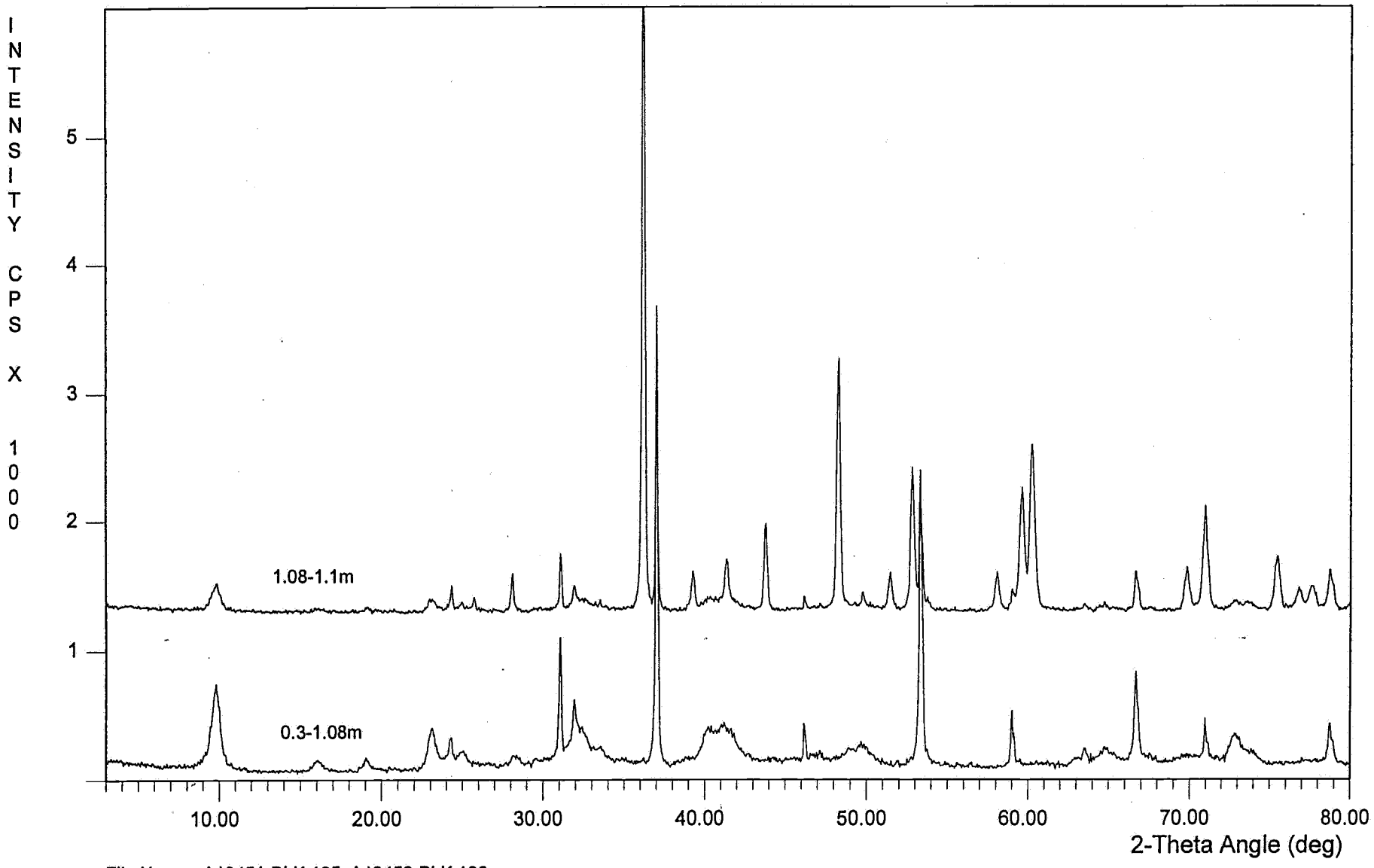


Fig. 1.30. XRD spectrum (Co Kα radiation, back pressed) of Garford palaeochannel samples P85.

0004432

Fig. 1.31. Garford Paleochannel Samples - P86 0.03-0.63m.

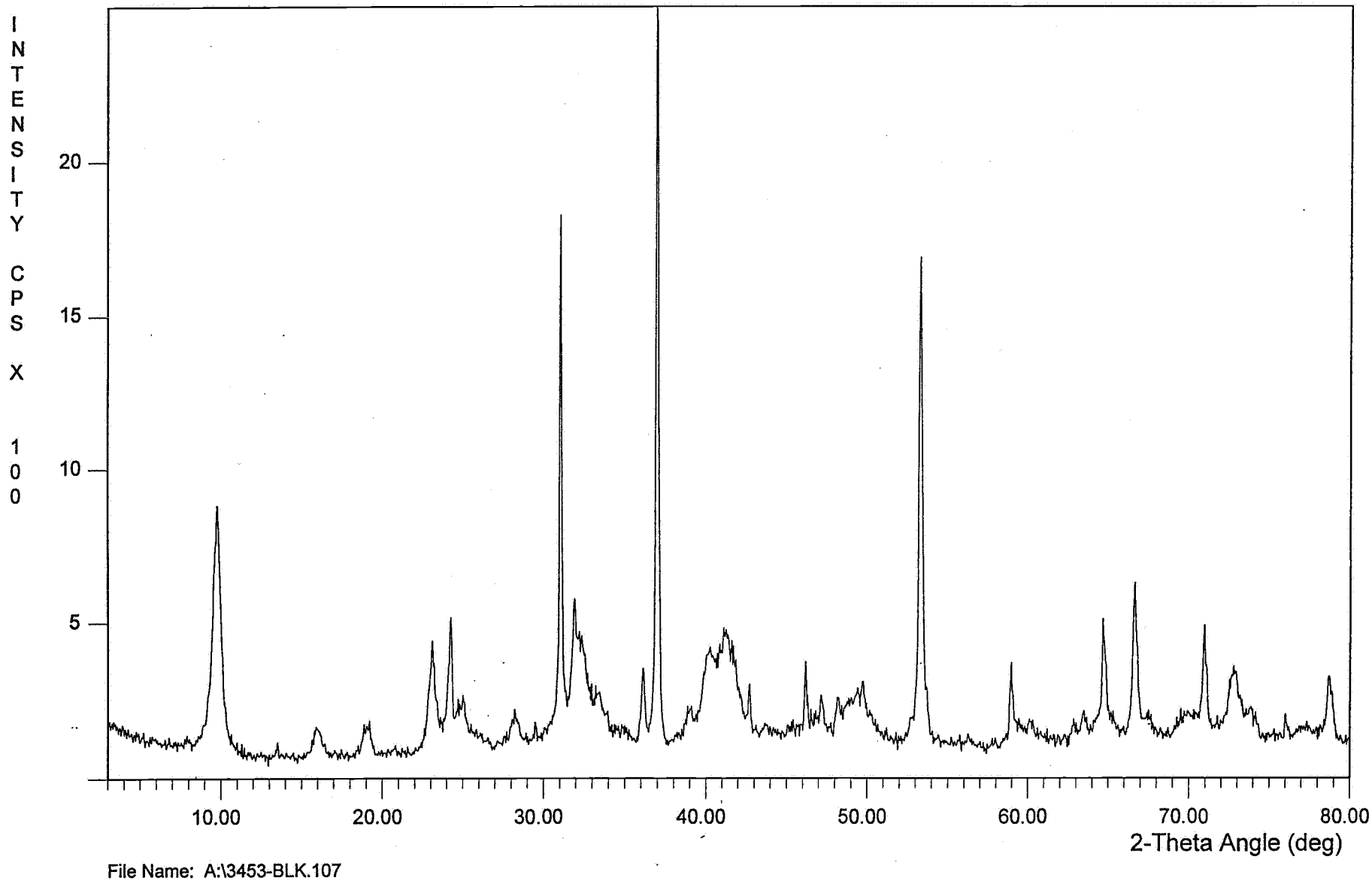


Fig. 1.31. XRD spectrum (Co Kα radiation, back pressed) of Garford palaeochannel sample P86 0.03-0.63m.

0004333

Fig. 1.32. Garford Paleochannel Samples - P87 0-0.6m.

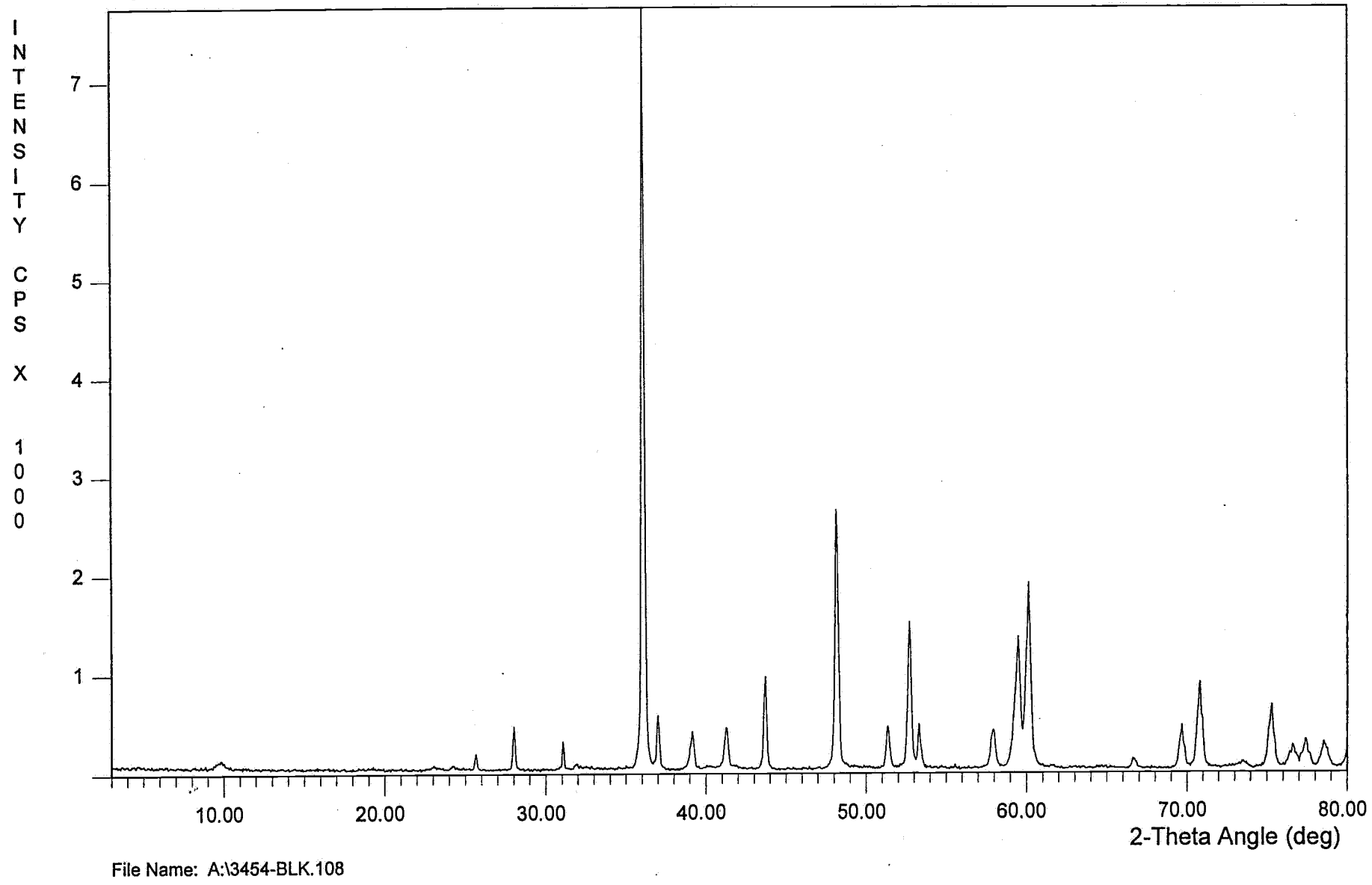


Fig. 1.32. XRD spectrum (Co Kα radiation, back pressed) of Garford palaeochannel sample P87 0.-0.6m.

Fig. 1.33. Garford Paleochannel Samples - P88.

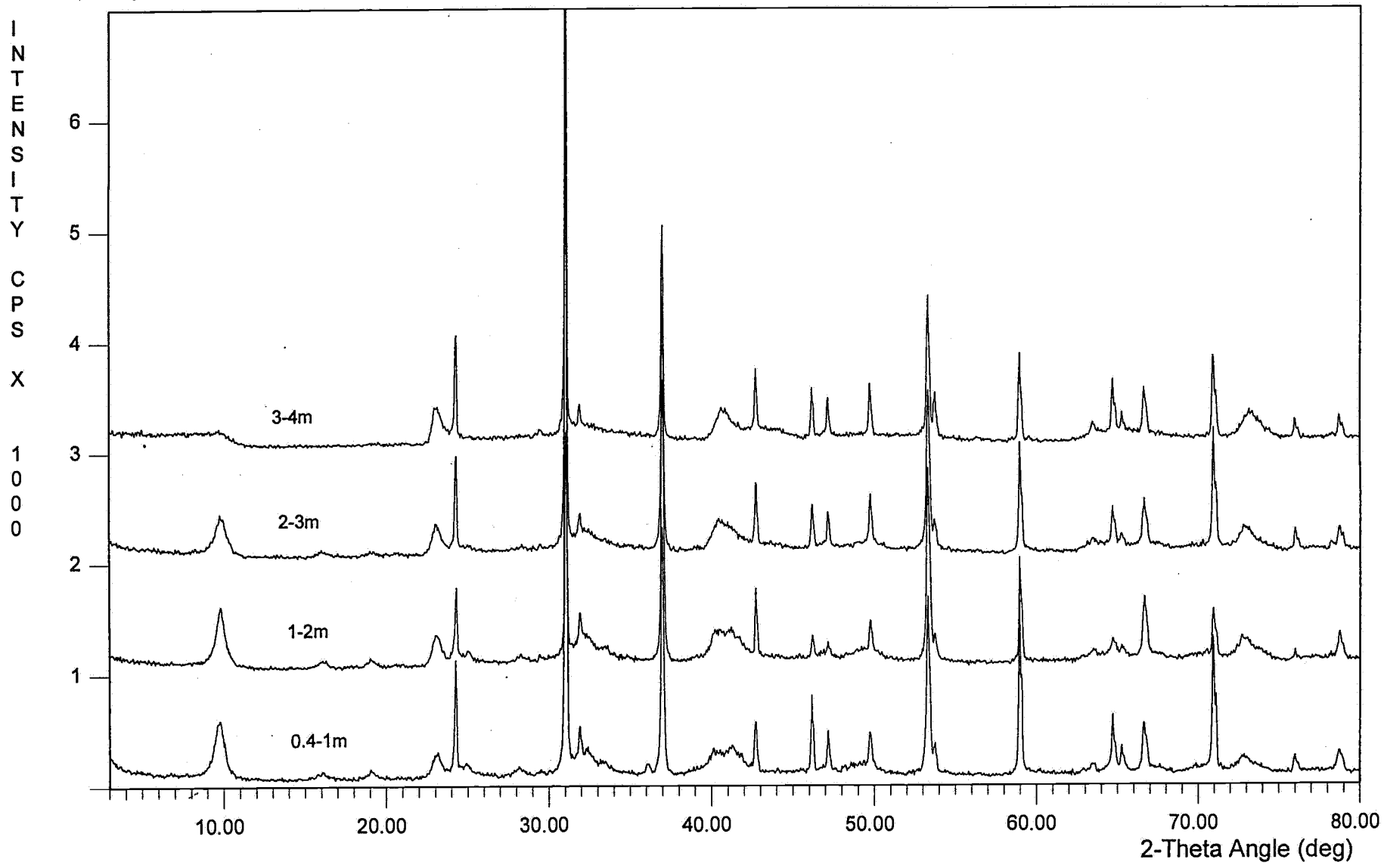


Fig. 1.33. XRD spectrum (Co Kα radiation, back pressed) of Garford palaeochannel samples P88.

CHAPTER 2. DOLOMITE REMOVAL BY DISSOLUTION IN ACID.

Introduction

Palygorskite bearing clays from the Garford palaeochannel can also contain significant amounts of dolomite (see previous Chapter and Raven *et al.*, 1995). Although small amounts of dolomite mixed with palygorskite may improve absorbency by propping open pore spaces, large amounts of dolomite reduce the desirable properties (i.e. absorbency and rheology) of palygorskite clays.

Although there is some evidence that dolomite can be separated by centrifugation (see previous Chapter), an obvious way to remove the dolomite is to dissolve it. The slight solubility of dolomite means that it can be removed by repeated washing of the clay. This would require approximately 70 litres of water per gram of dolomite (allowing for the precipitation of calcite).

The amount of solution required can be reduced by using acid solutions. However, acid washing needs to be carefully controlled because palygorskite will dissolve in solutions with pH lower than approximately 6 (Singer and Norrish, 1974). This is confirmed, to some extent, by Inukai *et al.* (1994) who used 4.5N HCl and 11N HCl to "purify" (i.e. remove dolomite from) a Turkish sepiolite. The high acid concentrations used by Inukai *et al.* (1994) caused considerable structural damage (Mg leaching) to the sepiolite well before all the dolomite was removed. Obviously, to achieve full removal of dolomite without damaging the clay, a lower concentration of acid is required.

Experimental Method

To study the dissolution of dolomite from Garford palaeochannel clays, HCl solution with a pH of approximately 2 (i.e. 0.01M HCl) was added to suspensions of the clay. (The actual value of the acid solution pH was 1.96.) Sample P35 6-7m was used in the experiments because it contained approximately 50% dolomite and 50% palygorskite (Raven *et al.*, 1995). Approximately 1gm of clay was dispersed in 250ml of RO water (pH 5 to 6). Acid solution was added to the dispersed-clay solution in amounts such that the combined solution pH could not exceed 3. For example, initial amounts of

added acid were 25ml. This amount was increased as the experiment proceeded and the total solution volume increased. The dispersed-clay solution was continuously stirred using a magnetic stirrer throughout each experiment. After each addition of acid the pH of the clay-water mix was monitored using a pH electrode and further acid was not added until equilibrium pH was reached.

Results and discussion

Initial experiments were carried out on a sample that had been in suspension for approximately 6 months. The pH of this suspension was between 9.5 and 10 which is high for a saturated dolomite/calcite solution. When as received P35 6-7m was used the initial pH was 8.1 to 8.2 which is reasonable for dolomite/calcite. This suggests that some reaction had taken place during the 6 months of suspension.

The changes in pH verses time after addition of various amounts of acid solution to a solution of dispersed as-received clay are shown in Fig. 2.1. The pH shows asymptotic (but not exponential decay) behaviour. After the addition of acid the pH rises rapidly for about 15 minutes at which stage there is a clear decrease in the rate of pH increase. It is possible that this rate change is caused by a lag in the response time of the pH electrode. Another, albeit smaller, change in rate of pH increase is seen after about 100 to 150 minutes. For example, at about 100 minutes after the addition of 250ml of acid solution and 150 minutes after the addition of 650ml of acid solution. Equilibrium pH is reached after approximately 400 minutes (approx. 7 hours).

Fig. 2.2 shows the equilibrium pH after addition of 0.01M HCl to a solution of dispersed as-received clay. Until the addition of approximately 300ml of acid the equilibrium pH falls slowly in an approximately linear fashion (from around 8.2 to 8.0). Addition of acid solution beyond 300ml causes a more rapid, but still linear, fall in equilibrium pH. The reasons for this change in rate of pH decrease are unknown to the authors but are possibly because of the formation of calcite or the reaction of silicates. Between the addition of a total of 600 to 650ml of acid solution there is a large decrease in pH with the equilibrium pH being approximately neutral. This indicates that the dispersed-clay solution is no longer buffered by dolomite.

After the addition of 650ml of 0.01M HCl solution the acid-treated clay was recovered by centrifugation and drying at 105°C. The amount of sample recovered was 40% of the original sample. XRD of the recovered sample (Fig. 2.3) showed that there was still between 3% and 5% dolomite remaining in the sample. The amount of dolomite calculated to be dissolved by the addition of 650ml of 0.01M HCl plus the 3% to 5% of dolomite in the recovered sample shows that the total dolomite in the sample is around 35% to 38%. This is in good agreement with the dolomite content reported by Raven *et al.* (1995).

XRD analysis of the recovered sample (Fig. 2.3) showed it to be high in palygorskite. The analysis also showed that the recovered sample contained appreciable amounts of illite. Illite was not reported by Raven *et al.* (1995).

In order to continue removal of dolomite from the sample the recovered sample was re-dispersed in 250ml of RO water. The equilibrium pH of this solution was 7.73. This is higher than the solution from which the sample was originally recovered (pH = 7.16) because the removal of Ca and Mg ions from solution by the recovery process allows the dolomite to further dissociate. Indeed, the presence of Ca and Mg ions released into solution during acid treatment inhibits the complete dissociation of dolomite at neutral to alkaline pH values. Fig. 2.4 shows the equilibrium pH as a function of Ca+Mg concentration in solution. The trends in pH variation are slightly clearer in Fig. 2.4 than in Fig. 2.2.

Addition of 25ml of 0.01M HCl to the re-dispersed-clay solution caused the pH of the solution to fall to an equilibrium value of 4.0. This indicates the complete dissolution of dolomite. XRD analysis of the sample recovered by centrifugation and 105°C drying (Fig. 2.5) confirmed the absence of dolomite.

XRD examination of the recovered clays (Fig. 2.6) showed no evidence of opaline material as was found when strong acid solutions were used to dissolve dolomite from clay (Inukai *et al.*, 1994). This suggests that although the pH did, at times, fall below

the stability field of palygorskite (i.e. <6) the solution was not at these pH values for long enough to cause significant dissolution of palygorskite.

XRD examination of recovered clays also revealed that when the starting material for acid treatment was P35 6-7m clay that had been left standing in water for 6 months there was less illite in the recovered acid-treated clay than in the recovered acid-treated clay from experiments when the starting material was as-received clay (Fig. 2.7). This, combined with the high pH values of dispersed-clay solutions made with P35 6-7m material that had been left standing in water for 6 months, suggests that some illite has been converted to palygorskite during the 6 months for which the material was left in water (OH is released on the conversion of illite to palygorskite). These observations, combined with the observation that palygorskite is found in the field at illite-dolomite interfaces (Keeling *et al.*, 1995), have implications in genesis mechanism for palygorskite in the Garford palaeochannel. The above results are not conclusive and further work is required to validate any hypothesis of palygorskite genesis.

Method for removal of dolomite from Garford palaeochannel clays

The above results suggest that a suitable method for removal of dolomite from Garford palaeochannel clay samples would be a two-stage process as follows.

1. Mix clay with sufficient water to allow easy stirring.
2. Auto-titrate with HCl maintaining the pH at 7. The dispersed-clay solution should be stirred at all times.
3. When acid requirement ceases, remove solids from suspension by centrifugation.
4. Resuspend recovered solids and add acid whilst stirring until pH is 6.
5. Remove solids from suspension by centrifugation and dry.

Whether this method is suitable for large scale, in-field operation remains to be tested. Given that a large resource of clay with high palygorskite content has been indicated as a result of the 1995 drilling programme, the use of acid treatment for beneficiation purposes may not be necessary. However, on the basis of the above results, a single acid-wash step was included in the method for removing quartz so as to remove any minor amounts of dolomite from samples (see Appendix 3).

References

Inukai, K., Miyawaki, R., Tomura, S., Shimosaka, K. and Irkeç, T. (1994). Purification of Turkish sepiolite through hydrochloric acid treatment. Applied Clay Science, **9**, 11-29.

Keeling, J.L., Ferris, G.M. and Statham-Lee, L. (1995). Palygorskite clay investigation, Garford palaeochannel, South Australia: Results of drilling April-May, 1995. Mines and Energy, South Australia, Report Book 95/48.

Raven, M.D., Abolins, N., Keeling, J.L. and Self, P.G. (1995). Absorbent Clay Project. Mineralogical characterisation of Garford palaeochannel clays. Supplementary Report to Mines and Energy, South Australia, April 1995. South Australian Department of Mines and Energy, Envelope 8785 (unpublished).

Singer, A. and Norrish, K. (1974). Pedogenic palygorskite occurrences in Australia. American Mineralogist, **59**, 508-517.

Fig. 2.1. Dissolution kinetics of dolomite dissolution from P35 6-7m.

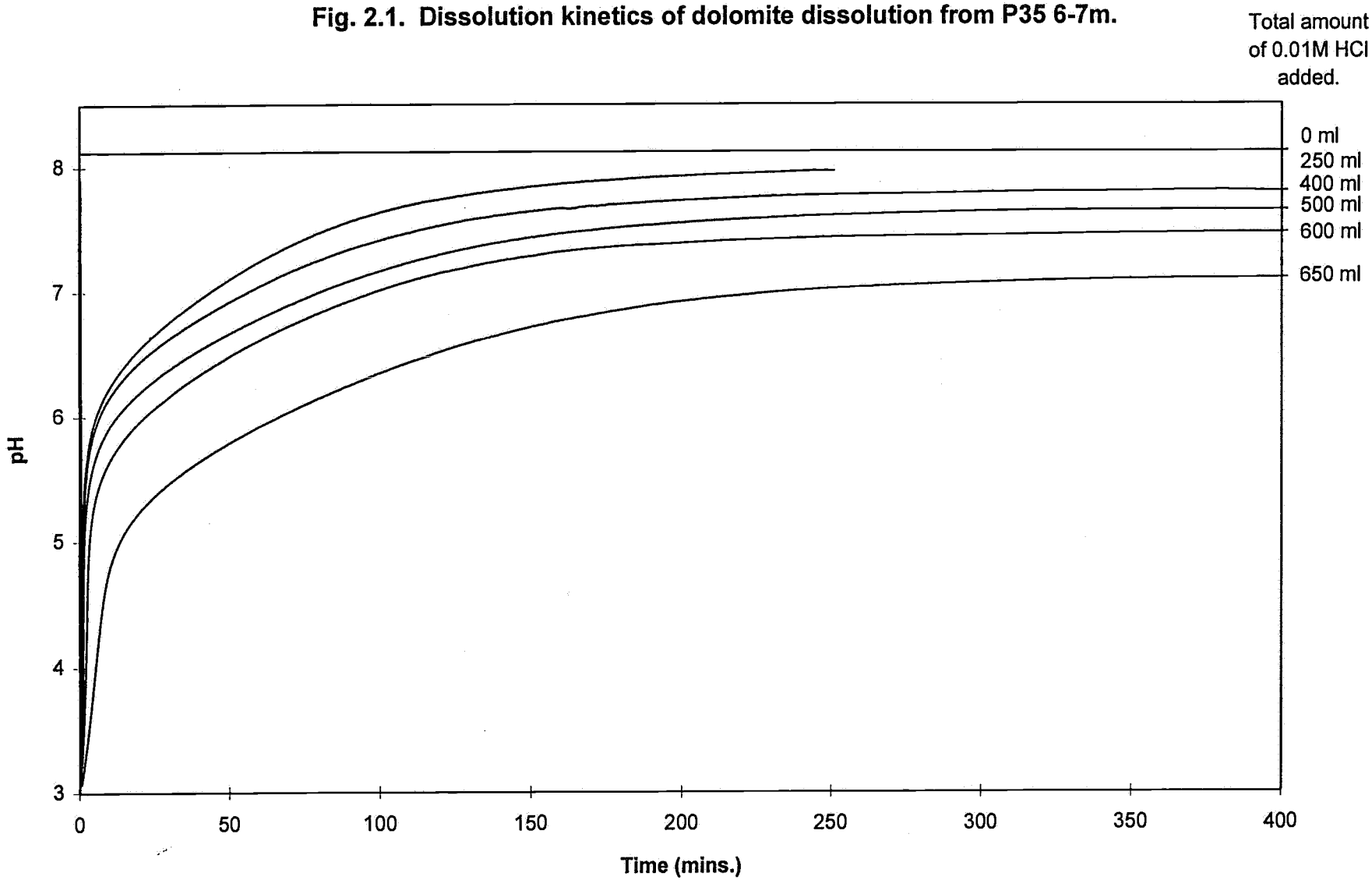


Fig. 2.1. Variation of pH with time after the addition of the indicated amounts of 0.01M HCl to sample P35 6-7m dispersed in water.

000441

Fig. 2.2. Acid dissolution of dolomite in P35 6-7m.

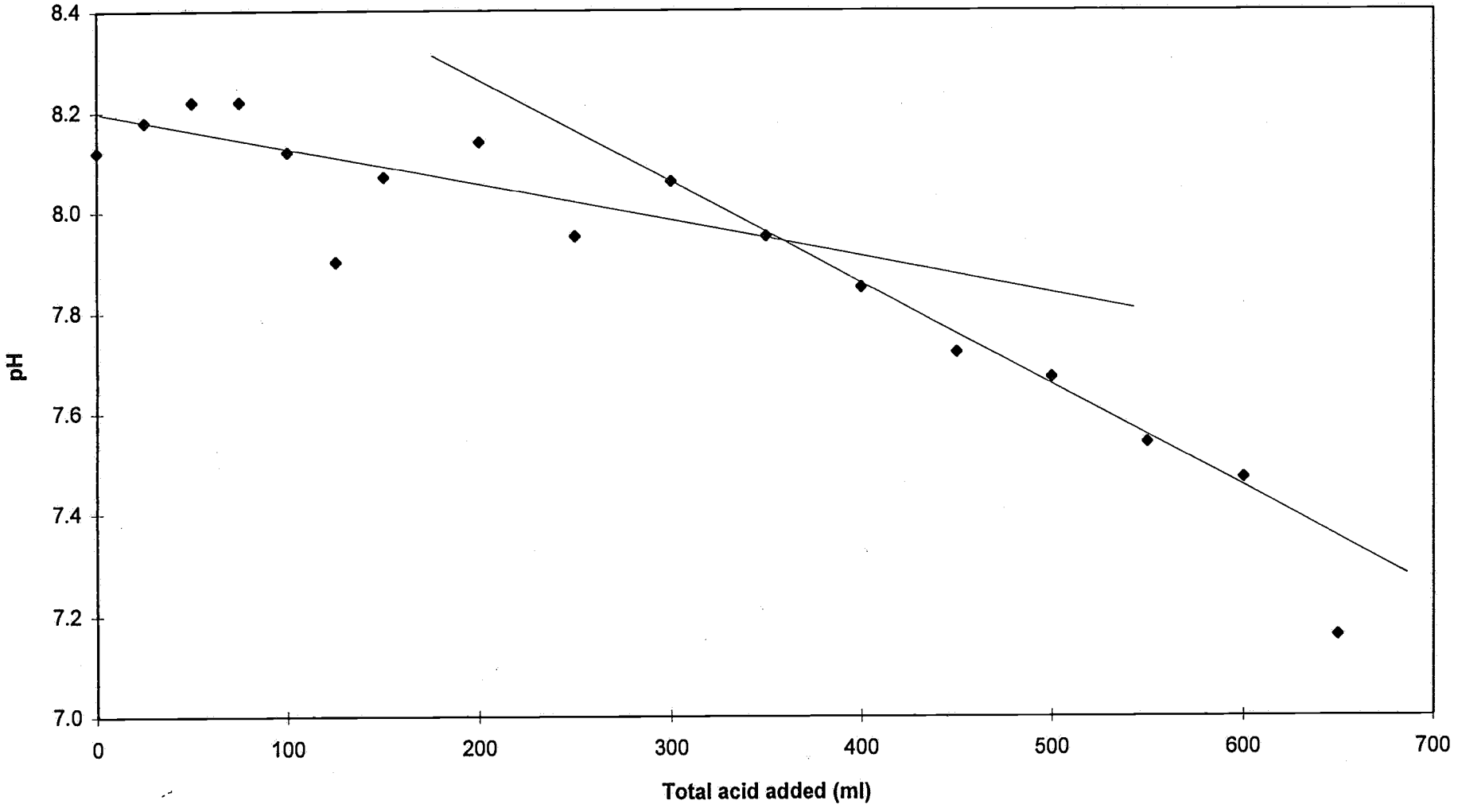


Fig. 2.2. Equilibrium pH after the addition of 0.01M HCl to sample P35 6-7m dispersed in water.

Fig. 2.3. Garford palaeochannel sample P35 6-7m. Residue after first acid treatment. Experiment 3.

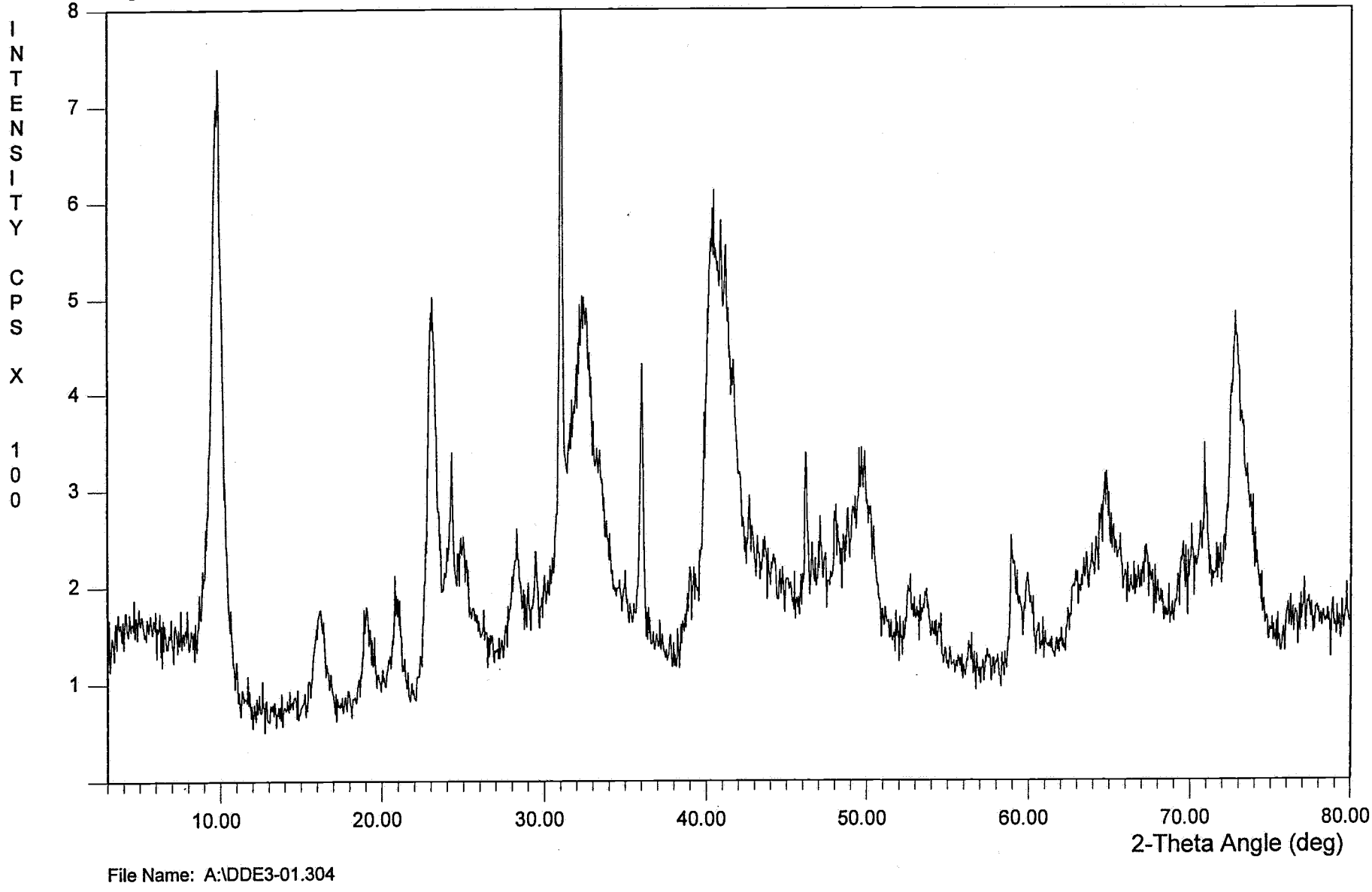


Fig. 2.3. XRD spectrum (Co Kα radiation, back pressed) of single acid treated sample P35 6-7m.

Fig. 2.4. Acid dissolution of dolomite in P35 6-7m.

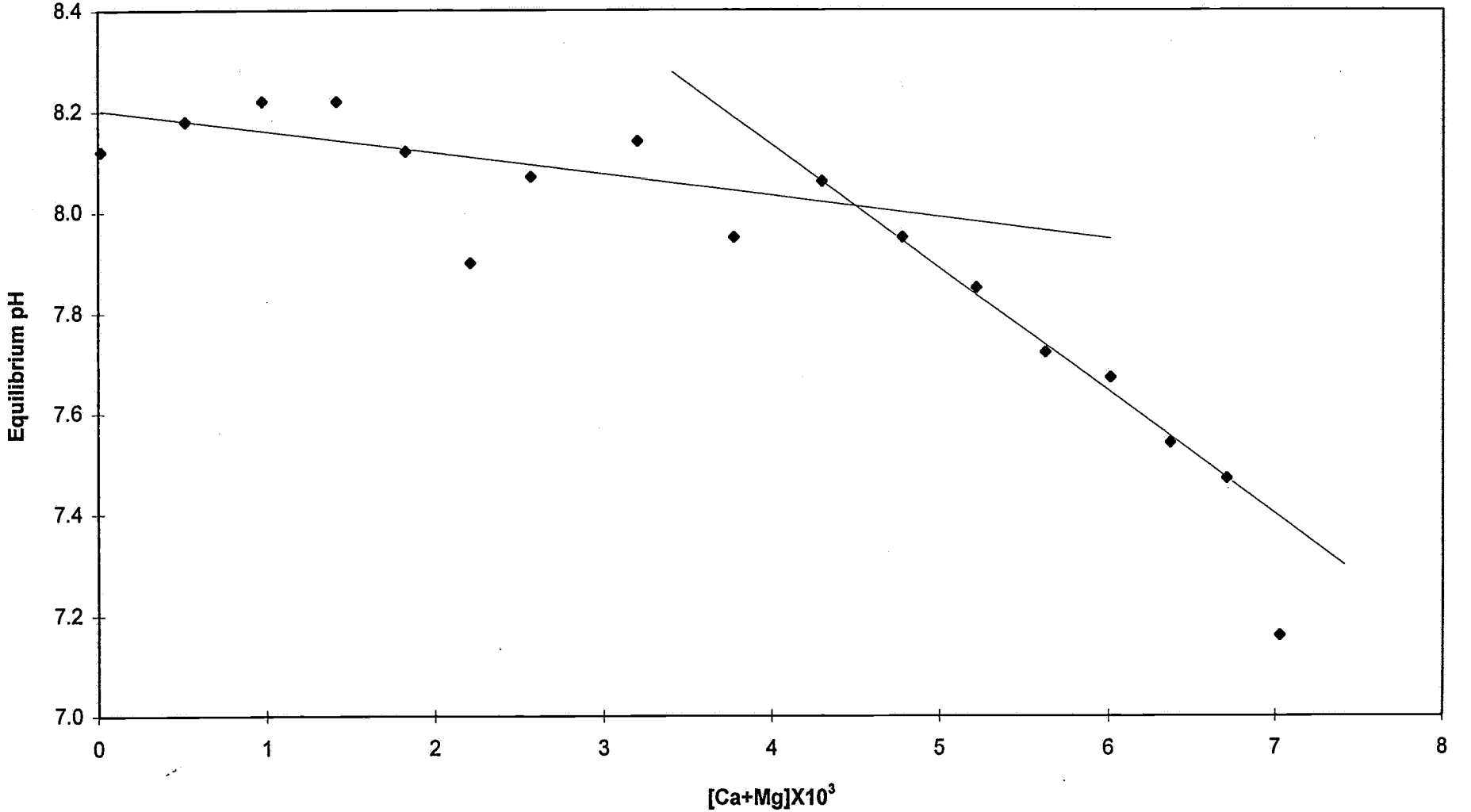


Fig. 2.4. Equilibrium pH verses Ca+Mg molar concentration after the addition of 0.01M HCl to sample P35 6-7m dispersed in water.

0004444

Fig. 2.5. Garford palaeochannel sample P35 6-7m. Residue after second acid treatment. Experiment 3.

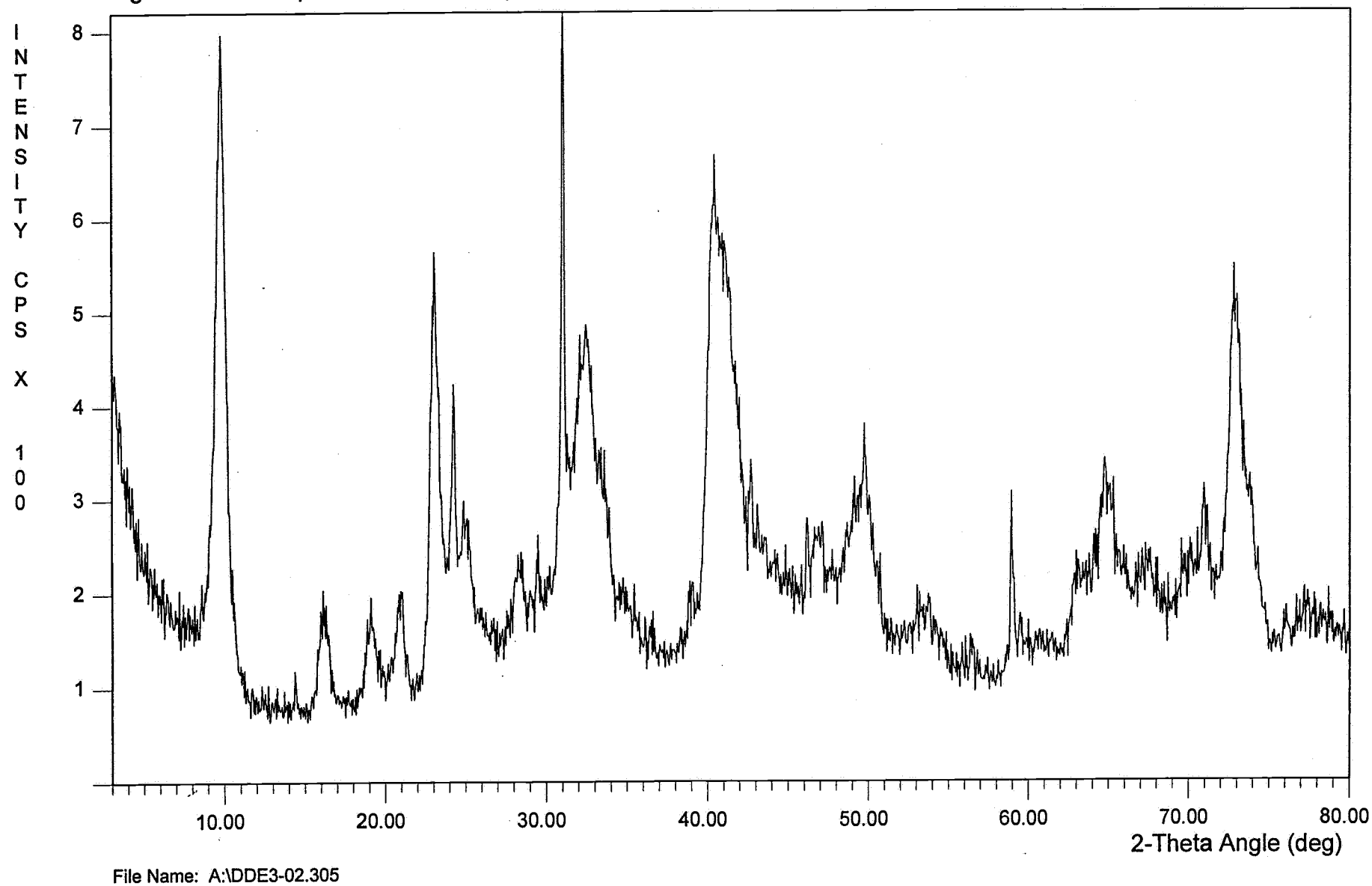


Fig. 2.5. XRD spectrum (Co Kα radiation, back pressed) of double acid treated sample P35 6-7m.

000445

Fig. 2.6. Garford palaeochannel sample P35 6-7m. Acid treated and untreated samples. Experiment 2.

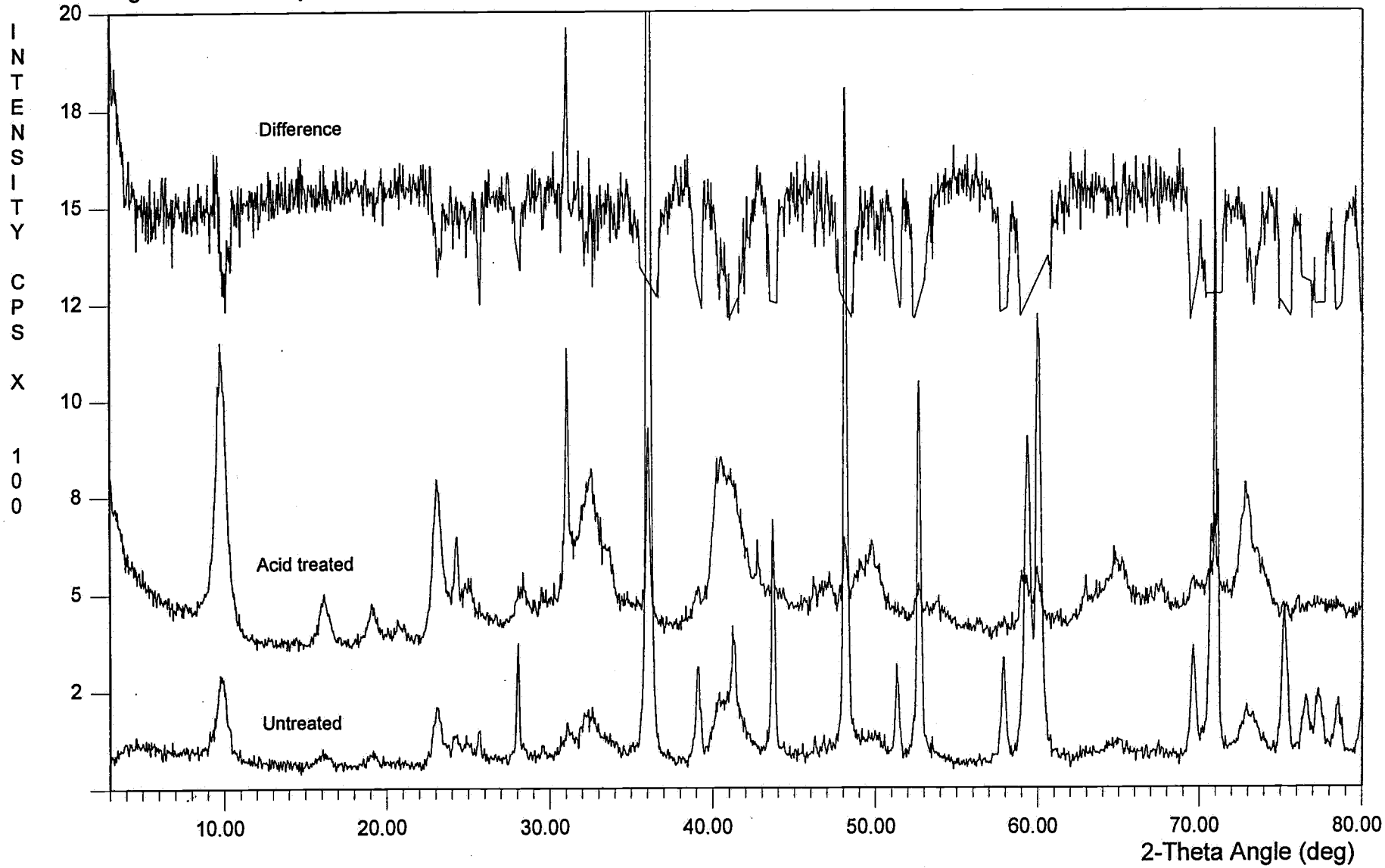


Fig. 2.6. Comparison of XRD spectra (Co Kα radiation, back pressed) of untreated and acid-treated sample P35 6-7m. The difference spectrum shows no evidence of amorphous silica.

Fig. 2.7. Garford palaeochannel sample P35 6-7m. As received sample and sample left in water for 6 months.

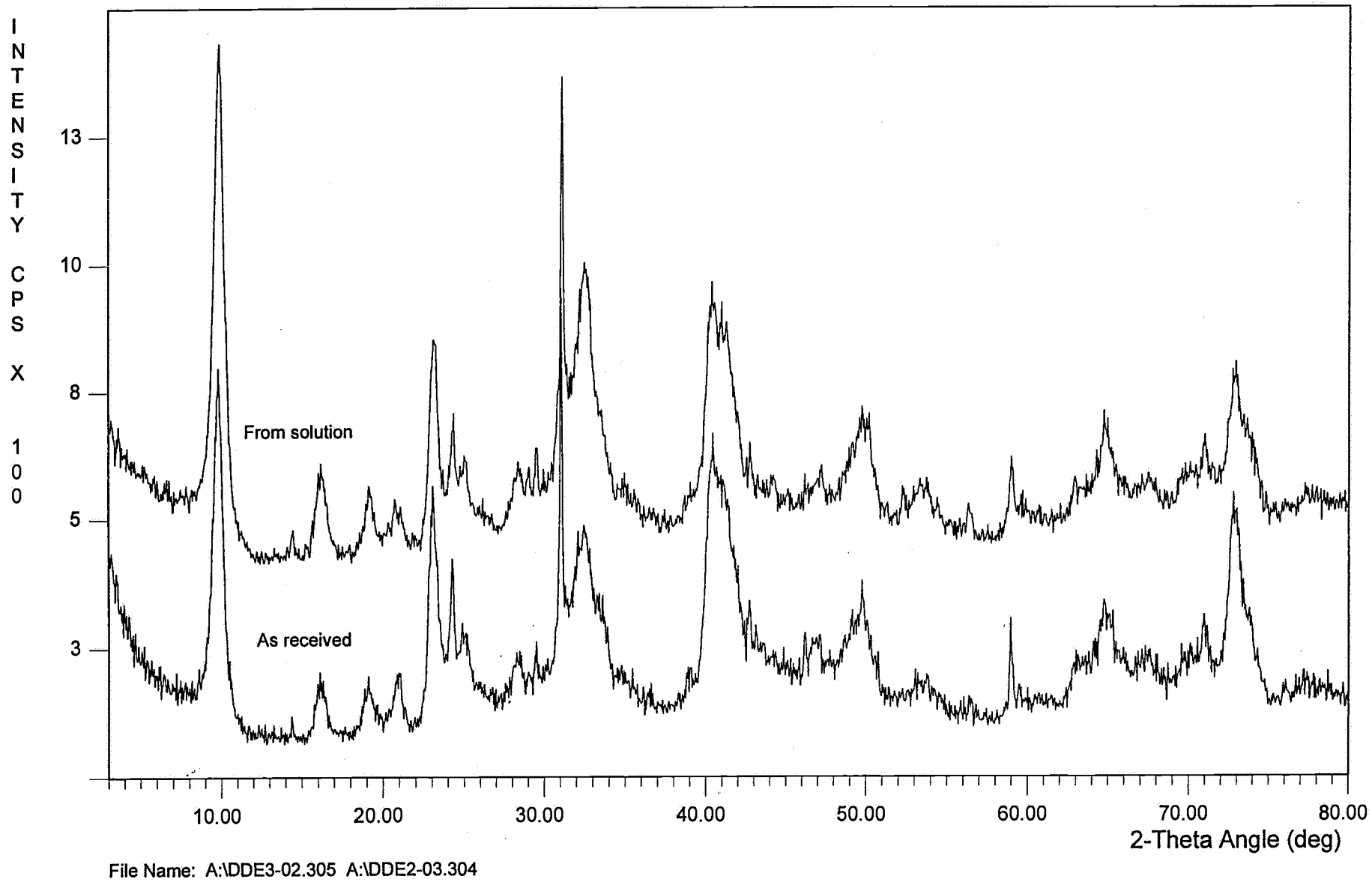


Fig. 2.7. Comparison of XRD spectra (Co Kα radiation, back pressed) of as-received sample and sample suspended in water for 6 months. Note the high illite content of the as-received sample (peak at 21° 2θ).

0004447

CHAPTER 3. PHYSICO-CHEMICAL PROPERTIES OF CLAYS AND MINERALS FROM THE GARFORD PALAEOCHANNEL.

Introduction

During the study of Garford palaeochannel clays several samples were identified that could be classed as mono-mineralic. These mono-mineralic samples can be used to characterise each of the major minerals in Garford palaeochannel clays, especially after beneficiation by techniques such as that described in Appendix 3. Careful characterisation of these samples was carried out by a combination of techniques including x-ray fluorescence spectroscopy (XRF), x-ray diffraction (XRD), thermal analysis and carbon analysis.

Quartz

The majority of quartz in Garford palaeochannel clays is >53μm in size. It is randomly distributed throughout the clay and is invariably coated with clay particles. The coating makes the quartz difficult to observe *in-situ* and in dried samples. It is readily discerned on dispersing the clays in water.

The quartz is a mixture of sub-rounded, frosted, white aggregates of small grains and sub-angular clear grains. Some particles show iron-oxide stains. Other minerals present in minor amounts with quartz in the >53μm size fraction are celestine, goethite, garnet, amphiboles and pyroxenes.

Illite

Illite and palygorskite are inseparable in the Garford palaeochannel samples. The grain size of the illite is very small (<0.2μm) (Raven *et al.*, 1995) but does not separate from the palygorskite during both sedimentation and centrifugation. The renormalised concentration of illite (Table 1.3) varies between 5wt.% and 30wt.% in samples containing high palygorskite and low dolomite. In general, increasing illite content in association with palygorskite in Garford palaeochannel clays corresponds with increased depth below the surface (Keeling *et al.*, 1995).

For XRF analysis sample P66 19-20m was used. This sample is very high in illite as shown by XRD analysis (Fig. 3.1). The chemical formula for Garford palaeochannel illite derived from the XRF analysis of this sample (Table 3.1) is:

$$(K_{0.92}\ Na_{0.07}\ Ca_{0.04})\ (Mg_{0.93}\ Fe^{3+}_{0.94}\ Al_{2.30})\ (Si_{7.37}\ Al_{0.63})\ O_{20}\ (OH)_4$$

Tetrahedral charge per formula unit = 0.63 electrons

Octahedral charge per formula unit = 0.43 electrons

Interlayer cation charge per formula unit = -1.06 electrons

(Note: An electron carries a negative charge and so a positive value in electron units corresponds to a net negative charge.)

The amount of K and Fe in the illite sample P66 19-20m is less than that of Muloorina illite (Churchman *et al.*, 1994). The lower Fe content would explain the brown colour of the Garford palaeochannel illite as opposed to the green colour of the high-Fe Muloorina illite.

As K content in Muloorina illite was used in earlier studies (Raven *et al.*, 1995) as a standard for the estimation of illite content in Garford palaeochannel clays, it is possible that these earlier studies under estimated illite content. This is not the case in this study because illite content was determined directly from XRD measurements using sample P66 19-20m as a standard.

Dolomite

Dolomite in Garford palaeochannel clays consists of irregular but sub-spherical aggregates formed as an agglomeration of several (approximately 10) smaller particles (Raven *et al.*, 1995). The aggregates are approximately 2μm in diameter. The size of the dolomite aggregates is such that they could probably be separated from other minerals in the Garford palaeochannel clays by controlled centrifugation. Alternatively, the dolomite can be removed by acid dissolution as described in the previous Chapter. Some samples with very-high dolomite were found during the 1995 drilling programme. Dolomite and dolomitic clays dominate the upper half of the Garford Formation sediments (Keeling *et al.*, 1995). Sample P33 Upper has been used for analytical

studies in this Report. The XRD pattern and XRF analysis of sample P33 Upper are shown in Fig. 3.2 and Table 3.1 respectively.

The XRF analysis indicates that the chemical formula for dolomite is:

$$Mg_{0.91}\,Ca_{1.09}\,(CO_3)_2$$

The dolomite is therefore depleted in Mg relative to the ideal composition (i.e. equal content of Mg and Ca).

Palygorskite

Several high-palygorskite samples were discovered amongst those taken during the 1995 drilling programme. The samples used for physico-chemical studies were P33 Lake Floor and P88 0.4-2m (see Chapter 1). XRD of sample P33 Lake Floor treated as described in Appendix 3 is shown in Fig. 3.3. Previous studies (Raven *et al.*, 1995) have shown that palygorskite from the Garford palaeochannel clays is fibrous and has a length of around 1μm and a diameter of around 0.015μm. Fibre length is correlated to the height and sharpness of XRD peaks especially those at 16° and 19° 2θ (Co Kα radiation). These peaks correspond to d-spacings of 6.35Å and 5.39Å respectively. The influence of fibre length on XRD spectra can be seen by comparing the XRD spectrum of Garford palaeochannel palygorskite with the spectra of palygorskite from Lake Nerramyne (Western Australia), Senegal and Xuyi (China) (Fig. 3.4 and Raven *et al.*, 1995). Lake Nerramyne palygorskite has a relatively short fibre length (approximately 0.5μm long by 0.015μm diameter) and shows broad and relatively weak XRD peaks (Raven *et al.*, 1995). Senegal (Appendix 4) and Xuyi palygorskites (Raven *et al.*, 1995) have long fibre lengths (approximately 2μm by 0.015μm diameter) and show strong, sharp XRD peaks. Garford palygorskite fibre length is slightly shorter than Senegal and Xuyi palygorskites but shows strong, sharp XRD peaks.

Dispersion and colloidal properties

During particle size fractionation (see Table 1.2) it was found that Garford palaeochannel palygorskite is self-flocculating in RO water (i.e. at approximately neutral pH). To further investigate the dispersion behaviour of Garford palaeochannel palygorskite, accurately-measured 0.5gm amounts of sample P88 0.4-2m treated as

described in Appendix 3 were dispersed in RO water by shaking for 20 minutes in a SPEX mill. The dispersed samples were then placed in 100ml measuring cylinders with an internal diameter of 2.7cm. At this point various amounts of either 0.01M HCl or 0.01M KOH were added to adjust the pH of the solution. RO water was then added to make the total volume 100ml and the solution agitated so that the clay was uniformly dispersed. The measuring cylinders were left at a constant temperature of 20°C. After 24 hours the top 10ml of the solutions were removed, placed in a beaker and stirred. The turbidity of 1ml of the stirred solution mixed with 29ml of RO water was then measured. The pH of the solution in the measuring cylinder was measured by a standard pH electrode. Where the sample flocculated and settled in the solution, the flocculated volume was measured by using the ml scale on the measuring cylinder. The results of the experiments are shown in Fig. 3.5. The absolute values of turbidity and flocculated volume are dependant on experimental conditions and the results should be used in a comparative way only.

The Garford palaeochannel palygorskite is dispersed at pH values above 6.5 and flocculated at pH values below 5.5. This indicates that the point of zero charge of the Garford palaeochannel palygorskite is around pH 6. The lowest measured flocculated volume was 50ml.

When the experiment was repeated at a pH of 7.7 but using a solution of 0.01M NaCl the palygorskite flocculated and compacted to a volume of 54ml. This is consistent with the results of Tama and El-Swaify (1978) who showed that using a 0.01M solution of mono-ionic species (KCl) was equivalent to a shift in pH of -2 units.

For comparison similar test were carried out on Lake Nerramyne, Senegal and Attagel 50 attapulgites. Lake Nerramyne showed similar behaviour to Garford palaeochannel palygorskite. The point of zero charge for Lake Nerramyne attapulgite was between pH values of 6.5 and 7.2. The as-received Attagel 50 and Senegal samples showed very high points of zero charge. For Attagel 50 it was between pH values of 9 and 9.5 and for Senegal attapulgite it was at a pH greater than 9.5. However, both of these materials show considerable pH buffering (because of the presence of calcite and dolomite) and so

there will be ions in solution that will cause a shift in the point of zero charge to higher pH values. Acid-washed Senegal attapulgite was found to have a point of zero charge at a pH value between 6 and 6.5. Acid-washed Attagel 50 was found to have a point of zero charge at a pH value of between 7.5 and 8.4. Lake Nerramyne attapulgite also showed a small amount of pH buffering and so it is probable that the point of zero charge for the Lake Nerramyne material is close to that of Garford palaeochannel palygorskite.

Attagel 50 was strongly buffered by dolomite/calcite and required double acid washing before an estimation of its true point of zero charge could be made. Although dolomite/calcite will detract from some properties there is a commercial advantage to buffering gellant material with dolomite. This is because the characteristics of the buffered material will remain constant over a seemingly wide range of chemical conditions.

Although dependant on experimental conditions, the volume into which the flocculated material compacts (Table 3.2) does give some information about the rheological properties of the sample. In a flocculated state, the particles are presumably in sufficient contact to form a self-supporting structure. The density of this structure will coincide with the onset of increased viscosity arising from particle-particle contact. Thus for Garford palaeochannel palygorskite viscosities significantly greater than that of water should occur when solutions are loaded at greater than 0.5gm per 50ml. This is about the twice the density for acid-washed Senegal attapulgite and Attagel 50. It is one fifth the density for Lake Nerramyne attapulgite.

The flocculated volume is dependant on pH and ionic species in solution (Table 3.2). For Garford palaeochannel palygorskite Na^+ solutions result in a lower flocculated volume than for Ca^{2+} solutions of equal charge concentration. This suggests that for Garford palaeochannel palygorskite Na^+ (and the associated water of hydrolisation) is more effective at neutralising the surface charge of the palygorskite than Ca^{2+} (and the associated water of hydrolisation). In contrast, for Senegal attapulgites, Ca^{2+} solutions

give a smaller flocculated volume than Na^+. This suggests that there is a variability in the nature of the surface of palygorskite from different locations.

Composition and cation exchange behaviour

To determine the composition of Garford palaeochannel palygorskite the sample P33 Lake Floor treated as described in Appendix 3 was used. XRF analysis was carried out on the sample in the as-received state and after being saturated with Mg, Ca, Na and K. These treatments enable the exchange properties to be determined. The results are shown in Table 3.1. Observations that can be made about these results are:

- In as-received, Mg-saturated and Ca-saturated samples the Na and K concentrations remain constant. When samples are Na- or K-saturated there is variation in Na, K, Mg and Ca contents.
- In as-received, Mg-saturated and Ca-saturated samples the water content of 105°C dried samples increases with increasing Ca content and decreasing Mg content. This is in accordance with the relative hydration energies of Mg and Ca and is similar to the behaviour of smectites. For Na- and K-saturated samples the water content remains as for the as-received material.

These observations are indicative of the two exchange mechanisms that are occurring. These mechanisms are exchange within the structural tunnels of palygorskite and exchange at the surfaces of the palygorskite. A third mechanism influencing the results is exchange at the surfaces of illite in the sample. It is assumed that the effect of illite will be small because of the low illite content and the low exchange capacity of illite. The observation that water content varies with Mg and Ca concentrations indicates that the water associated with these cations is not completely driven off at 105°C. This suggests that this water is located in the structural tunnels of the palygorskite and infers that Ca and Mg exchange predominantly within the tunnels. This is in agreement with the results of the flocculation experiments which showed that Ca was less effective at neutralising surface charge than Na.

On the assumption that no Na or K enter the tunnels and that Ca replaces all exchangeable Mg, the chemical formula of Garford palaeochannel palygorskite was determined to be:

$$(Mg_{2.75}\ Al_{1.12}\ Fe^{3+}_{0.37}\ \square_{0.76})\ (Si_{7.96}\ Al_{0.04})\ O_{20}\ (OH)_2\ (OH_2)_4 \bullet R^{2+}_{0.04}\ (H_2O)_4$$

where $\square$ represents octahedral vacancies and R^{2+} represents an exchangeable divalent cation.

Tetrahedral charge per formula unit = 0.04 electrons

Octahedral charge per formula unit = 0.04 electrons

(Note: An electron carries a negative charge and so a positive value in electron units corresponds to a net negative charge.)

Cation exchange capacity (CEC) = 10.5 ± 0.5 $cmol^+/kg$ of 1000°C ignited clay

(variance is based on average over three samples)

$(H_2O)_4$ is nominal

The formula for as-received Garford palygorskite is:

$$(Mg_{2.75}\ Al_{1.12}\ Fe^{3+}_{0.37}\ \square_{0.76})\ (Si_{7.96}\ Al_{0.04})\ O_{20}\ (OH)_2\ (OH_2)_4 \bullet Ca_{0.01}\ Mg_{0.03}\ (H_2O)_4$$

To allow for illite in the samples, all K was assigned to illite and then amounts of other oxides removed in accordance to the composition of illite as determined above.

This is not a complete formula because the XRF analysis shows that Na and K do replace Mg and Ca, especially Ca. Hence some Na and K must exchange within the tunnels of the palygorskite structure. By averaging the formula derived from all XRF results a structural formula that includes cations residing in the structural tunnels and on the surface of the palygorskite can be derived. This formula for as received Garford palaeochannel palygorskite is:

$$(Mg_{2.63}\ Al_{1.16}\ Fe^{3+}_{0.39}\ \square_{0.82})\ (Si_{7.91}\ Al_{0.09})\ O_{20}\ (OH)_2\ (OH_2)_4 \bullet R^{2+}_{0.07}\ R^{+}_{0.06}\ (H_2O)_4$$

where $\square$ represents octahedral vacancies. R^{2+} and R^+ represent an exchangeable divalent and monovalent cations respectively.

Tetrahedral charge per formula unit = 0.09 electrons

Octahedral charge per formula unit = 0.09 electrons

(Note: An electron carries a negative charge and so a positive value in electron units corresponds to a net negative charge.)

Cation exchange capacity (CEC) = 26.3 ± 0.5 $cmol^+/kg$ of 1000°C ignited clay

(variance is based on average over seven samples)

$(H_2O)_4$ is nominal

The formula for as-received Garford palygorskite is:

$$(Mg_{2.63}\ Al_{1.16}\ Fe^{3+}_{0.39}\ \square_{0.82})\ (Si_{7.91}\ Al_{0.09})\ O_{20}\ (OH)_2\ (OH_2)_4 \bullet Mg_{0.05}\ Ca_{0.02}\ Na_{0.02}\ K_{0.04}\ (H_2O)_4$$

To allow for the illite content of the samples it was assumed that the K in the Na-saturated sample (i.e. the sample with the lowest K content) was all associated with illite. This amount of illite was removed from all samples. Thus the amount removed was about 80% of that which would have been removed from the as-received, Mg-saturated and Ca-saturated samples had all the K in these samples been assigned to illite. It is therefore likely that assigning all K in a as-received sample to illite overestimates the illite content. This will counter act, in part, the underestimation of illite content by the use of Muloorina illite as a standard in the work of Raven *et al.* (1995). Hence, estimation of illite content by Raven *et al.* (1995) based on the K content of Muloorina illite is therefore likely to underestimate illite content in Garford palaeochannel clays by about 10% of the stated value.

The true structural formula for Garford palaeochannel palygorskite will lie somewhere between the two formulae given above. It is clear that the CEC value of the palygorskite is dependant on cationic species and that there seems to be a fair degree of specificity in the exchange properties of palygorskite. This specificity will be discussed in Chapter 5.

Absorption and organic carbon

In absorbency studies (Chapter 6) of high-palygorskite Garford palaeochannel clays it was found that some clays showed anomalously low water absorption. These clays were very dark (almost black) in colour in their wet, as-received state. It was postulated that organic matter may be binding the palygorskite fibres together thereby blocking pore space. Consequently the high-palygorskite clay P33 Lake Floor was analysed for total carbon by the high-frequency induction furnace (Leco) method (Rayment and Higginson, 1992, method 6B3), carbonate content by the manometric method (Rayment

and Higginson, 1992, method 19B1) and organic carbon by difference. The results are shown in Table 3.3.

The measured organic carbon content is low and would be insufficient to cause pore blockage. The value of CO_3 (dolomite) in the sample is as expected from XRD analysis.

An explanation for the low absorbency of some Garford palaeochannel clays is that the palygorskite fibres in these clays are bundled together and therefore do not have a high porosity in their natural state. The fibre bundling could be because the palygorskite of the Garford palaeochannel forms in a saline and therefore non-dispersive environment. Lake Nerramyne samples, which show high porosity and therefore high absorbency, do not contain halite or other soluble salts in the as-received state and may form in a more dispersive environment where the palygorskite fibres would not bundle.

Thermal characteristics

Thermogravimetric analysis and differential thermal analysis of Garford palaeochannel palygorskite (Fig. 3.6) shows that there are 3 steps in the dehydration of the palygorskite. The first step occurs in the temperature range 100°C to 175°C. XRD (Fig. 3.7) shows that, although there is a weight loss of around 7.5% over this temperature range, there is no structural change. The weight loss in this temperature range is caused by the loss of adsorbed and zeolitic water (Fig. 3.8a). This weight loss is fully reversible.

The second step occurs in the temperature range 225°C to 300°C. The weight loss that occurs in this temperature range is around 2.5%. Samples heated to temperatures within this range do not disperse as well as unheated samples. XRD (Fig 3.7) shows that accompanying this weight loss is a change in the structure of the palygorskite. The structural change causes a decrease in the strong palygorskite peak at 10°2θ, a shift in the peaks at 16°2θ and 19°2θ, a new peak to occur at 11°2θ and several new peaks to occur in the region 22°2θ to 25°2θ (Co Kα radiation). Although the sample contains illite and the XRD patterns clearly show the illite reflections, the changes in the patterns

are not caused by illite. This is confirmed by examination of pure illite samples which show that illite does not undergo any structural change up to temperatures of at least 700°C. The weight loss and structural change has been attributed to loss of half the bound water from the palygorskite structure (VanScoyoc *et al.*, 1979; Nagata *et al.*, 1974). When this amount of bound water is removed from the structure the tunnels collapse giving rise to a folded structure as shown in Fig. 3.8b. In the folded structure the b and c dimensions are reduced relative to the unheated structure. The peaks in the XRD pattern of the heated palygorskite can be indexed on the basis of the folded structure as shown in Fig. 3.9. The unit cell for the folded structure is a = 5.2Å, b = 15.6Å and csinβ = 11.0Å (assuming no change in the a dimension). This corresponds to a rotation of the silicate units by approximately 30°. Although on first examination it appears as though the c axis of the structure has not changed, this is not the case and arises from the coincidental equivalence of XRD reflections from the normal and folded structures.

The collapsed tunnels can be rehydrated by placing the heated palygorskite in water or a high relative-humidity atmosphere (Jones and Galan, 1988). The time and extent of rehydration is dependant on the highest temperature to which the palygorskite is heated. For example, Garford palaeochannel palygorskite heated to 280°C was completely rehydrated after being placed in water for 24 hours while the same palygorskite heated to 350°C did not completely rehydrate even after being placed in water for 48 hours.

Nathan (1969) proposed an alternate folded structure based on the alternate palygorskite structure of Gard and Follett (1968). The structural model proposed by Nathan (1969) would give rise to an (010) reflection (approximately 15.6Å) which is not observed in the XRD pattern of heated palygorskite. Hence, the structural model of Nathan (1969) for heated palygorskite is not preferred and, by implication, the structural model of Gard and Follett (1968) is also not preferred.

The third step in the dehydration of palygorskite is at temperatures above 400°C. In the temperature range 400°C to 500°C there is a 5% weight loss that has been attributed to the irreversible removal of all bound water and partial dehydroxylation of the structure

(Jones and Galan, 1988). Above 500°C there is a continuous slow decrease in weight corresponding to the slow dehydroxylation of the structure which suffers total collapse. The only significant peaks to remain in the XRD pattern of palygorskite heated above 500°C are the (021) and (012) reflections (see Figs. 3.7b and 3.9).

Genesis of palygorskite

The mechanisms of genesis of palygorskite are not readily apparent but field observation and laboratory analysis does provide some clues. Observations have shown that:

- palygorskite concentrations are highest at the interface between dolomitic (overlying) and illitic (underlying) clays (Keeling *et al.*, 1995),
- dolomite from directly above the palygorskite at site P33 is depleted in Mg,
- samples left in RO water for a long period of time show a reduced illite content relative to the original sample (see previous Chapter),
- samples left in RO water for a long period of time show a higher than expected pH (see previous Chapter).

These observations suggest that palygorskite forms by the dissolution of illite. The source of Mg for palygorskite formation is dolomite. Given the formula derived from XRF analysis, the reaction would be

$$\text{illite} + 1.75\text{Mg} + 0.54\text{Si} + 8\text{H}_2\text{O} \rightarrow$$

$$\text{palygorskite} + 0.87\text{Al} + 0.88\text{K} + 0.55\text{Fe}^{3+} + 0.05\text{Na} + 0.02\text{Ca} + 2(\text{OH}^-)$$

This reaction is plausible in some aspects but requires further explanation in others. The addition of Si, Mg and H_2O is plausible because these elements and compound are available in the lacustrine environment. The release of Fe is plausible because goethite is observed in the coarse fraction (>53μm) high-palygorskite samples. The release of relatively small amounts of Na and Ca is also plausible. However, the production of K and Al is questionable because no high-K or high-Al content minerals (other than illite) are observed in the field.

If the above illite to palygorskite genesis mechanism is correct, it is unlikely that illite forms a template for palygorskite growth because of the required transfer of atoms from

both the tetrahedral and octahedral sites. A more likely senario is dissolution of illite and precipitation of palygorskite.

It is possible that the association between illite an palygorskite is coincidental. There is an indication in some drill holes of illitisation of smectite. Therefore illite may be forming independently from but concurrently with palygorskite. The palygorskite may result from the dissolution of smectite in a high-Mg environment. Clearly further work needs to be carried out to fully understand the genesis of palygorskite in the Garford palaeochannel.

References

Churchman, G.J., Ferris, G.M., Keeling, J.L., McClure, S.G., Raven, M.D., Self, P.G. and Slade, P.G. (1994). Absorbent Clay Project. Characterisation of the selected clays. Progress Report No.1 to Mines and Energy, South Australia, June 1994. South Australian Department of Mines and Energy, Envelope 8785 (unpublished).

Gard, J.A. and Follett, E.A.C. (1968). A structural scheme for palygorskite. Clay Minerals, **7**, 367-370.

Jones, B.F. and Galan, E. (1988). Sepiolite and palygorskite. In: S.W. Bailey (Ed.), Hydrous Phyllosilicates (exclusive of the micas). Reviews in Mineralogy, **19**. Mineral Society of America.

Keeling, J.L., Ferris, G.M. and Statham-Lee, L. (1995). Palygorskite clay investigation, Garford palaeochannel, South Australia: Results of drilling April-May, 1995. Mines and Energy, South Australia, Report Book 95/48.

Nagata, H., Shimoda, S and Sudo, T. (1974). On dehydration of bound water of sepiolite. Clays and Clay Minerals, **22**, 285-293.

Nathan, Y. (1969). Dehydration of palygorskites and sepiolites. Proc. Int. Clay Conf., 91-98.

Raven, M.D., Abolins, N., Keeling, J.L. and Self, P.G. (1995). Absorbent Clay Project. Mineralogical characterisation of Garford palaeochannel clays. Supplementary Report to Mines and Energy, South Australia, April 1995. South Australian Department of Mines and Energy, Envelope 8785 (unpublished).

Rayment, G.E. and Higginson, F.R. (1992). Australian laboratory handbook of soil and water chemical methods. Inkata Press, Melbourne.

Tama, K. and El-Swaify, S.A. (1978). Charge, colloidal and structural stability interrelationships for oxidic soils. In: W.W. Emerson, R.D. Bond and A.R. Dexter, "Modification of Soil Structure". John Wiley and Sons, Chichester.

VanScoyoc, G.E., Serna, C.J. and Ahlrichs, J.L. (1979). Structural changes in palygorskite during dehydration and dehydoxylation. American Mineralogist, **64**, 215-223.

Table 3.1. XRF analysis (wt.%) of major minerals from the Garford palaeochannel clays. All samples <2μm >0.2μm unless otherwise stated. All analyses carried out on of 105°C dried samples.

	SiO_2	TiO_2	Al_2O_3	Fe_2O_3	MnO	MgO	CaO	Na_2O	K_2O	P_2O_5	SO_3	ZrO_2	Sr	Cl	F	Sum
Illite																
P66 19-20m																
<0.2μm	53.7	0.270	18.06	9.07	0.025	4.56	0.240	0.32	5.23	0.025	0.017	0.021	0.010	0.08	0.17	91.8
0.2-2μm	55.8	0.937	19.39	9.42	0.025	4.61	0.27	0.24	5.26	0.044	0.020	0.029	0.011	0.09	0.17	96.3
Dolomite																
P33 Upper																
As received	2.44	0.044	0.38	0.26	0.034	20.3	34.1	0.75	0.058	0.039	0.123	0.002	0.033	0.96	nm	59.5
Washed	2.24	0.040	0.42	0.30	0.035	20.5	34.0	0.04	0.29	0.034	0.018	0	0.031	0.04	nm	57.5
Palygorskite																
P33 Lake Floor																
As received	53.5	0.43	7.11	3.43	0.015	9.6	0.65	7.5	1.19	0.016	0.434	0.025	0.015	8.5	nm	92.4
Acid washed																
As received	58.3	0.530	10.08	4.94	0.023	11.6	0.125	0.11	1.25	0.027	0.023	0.020	0.003	0.03	0.18	87.3
As received	59.2	0.52	10.15	4.96	0.019	12.0	0.138	0.12	1.22	0.020	0.007	0.024	0.003	0.01	nm	88.3
As received	58.3	0.50	9.95	4.90	0.017	12.0	0.289	0.10	1.23	0.013	0.004	0.020	0.003	0.03	nm	87.4
Mg saturated	60.7	0.564	10.59	5.12	0.020	12.4	0.026	0.12	1.27	0.025	0.023	0.023	0.003	0.05	0.09	91.0
Ca saturated	57.1	0.525	9.94	4.96	0.016	11.3	0.263	0.14	1.17	0.024	0.027	0.019	0.003	0.04	0.28	85.8
Na saturated	59.0	1.41	9.94	4.77	0.018	11.6	0.056	0.34	1.05	0.051	0.011	0.036	0.003	0.02	nm	88.3
K saturated	59.3	0.78	10.10	4.92	0.018	11.8	0.042	0.16	1.60	0.031	0.006	0.027	0.002	0.02	nm	88.8

nm = not measured.

0004461

Table 3.2. Minimum flocculated volume of 0.5gm of various attapulgites in water.

	$(H_3O)^+$ ml	Ca^{2+} (0.01M) ml	Na^+ (0.02M) ml
P88 0.4-2m	50	55	44
Lake Nerramyne	10	nm	nm
Senegal attapulgite (acid washed)	96	55	96
Attagel 50 (acid washed)	75	nm	nm

nm = not measured.

Table 3.3. Carbon content (wt.%) of as-received, 105°C-dried Garford palaeochannel sample P33 Lake Floor.

Total C (Leco)	Organic C	CO_3 as dolomite
0.30	0.11	1.5

Fig. 3.1. Garford palaeochannel sample P66 19-20m. <0.2um. Illite.

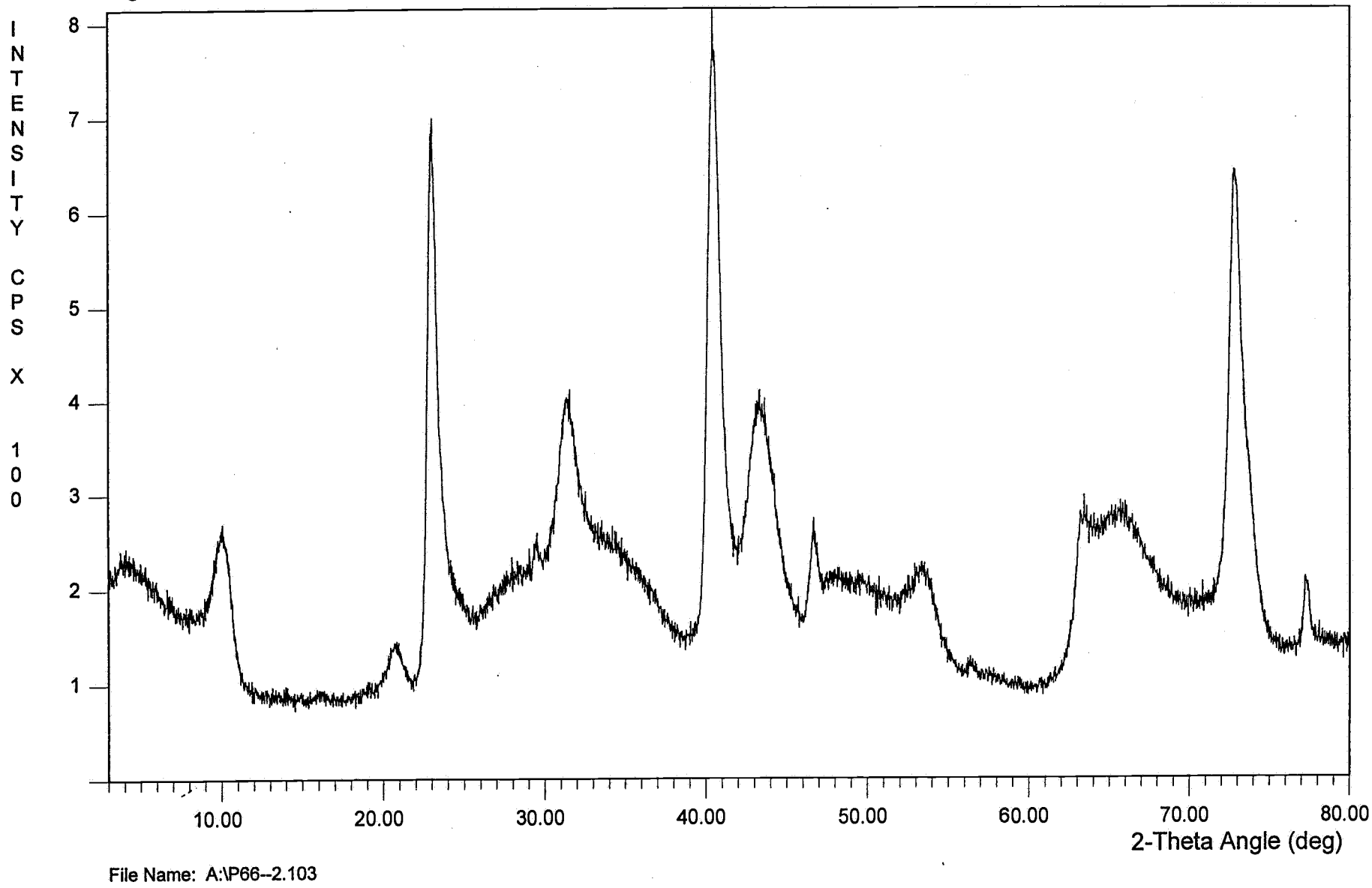


Fig. 3.1. XRD (Co Kα radiation, back pressed) of <0.2μm fraction of Garford palaeochannel sample P66 19-20m. This sample is virtually pure illite.

0004464
94

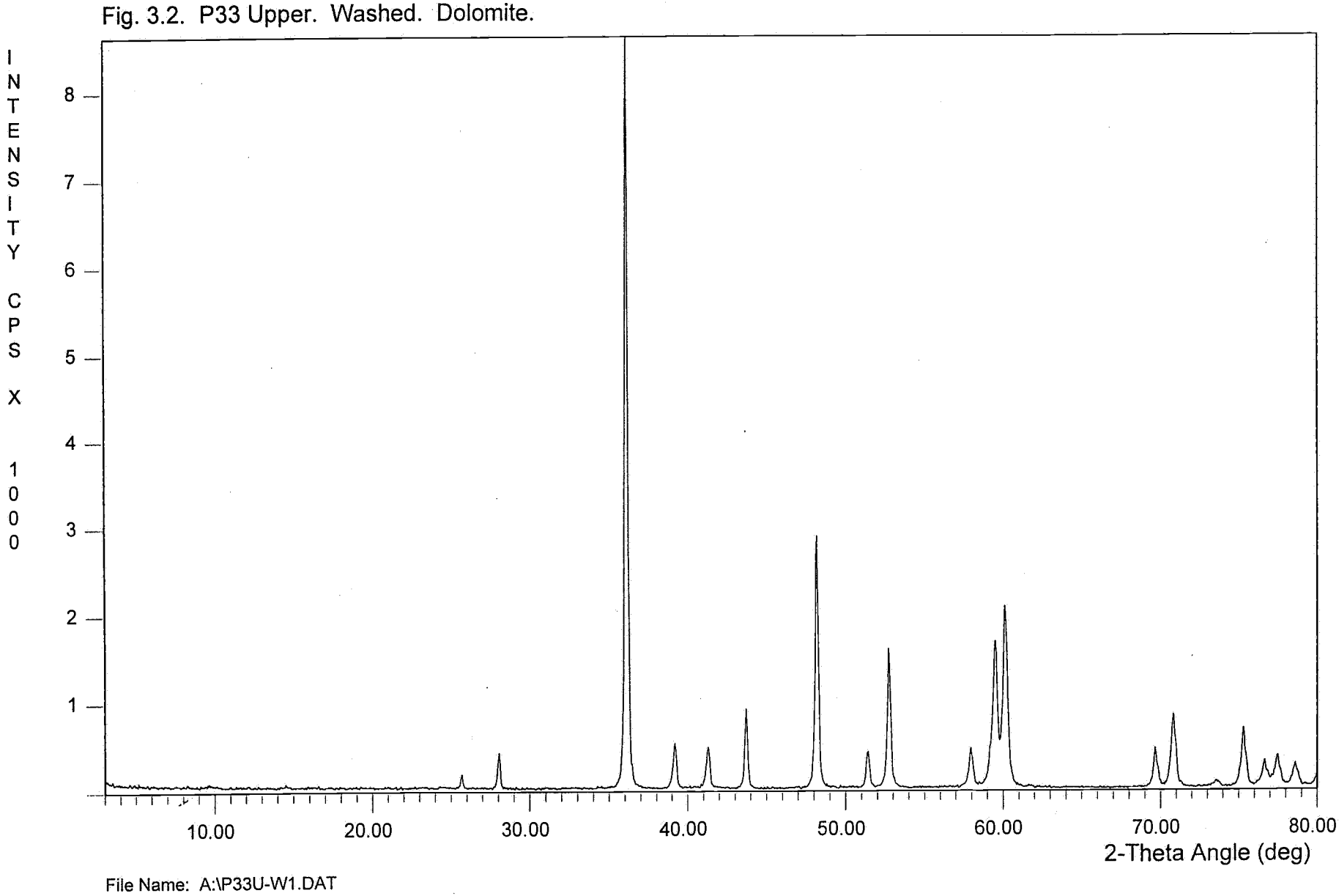


Fig. 3.2. XRD (Co Kα radiation, back pressed) of <0.2μm fraction of Garford palaeochannel sample P33 Upper. This sample is approximately 98% dolomite and 2% quartz.

0004655

Fig. 3.3. Garford palaeochannel sample P33 Lake Floor. Triple Washed. Palygorskite.

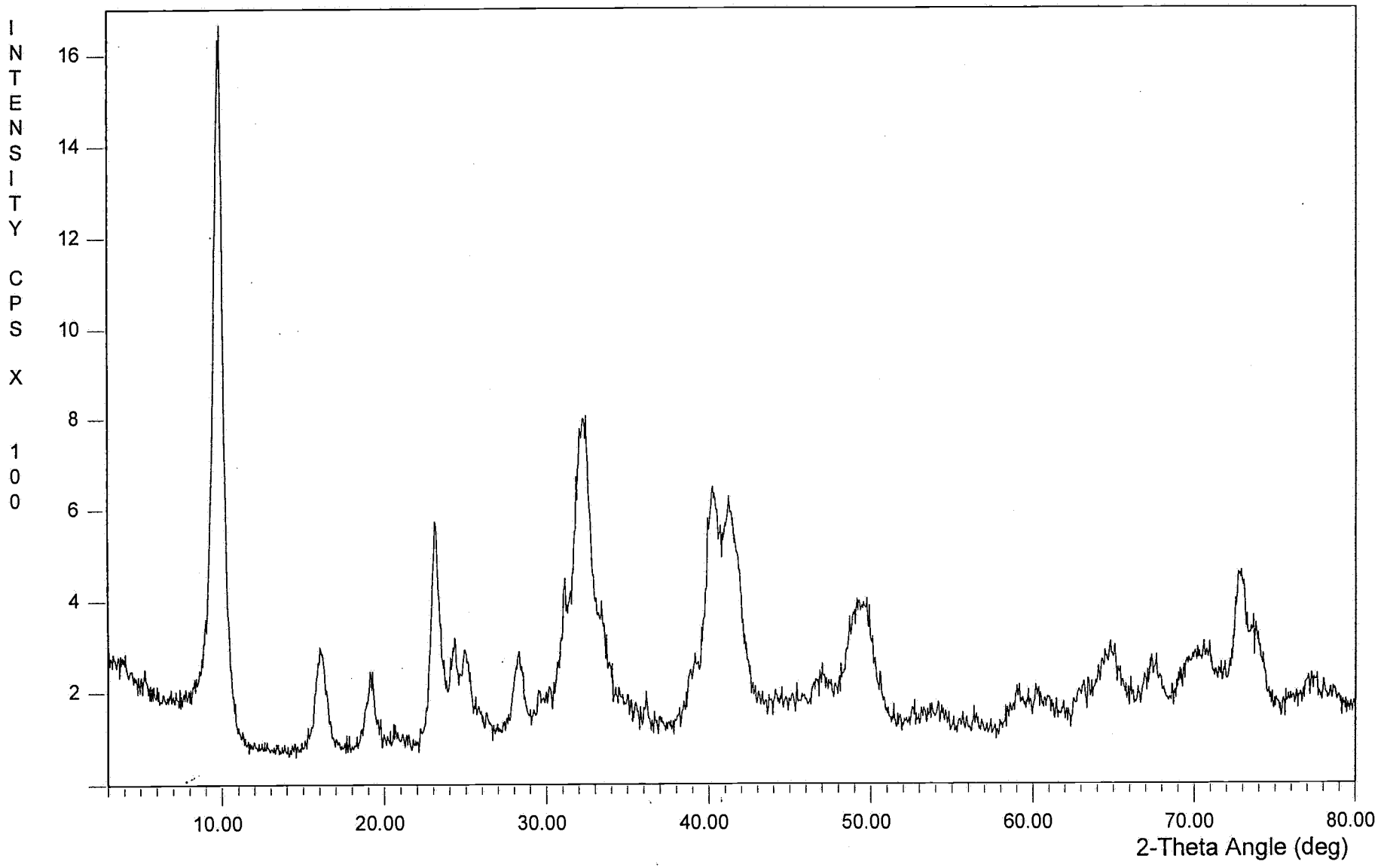


Fig. 3.3. XRD (Co Kα radiation, back pressed) of <10μm fraction of Garford palaeochannel sample P33 Lake Floor. This sample is virtually pure palygorskite.

0004466

Fig. 3.4. Comparison of Lake Nerramyne, Attagel, Garford palaeochannel, Xuyi and Senegal palygorskites.

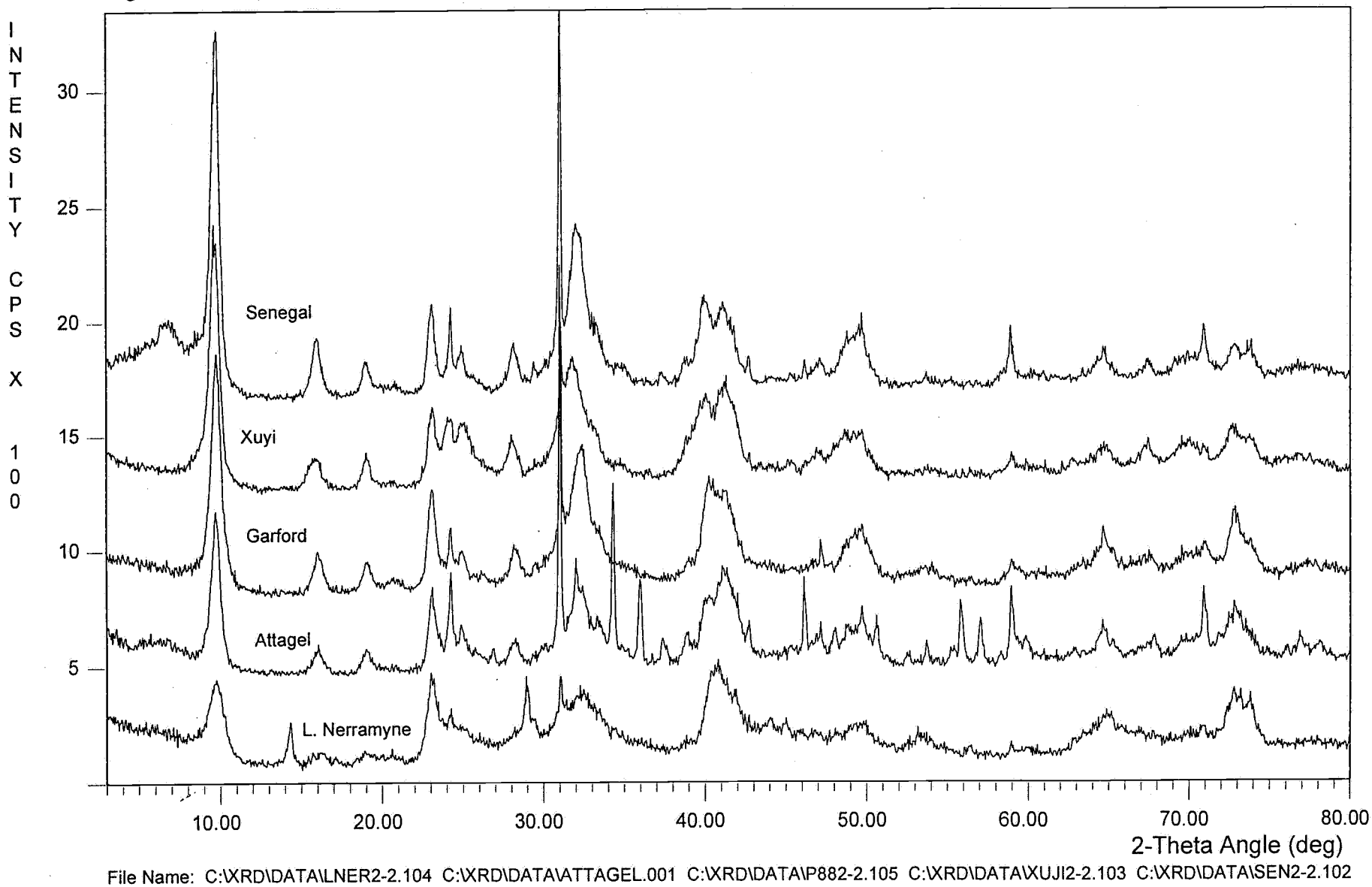
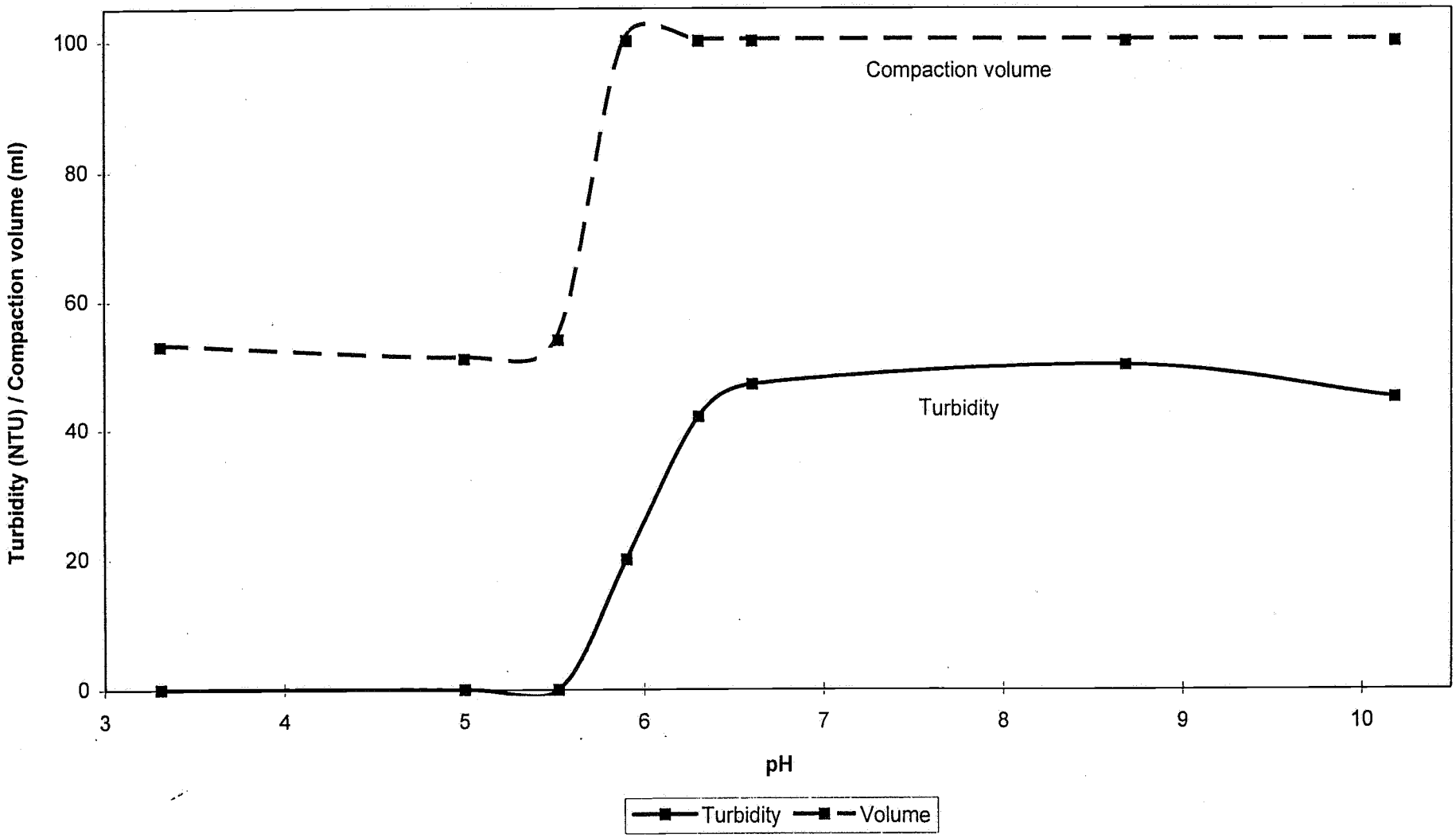


Fig. 3.4. Comparison of XRD spectra (Co Kα radiation, back pressed) of <2μm >0.2μm fractions of Lake Nerramyne, Attagel 50, Garford palaeochannel sample P88 0.4-2m, Xuyi No. 1 deposit and Senegal palygorskites.

0004067

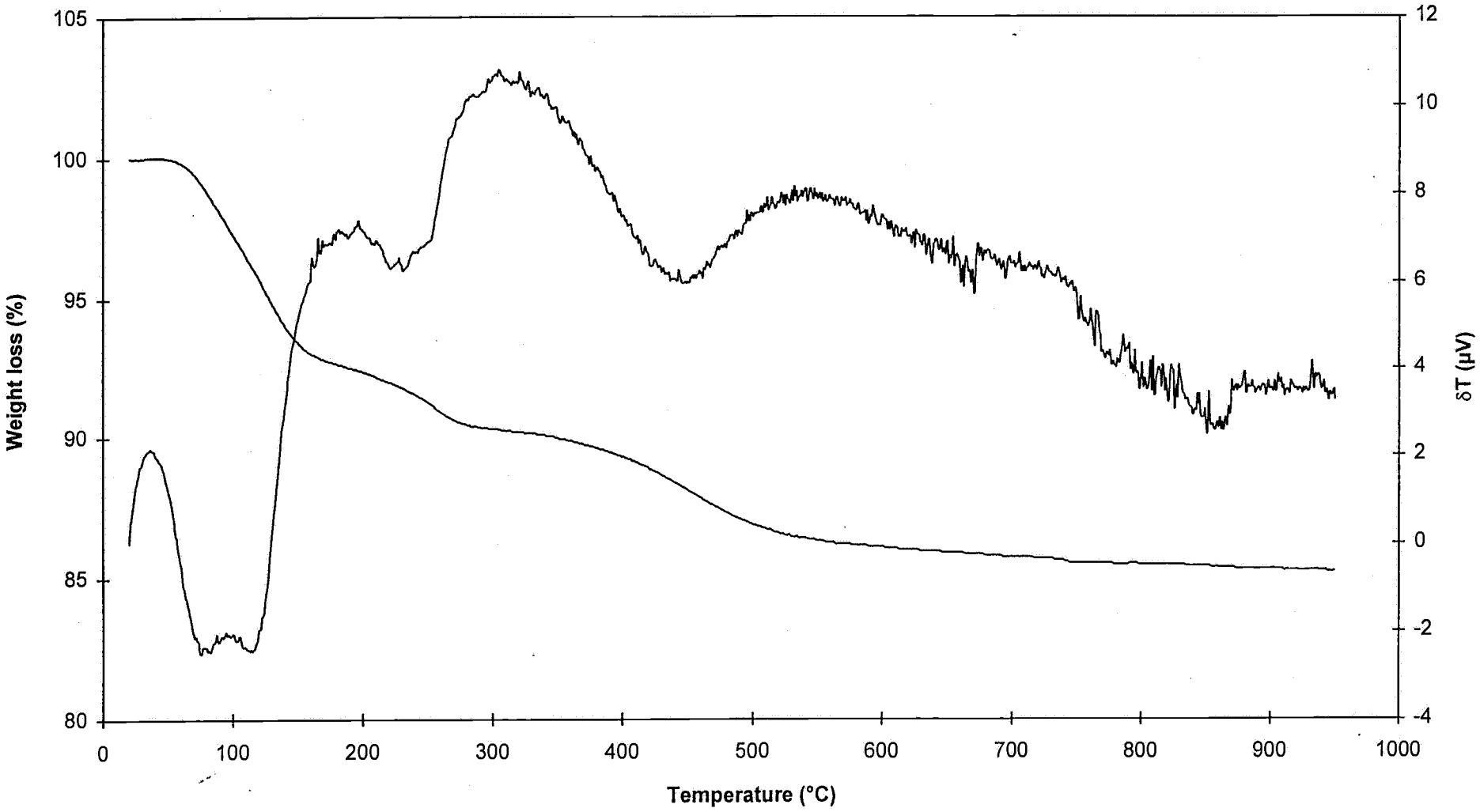
Fig. 3.5. Colloidal properties of Garford palaeochannel palygorskite P88 0.4-2m (<2µm >0.2µm).



0004468

Fig. 3.5. Colloidal properties of Garford palaeochannel palygorskite P88 0.4-2m, <2µm >0.2µm. See text for explanation.

Fig. 3.6. DTA and TGA of Garford palaeochannel sample P88 0.4-2m, <2µm >0.2µm.



0004469

Fig. 3.6. TGA and DTA (nitrogen atmosphere) of Garford palaeochannel palygorskite P88 0.4-2m, <2µm >0.2µm.

Fig. 3.7a. Garford palaeochannel palygorskite P88 0.4-2m. Heated 105C, 150C, 200C, 250C.

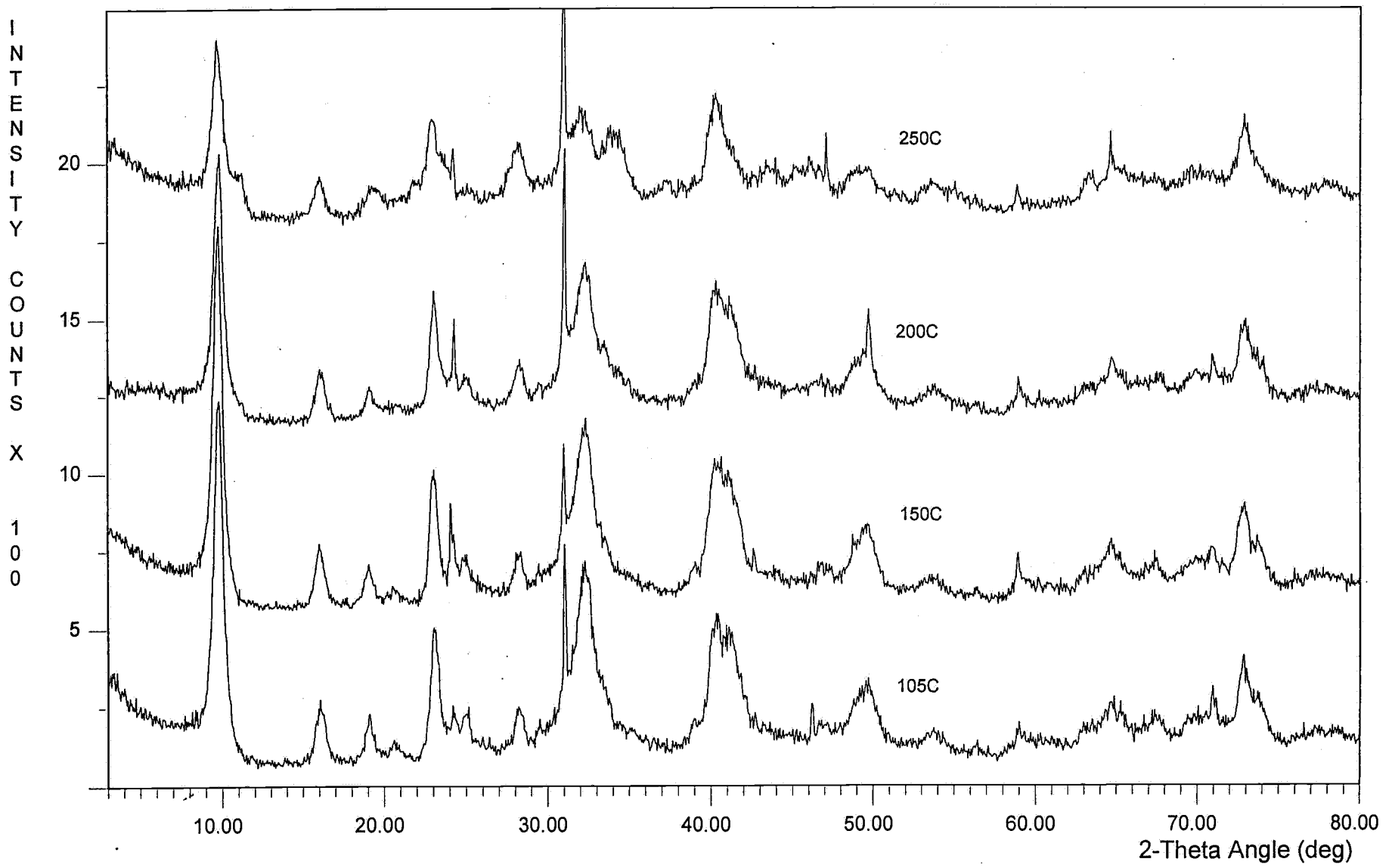
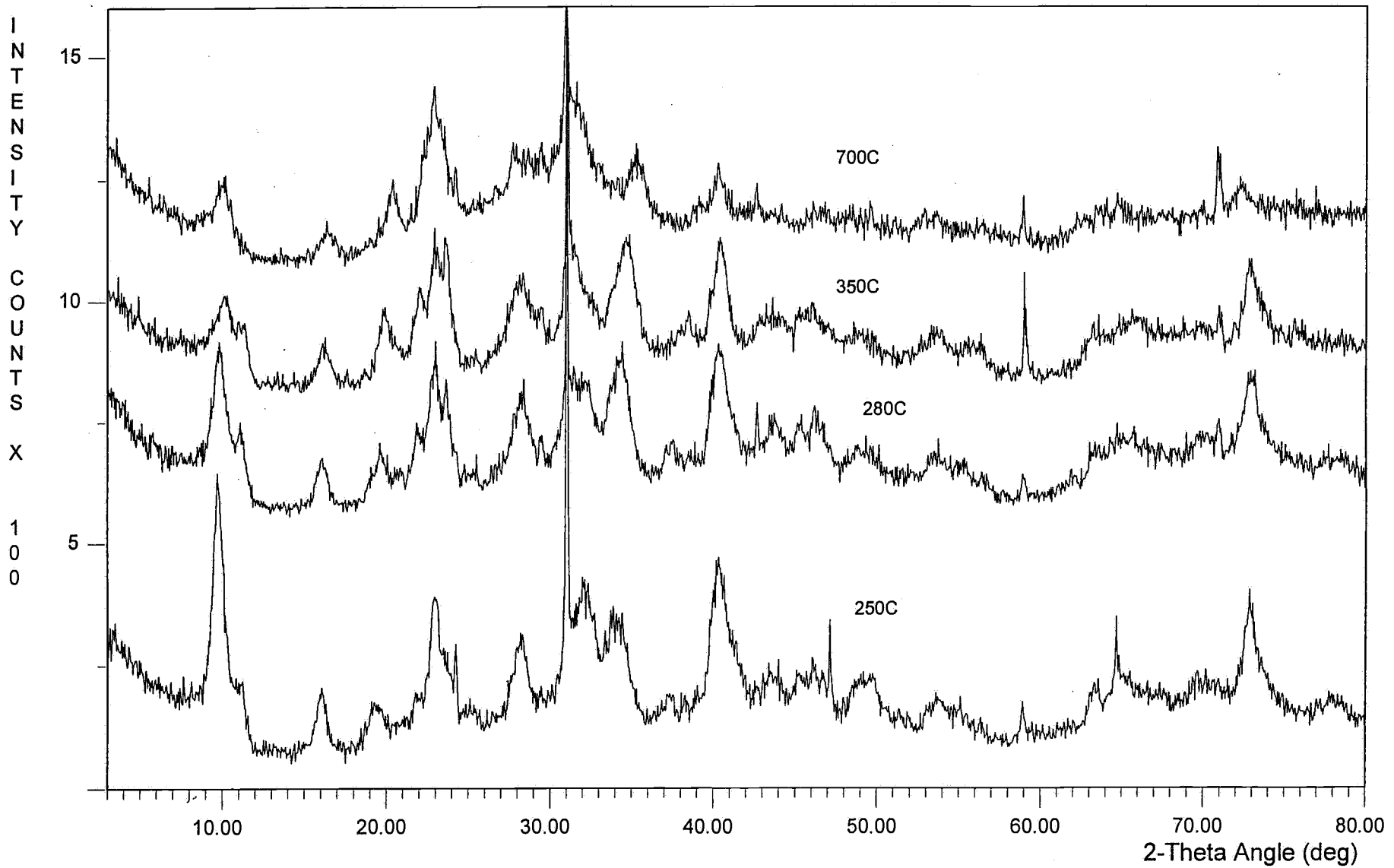


Fig. 3.7a. XRD (Co Kα radiation, back pressed) of Garford palaeochannel palygorskite P88 0.4-2m (<2μm >0.2μm) heated to 105°C, 150°C, 200°C and 250°C.

000470
100

Fig. 3.7b. Garford palaeochannel palygorskite P88 0.4-2m. Heated 250C, 280C, 350C, 700C.



File Name: c:\xrd\data\p88-250.101 c:\xrd\data\p88-280a.101 c:\xrd\data\p88-350.201 c:\xrd\data\p88-700.101

Fig. 3.7b. XRD (Co Kα radiation, back pressed) of Garford palaeochannel palygorskite P88 0.4-2m (<2μm >0.2μm) heated to 250°C, 280°C, 350°C and 700°C.

0004771
101

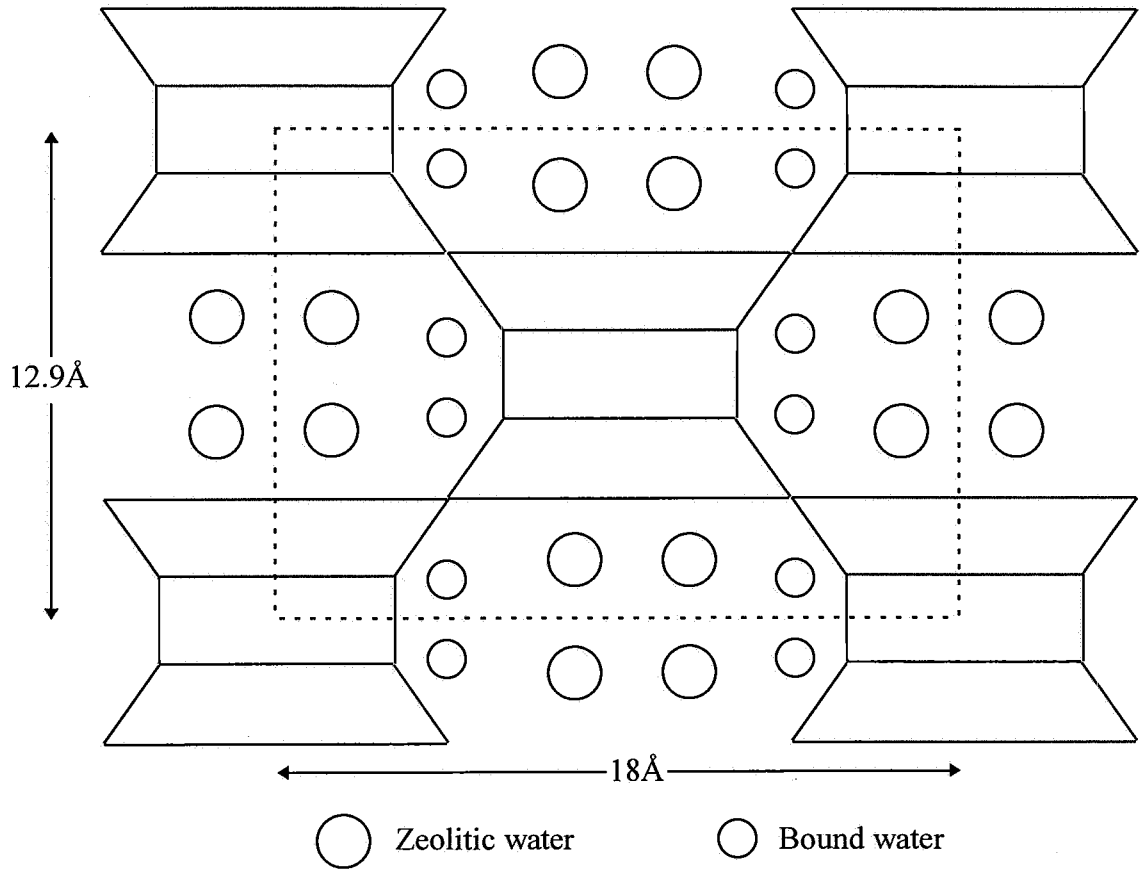


Fig. 3.8a. Schematic of the structure of palygorskite.

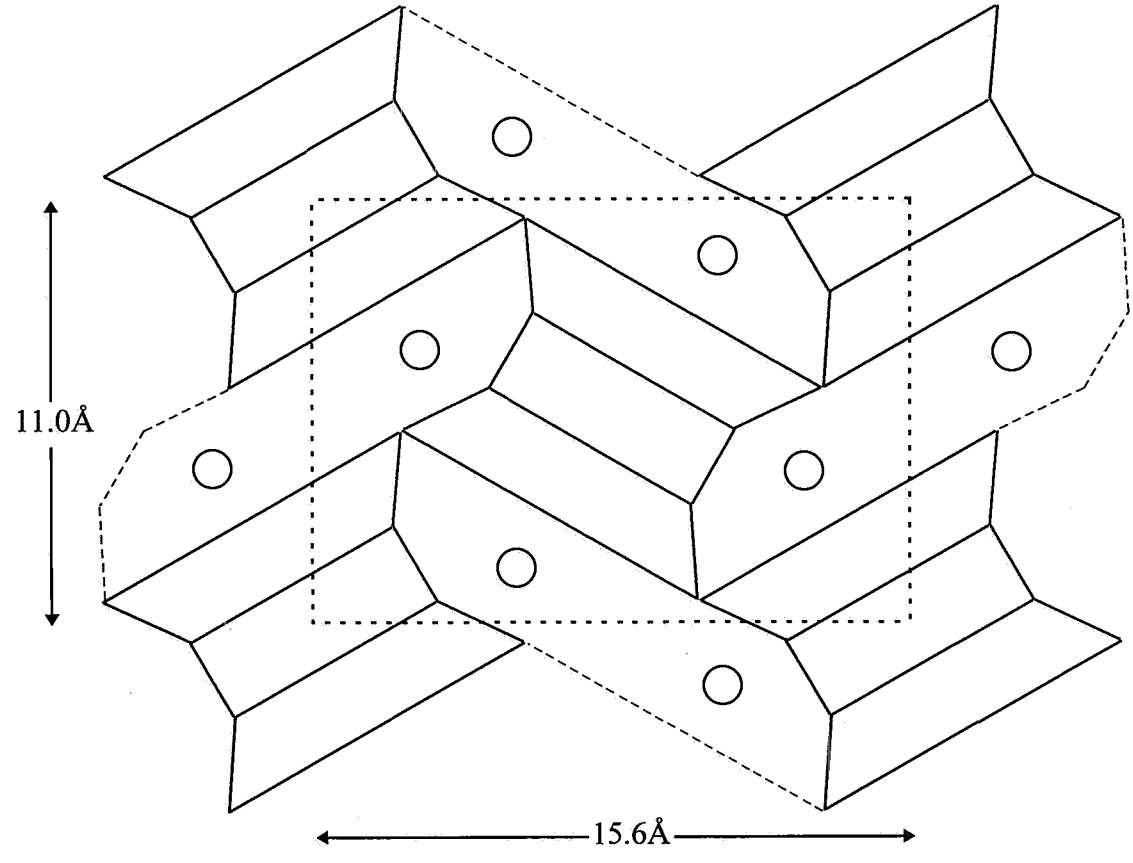


Fig. 3.8b. Schematic of the folded structure of palygorskite.

Fig. 3.9. Garford palaeochannel palygorskite P88 0.4-2m. Heated 105C and 350C. hkl indexing shown.

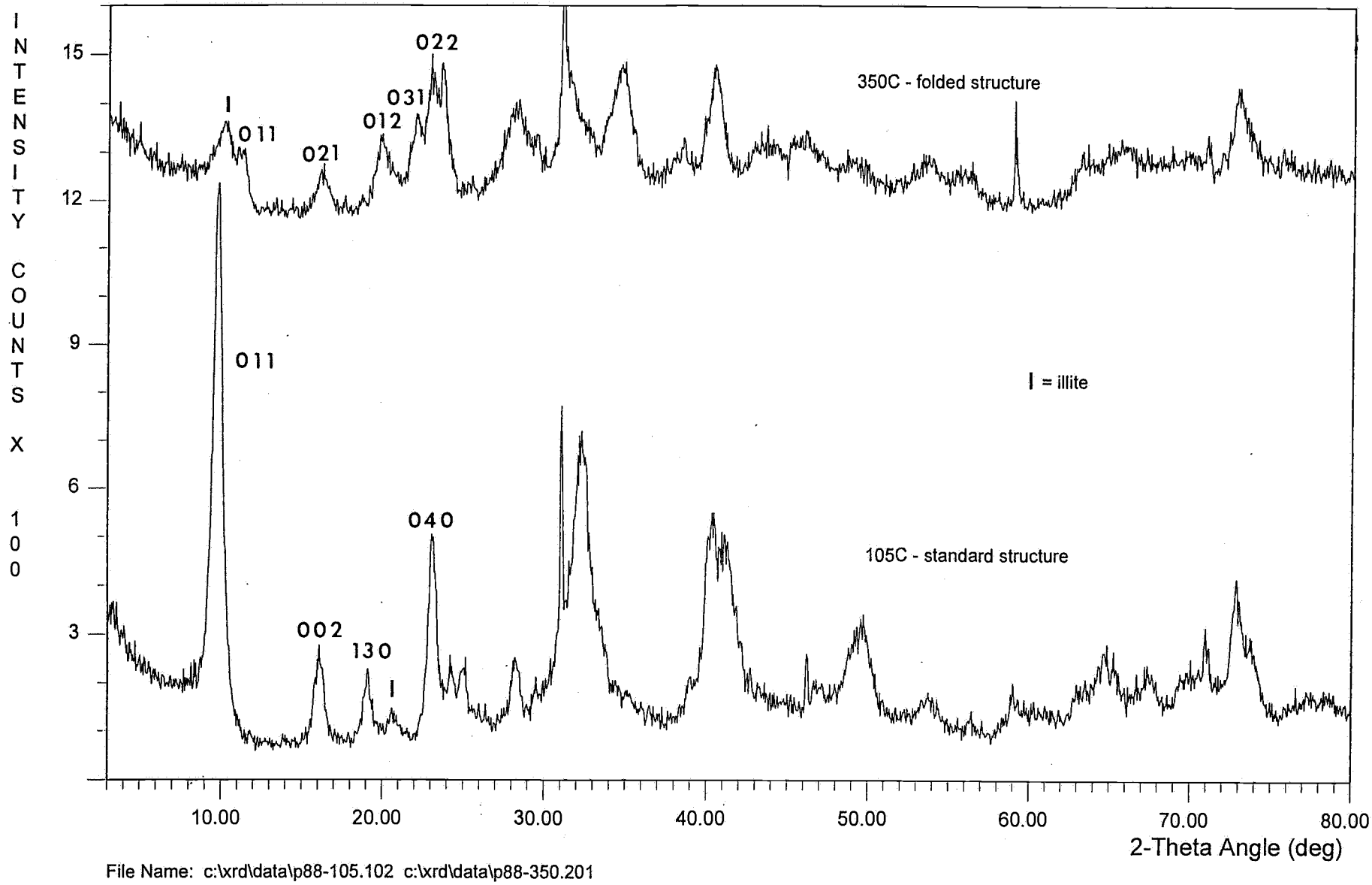
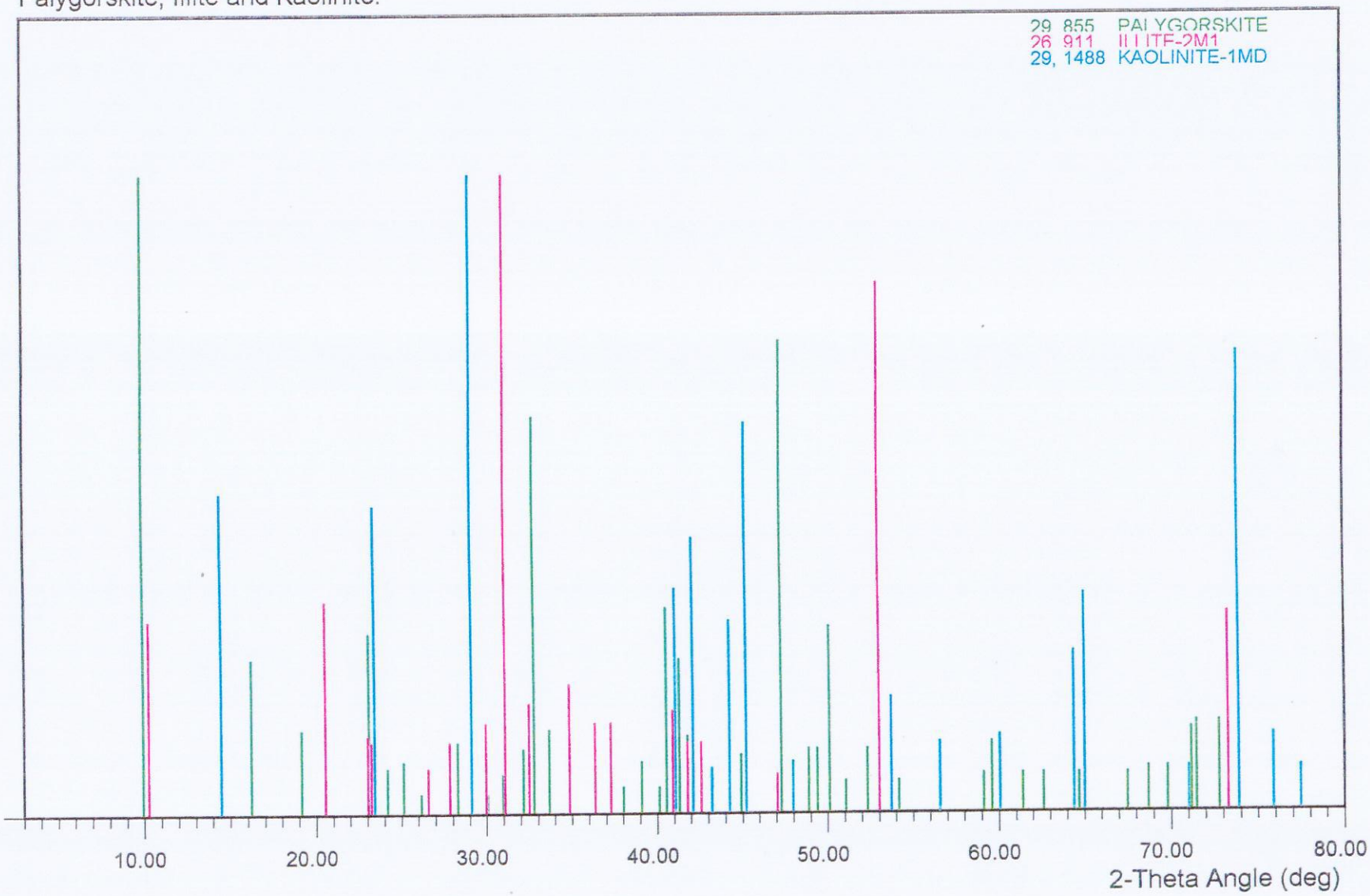


Fig. 3.9. XRD (Co Kα radiation, back pressed) of Garford palaeochannel palygorskite P88 0.4-2m (<2μm >0.2μm) heated to 105°C and 350°C. The hkl indexing for the standard and folded structures.

0004473
103

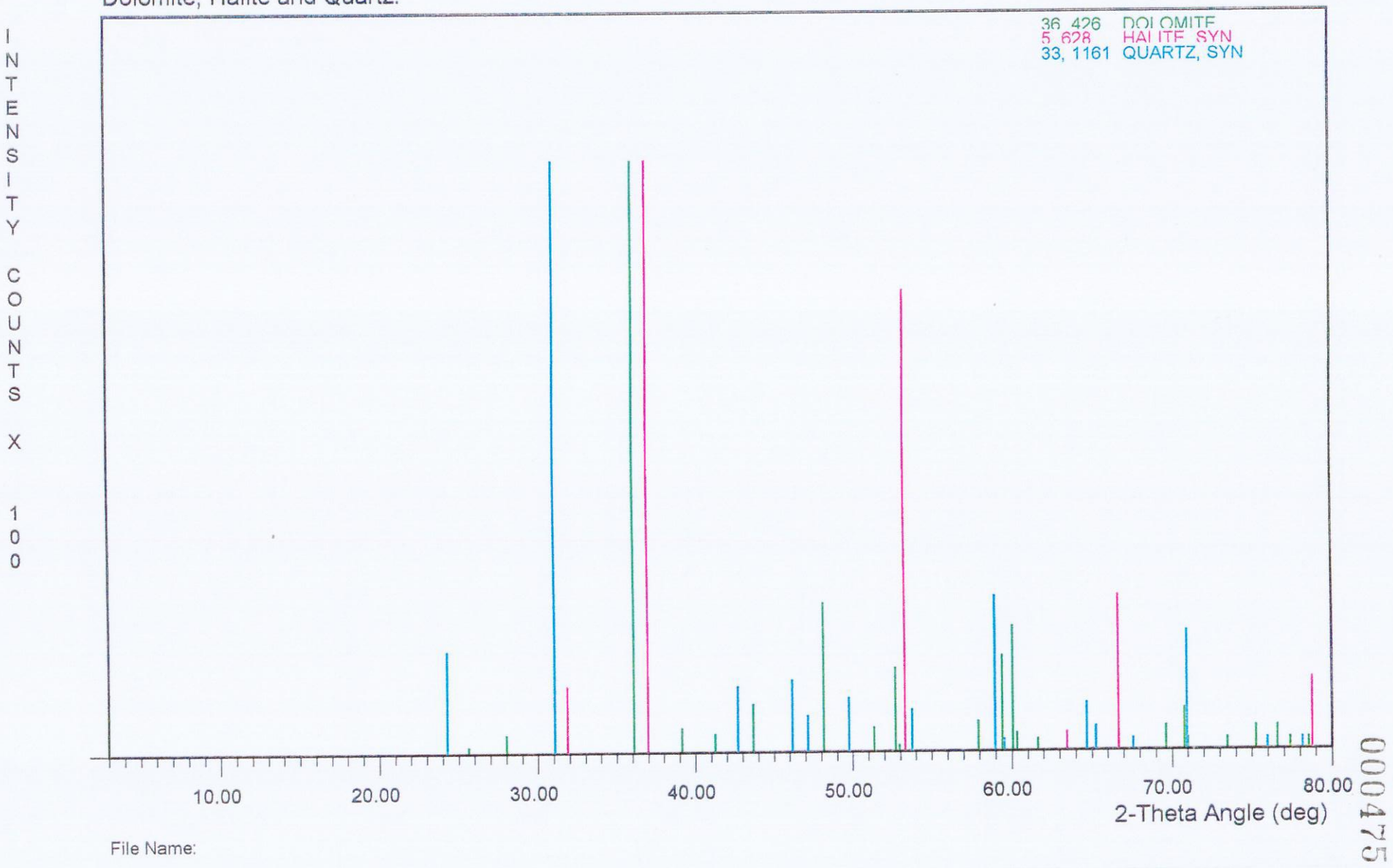
Palygorskite, Illite and Kaolinite.



File Name:

0004474

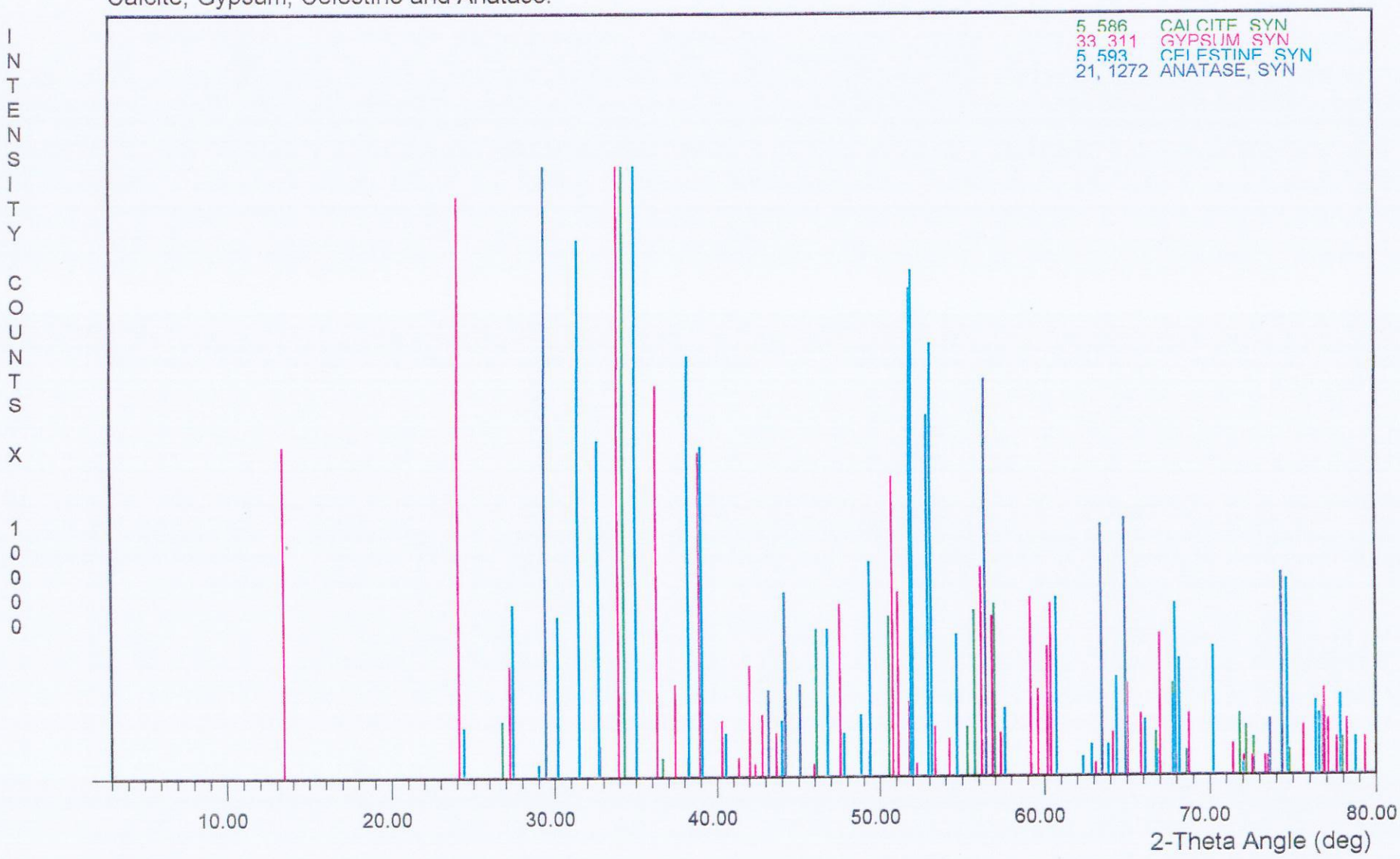
Dolomite, Halite and Quartz.



File Name:

000475

Calcite, Gypsum, Celestine and Anatase.



File Name:

0004276

CHAPTER 4. RHEOLOGY OF SELECTED SAMPLES FROM THE GARFORD PALAEOCHANNEL.

The fibrous morphology of palygorskite gives it rheological properties that are desirable for drilling muds, gellants and fillers. Factors other than morphology that can also effect the rheological properties of palygorskite suspensions include the degree of dispersion of palygorskite fibres (so that the particles in suspension are individual fibres rather than clumps), the proportion of non-fibrous mineral components and the electrolyte concentration in solution. To determine the rheological properties of Garford palaeochannel clays, clays with a range of mineralogical contents (but in general high palygorskite content) were selected for examination (Table 4.1). Several commercial attapulgites and bentonites (Table 4.1) were also examined for comparison.

Methods

Rheological properties were determined with reference to American Petroleum Institute (API) specifications for drilling-fluids (API specification 13A, 1993) but based on equipment available at CSIRO Division of Soils. For palygorskite-bearing materials, mixtures of 7.5% gm/ml, 5% gm/ml and 2.5% gm/ml (100% gm/ml equals 1gm per ml of solution) were made with either reverse osmosis (RO) water or saline-saturated (NaCl) solution. (The API specification is for 5.7% gm/ml suspensions.) The mixtures were shaken in a SPEX mill for 20 minutes immediately before rheological testing. For bentonites, mixture strengths were 10% gm/ml, 7.5% gm/ml and 5% gm/ml. (The API specification is for 6.4% gm/ml suspensions.) Mixtures were shaken in a SPEX mill for 20 minutes and then aged for 16 hours. The aged mixtures were shaken for 5 minutes immediately before rheological testing.

Some different mixture concentrations and mixing methods were used to define rheological properties under specific conditions. The details of these methods are given in the text.

The rheological properties of the mixtures were measured using a Brookfield RVDV-III rheometer. The small sample adaptor 13RP and spindles SC4-21 and SC4-27 were used

throughout. The sample volume used was approximately 15ml. Rheological properties were measured by stepping the shear rate up from zero to the maximum possible for the rheometer and spindle (maximum spindle rotation is 250rpm) and then stepping the shear rate back down to zero. Measurements of shear stress were made at each shear rate step. The total time for each measurement run was 20 minutes.

Results and discussion

Garford palaeochannel clays

The rheological properties of selected samples from the Garford palaeochannel mixed with RO water are shown in Fig. 4.1. The results are plotted as shear stress (dyne/cm^2) versus shear rate (sec^{-1}). Viscosity (cP) can be calculated as (100 x shear stress)/(shear rate). Thus the terms shear stress and viscosity can be used equally when describing overall trends in rheological data. For low shear rates, shear stress generally shows a rapid increase with increasing shear rate. At higher shear rates, shear stress approaches a constant value. With the exception of sample P88 2-3m (which has a high illite content), shear stress does not show any significant hysteresis effects. The clay-water mixtures show thixotropic behaviour with a noticeable increase in viscosity on standing. Viscosity of the mixtures is decreased by rapid shaking.

Shear stress (and therefore viscosity) at a given shear rate increases approximately as the square of the palygorskite content of the suspension. This indicates that palygorskite is the dominant mineral determining rheological properties of Garford palaeochannel clays. Thus when dolomite (Garford palaeochannel clay P33 Upper, <53μm) is added to a high palygorskite content clay (P88 0.4-2m, <2μm), the shear stress at a given shear rate decreases with decreasing palygorskite content (Fig. 4.2). The dolomite does not seem to contribute to the measured shear stress so that a 1:1 mixture of high palygorskite content clay and dolomite has almost identical shear stress characteristics as a suspension containing the same amount (absolute) of high palygorskite content clay but no dolomite (compare Fig. 4.2a with Fig. 4.2b). This result will be modified slightly by the particle size of the dolomite and the interaction between dolomite and other minerals in the clay. For example, the sample P84 7-10m (Fig. 4.1b) shows slightly higher shear stress values than would be predicted from the mixing experiments.

This may be attributed to the smaller particle size of dolomite in P84 7-10m (<2μm) compared with hand-ground dolomite used in the mixing experiment (P33 Upper, <53μm).

An increase in illite content in a palygorskite clay also decreases the shear stress (viscosity) on clay suspensions (compare P88 2-3m with P88 0.4-2m in Fig. 4.1c). In addition, the presence of illite causes hysteresis in the shear stress versus shear rate values.

Some clays, such as P86 0-0.63m and P84 12-14m, have lower than expected shear stress when compared with clays of similar mineralogy (i.e. P88 0.4-2m and P84 14-16m respectively). These low values of shear stress are attributed to insufficient dispersion. For example, when P86 0-0.63m is given 3 minutes of ultrasonic treatment using a Branson sonic probe, its rheological properties at high shear rates are close to those of sample P88 0.4-2m (Fig. 4.3). The ultrasonic treatment initially introduces hysteresis to the shear stress characteristics of the sample. This hysteresis disappears on aging and the rheological properties of the ultrasonically treated and aged P86 0-0.63m sample are similar to those of P88 0.4-2m.

Ultrasonic treatment of suspensions of high palygorskite content clays can produce almost a 50% increase in viscosity relative to the shaken suspensions (Fig. 4.4). Shaking in a SPEX mill for more than 20 minutes does not result in an increase in suspension viscosity. Hence, ultrasonic treatment is more effective in dispersing palygorskite relative to shaking in a SPEX mill. Thus, the amount of dispersion and therefore the rheological properties of a suspension are determined by the method used to prepare the suspension for testing. The fact that ultrasonic treatment does not cause a large relative increase in suspension viscosity (see bentonites) suggests that high palygorskite clays from the Garford palaeochannel are readily dispersable.

When mixed in saline-saturated solution the shear stress of each sample for a given shear rate decreases by a factor of approximately 2 (Fig. 4.5). The decrease in shear

stress (and therefore viscosity) is the result of the flocculation of the palygorskite as shown by the colloidal properties given in Chapter 3.

Dispersion of high palygorskite content clays in saline solutions is increased (and therefore the viscosity can be increased) by ultrasonic treatment using, for example, a Branson Sonic Probe (Fig. 4.6). However, on aging, viscosity falls back to the values obtained by shaking the samples in a SPEX mill. The time for the sample to return to the as-shaken values increases with increasing palygorskite content. This reflects the degree of resistance the palygorksite fibres experience when trying to flocculate. That is, the slower decay rate at higher palygorskite contents is simply the result of the higher viscosity of these suspensions.

Similar behaviour on ultrasonic treatment is shown by samples containing significant amounts of minerals other than palygorskite (sample P84 7-10m, Fig. 4.6).

The colloidal behaviour of palygorskite (Chapter 3) is such that palygorskite flocculates at low pH values. Hence, the viscosity of suspensions should also decrease with decreasing pH. Suspensions of 5% gm/ml of Garford palaeochannel clay P88 0.4-2m were made with solutions whose pH values were 5 (RO water), 3, 2 and 1. (The acid solutions were made by mixing a measured amount of 10M HCl with RO water.) The clay suspensions were shaken for 5 minutes in a SPEX mill and allowed to stand for 16 hours so that the pH would equilibrate. The aged, clay suspensions were then shaken for 20 minutes in a SPEX mill. The pH values of the shaken suspensions were measured immediately before rheological properties were determined. The measured pH values of the suspensions were 7.5, 6.5, 2.3 and 1. The increase in pH relative to the pH of the initial solutions is caused by the dissolution of dolomite in the samples (see Chapter 2). The rheological properties of the clays suspensions are shown in Fig. 4.7. The suspensions with pH 7.5 and 6.5 (initial pH 5 and 3) are virtually identical. The suspensions with pH 2.3 and 1 (initial pH 2 and 1) show a marked decrease in viscosity. The rheological behaviour of the clay suspension with pH 1 is comparable to that of a suspension made with a saline-saturated solution. The results from suspensions made

with solutions of different pH value show the value of dolomite as a buffer in palygorskite clays.

Commercial attapulgites (palygorskites)

The rheological properties of commercial attapulgites measured under the same conditions as for the Garford palaeochannel clays are shown in Figs. 4.8, 4.9 and 4.10. The overall properties of the commercial attapulgites and the Garford palaeochannel clays are similar. The viscosities of several high-palygorskite content clays from the Garford palaeochannel compare favourably with commercial attapulgites. Assuming that Senegal processed attapulgite and Attagel 50 are representative of material that meets API suspension specification, the minimum palygorskite content in Garford palaeochannel clays required to meet the suspension specification is approximately 70wt.%.

The Lake Nerramyne sample does not disperse readily and it shows very low shear stress after shaking in a SPEX mill for 20 minutes (Fig. 4.8). This is because of the low dispersability of Lake Nerramyne attapulgite. Ultrasonic treatment for 5 minutes markedly increases its shear stress characteristics but it still does not attain shear stress values as high as commercial attapulgites or high palygorskite content clays from the Garford palaeochannel (Fig. 4.8).

The effect of ultrasonic treatment on suspensions of commercial attapulgites (apart from Lake Nerramyne attapulgite) in saline-saturated solution (Fig. 4.10) is similar to that of clays from the Garford palaeochannel. Immediately after ultrasonic treatment the measured shear stress at a given shear rate increases significantly and then over a period of a few hours falls back to the value for the shaken-only sample.

Bentonites

The rheological properties of the selected bentonites mixed with RO water are shown in Fig. 4.11. As for attapulgites, for low shear rates, the shear stress of bentonite suspensions increases relatively rapidly with increasing shear rate. Unlike the attapulgites, at high shear rates, shear stress for bentonite suspensions becomes a

linearly increasing function of shear rate. Bentonites show a much more rapid variation in shear stress with suspension concentration relative to attapulgites. Empirically, the shear stress of bentonite suspensions at a given shear rate increases at approximately the 4th to 5th power of the bentonite concentration of the suspension. Consequently, viscosity of suspensions can be markedly increased by relatively small increases in suspension loadings. Thus, although Na-saturated Arumpo bentonite shows a lower viscosity than Volclay (and therefore presumably does not meet API specifications), the viscosity of a 11.5% gm/ml suspension of Na-saturated Arumpo bentonite would equal that of a 10% gm/ml of Volclay.

The bentonite suspensions show a much more marked increase in viscosity on aging than do the attapulgites. That is, the bentonites are more thixotropic than the attapulgites. Fig. 4.12 shows the change in shear stress of Na-saturated Arumpo bentonite (TP1) over a 4 hour period. During this time the shear stress at a given shear rate increases by approximately 50%. Shaking the suspension after aging reduces viscosity; this is characteristic of thixotropic suspensions. Hence, for the aged suspension, the shear stress is less on the downward run of the shear rate than on the upward run because of the mechanical energy put into the suspension during measurement.

Ultrasonification increases the viscosity of bentonite suspensions because it causes increased dispersion (Fig. 4.13). For Volclay the increase in shear stress after ultrasonic treatment is of the order of 20%. For the Arumpo bentonites the increase after ultrasonic treatment is very large (approximately 4 and 50 times for Na-saturated Arumpo bentonite and as-received Arumpo bentonite respectively). These results suggest that Volclay almost completely disperses after a shaking treatment while the Arumpo bentonites require much more mechanical effort to be fully dispersed.

Dispersion in bentonites can be achieved by both chemical and mechanical methods (or a combination of both). The standard chemical method of Na saturation neutralises both the internal and external surface charges of the bentonite allowing the fundamental units of the bentonite structure (i.e. the tetrahedral-octahedral-tetrahedral layers) to fall apart.

Mechanical methods rip the structure layers apart in much the same way as mica sheets can be peeled apart. As shown by Raven *et al.* (1992), Arumpo bentonites contain sub-spherical "onion" like particles that do not readily disperse. Hence, Na-saturation alone is not enough to disperse the bentonite layers. Although this is a disadvantage for applications requiring high viscosity at low concentrations (e.g. drilling muds) it is an advantage in applications requiring good absorbent properties. The relatively poor dispersion of the Arumpo bentonite will have little effect on its absorbent properties but will make recovery of the bentonite from solution by centrifugation or sedimentation easier because of the large particle size relative to a fully dispersed clay. It must be remembered that the rheology of only one sample from the Arumpo deposit has been tested and it is possible (indeed probable) that there is a variability in the dispersability of clay throughout the deposit.

When ultrasonically treated as-received Arumpo bentonite is dried at 60°C and then its rheological properties measured using the standard method (i.e. shaking only), the measured shear stresses are higher than for the original, shaken-only sample (Fig. 4.14). Thus it is possible that the viscosity of suspensions of Arumpo bentonite could be improved to meet API specifications by a combination of Na saturation and mechanical dispersion during processing. The viability of such a process requires further testing and the effects of other parameters such as drying temperature, method of Na saturation and variability in the ore would need to be investigated.

Bentonite flocculates in solutions with high salt concentrations. Thus bentonites suspended in saturated-saline solutions show a marked decrease in viscosity (Fig. 4.15) relative to suspensions in RO water (Fig. 4.11). Na-saturated Arumpo bentonite (TP1) shows an overall decrease in shear stress by a factor of approximately 5 and Volclay shows a decrease by a factor of approximately 20.

When bentonite, saturated-saline mixtures were left to stand overnight, the bentonite settled to the bottom of the container. The 5 minutes of shaking before measuring rheological properties brought the bentonite back into suspension. However, there was some flocculation and settling during rheological measurement as shown in Fig. 4.15.

When ultrasonically treated, the viscosity of the suspensions of bentonite in saline-saturated water increases (Fig. 4.16). For Volclay the ultrasonically treated saline suspensions have a viscosity of approximately one half of that of Volclay suspended in RO water (Fig. 4.11). The ultrasonically treated saline suspension of Na-saturated Arumpo bentonite has about the same viscosity as Na-saturated Arumpo bentonite suspended in RO water by shaking only (Fig. 4.11).

On aging, the viscosities of ultrasonically treated saline suspensions slowly decreases (Fig. 4.16). The rate of decrease is much slower than for attapulgites suspended in saturated-saline solution and ultrasonically treated (Fig. 4.5. and 4.10). This is presumably because of the greater resistance to movement experienced by bentonite particles with their sheet-like morphology than experience by palygorskite particles with their fibre morphology.

Conclusions

Examination of the rheological properties of selected clays from the Garford palaeochannel and several reference clays shows that the key parameters in determining rheological properties are particle morphology (including particle size) and the dispersibility of the particles. Particle morphology is characteristic of a particular clay and therefore is difficult to change. Dispersibility, on the other hand, can be changed by factors including mechanical treatment of the clays and varying ionic concentrations (including pH) of suspensions.

High palygorskite content clays from the Garford palaeochannel are readily dispersed and have rheological properties that compare favourably with commercial attapulgites that are used a drilling muds and gellants. In general, attapulgites that disperse readily are favoured for use as drilling muds and gellants while attapulgites with poor dispersion properties (such as Lake Nerramyne attapulgite) are favoured for applications requiring high absorbency. This is because clays with poor dispersibility are easier to recover from suspension that those that completely or almost completely disperse.

However, as is shown in Chapters 5 and 6, readily dispersible clays can have high absorption capacities.

Bentonites show different rheological behaviour relative to attapulgites but the values of viscosity of suspensions of bentonite and suspensions of attapulgite are comparable. Arumpo bentonite (TP1), even when fully Na-saturated, is not as dispersive as the commercial bentonites tested. Therefore suspensions of Arumpo bentonite have lower viscosities than suspensions of commercial bentonites when the suspensions are prepared in the same way. The viscosities of suspensions of Arumpo bentonite can be substantially improved by high energy mechanical treatment such as ultrasonification.

References

API Specification 13A (1993). Specification for drilling-fluid materials. API Specification 13A (Spec 13A), Fifteenth Edition, November, 1993. American Petroleum Institute, 1220L Street, Northwest Washington, DC 20005, USA.

Raven, M.D., Keeling, J.L., Self, P.G. and Slade, P.G. (1992). Mineralogical analysis of composite samples from the Arumpo bentonite deposit. CSIRO, Division of Soils, Technical Report 83/1992.

Table 4.1. Mineralogy of samples selected for rheological testing.

Sample	Mineralogy (wt.%)			
	Palygorskite	Illite	Dolomite	Quartz
P33 Lake Floor, <2μm >0.2μm	85-90	8-12	1	1
P84 7-10m, <2μm >0.2μm	7-10	1-3	88-92	<1
P84 12-14m, <2μm >0.2μm	45-50	8-12	40-45	<1
P84 14-16m, <2μm >0.2μm	45-50	8-12	40-45	<1
P86 0-0.63m, <2μm >0.2μm	72-77	10-15	5-9	4-7
P88 0.4-2m, <2μm >0.2μm	72-77	22-27	<1	1
P88 2-3m, <2μm >0.2μm	42-47	42-47	<1	7-11
Attagel 50, as received	80-90	5-15 (smectite)	2-5 (+ 4-7 calcite)	5-10
Senegal attapulgite, ore, <2μm >0.2μm	80-90	5-10 (smectite)	-	5-8
Senegal attapulgite, processed	75-85	10-20 (smectite)	1-2 calcite	3-7
Xuyi Attapulgite, <2μm >0.2μm	80-90	5-15	-	1-3
Lake Nerramyne attapulgite, <53μm	~70	~10 (includes kaolin)	~10	~10
Volclay premium gel, as received	Ca/Na montmorillonite 90-95	-	-	2-7 cristobalite 2-7
Arumpo bentonite, TP1, <2μm >0.2μm	Mg/Na montmorillonite 80-90	10-20	-	-
Arumpo bentonite, TP1, Na saturated, <2μm >0.2μm	Na montmorillonite 80-90	10-20	-	-

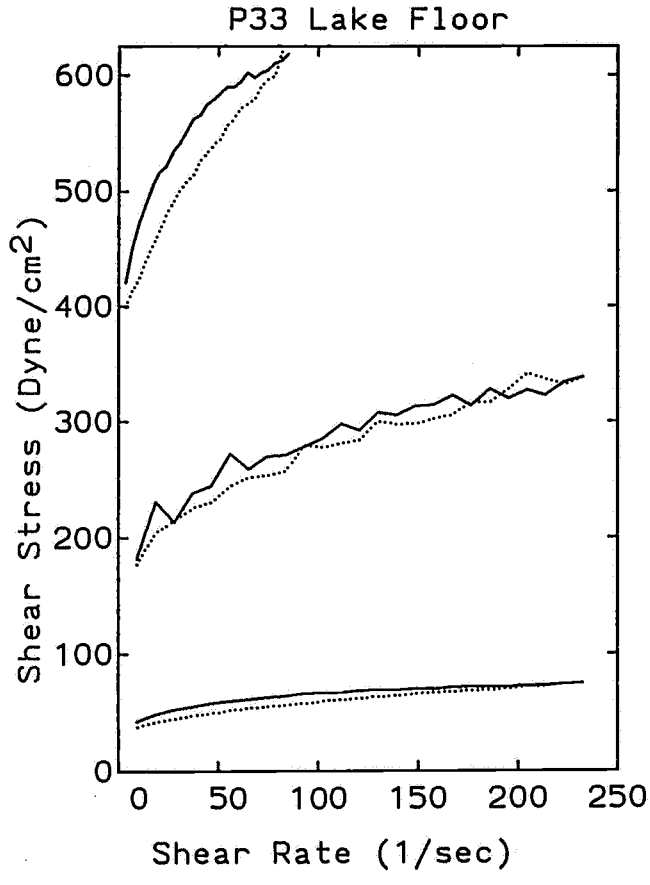


Fig. 4.1a. Rheological properties of selected Garford palaeochannel clays in RO water. The suspension concentrations are 7.5% gm/ml (upper line), 5% gm/ml (middle line) and 2.5% gm/ml (lower line). The solid line shows increasing shear rate and the dotted line shows decreasing shear rate. Note change of shear stress scale between samples.

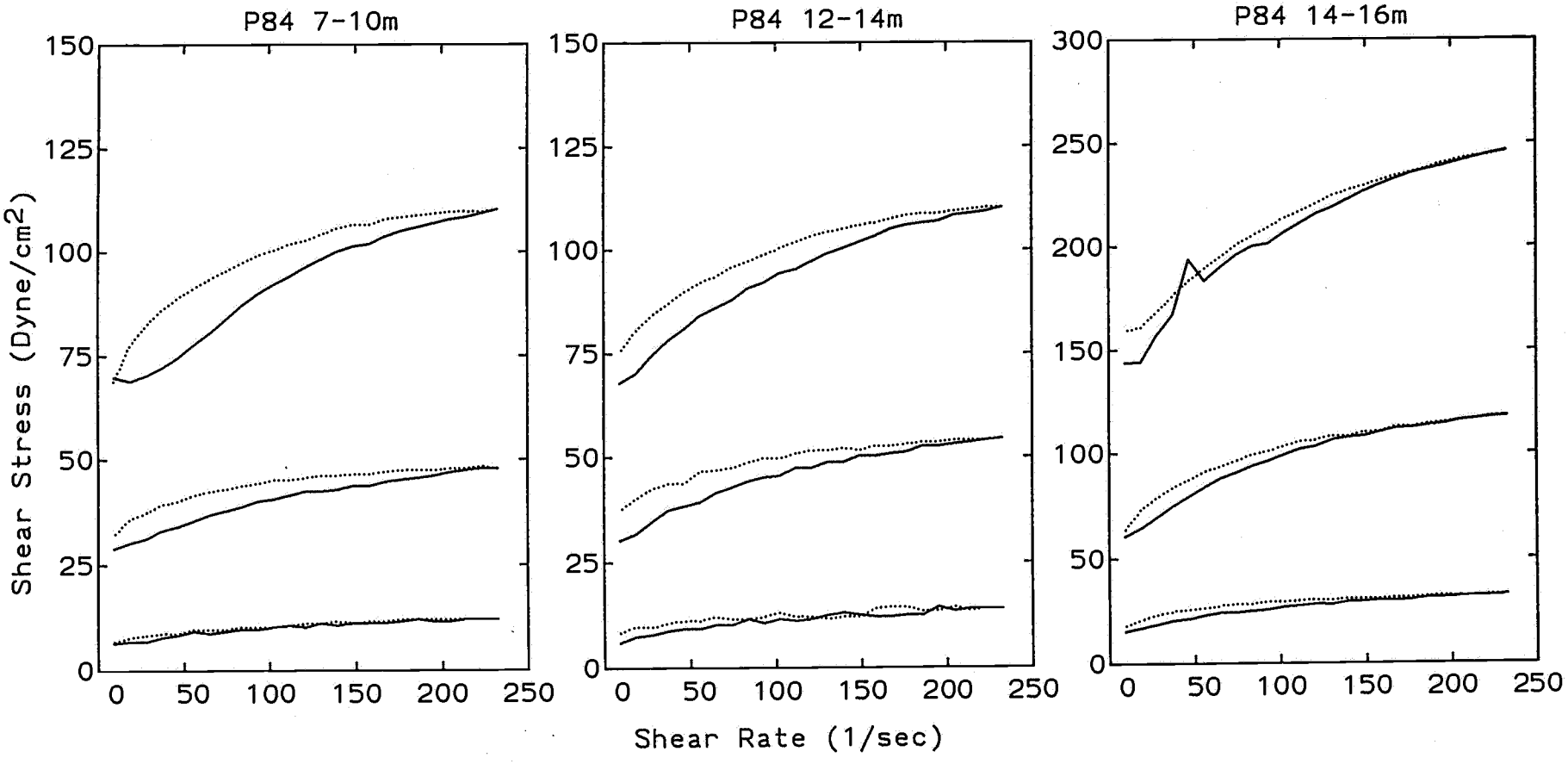


Fig. 4.1b. Rheological properties of selected Garford palaeochannel clays in RO water. The suspension concentrations are 7.5% gm/ml (upper line), 5% gm/ml (middle line) and 2.5% gm/ml (lower line). The solid line shows increasing shear rate and the dotted line shows decreasing shear rate. Note change of shear stress scale between samples.

0004489

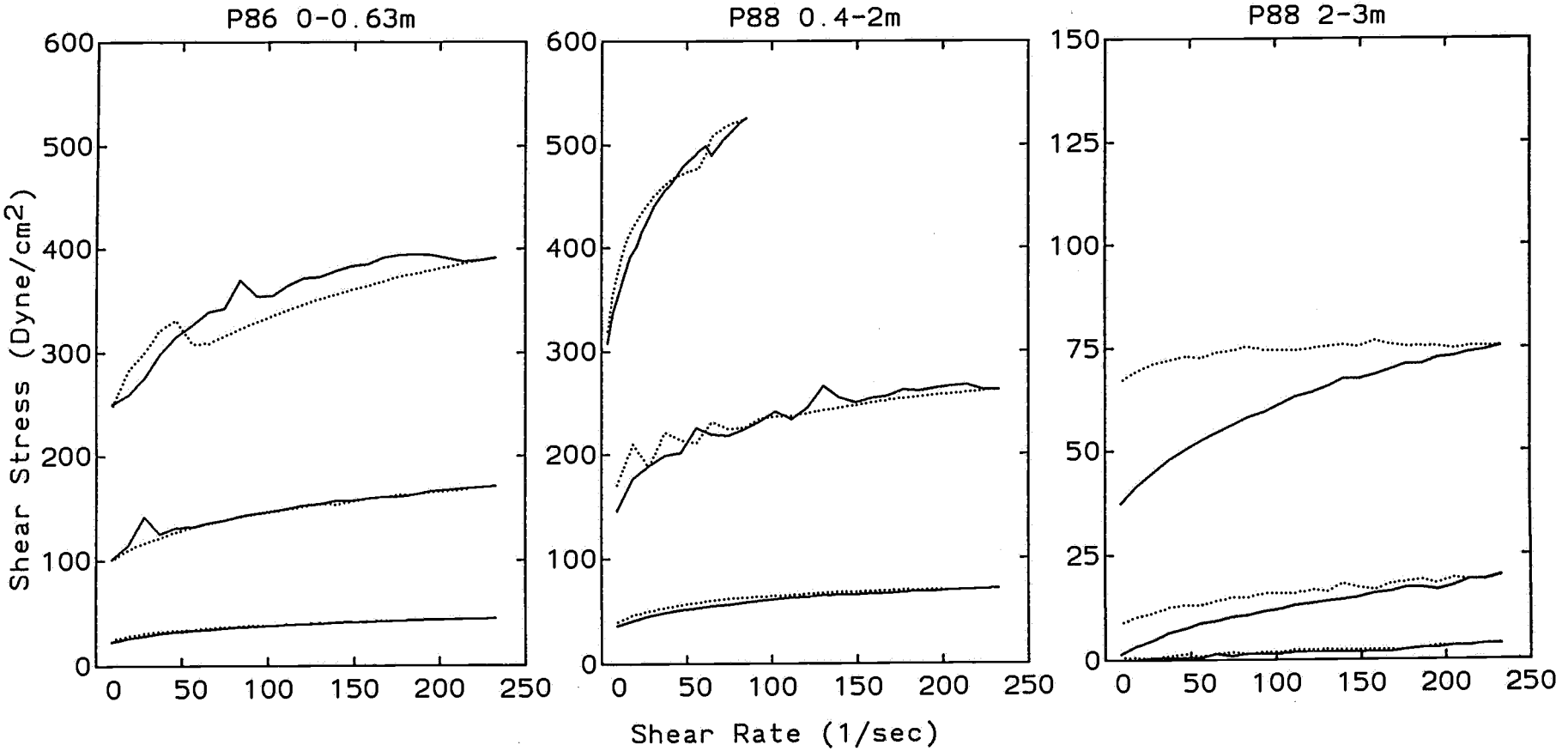


Fig. 4.1c. Rheological properties of selected Garford palaeochannel clays in RO water. The suspension concentrations are 7.5% gm/ml (upper line), 5% gm/ml (middle line) and 2.5% gm/ml (lower line). The solid line shows increasing shear rate and the dotted line shows decreasing shear rate. Note change of shear stress scale between samples.

0004480

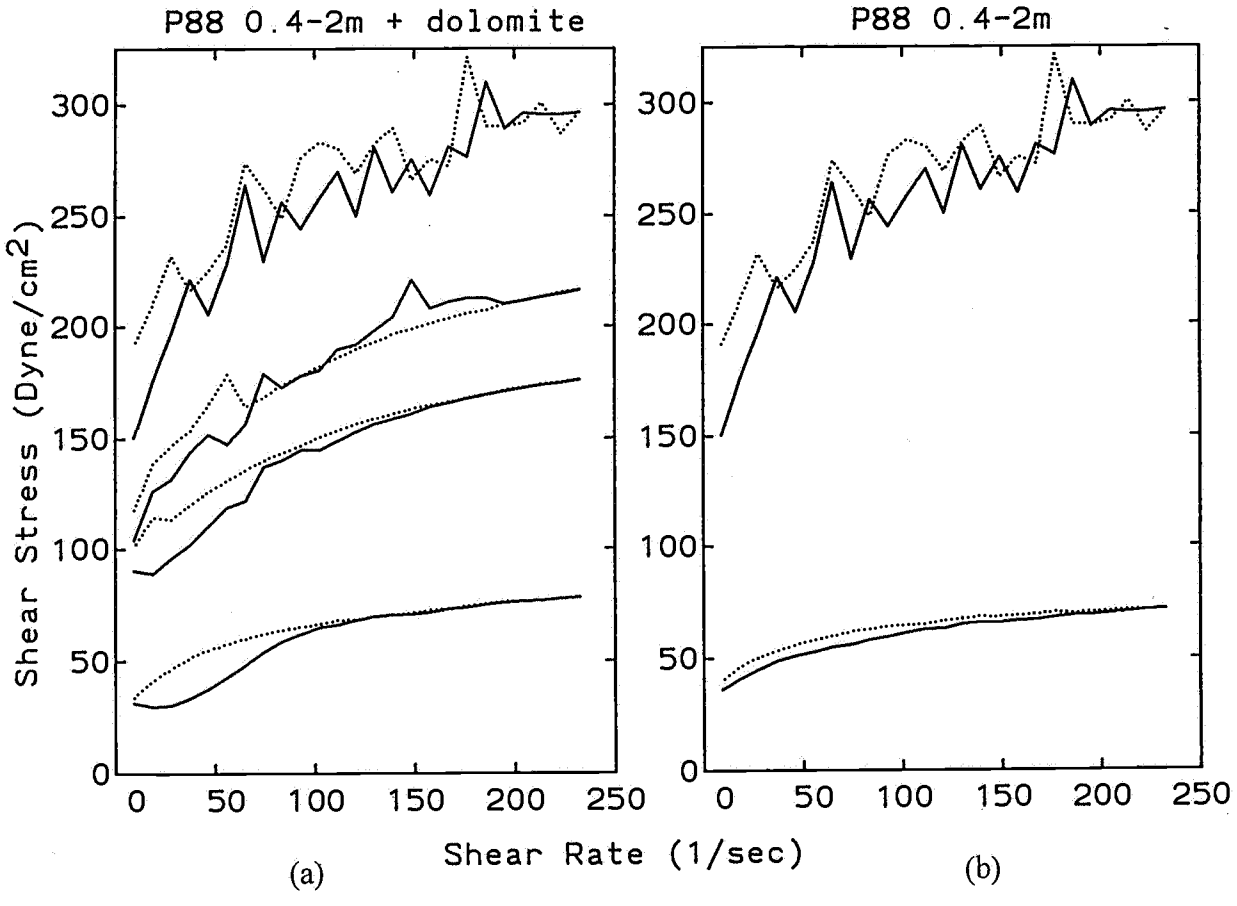


Fig. 4.2. Rheological properties of: (a) Garford palaeochannel sample P88 0.4-2m mixed with dolomite (P33 Upper) so that the total sample concentration in suspension is 5% gm/ml. The percentages of P88 0.4-2m in the mixture are 100% (top curve), 90%, 75% and 50% (bottom curve). (b) Garford palaeochannel sample P88 0.4-2m at concentrations of 5% gm/ml (upper) and 2.5% gm/ml (lower). All suspension in RO water. The solid line shows increasing shear rate and the dotted line shows decreasing shear rate.

0004911

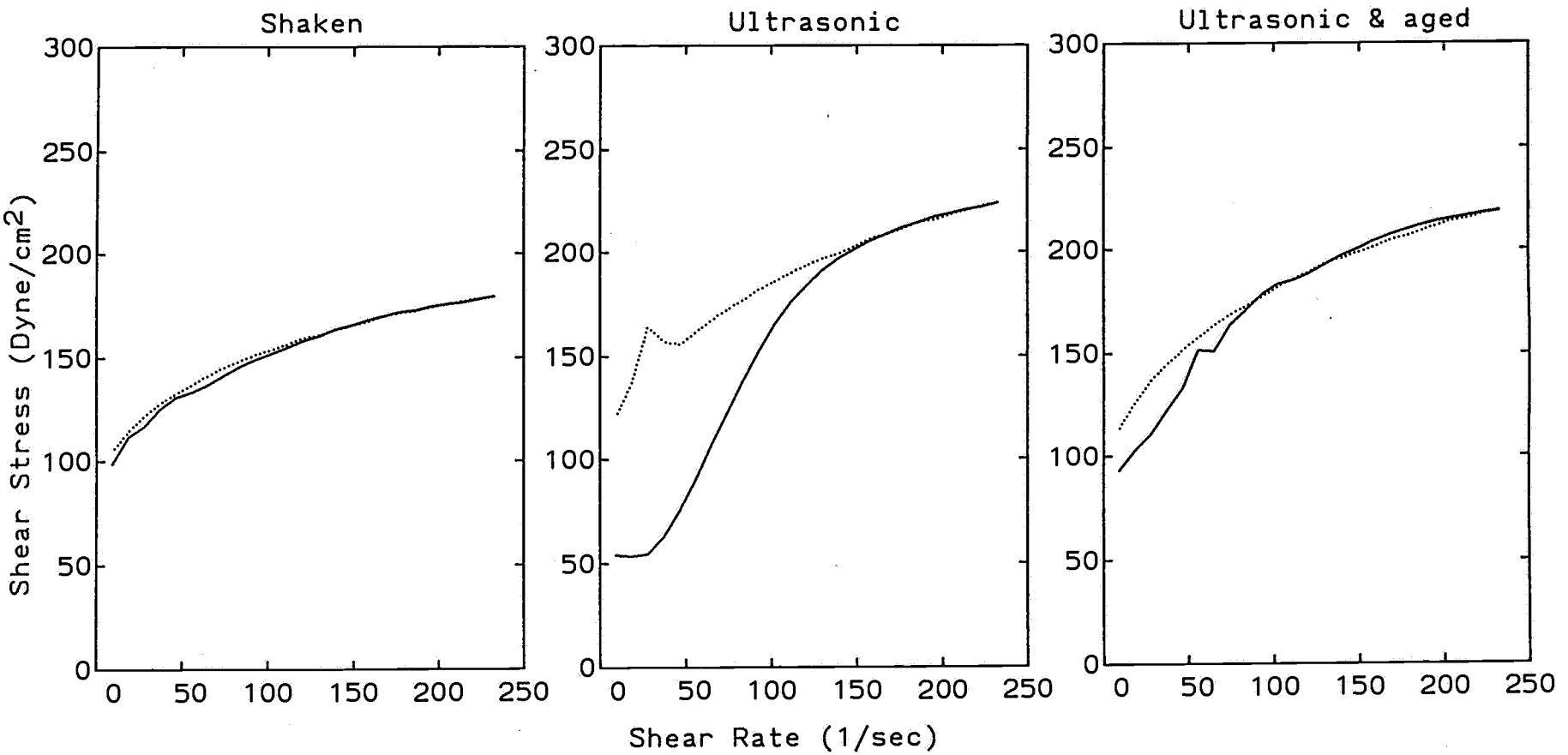


Fig. 4.3. Rheological properties of a 5% gm/ml suspension of Garford palaeochannel clay P86 0-0.63m in RO water after being shaken in a SPEX mill for 20 minutes (left), ultrasonically treated for 3 minutes (middle), and ultrasonically treated for 3 minutes and aged for 4 hours (right). The solid line shows increasing shear rate and the dotted line shows decreasing shear rate.

000492

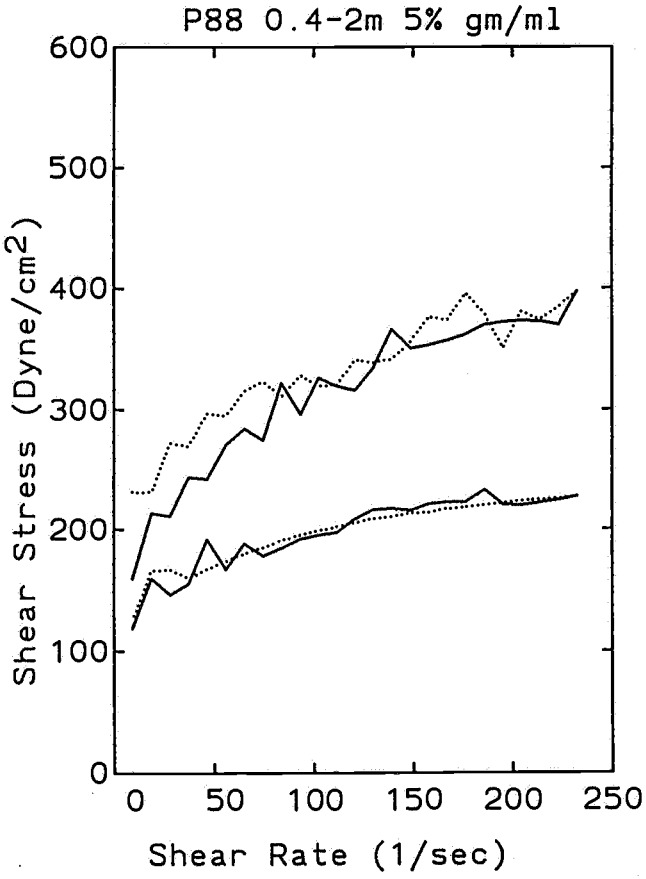


Fig. 4.4. Rheological properties of a 5% gm/ml suspension of Garford palaeochannel sample P88 0.4-2m in RO water. Lower curve was measured after shaking in a SPEX mill for 20 minutes. Upper curve was measured after 3 minutes of ultrasonic treatment. The solid line shows increasing shear rate and the dotted line shows decreasing shear rate.

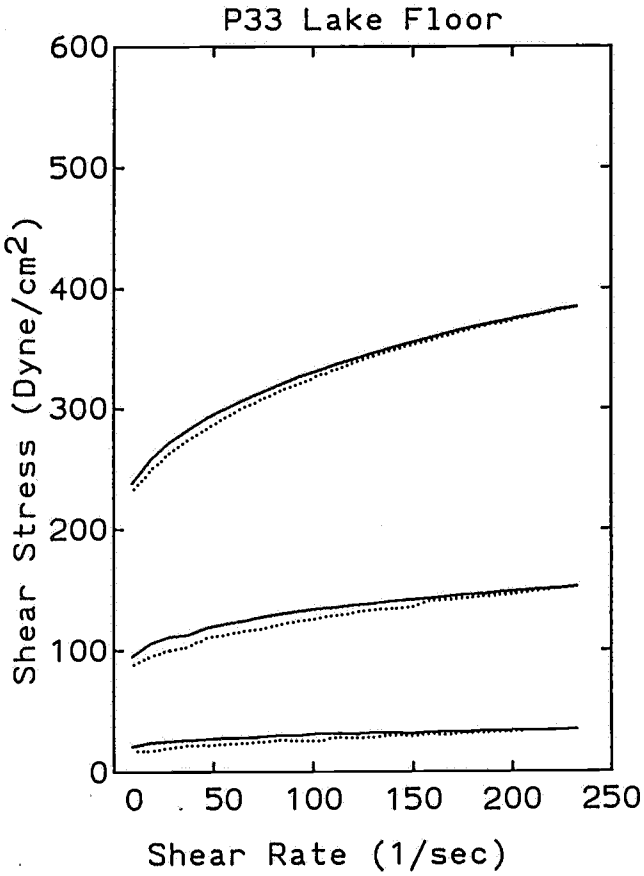


Fig. 4.5a. Rheological properties of selected Garford palaeochannel clays in saline-saturated solution. The suspension concentrations are 7.5% gm/ml (upper line), 5% gm/ml (middle line) and 2.5% gm/ml (lower line). The solid line shows increasing shear rate and the dotted line shows decreasing shear rate. Note change of shear stress scale between samples.

0004494

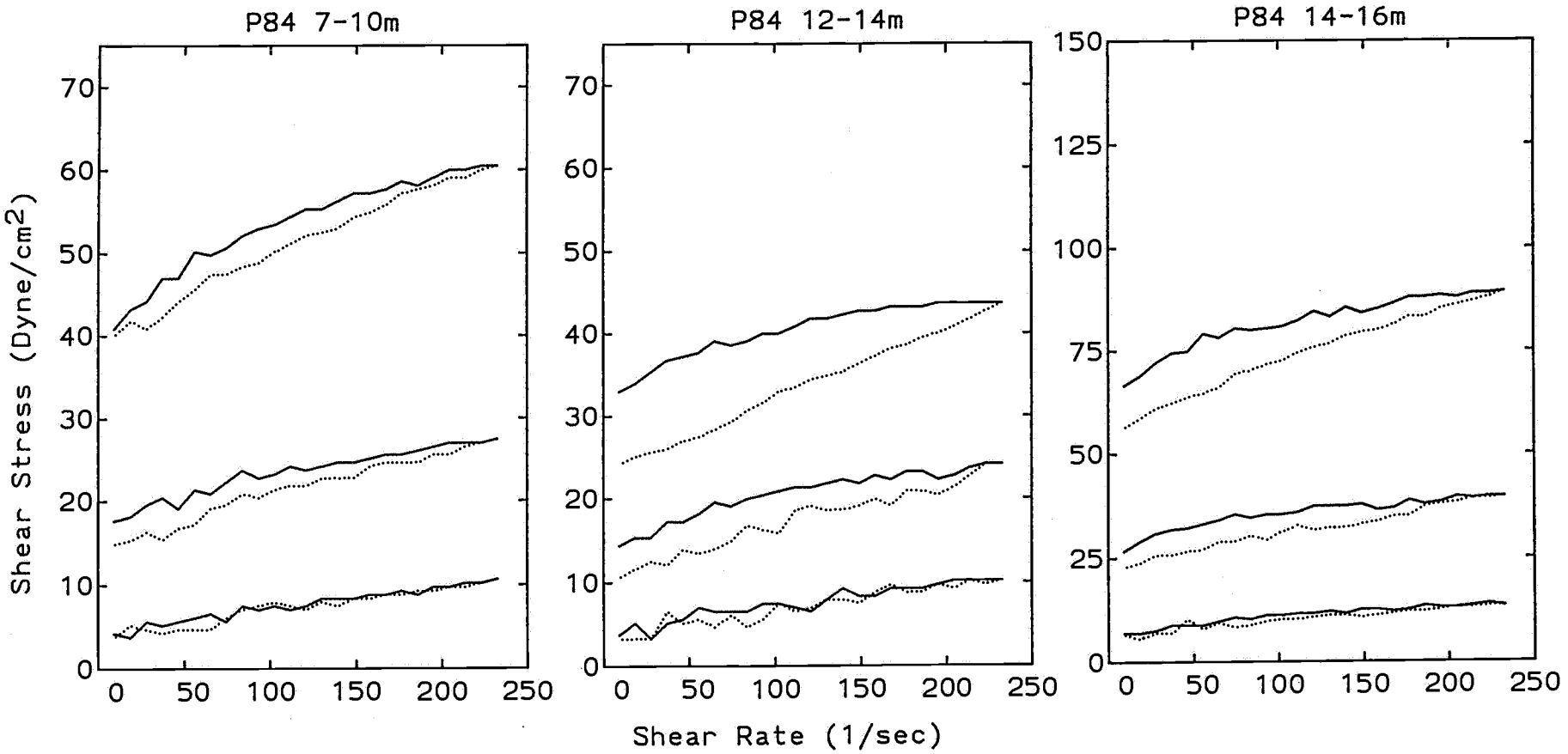


Fig. 4.5b. Rheological properties of selected Garford palaeochannel clays in saline-saturated solution. The suspension concentrations are 7.5% gm/ml (upper line), 5% gm/ml (middle line) and 2.5% gm/ml (lower line). The solid line shows increasing shear rate and the dotted line shows decreasing shear rate. Note change of shear stress scale between samples.

000495

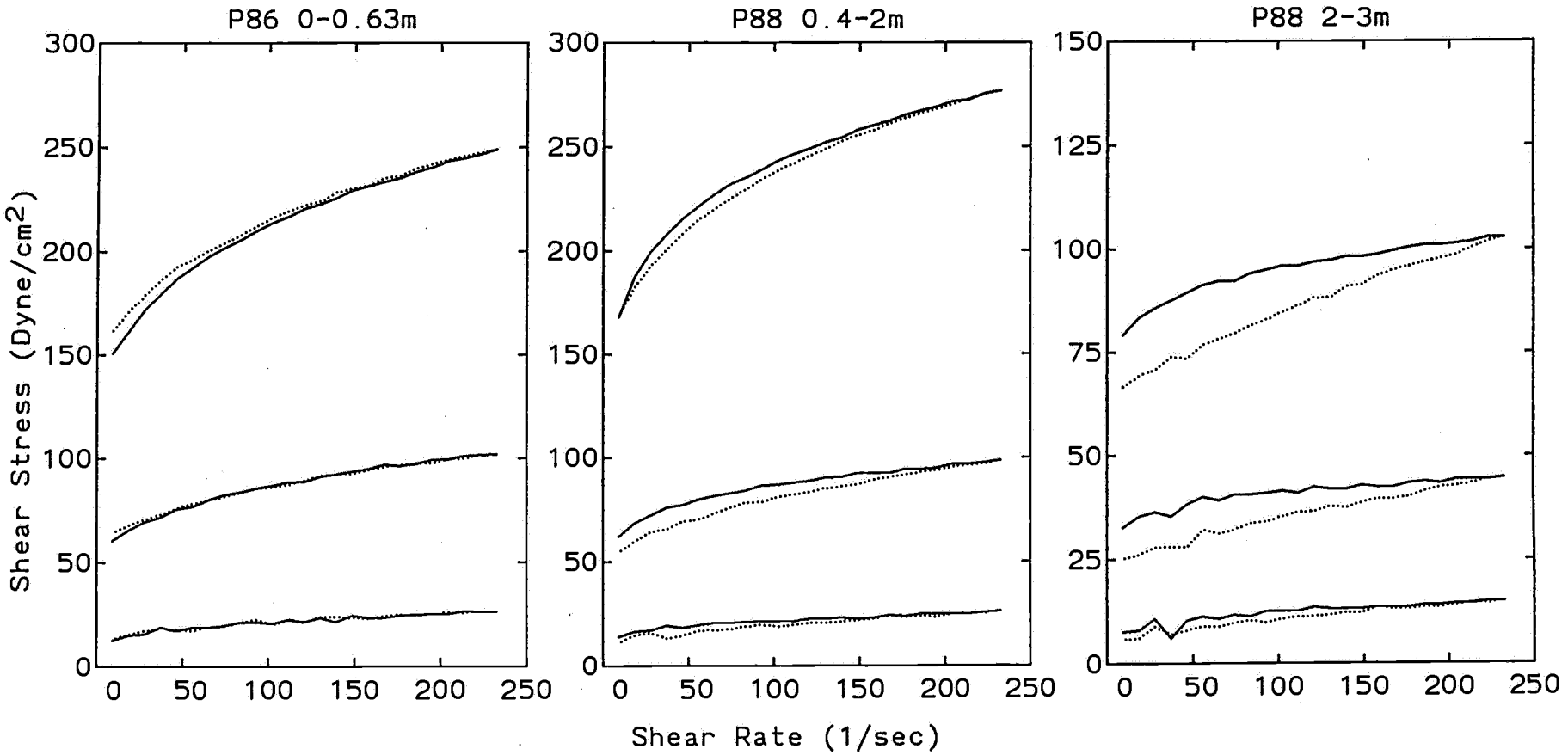


Fig. 4.5c. Rheological properties of selected Garford palaeochannel clays in saline-saturated solution. The suspension concentrations are 7.5% gm/ml (upper line), 5% gm/ml (middle line) and 2.5% gm/ml (lower line). The solid line shows increasing shear rate and the dotted line shows decreasing shear rate. Note change of shear stress scale between samples.

0004496

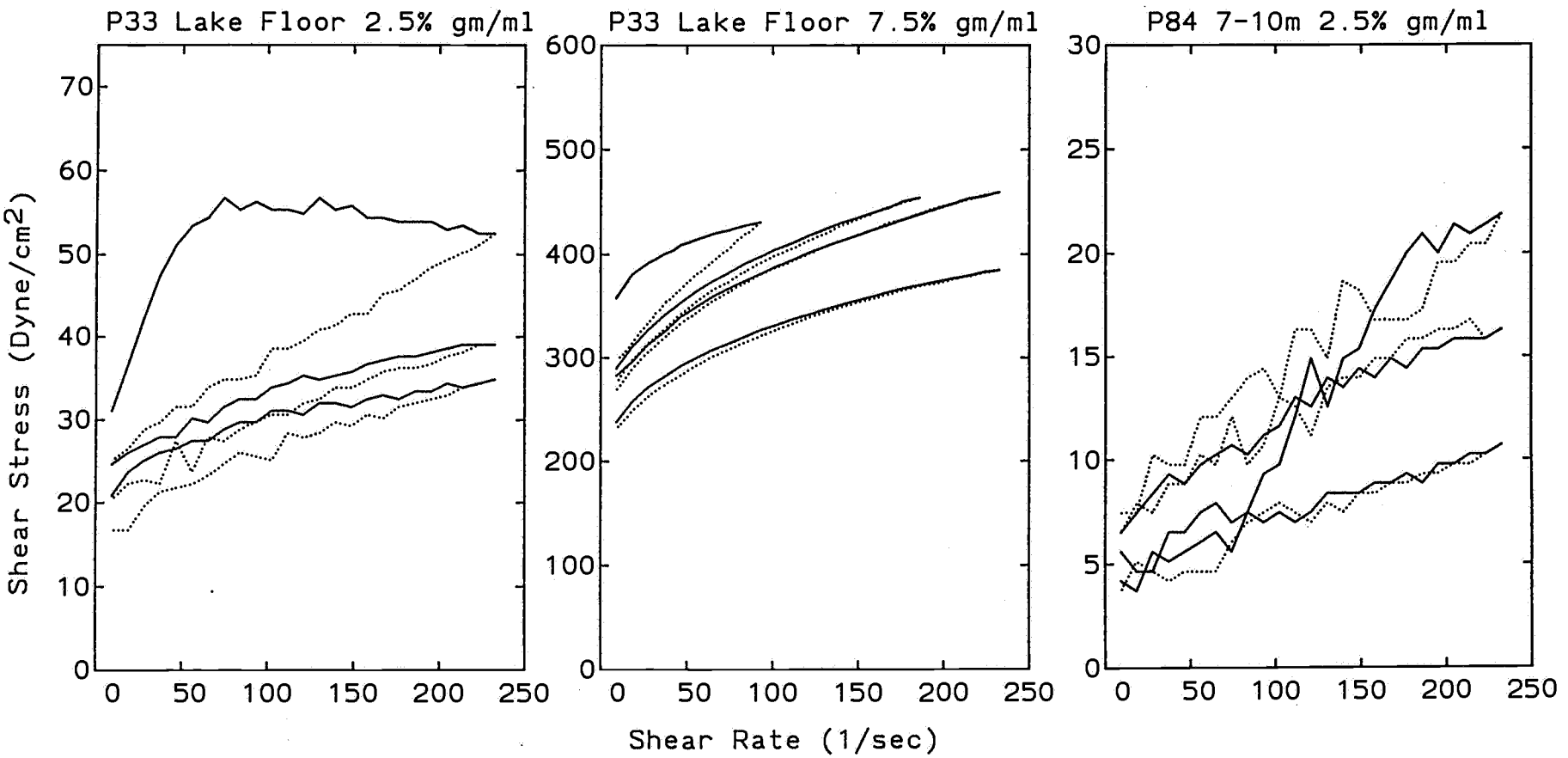


Fig. 4.6. Rheological properties of selected Garford palaeochannel clays in saline-saturated solution. The bottom curves are for the samples shaken in a SPEX mill for 20 minutes. The top curves are for the samples immediately after ultrasonification for 5 minutes. The middle curves show the decay with time (approximately 30 minutes between the beginning of each run) of the rheological properties of the ultrasonified samples. The solid line shows increasing shear rate and the dotted line shows decreasing shear rate.

0004497

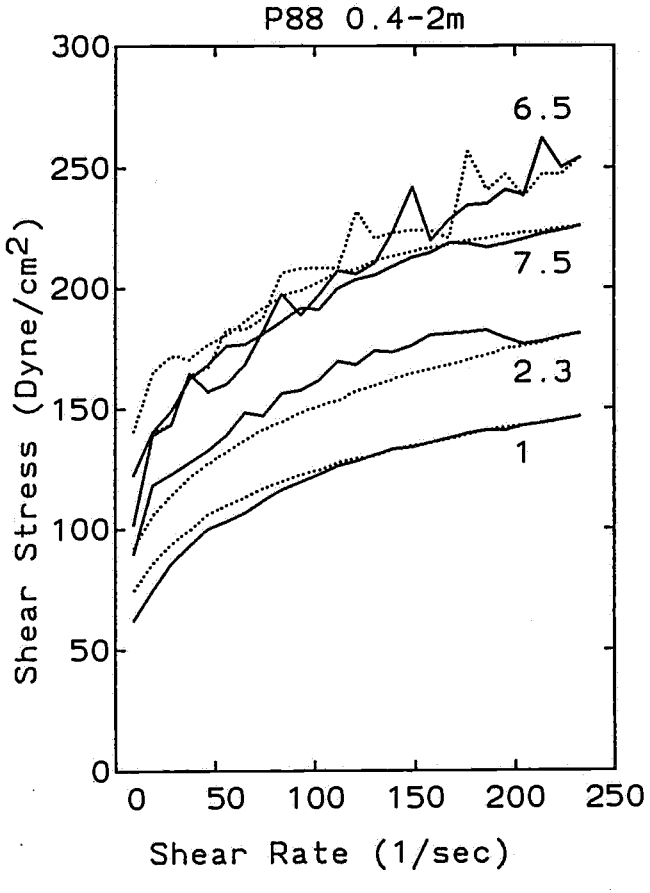


Fig. 4.7. Variation in rheological properties of sample P88 0.4-2m with solution pH (as marked). The suspension concentration is 5% gm/ml. The solid line shows increasing shear rate and the dotted line shows decreasing shear rate.

0000498
125

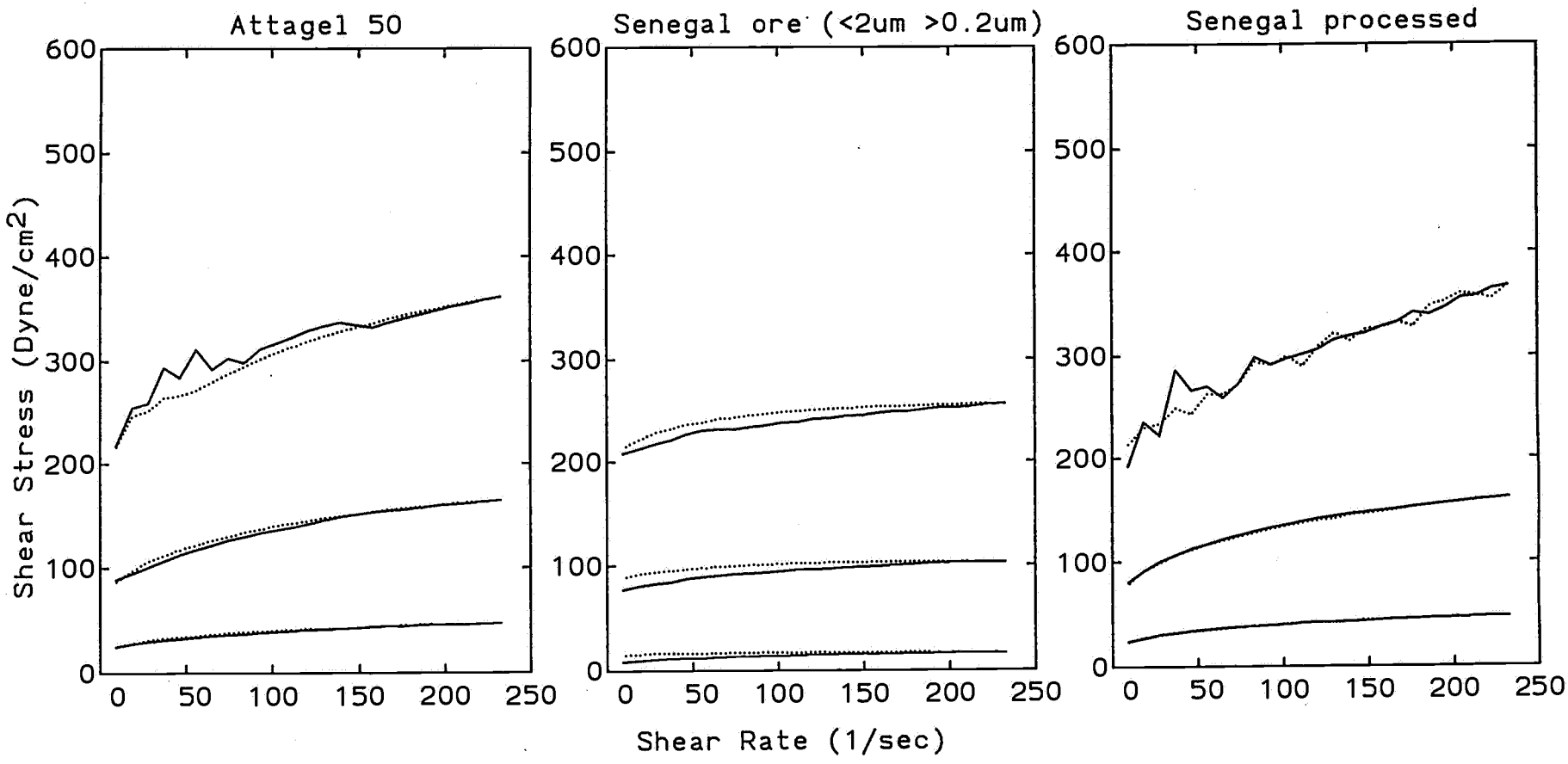


Fig. 4.8a. Rheological properties of commercial attapulgites in RO water. The suspension concentrations are 7.5% gm/ml (upper line), 5% gm/ml (middle line) and 2.5% gm/ml (lower line) except for the Lake Nerramyne samples that show only 7.5% gm/ml. The solid line shows increasing shear rate and the dotted line shows decreasing shear rate. Note change of shear stress scale between samples.

0000499

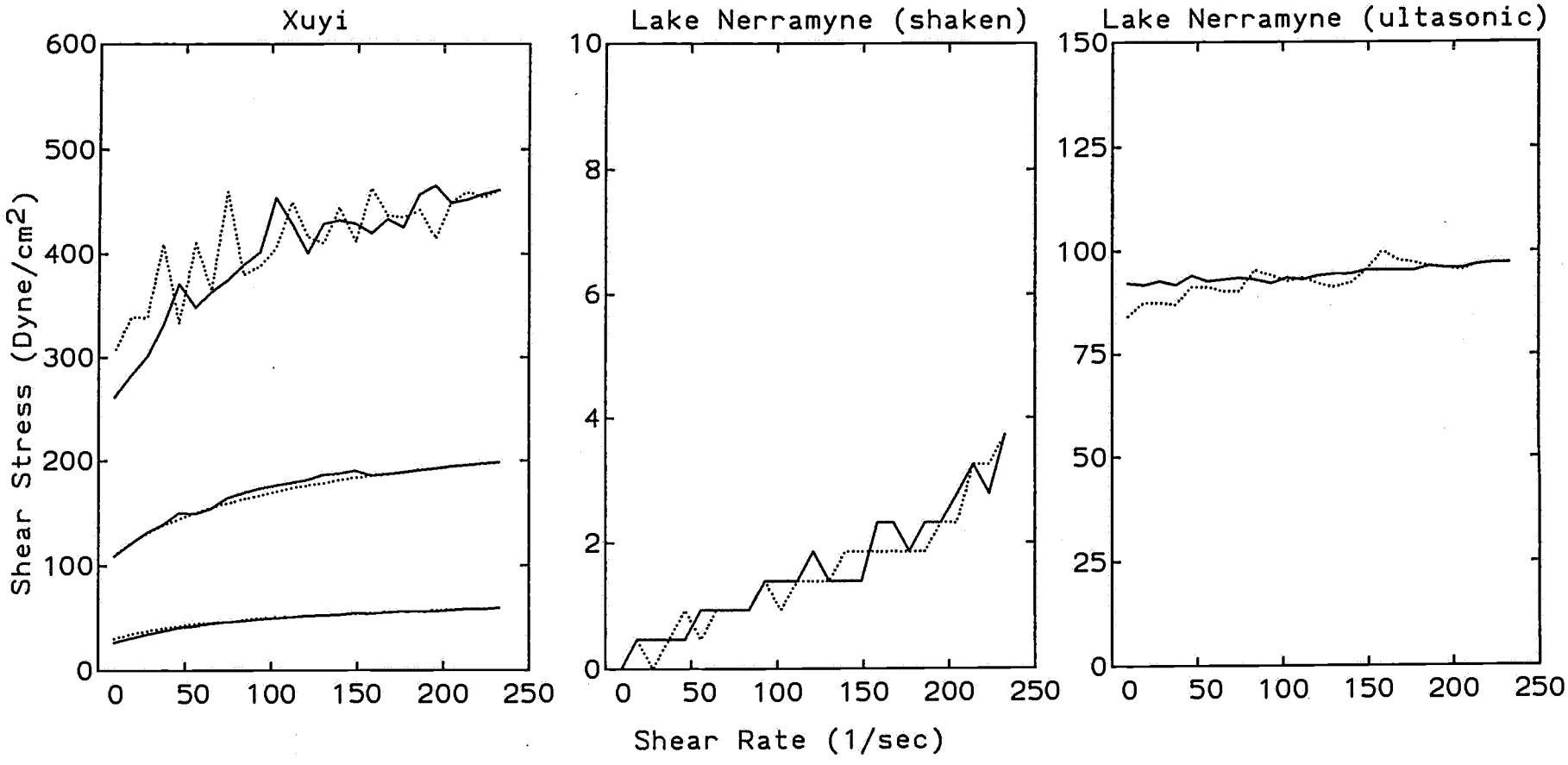


Fig. 4.8b. Rheological properties of commercial attapulgites in RO water. The suspension concentrations are 7.5% gm/ml (upper line), 5% gm/ml (middle line) and 2.5% gm/ml (lower line) except for the Lake Nerramyne samples that show only 7.5% gm/ml. The solid line shows increasing shear rate and the dotted line shows decreasing shear rate. Note change of shear stress scale between samples.

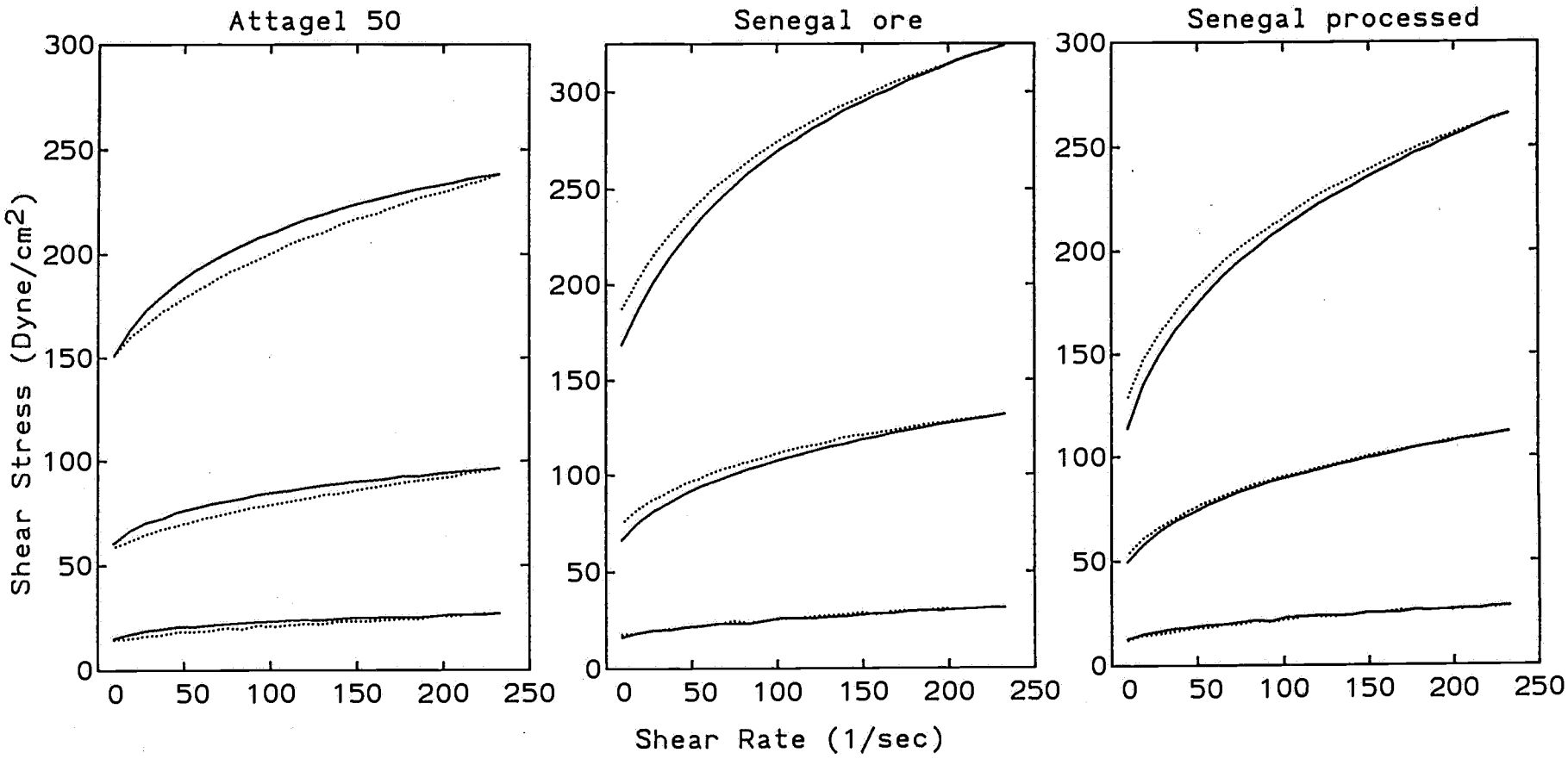


Fig. 4.9a. Rheological properties of commercial attapulgites in saline-saturated solution. The suspension concentrations are 7.5% gm/ml (upper line), 5% gm/ml (middle line) and 2.5% gm/ml (lower line) except for the Lake Nerramyne samples that show only 7.5% gm/ml. The solid line shows increasing shear rate and the dotted line shows decreasing shear rate. Note change of shear stress scale between samples.

0005011

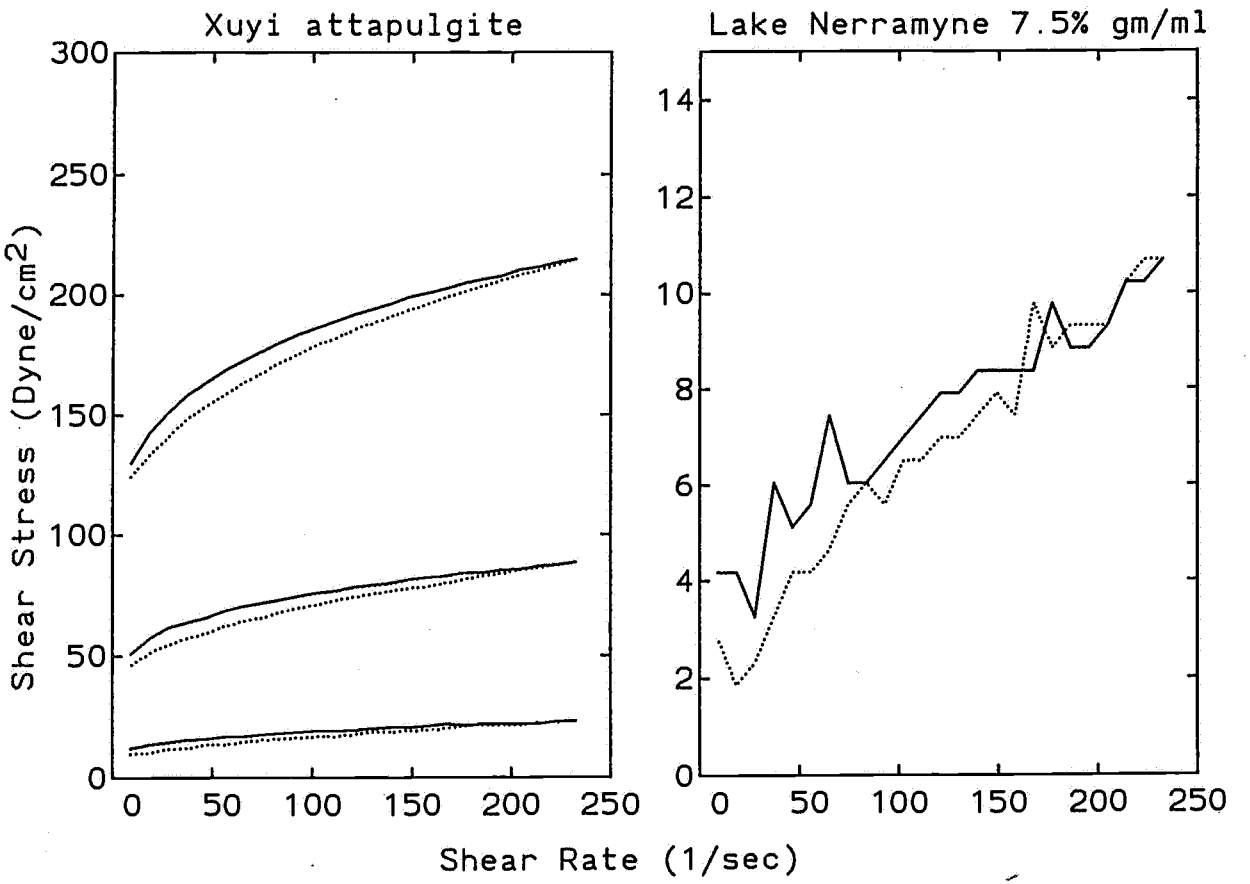


Fig. 4.9b. Rheological properties of commercial attapulgites in saline-saturated solution. The suspension concentrations are 7.5% gm/ml (upper line), 5% gm/ml (middle line) and 2.5% gm/ml (lower line) except for the Lake Nerramyne samples that show only 7.5% gm/ml. The solid line shows increasing shear rate and the dotted line shows decreasing shear rate. Note change of shear stress scale between samples.

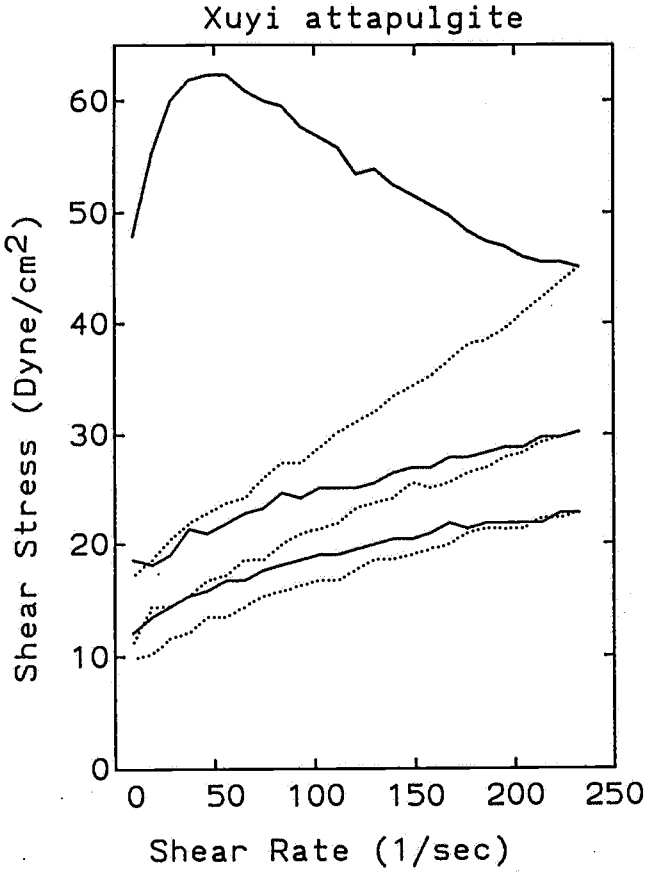


Fig. 4.10. Rheological properties of Xuyi attapulgite in saline-saturated solution (2.5% gm/ml). The bottom curve is for the sample shaken in a SPEX mill for 20 minutes. The top curve is for the sample immediately after ultrasonification for 5 minutes. The middle curve is for the ultrasonified sample and was measured immediately after the completion of the upper curve. The solid line shows increasing shear rate and the dotted line shows decreasing shear rate.

000503

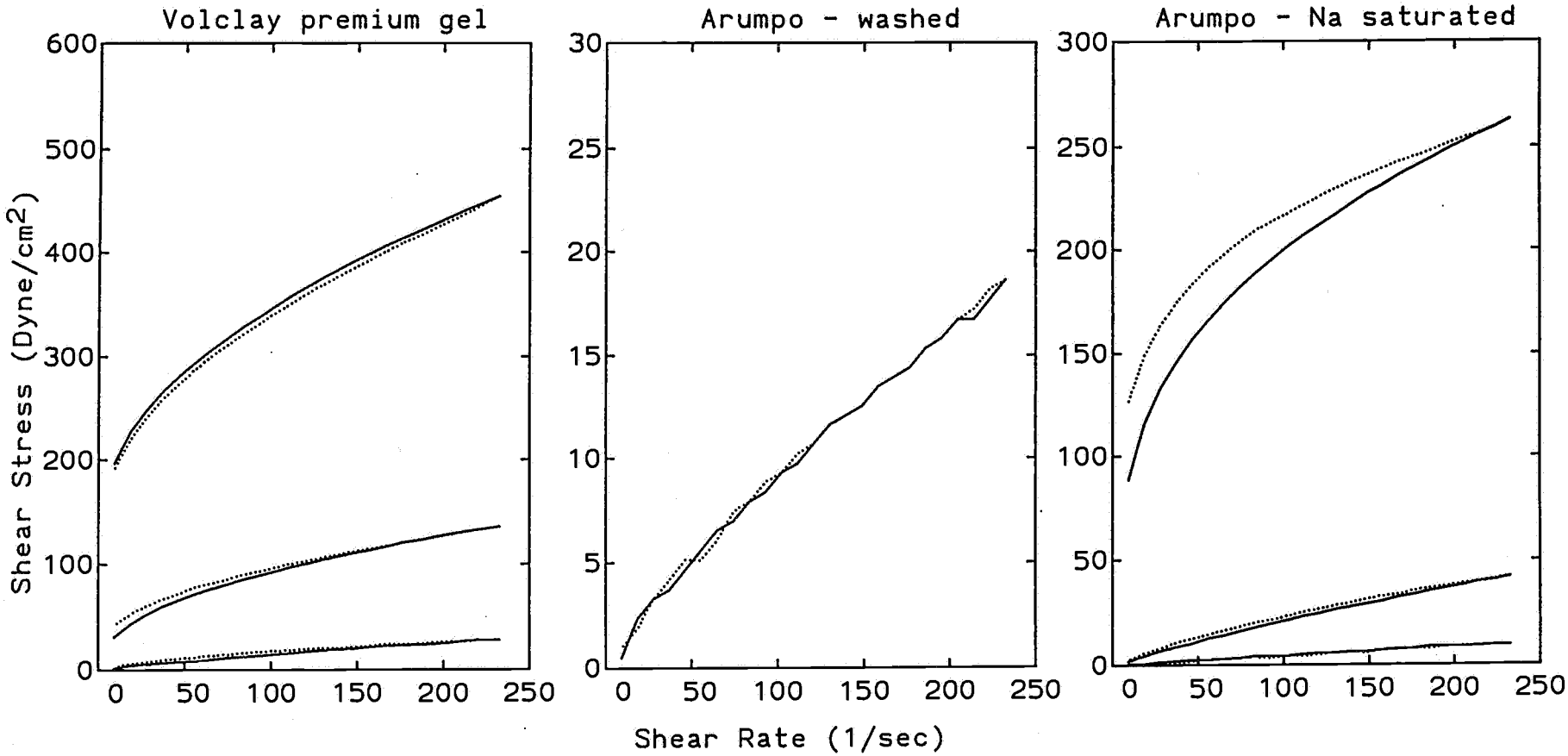


Fig. 4.11. Rheological properties of commercial bentonites in RO water. The suspension concentrations are 10% gm/ml (upper line), 7.5% gm/ml (middle line) and 5% gm/ml (lower line). The solid line shows increasing shear rate and the dotted line shows decreasing shear rate. Note change of shear stress scale between samples.

000504

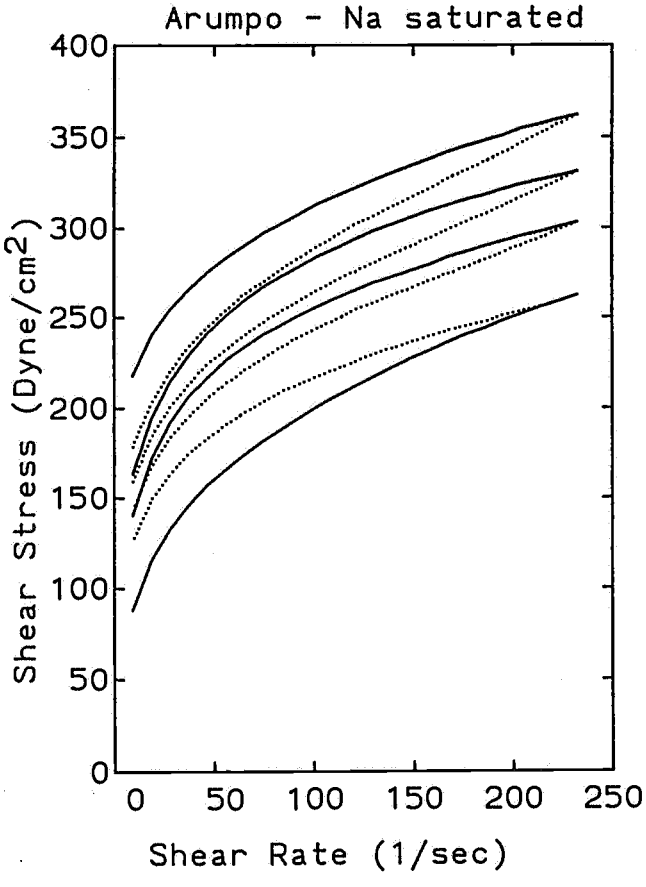


Fig. 4.12. Rheological properties of a 10% gm/ml suspension of Na-saturated Arumpo bentonite (TP1) in RO water. The curves from bottom (youngest) to top (oldest) are for a suspension aged over a period of 4 hours. The solid line shows increasing shear rate and the dotted line shows decreasing shear rate.

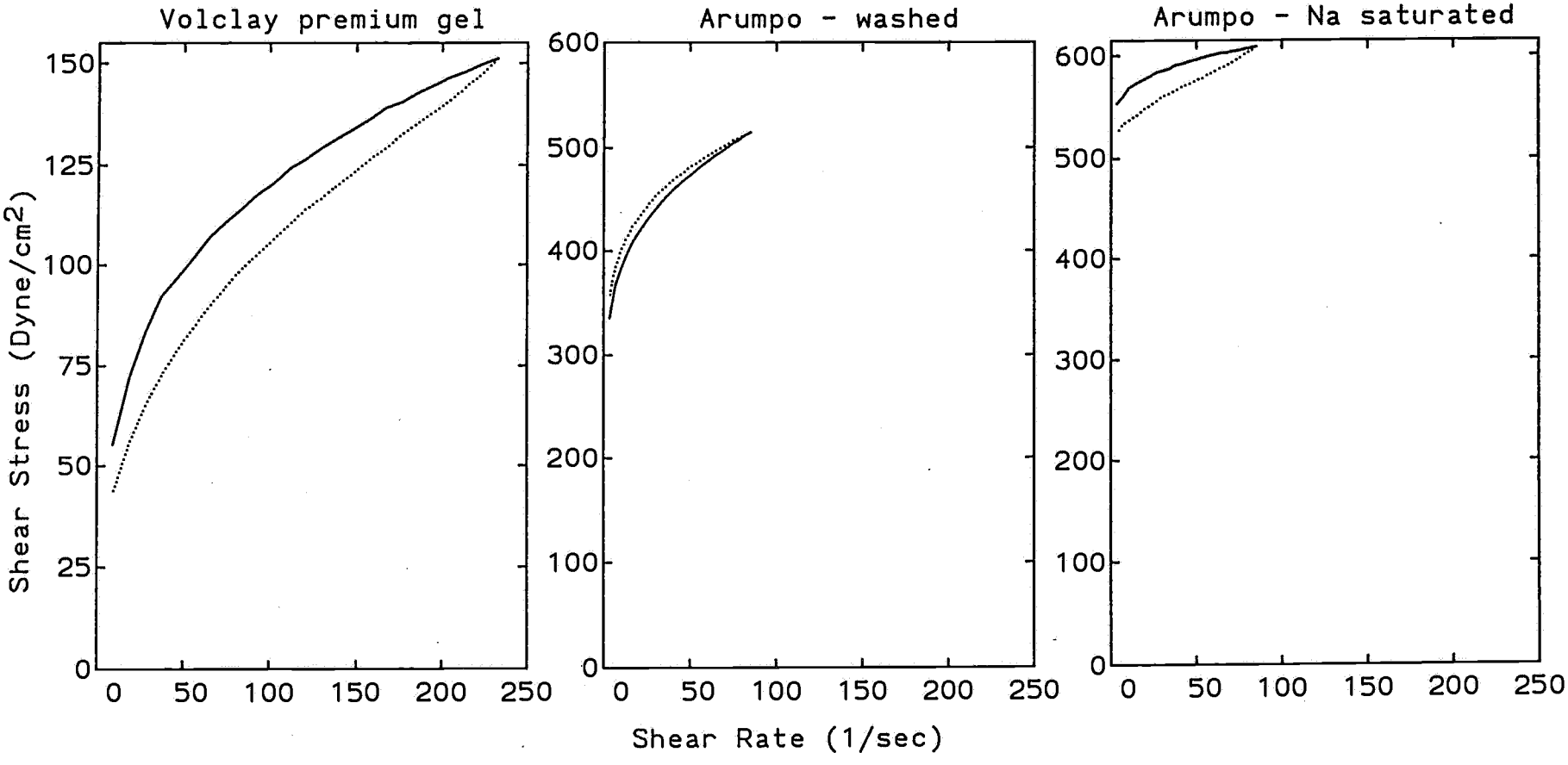


Fig. 4.13. Rheological properties of selected commercial bentonites after ultrasonic treatment for 3 minutes, aging for 4 hours and then shaking in a SPEX mill for 5 minutes. The Volclay suspension is 5% gm/ml and the Arumpo suspensions are 10% gm/ml. All suspensions in RO water. The solid line shows increasing shear rate and the dotted line shows decreasing shear rate.

0005096

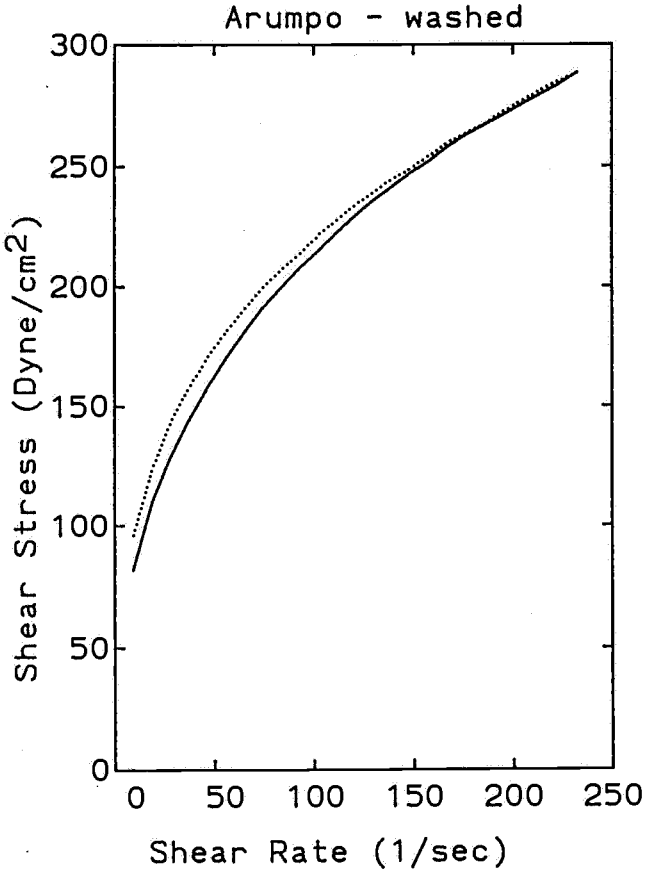


Fig. 4.14. Rheological properties of a 10% gm/ml suspension (RO water) of as-received Arumpo bentonite (TP1) after ultrasonic treatment for 3 minutes, drying at 60°C, shaking for 20 minutes, aging for 6 hours and shaking for 5 minutes. The solid line shows increasing shear rate and the dotted line shows decreasing shear rate.

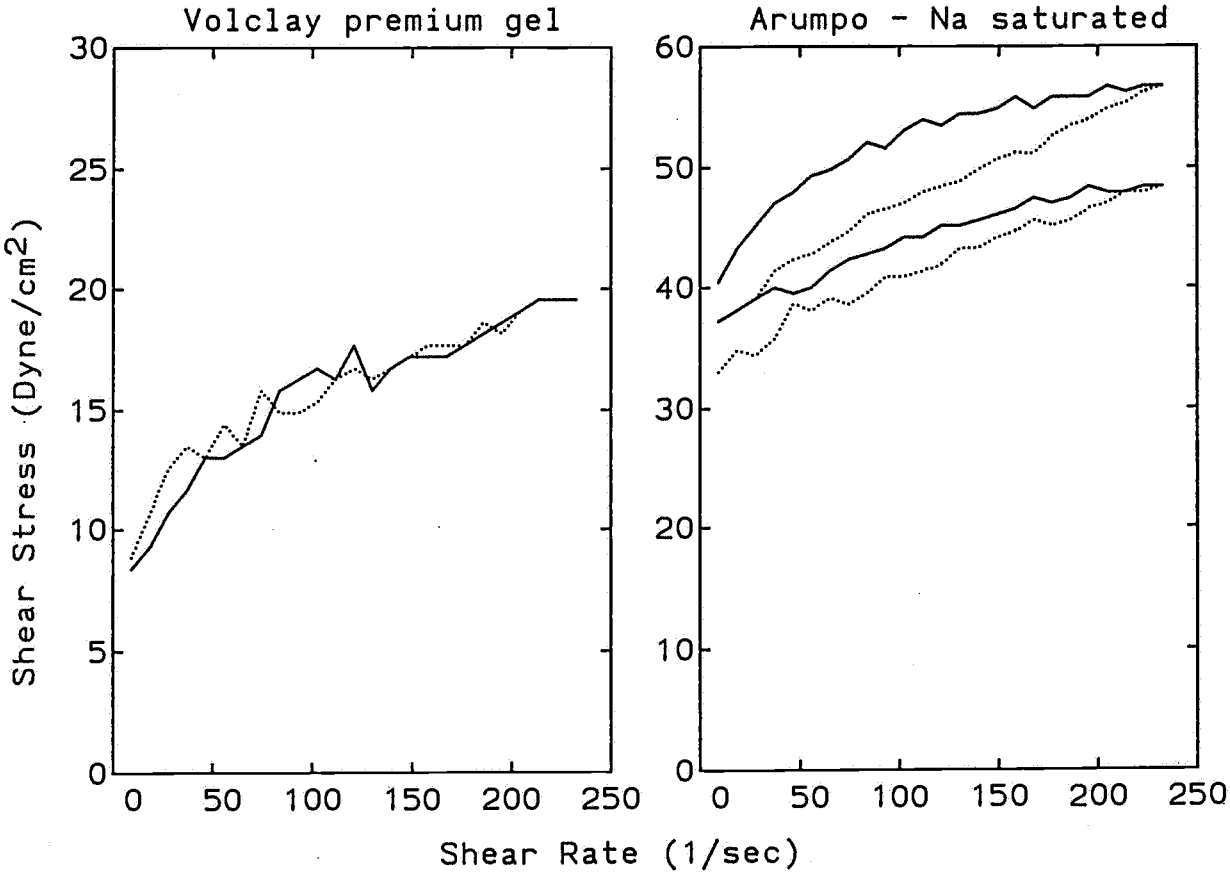


Fig. 4.15. Rheological properties of selected bentonites in saline-saturated solution (10% gm/ml). The lower curve for the Na-saturated Arumpo bentonite are results taken immediately after taking those in the upper curve. This shows the effects of flocculation and settling. The solid line shows increasing shear rate and the dotted line shows decreasing shear rate.

000508

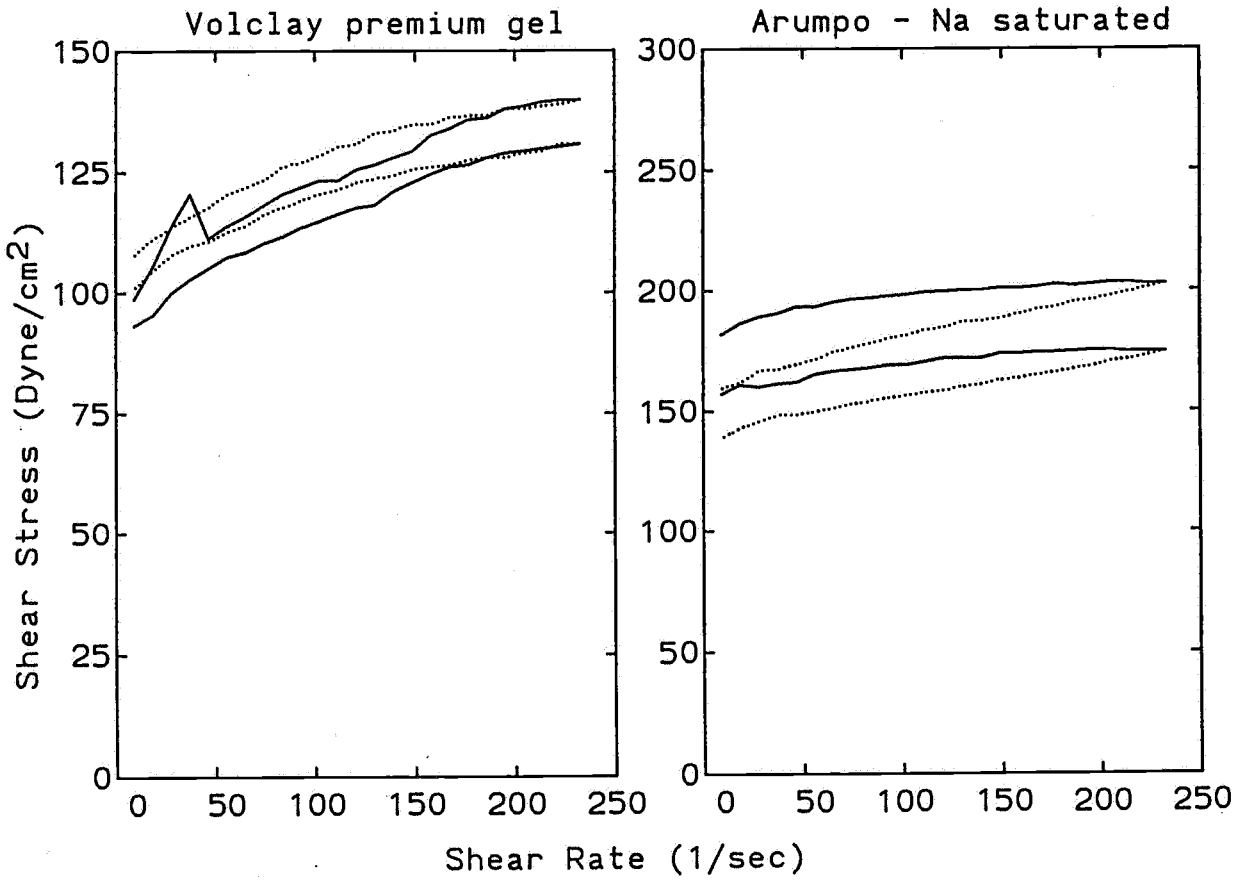


Fig. 4.16. Rheological properties of selected bentonites in saline-saturated solution. The bentonite concentration is 10% gm/ml. The upper curves a for suspensions that have been ultrasonically treated for 1 minute, aged for 3 hours and shaken in a SPEX mill for 5 minutes. The lower curves are for the sample aged for 1 hour after the initial measurement was made. The solid line shows increasing shear rate and the dotted line shows decreasing shear rate.

000509

CHAPTER 5. ABSORPTION PROPERTIES OF SELECTED SAMPLES.

Absorption of dyes

The fibrous nature of palygorskite gives it a high surface area and so it is reasonable to expect palygorskite to have good absorption properties. To test this expectation a suite of clays and other samples were selected for absorbency testing. These materials were

Garford palaeochannel sample P88 0.4-2m, <2μm >0.2μm	90% palygorskite
Garford palaeochannel sample P35 6-7m, <2μm >0.2μm	Approximately 50% palygorskite and 50% dolomite
Lake Nerramyne attapulgite, <53μm	Commercial high-absorbency clay
Volclay premium gel	Na bentonite
Magnesite [$Mg(CO_3)_2$]	Carbonate mineral
Iowaite [$Mg_4Fe(OH)_8OCl \cdot 2\text{-}4H_2O$]	Pyroaurite-sjögrenite (hydrotalcite) type mineral
$Ni_4Al(OH)_8OCl \cdot 2\text{-}4H_2O$	Pyroaurite-sjögrenite (hydrotalcite) type mineral
Wyoming bentonite	Na bentonite
Arumpo bentonite	Mg-Na bentonite

Magnesite and the pyroaurite-sjögrenite (hydrotalcite) type minerals are known for their good absorbency properties especially for anionic dyes.

The dyes chosen for the tests were red and blue food dyes. An advantage of these dyes is that, because of their low toxicity, they can be easily and safely handled and disposed of. Furthermore the amount of dye absorbed can be judged colourimetrically. These dyes are predominantly anionic in nature and have little to no effect on solution pH. The characteristics of these dyes are:

Red food dye:

National Food Authority (Canberra) number:	122
Colour Index (CI) number:	14720
Chemical Abstracts Services (CAS) number:	3567-69-9
Common names:	Carmoisine, azorubin

Description: Synthetic azodye. Anionic.

Chemical formula:

1-Naphthalenesulfonic acid, 4-hydroxy, 3-[(4-sulfo-1-naphthalenyl) azo], disodium salt.

Chemical structure: Fig. 5.1.

Blue food dye:

National Food Authority (Canberra) number: 133

Colour Index (CI) number: 42090

Chemical Abstracts Services (CAS) number: 3844-45-9

Common name: Brilliant blue FCF.

Description: Synthetic coal-tar dye. Anionic and cationic.

Chemical formula:

N-Ethyl-N-[4-[[4-[ethyl[(3-sulfophenyl)methyl]amino]phenyl] (2-sulfophenyl)methylene]-2,5-cyclohexadien-1-ylidene] - 3-sulfobenzenemethanaminium hydroxy inner salt, disodium salt.

Chemical structure: Fig. 5.2.

To test absorbency, stock solutions of red and blue dyes were prepared by adding 10 drops of concentrated dye to 1 litre of water. 75ml of stock solution was mixed with 0.5gm of sample by shaking in a SPEX mill. The resulting suspension was then allowed to stand at 20°C. After standing for 48 hours the supernatant was removed (using centrifugation where necessary) and its colour matched with that of the original stock solution diluted by a known amount. Results are shown in Table 5.1.

The amount of dye absorbed by clays varied between 15% and 60%. There was some colour change of solutions, particular for the red dye, suggesting that in bonding to the clay the optical-absorption properties of the dye are altered. To clear the solution centrifugation was required for P88 0.4-2m, Volclay premium gel, magnesite and for one of the pyroaurite-sjögrenite type minerals. Magnesite and the pyroaurite-sjögrenite type minerals absorbed almost all of the dye in solution. Magnesite took 48 hours to

clear the solution while the pyroaurite-sjögrenite type minerals took half an hour. Magnesite caused the solution pH to rise from approximately neutral to 10. Pyroaurite-sjögrenite type minerals vary in their effect on solution pH with values ranging between neutral and approximately 9.5. Clearly pyroaurite-sjögrenite type minerals are very efficient at removing anionic dyes from water and would be the preferred choice for absorbing anionic dyes.

Improved absorption properties are reported when palygorskite is heated to between 250°C and 400°C (Jones and Galan, 1988). Improvement in decolourising properties are reported when palygorskite is heated to around 700°C (Jones and Galan, 1988). Absorption results for Garford palaeochannel palygorskite P88 0.4-2m heated to 280°C, 350°C and 700°C are shown in Table 5.2. Heating improves the absorption of red food dye by palygorskite but has no effect on the absorption of blue food dye.

Absorption of organic compounds by clays can be improved by coating the clays with an organic compound. Selected clays were coated with excess amounts of poly diallyl dimethyl ammonium chloride (poly-DADMAC; Fig. 5.3) giving them an overall positive charge (Bernas *et al.*, 1995). This was achieved by mixing a known weight of poly-DADMAC with a known weight of clay in water and shaking vigorously for 10 minutes. The poly-DADMAC-clay complex is recovered by centrifugation followed by double washing with water and drying at 60°C (N. de Lacy, personal communication). The absorption results are shown in Table 5.3. The organic coating dramatically improved the absorption properties of the clays with the exception of red dye on Wyoming bentonite. These organo-clays are as effective as the pyroaurite-sjögrenite type minerals for the absorption of these anionic dyes although absorption times were of the order of a day.

Untreated or heated clays are moderate absorbers of the dyes and their real usefulness may be in their specificity for some dyes over others. The clays are very good absorbers of dyes when treated with an organic material such as poly-DADMAC. The variation in the way that individual clays react with the dyes and in the way particular clays react with dyes of different colour is indicative of a complex surface reaction that is

dependant on the surface charge distribution of the clays and how well this distribution matches the charge distribution of the dyes. Clearly, to study these mechanisms further, a technique that can directly view clay surfaces is required.

Specific absorption of cations

Slade and Kimber (1994) have investigated the absorption by palygorskite of divalent ions from mono-ionic solutions and found that palygorskite was a good absorber of these ions. Investigation of the cation exchange capacity of palygorskite (Chapter 3) indicated that palygorskite had different exchange capacities (and exchange mechanisms) for divalent and monovalent ions. Hence, in solutions containing a mixture of divalent and monovalent ions it is probable that ions of one valence will be absorbed preferentially to ions of the other valence.

Slade and Kimber (1994) tested cation uptake by placing 15gm of clay in 100ml of solution containing 1000ppm of a particular cation. To test cationic absorption from solutions containing both a divalent species and a monovalent species, the method of Slade and Kimber was modified in 2 ways. The first was to use a solution containing equal amounts (in terms of total charge) of Cd^{2+} and Na^{+} (as chlorides). The second was to use only 0.5gm of sample per 100ml of solution and allow for this by using a lower ionic concentration. The experiment was carried out by mixing 0.5gm of clay with 100ml of solution in a SPEX mill for 20 minutes. The mixture was then left to stand at 20°C for 24 hours. After this time the solution was passed through a 0.1μm filter and analysed using inductively coupled plasma spectroscopy. The cationic concentrations of the original (stock) solution and of solutions mixed with 3 clays are shown in Table 5.4.

In all cases Cd has been absorbed in preference to Na. The Garford palaeochannel sample P33 Lake Floor and the Lake Nerramyne sample have absorbed Cd exclusively. The amount of Cd absorbed is at the limit of the amount predicted by the CEC of these clays (approximately 10-20 $cmol^{+}/kg$). For both palygorskite samples the overall measured charge in solution is less than for the stock solution. This indicates that ions other than Cd^{2+} and Na^{+} have been released into solution. These other ions are almost

certainly Ca and Mg cations. Thus the palygorskites are behaving as would be predicted by a simple exchange mechanism.

The results are consistent with the hypothesis given in Chapter 3 that Na occupies exchange sites on the palygorskite external surfaces while divalent ions occupy the internal structural-tunnel sites. As the Garford palygorskite was obtained from an environment where halite is common, the external surfaces of the palygorskite are presumably saturated with Na and therefore do not have any capacity to take up more Na. If the external surfaces were saturated with another monovalent cation such a K then, presumably, Na would be absorbed from solution and K released into solution. Similarly, if the palygorskite was pre-saturated with Cd then there would be no absorption of Cd from solution.

The Na-saturated Arumpo bentonite also behaves in a way that can be predicted using a simple exchange mechanism. The Cd ions replace Na, releasing the latter into solution. The overall increase in measured charge suggests that the bentonite was not sufficiently washed during preparation. The Arumpo bentonite is a better absorber of Cd than the palygorskites. This is because of the bentonite's greater CEC (approximately 100cmol^{+}/kg). The amount of Cd absorbed by the bentonite is well below the maximum amount predicted from its CEC and thus the bentonite remains partially exchanged with Na. The fact that the bentonite has not absorbed all of the Cd is indicative of a partitioning of Cd between the solution and the exchange sites. Given the absorption is an exchange reaction, the bentonite saturated with a cation other than Na would have readily absorbed Na.

The nature of cation exchange by clays suggests that to remove a particular cation from a solution containing cations of more than one species, the absorbing clay should be pre-saturated with the cation or cations that are not to be removed from solution. Although palygorskite cannot absorb as many cations per unit weight as a bentonite (because of the lower CEC of palygorskite), palygorskite has the advantage of being more specific in terms of the absorption of di- and mono-valent cations.

To further understand the exchange mechanisms involved in cationic absorption it is necessary to determine whether cations can be back-exchanged from the surfaces and the relative cationic concentrations at which selective absorption no longer occurs.

References

Bernas, S.M., Oades, J.M., Churchman, G.J. and Grant, C.D. (1995). Comparison of the effects of latex and poly(DADMAC) of structural stability and strength of soil aggregates. Aust. J. Soil. Res., **33**, 369-380.

Jones, B.F. and Galan, E. (1988). Sepiolite and palygorskite. In: S.W. Bailey (Ed.), Hydrous Phyllosilicates (exclusive of the micas). Reviews in Mineralogy, **19**. Mineral Society of America.

Slade, P.G. and Kimber, R. (1994). Results on the uptake of cations of Ni, Cd, Cr and Pb, and benzene sorption by selected clays. Absorbent Clay project, Interim Progress report No. 2 to Mines and Energy, South Australia, November 1994. South Australian Department of Mines and Energy, Envelope 8785 (unpublished).

Table 5.1. Absorption of food dyes by various clays and other compounds. All samples dried at 105°C.

	Absorption (%)	
	Red food-dye	Blue food-dye
P88 0.4-2m	20-30	15-25
P35 6-7m	40-60[1]	15-25
Lake Nerramyne	40-60[1]	15-25
Volclay premium gel (Na bentonite)	40-60[1]	15-25
Magnesite [$Mg(CO_3)_2$]	95-100	95-100
Iowaite[2] [$Mg_4Fe(OH)_8OCl \cdot 2\text{-}4H_2O$]	95-100[3]	95-100[3]
[$Ni_4Al(OH)_8OCl \cdot 2\text{-}4H_2O$][2]	95-100[3]	85-95[3,4]

[1] Some colour change.
[2] Pyroaurite-sjögrenite type mineral.
[3] Rapid absorption (<30 min.)
[4] Colour caused by suspended particles.

Table 5.2. Absorption of food dyes by Garford palaeochannel palygorskite heated to various temperatures.

	Absorption (%)	
	Red food-dye	Blue food-dye
P88 0.4-2m, 105°C	20-30	15-25
P88 0.4-2m, 280°C	40-60[1]	15-25
P88 0.4-2m, 350°C	20-30	15-25
P88 0.4-2m, 700°C	40-60[1]	15-25

[1] Some colour change.

Table 5.3. Absorption of food dyes by various clays after treating with poly-DADMAC. The ratio given shows the weight of poly-DADMAC relative to the weight of clay in the sample.

	Absorption (%)	
	Red food-dye	Blue food-dye
P88 0.4-2m, DADMAC 5:1	85-95	95-100
Lake Nerramyne, DADMAC 5:1	90-95	95-100
Arumpo bentonite, DADMAC 5:1	95-100	95-100
Wyoming bentonite, DADMAC 8:1	40-50	95-100

Table 5.4. Effect of various clays on the concentration of Cd^{2+} and Na^{+} ions in a mixed solution of these ions. Clay was added at 0.5gm per 100ml of original (stock) solution.

Sample	Cd		Na		Total charge
	mg/l	mmol/l	mg/l	mmol/l	$mmol^{+}/l$
Stock solution	74.0	(0.66)	32.3	(1.41)	2.73
P33 Lake Floor	24.7	(0.22)	37.2	(1.62)	2.08
Lake Nerramyne	17.7	(0.16)	33.8	(1.47)	1.79
Na-saturated Arumpo bentonite	0.6	(0.01)	81.2	(3.53)	3.55

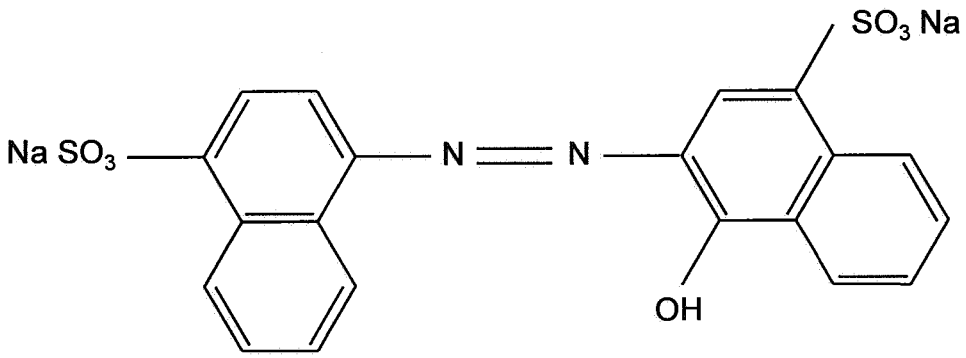


Fig. 5.1. Structure of red food dye.

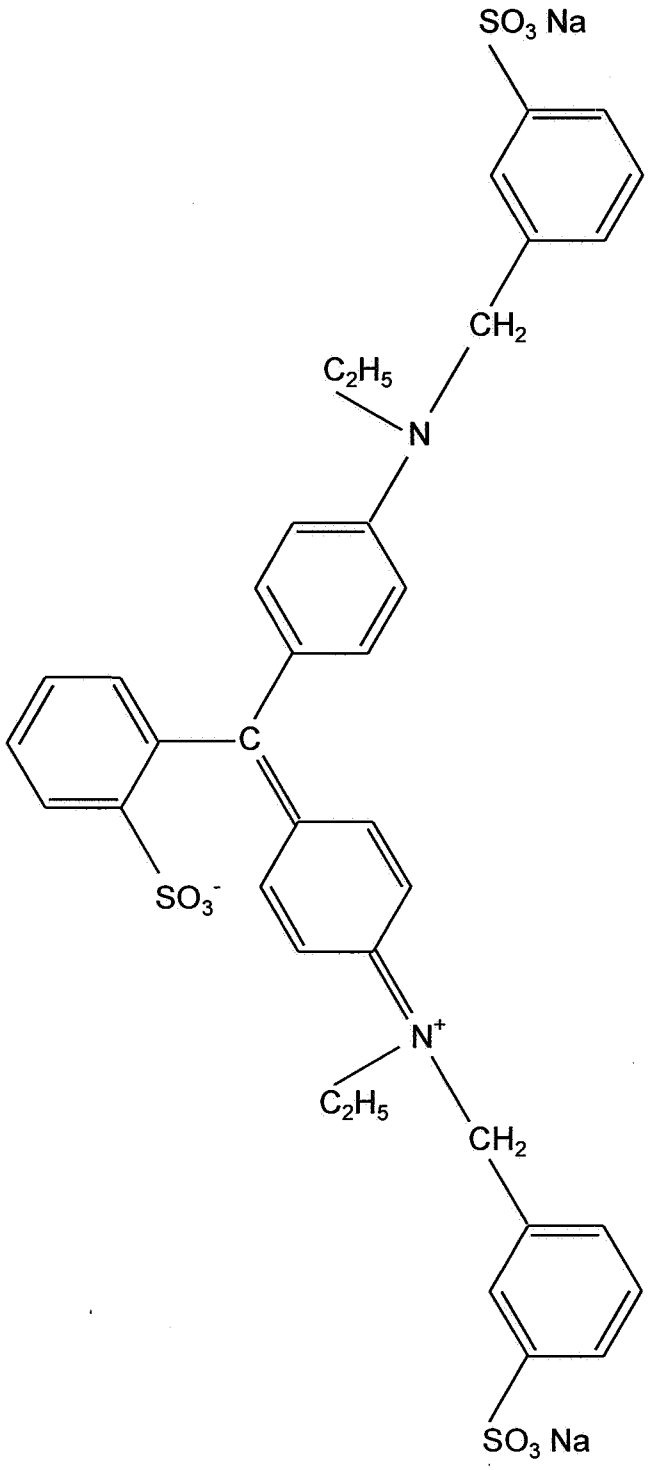


Fig. 5.2. Structure of blue food dye.

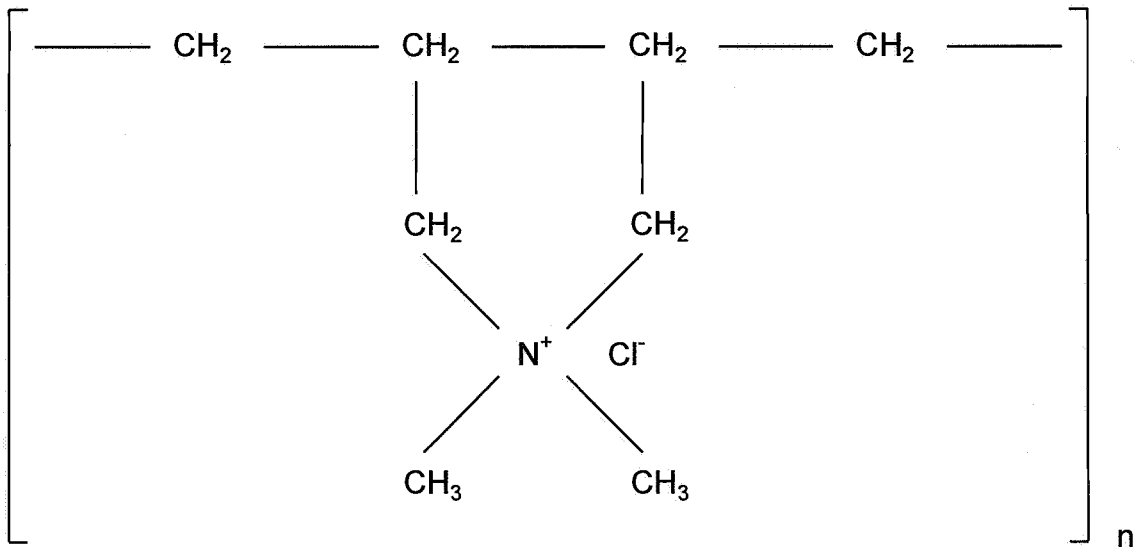


Fig. 5.3. Structure of poly-DADMAC.

CHAPTER 6. WATER SORPTION BY GARFORD PALAEOCHANNEL CLAYS.

The largest single market for palygorskite is as absorbent granules in pet litter. Water sorption measurement is a key parameter in comparing the performance of products.

Methods

Sub-samples of selected bulk samples from the 1995 drilling programme were taken for determination of water sorption capacity by the Westinghouse Method as described in Association Francais de Normalisation standard "Pet Litter - Determination of absorbent power - Water retention capacity", V19-002 December, 1990. Details of the method are given in Appendix 5.

Two sub-samples were taken of as-received bulk samples for each depth interval selected. These were dried at 105°C and 350°C respectively. The upper temperature was chosen based on concurrent work (Keeling *et al.*, in prep.) which showed that samples of Garford Formation clay require heating to at least 350°C in order that the clay granules retain their integrity when saturated. Drying at 350°C was done in a bench top electric kiln using a heating rate of 20°C per minute with a dwell time of 1 hour at maximum temperature, after which the sample was allowed to cool to 100°C.

Dried samples were crushed by hand and sieved to separate a minimum 60gm granular product in the size range >1mm, <6mm. Water sorption measurements were done in triplicate using 20gm samples.

Results and discussion

Results reported in Table 6.1 are the average of 3 tests by the Westinghouse method. Individual results were all within ±10% of the average value.

With the exception of two samples, P69 (9-10m) and P84 (10-11m), weight of water sorbed for samples dried at 105°C exceeded the original weight of the sample, that is water retention was ≥100%. High water sorption reflects the large surface area of samples due to the dominantly fine particle size of the mineral components (<5μm) and the degree of dispersion which allowed water to contact surfaces of individual particles. For samples

with <100% water sorption; P84 (10-11m) was predominantly re-cemented dolomite and did not disperse, while P69 (9-10m), which was also dolomitic, only partly dispersed.

Samples heated to 350°C showed little or no tendency to disperse. In all cases, there was some reduction of the water sorption capacity of the clays compared with those dried at 105°C. For samples heated to 350°C, water sorption capacity is influenced by additional factors of porosity and degree of permeability inherent in the raw clay sample.

The amount of water retained by samples showed a moderate degree of correlation with palygorskite content (Fig. 6.1). As expected, samples with highest water retention also had moderate to high palygorskite contents but there was considerable variation in their abilities to sorb and retain water. For example, P65 (13-14m) containing 44% palygorskite sorbed only 109% water when heated to 105°C compared with 203% water retention for sample P66 (16-17 m) with the same amount of palygorskite. On heating to 350°C both samples retained similar low amounts of water of 77% and 78% respectively.

The presence of higher amounts of illite and less dolomite in P65 (13-14m) compared with P66 (16-17 m) may have effected the dispersion of P65 or impeded access of water to the surface of palygorskite particles. The low water capacity of both samples when heated to 350°C suggests that the permeability characteristics of the raw clay were relatively poor.

The presence of halite is another factor affecting the water sorption capacity of samples. Halite will undergo some dissolution during sorption testing thereby reducing the sample weight and apparent water retention.

Sample P33 Lake Floor has a moderate palygorskite content (33-38%) but shows a substantial drop in sorption capacity when dried at 350°C (64%) compared with 105°C (144%). A fragment of raw clay dried at 105°C was coated with 30nm of gold and examined using a Cambridge S250 scanning electron microscope (SEM). The clay comprises compact, matted palygorskite fibres to around 1μm in length. These appear to be arranged in compressed and distorted layers (Fig. 6.2). Distortion of the layers may have occurred during sampling but the overall impression is of a clay with restricted porosity and permeability.

Sample P88 (0.4-2m), from the same lake as P33, showed similar low sorption capacity when heated to 350°C. This sample was readily beneficiated to around 88% palygorskite by removal of quartz and halite using the method described in Appendix 3. Water sorption for the beneficiated samples dried at 105°C and 350°C increased to 254% and 125% respectively, in line with the higher palygorskite content (Table 6.1). The results are comparable to, or better than, commercial palygorskite absorbent granules (~110%).

The results indicate that the sorption capacity of samples heated to 350°C may be substantially increased if the raw clay is initially processed in a manner that improves fibre dispersion and increases permeability.

Table 6.1. Water retention (wt.%) for Garford palaeochannel clays dried at 105°C and 350°C (Westinghouse Method).

Hole	Depth Interval (m)	Water Sorption (%) 105°C*	Water Sorption (%) 350°C	Mineralogy (by XRD using mineral standards, refer Chapter 1)
P33 Lake Floor		144	64	Paly 33-38%, Illite 4-6%, Halite 15-19%, Qtz 40-45%
P53	0.6 - 1.5	118	62	Paly 15-19%, Illite 2-5%, Dol 64-69%, Halite 6-8%, Qtz 4-6%
P54	0.1 - 0.6	106	66	Paly 13-16%, Illite 2-4%, Dol 70-74%, Halite 7-10%, Qtz 1-3%
P61	10 - 12	158	100	Paly 28-33%, Illite 16-18%, Dol 14-16%, Halite 4-5%, Qtz 30-34%
P61	12 - 14	128	68	Paly 29-34%, Illite 32-36%, Dol 5-8%, Halite 4-6%, Qtz 20-24%
P65	10 - 13	156	68	Paly 36-40%, Illite 18-23%, Dol 11-13%, Halite 5-7%, Qtz 15-19% Smectite 6-12%
P65	13 - 14	109	77	Paly 42-46%, Illite 23-28%, Dol 1-2%, Halite 5-7%, Qtz 8-11%, Smectite 10-15%
P66	15 - 16	138	73	Paly 24-28%, Illite 4-6%, Dol 50-55%, Halite 2-5%, Qtz 11-15%
P66	16 - 17	203	78	Paly 42-47%, Illite 6-10%, Dol 25-28%, Halite 5-9%, Qtz 4-6%, Smectite 5-10%
P66	17 - 18	116	74	Paly 9-13%, Illite 8-12%, Dol 6-10%, Halite 4-6%, Qtz 55-60%, Smectite 7-12%
P69	9 - 10	106	70	Paly 22-26%, Illite 17-21%, Dol 20-25%, Halite 1-3%, Qtz 27-33%, Smectite 0-5%
P69	10 - 11	87	49	Paly 13-16%, Illite 9-11%, Dol 45-50%, Halite 1-3%, Qtz 20-24%, Celestine 2-5%
P77	5 - 6	109	69	Paly 33-36%, Illite 5-9%, Dol 22-26%, Halite 4-6%, Qtz 8-12%, Smectite 15-20%, Gypsum 1-3%
P77	6 - 7	137	71	Paly 33-36%, Illite 9-12%, Dol 3-4%, Halite 5-9%, Qtz 27-33%, Smectite 15-20%

Table 6.1 cont. Water retention (wt.%) for Garford palaeochannel clays dried at 105°C and 350°C (Westinghouse Method).

Hole	Depth Interval (m)	Water Sorption (%) 105°C*	Water Sorption (%) 350°C	Mineralogy (by XRD using mineral standards, refer Chapter 1)
P77	7 - 8	170	100	Paly 45-50%, Illite 9-12%, Dol 1-2%, Halite 8-12%, Qtz 11-15%, Smectite 15-20%
P79	7 - 10	118	90	Paly 10-14%, Illite 1-2%, Dol 77-81%, Halite 1-3%, Qtz 5-7%
P84	10 - 11	43	33	Paly 4-8%, Illite 1-3%, Dol 87-93%, Halite 0-1%, Qtz 1-2%
P84	11 - 12	103	70	Paly 34-38%, Illite 2-5%, Dol 34-38%, Halite 2-3%, Qtz 20-23%
P84	12 - 14	114	71	Paly 43-47%, Illite 6-10%, Dol 8-12%, Halite 2-5%, Qtz 32-36%
P84	14 - 16	106	53	Paly 30-34%, Illite 3-6%, Dol 23-28%, Halite 2-4%, Qtz 30-34%, Smectite 0-5%
P85	0.1 - 1	169	75	Paly 55-60%, Illite 5-7%, Halite 26-30%, Qtz 6-10%
P86	0 - 0.6	158	74	Paly 57-63%, Illite 2-4%, Dol 1-2%, Halite 16-20%, Qtz 16-19%
P88	0.4 - 2	153	61	Paly 39-44%, Illite 5-8%, Dol 0-1%, Halite 12-15%, Qtz 35-40%
P88	2 - 3	136	106	Paly 35-40%, Illite 14-18%, Halite 12-15%, Qtz 31-35%
P88 washed	0.4 - 2	254	123	Paly 85%, Illite 13%, Dol 1%, Qtz ~1%

*All samples dried at 105°C, with the exception of P84 10-11m, became dispersed during the course of the test. In some cases a few milligrams of sample were lost through the cone mesh.

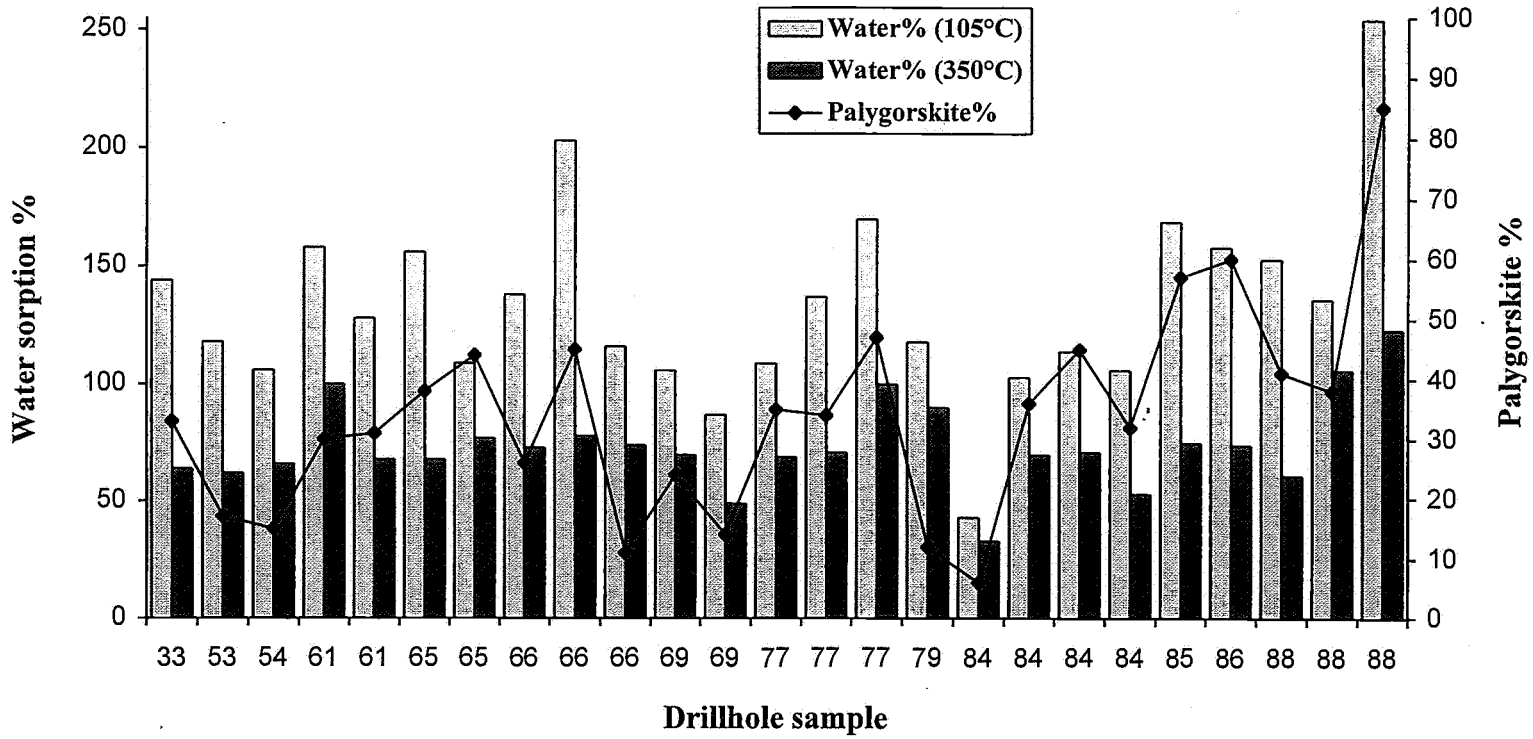


Fig. 6.1. Relationship between palygorskite content and water retained by samples dried at 105°C and 350°C.

(Sample number ordering as per Table 6.1.)

000527

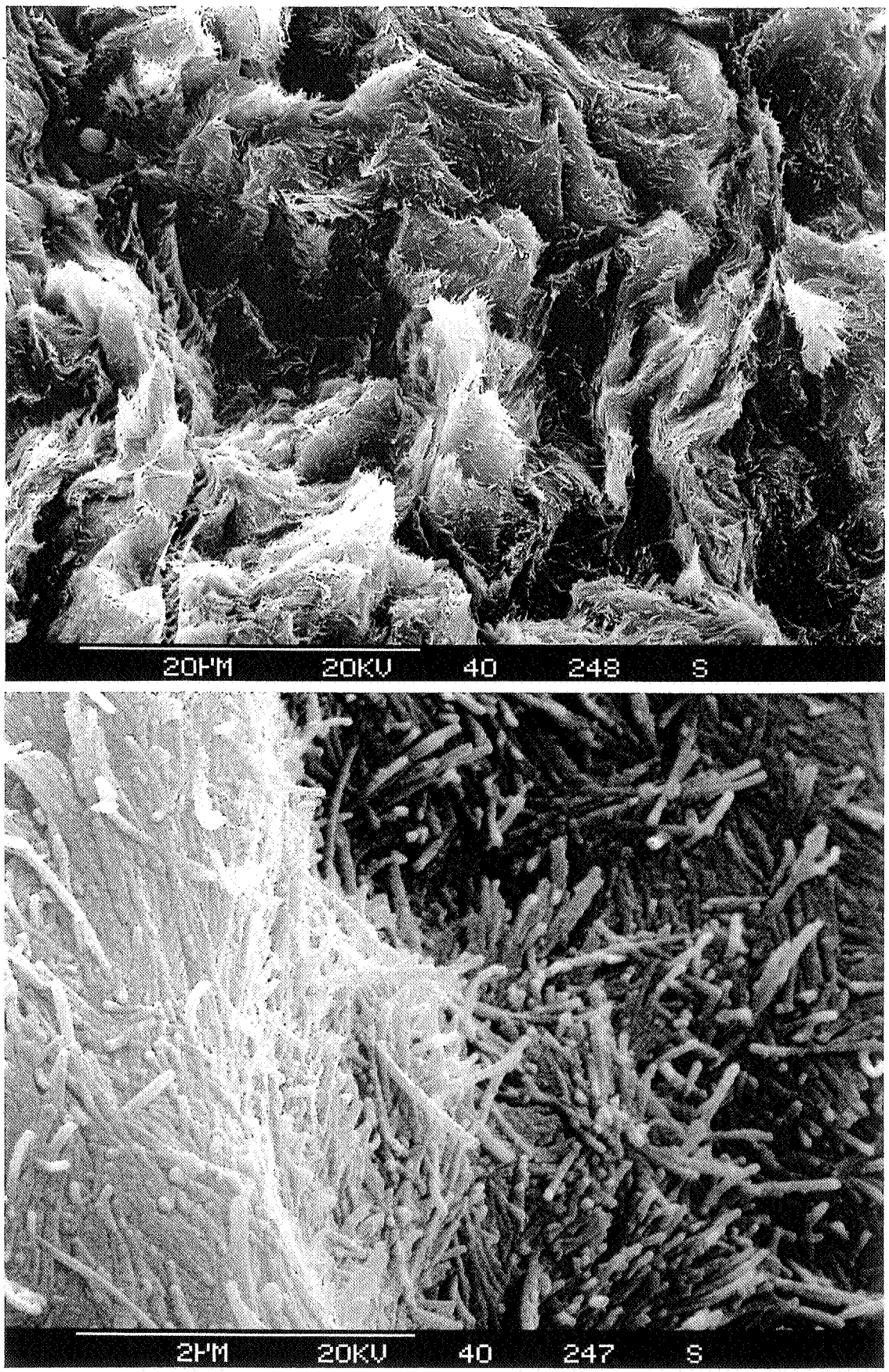


Fig. 6.2. P33 (Lake Floor): Scanning electron micrographs of compact matted palygorskite fibres to 1μm length from Garford Formation clays forming the floor of dry playa, Paly Lake, Garford palaeochannel. Micrograph Nos. 40/248 and 40/247.

ACKNOWLEDGMENTS.

The results in this Report were put together with the help of the following people:
A. Beech (chemical analysis), Dr G. Churchman (clay mineralogy), J. Coppi (photography), P. Davies (thermal analysis), Dr. W. Emerson (colloidal mechanics), P. Fazey (XRF), G. Ferris (water sorption), N. de Lacy (clay-organic complexes), S. McClure (SEM), Dr. K. Norrish (elemental analysis and mineralogy), G. Rinder (drafting), Dr. P. Slade (surface properties and mineralogy) and Dr. R. Taylor (pyroaurite minerals).

APPENDIX 1. QUANTIFICATION OF MINERAL CONTENT BY X-RAY DIFFRACTION.

In order to calibrate XRD for quantitative analysis, mixtures of standard minerals were prepared and the XRD patterns of these mixtures recorded and analysed. The standard samples were:

palygorskite	P33 Lake Floor, washed
dolomite	P33 Upper, washed
illite	P66 19-20m, <0.2μm, washed
halite	crushed analytical grade NaCl
quartz	crushed, acid-washed quartz

The first step in the calibration was to obtain high quality spectra of the standard materials (Figs. A1.1 to A1.5). In all cases Co Kα radiation was used and samples were back pressed into XRD specimen holders. From each XRD spectrum a number of high intensity peaks were chosen and their background-subtracted integrated peak areas obtained. In some cases (e.g. where strong peaks overlapped) a combination of peaks was used. The background subtracted integrated peak areas for the selected peaks are shown in Table A1.1. These values were obtained with a step size of 0.02° 2θ and a count time of 5 secs per step. The standard samples were also run consecutively on the x-ray diffractometer so that there would be no decrease in beam intensity from one sample to the next. The integrated peak areas provide the standards against which the mixtures are calibrated.

For the prepared mixtures of minerals the background subtracted integrated peak area of as many as possible of the standard peaks were measured and ratioed with the corresponding value obtained for the pure standard. In many cases the number of peaks was limited because of the overlap of peaks from the different minerals. The ratios of the peaks in the mixture with the pure samples where then averaged giving the average normalised intensity for each mineral in the sample. By averaging over a number of peaks, variations arising from orientation effects are minimised. The average normalised intensity for the various minerals were ratioed against the average normalised intensity for palygorskite from the sample and correlated with the known

composition of the mixture. The resulting correlations are used as calibrations for quantitative mineral analysis. As the method is based on ratios, changes in tube intensity, step size and count times do not effect the calibration.

Correlations are not valid outside the calibrated range. The calibration and quantification method is designed for samples with measurable palygorskite content, however, the calibrations can be adapted to give approximations to mineral content in samples containing little or no palygorskite by re-ratioing. It should be noted that, because XRD spectra are dependant on crystal shape and composition, the calibration will only be directly applicable to samples from the Garford palaeochannel and should only be used as a guide in other cases.

Dolomite

The correlation between the ratio of the averaged normalised intensity for dolomite and palygorskite and the ratio of illite and palygorskite contents are shown in Table A1.2 and Fig. A1.6. To a first approximation

$$\frac{\text{wt.\% palygorskite}}{\text{wt.\% dolomite}} = 1.53 \pm 0.06 \quad \frac{\text{Av. normalised intensity of palygorskite}}{\text{Av. normalised intensity of dolomite}}$$

or

$$\frac{\text{wt.\% dolomite}}{\text{wt.\% palygorskite}} = 0.65 \pm 0.03 \quad \frac{\text{Av. normalised intensity of dolomite}}{\text{Av. normalised intensity of palygorskite}}$$

Halite

For low halite concentrations the ratio of concentrations varies linearly with the ratio of average normalised intensity.

$$\frac{\text{wt.\% halite}}{\text{wt.\% palygorskite}} = 0.623 \pm 0.03 \quad \frac{\text{Av. normalised intensity of halite}}{\text{Av. normalised intensity of palygorskite}}$$

This relationship is valid only when $\frac{\text{wt.\% halite}}{\text{wt.\% palygorskite}} < 0.15$

Quartz

Quartz content determination is problematic because quartz often shows the effects of preferred orientation. These effects are seen when there is a large variation in the ratio of integrated peak intensities from the sample with unknown quartz content with the standard integrated peak intensities. There is an approximately linear relation between the ratio of concentrations and the ratio of average normalised intensity.

$$\frac{\text{wt.\% quartz}}{\text{wt.\% palygorskite}} = 1.15 \pm 0.10 \; \frac{\text{Av. normalised intensity of quartz}}{\text{Av. normalised intensity of palygorskite}}$$

This relationship is valid only when $\frac{\text{wt.\% quartz}}{\text{wt.\% palygorskite}} < 1$

The relationship rapidly becomes non-linear for concentration ratios greater than 1.

Illite

The determination of illite content requires a slightly different strategy than for other minerals. There are only 2 peaks, at 10.1°2θ and 20.7°2θ (Co Kα radiation), that are diagnostic for illite. The first of these peaks is obscured by the palygorskite peak at 9.8°2θ (Co Kα radiation) and the second is relatively weak and difficult to measure. The majority of the scattered intensity from illite is spread over all angles with no distinct peaks as such. Consequently, for illite it is necessary to use regions diagnostic for illite.

The region of the spectrum that is most suitable for measuring illite content is the angular range from 43.0°2θ to 44.4°2θ (Co Kα radiation) (labelled I in Table A1.1). The intensity in this region correlates strongly with illite content and is free of overlap from scattering by minerals commonly found in Garford palaeochannel samples. The sensitivity of the intensity in this region as a measure of illite content can be increased by subtracting a value representative of the background intensity. A region of background intensity is one that is insensitive to changes in mineral content. Five of these regions were distinguished and their angular ranges are listed in Table A1.1. Any of these 5 regions can be used for calibration purposes; in this study the region 45.8°2θ to 46.1°2θ (Co Kα radiation) was used.

The correlation between the background subtracted, normalised intensity for illite ratioed with the average normalised intensity for palygorskite and the ratio of illite and palygorskite contents are shown in Figs. A1.7a and A1.7b. The intensity ratio given in these figures is

$$(I-B)/[(I_n-B_n) \times (\text{Av. normalised intensity of palygorskite})$$

where

I is the intensity measured in the angular range 43.0°2θ to 44.4°2θ (Co Kα radiation),

B is the intensity measured in the angular range 45.8°2θ to 46.1°2θ (Co Kα radiation),

I_n is the standard intensity given for the angular range 43.0°2θ to 44.4°2θ (Co Kα radiation) in Table A1.1,

B_n is the standard intensity given for the angular range 45.8°2θ to 46.1°2θ (Co Kα radiation) in Table A1.1 and

Av. normalised intensity for palygorskite is the average of the measured palygorskite-peak intensities normalised relative to the intensities given in Table A1.1.

The sensitivity of the calibration can be increased by ratioing the intensity for the region from 43.0°2θ to 44.4°2θ (Co Kα radiation) with that from a region correlated with palygorskite (i.e. negatively correlated with illite). Two such regions are labelled P1 and P2 in Table A1.1. The calibration curves using these 2 regions are shown in Figs. A1.7c and A1.7d.

Although it is weak, the illite reflection at 20.7°2θ (Co Kα radiation) can be used as an approximate determination for illite content. This reflection approximately gives the following linear relationship:

$$\frac{\text{wt.\% illite}}{\text{wt.\% palygorskite}} = 0.625 \frac{\text{Normalised intensity of illite 20.7° peak}}{\text{Av. normalised intensity of palygorskite}} - 0.125$$

The offset (i.e. -0.125) required in this equation shows the approximate nature of the relationship.

Using the calibration

1. Collect spectrum of unknown sample. Step size and count time should be chosen to give enough resolution to adequately integrate peaks. Normally the maximum step size would be 0.05° and the minimum count time per step would be 1 second.
2. Identify minerals present.
3. Measure background subtracted integrated peak areas of as many peaks as possible for each mineral.
4. Ratio integrated peak areas with corresponding integrated peak areas for standard samples (Table A1.1).
5. Average ratios for each mineral thereby obtaining the averaged normalised intensity for each mineral.
6. Ratio average normalised intensity for each mineral with the average normalised intensity for palygorskite.
7. Use calibration, as outlined earlier under individual minerals, to obtain wt.% of mineral ratioed against wt.% palygorskite.
8. Normalise concentrations to 100%.

Table A1.1. Two theta angle (Co Kα radiation) and background-subtracted integrated peak intensities from standard samples.

Palygorskite	9.8°	16.1°	19.1°	20.7°	28.2°	46.9°	48.6°+49.6°			
	24046	3739	2268	433.6	2243	1401	8893			
Dolomite	36.1°	39.2°	41.3°	43.7°	48.2°	51.3°	52.7°	57.9°	59.5°+60.1°	
	44109	2924	2749	4122	14833	2059	8485	2794	29797	
Halite	37.0°	53.3°	63.4°	66.6°						
	100036	33410	1698	11384						
Quartz	24.3°	31.0°	42.7°	46.2°	47.2°	49.7°	53.7°	58.9°	70.9°	
	12931	63727	10836	6881	4290	4515	6488	32520	19997	
Illite			I	P1	P2	Background →				
	10.1°	20.7°	43.0°-44.4°	48.5°-50.0°	58.3°-61.0°	45.8°-46.1°	55.4°-56.0°	57.0°-57.4°	12.0°-13.0°	14.5°-15.0°
	3242	834	10007	6256	5318	1150	1416	875	1786	886

Table A1.2. Calibration for dolomite relative to palygorskite.

wt.% paly/wt.% dol	I_{paly}/I_{dol}	I_{dol}/I_{paly}	wt.% dol/wt.% paly
		0.00	0.00
		0.04	0.02
		0.06	0.04
		0.10	0.06
		0.14	0.08
		0.16	0.10
6.00	4.00	0.25	0.17
5.00	3.33	0.30	0.20
4.00	2.68	0.37	0.25
3.33	2.15	0.47	0.30
3.00	1.95	0.51	0.33
2.50	1.58	0.63	0.40
2.00	1.25	0.80	0.50
1.67	1.00	1.00	0.60
1.43	0.85	1.18	0.70
1.25	0.76	1.32	0.80
1.11	0.67	1.50	0.90
1.00	0.61	1.63	1.00
0.90	0.55	1.82	1.11
0.80	0.49	2.04	1.25
0.70	0.43	2.33	1.43
0.60	0.38	2.63	1.67
0.50	0.34	2.97	2.00
0.40	0.29	3.45	2.50
0.33	0.26	3.90	3.00
0.30	0.24	4.18	3.33
0.25	0.21	4.68	4.00
0.20	0.19	5.35	5.00
0.17	0.17	5.89	6.00
0.10	0.13		
0.08	0.10		
0.06	0.08		
0.04	0.06		
0.02	0.03		
0.00	0.00		

Fig. A1.1. Reference palygorskite. P33 Lake floor. Triple washed.

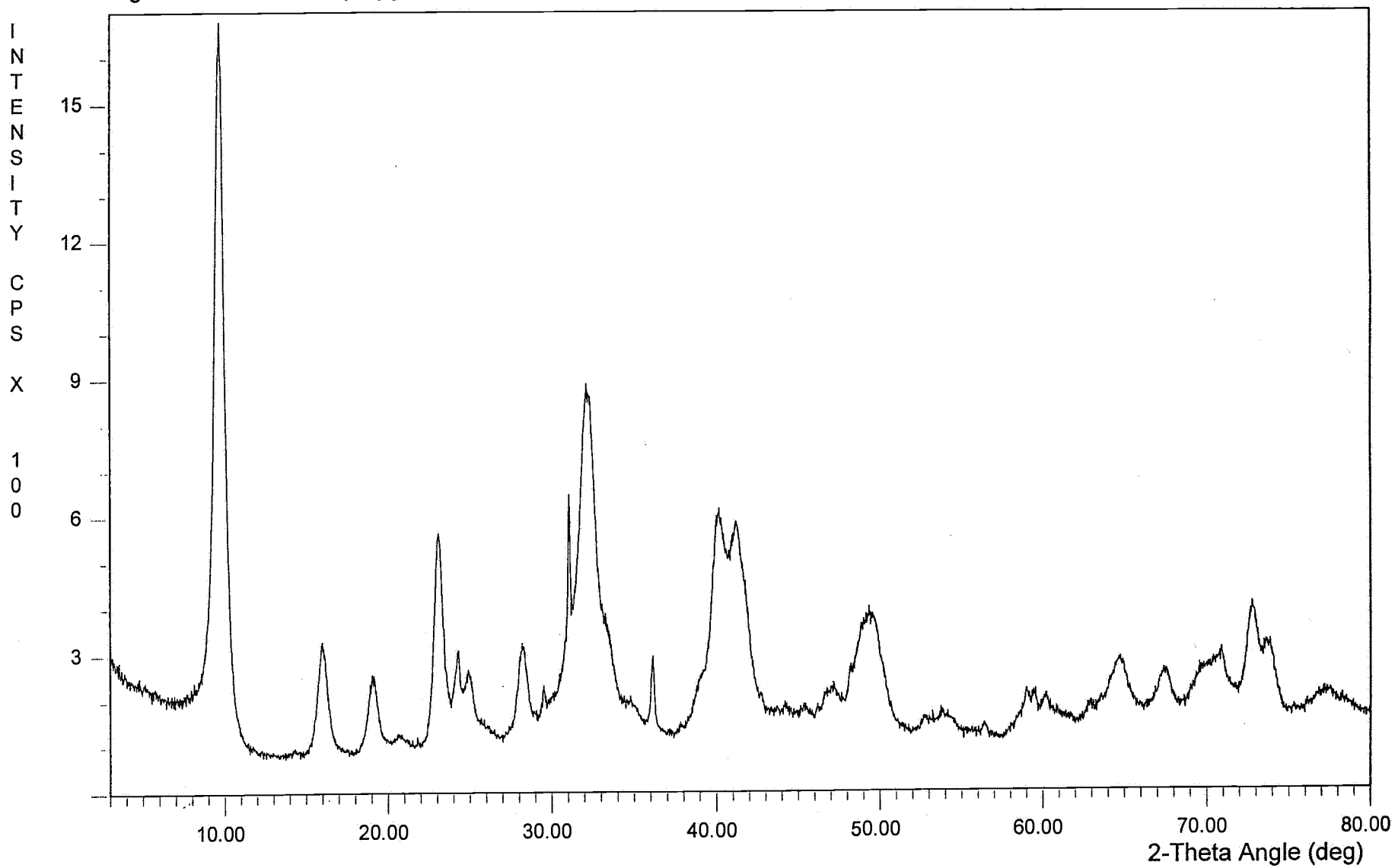


Fig. A1.1. XRD spectrum (Co Kα radiation, back pressed) of Garford palaeochannel sample P33 Lake Floor (palygorskite).

000537

Fig. A1.2. Reference dolomite. P33 Upper. Washed.

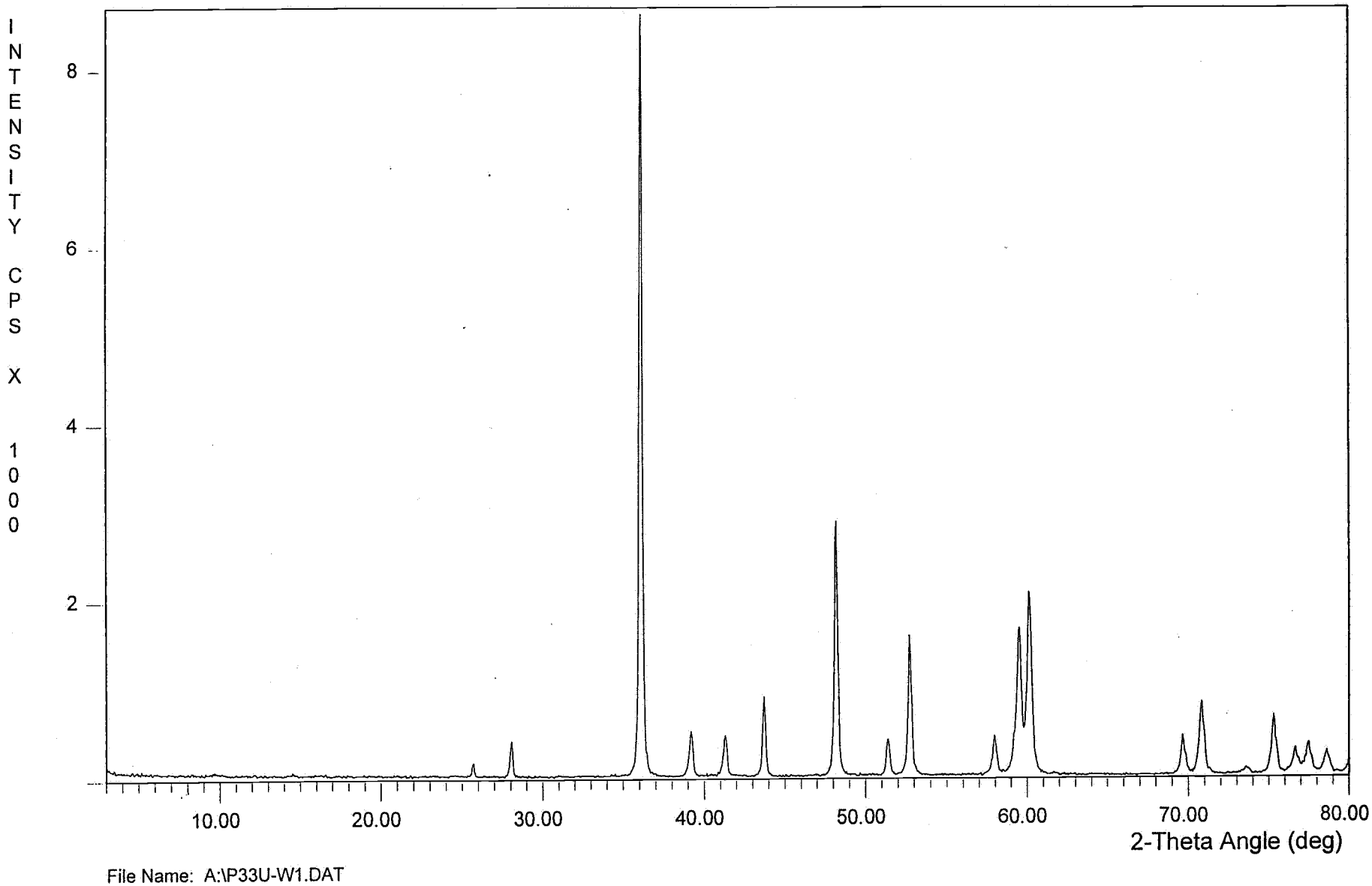


Fig. A1.2. XRD spectrum (Co Kα radiation, back pressed) of Garford palaeochannel sample P33 Upper (dolomite).

000538

Fig. A1.3. Reference halite. Crushed NaCl.

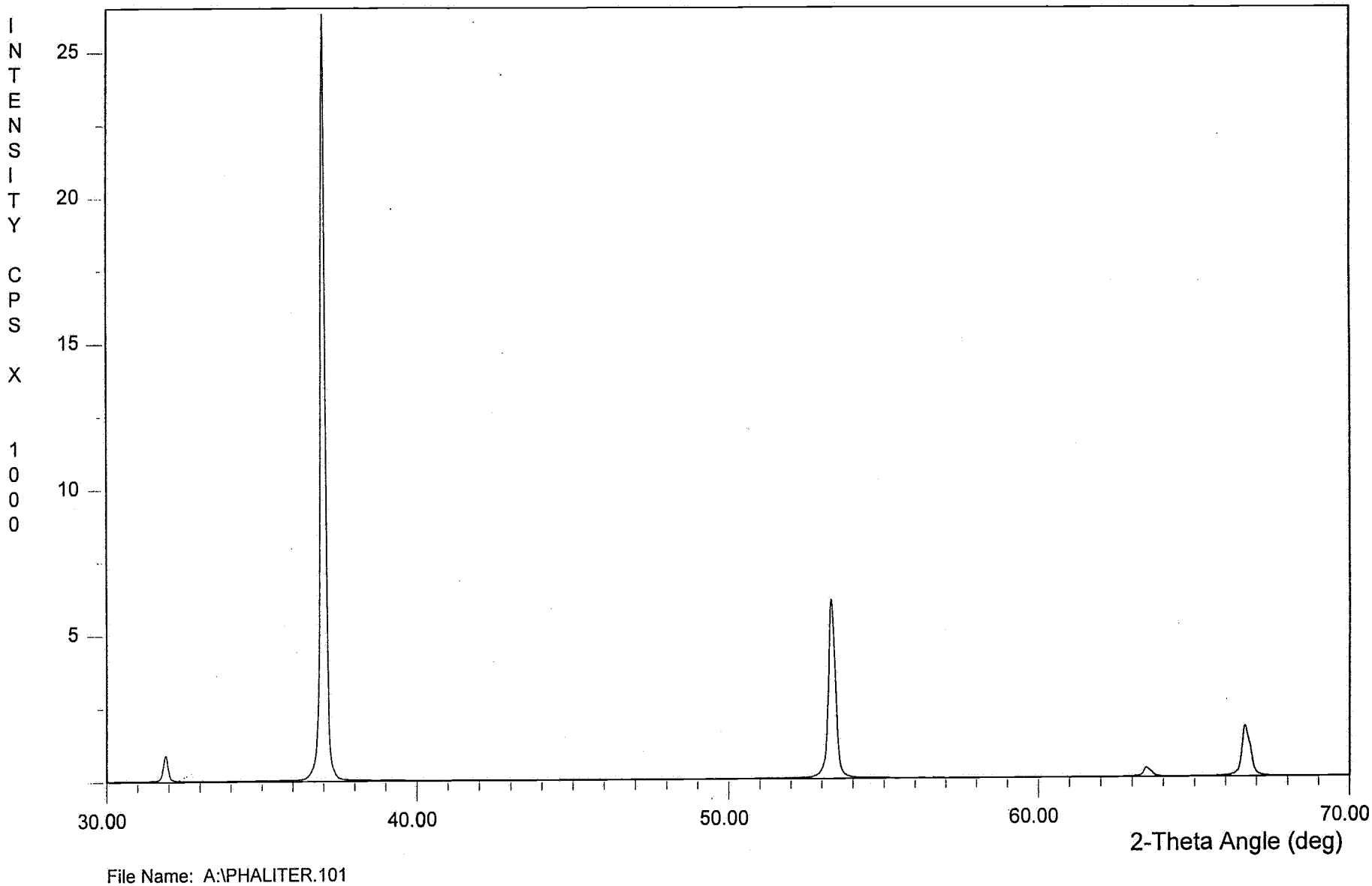


Fig. A1.3 XRD spectrum (Co Kα radiation, back pressed) of crushed NaCl (halite).

000539
166

Fig. A1.4. Reference quartz. Crushed acid-washed quartz.

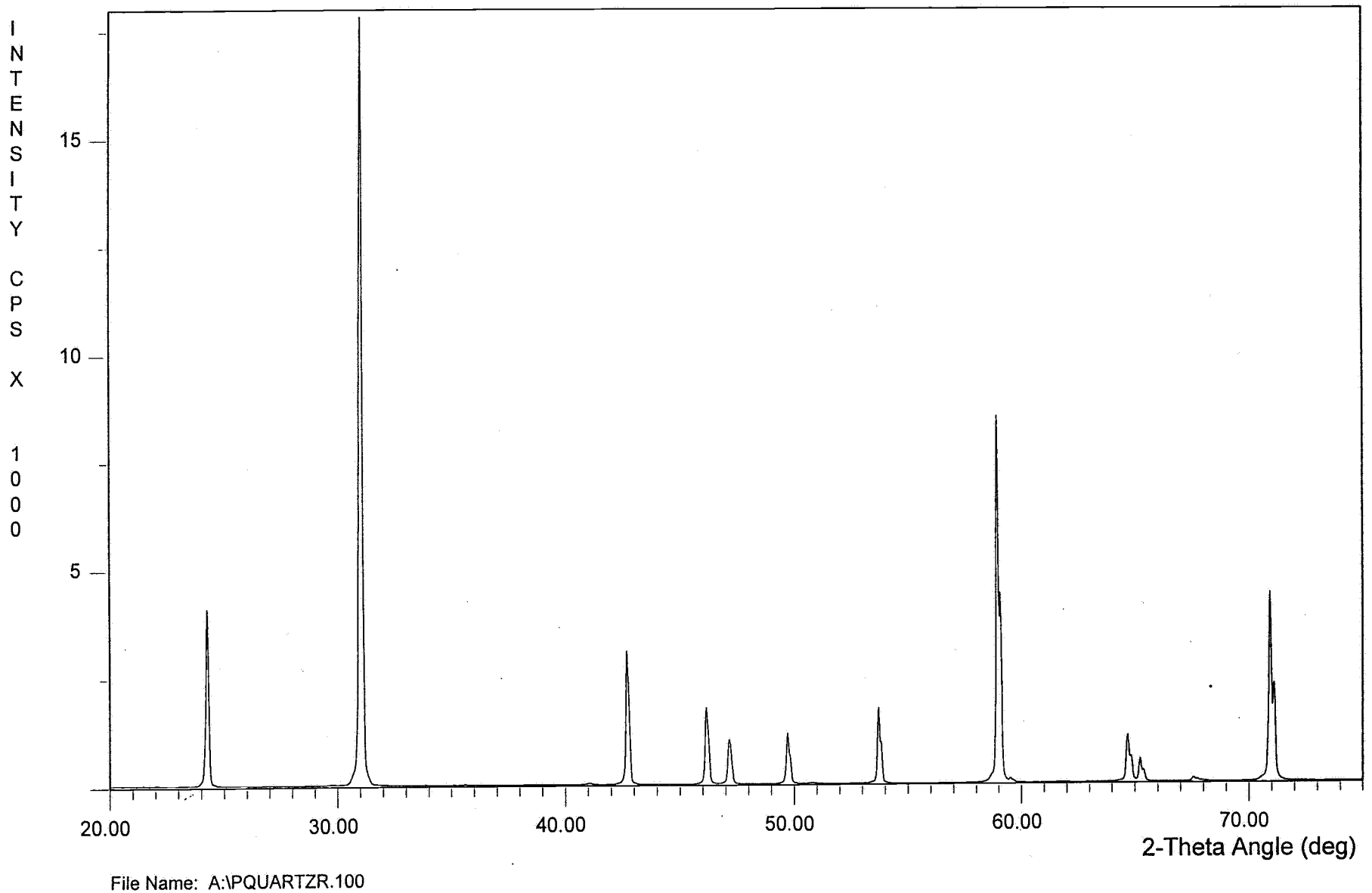


Fig. A1.4. XRD spectrum (Co Kα radiation, back pressed) of crushed acid-washed quartz.

Fig. A1.5. Reference illite. P66 19-20m. <0.2um.

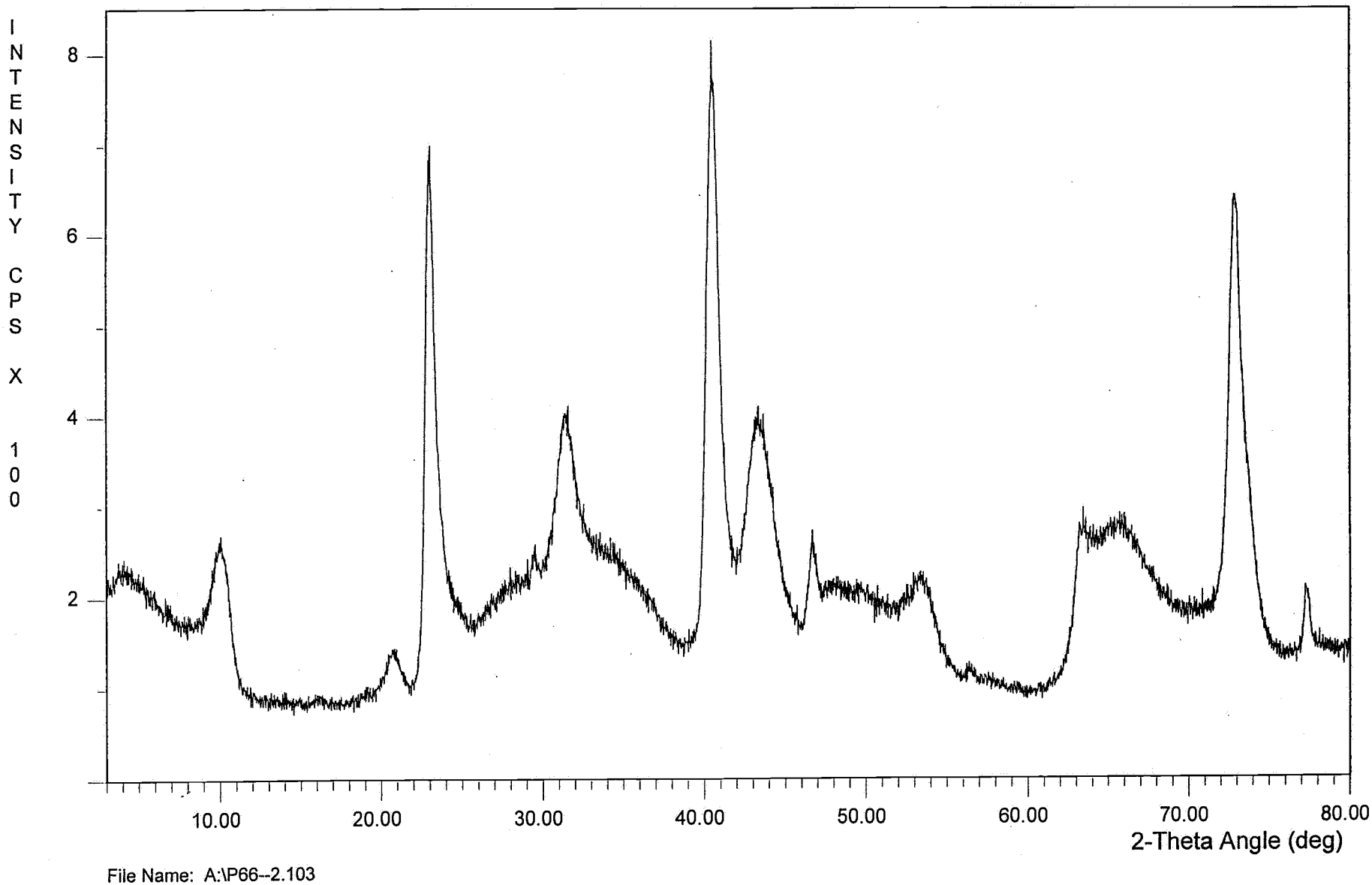


Fig. A1.5. XRD spectrum (Co Kα radiation, back pressed) of Garford palaeochannel sample P66 19-20m (illite).

000541
168

Fig. A1.6a. Calibration of dolomite relative to palygorskite.

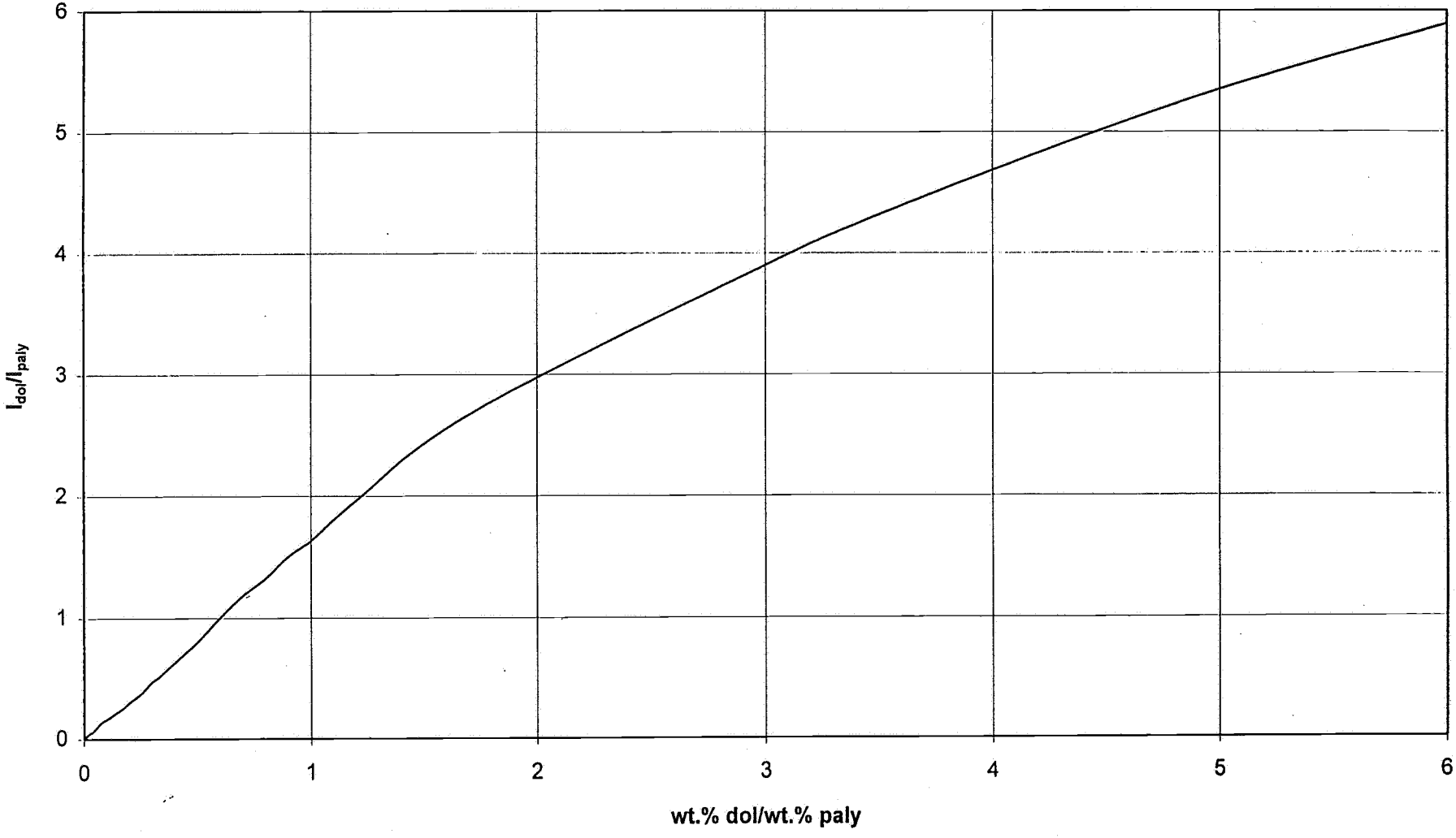


Fig. A1.6a. Calibration of dolomite content relative to palygorskite content using the ratio of averaged normalised intensities.

000542
169

Fig. A1.6b. Calibration of palygorskite relative to dolomite.

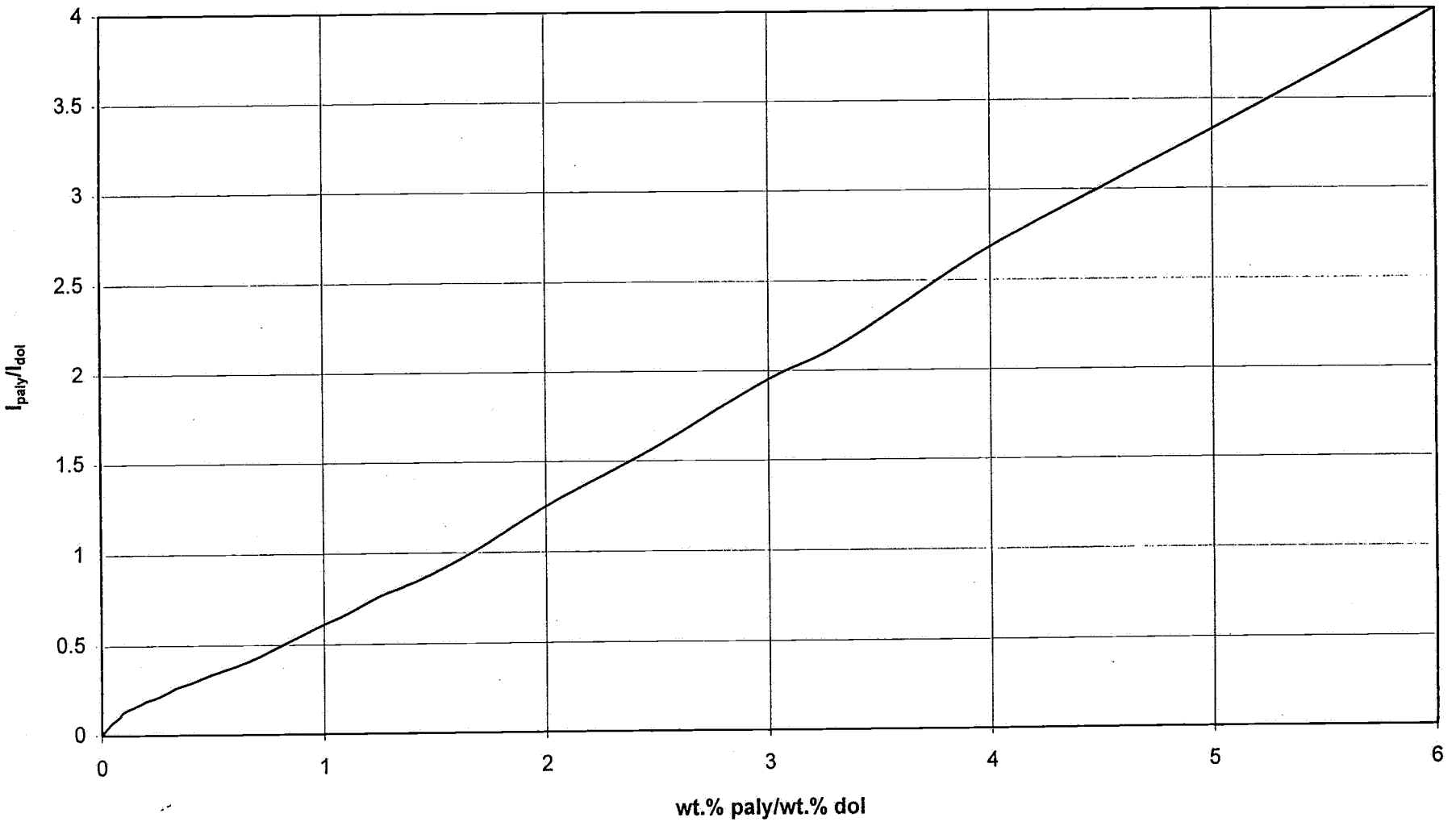


Fig. A1.6b. Calibration of palygorskite content relative to dolomite content using the ratio of averaged normalised intensities.

Fig. A1.7a. Calibration of illite relative to palygorskite.

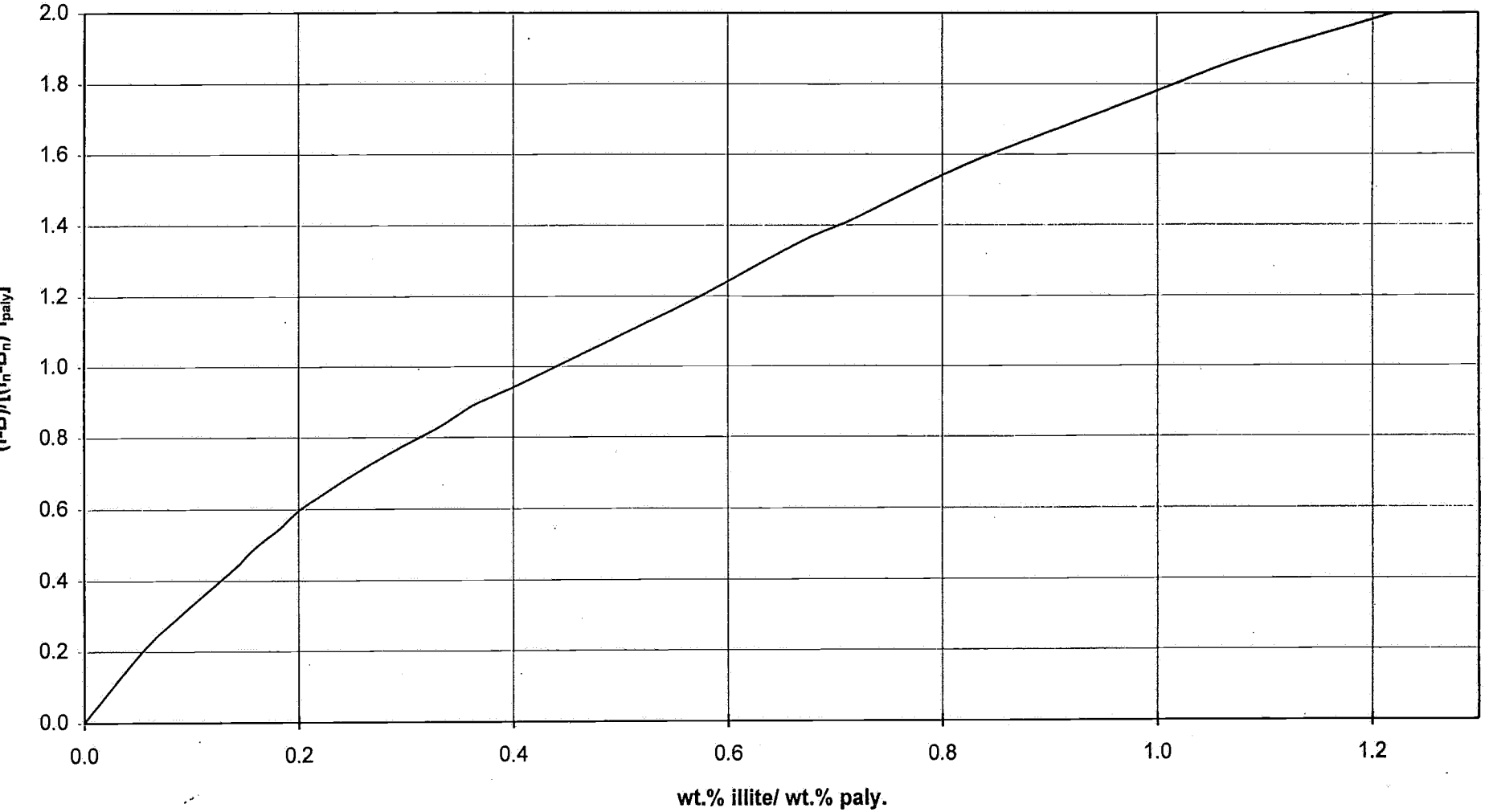
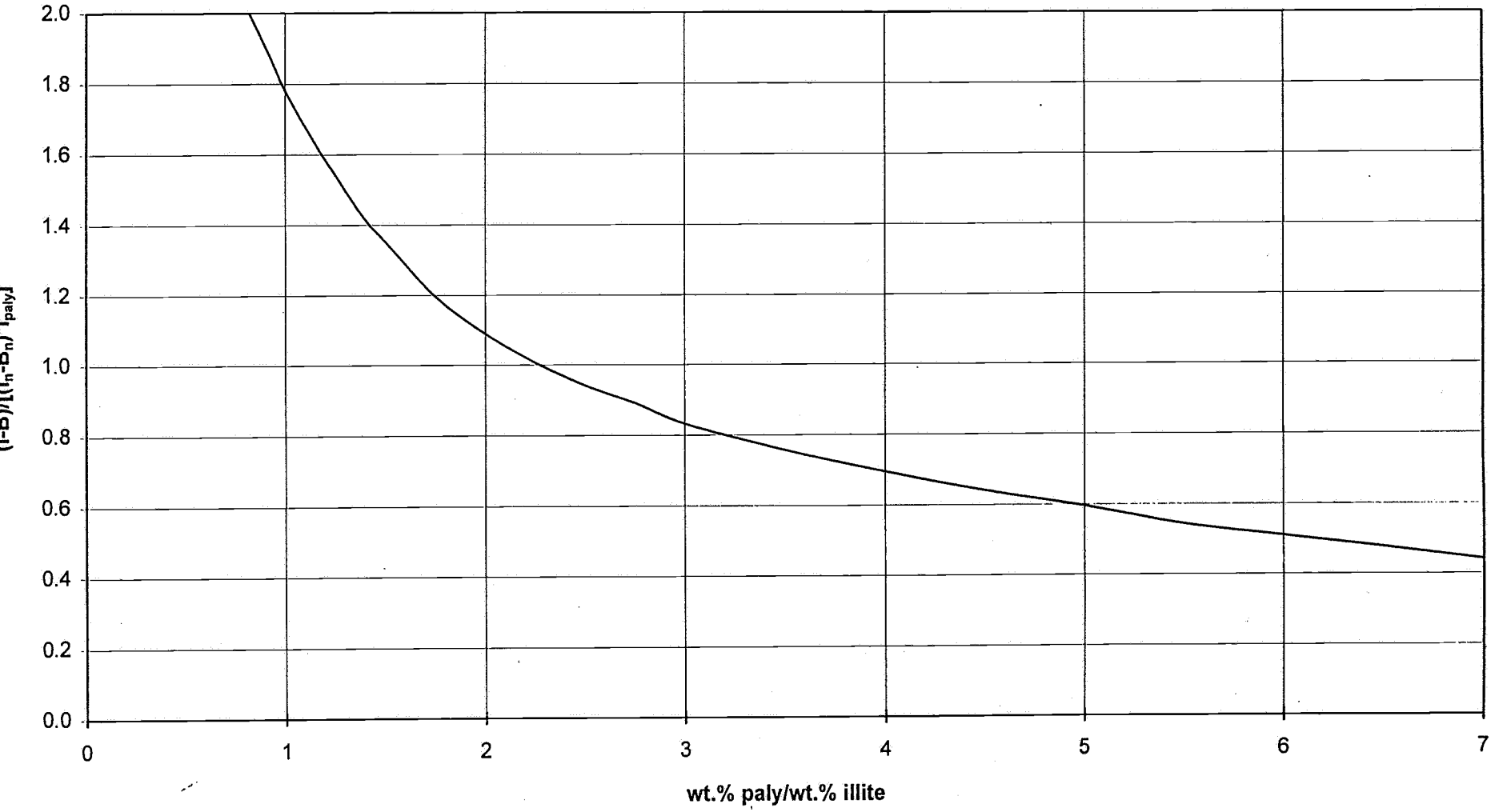


Fig. A1.7a. Calibration of illite content relative to palygorskite content using $(I-B)/[(I_n-I_{Bn})xI_{paly}]$ (see text).

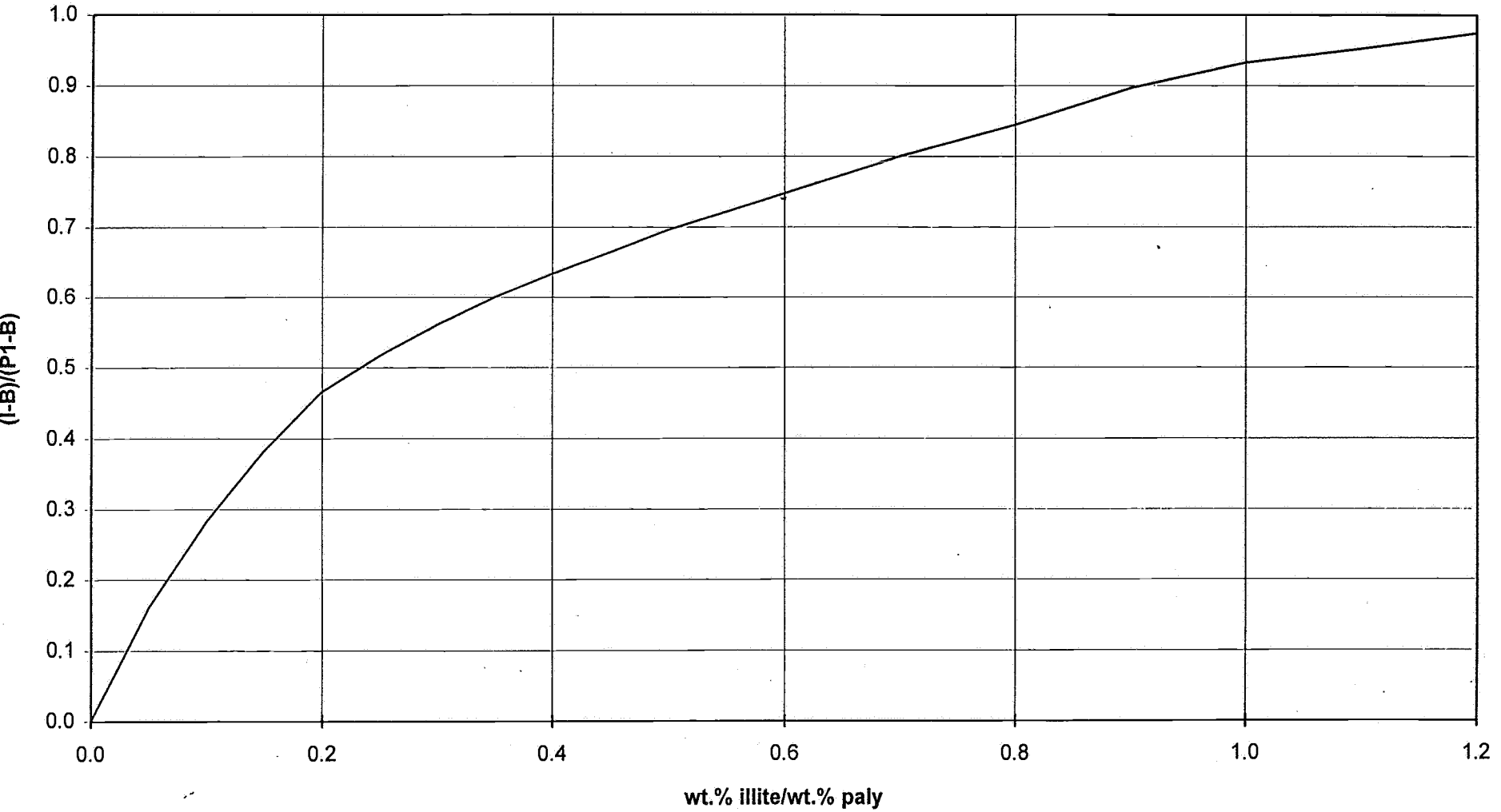
Fig. A1.7b. Calibration of palygorskite relative to illite.



000545
172

Fig. A1.7b. Calibration of palygorskite content relative to illite content using $(I-B)/[(I_n-I_{Bn})xI_{paly}]$ (see text).

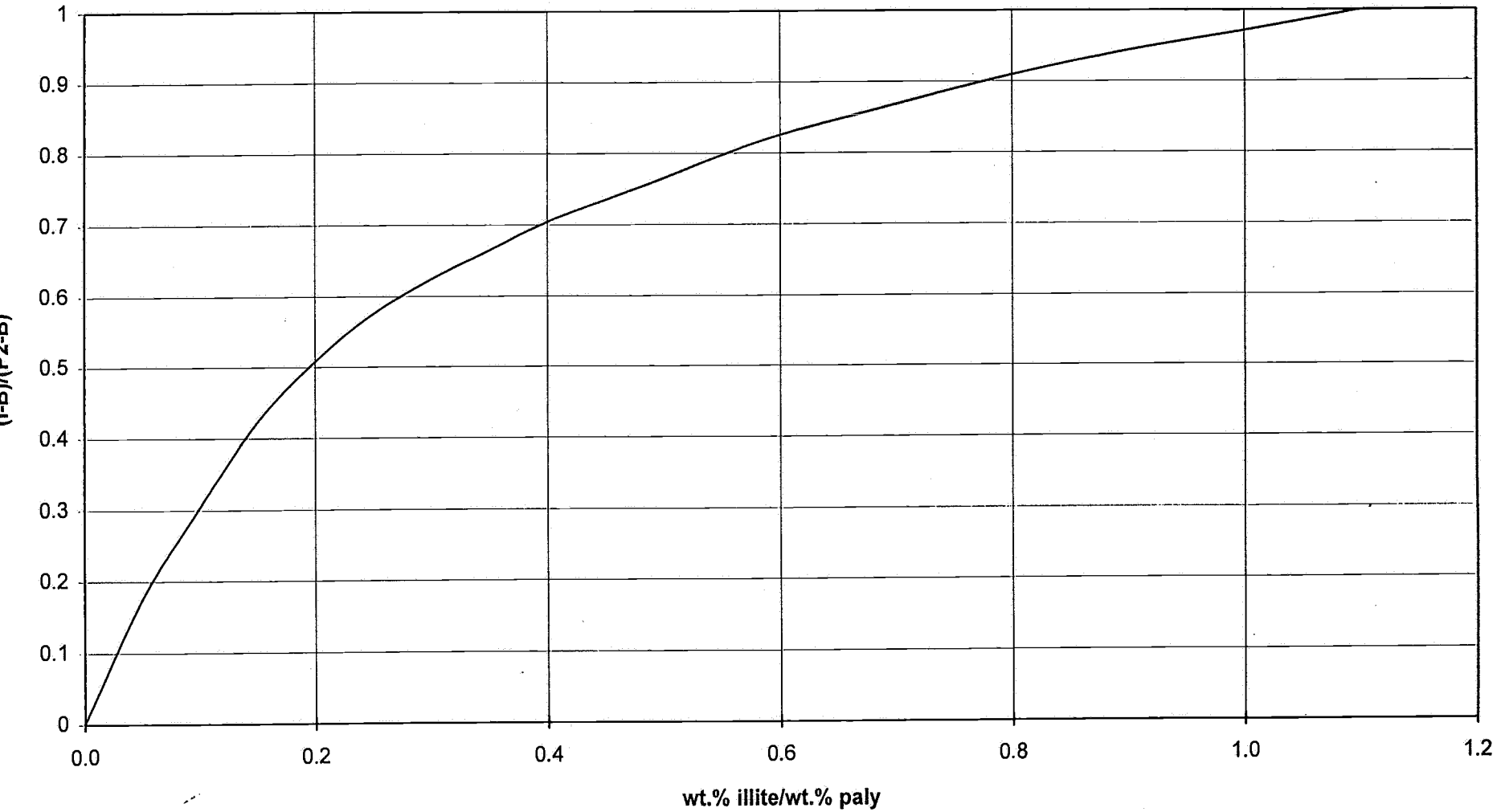
Fig. A1.7c. Calibration of illite relative to palygorskite.



0005546
173

Fig. A1.7c. Calibration of illite content relative to palygorskite content using (I-B)/(P1-B) (see text and Table A1.1).

Fig. A1.7d. Calibration of illite relative to palygorskite.



0000547
174

Fig. A1.7d. Calibration of illite content relative to palygorskite content using (I-B)/(P2-B) (see text and Table A1.1).

APPENDIX 2. MINERALOGY OF ALL SAMPLES FROM THE GARFORD PALAEOCHANNEL.

The tables presented in this Appendix list the mineralogy of a Garford palaeochannel samples studied in the course of the Absorbent Clay Project. Care should be taken when comparing the analyses of samples from previous studies (i.e. P24 to P43) with those from the present study because of the differences in the method of analysis. The second table lists the renormalised mineralogical content in order of decreasing palygorskite after the exclusion of quartz and halite.

The key to the mnemonics used in the tables is as follows:
Paly = palygorskite; Ill = illite; Dol = dolomite; Hal = halite; Qtz = quartz;
Smt = smectite (includes randomly interstratified and very-poorly crystalline material);
Kaol = kaolinite; Cal = calcite; Gyp = gypsum; Cel = celestine; An = anatase.
Tr = trace.

Table A2.1. Mineralogy (wt.%) of all studied samples from the Garford palaeochannel..

Sample	XRD File	Paly	Ill	Dol	Hal	Qtz	Smt	Kaol	Cal	Gyp	Cel	An	Other
P24 0-1m	P24-0-1.107	15	-	75	5	2	-	-	-	-	1	-	
P24 1-1.5m	P24-1-2.109	60	7	20	6	5	-	-	-	2	-	-	
P24 2-3m	P24-1-3.108	55	25	7	6	4	-	-	-	-	-	-	
P25 0-1m	P250-1	7	-	90	2	2	-	-	-	-	-	-	
P25 1-2m	P251-2	15	-	80	2	5	-	-	-	-	-	-	
P25 2-3m	P252-3	35	45	10	5	5	-	-	-	-	-	-	
P25 3-4m	P253-4	35	40	9	7	9	-	-	-	-	-	-	
P25 4-5m	P254-5	35	55	2	4	6	-	-	-	-	-	-	
P25 5-6m	P255-6	25	60	<1	4	8	-	-	-	-	-	-	
P25 6-7m	P256-7	20	65	<1	4	4	-	4	-	-	-	-	
P25 7-9m	P257-9	25	50	<1	5	9	-	8	-	-	-	-	
P26 0-1m	P260-1.101	15	-	80	3	4	-	-	-	-	<1	-	
P26 1-2m	P261-2.102	25	6	65	2	1	-	Tr	-	-	Tr	-	
P26 2-3m	P262-3.103	25	2	65	2	1	-	Tr	-	-	Tr	-	
P26 3-4m	P263-4A.DAT	35	-	60	2	1	-	-	-	-	Tr	-	
P26 4-5m	P264-5.105	15	-	80	3	1	-	Tr	-	-	Tr	-	
P26 5-6m	P265-6.106	15	-	80	3	Tr	-	Tr	-	-	Tr	-	
P26 6-6.5m	P266-7.107	10	20	-	5	15	45	Tr	-	-	-	Tr	
P29 6.9-9m	P29-6-9.DAT	10	-	85	1	1	-	-	-	1	-	-	
P30 0-1m	P300-1	7	10	65	2	15	-	-	-	-	-	-	
P30 1-2m	P301-2	15	-	85	2	<1	-	-	-	-	-	-	
P30 2-3m	P302-3	15	-	85	2	1	-	-	-	-	-	-	
P30 3-4m	P303-4	30	20	50	3	<1	-	-	-	-	-	-	
P30 4-6m	P304-5	7	-	45	3	3	40	-	-	-	2	-	
P31 2-3.5m	P312-3.108	10	-	90	1	1	-	-	-	-	-	-	
P31 3.5-5m	P314-5.110	8	-	90	1	2	-	-	-	-	-	-	
P31 5-6m	P315-6.111	20	-	80	1	1	-	-	-	-	-	-	
P31 6-7m	P316-7.112	-	-	-	6	-	90	Tr	-	-	-	-	
P33 0-1.5m	P33-0-1.106	90	-	3	4	2	-	Tr	-	-	-	-	
P33 1.5-2m	P33-1-2.107	20	-	75	2	2	-	-	-	-	-	-	
P33 2-3m	P33-2-3.108	30	-	60	5	5	-	Tr	-	-	-	-	

0005549

Table A2.1 (continued).

Sample	XRD File	Paly	Ill	Dol	Hal	Qtz	Smt	Kaol	Cal	Gyp	Cel	An	Other
P34 1-2m	P341-2	30	-	65	2	-	-	-	-	-	-	-	
P34 2-3m	P342-3	20	-	75	1	2	-	-	-	-	-	-	
P34 3-4m	P343-4	35	-	65	2	1	-	-	-	-	-	-	
P34 4-5m	P344-5	25	-	70	2	1	-	-	-	-	-	-	
P34 5-6m	P345-6	25	-	75	2	-	-	-	-	-	-	-	
P34 6-6.5m	P346-7	10	-	85	2	-	-	-	-	-	-	-	
P35 2-3m	P352-3.113	30	-	65	1	<1	-	-	-	-	-	-	
P35 3-4m	P353-4.114	35	-	65	1	1	-	-	-	-	-	-	
P35 4-5m	P354-5.115	35	-	65	1	<1	-	-	-	-	-	-	
P35 5-6m	P355-6.116	30	-	70	<1	1	-	-	-	-	-	-	
P35 6-7m	P356-7.117	50	-	45	5	<1	-	-	-	-	-	-	
P35 7-8m	P357-8.118	35	30	30	4	<1	-	-	-	-	-	-	
P35 8-9m	P358-9.119	20	15	60	3	<1	-	-	-	-	-	-	
P36 2-3m	P362-3.101	30	-	65	3	-	-	-	-	-	-	-	
P36 3-4m	P363-4.102	15	-	40	3	20	-	-	-	25	-	-	
P36 4-5m	P364-5.103	25	-	65	1	9	-	-	-	Tr	-	-	
P36 5-6m	P365-6.104	25	-	65	2	7	-	-	-	1	-	-	
P36 6-8m	P366-8.DAT	30	-	60	2	7	-	-	-	-	-	-	
P36 8-9m	P368-9.107	35	-	55	2	7	-	-	-	-	-	-	
P37 0-1m	P370-1.108	30	-	65	3	3	-	-	-	-	-	-	
P37 1-2m	P371-2.109	35	-	55	1	6	-	-	-	-	1	-	
P37 2-3m	P372-3.110	45	-	45	5	2	-	-	-	-	Tr	-	
P37 3-4m	P373-4.111	45	-	50	5	2	-	-	-	-	Tr	-	
P37 4-5m	P374-5.112	20	15	60	7	2	-	-	-	-	Tr	-	
P37 5-6m	P375-6.113	15	15	60	6	2	-	-	-	-	Tr	-	
P37 6-7.5m	P376-7.114	15	60	10	7	<1	-	-	-	-	-	-	
P38 1-2m	P381-2.115	45	-	55	2	1	-	-	-	-	-	-	
P38 3-4m	P383-4.116	30	15	45	3	<1	-	-	-	-	5	-	
P38 4-5m	P384-5.117	25	15	55	3	<1	-	-	-	-	-	-	
P38 5-5.5m	P385-6.118	25	10	55	3	<1	-	Tr	-	-	Tr	-	

Table A2.1 (continued).

Sample	XRD File	Paly	Ill	Dol	Hal	Qtz	Smt	Kaol	Cal	Gyp	Cel	An	Other
P40 0-1m	P40-0-1.201	20	-	75	5	<1	-	-	-	1	-	-	
P40 1-2m	P40-1-2.202	15	-	85	2	<1	-	-	-	-	-	-	
P40 2-3m	P40-2-3.203	20	Tr	75	3	-	-	-	-	-	-	-	
P40 3-4m	P40-3-4.204	30	-	60	7	1	-	-	-	-	1	-	
P40 4-5m	P40-4-5.205	20	-	70	5	5	-	-	-	-	<1	-	
P40 5-6m	P40-5-6.206	20	10	60	8	<1	-	-	-	1	-	-	
P40 6-7.5m	P40-6-7.207	10	45	15	15	6	-	-	-	-	1	-	
P41 0.3-1m	P41-0-1.301	20	-	65	2	10	-	-	-	-	-	-	
P41 1-2m	P41-1-2.302	25	-	70	3	2	-	-	-	-	-	-	
P41 2-3m	P41-2-3.303	30	5	55	5	1	-	-	-	-	-	-	
P41 3-4m	P41-3-4.304	20	7	60	6	<1	-	-	-	-	-	-	
P41 4-4.5m	P41-4-4~.305	50	10	20	15	2	-	-	-	-	-	-	
P42 0.3-1m	P420-1	50	-	50	6	5	-	-	-	-	-	-	
P42 1-2m	P421-2	35	-	55	4	3	-	-	-	-	-	-	
P42 2-3m	P422-3	30	-	50	7	15	-	-	-	-	Tr	-	
P42 3-5m	P423-4, 4-5	30	8	50	8	2	-	-	-	-	Tr		
P42 5-6m	P425-6	15	15	50	9	3	7	-	-	-	Tr	-	
P42 6-7m	P426-7	20	25	40	9	3	-	-	-	-	Tr	-	
P42 7-8m	P427-8	5	15	15	8	5	45	-	-	-	-	Tr	
P42 8-9m	P428-9	<1	5	6	5	40	40	-	-	-	-	Tr	
P43 0.1-1m	P43-0-1.101	25	-	70	5	<1	-	-	-	-	-	-	
P43 1-1.5m	P43-1-2.102	30	-	60	7	<1	-	-	-	-	-	-	
P43 1.5-2.5m	P43-2-2~.103	25	4	65	7	1	-	-	-	-	Tr	-	
P43 2.5-3m	P43-2~5-.104	40	8	30	15	<1	5	-	-	-	-	-	
Quartz Boulder	3249-BLK.101	-	~3	-	~6	~15	0-5	~75	-	-	-	-	
P33 Upper	3250-BLK.102	0-3	-	94-98	1-3	<1	-	-	-	-	-	-	
P33 Middle	3251-BLK.103	5-8	-	80-85	4-6	2-4	-	-	-	1-3	-	-	
P33 Lake Floor	3252-BLK.104	33-38	4-6	-	15-19	40-45	-	-	-	-	-	-	
P44 0-1m	3253-BLK.105	Tr	-	92-98	4-6	-	-	-	-	-	-	-	
P44 0.2-1m	3254-BLK.106	2-6	-	73-79	4-6	12-18	-	-	-	-	-	-	

000551

Table A2.1 (continued).

Sample	XRD File	Paly	Ill	Dol	Hal	Qtz	Smt	Kaol	Cal	Gyp	Cel	An	Other
P45 0-1m	3255-BLK.107	0-3	-	90-95	4-6	0-1	-	-	-	-	-	-	
P45 1-1.5m	3256-BLK.108	0-1	-	92-96	3-5	1-2	-	-	-	-	-	-	
P45 1.5-1.7m	3257-BLK.109	3-7	1-3	82-87	4-6	1-2	-	-	-	-	-	-	
P46 0-0.6m	3258-BLK.110	3-6	0-2	87-93	3-5	0-1	-	-	-	-	-	-	
P47 0-1m	3259-BLK.111	-	-	92-96	3-5	<1	0-2	-	-	Tr	-	-	
P48 Green clay	3260-BLK.112	-	8-12	-	2-4	62-68	5-10	5-10	-	Tr	-	Tr	Microcline ~ 5 Albite ~ 3
P48 0-1m	3261-BLK.113	0-2	-	94-98	1-3	<1	-	-	-	-	-	-	
P48 1-1.7m	3262-BLK.114	0-3	-	94-98	1-2	1-2	-	-	-	-	-	-	
P49 0-0.2m	3263-BLK.115	4-8	4-8	0-1	2-4	72-78	5-10	5-10	-	-	-	-	Microcline - Tr
P49 Black nodule	3264-BLK.116	-	-	-	-	12-18	-	-	~85	-	-	-	Microcline - Tr
P50 0-0.7m	3265-BLK.117	-	-	94-98	1-3	1-3	-	-	-	-	-	-	
P51 0-1m	3266-BLK.118	0-3	-	86-92	2-4	5-7	-	-	-	-	-	-	
P52 0-1m	3267-BLK.119	7-10	<1	76-82	4-6	2-4	-	-	-	3-6	-	Tr	Barite - Tr
P53 0.6-1m	3269-BLK.201	9-13	1-4	76-82	4-6	2-4	-	-	-	-	-	Tr	
P53 1-1.5m	3268-BLK.120	20-24	3-6	55-59	7-10	5-8	-	-	-	1-2	-	-	
P54 0.1-0.6m	3270-BLK.202	13-16	2-4	70-74	7-10	1-3	-	-	-	-	-	-	
P55 Upper grey clay	3271-BLK.203	3-7	3-7	-	6-10	38-42	15-20	1-5	1-2	~20	-	Tr	
P55 0-0.7m	3272-BLK.204	2-4	-	82-88	3-5	0-1	5-10	-	-	Tr	-	-	
P56 0.3-0.6m	3273-BLK.205	4-7	<1	86-92	2-4	2-3	-	-	-	-	-	-	
P57 0.1-0.6m	3274-BLK.206	19-23	4-6	58-62	7-10	5-7	-	-	-	-	-	-	
P61 6-8m	3375-BLK.101	5-10	20-30	1-5	1-3	20-30	5-10	20-30	1-5	-	-	Tr	
P61 8-10m	3376-BLK.102	5-10	20-30	15-25	1-4	15-25	5-10	10-20	1-3	-	-	Tr	
P61 10-11m	3377-BLK.103	33-38	20-22	18-20	5-7	18-20	-	-	-	-	-	-	
P61 11-12m	3378-BLK.104	23-28	12-15	11-13	4-6	42-48	-	-	Tr	-	-	-	
P61 12-13m	3379-BLK.105	36-40	10-12	9-11	3-5	36-39	-	-	Tr	-	-	-	
P61 13-14m	3380-BLK.106	23-28	55-60	2-5	5-7	5-10	-	-	-	-	-	-	
P61 14-15m	3381-BLK.107	15-20	60-65	1-4	<1	16-20	-	-	-	-	-	-	

Table A2.1 (continued).

Sample	XRD File	Paly	Ill	Dol	Hal	Qtz	Smt	Kaol	Cal	Gyp	Cel	An	Other
P65 6-7m	3382-BLK.108	11-15	0-2	80-85	1-3	2-5	-	-	-	-	-	-	
P65 7-8m	3383-BLK.109	1-3	<1	93-98	0-1	1-3	-	-	-	-	-	-	
P65 8-9m	3384-BLK.110	1-3	<1	93-98	1-2	1-2	-	-	-	-	-	-	
P65 9-10m	3385-BLK.111	39-43	6-8	31-35	5-7	11-15	-	-	-	-	-	-	
P65 10-11m	3386-BLK.112	39-43	23-28	2-3	5-7	20-25	1-5	-	-	-	-	-	
P65 11-12m	3387-BLK.101	31-34	23-28	1-2	5-7	20-25	10-15	-	-	-	-	Tr	
P65 12-13m	3388-BLK.102	39-43	9-13	31-35	3-5	7-9	1-5	-	-	-	-	Tr	
P65 13-14m	3389-BLK.103	42-46	23-28	1-2	5-7	8-11	10-15	-	-	-	-	Tr	
P65 14-15m	3390-BLK.104	5-10	35-40	0-1	2-3	30-35	15-20	-	-	-	-	Tr	
P65 15-16m	3391-BLK.105	4-7	55-60	<1	3-5	12-16	15-20	-	-	-	-	Tr	
P65 16-17.5m	3392-BLK.106	5-10	55-60	<1	4-6	11-15	15-20	-	-	-	-	Tr	
P66 14-15m	3393-BLK.107	9-13	0-2	80-85	1-3	3-6	-	-	-	-	-	-	
P66 15-16m	3394-BLK.108	24-28	4-6	50-55	2-5	11-15	-	-	-	-	-	-	
P66 16-17m	3395-BLK.109	42-47	6-10	25-28	5-9	4-6	5-10	-	-	-	-	Tr	
P66 17-18m	3396-BLK.110	9-13	8-12	6-10	4-6	55-60	7-12	-	-	-	-	Tr	
P66 18-19m	3397-BLK.111	7-10	45-55	1-2	3-5	17-20	15-20	-	-	-	-	Tr	
P66 19-20m	3398-BLK.112	2-5	65-75	0-1	4-6	4-7	15-20	-	-	-	-	-	
P67 14-15m	3399-BLK.100	30-35	8-12	39-43	5-9	5-10	0-5	-	-	-	-	-	
P67 15-16m	3400-BLK.101	22-27	19-23	37-41	4-6	5-10	0-5	-	-	-	-	-	
P67 16-17m	3401-BLK.102	35-40	25-30	2-4	6-9	15-20	5-10	-	-	-	-	-	
P68 11-12m	3402-BLK.104	27-33	30-35	15-19	3-5	7-11	5-10	-	-	-	-	-	
P68 12-13m	3403-BLK.105	11-15	8-12	67-73	1-3	1-3	0-5	-	-	-	-	-	
P68 13-14m	3404-BLK.106	10-14	8-12	62-67	1-3	7-12	0-5	-	-	-	-	-	
P69 9-10m	3405-BLK.107	22-26	17-21	20-25	1-3	27-33	0-5	-	-	-	Tr	-	
P69 10-11m	3406-BLK.108	13-16	9-11	45-50	1-3	20-24	-	-	-	-	2-5	-	
P70 9-10m	3407-BLK.109	22-26	7-10	7-9	1-3	52-58	0-5	-	-	-	-	-	
P74 10-11m	3408-BLK.110	2-6	0-1	87-93	0-2	3-7	-	-	-	-	-	-	
P74 11-12m	3409-BLK.111	3-7	0-1	87-93	0-2	3-7	-	-	-	-	-	-	

000553

Table A2.1 (continued).

Sample	XRD File	Paly	Ill	Dol	Hal	Qtz	Smt	Kaol	Cal	Gyp	Cel	An	Other
P76 6-7m	3410-BLK.112	3-7	0-1	73-79	1-2	16-20	-	-	-	-	-	-	
P76 7-8m	3411-BLK.101	25-30	1-3	57-63	3-5	2-5	0-5	-	-	0-1	-	-	
P76 8-9m	3412-BLK.102	10-13	1-2	75-80	2-4	5-7	-	0-1	-	-	-	-	
P76 9-10m	3413-BLK.103	15-18	1-3	60-65	3-7	10-13	0-5	-	-	-	-	-	
P76 10-11m	3414-BLK.104	29-33	1-3	36-42	4-8	18-22	0-5	-	-	-	-	-	
P76 11-12m	3415-BLK.105	8-12	<1	68-74	2-4	4-7	8-12	-	-	-	-	-	
P76 12-13m	3416-BLK.106	7-11	<1	70-75	2-4	3-6	8-12	-	-	-	-	-	
P76 13-14m	3417-BLK.107	3-7	<1	80-85	1-3	2-5	5-10	-	-	-	-	-	
P76 14-15m	3418-BLK.108	15-20	2-4	69-73	4-8	0-1	0-5	-	-	-	-	-	
P76 15-16m	3419-BLK.109	37-41	17-21	17-21	4-6	9-11	5-10	-	-	-	-	-	
P76 16-17m	3420-BLK.110	15-20	3-7	60-65	3-5	1-3	5-10	-	-	-	-	-	
P77 4-5m	3421-BLK.111	13-17	1-2	57-63	1-4	9-13	5-10	-	-	2-5	-	-	
P77 5-6m	3422-BLK.112	33-36	5-9	22-26	4-6	8-12	15-20	-	-	1-3	-	-	
P77 6-7m	3423-BLK.101	33-36	9-12	3-4	5-9	27-33	15-20	-	-	-	-	-	
P77 7-8m	3424-BLK.102	45-50	9-12	1-2	8-12	11-15	15-20	-	-	-	-	-	
P77 8-9m	3425-BLK.103	35-39	10-14	30-34	4-6	10-14	5-10	-	-	-	-	-	
P77 9-10m	3426-BLK.104	15-20	2-4	56-60	4-6	8-10	5-10	-	-	-	-	-	
P77 10-11m	3427-BLK.105	13-17	1-2	57-63	1-4	9-13	5-10	-	-	-	-	-	
P77 11-12m	3428-BLK.106	43-46	11-15	19-23	5-7	1-3	10-15	-	-	-	-	-	
P77 12-13m	3429-BLK.107	8-12	8-12	57-63	1-4	6-10	5-10	-	-	-	-	-	
P77 13-14m	3430-BLK.108	14-18	2-4	53-57	6-8	7-9	6-11	-	-	1-3	-	-	
P77 14-15m	3431-BLK.109	1-5	13-17	22-27	5-7	30-35	15-20	-	-	1-2	-	-	
P79 9-10m	3432-BLK.110	10-14	1-2	77-81	1-3	5-7	-	-	-	-	-	-	
P79 10-11m	3433-BLK.111	10-14	1-2	77-81	1-3	3-5	-	-	-	-	-	-	
P79 11-12m	3434-BLK.112	25-30	4-6	58-62	1-3	4-6	-	-	-	-	-	-	
P79 12-13m	3435-BLK.101	27-31	27-31	37-41	1-3	0-1	-	-	-	-	-	-	
P79 13-14m	3436-BLK.102	10-14	2-4	76-80	1-3	2-4	0-5	-	-	-	-	-	
P79 14-15m	3437-BLK.103	9-12	2-4	77-81	1-2	4-6	0-5	-	-	-	-	-	
P79 15-16m	3438-BLK.104	8-11	3-5	77-81	1-2	3-5	0-5	-	-	-	-	-	
P79 16-17m	3439-BLK.105	-	16-20	35-40	1-3	3-5	35-40	-	-	-	-	-	

Table A2.1 (continued).

Sample	XRD File	Paly	Ill	Dol	Hal	Qtz	Smt	Kaol	Cal	Gyp	Cel	An	Other
P84 6-7m	3440-BLK.106	1-2	2-4	0-2	-	65-70	5-15	15-20	-	-	-	Tr	
P84 7-8m	3441-BLK.107	5-9	3-5	-	0-1	70-75	5-15	1-5	-	-	-	Tr	
P84 8-9m	3442-BLK.108	55-61	7-10	5-7	1-3	20-25	0-5	-	-	-	-	Tr	
P84 9-10m	3443-BLK.109	17-20	4-7	70-75	1-2	1-5	-	-	-	-	-	-	
P84 10-11m	3444-BLK.110	4-8	1-3	87-93	0-1	1-2	-	-	-	-	-	-	
P84 11-12m	3445-BLK.111	34-38	2-5	34-38	2-3	20-23	-	-	-	-	-	-	
P84 12-13m	3446-BLK.112	44-48	5-9	6-10	2-5	34-37	-	-	-	-	-	-	
P84 13-14m	3447-BLK.101	42-46	6-10	10-14	3-5	30-34	-	-	-	-	-	-	
P84 14-15m	3448-BLK.102	10-13	1-3	42-48	1-2	35-39	0-5	-	-	-	-	-	
P84 15-16m	3449-BLK.103	50-55	6-10	5-7	3-5	24-28	0-5	-	-	-	-	-	
P84 16-17m	3450-BLK.104	37-42	10-14	14-18	2-3	26-30	0-5	-	-	-	-	-	
P85 0.3-1.08m	3451-BLK.105	55-60	5-7	-	26-30	6-10	-	-	-	-	-	-	
P85 1.08-1.1m	3452-BLK.106	15-20	<1	67-73	3-7	6-8	-	-	-	-	-	-	
P86 0.03-0.63m	3453-BLK.107	57-63	2-4	1-2	16-20	16-19	-	-	-	Tr	-	Tr	
P87 0-0.6m	3454-BLK.108	2-4	<1	87-93	3-5	1-3	-	-	-	-	-	-	
P88 0.4-1m	3455-BLK.109	37-41	2-4	1-2	12-15	40-45	-	-	-	-	-	-	
P88 1-2m	3456-BLK.110	40-45	7-10	-	12-15	33-37	-	-	-	-	-	Tr	
P88 2-3m	3457-BLK.111	35-40	14-18	-	12-15	31-35	-	-	-	-	-	Tr	
P88 3-4m	3458-BLK.112	-	-	-	12-15	42-47	40-45	-	-	-	-	Tr	

0005555

Table A2.2. Renormalised mineralogy (wt.%) of all studied samples from the Garford palaeochannel.

Paly	Ill	Dol	Sample	XRD File	Paly	Ill	Dol	Hal	Qtz	Smt	Kaol	Cal	Gyp	Cel	An	Other
97	0	3	P33 0-1.5m	P33-0-1.106	90	-	3	4	2	-	Tr	-	-	-	-	
93	5	2	P86 0.03-0.63m	3453-BLK.107	57-63	2-4	1-2	16-20	16-19	-	-	-	Tr	-	Tr	
91	9	0	P85 0.3-1.08m	3451-BLK.105	55-60	5-7	-	26-30	6-10	-	-	-	-	-	-	
90	7	3	P88 0.4-1m	3455-BLK.109	37-41	2-4	1-2	12-15	40-45	-	-	-	-	-	-	
88	12	0	P33 Lake Floor	3252-BLK.104	33-38	4-6	-	15-19	40-45	-	-	-	-	-	-	
83	17	0	P88 1-2m	3456-BLK.110	40-45	7-10	-	12-15	33-37	-	-	-	-	-	Tr	
77	15	8	P84 8-9m	3442-BLK.108	55-61	7-10	5-7	1-3	20-25	0-5	-	-	-	-	Tr	
76	15	9	P84 15-16m	3449-BLK.103	50-55	6-10	5-7	3-5	24-28	0-5	-	-	-	-	-	
75	11	13	P84 12-13m	3446-BLK.112	44-48	5-9	6-10	2-5	34-37	-	-	-	-	-	-	
70	30	0	P88 2-3m	3457-BLK.111	35-40	14-18	-	12-15	31-35	-	-	-	-	-	Tr	
69	13	19	P84 13-14m	3447-BLK.101	42-46	6-10	10-14	3-5	30-34	-	-	-	-	-	-	
69	8	23	P24 1-1.5m	P24-1-2.109	60	7	20	6	5	-	-	-	2	-	-	
64	19	17	P61 12-13m	3379-BLK.105	36-40	10-12	9-11	3-5	36-39	-	-	Tr	-	-	-	
63	29	8	P24 2-3m	P24-1-3.108	55	25	7	6	4	-	-	-	-	-	-	
63	13	25	P41 4-4.5m	P41-4-4~.305	50	10	20	15	2	-	-	-	-	-	-	
62	36	2	P77 7-8m	3424-BLK.102	45-50	9-12	1-2	8-12	11-15	15-20	-	-	-	-	-	
57	40	3	P65 10-11m	3386-BLK.112	39-43	23-28	2-3	5-7	20-25	1-5	-	-	-	-	-	
56	26	19	P70 9-10m	3407-BLK.109	22-26	7-10	7-9	1-3	52-58	0-5	-	-	-	-	-	
56	21	23	P84 16-17m	3450-BLK.104	37-42	10-14	14-18	2-3	26-30	0-5	-	-	-	-	-	
53	46	2	P65 13-14m	3389-BLK.103	42-46	23-28	1-2	5-7	8-11	10-15	-	-	-	-	Tr	
53	0	47	P35 6-7m	P356-7.117	50	-	45	5	<1	-	-	-	-	-	-	
52	42	5	P77 6-7m	3423-BLK.101	33-36	9-12	3-4	5-9	27-33	15-20	-	-	-	-	-	
51	18	31	P66 16-17m	3395-BLK.109	42-47	6-10	25-28	5-9	4-6	5-10	-	-	-	-	Tr	
51	9	41	P65 9-10m	3385-BLK.111	39-43	6-8	31-35	5-7	11-15	-	-	-	-	-	-	
50	26	24	P61 11-12m	3378-BLK.104	23-28	12-15	11-13	4-6	42-48	-	-	Tr	-	-	-	
50	46	4	P67 16-17m	3401-BLK.102	35-40	25-30	2-4	6-9	15-20	5-10	-	-	-	-	-	
50	0	50	P37 2-3m	P372-3.110	45	-	45	5	2	-	-	-	-	Tr	-	
50	0	50	P42 0.3-1m	P420-1	50	-	50	6	5	-	-	-	-	-	-	
49	28	23	P77 11-12m	3428-BLK.106	43-46	11-15	19-23	5-7	1-3	10-15	-	-	-	-	-	
48	16	36	P43 2.5-3m	P43-2~5-.104	40	8	30	15	<1	5	-	-	-	-	-	
48	5	48	P84 11-12m	3445-BLK.111	34-38	2-5	34-38	2-3	20-23	-	-	-	-	-	-	

000556

Table A2.2 (continued).

Paly	Ill	Dol	Sample	XRD File	Paly	Ill	Dol	Hal	Qtz	Smt	Kaol	Cal	Gyp	Cel	An	Other
47	28	25	P61 10-11m	3377-BLK.103	33-38	20-22	18-20	5-7	18-20	-	-	-	-	-	-	
47	16	38	P65 12-13m	3388-BLK.102	39-43	9-13	31-35	3-5	7-9	1-5	-	-	-	-	Tr	
47	0	53	P37 3-4m	P373-4.111	45	-	50	5	2	-	-	-	-	Tr	-	
46	31	22	P76 15-16m	3419-BLK.109	37-41	17-21	17-21	4-6	9-11	5-10	-	-	-	-	-	
45	53	2	P65 11-12m	3387-BLK.101	31-34	23-28	1-2	5-7	20-25	10-15	-	-	-	-	Tr	
45	0	55	P38 1-2m	P381-2.115	45	-	55	2	1	-	-	-	-	-	-	
42	48	11	P25 3-4m	P253-4	35	40	9	7	9	-	-	-	-	-	-	
42	30	29	P77 5-6m	3422-BLK.112	33-36	5-9	22-26	4-6	8-12	15-20	-	-	1-3	-	-	
42	22	36	P77 8-9m	3425-BLK.103	35-39	10-14	30-34	4-6	10-14	5-10	-	-	-	-	-	
42	6	52	P76 10-11m	3414-BLK.104	29-33	1-3	36-42	4-8	18-22	0-5	-	-	-	-	-	
39	50	11	P25 2-3m	P252-3	35	45	10	5	5	-	-	-	-	-	-	
39	0	61	P36 8-9m	P368-9.107	35	-	55	2	7	-	-	-	-	-	-	
39	0	61	P37 1-2m	P371-2.109	35	-	55	1	6	-	-	-	-	1	-	
39	0	61	P42 1-2m	P421-2	35	-	55	4	3	-	-	-	-	-	-	
38	60	2	P25 4-5m	P254-5	35	55	2	4	6	-	-	-	-	-	-	
38	15	48	P67 14-15m	3399-BLK.100	30-35	8-12	39-43	5-9	5-10	0-5	-	-	-	-	-	
38	0	63	P42 2-3m	P422-3	30	-	50	7	15	-	-	-	-	Tr	-	
37	32	32	P35 7-8m	P357-8.118	35	30	30	4	<1	-	-	-	-	-	-	
37	0	63	P26 3-4m	P263-4A.DAT	35	-	60	2	1	-	-	-	-	Tr	-	
35	32	33	P69 9-10m	3405-BLK.107	22-26	17-21	20-25	1-3	27-33	0-5	-	-	-	Tr	-	
35	0	65	P34 3-4m	P343-4	35	-	65	2	1	-	-	-	-	-	-	
35	0	65	P35 3-4m	P353-4.114	35	-	65	1	1	-	-	-	-	-	-	
35	0	65	P35 4-5m	P354-5.115	35	-	65	1	<1	-	-	-	-	-	-	
34	46	20	P68 11-12m	3402-BLK.104	27-33	30-35	15-19	3-5	7-11	5-10	-	-	-	-	-	
34	9	57	P42 3-5m	P423-4, 4-5	30	8	50	8	2	-	-	-	-	Tr	-	
33	17	50	P38 3-4m	P383-4.116	30	15	45	3	<1	-	-	-	-	5	-	
33	6	61	P41 2-3m	P41-2-3.303	30	5	55	5	1	-	-	-	-	-	-	
33	0	67	P33 2-3m	P33-2-3.108	30	-	60	5	5	-	Tr	-	-	-	-	
33	0	67	P36 6-8m	P366-8.DAT	30	-	60	2	7	-	-	-	-	-	-	
33	0	67	P40 3-4m	P40-3-4.204	30	-	60	7	1	-	-	-	-	1	-	
33	0	67	P43 1-1.5m	P43-1-2.102	30	-	60	7	<1	-	-	-	-	-	-	

0005527

Table A2.2 (continued).

Paly	Ill	Dol	Sample	XRD File	Paly	Ill	Dol	Hal	Qtz	Smt	Kaol	Cal	Gyp	Cel	An	Other
32	0	68	P34 1-2m	P341-2	30	-	65	2	-	-	-	-	-	-	-	
32	0	68	P35 2-3m	P352-3.113	30	-	65	1	<1	-	-	-	-	-	-	
32	0	68	P36 2-3m	P362-3.101	30	-	65	3	-	-	-	-	-	-	-	
32	0	68	P37 0-1m	P370-1.108	30	-	65	3	3	-	-	-	-	-	-	
31	6	63	P66 15-16m	3394-BLK.108	24-28	4-6	50-55	2-5	11-15	-	-	-	-	-	-	
30	70	0	P25 7-9m	P257-9	25	50	<1	5	9	-	8	-	-	-	-	
30	30	40	P79 12-13m	3435-BLK.101	27-31	27-31	37-41	1-3	0-1	-	-	-	-	-	-	
30	20	50	P30 3-4m	P303-4	30	20	50	3	<1	-	-	-	-	-	-	
30	5	65	P76 7-8m	3411-BLK.101	25-30	1-3	57-63	3-5	2-5	0-5	-	-	0-1	-	-	
30	5	65	P79 11-12m	3434-BLK.112	25-30	4-6	58-62	1-3	4-6	-	-	-	-	-	-	
30	0	70	P35 5-6m	P355-6.116	30	-	70	<1	1	-	-	-	-	-	-	
29	66	4	P61 13-14m	3380-BLK.106	23-28	55-60	2-5	5-7	5-10	-	-	-	-	-	-	
29	71	0	P25 5-6m	P255-6	25	60	<1	4	8	-	-	-	-	-	-	
29	71	0	P84 7-8m	3441-BLK.107	5-9	3-5	-	0-1	70-75	5-15	1-5	-	-	-	Tr	
29	51	21	P66 17-18m	3396-BLK.110	9-13	8-12	6-10	4-6	55-60	7-12	-	-	-	-	Tr	
28	27	45	P67 15-16m	3400-BLK.101	22-27	19-23	37-41	4-6	5-10	0-5	-	-	-	-	-	
28	11	61	P38 5-5.5m	P385-6.118	25	10	55	3	<1	-	Tr	-	-	Tr	-	
28	0	72	P36 4-5m	P364-5.103	25	-	65	1	9	-	-	-	Tr	-	-	
28	0	72	P36 5-6m	P365-6.104	25	-	65	2	7	-	-	-	1	-	-	
27	4	69	P43 1.5-2.5m	P43-2-2~.103	25	4	65	7	1	-	-	-	-	Tr	-	
27	2	71	P26 2-3m	P262-3.103	25	2	65	2	1	-	Tr	-	-	Tr	-	
27	0	73	P36 3-4m	P363-4.102	15	-	40	3	20	-	-	-	25	-	-	
26	16	58	P38 4-5m	P384-5.117	25	15	55	3	<1	-	-	-	-	-	-	
26	5	68	P53 1-1.5m	3268-BLK.120	20-24	3-6	55-59	7-10	5-8	-	-	-	1-2	-	-	
26	6	68	P26 1-2m	P261-2.102	25	6	65	2	1	-	Tr	-	-	Tr	-	
26	0	74	P34 4-5m	P344-5	25	-	70	2	1	-	-	-	-	-	-	
26	0	74	P41 1-2m	P41-1-2.302	25	-	70	3	2	-	-	-	-	-	-	
26	0	74	P43 0.1-1m	P43-0-1.101	25	-	70	5	<1	-	-	-	-	-	-	
25	0	75	P34 5-6m	P345-6	25	-	75	2	-	-	-	-	-	-	-	

Table A2.2 (continued).

Paly	Ill	Dol	Sample	XRD File	Paly	Ill	Dol	Hal	Qtz	Smt	Kaol	Cal	Gyp	Cel	An	Other
24	29	47	P42 6-7m	P426-7	20	25	40	9	3	-	-	-	-	Tr	-	
24	6	70	P57 0.1-0.6m	3274-BLK.206	19-23	4-6	58-62	7-10	5-7	-	-	-	-	-	-	
24	0	76	P41 0.3-1m	P41-0-1.301	20	-	65	2	10	-	-	-	-	-	-	
23	8	69	P41 3-4m	P41-3-4.304	20	7	60	6	<1	-	-	-	-	-	-	
22	78	0	P25 6-7m	P256-7	20	65	<1	4	4	-	4	-	-	-	-	
22	76	2	P49 0-0.2m	3263-BLK.115	4-8	4-8	0-1	2-4	72-78	5-10	5-10	-	-	-	-	Microcline - Tr
22	11	67	P40 5-6m	P40-5-6.206	20	10	60	8	<1	-	-	-	1	-	-	
22	0	78	P40 4-5m	P40-4-5.205	20	-	70	5	5	-	-	-	-	<1	-	
21	76	3	P61 14-15m	3381-BLK.107	15-20	60-65	1-4	<1	16-20	-	-	-	-	-	-	
21	16	63	P35 8-9m	P358-9.119	20	15	60	3	<1	-	-	-	-	-	-	
21	16	63	P37 4-5m	P374-5.112	20	15	60	7	2	-	-	-	-	Tr	-	
21	0	79	P33 1.5-2m	P33-1-2.107	20	-	75	2	2	-	-	-	-	-	-	
21	0	79	P34 2-3m	P342-3	20	-	75	1	2	-	-	-	-	-	-	
21	0	79	P40 0-1m	P40-0-1.201	20	-	75	5	<1	-	-	-	1	-	-	
21	0	79	P40 2-3m	P40-2-3.203	20	Tr	75	3	-	-	-	-	-	-	-	
20	12	67	P77 9-10m	3426-BLK.104	15-20	2-4	56-60	4-6	8-10	5-10	-	-	-	-	-	
20	14	66	P69 10-11m	3406-BLK.108	13-16	9-11	45-50	1-3	20-24	-	-	-	-	2-5	-	
20	5	75	P76 9-10m	3413-BLK.103	15-18	1-3	60-65	3-7	10-13	0-5	-	-	-	-	-	
20	0	80	P31 5-6m	P315-6.111	20	-	80	1	1	-	-	-	-	-	-	
20	0	80	P85 1.08-1.1m	3452-BLK.106	15-20	<1	67-73	3-7	6-8	-	-	-	-	-	-	
19	14	67	P77 13-14m	3430-BLK.108	14-18	2-4	53-57	6-8	7-9	6-11	-	-	1-3	-	-	
19	14	68	P76 16-17m	3420-BLK.110	15-20	3-7	60-65	3-5	1-3	5-10	-	-	-	-	-	
19	7	74	P84 14-15m	3448-BLK.102	10-13	1-3	42-48	1-2	35-39	0-5	-	-	-	-	-	
19	6	75	P84 9-10m	3443-BLK.109	17-20	4-7	70-75	1-2	1-5	-	-	-	-	-	-	
19	6	76	P76 14-15m	3418-BLK.108	15-20	2-4	69-73	4-8	0-1	0-5	-	-	-	-	-	
18	71	12	P37 6-7.5m	P376-7.114	15	60	10	7	<1	-	-	-	-	-	-	
18	11	71	P77 4-5m	3421-BLK.111	13-17	1-2	57-63	1-4	9-13	5-10	-	-	2-5	-	-	
18	11	71	P77 10-11m	3427-BLK.105	13-17	1-2	57-63	1-4	9-13	5-10	-	-	-	-	-	
17	25	57	P42 5-6m	P425-6	15	15	50	9	3	7	-	-	-	Tr	-	
17	17	67	P37 5-6m	P375-6.113	15	15	60	6	2	-	-	-	-	Tr	-	
17	0	83	P24 0-1m	P24-0-1.107	15	-	75	5	2	-	-	-	-	1	-	

000559

Table A2.2 (continued).

Paly	Ill	Dol	Sample	XRD File	Paly	Ill	Dol	Hal	Qtz	Smt	Kaol	Cal	Gyp	Cel	An	Other
16	80	5	P55 Upper grey clay	3271-BLK.203	3-7	3-7	-	6-10	38-42	15-20	1-5	1-2	~20	-	Tr	
16	3	80	P54 0.1-0.6m	3270-BLK.202	13-16	2-4	70-74	7-10	1-3	-	-	-	-	-	-	
16	0	84	P25 1-2m	P251-2	15	-	80	2	5	-	-	-	-	-	-	
16	0	84	P26 0-1m	P260-1.101	15	-	80	3	4	-	-	-	-	<1	-	
16	0	84	P26 4-5m	P264-5.105	15	-	80	3	1	-	Tr	-	-	Tr	-	
16	0	84	P26 5-6m	P265-6.106	15	-	80	3	Tr	-	Tr	-	-	Tr	-	
15	0	85	P30 1-2m	P301-2	15	-	85	2	<1	-	-	-	-	-	-	
15	0	85	P30 2-3m	P302-3	15	-	85	2	1	-	-	-	-	-	-	
15	0	85	P40 1-2m	P40-1-2.202	15	-	85	2	<1	-	-	-	-	-	-	
14	64	21	P40 6-7.5m	P40-6-7.207	10	45	15	15	6	-	-	-	-	1	-	
14	13	73	P68 12-13m	3403-BLK.105	11-15	8-12	67-73	1-3	1-3	0-5	-	-	-	-	-	
13	87	0	P26 6-6.5m	P266-7.107	10	20	-	5	15	45	Tr	-	-	-	Tr	
13	14	72	P68 13-14m	3404-BLK.106	10-14	8-12	62-67	1-3	7-12	0-5	-	-	-	-	-	
13	6	82	P79 13-14m	3436-BLK.102	10-14	2-4	76-80	1-3	2-4	0-5	-	-	-	-	-	
13	1	85	P65 6-7m	3382-BLK.108	11-15	0-2	80-85	1-3	2-5	-	-	-	-	-	-	
13	2	85	P79 9-10m	3432-BLK.110	10-14	1-2	77-81	1-3	5-7	-	-	-	-	-	-	
13	2	85	P79 10-11m	3433-BLK.111	10-14	1-2	77-81	1-3	3-5	-	-	-	-	-	-	
13	2	85	P76 8-9m	3412-BLK.102	10-13	1-2	75-80	2-4	5-7	-	0-1	-	-	-	-	
12	87	1	P65 14-15m	3390-BLK.104	5-10	35-40	0-1	2-3	30-35	15-20	-	-	-	-	Tr	
12	3	85	P53 0.6-1m	3269-BLK.201	9-13	1-4	76-82	4-6	2-4	-	-	-	-	-	Tr	
12	1	87	P66 14-15m	3393-BLK.107	9-13	0-2	80-85	1-3	3-6	-	-	-	-	-	-	
11	87	2	P66 18-19m	3397-BLK.111	7-10	45-55	1-2	3-5	17-20	15-20	-	-	-	-	Tr	
11	81	8	P61 6-8m	3375-BLK.101	5-10	20-30	1-5	1-3	20-30	5-10	20-30	1-5	-	-	Tr	
11	20	69	P77 12-13m	3429-BLK.107	8-12	8-12	57-63	1-4	6-10	5-10	-	-	-	-	-	
11	11	78	P76 11-12m	3415-BLK.105	8-12	<1	68-74	2-4	4-7	8-12	-	-	-	-	-	
11	6	83	P7914-15m	3437-BLK.103	9-12	2-4	77-81	1-2	4-6	0-5	-	-	-	-	-	
11	0	89	P29 6.9-9m	P29-6-9.DAT	10	-	85	1	1	-	-	-	1	-	-	
11	0	89	P34 6-6.5m	P346-7	10	-	85	2	-	-	-	-	-	-	-	

Table A2.2 (continued).

Paly	Ill	Dol	Sample	XRD File	Paly	Ill	Dol	Hal	Qtz	Smt	Kaol	Cal	Gyp	Cel	An	Other
10	62	29	P61 8-10m	3376-BLK.102	5-10	20-30	15-25	1-4	15-25	5-10	10-20	1-3	-	-	Tr	
10	11	79	P76 12-13m	3416-BLK.106	7-11	<1	70-75	2-4	3-6	8-12	-	-	-	-	-	
10	7	83	P79 15-16m	3438-BLK.104	8-11	3-5	77-81	1-2	3-5	0-5	-	-	-	-	-	
10	0	90	P31 2-3.5m	P312-3.108	10	-	90	1	1	-	-	-	-	-	-	
10	0	90	P52 0-1m	3267-BLK.119	7-10	<1	76-82	4-6	2-4	-	-	-	3-6	-	Tr	Barite - Tr
9	91	0	P65 16-17.5m	3392-BLK.106	5-10	55-60	<1	4-6	11-15	15-20	-	-	-	-	Tr	
9	12	79	P30 0-1m	P300-1	7	10	65	2	15	-	-	-	-	-	-	
8	43	49	P30 4-6m	P304-5	7	-	45	3	3	40	-	-	-	2	-	
8	0	92	P31 3.5-5m	P314-5.110	8	-	90	1	2	-	-	-	-	-	-	
7	93	0	P65 15-16m	3391-BLK.105	4-7	55-60	<1	3-5	12-16	15-20	-	-	-	-	Tr	
7	0	93	P33 Middle	3251-BLK.103	5-8	-	80-85	4-6	2-4	-	-	-	1-3	-	-	
7	0	93	P25 0-1m	P250-1	7	-	90	2	2	-	-	-	-	-	-	
6	75	19	P42 7-8m	P427-8	5	15	15	8	5	45	-	-	-	-	Tr	
6	2	92	P84 10-11m	3444-BLK.110	4-8	1-3	87-93	0-1	1-2	-	-	-	-	-	-	
6	1	93	P76 6-7m	3410-BLK.112	3-7	0-1	73-79	1-2	16-20	-	-	-	-	-	-	
6	0	94	P56 0.3-0.6m	3273-BLK.205	4-7	<1	86-92	2-4	2-3	-	-	-	-	-	-	
5	92	3	P84 6-7m	3440-BLK.106	1-2	2-4	0-2	-	65-70	5-15	15-20	-	-	-	Tr	
5	54	41	P77 14-15m	3431-BLK.109	1-5	13-17	22-27	5-7	30-35	15-20	-	-	1-2	-	-	
5	8	87	P76 13-14m	3417-BLK.107	3-7	<1	80-85	1-3	2-5	5-10	-	-	-	-	-	
5	2	92	P45 1.5-1.7m	3257-BLK.109	3-7	1-3	82-87	4-6	1-2	-	-	-	-	-	-	
5	1	94	P74 11-12m	3409-BLK.111	3-7	0-1	87-93	0-2	3-7	-	-	-	-	-	-	
5	1	94	P46 0-0.6m	3258-BLK.110	3-6	0-2	87-93	3-5	0-1	-	-	-	-	-	-	
5	0	95	P44 0.2-1m	3254-BLK.106	2-6	-	73-79	4-6	12-18	-	-	-	-	-	-	
4	96	1	P66 19-20m	3398-BLK.112	2-5	65-75	0-1	4-6	4-7	15-20	-	-	-	-	-	
4	1	95	P74 10-11m	3408-BLK.110	2-6	0-1	87-93	0-2	3-7	-	-	-	-	-	-	
3	8	89	P55 0-0.7m	3272-BLK.204	2-4	-	82-88	3-5	0-1	5-10	-	-	Tr	-	-	
3	0	97	P87 0-0.6m	3454-BLK.108	2-4	<1	87-93	3-5	1-3	-	-	-	-	-	-	

000561

Table A2.2 (continued).

Paly	Ill	Dol	Sample	XRD File	Paly	Ill	Dol	Hal	Qtz	Smt	Kaol	Cal	Gyp	Cel	An	Other
2	0	98	P65 7-8m	3383-BLK.109	1-3	<1	93-98	0-1	1-3	-	-	-	-	-	-	
2	0	98	P65 8-9m	3384-BLK.110	1-3	<1	93-98	1-2	1-2	-	-	-	-	-	-	
2	0	98	P51 0-1m	3266-BLK.118	0-3	-	86-92	2-4	5-7	-	-	-	-	-	-	
2	0	98	P45 0-1m	3255-BLK.107	0-3	-	90-95	4-6	0-1	-	-	-	-	-	-	
2	0	98	P33 Upper	3250-BLK.102	0-3	-	94-98	1-3	<1	-	-	-	-	-	-	
2	0	98	P48 1-1.7m	3262-BLK.114	0-3	-	94-98	1-2	1-2	-	-	-	-	-	-	
1	0	99	P48 0-1m	3261-BLK.113	0-2	-	94-98	1-3	<1	-	-	-	-	-	-	
1	0	99	P45 1-1.5m	3256-BLK.108	0-1	-	92-96	3-5	1-2	-	-	-	-	-	-	
0	100	0	P31 6-7m	P316-7.112	-	-	-	6	-	90	Tr	-	-	-	-	
0	100	0	Quartz Boulder	3249-BLK.101	-	~3	-	~6	~15	0-5	~75	-	-	-	-	
0	100	0	P48 Green clay	3260-BLK.112	-	8-12	-	2-4	62-68	5-10	5-10	-	Tr	-	Tr	Microcline ~ 5 Albite ~ 3
0	100	0	P88 3-4m	3458-BLK.112	-	-	-	12-15	42-47	40-45	-	-	-	-	Tr	
0	88	12	P42 8-9m	P428-9	<1	5	6	5	40	40	-	-	-	-	Tr	
0	60	40	P79 16-17m	3439-BLK.105	-	16-20	35-40	1-3	3-5	35-40	-	-	-	-	-	
0	1	99	P47 0-1m	3259-BLK.111	-	-	92-96	3-5	<1	0-2	-	-	Tr	-	-	
0	0	100	P44 0-1m	3253-BLK.105	Tr	-	92-98	4-6	-	-	-	-	-	-	-	
0	0	100	P49 Black nodule	3264-BLK.116	-	-	-	-	12-18	-	-	~85	-	-	-	Microcline - Tr
0	0	100	P50 0-0.7m	3265-BLK.117	-	-	94-98	1-3	1-3	-	-	-	-	-	-	

APPENDIX 3. LABORATORY METHOD FOR SEPARATION OF QUARTZ AND DOLOMITE FROM GARFORD PALAEOCHANNEL CLAY SAMPLES.

1a. Place 2gms of sample in Waring laboratory blender, add water and mix at low speed for 20secs and then high speed for 20secs.

Alternatively

1b. Place 2gms of sample in specimen jar, add water and place on wrist shaker (SPEX mill) for 20mins. Place mixture in beaker and add approximately 750ml of water.

2. Pass suspension through sieve (250μm will do but finer will assist in centrifugation) over 2 litre beaker. Wash sieve and discard oversize.

3. Ultrasonically treat in ultrasonic bath for 5mins.

4. Decant suspension to another beaker. Discard sediment in bottom of beaker.

5. Centifuge for 10mins at 6000rpm. Discard supernatant (thereby removing salt).

6. Resuspend in 800ml of water.

7. Centrifuge for <2μm fraction keeping both the <2μm fraction and >2μm fraction.

8. Check that the <2μm fraction is free of quartz. If pure retain as <2μm fraction, if impure add to >2μm fraction.

9. Ultrasonic >2μm fraction and then repeat steps 7, 8 and 9 until a quartz free sample is obtained.

10. Acid wash with 0.01M HCl to remove dolomite. The amount of HCl required will depend on the concentration of dolomite in the sample. For samples with less than 5wt% dolomite approximately 25ml of 0.01M HCl per gram of sample is sufficient. (The dolomite is removed when the pH of the suspension remains below 7 for 24hrs after the addition of HCl.)

11. Wash, centrifuge and dry at 105°C to recover sample.

APPENDIX 4. ANALYSES OF REFERENCE SAMPLES.

Several samples have been used in this study as standard reference materials. These samples are:

Attagel 50 (commercial gellant attapulgite)

Senegal attapulgite, ore and processed (commercial drilling mud)

Lake Nerramyne attapulgite (commercial absorbent)

Xuyi No. 1 deposit attapulgite (high quality palygorskite from China)

Arumpo bentonite, from test pit 1 (TP1)

Volclay premium gel (commercial gelant Na bentonite).

Most of the samples have been described in other Absorbent Clay Project Reports. The Mineralogy of specific reference materials is presented in Table 4.1. Table A4.1 shows XRF analyses of reference samples that have not been presented elsewhere in the Reports from the Absorbent Clay Project. Figs. A4.1 to A4.6 show XRD patterns for the reference samples. Transmission electron micrographs of Senegal attapulgite are shown in Fig. A4.7. The colour (light brown) and mineralogy of processed Senegal attapulgite is the same as the unprocessed ore suggesting that, other than crushing and perhaps the addition of a small amount of calcite, Senegal ore is given minimal processing. The colour of the <2μm fraction of Senegal attapulgite is very-pale yellow.

The exchange properties of the commercial Na-bentonite Volclay premium gel has been characterised by saturation with various cations. From the XRF analyses the structural formula for the <2μm >0.2μm fraction of Volclay premium gel is:

$(Na_{0.46}\ Ca_{0.13}\ Mg_{0.02}\ K_{0.02})\ (Al_{3.10}\ Mg_{0.51}\ Fe_{0.37})\ (Si_{7.77}\ Al_{0.23})\ O_{20}\ (OH)_4 \bullet nH_2O$

This formula was derived after subtracting 5wt.% SiO_2 (2.4wt.% quartz and 2.6wt.% cristobalite) that was shown to be present by XRD. The cation exchange capacity derived from this formula is 109.7 $cmol^+/kg$ of ignited clay. The exchangeable cations on an individual basis are:

Ca	Mg	Na	K	Total
		$cmol^+/kg$ of ignited clay		
36.6	5.6	64.7	2.8	109.7

Table A4.1. XRF analyses of 105°C dried reference samples. All samples <2μm >0.2μm unless otherwise stated.

	SiO_2	TiO_2	Al_2O_3	Fe_2O_3	MnO	MgO	CaO	Na_2O	K_2O	P_2O_5	SO_3	ZrO_2	Sr	Cl	F	Sum
Attagel 50	57.7	0.46	10.74	3.49	0.052	10.8	2.88	0.12	0.66	0.98	0.019	0.010	0.007	0.01	nm	88.0
Xuyi attapulgite	62.5	0.56	6.54	4.39	0.061	13.3	0.165	0.10	0.86	0.019	0.004	0.009	0.001	0.01	nm	88.6
Lake Nerramyne																
<53μm >2μm	54.6	0.78	14.77	4.79	0.062	7.3	2.88	0.29	2.06	0.012	0.020	0.027	0.008	0.06	nm	87.6
<2μm >0.2μm	56.3	0.76	17.36	5.24	0.033	6.7	0.492	0.59	2.08	0.009	0.026	0.021	0.005	0.25	nm	89.7
Senegal ore	62.1	0.47	8.79	4.47	0.016	11.1	1.11	0.13	0.483	0.512	0.017	0.016	0.005	0.03	nm	89.2
Senegal processed (acid washed)	59.3	0.40	8.61	4.52	0.022	11.4	0.90	0.09	0.396	0.287	0.019	0.009	0.004	0.01	nm	86.0
Volclay (premium gel)																
As received (bulk)	63.2	0.15	20.41	3.74	0.008	2.47	1.17	2.4	0.502	0.038	0.252	0.031	0.033	0.07	nm	94.5
As received	63.5	0.12	21.13	3.74	0	2.70	0.95	1.9	0.140	0.018	0.028	0.023	0.030	0.07	nm	94.3
Ca saturated	63.2	0.13	21.21	3.76	0.005	2.56	2.49	0.15	0.089	0.019	0.027	0.024	0.003	0.05	nm	93.7
Mg saturated	62.2	0.12	20.92	3.71	0.004	4.23	0.068	0.15	0.091	0.012	0.026	0.022	0.002	0.02	nm	91.6
Na saturated	64.3	0.13	21.34	3.84	0.003	2.62	0.71	2.0	0.116	0.021	0.033	0.025	0.022	0.04	nm	95.2

nm = not measured.

Fig. A4.1. Attagel 50. Omya Southern. As received and acid washed.

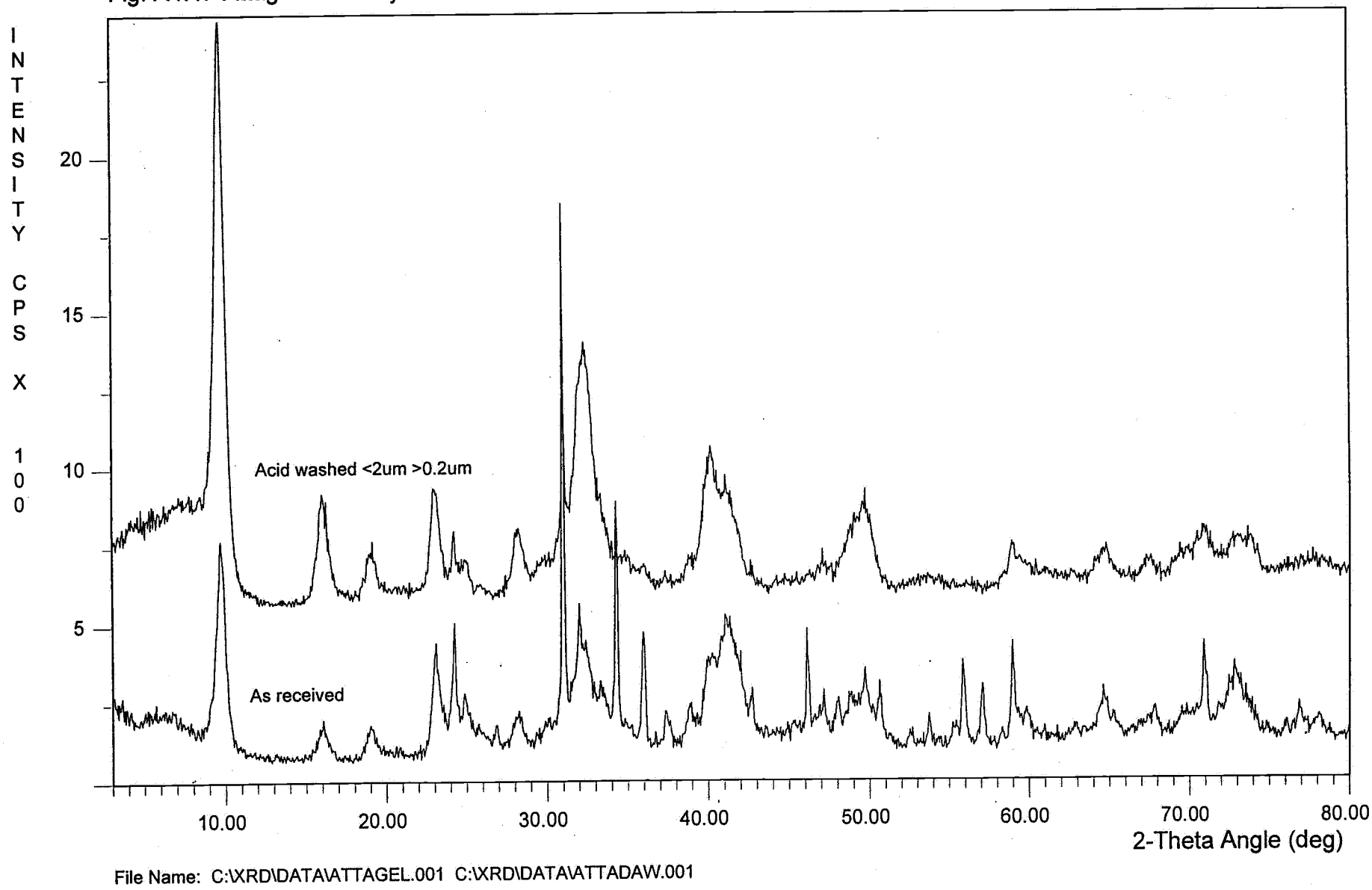


Fig. A4.1. XRD spectra (Co Kα radiation, back pressed) of as-received and acid-washed Attagel 50.

0005566

Fig. A4.2. Xuyi attapulgite. <2um >0.2um.

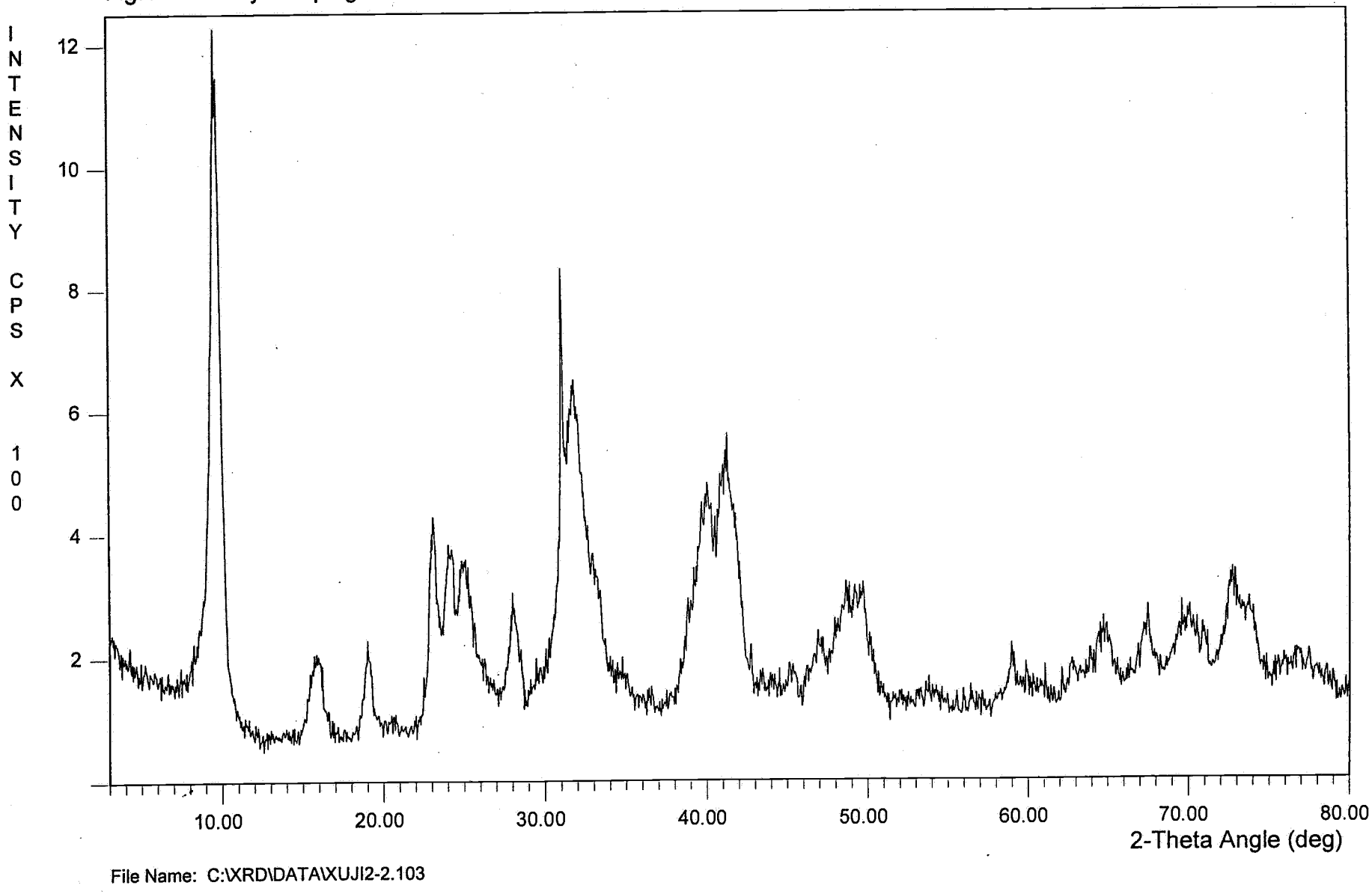


Fig. A4.2. XRD spectra (Co Kα radiation, back pressed) of <2μm >0.2μm fraction of attapulgite from Xuyi No. 1 deposit (China).

000567

Fig. A4.3. Lake Nerramyne. As sold.

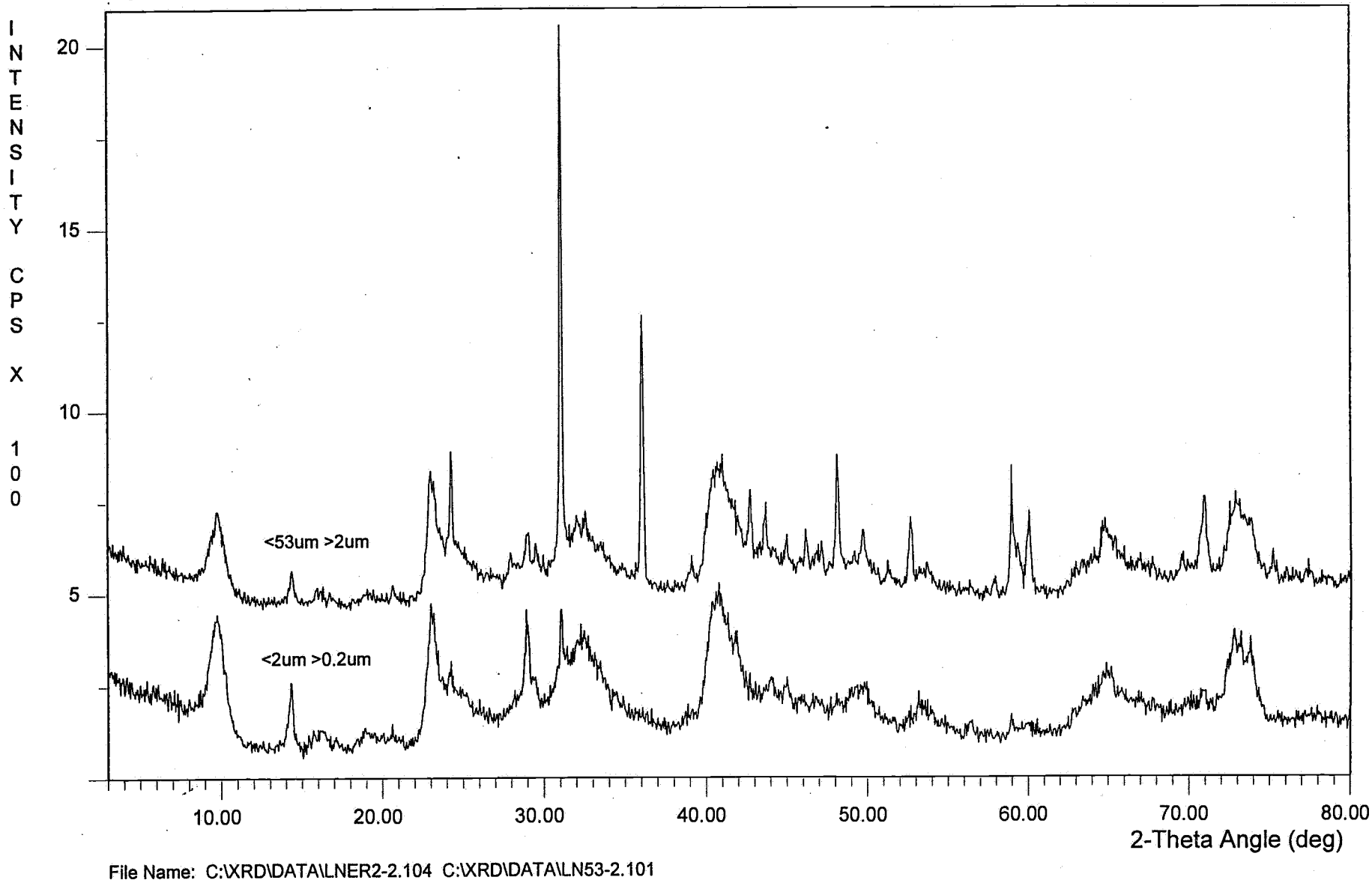
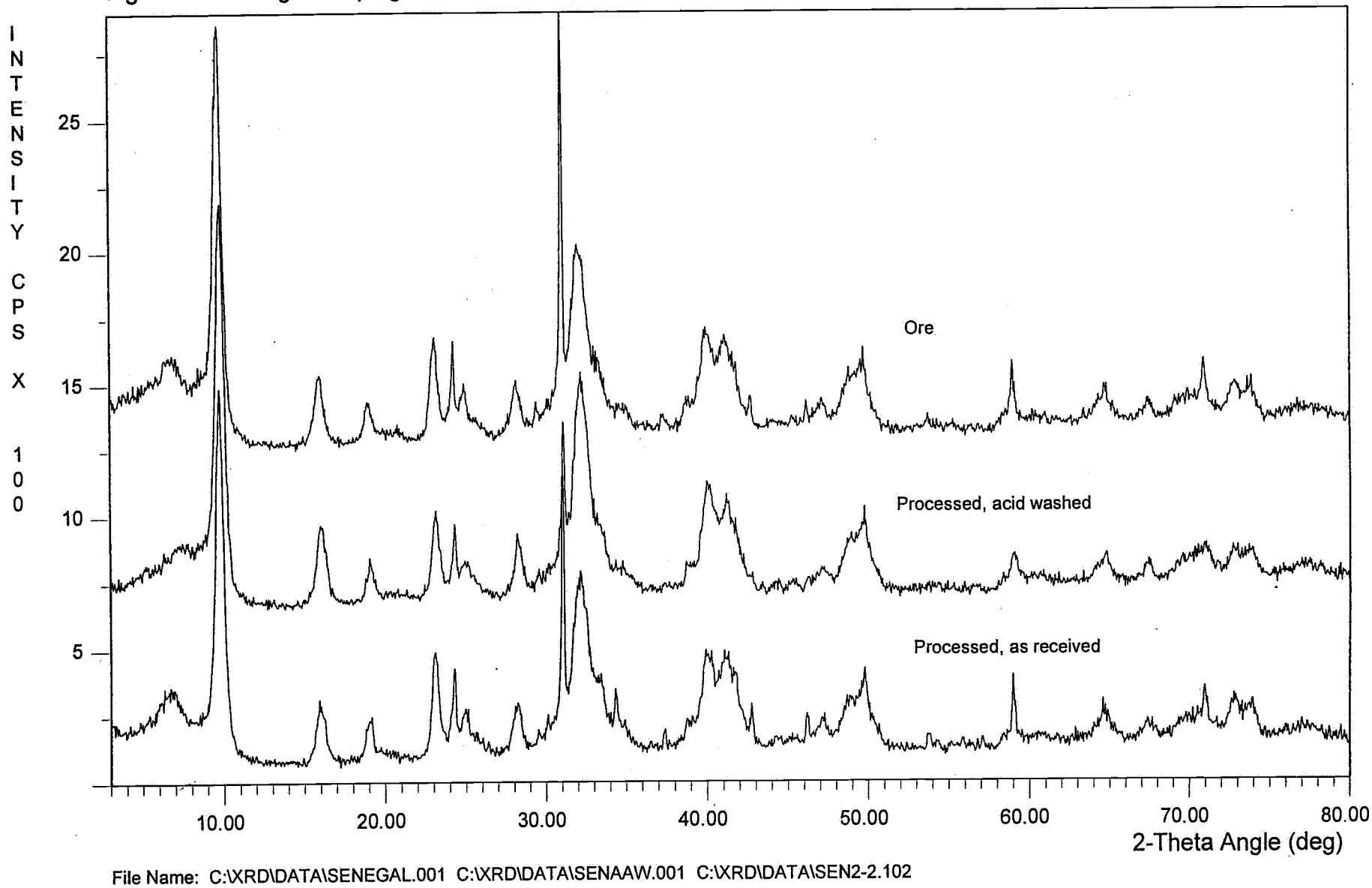


Fig. A4.3. XRD spectra (Co Kα radiation, back pressed) of <53μm >2μm and <2μm >0.2μm fractions of Lake Nerramyne attapulgite.

000568

Fig. A4.4. Senegal attapulgite. Processed (as received and acid washed) and ore (<2μm >0.2μm).



File Name: C:\XRD\DATA\SENEGAL.001 C:\XRD\DATA\SENAAW.001 C:\XRD\DATA\SEN2-2.102

Fig. A4.4. XRD spectra (Co Kα radiation, back pressed) of <2μm >0.2μm fraction of as-received Senegal ore and as-received and acid-washed processed Senegal attapulgite.

000569

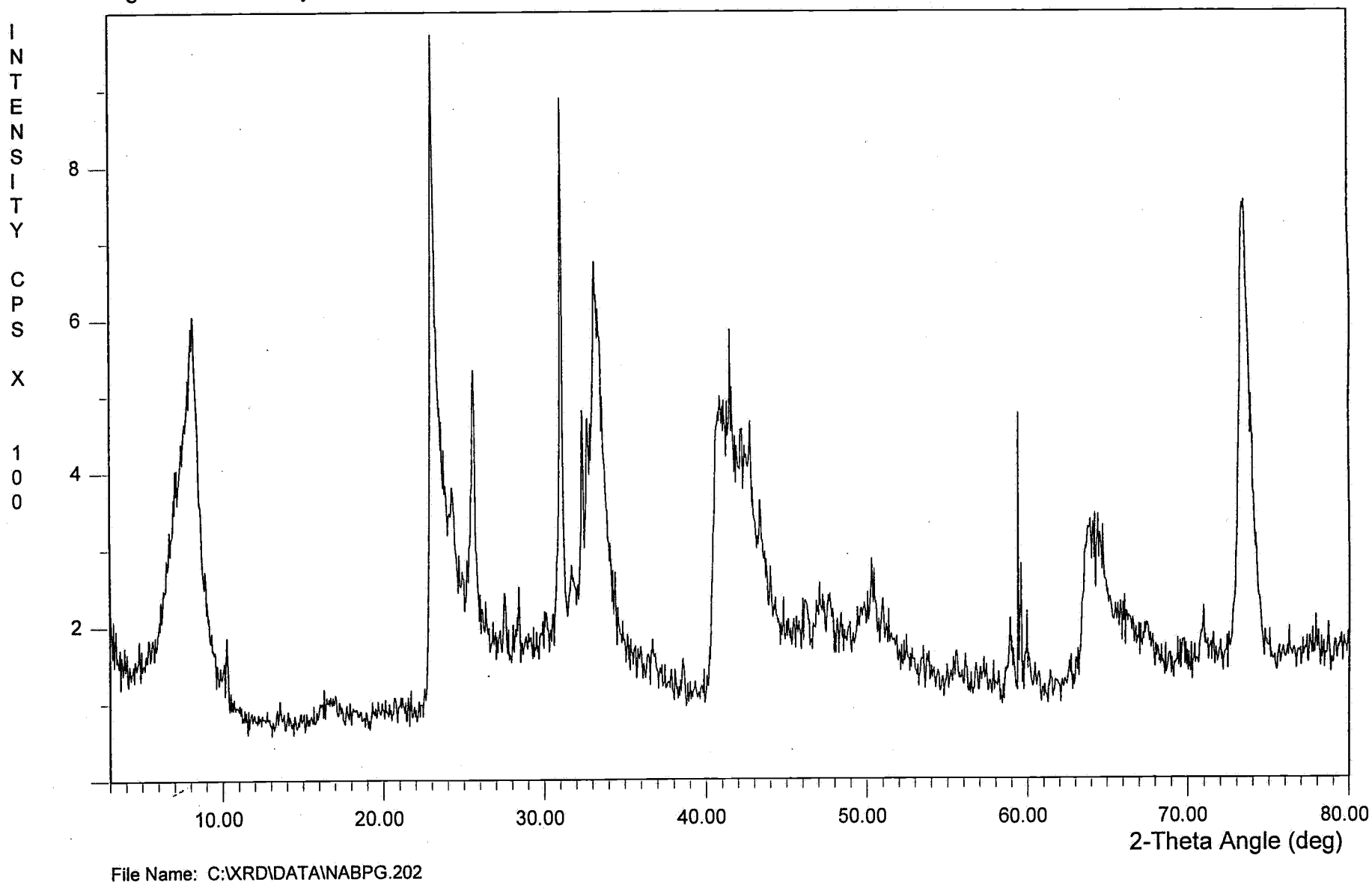


Fig. A4.5a. XRD spectra (Co Kα radiation, back pressed) of as-received Volclay premium gel (Na bentonite).

000520
197

Fig. A4.5b. Volclay premium gel. As-received and Na saturated. <2um >0.2um.

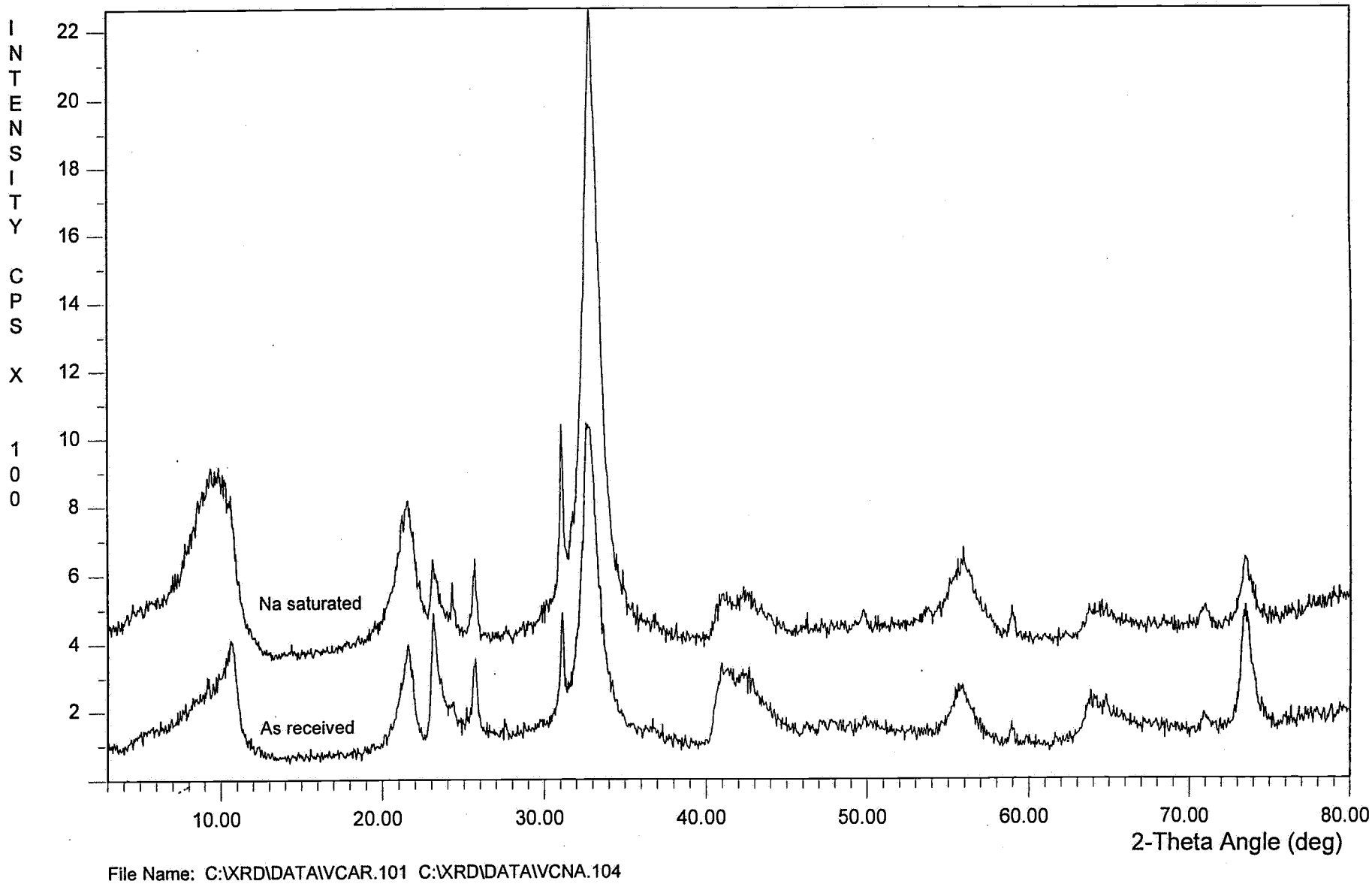


Fig. A4.5b. XRD spectra (Co Kα radiation, back pressed) of <2μm >0.2μm fraction of as-received and Na-saturated Volclay premium gel.

000571
198

Fig. A.4.5c. Volclay premium gel. Mg saturated and Ca saturated. <2um >0.2um.

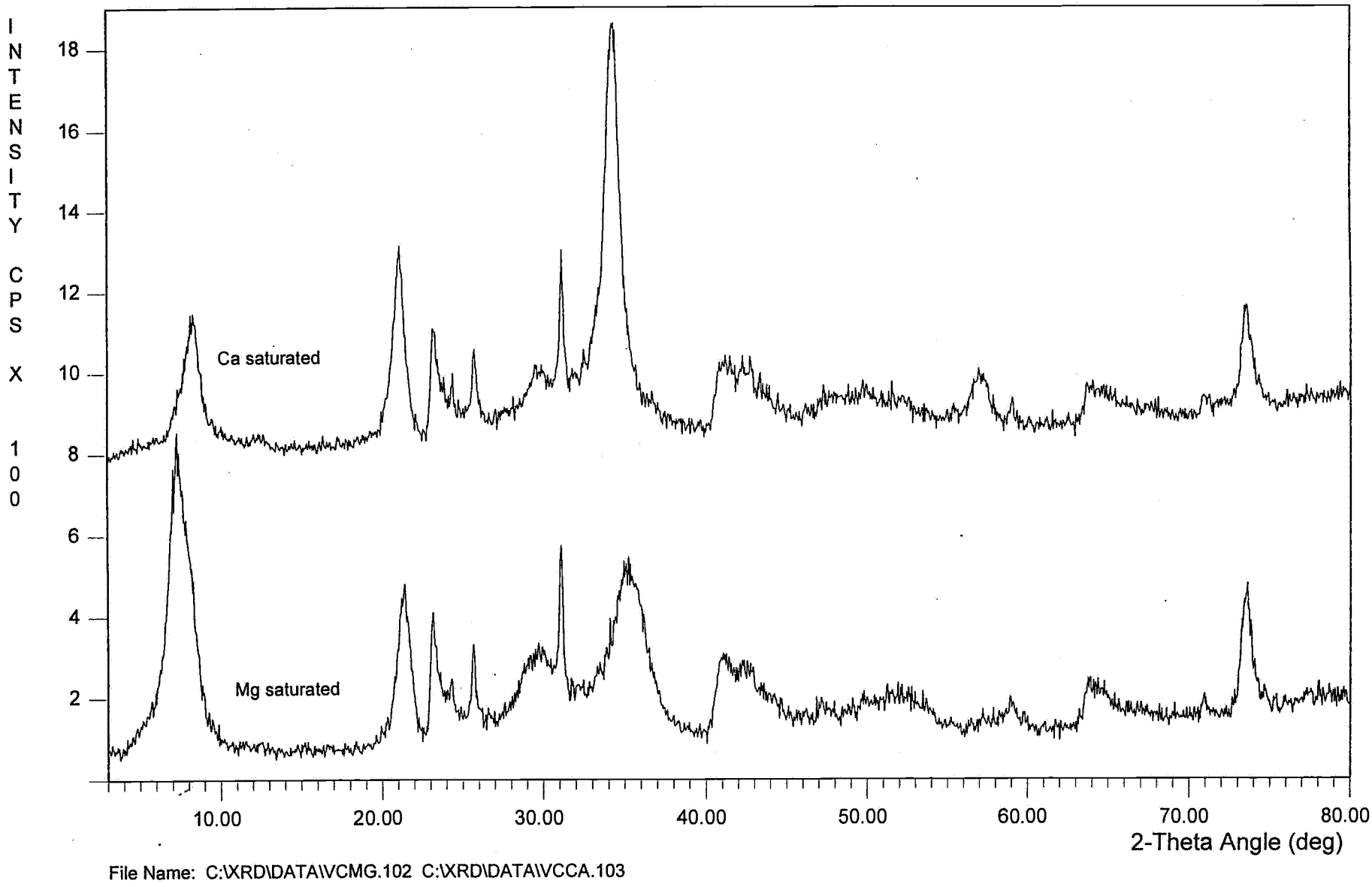


Fig. A4.5c. XRD spectra (Co Kα radiation, back pressed) of <2μm >0.2μm fraction of Ca-saturated and Mg-saturated Volclay premium gel.

000572
199

Fig. A4.6. Arumpo bentonite (TP1). As received and Na saturated. <2um >0.2um.

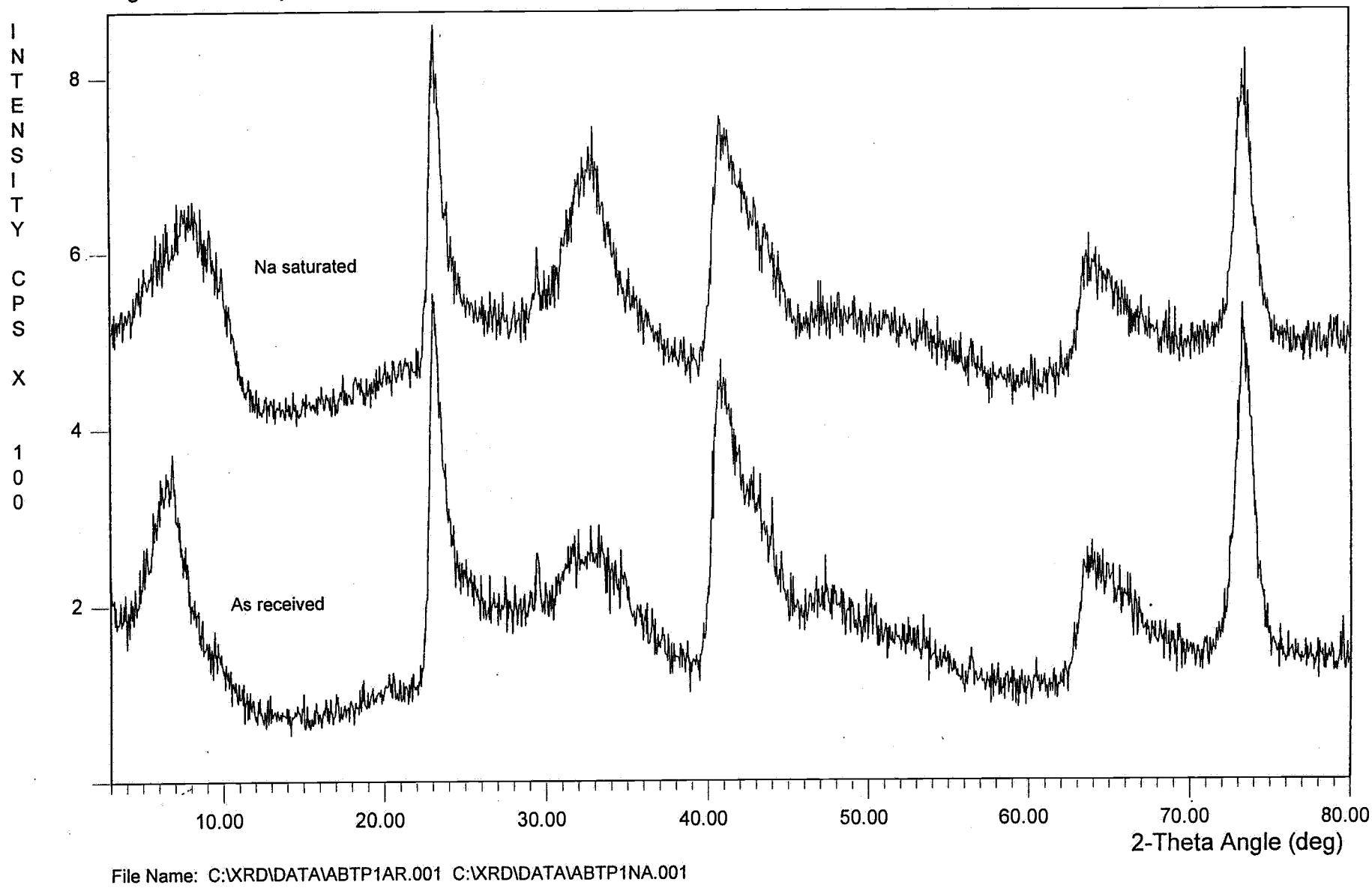


Fig. A4.6. XRD spectra (Co Kα radiation, back pressed) of <2μm >0.2μm fraction of as-received and Na-saturated Arumpo bentonite (TP1).

000573
200

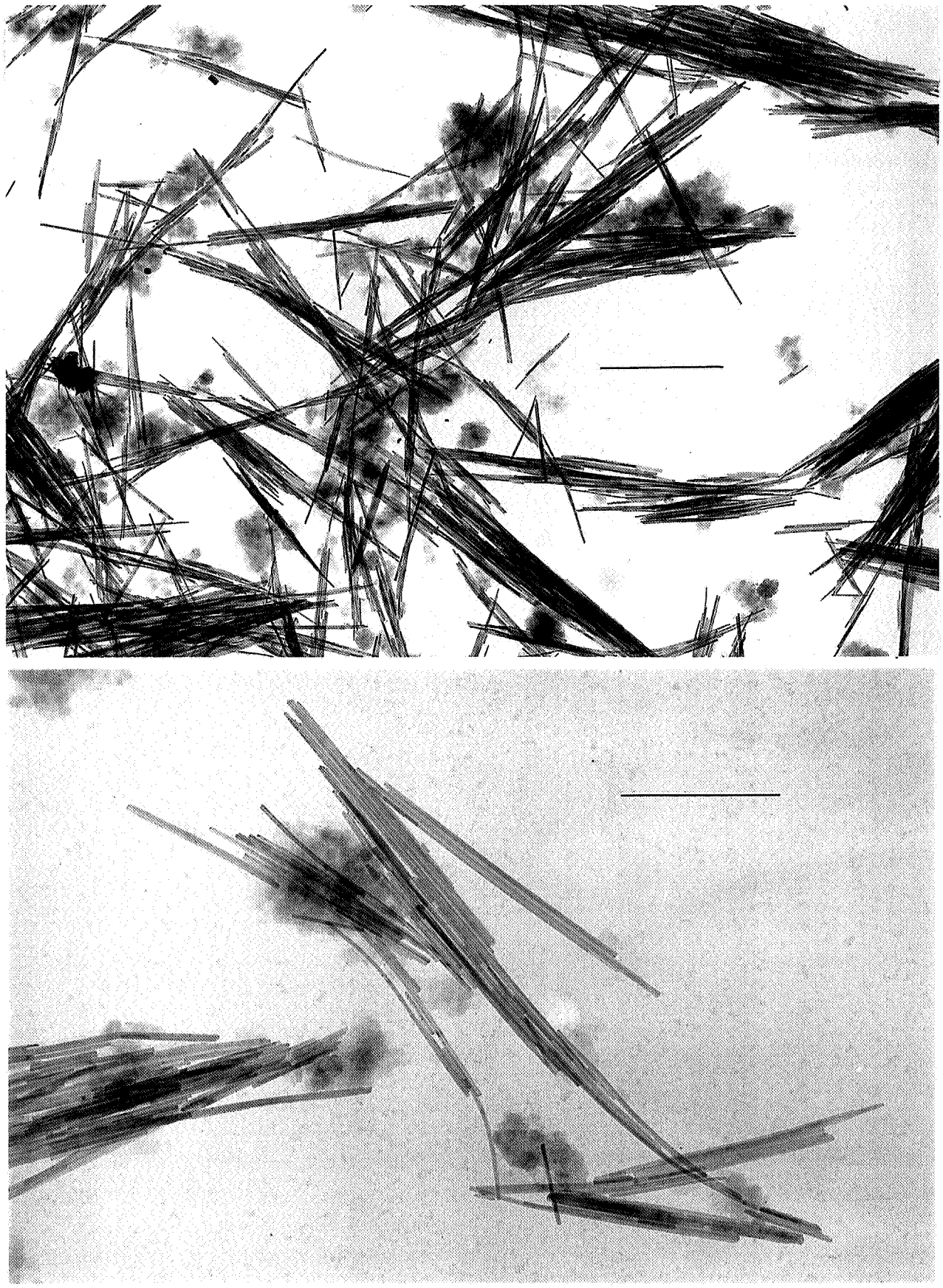


Fig. A4.7. Transmission electron micrographs of as-received Senegal attapulgite. Scale bars: 1μm (upper) and 0.5μm (lower). Plates: 022095 and 022098.

APPENDIX 5. WATER SORPTION BY WESTINGHOUSE METHOD.

Test based on Westinghouse Method to determine the absorbed water content of a given mass of sample as described in French Standard V19-002, December 1990 - "Pet Litter - Determination of absorbent power - Water retention capacity".

Sample requirements: Clay granules 1 to 6mm diameter.

Apparatus

- Balance with an accuracy of ±0.1gm.
- Cone made from stainless steel mesh with 0.35mm openings and wire diameter 0.22mm. Cone diameter 70mm, height 75mm, as per Fig. A5.1.

Method

- Weigh the cone = M_0 (±0.1gm).
- Weigh 20gm of sample = M_1 (±0.1gm). Place in cone.
- Immerse cone and sample in water and allow to soak for 20 minutes.
- Remove cone and sample and stand to drain for 30 minutes.
- Weigh the cone and saturated sample = M_2 (±0.1gm).
- Do three complete determinations for each sample.

Results

The water absorbing capacity, in mass %, equals:

$$\frac{M_2 - M_1 - M_0}{M_1} \times 100$$

Report the average of the three measurements.

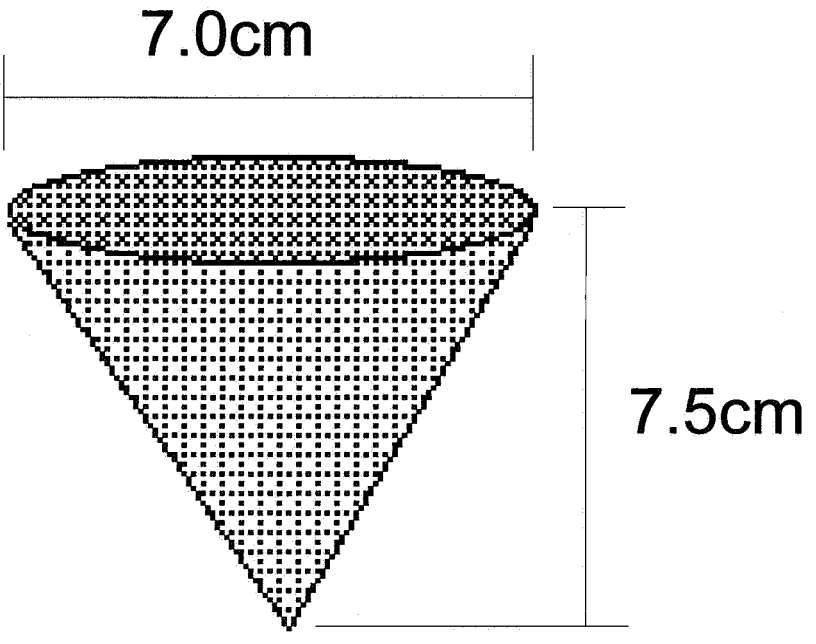
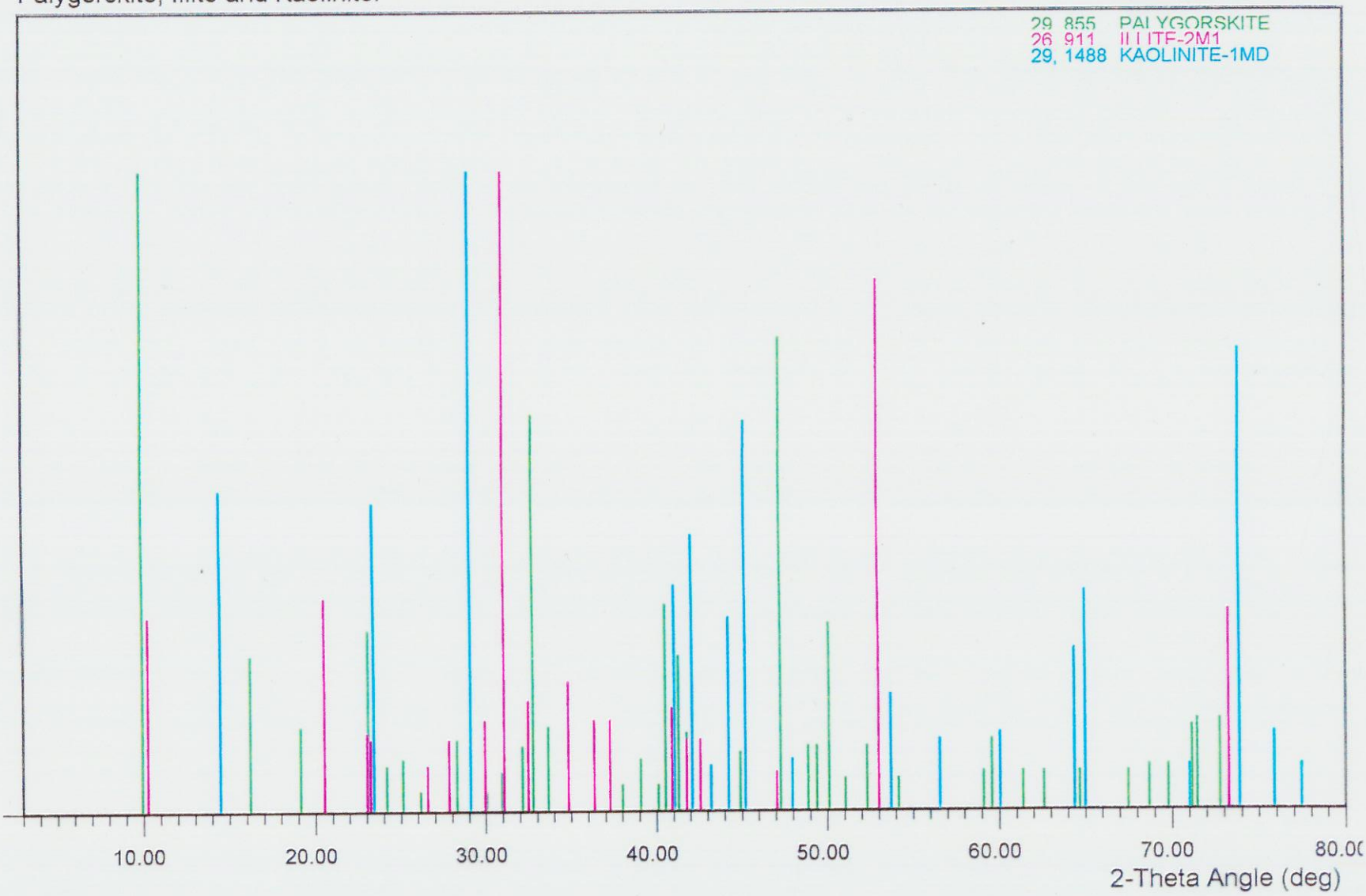


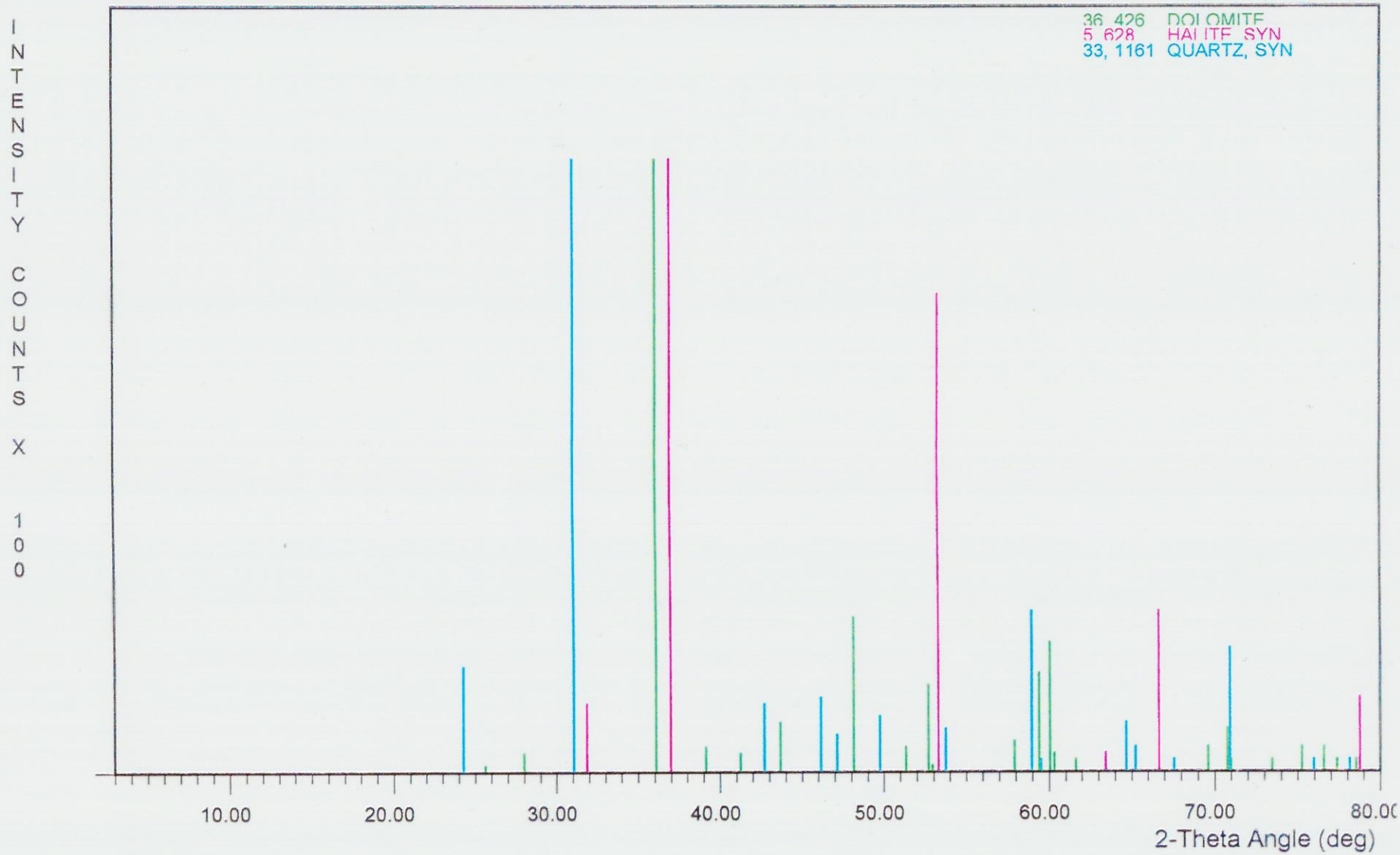
Fig. A5.1. Cone dimensions

Palygorskite, Illite and Kaolinite.



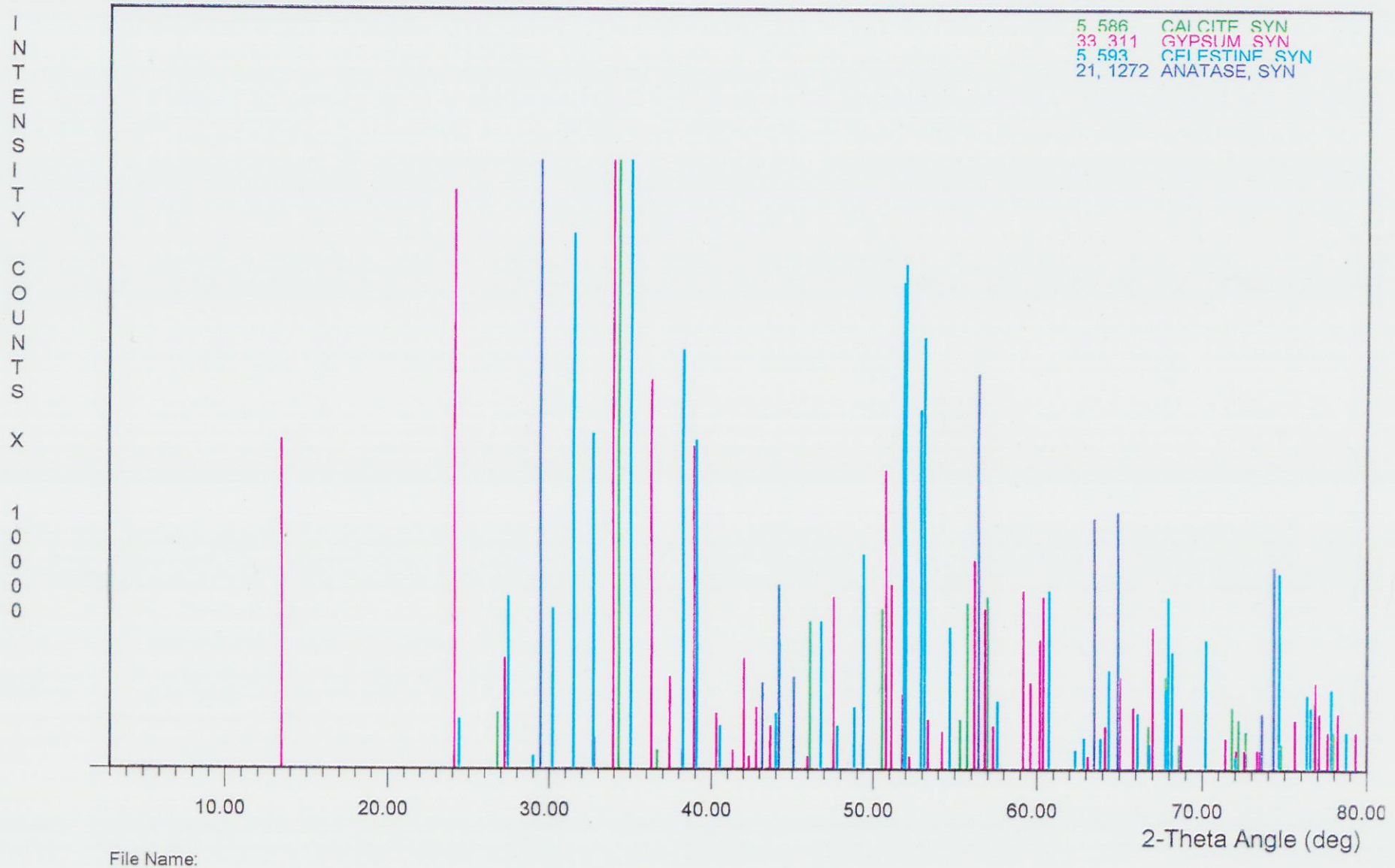
File Name:

Dolomite, Halite and Quartz.



File Name:

Calcite, Gypsum, Celestine and Anatase.



File Name: